

VOL. 469 MAY 19, 1989
COMPLETE IN ONE ISSUE

JOURNAL OF

CHROMATOGRAPHY

INTERNATIONAL JOURNAL ON CHROMATOGRAPHY, ELECTROPHORESIS AND RELATED METHODS

EDITORS

R. W. Giese (Boston, MA)
J. K. Haken (Kensington, N.S.W.)
K. Macek (Prague)
L. R. Snyder (Orinda, CA)

EDITOR, SYMPOSIUM VOLUMES, E. Heftmann (Orinda, CA)

EDITORIAL BOARD

D. W. Armstrong (Rolla, MO)
W. A. Aue (Halifax)
P. Boček (Brno)
A. A. Boulton (Saskatoon)
P. W. Carr (Minneapolis, MN)
N. H. C. Cooke (San Ramon, CA)
V. A. Davankov (Moscow)
Z. Deyl (Prague)
S. Dilli (Kensington, N.S.W.)
H. Engelhardt (Saarbrücken)
F. Erni (Basle)
M. B. Evans (Hatfield)
J. L. Glajch (N. Billerica, MA)
G. A. Guiochon (Knoxville, TN)
I. M. Hais (Hradec Králové)
W. S. Hargcock (San Francisco, CA)
S. Hjertén (Uppsala)
Cs. Horváth (New Haven, CT)
J. F. K. Huber (Vienna)
K.-P. Hupe (Waldbronn)
T. W. Hutchens (Houston, TX)
J. Janák (Brno)
P. Jandera (Pardubice)
B. L. Karger (Boston, MA)
E. sz. Kováts (Lausanne)
A. J. P. Martin (Cambridge)
L. W. McLaughlin (Chestnut Hill, MA)
R. P. Patience (Sunbury-on-Thames)
J. D. Pearson (Kalamazoo, MI)
H. Poppe (Amsterdam)
F. E. Regnier (West Lafayette, IN)
P. G. Righetti (Milan)
P. Schoenmakers (Eindhoven)
G. Schomburg (Mülheim/Ruhr)
R. Schwarzenbach (Dübendorf)
R. E. Shoup (West Lafayette, IN)
A. M. Sioffi (Marseille)
D. J. Strydom (Boston, MA)
K. K. Unger (Mainz)
J. T. Watson (East Lansing, MI)
B. D. Westerlund (Uppsala)

EDITORS, BIBLIOGRAPHY SECTION

Z. Deyl (Prague), J. Janák (Brno), V. Schwarz (Prague), K. Macek (Prague)

ELSEVIER

Scope. The *Journal of Chromatography* publishes papers on all aspects of chromatography, electrophoresis and related methods. Contributions consist mainly of research papers dealing with chromatographic theory, instrumental development and their applications. The section *Biomedical Applications*, which is under separate editorship, deals with the following aspects: developments in and applications of chromatographic and electrophoretic techniques related to clinical diagnosis or alterations during medical treatment; screening and profiling of body fluids or tissues with special reference to metabolic disorders; results from basic medical research with direct consequences in clinical practice; drug level monitoring and pharmacokinetic studies; clinical toxicology; analytical studies in occupational medicine.

Submission of Papers. Papers in English, French and German may be submitted, in three copies. Manuscripts should be submitted to: The Editor of *Journal of Chromatography*, P.O. Box 681, 1000 AR Amsterdam, The Netherlands, or to: The Editor of *Journal of Chromatography, Biomedical Applications*, P.O. Box 681, 1000 AR Amsterdam, The Netherlands. Review articles are invited or proposed by letter to the Editors. An outline of the proposed review should first be forwarded to the Editors for preliminary discussion prior to preparation. Submission of an article is understood to imply that the article is original and unpublished and is not being considered for publication elsewhere. For copyright regulations, see below.

Subscription Orders. Subscription orders should be sent to: Elsevier Science Publishers B.V., P.O. Box 211, 1000 AE Amsterdam, The Netherlands, Tel. 5803 911, Telex 18582 ESPA NL. The *Journal of Chromatography* and the *Biomedical Applications* section can be subscribed to separately.

Publication. The *Journal of Chromatography* (incl. *Biomedical Applications*) has 37 volumes in 1989. The subscription prices for 1989 are:

J. Chromatogr. + Biomed. Appl. (Vols. 461-497):
Dfl. 6475.00 plus Dfl. 999.00 (p.p.h.) (total ca. US\$ 3737.00)

J. Chromatogr. only (Vols. 461-486):
Dfl. 5200.00 plus Dfl. 702.00 (p.p.h.) (total ca. US\$ 2951.00)

Biomed. Appl. only (Vols. 487-497):
Dfl. 2200.00 plus Dfl. 297.00 (p.p.h.) (total ca. US\$ 1248.50).

Our p.p.h. (postage, package and handling) charge includes surface delivery of all issues, except to subscribers in Argentina, Australia, Brasil, Canada, China, Hong Kong, India, Israel, Malaysia, Mexico, New Zealand, Pakistan, Singapore, South Africa, South Korea, Taiwan, Thailand and the U.S.A. who receive all issues by air delivery (S.A.L. — Surface Air Lifted) at no extra cost. For Japan, air delivery requires 50% additional charge; for all other countries airmail and S.A.L. charges are available upon request. Back volumes of the *Journal of Chromatography* (Vols. 1-460) are available at Dfl. 195.00 (plus postage). Claims for missing issues will be honoured, free of charge, within three months after publication of the issue. Customers in the U.S.A. and Canada wishing information on this and other Elsevier journals, please contact Journal Information Center, Elsevier Science Publishing Co. Inc., 655 Avenue of the Americas, New York, NY 10010. Tel. (212) 633-3750.

Abstracts/Contents Lists published in Analytical Abstracts, ASCA, Biochemical Abstracts, Biological Abstracts, Chemical Abstracts, Chemical Titles, Chromatography Abstracts, Current Contents/Physical, Chemical & Earth Sciences, Current Contents/Life Sciences, Deep-Sea Research/Part B: Oceanographic Literature Review, Excerpta Medica, Index Medicus, Mass Spectrometry Bulletin, PASCAL-CNRS, Referativnyi Zhurnal and Science Citation Index.

See inside back cover for Publication Schedule, Information for Authors and information on Advertisements.

© ELSEVIER SCIENCE PUBLISHERS B.V. — 1989

0021-9673/89/503.50

All rights reserved. No part of this publication may be reproduced, stored in a retrieval system or transmitted in any form or by any means, electronic, mechanical, photocopying, recording or otherwise, without the prior written permission of the publisher, Elsevier Science Publishers B.V., P.O. Box 330, 1000 AH Amsterdam, The Netherlands.

Upon acceptance of an article by the journal, the author(s) will be asked to transfer copyright of the article to the publisher. The transfer will ensure the widest possible dissemination of information.

Submission of an article for publication entails the authors' irrevocable and exclusive authorization of the publisher to collect any sums or considerations for copying or reproduction payable by third parties (as mentioned in article 17 paragraph 2 of the Dutch Copyright Act of 1912 and the Royal Decree of June 20, 1974 (S. 351) pursuant to article 16 b of the Dutch Copyright Act of 1912) and/or to act in or out of Court in connection therewith.

Special regulations for readers in the U.S.A. This journal has been registered with the Copyright Clearance Center, Inc. Consent is given for copying of articles for personal or internal use, or for the personal use of specific clients. This consent is given on the condition that the copier pays through the Center the per-copy fee stated in the code on the first page of each article for copying beyond that permitted by Sections 107 or 108 of the U.S. Copyright Law. The appropriate fee should be forwarded with a copy of the first page of the article to the Copyright Clearance Center, Inc., 27 Congress Street, Salem, MA 01970, U.S.A. If no code appears in an article, the author has not given broad consent to copy and permission to copy must be obtained directly from the author. All articles published prior to 1980 may be copied for a per-copy fee of US\$ 2.25, also payable through the Center. This consent does not extend to other kinds of copying, such as for general distribution, resale, advertising and promotion purposes, or for creating new collective works. Special written permission must be obtained from the publisher for such copying.

No responsibility is assumed by the Publisher for any injury and/or damage to persons or property as a matter of products liability, negligence or otherwise, or from any use or operation of any methods, products, instructions or ideas contained in the materials herein. Because of rapid advances in the medical sciences, the Publisher recommends that independent verification of diagnoses and drug dosages should be made.

Although all advertising material is expected to conform to ethical (medical) standards, inclusion in this publication does not constitute a guarantee or endorsement of the quality or value of such product or of the claims made of it by its manufacturer.

This issue is printed on acid-free paper.

CONTENTS

(Abstracts/Contents Lists published in Analytical Abstracts, ASCA, Biochemical Abstracts, Biological Abstracts, Chemical Abstracts, Chemical Titles, Chromatography Abstracts, Current Contents/Physical, Chemical & Earth Sciences, Current Contents/Life Sciences, Deep-Sea Research/Part B: Oceanographic Literature Review, Excerpta Medica, Index Medicus, Mass Spectrometry Bulletin, PASCAL-CNRS, Referativnyi Zhurnal and Science Citation Index)

Publisher's Note	1
Interplay of hydrophobic and electrostatic interactions in biopolymer chromatography. Effects of salts on the retention of proteins by W. R. Melander, Z. El Rassi and Cs. Horváth (New Haven, CT, U.S.A.) (Received February 1st, 1989)	3
Mathematical modelling of the peak in liquid chromatography by J. Plicka, V. Svoboda, I. Kleinmann and A. Uhlířová (Prague, Czechoslovakia) (Received January 24th, 1989)	29
Optimization of the gas chromatographic separation of five-membered ring polyarenes with an admixed BPhBT liquid crystal-Dexsil 300 stationary phase by G. M. Janini and N. T. Filfil (Kuwait, Kuwait) (Received January 17th, 1989)	43
Contribution of longitudinal diffusion to band broadening in liquid chromatography by A. Berthod, F. Chartier and J.-L. Rocca (Villeurbanne, France) (Received January 20th, 1989)	53
Discussion of a controversial chiral recognition model by W. H. Pirkle and J. E. McCune (Urbana, IL, U.S.A.) (Received February 1st, 1989)	67
Resolution of a coeluting chromatographic pair using Kalman filtering by T. Barker and S. D. Brown (Newark, DE, U.S.A.) (Received January 31st, 1989)	77
Use of a centrifugal partition chromatography for assessing partition coefficients in various solvent systems by N. El Tayar, A. Marston, A. Bechalany, K. Hostettmann and B. Testa (Lausanne, Switzerland) (Received January 20th, 1989)	91
π -Acceptor amide group for liquid chromatographic chiral separations with special emphasis on the 3,5-dinitrobenzoyl amide by R. Däppen, H. R. Karfunkel and F. J. J. Leusen (Basle, Switzerland) (Received January 12th, 1989)	101
Ionization of DEAE-cellulose. Dependence of pK on ionic strength by M. A. Smith and P. C. Gillespie (Provo, UT, U.S.A.) (Received January 5th, 1989)	111
Study of the lipophilic character of a series of β -carboline by G. L. Biagi (Bologna, Italy), M. C. Pietrogrande (Ferrara, Italy), A. M. Barbaro and M. C. Guerra (Bologna, Italy), P. A. Borea (Ferrara, Italy) and G. Cantelli Forti (Bologna, Italy) (Received January 31st, 1989)	121
Normalisation of high-performance liquid chromatography peak retention times for computerised comparison of wheat prolamin chromatograms by H. C. Sapirstein, M. G. Scanlon and W. Bushuk (Winnipeg, Canada) (Received January 24th, 1989)	127
Analytical resolution of 4(5)-alkylated γ -(δ)-lactones by high-performance liquid chromatography on a silica-bonded chiral polyacrylamide sorbent. Chromatographic characterization of a stationary phase by M. Huffer and P. Schreier (Würzburg, F.R.G.) (Received January 13th, 1989)	137

(Continued overleaf)

(Contents continued)

Gas chromatographic and sorption properties of macroporous methacrylate copolymers by J. Hradil and F. Švec (Prague, Czechoslovakia), N. P. Platonova and L. D. Belyakova (Moscow, U.S.S.R.) and V. Maroušek (Prague, Czechoslovakia) (Received January 27th, 1989)	143
Use of crown ethers in gas chromatography by Y. Jin and R. Fu (Beijing, China) and Z. Huang (Wuhan, China) (Received January 13th, 1989)	153
Analysis of solvent residues in pharmaceutical bulk drugs by wall-coated open tubular gas chromato- graphy by D. W. Foust and M. S. Bergren (Kalamazoo, MI, U.S.A.) (Received February 10th, 1989)	161
Separation of 4-(2-pyridylazo)resorcinolato metal chelates by micellar electrokinetic capillary chro- matography by T. Saitoh, H. Hoshino and T. Yotsuyanagi (Sendai, Japan) (Received January 30th, 1989)	175
Chromatographic approaches to the quality control of chiral proprionate anti-inflammatory drugs and herbicides by B. Blessington, N. Crabb, S. Karkee and A. Northage (Bradford, U.K.) (Received Febru- ary 14th, 1989)	183
Derivatization of N-methyl and cyclic amino acids with dimethylformamide dimethyl acetal by M. F. Grubb and P. S. Callery (Baltimore, MD, U.S.A.) (Received January 20th, 1989)	191
Degradation and analysis of polyoxyethylene monoalkyl ethers in the presence of acetyl chloride and ferric chloride by J. Szymanowski (Poznań, Poland) and P. Kusz, E. Dziwiński, H. Szewczyk and K. Pyżal- ski (Kedzierzyn-Koźle, Poland) (Received January 16th, 1989)	197
Mass spectral investigations on trichothecene mycotoxins. VII. Liquid chromatographic-thermo- spray mass spectrometric analysis of macrocyclic trichothecenes by T. Krishnamurthy (Aberdeen Proving Ground, MD, U.S.A.), D. J. Beck and R. K. Isensee (Whitesboro, NY, U.S.A.) and B. B. Jarvis (College Park, MD, U.S.A.) (Received January 6th, 1989)	209
Sample-induced internal gradient of ionic strength in ion-exclusion microcolumn liquid chromato- graphy by K. Šlais (Brno, Czechoslovakia) (Received February 10th, 1989)	223
Formic acid as a milder alternative to trifluoroacetic acid and phosphoric acid in two-dimensional peptide mapping by D. J. Poll and D. R. K. Harding (Palmerston North, New Zealand) (Received January 18th, 1989)	231
Determination of polycyclic aromatic hydrocarbons in lubricating oil base stocks using high-per- formance liquid chromatography and gas chromatography-mass spectrometry by J.-P. F. Palmentier, A. J. Britten, G. M. Charbonneau and F. W. Karasek (Waterloo, Canada) (Received January 23rd, 1989)	241
Adsorption chromatography on cellulose. IV. Separation of D- and L-tryptophan and D- and L- methyltryptophan on cellulose with aqueous solvents by A. O. Kuhn and M. Lederer (Lausanne, Switzerland) and M. Sinibaldi (Monterotondo Scalo, Italy) (Received November 15th, 1988)	253
Separation of <i>cis</i> and <i>trans</i> isomers of unsaturated fatty acids by high-performance liquid chromato- graphy in the silver ion mode by W. W. Christie and G. H. McG. Breckenridge (Ayr, U.K.) (Received November 10th, 1988)	261

Separation of major phospholipid classes by high-performance liquid chromatography and subsequent analysis of phospholipid-bound fatty acids using gas chromatography by M. Seewald and H. M. Eichinger (Kranzberg, F.R.G.) (Received January 2nd, 1989)	271
Analysis of warfarin and its metabolites by reversed-phase ion-pair liquid chromatography with fluorescence detection by Y. W. J. Wong and P. J. Davis (Austin, TX, U.S.A.) (Received January 11th, 1989)	281
Separation of fungal sterols by normal-phase high-performance liquid chromatography. Application to the evaluation of ergosterol biosynthesis inhibitors by G. A. Peacock and M. W. Goosey (Wantage, U.K.) (Received January 24th, 1989)	293
Use of liquid chromatography in the synthesis of isoluminol-labelled medroxyprogesterone acetate and zeranol by H. Koehler, L. Larocque and S. Sved (Ottawa, Canada) (Received February 3rd, 1989)	305
Determination of preservatives in cosmetic products. II. High-performance liquid chromatographic identification by N. de Kruijf, A. Schouten, M. A. H. Rijk and L. A. Pranoto-Soetardhi (Zeist, The Netherlands) (Received January 18th, 1989)	317
Characterization of indirect photometry for the determination of inorganic anions in natural water by ion chromatography by N. Chauret and J. Hubert (Montreal, Canada) (Received January 11th, 1989)	329
Isocratic elution of sodium, ammonium, potassium, magnesium and calcium ions by ion-exchange chromatography by H. Sato (Yokohama-shi, Japan) (Received January 16th, 1989)	339
Capillary gas chromatographic-mass spectrometric determination of acid herbicides in soils and sediments by T. Tsukioka (Nagano, Japan) and T. Murakami (Tokyo, Japan) (Received January 11th, 1989)	351
Rapid high-performance liquid chromatographic separation of barley malt α -amylase on cyclobond columns by C. A. Henson and J. M. Stone (Madison, WI, U.S.A.) (Received January 24th, 1989)	361
Quantitative analysis of thorium in plutonium using reversed-phase liquid chromatography and spectrophotometric detection by V. T. Hamilton, W. D. Spall, B. F. Smith and E. J. Peterson (Los Alamos, NM, U.S.A.) (Received January 12th, 1989)	369

Notes

Influence of the cellulose content of cellulose gels on the electrophoretic mobility by M. Wroński (Łódź, Poland) (Received January 24th, 1989)	378
Chromatographic studies of metal complexes. V. Thin-layer chromatography of some octahedral cobalt(III) and nickel(II) complexes by R. K. Ray and M. K. Bandyopadhyay (Parganas, India) and G. B. Kauffman (Fresno, CA, U.S.A.) (Received January 21st, 1989)	383
Use of absorbance ratios in densitometric measurements for the characterization and identification of natural products of pharmacological interest by M. I. Walash and O. M. Salama (Mansoura, Egypt) and M. M. Bishr (Saffat, Kuwait) (Received December 27th, 1989)	390
Simple method for the preparation of spherical agarose and composite gel particles by E. Presecan, H. Porumb and I. Lascu (Cluj-Napoca, Romania) (Received January 31st, 1989)	396

(Continued overleaf)

Improvement of a carbon-nitrogen elemental analyser for marine samples collected on glass-fibre filters by C. Bechemin, D. Delmas and M.-J. Garet (Nieul-sur-Mer, France) (Received January 30th, 1989)	399
Large-volume spotting apparatus and its application to the semi-quantitative determination of organochlorine pesticides in tea by H. Wan (Hangzhou, China) (Received January 27th, 1989)	403
Traditional oriental medicines. I. Black Pearl: identification and chromatographic determination of some undeclared medicinal ingredients by A. By, J. C. Ethier, G. Lauriault, M. LeBelle, B. A. Lodge, C. Savard, W.-W. Sy and W. L. Wilson (Ottawa, Canada) (Received February 9th, 1989)	406
Resolution of neuroactive non-protein amino acid enantiomers by high-performance liquid chromatography utilising pre-column derivatisation with <i>o</i> -phthalaldehyde-chiral thiols. Application to 2-amino- <i>ω</i> -phosphonoalkanoic acid homologues and α -amino- β -N-methylaminopropionic acid (β -methylaminoalanine) by M. R. Euerby, L. Z. Partridge and P. B. Nunn (London, U.K.) (Received February 14th, 1989)	412
Application of correlation chromatography to the investigation of biopolymers in wines by I. Sh. Shatirishvili (Tbilisi, U.S.S.R.) (Received January 16th, 1989)	420
High-performance liquid chromatography of brassinosteroids in plants with derivatization using 9-phenanthreneboronic acid by K. Gamoh (Kochi-shi, Japan) and K. Omote, N. Okamoto and S. Takatsuto (Niigata, Japan) (Received January 24th, 1989)	424
Liquid chromatographic separation of racemates on acetylated or carbamoylated β -cyclodextrin-bonded stationary phases by M. Tanaka and T. Shono (Osaka, Japan), D.-Q. Zhu (Dalian, China) and Y. Kawaguchi (Kanagawa, Japan) (Received February 15th, 1989)	429
Milligram-scale separation of optical isomers of 2-pentafluoroethylalanine and 2-trifluoromethylalanine by medium-performance reversed-phase chromatography by J. W. Keller and K. Niwa (Fairbanks, AK, U.S.A.) (Received February 21st, 1989)	434
Isocratic reversed-phase high-performance liquid chromatographic assay for a cryptand-cryptate-free metal ion system by W. A. Pettit, B. K. Swailes and R. E. Peterson (Iowa City, IA, U.S.A.) (Received February 27th, 1989)	440
Use of free-flow electrophoresis for the purification of components separated by ion-pair chromatography by R. Kessler, H. J. Manz and G. Székely (Basle, Switzerland) (Received February 2nd, 1989)	444
Purification of yeast killer toxin KT28 by receptor-mediated affinity chromatography by M. Schmitt and F. Radler (Mainz, F.R.G.) (Received January 27th, 1989)	448
Author Index	453

*
* In articles with more than one author, the name of the author to whom correspondence should be addressed is indicated in the
* article heading by a 6-pointed asterisk (*)
*

JOURNAL OF CHROMATOGRAPHY

VOL. 469 (1989)

JOURNAL *of* CHROMATOGRAPHY

INTERNATIONAL JOURNAL ON CHROMATOGRAPHY,
ELECTROPHORESIS AND RELATED METHODS

EDITORS

R. W. GIESE (Boston, MA), J. K. HAKEN (Kensington, N.S.W.), K. MACEK (Prague),
L. R. SNYDER (Orinda, CA)

EDITOR, SYMPOSIUM VOLUMES

E. HEFTMANN (Orinda, CA)

EDITORIAL BOARD

D. W. Armstrong (Rolla, MO), W. A. Aue (Halifax), P. Boček (Brno), A. A. Boulton (Saskatoon), P. W. Carr (Minneapolis, MN), N. H. C. Cooke (San Ramon, CA), V. A. Davankov (Moscow), Z. Deyl (Prague), S. Dilli (Kensington, N.S.W.), H. Engelhardt (Saarbrücken), F. Erni (Basle), M. B. Evans (Hatfield), J. L. Glajch (N. Billerica, MA), G. A. Guiochon (Knoxville, TN), I. M. Hais (Hradec Králové), W. S. Hancock (San Francisco, CA), S. Hjertén (Uppsala), Cs. Horváth (New Haven, CT), J. F. K. Huber (Vienna), K.-P. Hupe (Waldbronn), T. W. Hutchens (Houston, TX), J. Janák (Brno), P. Jandera (Pardubice), B. L. Karger (Boston, MA), E. sz. Kováts (Lausanne), A. J. P. Martin (Cambridge), L. W. McLaughlin (Chestnut Hill, MA), R. P. Patience (Sunbury-on-Thames), J. D. Pearson (Kalamazoo, MI), H. Poppe (Amsterdam), F. E. Regnier (West Lafayette, IN), P. G. Righetti (Milan), P. Schoenmakers (Eindhoven), G. Schomburg (Mülheim/Ruhr), R. Schwarzenbach (Dübendorf), R. E. Shoup (West Lafayette, IN), A. M. Siouffi (Marseille), D. J. Strydom (Boston, MA), K. K. Unger (Mainz), J. T. Watson (East Lansing, MI), B. D. Westerlund (Uppsala)

EDITORS, BIBLIOGRAPHY SECTION

Z. Deyl (Prague), J. Janák (Brno), V. Schwarz (Prague), K. Macek (Prague)



ELSEVIER

AMSTERDAM — OXFORD — NEW YORK — TOKYO

J. Chromatogr., Vol. 469 (1989)

All rights reserved. No part of this publication may be reproduced, stored in a retrieval system or transmitted in any form or by any means, electronic, mechanical, photocopying, recording or otherwise, without the prior written permission of the publisher, Elsevier Science Publishers B.V., P.O. Box 330, 1000 AH Amsterdam, The Netherlands.

Upon acceptance of an article by the journal, the author(s) will be asked to transfer copyright of the article to the publisher. The transfer will ensure the widest possible dissemination of information.

Submission of an article for publication entails the authors' irrevocable and exclusive authorization of the publisher to collect any sums or considerations for copying or reproduction payable by third parties (as mentioned in article 17 paragraph 2 of the Dutch Copyright Act of 1912 and the Royal Decree of June 20, 1974 (S. 351) pursuant to article 16 b of the Dutch Copyright Act of 1912) and/or to act in or out of Court in connection therewith.

Special regulations for readers in the U.S.A. This journal has been registered with the Copyright Clearance Center, Inc. Consent is given for copying of articles for personal or internal use, or for the personal use of specific clients. This consent is given on the condition that the copier pays through the Center the per-copy fee stated in the code on the first page of each article for copying beyond that permitted by Sections 107 or 108 of the U.S. Copyright Law. The appropriate fee should be forwarded with a copy of the first page of the article to the Copyright Clearance Center, Inc., 27 Congress Street, Salem, MA 01970, U.S.A. If no code appears in an article, the author has not given broad consent to copy and permission to copy must be obtained directly from the author. All articles published prior to 1980 may be copied for a per-copy fee of US\$ 2.25, also payable through the Center. This consent does not extend to other kinds of copying, such as for general distribution, resale, advertising and promotion purposes, or for creating new collective works. Special written permission must be obtained from the publisher for such copying.

No responsibility is assumed by the Publisher for any injury and/or damage to persons or property as a matter of products liability, negligence or otherwise, or from any use or operation of any methods, products, instructions or ideas contained in the materials herein. Because of rapid advances in the medical sciences, the Publisher recommends that independent verification of diagnoses and drug dosages should be made. Although all advertising material is expected to conform to ethical (medical) standards, inclusion in this publication does not constitute a guarantee or endorsement of the quality or value of such product or of the claims made of it by its manufacturer.

This issue is printed on acid-free paper.

PUBLISHER'S NOTE

This volume of the *Journal of Chromatography* is remarkable in that it ushers in a new era in the history of the journal. As our readers will know, Michael Lederer has been its editor since it first appeared more than 30 years ago. In that time we have seen it grow from one volume per year in bimonthly issues, to 37 volumes per year in 60 issues, so that there is now more than one issue per week.

During these years, Michael Lederer has amply demonstrated his encyclopaedic knowledge of the field of chromatography and has amazed many an author by his recollection of references bearing on the author's own work, but performed decades earlier. His editorial work has been of great benefit to the journal and has certainly assisted in its development towards the position it holds today.

Turning to the future, it was decided that with a view to the continuity of the journal a number of editors should take over the helm so that the increasing diversity of methods and applications could adequately be dealt with. These considerations led to the appointment of a team of five new editors, each of them active in a different field. Tragically, one of them, Roland Frei, died before the transition could take place, so that four now remain. They are supported by the reconstructed editorial board of the main part of the journal, and that of the biomedical section.

The general structure with the "black" main part of the journal, including the symposium volumes, and the "red" biomedical applications section, will be maintained. The types of papers published will remain unchanged, but special issues will be introduced into the main part dealing with particular themes of current interest. These will consist both of reviews and of original papers.

The reputation of any scientific journal naturally depends on the quality of the papers published. This in turn depends on the unstinted efforts of editors, editorial board members and referees. The new team of editors is determined to ensure that high standards are maintained, and know that most authors give preference to a journal where this is the case. The publishers will continue to strive to achieve the shortest possible publication time consistent with the refereeing and production stages.

Summarising, we would like to express our thanks to the authors (upon whose submissions the journal ultimately depends) the editors, the board members, and certainly the referees who together have ensured that the journal is the leader in the field. It is our conviction that with the new editorial team it will continue this worthy tradition.

And in conclusion, it is clear that the science of chromatography owes a debt of gratitude to Michael Lederer for all the efforts he has untiringly devoted in the course of several decades to the furtherance of the field, and to the stimulation of the publication of its results.

Our best efforts will be devoted to maintaining the high quality of the journal to which Michael Lederer has contributed so much. Profound thanks are his due.

CHROM. 21 393

INTERPLAY OF HYDROPHOBIC AND ELECTROSTATIC INTERACTIONS IN BIOPOLYMER CHROMATOGRAPHY

EFFECT OF SALTS ON THE RETENTION OF PROTEINS^a

WAYNE R. MELANDER^b, ZIAD EL RASSI^c and CSABA HORVÁTH*

Department of Chemical Engineering, Yale University, P.O. Box 2159, Yale Station, New Haven, CT 06520 (U.S.A.)

(Received February 1st, 1989)

SUMMARY

The effect of salt on the retention behavior of proteins in electrostatic and hydrophobic interaction chromatography is described by a three-parameter equation, $\log k' = A - B \log m_s + C m_s$, where k' is the retention factor and m_s is the molality of the salt in the eluent. Parameter B , termed the electrostatic interaction parameter, depends on the characteristic charge of the protein and the salt counterion and governs the change of retention with the salt concentration in ion-exchange chromatography. According to the model the magnitude of the hydrophobic interaction parameter C is determined by the hydrophobic contact area upon protein binding at the stationary phase surface and the properties of the salt as measured by its molal surface tension increment. Retention data measured at different salt concentrations in the eluent on a variety of ion exchangers can be fitted to the above equation which yields U-shaped plots of $\log k'$ against $\log m_s$. The limiting slopes of the appropriate plots at sufficiently low and high salt concentrations can be used to evaluate the electrostatic and hydrophobic interaction parameters, respectively. The approach, which is based on a combination of established treatments of electrostatic and hydrophobic interactions offers a convenient framework for analyzing retention data in biopolymer high-performance liquid chromatography and for the characterization of stationary phases. Furthermore, it may facilitate some characterization of protein molecules on the basis of their retention behavior as a function of the concentration and nature of the salt in the eluent.

In the treatment of electrostatic interactions use is made of the counterion condensation theory that is believed to make possible a more comprehensive analysis

^a Presented at the *9th International Symposium on Column Liquid Chromatography*, Edinburgh, July 1-5, 1985. The majority of the papers presented at this symposium have been published in *J. Chromatogr.*, Vols. 352 (1986) and 353 (1986).

^b Present address: E. I. duPont de Nemours and Company, Inc., Medical Products Department, Diagnostics Systems Research and Development Division, Glasgow Site, Mailbox 122, Wilmington, DE 19898, U.S.A.

^c Present address: Department of Chemistry, Oklahoma State University, Stillwater, OK 74078-0447, U.S.A.

than the traditional stoichiometric ion-exchange model which assumes binding of the proteins by coulombic interactions at discrete sites. The treatment of hydrophobic interactions is based on an adaptation of the solvophobic theory which predicts that the hydrophobic portion of the free energy of binding is proportional to the hydrophobic contact area and the microthermodynamic surface tension of the aqueous salt solution. Despite its simplicity the theory was successful in explaining the observed effect of the nature and concentration of salt in the eluent, the pH and the effect of the density of fixed charges at the surface of the stationary phase in the absence of specific salt effects.

INTRODUCTION

Electrostatic interaction (ion-exchange) and hydrophobic interaction chromatography (HIC) with high-performance columns and equipment are emerging as major branches of biopolymer chromatography both on an analytical and preparative scale. As the nature and concentration of the salt in the eluent is the basic retention modulator in both types of chromatography, the effect of salt is of fundamental significance. Since in many instances both types of interactions are involved in the retention process it is of interest to develop a comprehensive treatment of the underlying physico-chemical phenomena. In this work we attempt to account for the salt effect on electrostatic and hydrophobic interactions responsible for the retention of biopolymeric eluents.

The classical stoichiometric theory of salt elution in ion-exchange chromatography of biopolymers was developed by Boardman and Partridge¹ and a more detailed treatment can be found in the monograph of Morris and Morris². Recently the theory was expanded by Regnier and co-workers^{3,4} who presented retention data obtained from measurements by using high-performance liquid chromatography (HPLC). A major shortcoming of the stoichiometric theories, however, is their failure to consider explicitly stationary phase properties and the implications of hydrophobic interactions which may occur concomitantly with electrostatic interactions. The "ion-exchange" model assumes that the polyion is site bound, and its popularity stems from the simplicity of the appurtenant stoichiometric treatment. Moreover, no other models are currently available because of the lacuna in applying modern polyelectrolyte theories to such complex systems.

Another way of looking at the problem is to assume that both the salt and polyionic elute are territorially or atmospherically bound, *i.e.*, they are retained by the electrostatic field at the stationary phase surface, but remain free to move within a certain layer above it. In such a case, the biopolymeric elute is expected to experience little change in hydration upon transfer from the bulk mobile phase to the stationary phase domain. A modified Poisson-Boltzmann theory or its descendant, the Gouy double-layer theory, could be of interest here for treatment of electrostatic interactions. We have chosen instead to adopt Manning's counterion condensation theory because of the analytical solutions it has provided⁵⁻¹⁰ and its experimental verification^{11,12}. For the treatment of hydrophobic interactions we have employed our earlier adaptation of Sinanoglu's¹³ solvophobic theory to the salting-out of proteins and their retention in hydrophobic interaction chromatography^{14,15}. The three-parameter equation that we obtain by combining the electrostatic and hydrophobic theory offers

a means to interpret the physico-chemical phenomena underlying the retention process and a method to characterize the properties of the stationary phase. In this paper, this approach is used to analyze isocratic retention data obtained with siliceous ion exchangers having a "soft" surface composed of a highly hydrated polymeric layer in a broad range of salt concentration in the eluent.

THEORY

Simplified model of retention

A simplified model is proposed to describe the effect of salt concentration on retention in biopolymer chromatography with stationary phases which have a "soft", highly hydrated surface with fixed charges or weakly hydrophobic binding sites or both. It is based on the following assumptions. (i) The dimensions of the smooth walled pores of the rigid support are large with respect to the size of the elute molecules so that pores can be approximated by cylinders of infinite radius and size-exclusion effects are absent. (ii) The fixed charges and hydrophobic binding sites are uniformly spaced and equi-accessible in the hydrated stationary phase layer at the pore wall. (iii) The biopolymer elutes are spherical molecules with uniformly distributed and equi-accessible fixed charges and hydrophobic patches at the surface. (iv) The conformation of the biopolymer molecule upon transfer between the two phases and interaction with the functional groups in the stationary phase domain is conserved. (v) A single valued phase ratio expresses the ratio of the volume occupied by the fixed charges and hydrophobic binding sites, and the volume of the mobile phase in the column. (vi) Conditions of linear elution chromatography prevail, *i.e.*, only a small fraction of the binding domains are occupied by the elute. (vii) No specific interactions of the eluting salt with the biopolymer have to be considered.

The magnitude of the retention when both electrostatic and hydrophobic interactions are involved is determined by the sum of the free energies for the equilibrium distribution of the biomacromolecular elute between the bulk mobile phase and the stationary phase domains. The corresponding equilibrium constant, K , can be written formally as

$$\log K = (-\Delta G_{es}^{\circ}/2.3RT) - (\Delta G_{h\phi}^{\circ}/2.3RT) \quad (1)$$

where ΔG_{es}° and $\Delta G_{h\phi}^{\circ}$ are the Gibbs free energies for retention by electrostatic and hydrophobic interactions, respectively, T is the absolute temperature and R is the universal gas constant.

We assume that the retention factor, k' , which can be directly measured from the chromatogram, is related to K as

$$k' = \phi K \quad (2)$$

where ϕ is the phase ratio, *i.e.*, the ratio of the two appurtenant domains of the stationary and mobile phases.

Electrostatic interactions between biopolymers and the stationary phase

Recent developments in polyelectrolyte theory, particularly the counterion

condensation theory of Manning⁵⁻¹⁰ as well as Record and co-workers^{11,12} provides the basis for our analysis of the pertinent retention thermodynamics in electrostatic interaction chromatography. Although the counterion condensation theory is particularly appropriate to linear polyelectrolytes with discrete charges, we assume that it is applicable to electrostatic interaction chromatography with stationary phases which contain wide cylindrical pores and an array of fixed charge bound via the organic moiety to the pore walls¹⁶⁻¹⁸. The validity of this assumption is discussed later.

A detailed description of the counterion condensation theory is found in Manning's review⁵. In his treatment the charged surface is characterized by a dimensionless structural parameter ξ , that is given by

$$\xi = q^2/ebk_B T \quad (3)$$

where q is the protonic charge, ϵ is the dielectric constant of the bulk mobile phase, b is the average spacing of fixed charges on the surface and k_B is Boltzmann's constant. It is assumed that the polyionic protein having a characteristic charge of Z_p is

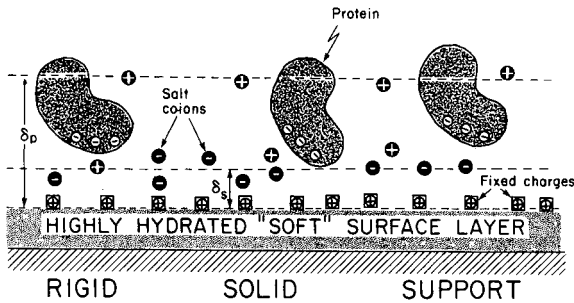


Fig. 1. Schematic illustration of atmospheric binding of proteins in view of the counterion condensation theory. The thickness of the layers containing the condensed salt counterions and the bound protein molecules is given by δ_s and δ_p , respectively. The protein, as illustrated, carries a characteristic charge of -3 .

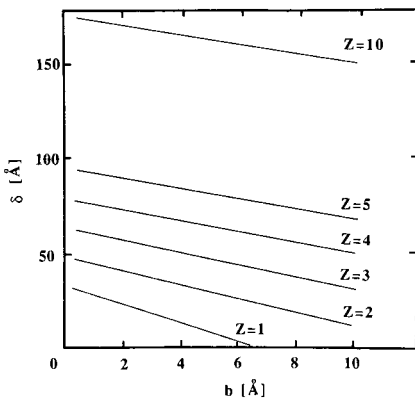


Fig. 2. Plot of the thickness, δ , of the layer containing condensed counterions against the distance between the fixed charges at the surface, b , with the charge on the counterion, Z , as the parameter. The following values were used in the calculation: $q = 4.8 \cdot 10^{-10}$ e.s.u.; $\epsilon = 80$; $k_B T = 4.11 \cdot 10^{-14}$ ergs.

atmospherically bound and found in a "condensation" layer having a thickness of δ_p over the surface of the stationary phase where each fixed charge occupies an area of b^2 . For our case, the treatment by Manning⁵ has been adapted to evaluate the relationship:

$$\delta_p = be(1 + Z_p)(\xi - Z_p^{-1}) \quad (4a)$$

where e is the base of the natural logarithm.

The corresponding layer thickness for salt counter-ions having a valence of Z_s is given by

$$\delta_s = be(1 + Z_s)(\xi - Z_s^{-1}) \quad (4b)$$

The free energy of binding of the polyionic eluite to the oppositely charged surface of the stationary phase in the presence of the salt counterion that is expelled in the process, is found to be

$$-\Delta G_{es}^0/2.3RT = \log(N_{AV}b^2\delta_p/1000e) + (Z_p/Z_s)\log[1000e/(N_{AV}b^2\delta_s m_s)(1 - Z_s\xi)] \quad (5)$$

where m_s is the molal salt concentration and N_{AV} is Avogadro's number.

The atmospheric binding of the protein and the salt counterions is schematically illustrated in Fig. 1. It is seen that the protein molecules are not bound to any of the charged sites at the surface but are kept in the stationary phase domain by the electrostatic field generated by the plurality of fixed charges in close proximity at the surface. A feature of such territorial binding is believed to be the freedom for lateral movement by the bound species. Fig. 2 represents a graphical illustration of eqn. 4 and shows the dependence of the thickness of the counterion condensation layer on the distance between the charges for counterions having different electronic charges.

Hydrophobic interactions between biopolymer and stationary phase

In the present treatment of the energetics of retention in hydrophobic interaction chromatography, retention is assumed to occur due to contact between the hydrophobic patches at the biopolymer surface and the hydrophobic binding sites on the stationary phase as illustrated in Fig. 3. In the hermeneutics of the solvophobic theory¹³, the free energy change for hydrophobic interactions, $\Delta G_{h\phi}^0$ has been expressed as

$$\Delta G_{h\phi}^0 = \Delta G_{es}^0 + \Delta G_{vdw}^0 + \Delta G_{assoc}^0 + \Delta G_{red}^0 + N_{AV}(\gamma'_S A_S - \gamma'_M A_M) + RT \ln(RT/P^0V) \quad (6)$$

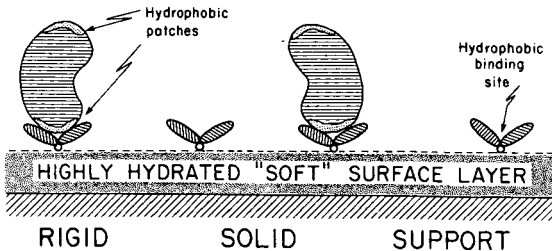


Fig. 3. Illustration of hydrophobic interactions between the hydrophobic ligates of the stationary phase and the hydrophobic patches on the surface of the protein.

where, according to the previous treatment¹⁴, $\Delta G_{\text{es}}^{\circ}$ is the free energy change associated with electrostatic effects upon binding, $\Delta G_{\text{assoc}}^{\circ}$ is the free energy change for eluite–ligate association in the absence of surrounding solvent, *i.e.*, in the gas phase, and $\Delta G_{\text{vdw}}^{\circ}$ is the free energy change due to Van der Waals interactions. $\Delta G_{\text{red}}^{\circ}$ expresses the reduction of free energy due to solvent–ligate and solvent–eluite interactions not treated in the preceding terms. In the last term which takes care of the free volume, V and P° are the mean molar volume of solvent and the standard pressure, respectively. The respective microthermodynamic surface tensions pertinent to the mobile and stationary phase domains are γ'_{M} and γ'_{S} , whereas the molecular surface areas of the free and bound eluite exposed to the aqueous mobile phase are A_{M} and A_{S} , respectively.

Electrostatic effects indicated by the term $\Delta G_{\text{es}}^{\circ}$ in eqn. 6 had been evaluated by combining the Debye–Hückel treatment with the solvophobic theory^{15,19}. In the absence of fixed charges at the surface the electrostatic contribution would be solely determined by this term, which vanishes at sufficiently high salt concentrations. When there are fixed charges at the stationary surface eqn. 5 can be used to determine the value of $\Delta G_{\text{es}}^{\circ}$.

Examination of eqn. 6 suggests that biopolymer size does not enter explicitly into the calculation of retention energetics. The important quantity is the change in the molecular surface area $\Delta A'$, which is given by the change in the total surface area upon hydrophobic binding ($A'_{\text{M}} - A'_{\text{S}}$) and is thus proportional to the “hydrophobic contact surface area”. In general, the total hydrophobic surface area is expected to increase with the molecular weight of the biopolymer eluite. Of course, the hydrophobic surface area of each protein will be determined by its primary, secondary, and tertiary structure under the prevailing experimental conditions.

In the present treatment it is assumed that the sole effect of increasing salt concentration at sufficiently high salt concentrations is to increase the microthermodynamic surface tension and to augment hydrophobic interactions^{15,20,21}. Thus, specific interactions between the biopolymeric eluite and the salt are assumed to be absent. As the surface tension of salt solutions is often a linear function of the salt concentration in such cases, the logarithmic equilibrium constant is expected to increase linearly with the salt concentration in the mobile phase when hydrophobic interactions dominate retention. We also may assume as a first approximation, that with stationary phases having “soft”, *i.e.*, very hydrophilic surface in contact with neat water the microthermodynamic surface tension is the same in both the mobile and stationary phase domains and given by γ so that $\gamma \equiv \gamma'_{\text{M}} \equiv \gamma'_{\text{S}}$. On the other hand, for salt solutions the appropriate surface tension can be expressed by adapting earlier treatment as $\gamma = \gamma_0 + \sigma_{\text{s}}m_{\text{s}}$ where γ_0 is the surface tension of the neat water, σ_{s} is the molal surface tension increment of the neutral salt and m_{s} is the molal salt concentration¹⁵.

The simple approach outlined above allows us to express the dependence of the free energy of hydrophobic interactions on the molal surface tension increment of the neutral salt, σ_{s} , in the absence of specific salt effects¹⁵ as

$$\Delta G_{\text{h}\phi}^{\circ} = \Delta G_{\text{aq}}^{\circ} - \Delta A' \sigma_{\text{s}} m_{\text{s}} \quad (7a)$$

where $\Delta G_{\text{aq}}^{\circ}$ includes all contributions to the retention free energy in the system under

investigation according to eqn. 6, except that due to salt mediated hydrophobic interactions and is given by

$$\Delta G_{\text{aq}}^{\circ} = \Delta G_{\text{es}}^{\circ} + \Delta G_{\text{assoc}}^{\circ} + \Delta G_{\text{red}}^{\circ} - \Delta A' \gamma_0 + RT \ln(RT/P^{\circ}V) \quad (7b)$$

Thus the product $\Delta A' \gamma_0$ accounts for free energy differences of cavity formation in neat solvent in the absence of any electrostatic effects.

Retention by combined coulombic and hydrophobic interactions

In order to express the dependence of the retention factor on the salt concentration in the eluent when both electrostatic and hydrophobic interactions are involved, eqns. 1-7 are combined to yield

$$\log k' = \log(N_{\text{AV}} b^2 \delta_{\text{P}} / 1000e) + (Z_{\text{p}} / Z_{\text{s}}) \log[1000e / (N_{\text{AV}} b^2 \delta_{\text{s}} m_{\text{s}}) (1 - Z_{\text{s}} \xi)] - (\Delta G_{\text{aq}}^{\circ} / 2.3RT) + (\Delta A' \sigma_{\text{s}} m_{\text{s}} / 2.3RT) + \log \phi \quad (8)$$

where ϕ is the phase ratio.

In view of eqn. 8 the dependence of the logarithmic retention factor on the salt concentration for the combined effect of hydrophobic and electrostatic interactions can be expressed in a simplified form as

$$\log k' = A - B \log m_{\text{s}} + C m_{\text{s}} \quad (9)$$

where B and C are the appropriate electrostatic and hydrophobic interaction parameters, respectively, and A is a constant encompassing all characteristic system parameters. The value of the parameters in eqn. 9 depends, among other factors, on the number, size, and distribution of charges and hydrophobic sites of the biopolymer, as well as on the nature and density of the binding sites on the stationary phase.

Comparison of eqns. 8 and 9 yields for parameter A the following expression

$$A = \log(N_{\text{AV}} b^2 \delta_{\text{P}} / 1000e) + (Z_{\text{p}} / Z_{\text{s}}) \log[1000e / (N_{\text{AV}} b^2 \delta_{\text{s}}) (1 - Z_{\text{s}} \xi)] - \Delta G_{\text{aq}}^{\circ} / 2.3RT + \log \phi \quad (10)$$

The electrostatic interaction parameter B is evaluated in a similar fashion as

$$B = Z_{\text{p}} / Z_{\text{s}} \quad (11)$$

The expression for the hydrophobic interaction parameter C is obtained as

$$C = \Delta A' \sigma_{\text{s}} / 2.3RT \quad (12)$$

The analysis is further complicated if n co-ions accompanying the biopolymer are expelled when the biopolymer is bound to the stationary phase. In such a case with monovalent salt, the electrostatic interaction parameter may be modified¹² as

$$B = (Z_{\text{p}} / Z_{\text{s}}) + n \quad (13)$$

Eqn. 9 expresses the relationship between the retention factor and the molality of salt in the mobile phase, when chromatography proceeds within the constraints of the simplifying assumptions stated above, via electrostatic interactions, hydrophobic interactions or both. The equation implies that under conditions of purely hydrophobic interaction chromatography, the plots of $\log k'$ against m_s will be linear, whereas plots of $\log k'$ against $\log m_s$ yield straight lines under conditions of electrostatic interaction chromatography over a certain range of salt concentrations.

The salt concentration $m_{s,0}$ at the minimum of $\log k'$ in such plots is determined by differentiating eqn. 9 with respect to concentration and is given by

$$m_{s,0} = B/2.3C \quad (14)$$

In view of the previous treatment, $m_{s,0}$ is a complex function of the properties of the salt, the stationary phase and the macromolecule. The minimum retention factor, k'_{\min} at salt concentration $m_{s,0}$ is given by

$$\log k'_{\min} = A - B \log(B/2.3C) + B/2.3 \quad (15)$$

so that the minimum value of the retention factor is a single function of the three parameters in eqn. 9. Although at $\log k'_{\min}$ there may be no interaction between the biopolymeric eluite and the stationary phase surface, significant size exclusion effects still may yield a measurable value for k'_{\min} (ref. 22).

We would expect the eluent pH to have no effect on the value of ξ which expresses the charge density on stationary phases having the properties of strong anion or strong cation exchangers. On the other hand, weak anion and weak cation exchangers have ionogenic functions which may dissociate to different degrees in the operational pH range of mobile phase. Hence, their values may be dependent on the eluent pH used in the experiment. Although Manning⁵ does not consider such titratable sites independent and equivalent, we may make this simplifying approximation to express the pH dependence of ξ for anion exchangers as

$$\xi = \xi_{\max}[1/(1 + 10^{\text{pH} - \text{p}K_a})] \quad (16)$$

and for cation exchangers as

$$\xi = \xi_{\max}[10^{\text{pH} - \text{p}K_a}/(1 + 10^{\text{pH} - \text{p}K_a})] \quad (17)$$

where ξ_{\max} is the value of the ξ parameter when all fixed ionogenic groups at the surface are dissociated and $\text{p}K_a$ is the negative logarithm of their acid dissociation constant.

Another effect of pH is to modify the value of the protonic charge on the biomacromolecule. Thus, the overall effect of pH on the retention is the result of changing the electrostatic potential of both the stationary phase and the biopolymeric eluite. As a result both electrostatic and hydrophobic interactions are affected by the change in pH.

Apparent values of the interaction parameters

Evaluation of the parameters A , B and C requires retention data measured over

a sufficiently wide range of salt concentrations in the eluent. In the domain of electrostatic interaction chromatography, *i.e.*, at relatively low salt concentrations, it has been customary to make $\log k'$ vs. $\log m_s$ plots which yield apparent straight lines with slope denoted by the symbol B' here. In the literature the symbol Z has frequently been used for the slope thus obtained¹⁻³.

Neglect of solvophobic effects by omitting the linear dependence of the logarithmic retention factor on the salt concentration in eqn. 9 modifies the interpretation of the coefficients A and B . Eqn. 9 can be differentiated with respect to logarithmic salt concentration to obtain A' and B' , the apparent values of A and B respectively as given by

$$A' = A + Cm_s(1 - 2.3 \log m_s) \quad (18)$$

and

$$B' = B - 2.3Cm_s \quad (19)$$

At low salt concentrations the magnitude of the product of the hydrophobic interaction parameter and salt molality, Cm_s , is usually negligible with respect to B and only minor deviations from linearity are expected in plots of $\log k'$ vs. $\log m_s$ at low salt concentrations. According to eqn. 11, the coefficient B is equal to Z_p/Z_s , *i.e.*, the ratio of the effective charges on the biopolymeric and the salt counterions, but as seen from eqn. 19, hydrophobic interactions may also affect the value of the slope of such a plot of experimental data. Nevertheless, even at salt concentrations of the order of 0.1 m the value of the term $2.3 Cm_s$ in eqn. 19 is only slightly greater than 20% of B when B and C are of similar magnitude. This condition is satisfied for the proteins examined here. However, the similarity in magnitude of B and C parameters needs to be determined for each protein and set of experimental conditions, because, if C is significantly greater than B at the error in evaluating B at $m_s > 0.1$ from a quasi-linear plot can be more substantial. In these cases, the measured value of Z_p would be significantly affected by the magnitude of hydrophobic interactions as well, as illustrated in Fig. 4.

The implications of eqns. 18 and 19 are schematically illustrated in Fig. 4. Fig. 4a

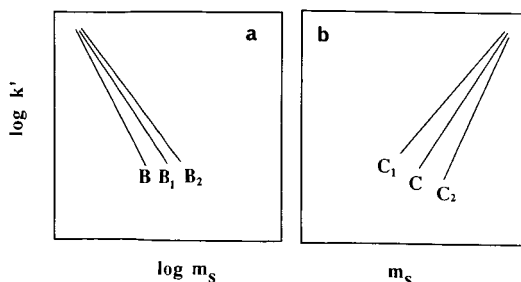


Fig. 4. Schematic illustration of the true and apparent interaction parameters. (a) When hydrophobic interactions are significant at low salt concentrations experiments may yield instead of the intrinsic electrostatic interaction parameter B the apparent values of B_1 or B_2 . (b) Attractive or repulsive electrostatic interactions can affect the apparent value of the hydrophobic interaction parameter, and experiments may yield the respective slopes C_1 or C_2 instead of the intrinsic hydrophobic interaction parameter C .

shows the $\log k'$ vs. $\log m_s$ plots obtained in the low salt concentration regime at three different values of C . As the value of C increases, the slope of the curve decreases and so the apparent value of B decreases as suggested on the graph by B_1 and B_2 . Fig. 4b shows that neglect of electrostatic effects in the high salt concentration regime may produce analogous ambiguities in the estimated value of C . The line marked C corresponds to the true value of the hydrophobic interaction parameter obtained if electrostatic effects are absent or correctly treated, whereas C_1 and C_2 show the effect when electrostatic effects are present but neglected. Similar results could be expected for instance in hydrophobic interaction chromatography on ion exchangers or other stationary phases with fixed charges at high salt concentrations.

EXPERIMENTAL

Materials

Cytochrome c from horse heart, ovalbumin, myoglobin from equine skeletal muscle, ribonuclease A, and α -chymotrypsinogen A, both from bovine pancreas, bovine serum albumin, lysozyme from chicken egg white and Tris were purchased from Sigma (St. Louis, MO, U.S.A.). H_3PO_4 , NaH_2PO_4 , Na_2HPO_4 , $(NH_4)SO_4$, HCl, NaOH, NaCl, $MgSO_4$, acetic and citric acids were supplied by Fisher Scientific (Pittsburgh, PA, U.S.A.). Distilled water was prepared with a Barnstead Nano pure unit.

Instruments

The liquid chromatograph was assembled from a Model 750 solvent delivery pump with a Model 753 ternary solvent mixer and a Model 740 control module supplied by Micromeritics (Norcross, GA, U.S.A.) or of two Model 100A pumps, a Model 420 gradient controller, an Altex (Berkeley, CA, U.S.A.) magnetic mixer, a Rheodyne (Berkeley, CA, U.S.A.) Model 7010 sampling valve with 20- or 100- μ l sample loop and a Kratos (Ramsey, NJ, U.S.A.) Model 770R variable-wavelength UV detector. The column effluent was monitored at 280 nm, and chromatograms were obtained with a Schlumberger (Benton Harbor, MI, U.S.A.) Model SR-204 strip chart recorder or with a Shimadzu (Columbia, MD, U.S.A.) Model Chromatopac C-R3A recording data processor.

Columns

The Zorbax BioSeries 80 \times 6.2 mm I.D. columns WCX-300, WAX-300, SCX-300 and SAX-300 were gifts from DuPont (Wilmington, DE, U.S.A.). The acronyms used for column designation are as follows: WCX, weak cation exchanger; WAX, weak anion exchanger; SCX, strong cation exchanger; SAX, strong anion exchanger.

Data analysis

Retention factors determined under isocratic conditions were fitted to eqn. 9 by non-linear regression analysis and thus the coefficients, A , B and C were evaluated. The degree of fit was checked by comparison of experimental values to those calculated by use of the fitted parameters.

RESULTS AND DISCUSSION

The aim of this paper is to analyze biopolymer retention over a wide range of salt concentrations in a more comprehensive way than is possible by previous treatments. By considering both hydrophobic and electrostatic effects, the two chief factors which determine the magnitude of retention are treated conjointly. Although greatly oversimplified and restricted to "well behaved" systems, the analysis can provide a means to extract from experimental data parameters which are related to the properties of the biopolymer eluite and the salt in a given chromatographic system. Furthermore, these parameters could be useful in characterizing the stationary phases used in this kind of chromatography.

The electrostatic interaction parameter B , as defined in eqn. 11, is independent of the charge density ξ at the surface. This may correspond to a situation of low counterion condensation according to Manning⁵ and is of interest in linear elution chromatography for which eqn. 5 is believed to apply. When the electrostatic interaction between the polyionic eluite and the stationary phase is very strong, a high level of condensation occurs⁵. Binding of proteins by ion exchangers at very low salt concentrations, such as observed in preparative chromatography under certain conditions, may exemplify this condition. The value of the electrostatic interaction parameter for high levels of condensation, B^* , is obtained from Manning⁵ as

$$B^* = Z_p \xi (1 - Z_p \theta_p) / Z_s \quad (20)$$

where θ_p is the number of protein counterions associated with a fixed charge at the surface. A significant conclusion from eqn. 20 is that at high level of condensation the charge density of the ion exchanger has a strong effect on the electrostatic interaction parameter and a comparison of eqns. 11 and 20 shows that the electrostatic interaction parameters at low and high levels of condensation differ by a factor of $\xi(1 - Z_p \theta_p)$. The following discussion will be restricted to low levels of condensation believed to occur in ion-exchange chromatography with salt elution.

Record has given an alternative formulation of the electrostatic interaction parameter, B^{**} (refs. 11 and 12) that applies to situations of low levels of counterion condensation. The dependence on the charge density is as follows

$$B^{**} = (Z_p / Z_s) [1 - (2\xi)^{-1}] \quad (21)$$

According to this relationship, the absolute value of B is expected to increase with the charge density, *i.e.*, with decreasing spacing between the fixed charges at the surface of the stationary phase. From this it follows that the shape of the $\log k'$ vs. logarithmic salt concentration plots will also depend on the charge density of the ion exchanger even at low levels of condensation.

Thus, the electrostatic interaction parameter B provides a measure of electrostatic effects and is a function of Z_p , the effective charge on the biopolymer eluite. It is an indirect function of the charge density on the surface of the stationary phase. The counterion condensation theory begins with the insight that in order to interact charges must be within the Bjerrum length. This length is defined as the distance at which two unit charges interact with an energy of $k_B T$ in the relevant dielectric medium

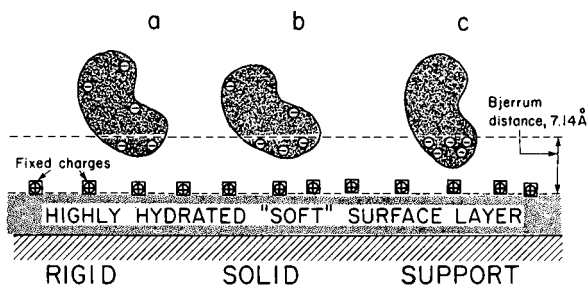


Fig. 5. Schematic illustration of the atmospheric binding of proteins having the same net charge (-5) but (a) uniform, (b) moderately asymmetric and (c) highly asymmetric charge distribution. It is seen that the effective (characteristic) charge on the protein, which is represented by these charges present within the layer of a thickness equal to the Bjerrum distance, is determined by the charge distribution.

and its value is 7.14 \AA in water at 25°C . Many proteins can be regarded as spherical molecules having diameters in excess of this value with charges randomly dispersed on the protein surface. Therefore, only a fraction of the total charges on the protein molecule can interact with the charged surface of the stationary phase unless the charge distribution on the protein is highly asymmetrical as suggested by the schematic illustrations in Fig. 5. Thus, in the usual case, the magnitude of Z_p does not reflect the macromolecular net charge but an "effective" or "characteristic" charge of the protein. This "effective" charge can probably be regarded as the number of charges involved in the most energetically favorable interactions between protein and stationary phases.

The hydrophobic interaction parameter C is expected to depend on that hydrophobic surface area of the eluite that contacts the hydrophobic ligates at the stationary phase surface^{15,19,20}. Thus it will increase with the density and size of hydrophobic patches on the surface of the protein. Generally, C is likely to increase with the molecular size of the protein, and decrease with the number of ionized groups on the protein. Concomitantly, C is expected to increase with the density and size of the hydrophobic binding sites at the stationary phase surface, particularly at low ligate concentrations. The nature of the salt used in the eluent also affects the value of C , which increases in the absence of specific salt effects with the molal surface tension increment¹⁵. In many cases, salts may enter into dipole-dipole interactions with the large dipolar protein molecules (see refs. in ref. 15), and other types of specific ion binding may also occur²³. In such cases the above simple interpretation of the hydrophobic interaction parameter is not expected to be applicable.

The theoretical treatment presented here facilitates the interpretation of retention data obtained in protein chromatography with stationary phases having fixed charges at the surface and with increasing and decreasing salt gradients in the electrostatic and in hydrophobic interaction modes of chromatography, respectively. Since different physico-chemical properties of the proteins are responsible for their retention in the two techniques, widely different separation selectivities can be achieved by using the same column in the dual operation mode. The theory allows us to evaluate the interaction parameters that determine the effect of salt on the retention over a wide range of conditions, and at the same time, are characteristic of both the protein and the chromatographic system. Fig. 6 illustrates the effect of these

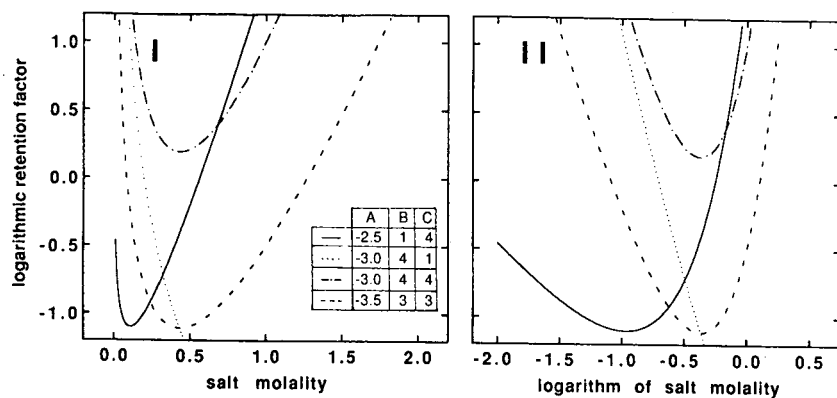


Fig. 6. Graphs illustrating the dependence of the logarithmic retention factor against the salt molality (I) and against the logarithmic salt molality (II) for the parameter values A , B and C .

parameters on protein retention. Plots similar to those shown in Fig. 6I and II can be used to evaluate from the respective limiting slopes the electrostatic and hydrophobic interaction parameters.

The effect of salt concentration on protein retention has been investigated under various experimental conditions; representative plots of the measured logarithmic retention factors against the salt concentration in the eluent are shown in Figs. 7–9, where the solid lines were drawn by fitting the data points according to eqn. 9. The corresponding parameter values calculated are listed in Table I.

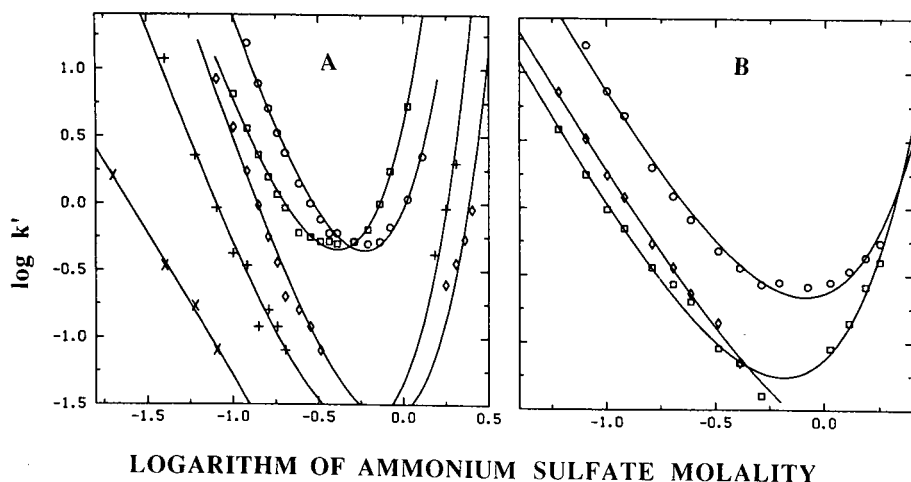


Fig. 7. Plot of the logarithmic retention factor of proteins obtained on weak cation-exchange (A) and strong cation-exchange (B) columns against the logarithmic molality of ammonium sulfate in the mobile phase. The solid curves were obtained by use of eqn. 9 and the parameters listed in Table I. Column, 80×6.2 mm I.D.; mobile phase, 20 mM phosphate buffer containing ammonium sulfate, pH 6.0; flow-rate, 1.5 ml/min; temperature, 25°C; UV detection at 280 nm. Sample components, (x) myoglobin; (+) ribonuclease; (\diamond) cytochrome c ; (\square) α -chymotrypsinogen A; (O) lysozyme.

Fig. 7 shows results obtained with the use of a weak and a strong cation exchanger and ammonium sulfate in the eluent at pH 6.0. It is seen that on both columns the isocratic retention factor first decreases with increasing salt concentration in the mobile phase until a minimum is reached after which further increase in salt concentration results in increasing retention factors in accordance with the predictions of eqn. 9. Fig. 8 shows results obtained by using weak and strong anion exchanger columns and salt at pH 7.8 with another set of proteins. As seen in Fig. 8A, the value of B for α -chymotrypsinogen on both the weak and strong anion-exchange columns is rather small. This is not surprising because this protein has a net positive charge at the pH of the eluent. On the other hand ovalbumin and bovine serum albumin were not retained on weak anion exchangers by eluents having ammonium sulfate concentrations in the range 0.25–2.0 m .

Fig. 8B shows results obtained with the same proteins on a strong anion exchanger. Both bovine serum albumin and α -chymotrypsinogen A are retained by electrostatic and hydrophobic interactions at low and high salt concentrations, respectively, whereas ovalbumin is retained only by electrostatic interactions in the experimental salt concentration range.

Fig. 9 illustrates results obtained with α -chymotrypsinogen A on a weak cation exchanger column by using isocratic elution with 25 mM phosphate buffer, pH 6.0, that contained sodium acetate, sodium chloride or ammonium sulfate over a wide range of concentration. As expected the B values are of the same order of magnitude within experimental error given the fact that the valence of the salt counterion, Z_p , is the same in all cases and equal to unity. In contradistinction, the value of the hydrophobic interaction parameter, C , is a function of the molal surface tension increment of salts; therefore, the decreasing order of C values for ammonium sulfate, sodium acetate and sodium chloride reflects the relative magnitude of the σ_s values.

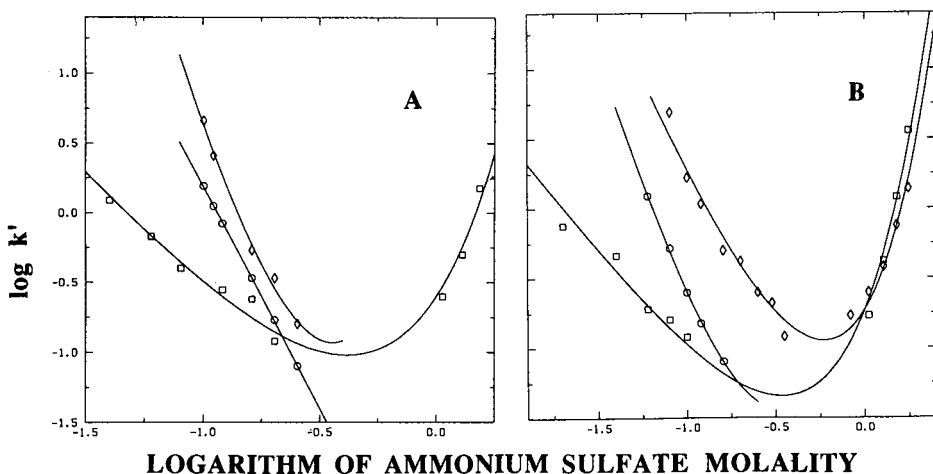


Fig. 8. Plot of the logarithmic retention factor of proteins obtained on weak anion-exchange (A) and strong anion-exchange (B) columns against the logarithmic molality of ammonium sulfate in the mobile phase. The solid curves were obtained by use of eqn. 9 with the parameters listed in Table I. Mobile phase, 20 mM Tris-HCl containing ammonium sulfate, pH 7.8. Sample components, (\square) α -chymotrypsinogen, (\circ) ovalbumin, (\diamond) bovine serum albumin. Other conditions as in Fig. 7.

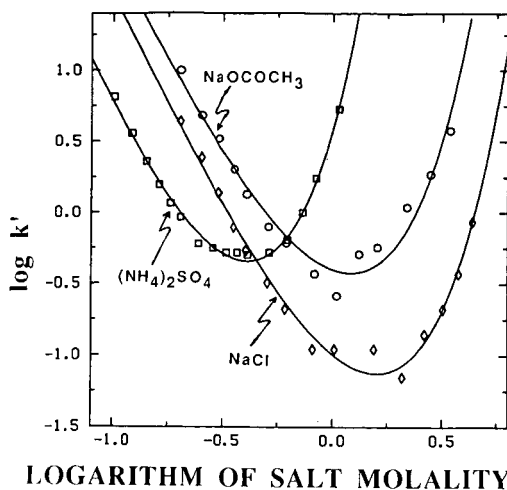


Fig. 9. Graph illustrating plots of the logarithmic retention factor of α -chymotrypsinogen A against the concentration of various salts in the eluent. The solid curves were obtained by use of eqn. 9 with the parameters listed in Table IV. Column: WCX, 80×6.2 mm I.D.; mobile phase, 20 mM phosphate buffer, pH 6.0 containing various salts; flow-rate, 1.5 ml/min; temperature, 25°C.

Figs. 7-9 suggest that the present analysis of salt effects probably is of broad applicability. Indeed, data obtained with a limited number of salts but with a variety of proteins and other polyionic biological substances on stationary phases of various provenance conforms at least qualitatively to the predicted shape of the logarithmic retention factor *versus* salt concentration plots. The pore morphology of the silica

TABLE I

PARAMETERS OF EQN. 9 FOR VARIOUS PROTEINS AND ION EXCHANGERS

Retention data were measured with buffered eluents containing different concentrations of $(\text{NH}_4)_2\text{SO}_4$.

Protein	Stationary phase	Parameter		
		A	B	C
Lysozyme	WCX ^a	-3.17	4.25	3.12
	SCX ^a	-2.15	2.87	1.51
α -Chymotrypsinogen A	WCX ^a	-3.58	3.94	4.16
	SCX ^a	-2.93	2.78	1.84
	WAX ^b	-2.51	1.83	1.91
	SAX ^b	-2.82	1.64	2.07
Cytochrome <i>c</i>	WCX ^a	-3.83	4.13	2.20
	SCX ^a	-2.06	2.35	—
Ribonuclease A	WCX ^a	-3.99	3.46	2.69
Bovine serum albumin	WAX ^b	-2.96	3.55	—
	SAX ^b	-2.92	2.99	2.18
Ovalbumin	WAX ^b	-2.98	3.18	—
	SAX ^b	-3.37	2.81	—

^a 20 mM phosphate buffer, pH 6.0.

^b 20 mM Tris buffer, pH 7.8.

support often has a great influence on the retention behavior of proteins, but little is known about either the detailed pore topology of the various stationary phase supports or the nature of its effect on retention. In order to facilitate the comparison of the results presented here, therefore, Zorbax BioSeries ion exchangers, which are based on the same silica gel support, were used throughout the study.

Effect of ligate density

The density of the ligates, *i.e.*, the covalently bound functions serving as the binding sites at the stationary phase surface cannot usually be measured directly with confidence. However, as discussed above, the value of the electrostatic parameter B for a given protein is likely to be directly proportional to the surface density of the ionized ligates on the stationary phase. Thus, by comparing the values of B , obtained from retention data measured on different stationary phases, we can estimate the relative concentrations of fixed charges at their surface.

In general, the ratio of ligate densities can be estimated from the results of appropriate elemental analysis of the stationary phases provided they were made from the same support by using similar chemistries. In our case, the ratio of ligate densities, δ_1/δ_2 , was calculated by using data from the supplier²⁴ as 1.07 and 1.78 for the stationary pairs WAX/SAX and WCX/SCX, respectively. As shown in Table II, the electrostatic interaction parameters measured with different proteins on these ion exchangers yield ratios that are fairly constant and commensurate to the above values. Moreover, the ratios of the pertinent B parameters are nearly invariant with protein, and this observation also supports the usefulness of this approach.

TABLE II

VALUES OF THE ELECTROSTATIC INTERACTION PARAMETER, B , OBTAINED UNDER VARIOUS EXPERIMENTAL CONDITIONS AND THE EFFECT OF THE RELATIVE LIGATE DENSITY AT THE STATIONARY PHASE SURFACE, δ_1/δ_2

Retention data were measured on Zorbax BioSeries columns and with $(\text{NH}_4)_2\text{SO}_4$ in the eluent. Subscripts denote the column number.

Protein	pH	Column		B_2	B_1/B_2	δ_1/δ_2
		1	2			
α -Chymotrypsinogen A	6.0	WAX	SAX	1.43	1.29	1.07
	7.0	WAX	SAX	1.66	1.10	1.07
	7.8	WAX	SAX	1.64	1.12	1.07
Ovalbumin	6.0	WCX	SCX	2.78	1.42	1.78
	6.0	WAX	SAX	3.08	0.98	1.07
	7.0	WAX	SAX	2.47	1.47	1.07
α -Chymotrypsinogen A	7.8	WAX	SAX	2.82	1.13	1.07
	6.0	WCX ^a	WCX ^b	3.94	0.78	—
	7.0	WCX ^a	WCX ^b	4.11	0.87	—
Lysozyme	6.0	WCX ^a	WCX ^b	4.25	0.79	—
	7.0	WCX ^a	WCX ^b	4.17	0.90	—
	6.0	WCX	SCX	4.25	1.48	1.78
Cytochrome <i>c</i>	6.0	WCX	SCX	4.13	1.54	1.78

^a Column after losing a part of its retentive capacity.

^b Column before losing a part of its retentive capacity.

In the course of the experiments, the weak cation-exchange column was operated at elevated temperatures with concomitant reduction of its retentive properties due to loss of organic ligates. The B values calculated from the data obtained on this cation-exchange column before and after the drop in its retention capacity were compared to gain information on the effect of reduced ligate density. Although the actual reduction can only be inferred from the significantly lower retention factors measured upon the heat treatment of the column, the B_1 to B_2 ratios in Table II clearly indicate a loss of surface charges. It should also be noted that this analysis confirms the general observation that the surface density of the negatively charged groups is significantly greater for the weak than the strong cation exchanger. Repulsion between the negatively charged sulfonic acid groups may hinder the attainment of such a high charge density at the surface that is possible with neutral carboxyl groups in the preparation of the stationary phase at sufficiently low pH. Therefore, the "weak" ion exchangers may have greater capacity than do "strong" ion exchangers.

The ratio of the two parameters B and C may also be of significance in the characterization of stationary phases. The value of B/C expresses the relative magnitude of the two major salt-mediated interactions that determine retention. The values of B/C have been calculated for several proteins on various columns and are presented in Table III. In order to assure that parameter C employed in the calculations truly represents hydrophobic interactions, only data obtained with

TABLE III

RATIOS OF THE ELECTROSTATIC, B , AND HYDROPHOBIC, C , INTERACTION PARAMETERS OBTAINED FROM THE RETENTION DATA OF VARIOUS PROTEINS ON DIFFERENT ION-EXCHANGE COLUMNS WITH AMMONIUM SULFATE IN THE ELUENT

<i>Protein</i>	<i>pH</i>	<i>Column</i>	<i>B/C</i>
α -Chymotrypsinogen A	6.0	SCX	1.51
Lysozyme	6.0	SCX	1.90
Bovine serum albumin	6.0	SAX	1.19
	7.0	SAX	1.31
	7.8	SAX	1.37
α -Chymotrypsinogen A	6.0	SAX	0.71
	7.0	SAX	0.77
	7.8	SAX	0.79
	6.0	WAX	0.83
	7.0	WAX	0.91
	7.8	WAX	0.96
	6.0	WCX ^a	0.95
	6.0	WCX ^b	0.99
	7.0	WCX ^a	1.10
	7.0	WCX ^b	1.15
Lysozyme	6.0	WCX ^a	1.36
	6.0	WCX ^b	1.47
	7.0	WCX ^a	1.60
	7.0	WCX ^b	1.62

^a Column before losing a part of its retentive capacity.

^b Column after losing a part of its retentive capacity.

proteins which exhibited a major increase in retention with the salt concentration are included in Table III. As seen the B/C values for a given protein depend only weakly on the eluent pH. This is expected because the extent of ionization of the major acidic or basic groups and consequently the density of the cationic and anionic charges on the proteins may not change significantly in the pH range studied here. The B to C ratios obtained from data on the weak cation exchanger before and after the reduction in its retention capacity are very similar. This finding suggests that loss of both hydrophobic and charged functions occurred to the same extent. This is not unexpected because each ligate embodies both kinds of functions and therefore their densities are likely to be proportional. The B to C ratio obtained on a given ion exchanger with different proteins can also be interpreted as some kind of a weighted number of charges per unit hydrophobic area of protein and such values measured for various proteins on a given stationary phase can be used to rank them according to their charge density thus defined. Accordingly the data in Table III suggests that both the anionic charge density on bovine serum albumin and the cationic charge density on lysozyme are greater than the respective charge densities on α -chymotrypsinogen A. In turn, B/C data obtained with selected proteins on various columns may be useful to gain information on the relative densities of the electrostatic and hydrophobic functions on the surface of different stationary phases. For instance, such information can be extracted from the B to C ratio for α -chymotrypsinogen at pH 6.0 that is greater on the strong than on the weak cation exchanger and greater on the weak than on the strong anion exchanger.

Effect of salt on the electrostatic interaction parameter

The stoichiometric model of Boardman and Partridge¹ for electrostatic interaction chromatography, in agreement with eqn. 11, predicts that the electrostatic interaction parameter B , is directly proportional to the characteristic charge on the protein, and inversely proportional to the charge on the salt co-ion. On the other hand, the model of Regnier and co-workers^{3,4} postulates a more complex relationship for the dependence of B on the valence of the salt co-ion.

Values of the parameter B obtained on a weak cation exchanger for several proteins are shown in Table IV. The data, which were obtained at pH 6.0 and 7.0 with univalent and divalent salt in the eluent, suggests an inverse dependence of the parameter B on the valence of the salt co-ion. In view of eqn. 11 the parameter B measured on the cation exchanger with a sodium salt should be twice as large as that measured with magnesium salt for a given protein in the event of simple ion exchange. It is seen from Table IV, however, that it is not the case and this discrepancy can be explained by the well known specific binding of Mg^{2+} in proteins that has been found to result in a deviation from the usual salt effect on hydrophobic interactions^{2,3}.

In order to investigate this phenomenon we used the B values in Table IV and estimated the magnitude of magnesium binding assuming that eqn. 13 is applicable. The corresponding numbers of Mg^{2+} ions bound, n , per molecule of cytochrome c , α -chymotrypsinogen A and lysozyme were 1.24, 0.86, and 0.79, respectively. This finding suggests that in the case of specific salt binding the physico-chemical phenomena determining the value of B are more complex than those considered in the present treatment.

According to the theory, the interaction strength should be proportional to the

TABLE IV

EFFECT OF SALT ON THE ELECTROSTATIC INTERACTION PARAMETER B

The retention data were obtained on the weak cation-exchange column of reduced retentive capacity

<i>Protein</i>	<i>pH</i>	<i>Salt</i>	<i>B</i>
Cytochrome <i>c</i>	6.0	Sodium acetate	3.26 ^a
	6.0	NaCl	3.07
	6.0	(NH ₄) ₂ SO ₄	2.31 ^a
	6.0	Sodium citrate	2.03
	7.0	MgSO ₄	2.29 ^a
	7.0	(NH ₄) ₂ SO ₄	2.99 ^a
α-Chymotrypsinogen A	6.0	Sodium acetate	3.11
	6.0	NaCl	3.48
	6.0	(NH ₄) ₂ SO ₄	3.08
	6.0	Sodium citrate	3.33
	7.0	MgSO ₄	3.02
	7.0	(NH ₄) ₂ SO ₄	3.56
Lysozyme	6.0	Sodium acetate	3.43
	6.0	NaCl	3.48
	6.0	(NH ₄) ₂ SO ₄	3.38
	6.0	Sodium citrate	3.16
	7.0	MgSO ₄	2.73
	7.0	(NH ₄) ₂ SO ₄	3.75

^a Insufficient data in the hydrophobic interaction domain at high salt concentrations.

effective charge on the macromolecule and the electrostatic potential at the stationary phase surface. The effective or characteristic charge at present has to be obtained from experimental data since it is not necessarily the same as the net charge on the protein, *e.g.*, due to asymmetric charge distribution. This can dramatically affect retention behavior; for instance, Haff *et al.*²⁵ and Fausnaugh *et al.*²⁶ have found that β-lactoglobulin A was retained on anion exchangers at eluent pH values equal to or even below the isoelectric point of the protein.

Effect of eluent pH

According to the model, parameters B and C are directly proportional to the characteristic charge on the biopolymer eluite and to the net decrease in exposed surface area upon its binding to the stationary phase ligates, respectively. As the number of anionic and cationic sites on the macromolecule changes with the pH at least parameter B is strongly pH dependent even with strong ion exchangers. The degree of ionization of weak cation and anion exchangers may also change with the pH so that more complex pH dependence of the parameter B is expected with such stationary phases. The hydrophobic interaction parameter C may be affected by pH dependent changes in certain binding sites on the stationary phase and a marked pH dependence is expected when the hydrophobic binding sites contain ionogenic groups. The situation might further be complicated by pH induced conformation changes in the eluite molecule or in the ligates at the surface of the stationary phase.

Fig. 10 illustrates the pH dependence of each parameter. For the proteins under investigation, data were obtained over a sufficiently broad range of salt concentration to assure reliable values of both parameters. The observed dependence of B on the

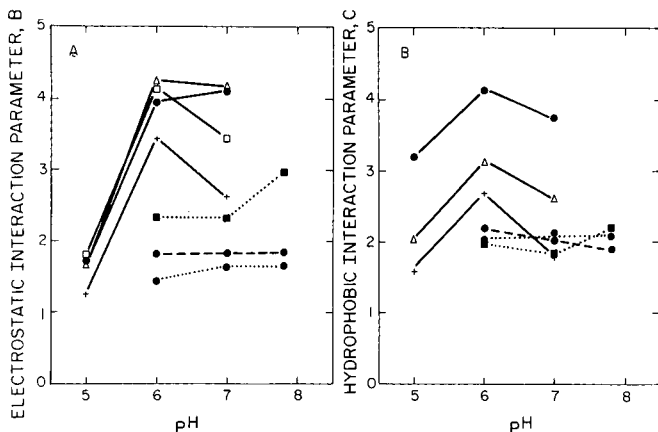


Fig. 10. Graphs illustrating the dependence of the electrostatic interaction (A) and the hydrophobic interaction (B) parameters on the pH of the eluent containing ammonium sulfate. Columns: WCX (—); WAX (---); SAX (···). Mobile phase, 20 mM phosphate at pH 5.0 and 6.0, or 20 mM Tris-HCl at pH 7.0 and 7.8. Sample components: (●) α -chymotrypsinogen A; (Δ) lysozyme; (+) ribonuclease A; (■) bovine serum albumin; (□) cytochrome *c*.

eluent pH, depicted in Fig. 10A, is generally consistent with the behavior inferred above. The *B* values obtained for α -chymotrypsinogen A on both strong and weak anion exchangers were nearly constant or increased slightly with pH because this protein has a relatively high *pI* value. However, the value of *B* for bovine serum albumin increased with the eluent pH, indicating an increase in the dissociation of the side chain carboxylic acids of this acidic protein (*pI* = 4.5).

As mentioned above, the interpretation of the results obtained with the weak cation exchanger is less straightforward. The electrostatic interaction parameters for lysozyme, ribonuclease A, cytochrome *c* and α -chymotrypsinogen A all increase upon a change in pH from 5 to 6, but only for α -chymotrypsinogen A is seen an increase in the value of *B* between pH 6 and 7. The general increase in the pH range from 5 to 6 is probably due to the increasing degree of ionization of the carboxylic groups on the stationary phase, since changes in the degree of ionization of cationic groups on the protein, *i.e.*, the histidine, lysine and arginine side chains, are very small in this pH range. In contrast, the ionization of the carboxylic ligates would not be expected to increase significantly in the pH range from 6 to 7. Where protonation of the histidine side chains occurs in the pH domain, the retention can either decrease or increase according to the relative significance of the histidine ionization.

The pH dependence of the hydrophobic interaction parameter *C* is shown in Fig. 10B. On both types of anion exchangers the valence of the parameter is practically independent of pH over the range from pH 6.0 to 7.8. However, the results on the weak cation exchanger are more complex. The values of *C* are lower at pH 7 than at pH 6, suggesting that the number of hydrophobic binding sites on the stationary phase decreases due to increasing ionization of the carboxylic functions. The observed increase in *C* between pH 5 and 6, which should reflect an increase in the hydrophobicity characteristic of the protein over that pH range, is more difficult to explain. The two major groups which undergo ionization in that pH range are the

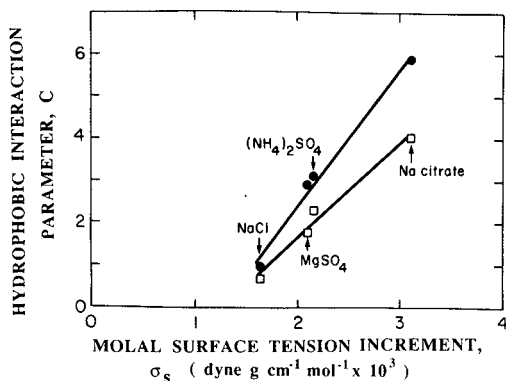


Fig. 11. Graph illustrating the dependence of the hydrophobic interaction parameter on the molal surface tension increment of the salt in the eluent. Weak cation-exchange column was used with NaCl, MgSO₄, (NH₄)₂SO₄ and sodium citrate in the eluent and the proteins were (●) α -chymotrypsinogen A and (□) lysozyme. The values of the surface tension increment were taken from ref. 15.

carboxyls of the glutamic and aspartic acid side chains and the basic group of histidine. Only the latter would be expected to become more hydrophobic with increasing pH so that the ionization of these groups and/or pH induced configuration changes may be responsible for the observed effect.

Effect of salt on the hydrophobic interaction parameter

The data of Fausnaugh *et al.*²⁶ support the theoretical prediction¹⁵ that the retention augmenting effect of neutral salts parallels their molal surface tension increment in hydrophobic interaction chromatography. Gooding *et al.*²⁷ investigated the effect of sodium chloride and ammonium sulfate on the retention of seven proteins by using two kinds of stationary phases in hydrophobic interaction chromatography and their results are also in qualitative agreement with the expected behavior.

According to eqn. 12, which stems from a rather simple approach to the effect of neutral salts on protein interactions, the hydrophobic interaction parameters should be a linear function of the molal surface tension increment¹⁵.

In this study, values of C were obtained for α -chymotrypsinogen and lysozyme from retention data on a weak cation exchanger with sodium chloride, ammonium sulfate, sodium citrate and magnesium sulfate at pH 6 and 7, respectively. Fig. 11 shows plots of parameter C against the molal surface tension increment that have the dimensions of $(\text{dyne g cm}^{-1} \text{ mol}^{-1}) \cdot 10^3$. The values used were 1.64 for NaCl, 2.10 for MgSO₄, 2.16 for (NH₄)₂SO₄ and 3.12 for sodium citrate¹⁵. The hydrophobic interaction parameters obtained with ammonium sulfate at pH 6 and 7 were 3.11 and 3.10 for α -chymotrypsinogen A and 2.29 and 2.32 for lysozyme, respectively. The plots of the C values obtained with NaCl, MgSO₄, (NH₄)₂SO₄ and citrate yield straight lines for both proteins. Thus, the results are in agreement with the predictions of the model presented here. Nevertheless, we recognize that the surface tension argument is an oversimplification when dealing with such a complex system as protein binding and cannot be generally applicable in view of specific salt binding effects. Nevertheless, in many cases it offers a very convenient approach to explain the effects of salt on

hydrophobic interactions. Only values for preferential hydration²³, which were found to parallel the C parameters measured with different salts in the eluent for lysozyme²⁸, might offer an alternative.

Effect of salt concentration on column efficiency

The concentration of the eluting salt affects not only the magnitude of retention but also the efficiency of the column with isocratic elution as shown in Fig. 12. On a given ion exchanger many proteins can be retained to a similar extent by electrostatic and hydrophobic interactions at low and high salt concentrations, respectively. We have found that for a given protein and retention factor the efficiency of the column under conditions of isocratic elution as measured by the plate height is significantly lower at high than at low salt concentrations in the eluent, *i.e.*, the same column exhibits a lower efficiency in the hydrophobic than in the electrostatic interaction mode with the columns under investigation. Two factors may be responsible for this behavior. First, the viscosity of the mobile phase increases with the salt concentration and concomitantly the diffusivity of the eluite decreases. Second, the binding kinetics for hydrophobic interactions, which are believed to involve contact between the hydrophobic moieties of the protein and stationary phase ligates, are expected to be less favorable than those for electrostatic interactions, which involve atmospheric binding, according to the treatment presented here. However, since most commonly gradient elution is used in both electrostatic or hydrophobic interaction chromatography, in practice, the apparent column efficiencies may not differ appreciably. It should also be noted that in bona fide hydrophobic interaction chromatography with mildly hydrophobic stationary phases that do not have fixed charges, lower salt concentration in the eluent suffices to retain the proteins than in the cases discussed here.

Potential use of the interaction parameters

In light of the above analysis parameters B and C may provide some physico-chemical information on the eluite molecule upon comparing data obtained

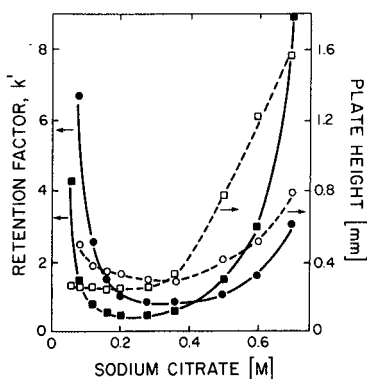


Fig. 12. Effect of salt concentration in the eluent on the magnitude of retention factor and column efficiency. Column: Zorbax BioSeries WCX 300, 80×6.2 mm I.D. Eluent: 20 mM phosphate buffer, pH 6.0, containing sodium citrate; flow-rate, 1.5 ml/min; temperature 25°C; UV detection at 280 nm. Sample components: (\square and \blacksquare) α -chymotrypsinogen A; (\circ and \bullet) lysozyme.

on reference columns under different elution conditions. The dependence of B on salt type is likely to give insight into salt binding by the proteins in solution and the corresponding stoichiometric coefficients. The equilibrium constants for these interactions are implicit in the parameter B and it may be possible to extract them mathematically. On the other hand, the hydrophobic surface of the eluite is characterized by the parameter C . Therefore, ranking of elutes in ascending order of the parameter obtained from data measured on a suitable HIC column C can provide a semi-quantitative scale of the hydrophobic character of the surface for biopolymer elutes. Since C is a measure of eluite interaction with a hydrophobic surface, the information thus obtained may afford further insights into the interactions of proteins with membranes or other surfaces of biological interest.

Alternatively, the interaction parameters may be used to characterize columns by comparing data obtained on different columns with an appropriately chosen set of elutes used as probes. The charge density of a given stationary phase relative to that of a reference stationary phase having similar properties can be inferred from the comparison of the corresponding values of parameter B obtained with such standard elutes. That should provide a valid basis for intercolumn comparison. In similar fashion, the relative magnitude of parameter C obtained with retention data of the standard elutes on different stationary phases should give a comparison of the effective size and/or density of the hydrophobic functions at the surface. We note that in general no such information can be obtained from a comparison of retention factors measured with different columns at the same salt concentration in the eluent, as seen from the illustration of simulated data in Fig. 6.

Interrelationship of the interaction parameters

Parameter A contains information on both electrostatic and hydrophobic interactions as seen from eqns. 10–12 that reveal a mathematically simple relationship between the three parameters. Eqn. 10 contains the ratio Z_p/Z_s which is identical to B in the simple case represented by eqn. 11, and suggests a linear relationship between

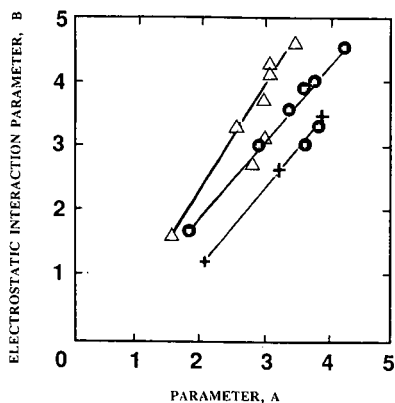


Fig. 13. Illustration of the relationship between parameters A and B . The data were obtained from measurements on weak ion exchange columns in a wide range of eluent pH and salts. Each data point represents a pair of parameters evaluated from measurements with the same salt at the same pH. Sample components: (Δ) lysozyme; (\bullet) α -chymotrypsinogen A; ($+$) ribonuclease A.

A and B . Indeed, the plots of the parameters obtained from experimental data shown in Fig. 13 confirm the prediction. On the other hand the term $-\Delta G_{\text{aq}}^{\circ}/2.3RT$ in eqn. 10 is directly proportional to the molecular surface area change, $-\Delta A'$, the term C . This implies that electrostatic effects or hydrophobic interactions contribute to retention even outside the salt concentration range where they are predominant. For example, the intercepts of $\log k'$ vs. m_s plots in the domain of hydrophobic interaction chromatography should have increasingly greater negative intercepts when the characteristic charge of the elute, Z_p increases or its hydrophobic character as measured by the $\Delta G_{\text{hp}}^{\circ}$ term decreases. Usually, the apparent intercept of $\log k'$ vs. $\log m_s$ plots increases with Z_p and decreases with the appropriate hydrophobic surface area. The determination of pertinent equilibrium constants from the values of A , B and C would be theoretically possible but difficult in practice due to experimental uncertainties and the simplifying assumptions underlying the model.

CONCLUSION

Elucidation of the physico-chemical phenomena underlying the retention process of complex molecules in interactive chromatography is one of the greatest challenges for chromatographic science today. The intricate properties of the dynamic surface of the biopolymeric elutes are still largely unknown and therefore a detailed mechanistic study of the interactions is not yet possible. This paper represents an attempt to treat together both electrostatic and hydrophobic interactions which are implicated in salt mediated elution chromatography of proteins. Although it inevitably entails gross oversimplifications, it provides a framework for the analysis of chromatographic data and facilitates the study of the effect on the retention of the surface properties of both the biopolymer and the stationary phase as well as of mobile phase components. The concepts presented here are not restricted to linear elution chromatography and can be extended to non-linear chromatography of proteins, which is of growing interest in preparative scale separations.

ACKNOWLEDGEMENTS

The authors thank Guhan Subramanian for valuable assistance in the experiments and Firoz Antia for helpful discussions. The work was supported by grants Nos. GM20993 and CA 21948 from the U.S. Public Health Service, Department of Health and Human Services.

REFERENCES

- 1 N. K. Boardman and S. M. Partridge, *Biochem. J.*, 59 (1955) 543.
- 2 C. J. O. R. Morris and P. Morris, *Separation Methods in Biochemistry*, Wiley, New York, 1976, pp. 86-87.
- 3 W. Kopaciewicz, M. A. Rounds, J. Fausnaugh and F. E. Regnier, *J. Chromatogr.*, 266 (1983) 3.
- 4 M. A. Rounds and F. E. Regnier, *J. Chromatogr.*, 283 (1984) 37.
- 5 G. S. Manning, *Q. Rev. Biophys.*, 11 (1978) 179.
- 6 G. S. Manning, *J. Phys. Chem.*, 85 (1981) 870.
- 7 G. S. Manning, *J. Phys. Chem.*, 85 (1981) 1506.
- 8 G. S. Manning, *Biopolymers*, 22 (1983) 689.
- 9 G. S. Manning, *J. Phys. Chem.*, 88 (1984) 6654.

- 10 R. W. Wilson, D. C. Rau and V. A. Bloomfield, *Biophys. J.*, 30 (1980) 317.
- 11 M. T. Record, Jr., C. F. Anderson and T. M. Lohman, *Q. Rev. Biophys.*, 11 (1978) 103.
- 12 C. F. Anderson and M. T. Record, Jr., *Annu. Rev. Phys. Chem.*, 33 (1982) 191-222.
- 13 O. Sinanoğlu, in H. Ratajczak and W. J. Thomas-Orville (Editors), *Molecular Interactions*, Vol. 3, Wiley, New York, 1982, p. 283.
- 14 Cs. Horváth, W. Melander and I. Molnár, *J. Chromatogr.*, 125 (1976) 129.
- 15 W. Melander and Cs. Horváth, *Arch. Biochem. Biophys.*, 183 (1977) 393.
- 16 M. Gueron and G. Weisbuch, *Biopolymers*, 19 (1980) 353.
- 17 B. H. Zimm and M. Le Bret, *J. Biomol. Struct. Dynamics*, 1 (1983) 461.
- 18 M. Le Bret and B. H. Zimm, *Biopolymers*, 23 (1984) 287.
- 19 Cs. Horváth, W. Melander and I. Molnár, *Anal. Chem.*, 49 (1977) 142.
- 20 W. R. Melander and Cs. Horváth, *J. Solid-Phase Biochem.*, 2 (1977) 141.
- 21 W. R. Melander, D. Corradini and Cs. Horváth, *J. Chromatogr.*, 317 (1984) 67.
- 22 E. Pfannkoch, K. C. Lu, F. E. Regnier and H. G. Barth, *J. Chromatogr. Sci.*, 18 (1980) 430.
- 23 T. Arakawa and S. N. Timasheff, *Biochemistry*, 23 (1984) 5912.
- 24 R. W. Stout, personal communication.
- 25 L. A. Haff, L. G. Fägerstam and A. R. Barry, *J. Chromatogr.*, 266 (1983) 409.
- 26 J. L. Fausnaugh, L. A. Kennedy and F. E. Regnier, *J. Chromatogr.*, 317 (1984) 141.
- 27 D. L. Gooding, M. N. Schmuck and K. M. Gooding, *J. Chromatogr.*, 296 (1984) 107.
- 28 E. S. Parente and D. B. Wetlaufer, *J. Chromatogr.*, 288 (1984) 389.

CHROM. 21 352

MATHEMATICAL MODELLING OF THE PEAK IN LIQUID CHROMATOGRAPHY

JAN PLICKA, VRATISLAV SVOBODA*, IMRICH KLEINMANN and ALENA UHLÍŘOVÁ

Institute for Research, Production and Application of Radioisotopes, Radiová 1, 102 27 Prague 10 (Czechoslovakia)

(First received November 1st, 1988; revised manuscript received January 24th, 1989)

SUMMARY

A program for the numerical solution of the transport differential equation describing the behaviour of a peak on a chromatographic column for an arbitrary shape of the equilibrium isotherm and an arbitrary amount injected for one- and two-component systems is presented. For one component, the influence of the axial dispersion coefficient, the separation coefficient, the curvature of the equilibrium isotherm and the apparatus function of the detector were examined. For a two-component system, the column overloading for pairs of components with various mutual influences was studied.

INTRODUCTION

Owing to the increasing availability of larger computers in chemical laboratories and the growing mathematical expertise of research chemists, mathematical modelling is an expanding technique. An exact mathematical model is a tool that permits both a deeper understanding of a process being studied and the optimization of parameters that influence this process, together with the prediction of results for arbitrary conditions. The development of the model is the first step in this procedure.

The fundamental mathematical description of the chromatographic process is based on the transport differential equation, defined for example by Deyl *et al.*¹ (see eqn. 1). Different approaches to the solution of this equation, leading to an analytical expression or to a numerical solution, can be found in the literature. The analytical solution for a linear equilibrium isotherm and a Dirac-shaped injected peak^{2,3} is regarded as valuable. As follows from the relationship for reduced statistical moments⁴, the axial dispersion coefficient D has a dominant influence on the width and asymmetry of a peak. The analytical solution considering the axial dispersion and non-linear equilibrium isotherms, approximated by a second-order polynomial, were demonstrated by Jaulman and co-workers^{5,6}, including the successful experimental verification of the suitable concentration range. The problem of the mathematical modelling of non-ideal, non-linear equilibrium chromatography using eqn. 1 was

described thoroughly by Smit *et al.*^{7,8}. The algorithm of the numerical procedure is based on an explicit method for the solution of partial differential equations.

The numerical solution of eqn. 1 for the boundary conditions corresponding to the scale-up of liquid chromatography was given by Cowan *et al.*⁹ for non-equilibrium chromatography. They applied a kinetic function describing a first-order reversible reaction.

Guiochon and co-workers¹⁰⁻¹⁵ applied a non-traditional approach to the solution of eqn. 1. They used the observation that the solution of eqn. 1 is similar to the numerical solution of a simpler equation for an ideal model, provided that the increments of space and time are suitably chosen (not too small).

The aim of this work was to construct a computer program for the numerical solution of eqn. 1 for an arbitrary case of the equilibrium isotherm and for an arbitrary volume and concentration of sample injected that should also be applicable for a two-component system.

THEORY

Development of the model

The model is based on the well known differential equation describing the mass balance of the component examined on the column at a point x and time t :

$$\frac{\partial C(x, t)}{\partial t} + \frac{1 - \varepsilon}{\varepsilon} \cdot \frac{\partial \bar{C}(x, t)}{\partial t} = D \cdot \frac{\partial^2 C(x, t)}{\partial x^2} - u \cdot \frac{\partial C(x, t)}{\partial x} \quad (1)$$

where u is the linear velocity of the mobile phase (cm/s), D the axial dispersion coefficient (cm²/s), ε the void fraction of the bed, \bar{C} the concentration of the examined component in the stationary phase (mol/l of the stationary phase) and C the concentration of the examined component in the mobile phase (mol/l).

The velocity is assumed to be constant within the whole column cross-section S ($u = Q/S\varepsilon$), where Q is the flow-rate (cm³/s). The coefficient D is also assumed to be constant for the given experimental conditions, *i.e.*, for a given temperature, viscosity, density and velocity of the mobile phase, sorbent particle size, examined component, column diameter, etc. To determine its value, a chromatographic experiment under the conditions when the component examined is not retained must be performed and evaluated, *e.g.*, by using the analytical solution⁴. As far as the change in mass with time on the sorbent, $\partial \bar{C}/\partial t$, is concerned, it can be assumed that the whole process is at equilibrium and that the functional dependence between C and \bar{C} [$\bar{C} = \bar{C}(C)$, the equilibrium isotherm] exists. The experimental procedures that enable this dependence to be found have already been described^{16,17}. It is obvious that all the parameters characterizing the column, the mobile phase, the examined component and the experimental conditions necessary for the solution of eqn. 1, *i.e.*, for the determination of the course of the function $C(x, t)$, are easily accessible experimentally.

Numerical solution

Replacing the term $\partial \bar{C}/\partial t$ by the term $(\partial \bar{C}/\partial C)(\partial C/\partial t)$ and introducing the dimensionless variables $\tilde{x} = x/L$ and $\tilde{t} = t/t_0$, where L is the column length and $t_0 = L/u$, eqn. 1 can be written as

$$\left(1 + \frac{1 - \varepsilon}{\varepsilon} \cdot \frac{\partial \bar{C}}{\partial C}\right) \frac{\partial C(\tilde{x}, \tilde{t})}{\partial \tilde{t}} = \frac{1}{Pe} \cdot \frac{\partial^2 C(\tilde{x}, \tilde{t})}{\partial \tilde{x}^2} - \frac{\partial C(\tilde{x}, \tilde{t})}{\partial \tilde{x}} \quad (2)$$

where $Pe = uL/D$ is the Peclet number. The boundary conditions are given by the equations

$$P = C - \frac{1}{Pe} \cdot \frac{\partial C}{\partial \tilde{x}}; \quad \tilde{x} = 0, \tilde{t} \geq 0$$

$$\frac{\partial C}{\partial \tilde{x}} = 0; \quad \tilde{x} = 1, \tilde{t} \geq 0 \quad (3)$$

where P is the substance concentration in the input mobile phase. The following initial condition is assumed:

$$C(\tilde{x}, 0) = 0; \quad \tilde{x} \in \langle 0, 1 \rangle \quad (4)$$

To solve eqn. 2, we use the Cranck–Nicolson implicit method¹⁸. The interval defined by the chromatographic peak is divided into n parts and the substitution of the derivations in eqn. 2 is performed in the usual way. For the expression in parentheses on the left hand side of eqn. 2 we introduce the symbol F ; it is obvious that F is a function of C . This term can be replaced, in the agreement with the Cranck–Nicolson method, by the average:

$$F_i^{j+1/2.(m+1)} \approx \frac{1}{2} [F_i^{j+1.(m+1)} + F_i^j] \quad (5)$$

where j is related to the time level, i to the spatial coordinate and m is the iterative step of the solution of eqn. 2; for $m = 0$ we choose $F_i^{j+1.(0)} = F_i^j$.

Eqn. 1 or 2 can also be applied for the description of a chromatographic process for a two-component mixture with components 1 and 2. If the equilibrium isotherms expressed generally as $\bar{C}_k = \bar{C}_k(C_1, C_2)$, where $k = 1$ or 2, are assumed, then instead of eqn. 2 we have a system of two partial differential equations:

$$\left(1 + \frac{1 - \varepsilon}{\varepsilon} \cdot \frac{\partial \bar{C}_k}{\partial C_k}\right) \frac{\partial C_k}{\partial \tilde{t}} + \frac{1 - \varepsilon}{\varepsilon} \cdot \frac{\partial \bar{C}_k}{\partial C_l} \cdot \frac{\partial C_l}{\partial \tilde{t}} = \frac{1}{Pe_k} \cdot \frac{\partial^2 C_k}{\partial \tilde{x}^2} - \frac{\partial C_k}{\partial \tilde{x}} \quad (6)$$

$$k, l = 1, 2, k \neq l$$

The value of the derivation $\partial \bar{C}_k / \partial C_k$ or $\partial \bar{C}_k / \partial C_l$ can be approximated by an equation analogous to eqn. 5. For the derivations in eqn. 6 we use the following substitutions:

$$\frac{\partial C_k}{\partial \tilde{t}} \approx \frac{C_{k,i}^{j+1.(m+1)} - C_{k,i}^j}{\Delta \tilde{t}} \quad (7)$$

$$\frac{\partial C_k}{\partial \tilde{x}} \approx \frac{1}{2} \left[\frac{C_{k,i+1}^{j+1,(m+1)} - C_{k,i-1}^{j+1,(m+1)}}{2\Delta\tilde{x}} + \frac{C_{k,i+1}^j - C_{k,i-1}^j}{2\Delta\tilde{x}} \right] \quad (8)$$

$$\frac{\partial^2 C_k}{\partial \tilde{x}^2} \approx \frac{1}{2} \left[\frac{C_{k,i+1}^{j+1,(m+1)} - 2C_{k,i}^{j+1,(m+1)} + C_{k,i-1}^{j+1,(m+1)}}{2\Delta\tilde{x}^2} + \frac{C_{k,i+1}^j - 2C_{k,i}^j + C_{k,i-1}^j}{2\Delta\tilde{x}^2} \right] \quad (9)$$

for $m = 0$ we choose $C_{k,i}^{j+1,(0)} = C_{k,i}^j$.

After the substitution of these approximations into eqn. 6, we obtain (in agreement with the Cranck-Nicolson method) a system of linear equations for unknown $C_{k,i}^{j+1}$ ($k = 1, 2; i = 1, 2, \dots, n + 1$). It is evident that the matrix of this system is tridiagonal.

The concept of the program is as follows. A number of iteration steps are tested on the basis of comparison of an integral value corresponding to the amount of substances contained in the chromatographic peaks with the amount of substances injected on to the column. The difference in these two values must be less than 0.1%. After the computation of a concentration profile for each time level, the initial and end points of the peak are determined as a concentration C greater than or equal to one thousandth of the maximum concentration in the peak. The magnitude of a differential step in the coordinate ($\Delta\tilde{x}$) is adjusted so that the maximum number of points in the peak is 500. The differential step in time ($\Delta\tilde{t}$) is chosen first to be 0.0001 and after the peak end has passed the beginning of the column $\Delta\tilde{t} = 0.001$.

In the computation, the following equations were used to describe the isotherms: one-component system:

$$\bar{C} = \frac{AC}{1 + BC} \quad (10)$$

two-component system:

$$\bar{C}_k = \frac{A_k C_k}{1 + B_1 C_1 + B_2 C_2}, \quad k = 1, 2 \quad (11)$$

where A and B are constants.

A rectangular shape was assumed for the input signal, *i.e.*, P in eqn. 3 takes the value C_0 (the concentration of a component determined in an injected sample), and for the time greater than the time necessary for the passing of the injected volume, the value 0.

The input data for the program are as follows: the column length L , its diameter $I.D.$, the void fraction of the bed ε , the mobile phase flow-rate Q , the volume injected V_D , the concentration in the injected sample C_{0k} , the axial dispersion coefficients D_k and the equilibrium isotherm parameters A_k and B_k . The program output represents the time course of the concentration at the end of the column, $C_k(L, t)$, or at an arbitrary point, as the case may be. The parameters used for the characterization of the chromatographic peaks, *i.e.*, the statistical moments (from the first to the fourth reduced statistical moment), the capacity factor, the plate number, etc., can be determined from this concentration course.

All the computations were performed using a PDP 11/23 microcomputer with a 128K memory under the RSX 11 M system. The programs were written in Fortran F 77. The computation of the chromatogram for one component took 2–3 h and for a two-component system 8–12 h.

RESULTS AND DISCUSSION

The accuracy of the program for a one-component system was verified for a linear isotherm by comparison with the analytical expression for the statistical moments. For $L = 25$ cm, $I.D. = 0.8$ cm, $\varepsilon = 0.375$, $Q = 0.6$ ml/min, $V_D = 0.1$ ml, $D = 0.0008$ cm²/s, $A = 1.5$ and $B = 0.0$, the difference was 0.17% for the first, 2.5% for the second and 4.2% for the third moments. These differences are regarded as negligible. For a non-linear isotherm, the analytical expression reported by Jaulmes *et al.*⁶ was used for the comparison. The course of the isotherm described both by eqn. 10 and by the second-order polynomial (the expression for which the analytical relationship was derived) is illustrated in Fig. 1a. Fig. 1b, c and d show that the difference in the courses of the peaks obtained by the two methods of computation increases with increasing load of the column, *i.e.*, in a region of concentrations such that the corresponding isotherms differ. When in the numerical computation the same polynomial was used for the description of the equilibrium dependence $\bar{C} \sim C$, the courses of the peaks were identical even for greater loadings of the column.

For a linear isotherm, the well known relationships between the separation coefficient K_D (see eqn. 10) ($K_D = A$ for $B = 0$) and the capacity factor k' [$k' = K_D(1 - \varepsilon)/\varepsilon$] and the linearity between the number of plates N and the column length L were verified. In instances the result was in good agreement with theory¹. The influence of the coefficient D on the width and asymmetry of a chromatographic peak is evident from Fig. 2a. The influence of the separation coefficient K_D on the peak width is shown in Fig. 2b and demonstrates the course of the amount of substance on the column at various times. The time points are chosen so that the leading edges of the peaks cover the same distances. Fig. 2b shows that a peak moving more slowly (with a higher K_D value) is narrower inside the column. The reality that at the column outlet it is broader is due to the fact that it flows out more slowly from the column.

The influence of a non-linear course of the equilibrium isotherm on the peak asymmetry and on the position, *i.e.*, on the capacity factor, is evident from Fig. 3. Although the non-linearity of the isotherm is not very pronounced ($B = \pm 0.2$), the courses of both peaks (Fig. 3b and c) differ considerably from that for a linear isotherm (Fig. 3a).

The program constructed for one component was used for the evaluation of the influence of the real apparatus function of the detector (a flow-through radioactivity detector designed in our laboratory) (see Fig. 4a) on the peak leaving the column. Fig. 4b and c compare the peaks before and after the convolution with the detector apparatus function. It is evident that for a 250×8 mm I.D. column an injection volume of 100 μ l, the influence of the detector is negligible.

On the basis of the results obtained, we conclude that the program for the numerical solution of eqn. 1 for one component is correct and can be used for experimental verification.

This program constructed for one component formed the basis of the

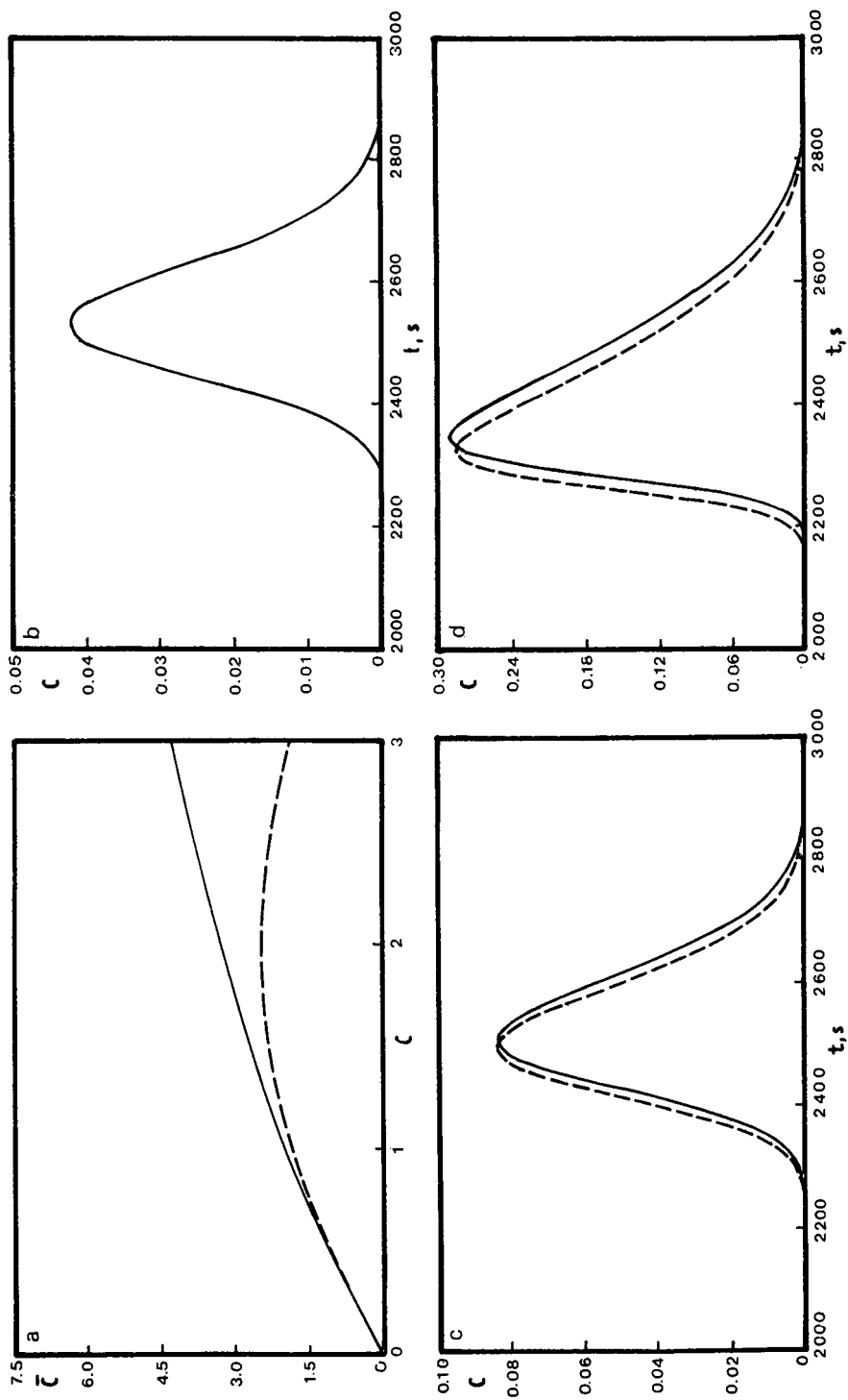


Fig. 1. Comparison of the numerical solution (solid line) of eqn. 1 for the Langmuir isotherm, $\bar{C} = 2.5C/(1 + 0.25C)$, with the analytical solution⁶ (broken line) for the second-order polynomial, $\bar{C} = 2.5C - 0.625C^2$. (a) The course of the isotherm. (b-d) $L = 29.2$ cm, $I.D. = 0.8$ cm, $\varepsilon = 0.5$, $\bar{Q} = 0.6$ ml/min, $D = 8 \cdot 10^{-4}$ cm²/s; (b) $V_D = 0.1$ ml, $C_0 = 1.0$; (c) $V_D = 0.1$ ml, $C_0 = 2.0$; (d) $V_D = 0.25$ ml, $C_0 = 3.0$.

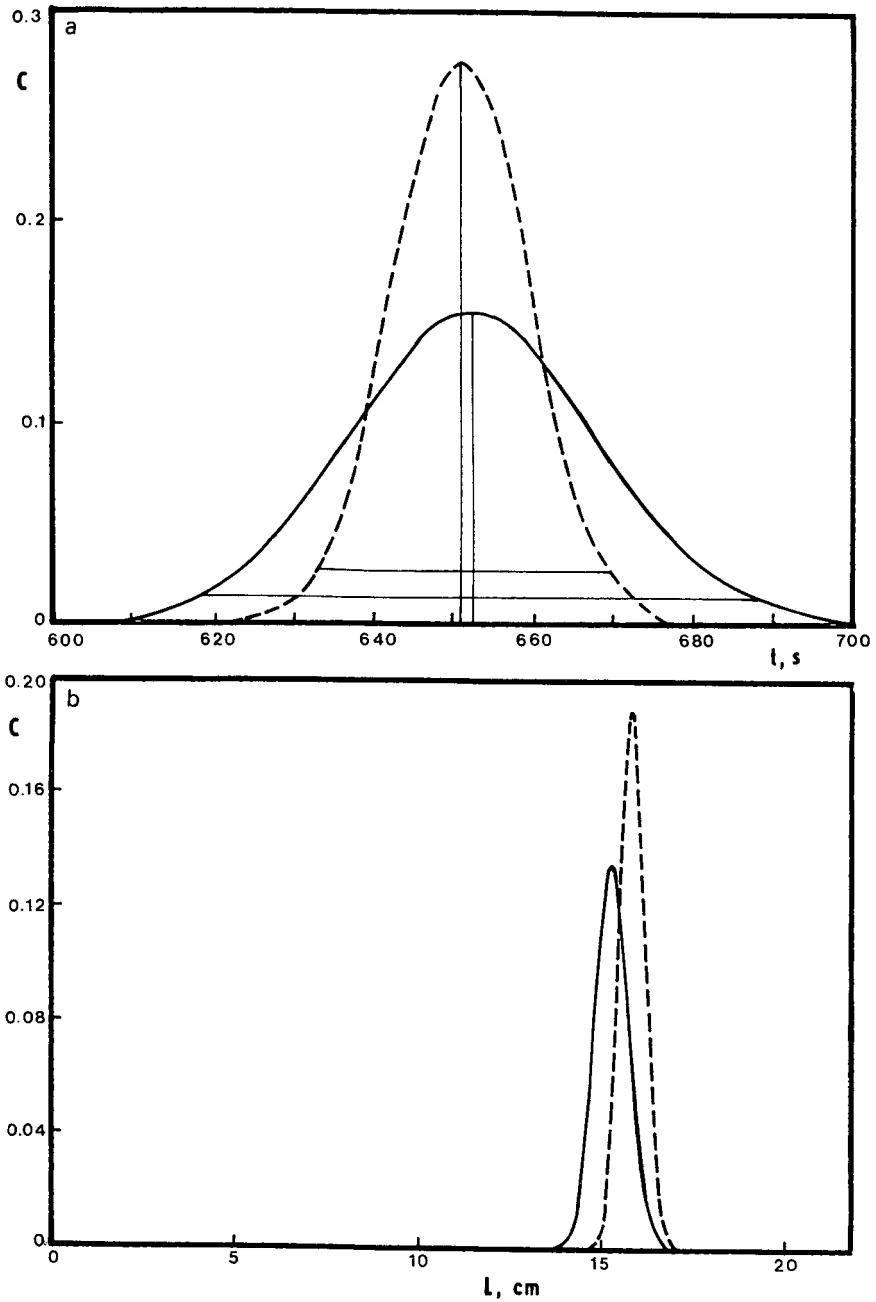


Fig. 2. Computations for linear chromatography: $L = 25$ cm, $I.D. = 0.4$ cm, $\varepsilon = 0.375$, $Q = 0.2$ ml/min, $V_D = 0.02$ ml, $C_0 = 1.0$. (a) Influence of the axial dispersion coefficient: $D = 1.5 \cdot 10^{-4}$ cm²/s (broken line), $D = 5 \cdot 10^{-4}$ cm²/s (solid line), $K_D = 0.5$. (b) Influence of the separation coefficient: $K_D = 0.5$ (solid line), $K_D = 2.0$ (broken line), $D = 5 \cdot 10^{-4}$ cm²/s.

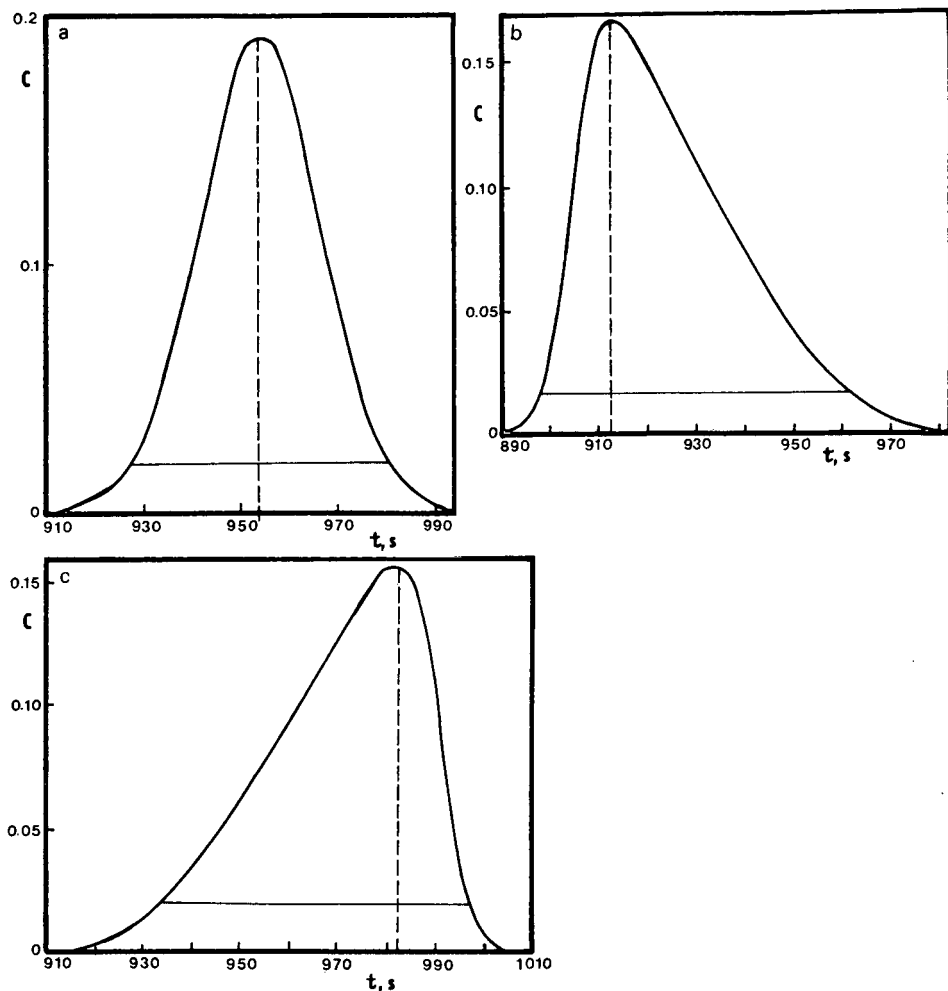


Fig. 3. Influence of the shape of the isotherm on the shape of the peak for the following conditions: $L = 25$ cm, $I.D. = 0.4$ cm, $\epsilon = 0.375$, $Q = 0.2$ ml/min, $V_D = 0.02$ ml, $C_0 = 1.0$, $D = 1.5 \cdot 10^{-4}$ cm²/s. (a) $A = 1.0$, $B = 0.0$; (b) $A = 1.0$, $B = 0.2$; (c) $A = 1.0$, $B = -0.2$.

construction of a program for two components. As an equilibrium function we used eqn. 11, which represents the Langmuir isotherm^{19,20} for positive values of the coefficients B . For negative coefficients B , only the range of concentrations when the denominator of eqn. 11 is positive has a physical sense.

The aim of the numerical experiments was to verify the accuracy of the program on the basis of the influence of column overloading on the shape and resolution of peaks for various equilibrium isotherms given by eqn. 11, *i.e.*, for various values of B under the same conditions (see Figs. 5, 6 and 7).

With negative values of B and considering the limited definition range, overloading may be realized by increasing the volume injected and not the concentration. Therefore, the results of both methods of overloading were compared

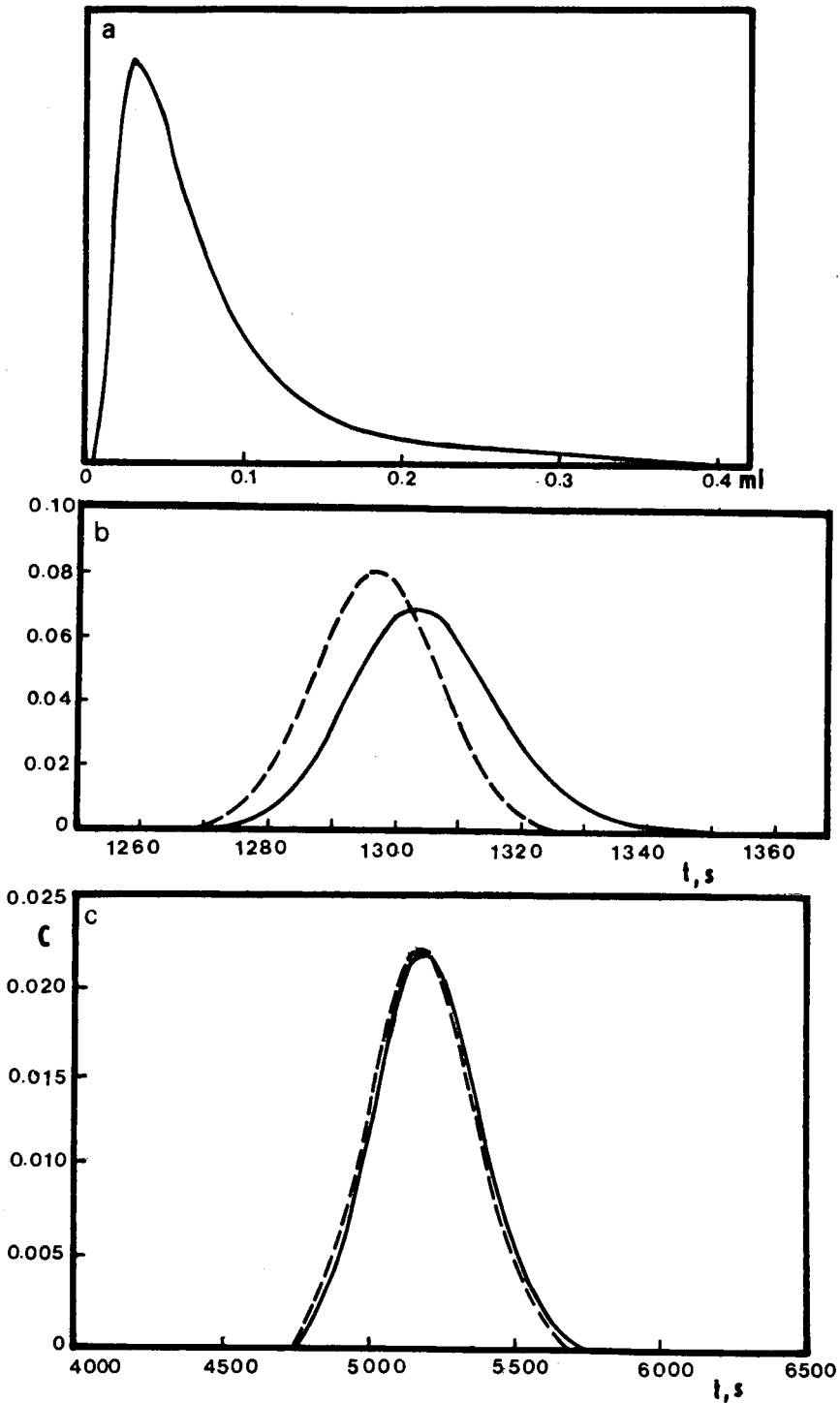


Fig. 4. Comparison of the chromatographic peak before convolution (broken line) and after convolution (solid line) with the apparatus function of a flow-through radioactivity detector. Conditions used: $L = 25$ cm, $\epsilon = 0.375$, $Q = 0.6$ ml/min, $C_0 = 1.0$, $A = 6.0$, $B = 0.0$. (a) Shape of the apparatus function; (b) $I.D. = 0.4$ cm, $V_D = 0.02$ ml, $D = 1.5 \cdot 10^{-4}$ cm²/s; (c) $I.D. = 0.8$ cm, $V_D = 0.1$ ml, $D = 8 \cdot 10^{-4}$ cm²/s.

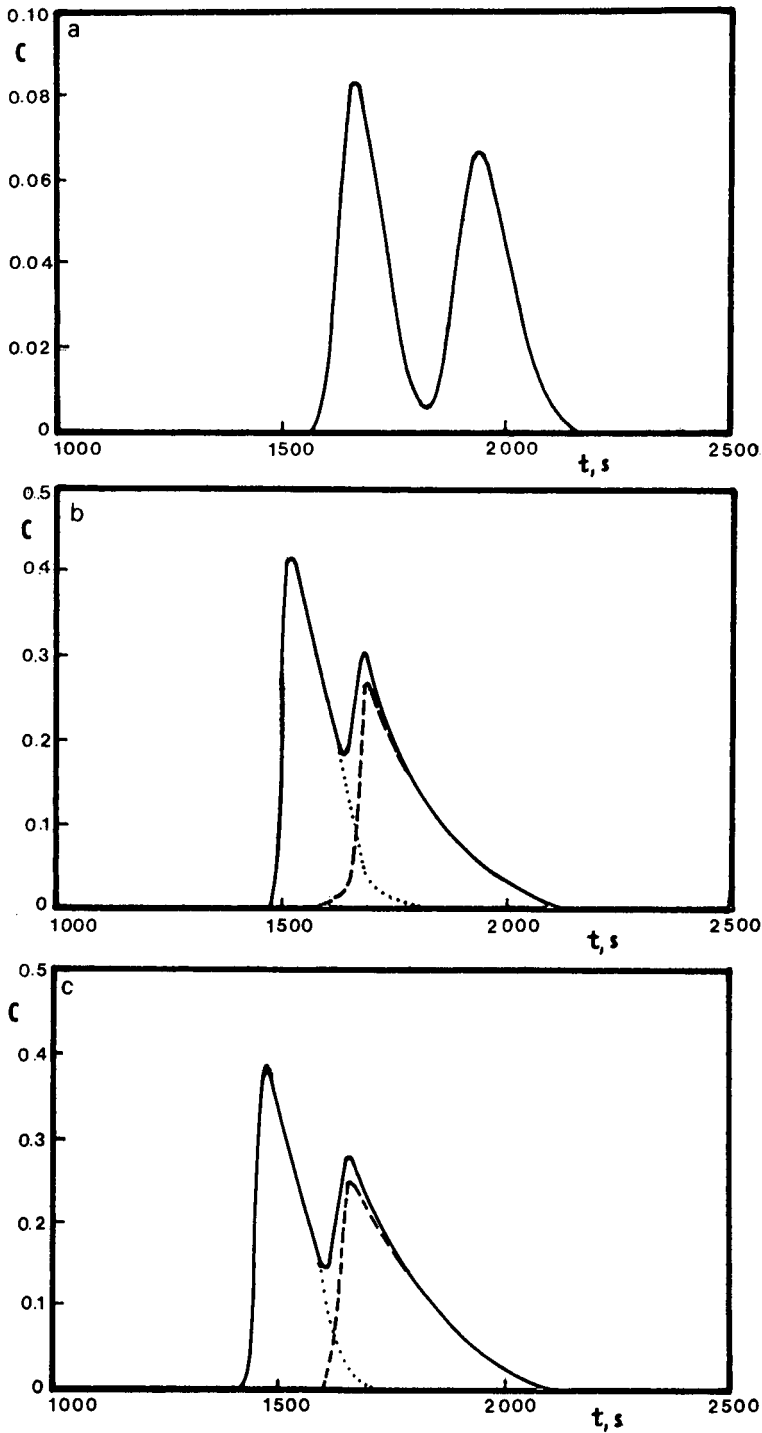


Fig. 5. Computation of a chromatogram for the two-component system (see eqn. 6). $L = 25$ cm, $I.D. = 0.8$ cm, $\varepsilon = 0.375$, $Q = 0.6$ ml/min, $D_1 = D_2 = 5 \cdot 10^{-4}$ cm²/s, $A_1 = 1.6$, $B_1 = 0.3$, $A_2 = 1.96$, $B_2 = 0.3$. (a) $V_D = 0.1$ ml, $C_{01} = C_{02} = 1.0$; (b) $V_D = 0.5$ ml, $C_{01} = C_{02} = 1.0$; (c) $V_D = 0.1$ ml, $C_{01} = C_{02} = 5.0$. The individual components are marked by the broken line.

first for the case when the definition range of eqn. 11 was unlimited (both coefficients B were positive). As follows from Fig. 5b and c, the difference is not pronounced; for the higher concentrations the retention times are slightly lower and the resolution higher.

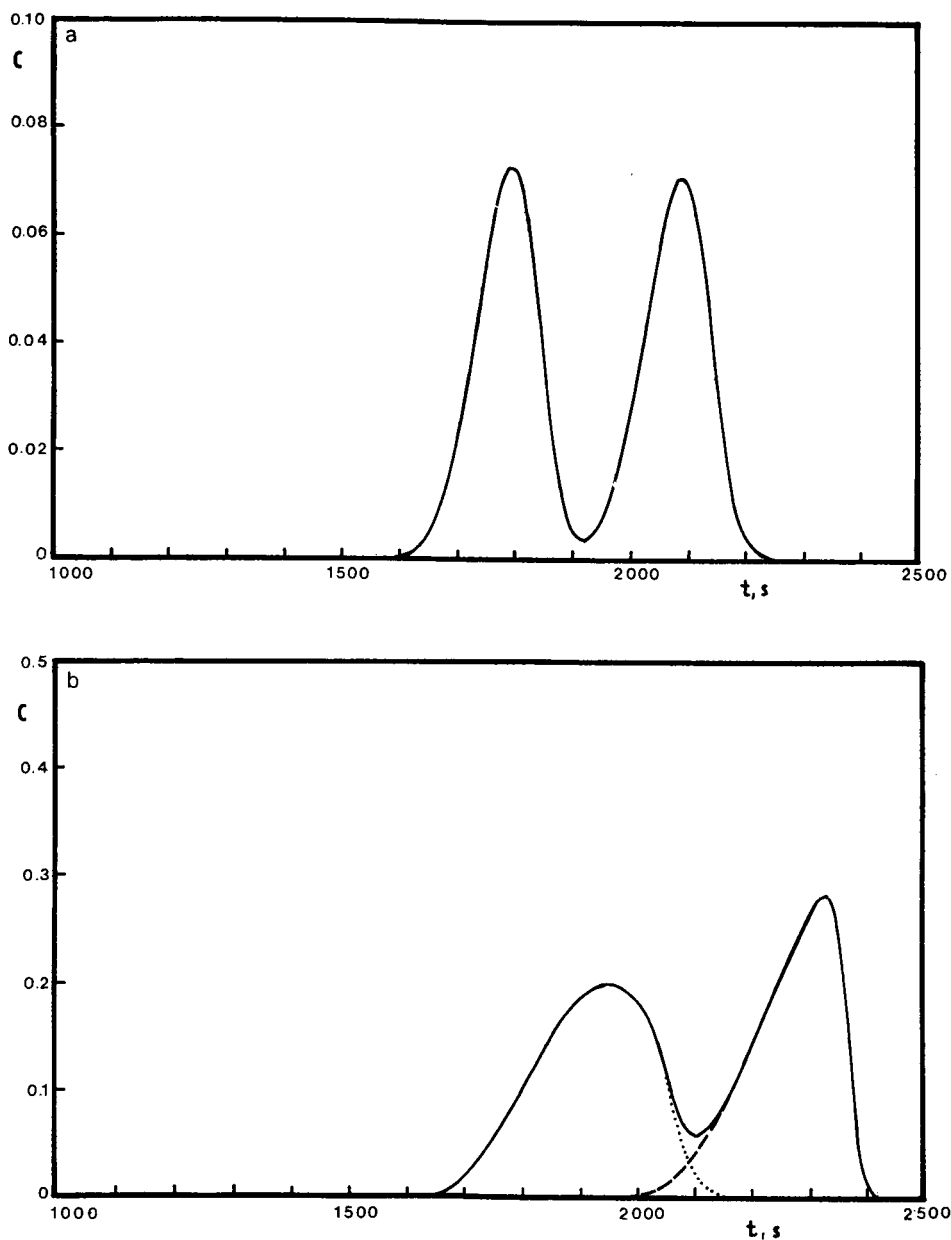


Fig. 6. Computation of a chromatogram for the two-component system. $A_1 = 1.6$, $B_1 = -0.3$, $A_2 = 1.96$, $B_2 = -0.3$. (a) $V_D = 0.1$ ml, $C_{01} = C_{02} = 1.0$; (b) $V_D = 5.0$ ml, $C_{01} = C_{02} = 1.0$. Other conditions as in Fig. 5.

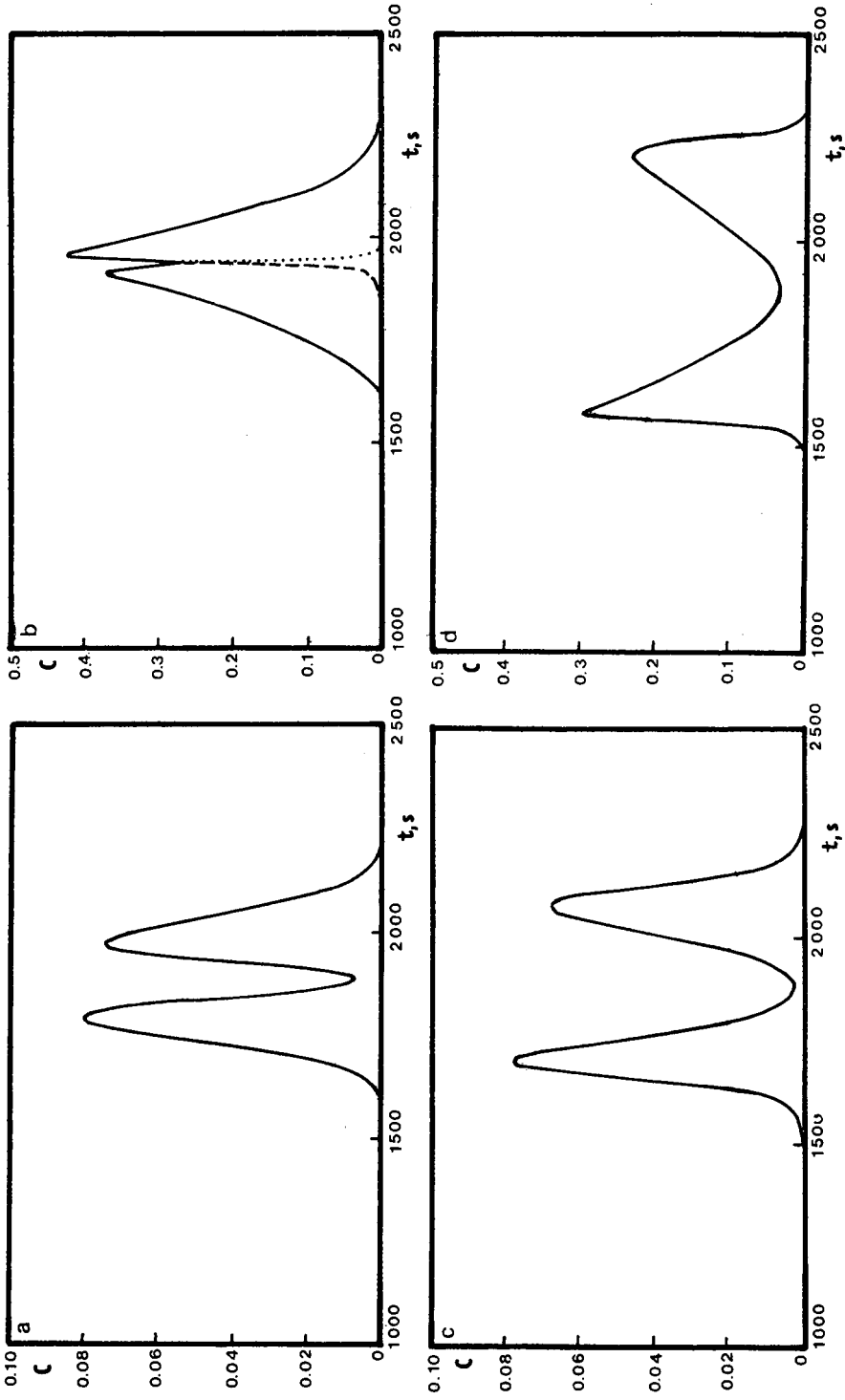


Fig. 7. Computation of a chromatogram for the two-component system. (a) $A_1 = 1.6, B_1 = -0.3, A_2 = 1.96, B_2 = 0.3, V_D = 0.1 \text{ ml}, C_{01} = C_{02} = 1.0$; (b) A_1, B_1, A_2 and B_2 as in (a), $V_D = 0.5 \text{ ml}, C_{01} = C_{02} = 1.0$; (c) $A_1 = 1.6, B_1 = 0.3, A_2 = 1.96, B_2 = -0.3, V_D = 0.1 \text{ ml}, C_{01} = C_{02} = 1.0$; (d) A_1, B_1, A_2 and B_2 as in (c), $V_D = 0.5 \text{ ml}, C_{01} = C_{02} = 1.0$. Other parameters as in Fig. 5.

The chromatograms in Figs. 5–7 demonstrate that in all instances, when the amount injected is increased, the retention times t_R are shifted to lower or higher values depending on whether B is positive or negative. From the standpoint of the resolution, the most disadvantageous case is when $B_1 < 0$ and $B_2 > 0$. To judge the effect of the mutual influence of the first and second components, let us compare the retention times of one component (for a given value of B) with the retention times of the same component but for another value of B of the second component. For example, the retention times of the first component t_{R1} on the chromatograms in Fig. 7a and b are lower than t_{R1} in Fig. 6a and b, but t_{R2} on the same chromatograms (Fig. 7a and b) are higher than t_{R2} in Fig. 5a and b. Similarly, we can compare Fig. 7c and d with Fig. 5a and b for the first component and with Fig. 6a and b for the second component. All these comparisons show the influence of the second component (or its corresponding B value) on the retention time of the competitive component.

The program may be used for a real system on the condition that the real values ε , D_k , $\bar{C}_k = \bar{C}_k(C_1, C_2)$ and possibly the shape of the input signal have been determined.

CONCLUSION

The various methods for modelling of the chromatographic process can be found in the literature^{21–24}. We decided to solve eqn. 1 using the procedure that, according to Guiochon and Katti's review dealing on preparative chromatography²⁵, belongs to the group of solutions that are available for the quasi-ideal problem, *i.e.*, the kinetics of mass transfer must be rapid and independent of the concentration, and must be accounted for by an apparent diffusion coefficient. The advantage of this approach consists in its applicability to multi-component systems, whereas the approach based on the real kinetic function of mass transfer and a non-linear isotherm is not applicable to the study of the separation between two compounds.

In subsequent work we shall examine the experimental verification of the numerical solution discussed above. In addition, we shall compare the results with those obtained following an approach similar to the work of Ghodbane and Guiochon¹³ and with the data obtained in different ways (mixed cells model) developed in our laboratory²⁴.

REFERENCES

- 1 Z. Deyl, K. Macek and J. Janák (Editors), *Liquid Column Chromatography — A Survey of Modern Techniques and Applications*, Elsevier, Amsterdam, 1975.
- 2 H. Röck, *Chem.-Ing.-Tech.*, 28 (1956) 489.
- 3 J. J. Carberry, *Nature (London)*, 189 (1961) 391.
- 4 E. Kučera, *J. Chromatogr.*, 19 (1965) 237.
- 5 A. Jaulmes, C. Vidal-Madjar, A. Ladurelli and G. Guiochon, *J. Phys. Chem.*, 88 (1984) 5379.
- 6 A. Jaulmes, C. Vidal-Madjar, H. Colin and G. Guiochon, *J. Phys. Chem.*, 90 (1986) 207.
- 7 J. C. Smit, H. C. Smit and E. M. de Jager, *Anal. Chim. Acta*, 122 (1980) 1.
- 8 J. C. Smit, H. C. Smit and E. M. de Jager, *Anal. Chim. Acta*, 122 (1980) 151.
- 9 G. H. Cowan, I. S. Gosling, J. F. Laws and W. P. Sweetenham, *J. Chromatogr.*, 363 (1986) 37.
- 10 P. Rouchon, P. Valentin, M. Schonauer and G. Guiochon, *Sep. Sci. Technol.*, 22 (1987) 1793.
- 11 G. Guiochon, S. Golshan-Shirazi and A. Jaulmes, *Anal. Chem.*, 60 (1988) 1856.
- 12 G. Guiochon and S. Ghodbane, *J. Phys. Chem.*, 92 (1988) 3682.
- 13 S. Ghodbane and G. Guiochon, *J. Chromatogr.*, 444 (1988) 275.
- 14 A. Katti and G. Guiochon, *J. Chromatogr.*, 449 (1988) 25.

- 15 S. Ghodbane and G. Guiochon, *J. Chromatogr.*, 450 (1988) 27.
- 16 J.-X. Huang and Cs. Horváth, *J. Chromatogr.*, 406 (1987) 285.
- 17 W. Kopaciewicz, S. Fulton and S. Y. Lee, *J. Chromatogr.*, 409 (1987) 111.
- 18 M. E. Davis, *Numerical Methods and Modelling for Chemical Engineers*, New York, Chichester, Brisbane, Toronto, Singapore, 1984.
- 19 F. G. Helfferich and G. Klein, *Multicomponent Chromatography — Theory of Interference*, Marcel Dekker, New York, 1970.
- 20 M. D. LeVan and T. Vermeulen, *J. Phys. Chem.*, 85 (1981) 3247.
- 21 J. E. Eble, R. L. Grob, P. E. Antle and L. R. Snyder, *J. Chromatogr.*, 384 (1987) 25.
- 22 J. E. Eble, R. L. Grob, P. E. Antle and L. R. Snyder, *J. Chromatogr.*, 405 (1987) 1.
- 23 J. Villermaux, *J. Chromatogr.*, 406 (1987) 11.
- 24 V. Svoboda, *J. Chromatogr.*, 464 (1989) 1.
- 25 G. Guiochon and A. Katti, *Chromatographia*, 24 (1987) 165.

CHROM. 21 324

OPTIMIZATION OF THE GAS CHROMATOGRAPHIC SEPARATION OF FIVE-MEMBERED RING POLYARENES WITH AN ADMIXED BPhBT LIQUID CRYSTAL-DEXSIL 300 STATIONARY PHASE

G. M. JANINI* and N. T. FILFIL

Department of Chemistry, Kuwait University, P.O. Box 5969, Kuwait 13060 (Kuwait)

(First received November 8th, 1988; revised manuscript received January 17th, 1989)

SUMMARY

A window diagram constructed with the liquid crystal BPhBT in admixtures with the gum phase Dexsil 300 gave the optimum mixing ratio for the gas chromatographic resolution of five-membered ring polycyclic aromatic hydrocarbon solutes. The window diagram was constructed from relative retention data obtained from specific retention volume measurements. Plots of the specific retention volumes versus percentage of BPhBT in the blend were linear to within $\pm 5\%$ for all solutes. Further, intimately blended phases gave specific retention volumes virtually identical with those of mechanically mixed phases, within experimental error, when the same mixing ratios were compared. This suggests that the liquid crystal is only dispersed (as opposed to dissolved) in Dexsil 300 and that the two phases act independently of each other in the blends. This contention is supported by differential scanning calorimetric measurements. The use of the retention index scheme for the purpose of window diagram construction is shown not to be a valid option for this system.

INTRODUCTION

Comprehensive theoretical and experimental studies by Laub, Purnell and co-workers¹⁻⁹ have established that solute retention with mixed gas chromatographic stationary phases can be predicted from retention data with each of the pure phases. The subject has been comprehensively reviewed by Laub¹⁰ and by Laub and Wellington¹¹. The theoretical basis of this approach rests on a solution model in which the mixed phases are considered to be mutually immiscible. Thus,

$$K_{R(M)} = \varphi_A K_{R(A)}^0 + \varphi_B K_{R(B)}^0 \quad (1)$$

where K_R^0 is the partition coefficient of a solute with pure phases A and B, $K_{R(M)}$ is the partition coefficient with any combination of the two pure phases and φ_i is the volume fraction of component i .

As was first deduced by Primavesi¹², eqn. 1 can be put alternatively in terms of solute specific retention volume (V_g^0):

$$V_{g(M)}^0 = w_A V_{g(A)}^0 + w_B V_{g(B)}^0 \quad (2)$$

where w_i is the mass fraction of component i .

Pecsok and Apffel¹³ have also shown that for several binary stationary phases, eqn. 1 can be cast in terms of the retention index, I :

$$I_{(M)} = \varphi_{(A)} I_{(A)}^0 + \varphi_{(B)} I_{(B)}^0 \quad (3)$$

Further, for columns of equal phase ratio per unit length, eqn. 1 can be put in terms of capacity factors, k' :

$$k'_{(M)} = w_{(A)} k'_{(A)} + w_{(B)} k'_{(B)} \quad (4)$$

However, some modification of eqn. 4 is required when the capacity factor data are obtained with packings of unequal liquid loadings and/or particle size^{8,9}.

Any variant of eqn. 1 can be used for the prediction of the optimum mixed phase for the resolution of a given solute mixture. For example, employing eqn. 2 the relative retention of two solutes ($\alpha_{2/1}$) is given by

$$\alpha(2/1) = \frac{[w_{(A)} V_{g(A)}^0 + w_{(B)} V_{g(B)}^0]_2}{[w_{(A)} V_{g(A)}^0 + w_{(B)} V_{g(B)}^0]_1} \quad (5)$$

Thus plots of $\alpha(2/1)$ versus $w_{(A)}$ (window diagram) allows the prediction of the optimum α value for the most difficult solute pair. Consequently, the number of theoretical plates and, hence, the column length required to affect the resolution can then be calculated¹⁴.

Examination of eqn. 1 and its variants by several workers showed that it is valid for a wide variety of mixed solvents and solute classes^{10,11}. However, several studies¹⁵⁻²⁰ have shown that the relationship is accurate to no better than 20% for several systems examined with intimately blended stationary phases. For example, curvature of the plots of $K_{(M)}$ versus φ_A was observed for a number of solutes with squalane in admixture with dinonyl phthalate as stationary phase at 30°C²¹. On the other hand, and as argued by many workers^{3,11,20}, retention with mechanically mixed stationary phases must conform with eqn. 1 and its variants because the phases are physically separated in the column.

In this work, we have examined the linearity of plots of $V_{g(M)}^0$ versus $w_{(A)}$ for mixed liquid crystal-polymeric gum phases. Two sets of columns were constructed to assess this effect, one with mechanically mixed phases and the other with intimately blended phases. A window diagram constructed from the data generated by these columns gave the optimum mixed-bed composition for the separation of five-membered ring polycyclic aromatic hydrocarbons.

EXPERIMENTAL

N,N'-Bis(*p*-phenylbenzylidene)- α,α' -bi-*p*-toluidine (BPhBT) was synthesized by the reaction of 2 mol of *p*-phenylbenzaldehyde with 1 mol of α,α' -bi-*p*-toluidine. The mixture was allowed to reflux in absolute ethanol for 24 h, then the product was

recrystallized twice from hot chloroform. The solid–nematic transition temperature (257°C) and the nematic–isotropic transition temperature (403°C) were measured by differential scanning calorimetry (DSC) and were confirmed by hot-stage microscopy. Dexsil 300 and Chromosorb W HP (100–120 mesh) were purchased from Applied Science Labs. (State College, PA, U.S.A.).

The column packings were prepared by dissolving weighed amounts of the appropriate stationary phase in chloroform and transferring it into a chloroform slurry of weighed solid support in a round-bottomed flask. Excess of solvent was gently removed using a rotary evaporator and the slurry was then sieved to the appropriate mesh size. The percentage loading (10–11%) of each packing was determined to $\pm 2\%$ by exhaustive duplicate extractions. The columns used were 1/4 in. O.D. Pyrex glass.

A Perkin-Elmer Sigma 1B gas chromatograph equipped with dual column, forced-air oven, two flame ionization detectors, electronic carrier gas flow controllers and a Sigma 10 data station was employed. The column outlet pressure was read off a barometer and the column inlet pressure was measured with an auxiliary pressure gauge to ± 0.2 p.s.i. The oven temperature was independently calibrated with a thermocouple. The temperature control at 265°C was accurate to within $\pm 3^\circ\text{C}$.

Retention data were directly recorded by the on-line data station. An average of three measurements were taken for each point. The retention time of benzene was used to correct for the dead time. The minimum sample size was used to ensure that all peaks are symmetric. Helium carrier gas flow-rates were read off the digital display and were also checked with a calibrated soap-bubble flow meter.

Specific retention volumes were calculated from primary chromatographic data by the expression

$$V_g^0 = t' F_c^0 / g \quad (6)$$

where t' is the corrected solute retention time, F_c^0 is the volume flow rate of the carrier gas adjusted to the mean column pressure and 0°C and g is the mass of the liquid stationary phase in the column.

RESULTS AND DISCUSSION

The use of liquid crystals as stationary phases for the separation of rigid geometric isomers is gaining interest, especially after the introduction of polymeric varieties of these materials^{22,23}. A considerable improvement in column efficiency is achieved when liquid crystals are used in admixtures with gum phases²⁴. Of particular importance is the fact that dispersion of the liquid crystalline material in the gum solvent (up to 25%, w/w) does not destroy but only dilutes the ordered molecular orientation of the liquid crystal, which is responsible for its unique selectivity towards rigid geometric isomers²⁴. This suggests that at least for the systems studied so far^{24,25} the liquid crystal phase is immiscible in the gum solvent. Hence eqns. 1 and 2 ought to be valid for such systems despite the fact that the two phases differ widely in their solvent properties.

To test this hypothesis we selected the liquid crystal BPhBT and the gum phase Dexsil 300. Fig. 1 shows DSC thermograms for (a) neat BPhBT, (b) a 10% (w/w)

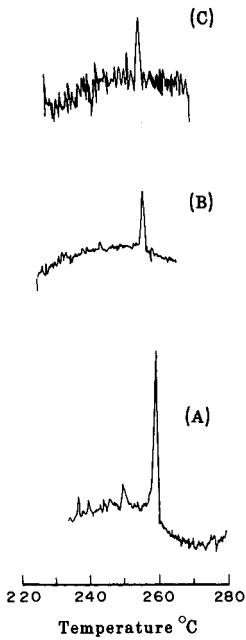


Fig. 1. DSC scans of (A) bulk BPhBT, (B) 10% (w/w) coating of BPhBT on Chromosorb W HP and (C) 10% (w/w) coating of a blend of BPhBT-Dexsil 300 (55.6:44.4) on Chromosorb W HP. Scan rate, 10°C/min.

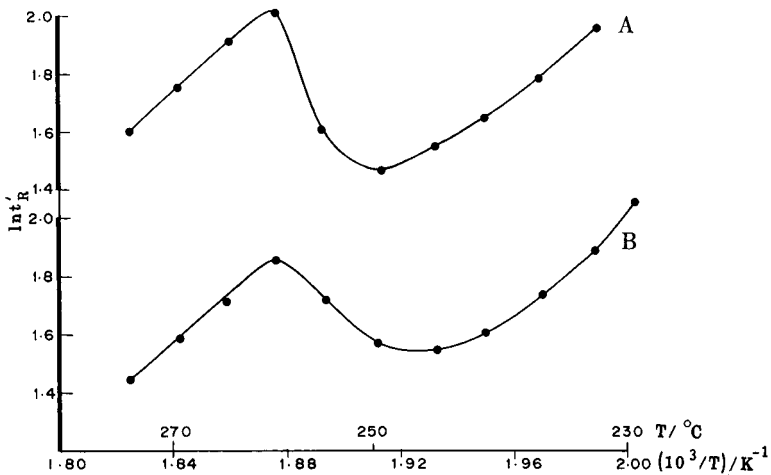


Fig. 2. Plots of the logarithm of the retention time (t'_R) of benzo[a]pyrene as a function of reciprocal temperature on (A) mechanically mixed and (B) intimately blended columns of BPhBT-Dexsil 300. Each packing contained 56.6% BPhBT.

TABLE I

SPECIFIC RETENTION VOLUMES OF SOLUTES [$V_g^0 \pm 5\%$ (ml g^{-1})] WITH NEAT BPhBT, NEAT DEXSIL 300 AND INTIMATE BLENDS OF THE TWO PHASES AT 265°C

Solute	BPhBT (mass%)					
	0	9.5	23.9	55.6	73.9	100
Triphenylene	247.6	264.3	298.1	322.2	337.9	404.4
Benz[a]anthracene	242.2	260.4	316.8	409.9	478.7	547.2
Chrysene	243.2	280.6	376.0	502.3	584.9	709.7
Benzo[k]fluoranthene	530.0	632.5	831.8	1153	1306	1644
Benzo[e]pyrene	644.5	760.5	890.1	1146	1298	1504
Perylene	702.7	832.7	1037	1350	1659	1918
Benzo[a]pyrene	658.7	818.2	1129	1633	2097	2483

coating of BPhBT on Chromosorb W HP (100–120 mesh) and (c) a 10% (w/w) coating of BPhBT–Dexsil 300 (55.6:44.4) on Chromosorb W HP (100–120 mesh). There is a slight shift in the solid–nematic transition temperature of coated BPhBT in comparison with neat BPhBT. However, no difference is observed between coatings of neat BPhBT and those of its blend with Dexsil 300, indicating that the liquid crystal is only dispersed in Dexsil 300 because real solution behaviour would shift the BPhBT transition temperature to lower values and eventually disrupt the mesomorphic order as the percentage of Dexsil 300 is increased. Further evidence is provided in Fig. 2, which presents Van 't Hoff plots of the logarithm of the retention time of a solute (benz[a]anthracene) as a function of reciprocal temperature on two admixed BPhBT–Dexsil 300 columns, one mechanically mixed and the other intimately blended. The two curves are essentially identical, showing no appreciable difference in the BPhBT phase transition for the two types of phase mixing.

TABLE II

COMPARISON OF SPECIFIC RETENTION DATA WITH COLUMNS OF 10% (w/w) MECHANICALLY MIXED PACKING AND 10% (w/w) INTIMATELY BLENDED PACKING AT 265°C

BPhBT in each column: 55.6% (w/w).

Solute	$V_g^0 \pm 5\%$ (ml g^{-1})	
	Mechanically mixed packing ^a	Intimately blended packing ^b
Triphenylene	331.0	322.2
Benz[a]anthracene	419.0	409.9
Chrysene	497	502.3
Benzo[k]fluoranthene	1182	1153
Benzo[e]pyrene	1139	1146
Perylene	1332	1350
Benzo[a]pyrene	1701	1633

^a Mechanically mixed 10% (w/w) BPhBT packing and 10% (w/w) Dexsil 300 packing.

^b 10% packing of intimately blended BPhBT (56.6%) and Dexsil 300 (44.4%).

Table I gives the specific retention volumes of seven polycyclic aromatic solutes on six columns with different blending ratios of BPhBT to Dexsil 300. Although specific retention data could be measured to $\pm 1\%$ with high-precision instruments, we estimate the error in our V_g^0 data to be within $\pm 5\%$. This estimate is based on the reproducibility of V_g^0 data from two independent measurements using our experimental set-up with two columns having the same proportion of 55.6% BPhBT in the blend. Also, when experimentally determined V_g^0 data were compared with smoothed values obtained from plots of V_g^0 versus mass percentage of BPhBT, a scatter well within $\pm 5\%$ was observed.

Further, two columns were compared, one with a mechanically mixed and the other with an intimately blended packing. The percentage of BPhBT in each was 55.6%, and the loading of each was 10% (w/w) on Chromosorb W HP (100–200 mesh). The results presented in Table II show that the difference from solute to solute is within $\pm 5\%$. This further demonstrates that there is no systematic variation in the data generated with these two types of phase mixing.

Fig. 3 shows plots of V_g^0 values obtained with intimately blended phases versus the percentage of BPhBT, which were linear, and linear regression analysis on the data for each solute yielded correlation coefficients in excess of 0.99. Fig. 4 is a window diagram constructed by plotting the relative retention (α) values for each pair of solutes

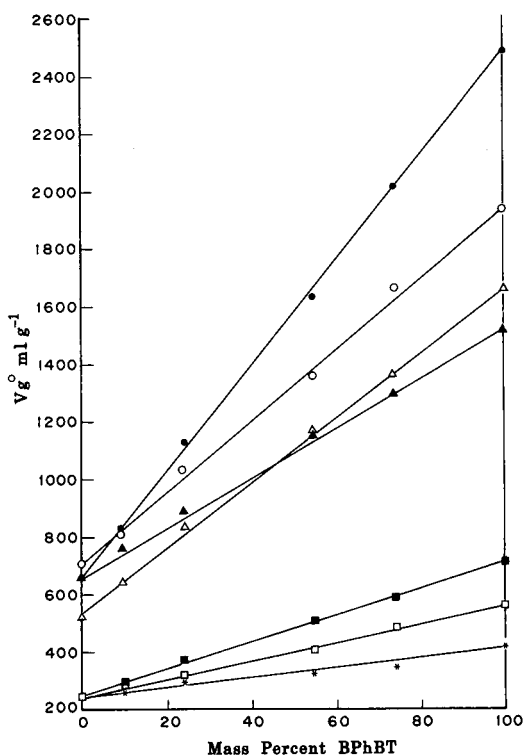


Fig. 3. Plots of the specific retention volume versus mass percentage of BPhBT for various solutes at 265°C. Solutes: ● = benzo[a]pyrene; ○ = perylene; △ = benzo[k]fluoranthene; ▲ = benzo[e]pyrene; ■ = chrysenes; □ = benz[a]anthracene; * = triphenylene.

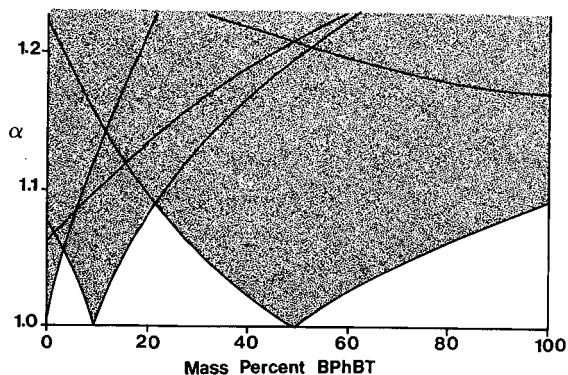


Fig. 4. Window diagram calculated from relative retention data from Table I and Fig. 3. Optimum predicted BPhBT mass percentage is 23%.

for the five-membered ring compounds. An interesting feature is that the plot shows that a column that contains only about 23% of BPhBT will easily resolve all the components of the mixture. Although neat BPhBT is more selective (*i.e.*, gives higher α values), an increase in column efficiency is gained by using columns with the optimum phase ratio. To illustrate this, Fig. 5 shows the resolution of five-membered ring polyarenes on a column packed with BPhBT-Dexsil 300 (23:77). The elution order is benzo[*k*]fluoranthene < benzo[*e*]pyrene < perylene < benzo[*a*]pyrene. The elution order of the first two compounds is the opposite of that with neat BPhBT. In

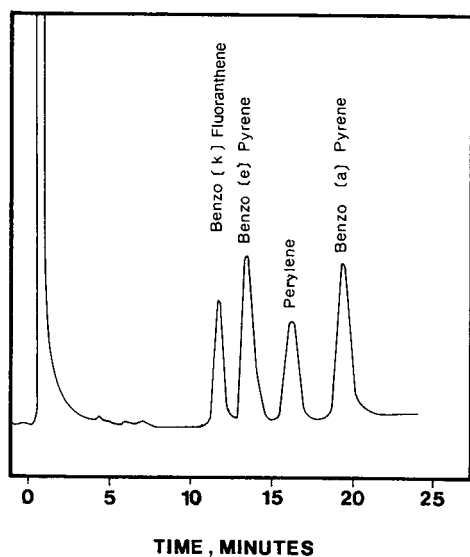


Fig. 5. Chromatogram of four pentacyclic aromatic hydrocarbons. Column: 1.8 m \times 2 mm I.D. Pyrex glass. Packing: 3% (w/w) on Chromosorb W HP (100–120 mesh). Stationary phase: BPhBT-Dexsil 300 (23:77). Conditions: oven, 265°C; injector, 270°C; detector, 270°C; carrier gas, helium; flow-rate, 40 cm³ min⁻¹.

contrast, benzo[*e*]pyrene and benzo[*a*]pyrene co-elute on neat Dexsil 300 columns and they are not resolved from the other two compounds.

It is concluded that the separation of polycyclic aromatic hydrocarbons, or for that matter any set of rigid geometric isomers, can be optimised by using admixtures of liquid crystals and gum phases. The optimization procedure requires only the measurement of V_g^0 data for each solute with the two neat phases. It should be noted that although several workers have observed systematic differences between the partition coefficient data generated with intimately blended and mechanically mixed phases²⁶, no such non-linear behaviour is apparent in this study, despite the wide difference in the solution properties of the liquid crystal and the gum phase.

An obvious drawback to this approach is that it requires the measurement of V_g^0 data, which may present some practical difficulties especially when gum silicone phases are used.

Window diagrams can be constructed with retention indices data via eqn. 3; however, this approach requires that the retention index of each compound should not be widely different with the two neat phases. In this work we measured the retention indices of the set of solutes with the two neat phases and found that the values for the four-membered ring compounds with BPhBT are higher than those with Dexsil 300 by more than 1500 units. For the five-membered ring compounds the difference is over 2000 units. Hence this approach is rendered impractical. Further, the alternative use of capacity factor data also requires some stringent conditions in column fabrication.

ACKNOWLEDGEMENTS

Support for this work was provided jointly by Kuwait University and the Kuwait Foundation for the Advancement of Science under project No. SC035/86-13-03. Helpful discussions with R. J. Laub are greatly appreciated.

REFERENCES

- 1 R. J. Laub and J. H. Purnell, *J. Chromatogr.*, 112 (1975) 71.
- 2 R. J. Laub and J. H. Purnell, *Anal. Chem.*, 48 (1976) 799.
- 3 R. J. Laub and J. H. Purnell, *Anal. Chem.*, 48 (1976) 1720.
- 4 R. J. Laub, J. H. Purnell and P. S. Williams, *J. Chromatogr.*, 134 (1977) 249.
- 5 W. K. Al-Thamir, R. J. Laub and J. H. Purnell, *J. Chromatogr.*, 142 (1977) 3.
- 6 R. J. Laub, J. H. Purnell and P. S. Williams, *Anal. Chim. Acta*, 95 (1977) 135.
- 7 R. J. Laub, J. H. Purnell, D. M. Summers and P. S. Williams, *J. Chromatogr.*, 155 (1978) 1.
- 8 R. J. Laub and J. H. Purnell, *J. Chromatogr.*, 161 (1978) 49.
- 9 R. J. Laub and J. H. Purnell, *J. Chromatogr.*, 161 (1978) 59.
- 10 R. J. Laub, in T. Kuwana (Editor), *Physical Methods of Modern Chemical Analysis*, Vol. 3, Academic Press, New York, 1983, p. 250.
- 11 R. J. Laub and C. A. Wellington, in R. Foster (Editor), *Molecular Association*, Academic Press, London, 1979, Ch. 3.
- 12 G. R. Primavesi, *Nature (London)*, 184 (1959) 2010.
- 13 R. L. Pecsok and J. Appfel, *Anal. Chem.*, 51 (1979) 594.
- 14 J. H. Purnell, *J. Chem. Soc.*, (1960) 1268.
- 15 A. J. Ashworth and D. M. Hooker, *J. Chromatogr.*, 131 (1977) 399.
- 16 J. F. Parcher and T. N. Westlake, *J. Phys. Chem.*, 81 (1977) 307.
- 17 S. D. Christian, E. E. Tucker and A. Mirta, *J. Chem. Soc., Faraday Trans. 1*, 73 (1977) 537.
- 18 E. E. Tucker and S. D. Christian, *J. Am. Chem. Soc.*, 100 (1978) 1418.
- 19 W. E. Acree, Jr. and G. L. Bertrand, *J. Phys. Chem.*, 83 (1979) 2355.

- 20 P. F. Tiley, *J. Chromatogr.*, 179 (1979) 247.
- 21 M. W. P. Harbison, R. J. Laub, D. E. Martire, J. H. Purnell and P. S. Williams, *J. Phys. Chem.*, 83 (1979) 1262.
- 22 G. M. Janini, *Adv. Chromatogr.*, 17 (1979) 231.
- 23 M. A. Apfel, H. Finkelmann, G. M. Janini, R. J. Laub, B.-H. Luhmann, A. Price, W. L. Roberts, T. J. Shaw and C. A. Smith, *Anal. Chem.*, 57 (1985) 651.
- 24 G. M. Janini, G. M. Muschik, H. J. Issaq and R. J. Laub, *Anal. Chem.*, 60 (1988) 1119.
- 25 R. J. Laub, W. L. Roberts and C. A. Smith, *J. High Resolut. Chromatogr. Chromatogr. Commun.*, 3 (1980) 355.

CHROM. 21 335

CONTRIBUTION OF LONGITUDINAL DIFFUSION TO BAND BROADENING IN LIQUID CHROMATOGRAPHY

ALAIN BERTHOD*, FRÉDÉRIC CHARTIER and JEAN-LOUIS ROCCA

Laboratoire des Sciences Analytiques, UA CNRS 435, Université de Lyon 1, 69622 Villeurbanne Cédex (France)

(First received December 27th, 1988; revised manuscript received January 20th, 1989)

SUMMARY

The contribution of longitudinal diffusion to band broadening in liquid chromatography was studied with a laboratory-made densely grafted stationary phase. Nucleosil 100-5 was used as the silica base. Tetradecyldimethyl(dimethylamino)silane was the bonding reagent used to obtain a brush-type monolayer phase with an 18% carbon load and $3.5 \mu\text{mol}/\text{m}^2$ bonding coverage. The phase was fully characterized for surface area, porosity and mean pore diameter. A $15 \text{ cm} \times 4 \text{ mm I.D.}$ column was slurry packed with the phase and used to obtain Knox plots: h , the reduced plate height, versus v , the reduced linear mobile phase velocity. All efficiency values were measured using the moment method. A , B and C terms of the Knox equation were determined at two temperatures, 25 and 40°C , and for four solutes, benzene, toluene, ethylbenzene and propylbenzene. As longitudinal diffusion is dependent on B , B values were also determined by the arrested elution method (static method). Static and dynamic plots of B versus k' led to obstruction factors, γ_m , of 1.10 ± 0.1 and 1.32 ± 0.16 , respectively. If obstruction factors higher than unity are found with other phases, it may be thought that the established chromatographic theory overlooked some phenomena occurring in porous and densely bonded phases.

INTRODUCTION

One of the constant trends in liquid chromatography (LC) is attempts to achieve more efficient systems. The understanding of the causes of band broadening is the obvious way to control and to reduce it. The earliest mathematical description of the general phenomena occurring in a chromatographic column was developed by Martin and Synge¹, who introduced the plate model still in use today. This model was refined by several workers, specially Giddings² and Knox and co-workers³⁻⁷. Several models, such as the mass balance model, were developed. The random walk model and the non-equilibrium treatment were both initiated by Giddings². Using these models, different plate-height equations were derived by Giddings², Snyder⁸, Huber⁹ and Knox and co-workers^{3,4}. Such equations relate the reduced plate height to the reduced mobile phase velocity. With a set of experiments at different flow-rates, it is possible to obtain an insight into the solute exchange between phases in the column.

The aim of this work was to study the contribution of the longitudinal diffusion to band broadening. The B term of the Knox equation is directly related to the longitudinal or axial molecular diffusion. The Knox equation is

$$h = Av^{1/3} + B/v + Cv \quad (1)$$

in which A , B and C are dimensionless solute and stationary zone-dependent constants, h is the dimensionless reduced plate height [$h = H/d_p$, where H is the height equivalent to a theoretical plate (HETP) and d_p is the particle diameter] and v is the dimensionless reduced velocity:

$$v = ud_p/D_m \quad (2)$$

where u is the mobile phase linear velocity (cm/s), and D_m the solute diffusion coefficient in the mobile phase (cm²/s). It is relatively easy to obtain the A , B and C terms of the Knox equation by measuring efficiencies at different mobile phase flow-rates.

In most studies, the chromatographic peak efficiencies were derived from peak-width measurements assuming a Gaussian peak shape. Such calculations always produce overestimated plate numbers. Throughout this work, the moment method was used for efficiency measurement, as it is the only method that makes no assumptions about the peak shape².

Such efficiency experiments were usually done with commercial stationary phases for which the physico-chemical properties are not fully known. In order to work on a well characterized phase, we synthesized it and packed a column with it. To cross-check the results obtained dynamically (Knox equation), static experiments (non-elution chromatography) were carried out with the same column.

THEORETICAL

The HETP is the ratio of the column length, L , to the plate number, N :

$$H = L/N \quad (3)$$

Expressing the peak variance, σ^2 , in length units, the HETP becomes

$$H = \sigma^2/L \quad (4)$$

Variances are additive. The total variance, σ^2 , is the sum of several contributions:

$$\sigma^2 = \sigma_{\text{ext}}^2 + \sigma_{\text{fl}}^2 + \sigma_{\text{ld}}^2 + \sigma_{\text{mt}}^2 \quad (5)$$

where the subscripts ext, fl, ld and mt represent the extra-column contributions (injector, detector, tubing), the flow contribution (eddy diffusion and flow anisotropy), the longitudinal diffusion contribution (the term investigated in this study) and the mass transfer term, respectively.

For a column packed with porous particles, the general plate height expression was written as²

$$H = 2\lambda d_p + 2\gamma D_m/u + \frac{qk'd_f^2u}{(1+k')^2D_s} + \frac{[\Omega f(k') + f(\varphi)g(k')]ud_p^2}{D_m} \quad (6)$$

where λ , γ , q and Ω are geometrical factors, D_m and D_s are the diffusion coefficients of the solute in the mobile and the stationary phase, respectively, k' is the capacity factor, d_f is the stationary phase thickness, φ is the fraction of the mobile phase inside the porous bed and $f(k')$, $g(k')$ and $f(\varphi)$ are mathematical functions.

Knox⁶ showed that the flow contribution to the plate height equation could be represented to a high degree of approximation by

$$H_{fl} = [1/(\alpha + \beta u^{-n})] \quad \text{with } n < 1 \quad (7)$$

where α and β are constants and n , determined empirically, has a value between 0.2 and 0.5. Using the reduced parameters h and v , Knox further simplified eqn. 7 to

$$h_{fl} = Av^{1/3} \quad (8)$$

The constant A depends critically on the regularity of the column packing. A very uniform column packing may produce an A value as low as 0.5. Values of A larger than 3 usually indicate a poorly packed column⁶.

The C term of the Knox equation (eqn. 1) represents the mass transfer contribution. According to Giddings², Knox⁶ and Knox and Scott¹⁰, it can be written as

$$C = q \left(\frac{k' + \varphi}{1 + k'} \right)^2 \left(\frac{D_m}{\gamma_{sm}\varphi D_m + k'\gamma_s D_s} \right) \quad (9)$$

where the subscript sm represents the stagnant mobile phase and the γ terms are obstruction factors for diffusion through granular and/or porous materials. The geometrical factor q is dependent on porosity². For a stationary phase in a spherical configuration and medium pores, $q = 1/30$. For narrow pores whose cross-sectional area, a , increases from the bottom as $a = a_0x^n$, where x is the distance from the bottom of the pore and n is the taper factor, q becomes $2/[(n+1)(n+3)]$. For example, when the taper factor is 2, $q = 2/15$.

The B term of the Knox equation is the term of interest in longitudinal diffusion studies. Using the random walk model and the Einstein equation for molecular diffusion¹¹, which is

$$d^2 = 2Dt_d \quad (10)$$

where t_d is the average time which a molecule needs to diffuse a distance d from its starting point, Giddings² showed that the longitudinal molecular diffusion contribution is the sum of three terms:

a stationary phase term:

$$\sigma_s^2 = 2\gamma_s D_s k' V_m \quad (11)$$

a moving mobile phase term (subscript mm):

$$\sigma_{mm}^2 = 2\gamma_{mm} D_m (1 - \phi) V_m \quad (12)$$

and a stagnant mobile phase term:

$$\sigma_{sm}^2 = 2\gamma_{sm} D_m \phi V_m \quad (13)$$

Using the reduced parameters h and ν and restricting the sum $[\gamma_{mm}(1 - \phi) + \gamma_{sm}\phi]$ to γ_m , the B term can be written as

$$B = 2 [\gamma_m + \gamma_s (D_s/D_m) k'] \quad (14)$$

SYNTHESIS AND CHARACTERIZATION OF THE STATIONARY PHASE

The stationary phase was synthesized following the aminosilane route described by Kováts and co-workers^{12,13}. Aminosilanes are known to produce highly dense and reproducible organosiloxy brush-type layers¹².

It was shown by Morel and co-workers^{14,15} that thermal phase transitions occurred for densely grafted alkyl phases. The transition temperature was closely related to the melting point of the corresponding linear alkane. For example, the transition zone of brush-type octadecylsilane (ODS, C₁₈) phases was between 7 and 27°C and the melting point of *n*-octadecane is 28°C. This phase transition for ODS-bonded silica corresponds to the most usual working temperatures and may be responsible for the lack of reproducibility obtained using such phases. We chose to prepare a tetradecyl (C₁₄) bonded phase because the melting point of tetradecane is 5°C and, hopefully, the thermal transition zone will be well below room temperature.

Synthesis

A thorough description of the stationary phase synthesis and characterization was given in a recent paper¹⁶. Nucleosil 100-5 silica base was obtained from Macherey, Nagel & Co. (Düren, F.R.G.). This spherical silica was stated to have a mean particle size, mean pore diameter and pore volume of 5 μm, 10 nm and 1 ml/g, respectively. The actual values for the batch used were measured and are given in Table I. The pore volume and diameter were 38% and 27%, respectively, lower than the supplier's stated values. The bonding reagent was tetradecyl(dimethylamino)silane prepared from tetradecene¹⁶.

Characterization

Table I lists the physico-chemical parameters of the bare Nucleosil 100-5 compared with these of the bonded material. Surface areas were measured using the BET method. Pore size and pore volume were obtained by the mercury intrusion method. A Carlo Erba mercury porosimeter was used. Carbon loading percentages

TABLE I
STATIONARY PHASE PARAMETERS

Stationary phase	Surface area (m ² /g)	Particle diameter (μm)	Pore volume (ml/g)	Mean pore diameter (nm)	Carbon load (%)	Bonding coverage (μmol/m ²)
Nucleosil 100-5	350	5	0.63	7.3	—	—
C ₁₄ bonded phase	210	5	0.45	8.6	17.9	3.5

and bonding coverage were calculated using C and H microanalysis measurements performed by the Service Central d'Analyses, CNRS (Solaize, France).

Nucleosil 100-5 silica gel is a highly porous material. More than 98% of the surface area is due to pores, *i.e.*, the total surface area is mainly particle internal area. The bonding procedure decreased both the surface area and pore volume. However, it seemed to increase the mean pore diameter. This value was calculated using the surface area, S , the pore volume, V_{pore} , and assuming cylindrical pores of constant diameter, d_{pore} :

$$d_{\text{pore}} = 4V_{\text{pore}}/S \quad (15)$$

The mercury intrusion curves indicated a high pore dispersity. Hence the mean pore diameter given by eqn. 15 is only indicative. However, the increase in d_{pore} after bonding was a good indication of possible clogging of filling of smaller pores due to the bonding process.

The high carbon load (17.9% for C₁₄) corresponded to a high bonding coverage (3.5 μmol/m²) of the monolayer brush type. This bonding coverage corresponded to 78% of the theoretical maximum monolayer concentration (4.5 μmol/m²) (ref. 17).

EXPERIMENTAL

Chromatograph system

All measurements were carried out using a standard high-performance liquid chromatography system with methanol–water (70:30, v/v) as the mobile phase at 25 or 40°C. The pump was a Shimadzu Model LC-5A (Touzart & Matignon, Paris, France). A Model 7520 0.5-μl injection valve (Rheodyne, Cotati, CA, U.S.A.) and a Shimadzu SPD-6A UV detector with a 0.5-μl cell were connected with a 15 cm × 4 mm I.D. column slurry packed with the C₁₄ bonded silica described previously. The column was immersed in a constant-temperature water-bath at 25 or 40 ± 0.1°C. The solutes, benzene, toluene, ethylbenzene and propylbenzene, supplied by Merck (Darmstadt, F.R.G.), were detected at 254 nm.

Column parameters

Table II lists the column parameters. The mobile phase volume, V_m , was obtained through the density method¹⁰. The column was filled first with chloroform, weighed, rinsed and then filled with hexane and weighed again. The difference in weights divided by the difference in liquid densities gave V_m . The extra-particle

TABLE II
COLUMN PARAMETERS

<i>Parameter</i>	<i>Value</i>	<i>Parameter</i>	<i>Value</i>
Column length, L	15 cm	Stagnant mob. phase fraction,	
Column I.D.	4 mm	$\phi = (V_m - V_{ext})/V_m$	0.37
Column volume, V_c	1885 μl	Total column porosity,	
Stationary phase volume, V_s	509 μl	$\varepsilon_T = V_m/V_c$	0.73
Mobile phase volume, V_m	1376 μl	Extra particle porosity,	
Extra particle volume, V_{ext}	868 μl	$\varepsilon_e = V_{cm}/V_c$	0.46
Pore volume, V_{int}	508 μl	Column permeability factor, Φ	1500

volume, V_{cm} , was obtained using sulphanic acid. This solute is fully excluded with methanol and sodium nitrate (10^{-3} mol/l) as the mobile phase¹⁰.

Efficiency measurements

To be able to obtain a meaningful Knox plot, the plate count must be significant. The moment method is the only method that gives the plate number of a peak with no shape assumptions¹⁸. Peak area is the zeroth moment, μ_0 , calculated as

$$\mu_0 = \int C(t) dt \quad (16)$$

where $C(t)$ is the detector signal. The mean is the first moment, μ_1 , of the elution curve and it occurs at the centre of mass of the peak:

$$\mu_1 = \left[\int tC(t) dt \right] / \mu_0 \quad (17)$$

The second central reduced moment, μ'_2 , is the peak variance. The third moment measures the peak skewness and is not needed for plate count determination. The plate number is determined as

$$N = \mu_1^2 / \mu'_2 \quad (18)$$

Moments were calculated using a Hewlett-Packard HP-85 microcomputer and a data acquisition technique. The analogue detector output was digitized by a 760 A-D interface (Nelson Analytical, Santa Clara, CA, U.S.A.). The computation method has been described elsewhere¹⁹.

Diffusion coefficient measurements

The Taylor-Aris method²⁰ was used for diffusion coefficient determinations. In an open straight tube of length L and radius r , the band broadening due to the flow-rate, F , produces a variance, σ^2 , dependent on the solute diffusion coefficient, D_m , according to²¹

$$\sigma^2 = \pi r^4 L F / (24 D_m) \quad (19)$$

We used a water-jacketed straight tube of 1.60 m \times 0.254 mm (1/100 in.) I.D. and an internal volume of 83 μ l. Total variances were determined for five different flow-rates, 10, 20, 50, 100 and 200 μ l/min. They were corrected for the extra-column band broadening (Fig. 1). D_m was obtained from the slopes of the σ^2 versus F plots.

Arrested elution method

All B values were checked by the arrested elution method²². Band broadening arising from longitudinal diffusion is independent of whether the band is moving or stationary. If the solute is stopped inside the column for a time t_r , axial diffusion occurs and induces an additional variance, σ_z^2 , which increases the total variance:

$$\sigma_z^2 = 2D_{\text{eff}}t_r \quad (20)$$

where D_{eff} is the effective diffusion coefficient of the solute in the column. t_r was varied from 2 to 15 h. The plots of the total variance, σ^2 , versus t_r gave straight lines whose slopes led to D_{eff} ^{10,22}. D_{eff} is related to γ_m , k' and γ_s by¹⁰

$$D_{\text{eff}} = (\gamma_m D_m + k' \gamma_s D_s) / (1 + k') \quad (21)$$

Eqns. 14 and 21 give:

$$B = 2(1 + k') D_{\text{eff}} / D_m \quad (22)$$

Extra-column band broadening

Eqn. 5 shows an extra-column contribution, σ_{ext}^2 , to the total measured variance, σ^2 . This contribution was calculated by measuring the variance obtained with the injection valve directly connected to the UV detector, without a column or straight tube. Fig. 1 shows the external variance versus flow-rate. All measured variances were corrected for the corresponding σ_{ext}^2 value.

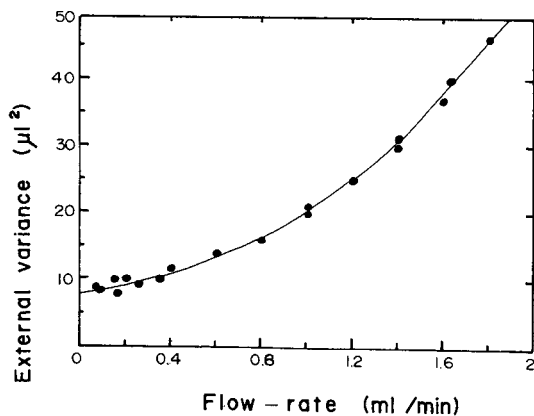


Fig. 1. Dependence of the external variance on the flow-rate. Mobile phase, methanol-water (70:30, v/v); test solute, benzene; variances measured with the moment method.

RESULTS AND DISCUSSION

Diffusion coefficient measurements

Table III lists the diffusion coefficients, D_m and D_{eff} , for the four solutes studied at 25 and 40°C. All D_m values at 40°C were obtained by correcting the corresponding 25°C D_m value for temperature, T , and viscosity, η , changes:

$$D_{m40} = D_{m25} (313/298) (\eta_{25}/\eta_{40}) = 1.355 D_{m25} \quad (23)$$

A, B and C terms of the Knox equation

Table IV gives the efficiency obtained at different flow-rates. Plate numbers, N , as high as 7000 were obtained for a 15-cm column, corresponding to about 50 000 plate/m [70 000 plate/m assuming a Gaussian shape for the peaks (0.6H method)]; 0.6H N values are given for information but were not used in this work. The moment values of N are generally smaller than the 0.6H values by a factor of 40%. The 0.6H values were corrected for extra-column effects using the external variances (Fig. 1) obtained with the moment method. The corresponding external variances calculated by the 0.6H method would be lower. Then the corrected 0.6H plate values would also be lower. This would bring the two values more closely into line. As the experimental system was optimized to reduce all external contribution (Fig. 1), the typical N discrepancy would stay in the region of 30%.

Table V lists the computer-fitted values (least-squares method) of the A , B and C terms of the Knox equation together with the capacity factors, k' , at 25 and 40°C. The A term, close to unity, is an indication of a correctly packed column³⁻⁷. For the four solutes studied, A seems not to be dependent on k' and slightly dependent on temperature. The mean values were 1.1 and 0.9 at 25 and 40°C, respectively.

The C term measures the efficiency of the mass transfer. The column and stationary phase particles that we used were not well suited for a reliable C determination. The maximum reduced velocity value that we were able to obtain was lower than 20 in order to work with a reasonable column pressure drop. Knox and Pryde²³ recommend the use of v values higher than 100 in order to obtain a significant C evaluation. Knox and Scott¹⁰ used v values as high as 5000 with 540- μm particles. This was impossible with 5- μm particles and 15-cm columns as the inlet pressure very rapidly became the limiting factor. At 25°C, the C values decreased as k' increased (Table V). An identical trend was reported by Stout *et al.*²⁴. They thought that the

TABLE III
SOLUTE DIFFUSION COEFFICIENTS ($\times 10^6 \text{ cm}^2/\text{s}$)

Coefficient	Temperature (°C)	Solute			
		Benzene	Toluene	Ethylbenzene	Propylbenzene
D_m	25	8.65	8.0	7.4	6.5
	40	11.8	10.8	10.0	8.8
D_{eff}	25	5.6	4.45	3.3	2.5
	40	7.9	6.7	5.0	4.2

TABLE IV
EFFICIENCY MEASUREMENTS AT 25°C

Plate count obtained by the moment method or by $N = 4(t_r/W_{0.6H})^2$ for the $N(0.6H)$ columns. Average of at least three coherent (within 5%) experiments.

Flow-rate (ml/min)	Benzene		Toluene,	Ethylbenzene,	Propylbenzene	
	<i>N</i>	<i>N</i> (0.6 <i>H</i>)	<i>N</i>	<i>N</i>	<i>N</i>	<i>N</i> (0.6 <i>H</i>)
0.078	5860	6070	5670	—	—	—
0.088	6060	5920	6030	5240	4610	4870
0.099	7335	7360	6145	5860	5190	5375
0.196	9110	11 010	9160	6720	5585	5940
0.291	9260	11 475	9880	8860	8490	8810
0.389	8260	10 800	9160	9070	8810	9890
0.489	8630	10 190	9055	8400	8210	10 150
0.569	7620	11 680	8250	8110	8200	9770
0.688	6695	11 030	7780	6880	7430	9620
0.791	6330	9980	7310	6980	7550	10 460
0.891	6070	10 600	7045	6730	6780	9770
0.985	6570	10 800	7305	5930	6590	10 190
1.080	6120	11 610	6665	5890	6650	10 035
1.160	6110	11 550	6485	5290	6200	10 225
1.230	6285	11 920	5860	5090	6050	9850

decrease in C with increasing k' was due to surface diffusion as the effective diffusion coefficient of solute molecules would be greater within the particle pores as a result of surface diffusion. Horváth and Lin²⁵ also demonstrated that the plate height contribution of kinetic resistances was dependent on k' . The decrease in C with increase in k' was less obvious at 40°C. The general trend is an increase in C with increase in temperature. This may be due to the temperature dependence of diffusion coefficients, as shown by eqn. 9 and Table III.

TABLE V
KNOX PARAMETERS AND CAPACITY FACTORS

Error limits in parentheses. Range of v , 0.7–16; number of data points, 15 (see Table IV).

Solute	25°C					40°C				
	<i>A</i>	<i>B</i>	<i>B</i> ^a	<i>C</i>	<i>k'</i>	<i>A</i>	<i>B</i>	<i>B</i> ^a	<i>C</i>	<i>k'</i>
Benzene	1.1 (0.15)	3.1 (0.2)	2.72 (0.03)	0.22 (0.02)	1.1	1.1 (0.25)	4.5 (0.7)	2.54 (0.03)	0.2 (0.04)	0.9
Toluene	1.05 (0.15)	3.5 (0.2)	3.45 (0.03)	0.16 (0.02)	2.1	0.85 (0.25)	4 (0.7)	3.22 (0.03)	0.34 (0.04)	1.6
Ethylbenzene	1.1 (0.15)	3.8 (0.4)	4.01 (0.04)	0.15 (0.02)	3.5	0.9 (0.15)	3.5 (0.4)	3.60 (0.04)	0.32 (0.03)	2.6
Propylbenzene	1.3 (0.15)	5.0 (0.4)	5.38 (0.04)	0.09 (0.02)	6.0	0.8 (0.10)	5.0 (0.5)	5.15 (0.04)	0.21 (0.02)	4.4

^a *B* values obtained by the arrested elution method (eqn. 22).

Table VI lists the characteristics of the plots of $(q/C) [(k' + \varphi)/(1 + k')]^2$ versus k' . According to eqn. 9, these plots must be linear with $\gamma_s D_s/D_m$ as the slope and $\gamma_{sm}\varphi$ as the intercept. Two q values were used to obtain these plots; $q = 1/30$ is the value usually chosen for porous spherical particles and $q = 2/15$ corresponds to a stationary phase with narrow pores and a taper factor of 2 (from ref. 2, p. 190). Given the low accuracy of C determination, the linearity was not very good (regression factors $r^2 = 0.979$ and 0.715 at 25 and 40°C , respectively). For comparison, the values in ref. 24 were plotted using the same procedure. The results in Table VI were compared with those obtained by static and dynamic experiments leading to the B term which is the term of interest in longitudinal diffusion studies. Table V gives the B terms obtained by dynamic and static experiments.

Comparison of dynamic and static results

The B values obtained by fitting the h versus v plots with the Knox equation were in agreement with those obtained by the arrested elution method for all sets of experiments except with benzene and toluene at 40°C . Attempts were made to fit the dynamic experimental results using the static B values. The A and C values resulting from such a fitting procedure were within the limits indicated in Table V, except for benzene and toluene at 40°C .

Plots of B versus k' at 25 and 40°C are shown in Fig. 2A and B, respectively. The static B values obtained from Table III and eqn. 22 correspond to open symbols and the dynamic values (Table V, eqn. 14) to closed symbols. Lines 2 and 3 match the maximum and minimum errors in Table V to give an idea of the uncertainty in γ_m . Table VII lists the slopes, intercepts, regression coefficients and calculated chromatographic parameters. The surprising result is the high value of γ_m , the mobile phase obstruction factor. At 25°C , the intercepts led to γ_m values of 1.32 ± 0.16 and 1.10 ± 0.04 for dynamic and static experiments, respectively. These results cannot be attributed to experimental errors, given the relatively low scatter of data and the same trend obtained by two different approaches. Values very close to unity were obtained for the obstruction factor γ_m^{7-10} . B data from ref. 24 were calculated from peak

TABLE VI
PARAMETERS CORRESPONDING TO C VALUES

Slopes and intercepts of the $(q/C) [(k' + \varphi)/(1 + k')]^2$ versus k' plots (eqn. 9); n = number of points.

q	Temperature ($^\circ\text{C}$)	Slope ($\gamma_s D_s/D_m$)	Intercept ($\gamma_{sm}\varphi$)	r^2	n	γ_{sm}
1/30	25	0.046	0.023	0.979	4	0.062
		0.016	0.042	0.715	4	0.113
	22	0.063 ^a	0.27 ^a	0.764 ^a	9 ^a	0.900 ^a
2/15	25	0.046 ^b	0.05 ^b	0.826 ^b	16 ^b	0.255 ^b
		0.184	0.092	0.979	4	0.248
	22	0.065	0.170	0.715	4	0.460
		0.252 ^a	1.09 ^a	0.764 ^a	9 ^a	3.650 ^a
		0.182 ^b	0.20 ^b	0.826 ^b	16 ^b	1.020 ^b

^a 3- and 6- μm Zorbax C_8 phase.

^b 3- and 6- μm Zorbax C_{18} phase, from Table I in ref. 24.

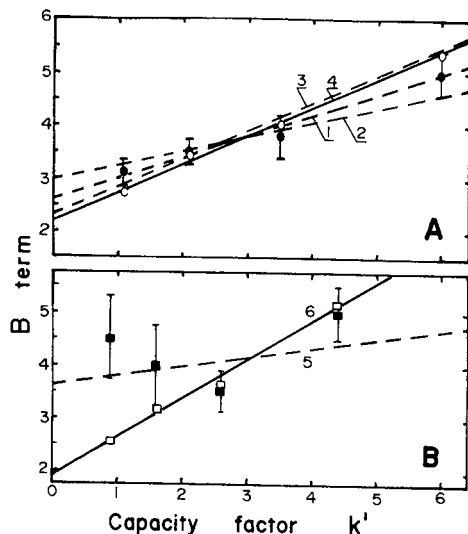


Fig. 2. Plots of B versus k' . Open symbols and solid lines: static determination (eqn. 22 and Table III). Closed symbols and dashed lines: dynamic determination (Knox plots, Table V). Column, 15 cm \times 4 mm I.D.; C_{14} stationary phase; mobile phase, methanol-water (70:30, v/v). (A) 25°C. 1, Dynamic determination, mean; 2, dynamic determination, minimum; 3, dynamic determination, maximum; 4, static determination, see Table VII. (B) 40°C. 5, Dynamic determination; 6, static determination.

efficiencies obtained using the moment method. These data were force-fitted to a γ_m value of 0.64. Although the scatter of these data were not completely inconsistent with $\gamma_m = 0.64$, Fig. 3 in ref. 24 appears unusual. We further used them to construct B versus k' plots, without any force-fitted value. The slopes and intercepts of such plots are listed in Table VII. This allowed us to calculate γ_m values higher than unity for porous Zorbax commercial stationary phases, considering plots with r^2 lower than 0.95 are significant. A γ_m value higher than 1 is theoretically impossible²; it would mean that solute diffusion in the mobile phase inside the glutted stationary phase is easier and

TABLE VII
PARAMETERS CORRESPONDING TO FIG. 2
Lines 4 and 6 correspond to static determinations.

Temperature ($^{\circ}$ C)	Line No.	Slope	Intercept	r^2	γ_m	$\gamma_s D_s / D_m$
25	1	0.380	2.64	0.990	1.32	0.190
	2	0.265	3.00	—	1.50	0.135
	3	0.510	2.34	—	1.17	0.255
	4	0.528	2.215	0.997	1.11	0.264
40	5	0.172	3.62	0.652	1.81	0.086
	6	0.721	1.92	0.991	0.96	0.361
22	— ^a	0.254	2.07	0.824	1.04	0.127
	— ^b	0.314	2.33	0.924	1.17	0.159

^a 3- and 6- μ m Zorbax C_8 phase.

^b 3- and 6- μ m Zorbax C_{18} phase, from Table I in ref. 24.

faster than diffusion in the bulk mobile phase. Given the porous structure of the packing material, this seems highly unlikely.

The model we used may be questioned. Crombeen *et al.*²⁶ showed that the additivity of diffusional fluxes, as used in eqns. 14, 21 and 22, only applied in cases where diffusion pathways in the two phases were parallel. In a random structure such as a porous particle packing material, a non-linear model must be set up²⁶. In contrast, to explain the high B values that they obtained, Stout *et al.*²⁴ suggested again the possible importance of surface diffusion.

We think that the main reason why γ_m factors higher than unity were not previously reported is the use of the efficiency computation method. In most previous studies^{3-10,22,23,26}, band broadening was calculated assuming Gaussian peaks. The raw efficiency data in Table IV show that the higher the flow-rate, the greater is the overestimation of the Gaussian plate number. The overestimation was between 3% at lower flow-rates (78 $\mu\text{l}/\text{min}$) and 90% at higher values (1.25 ml/min). Reduced plate heights calculated from overestimated plate numbers are obviously lower than those which we calculated using the exact second moment method. This led to different computer fits with the Knox equation, namely lower A , B and C values. The pertinence of the use of the moment method was shown in the static method measurements: the D_{eff} coefficients, obtained using the moment method (Table III and Fig. 2), were significantly less scattered than the same coefficients obtained by Knox and Scott¹⁰ using the Gaussian $0.6H$ method.

At 40°C, Fig. 2B shows that the B values were scattered ($r = 0.652$, Table VII). The results for benzene and toluene were poorly reproducible for unknown reasons (relative standard deviations 20, 20, 11 and 10% for benzene, toluene, ethylbenzene and propylbenzene, respectively). However, the results of the arrested elution method were less scattered and produced a significant straight line ($r = 0.991$, Table VII). This line gave an intercept allowing a γ_m factor of 0.96 to be calculated.

The $\gamma_s D_s/D_m$ values were between 0.13 and 0.27 at 25°C and 0.36 at 40°C. They can be compared with the slopes of the $(q/C)[(k' + \phi)/(1 + k')]^2$ versus k' plots (Table VI). Both sets of data seem consistent with $q = 2/15$. The slopes obtained with $q = 1/30$ in eqn. 9 are too low. For valid C values, the γ_{sm} values were lower than unity. The $\gamma_s D_s/D_m$ values obtained using the C values in ref. 24 would be consistent with those obtained using the corresponding B values with $q = 1/15$ in eqn. 9. However, the γ_{sm} value obtained for Zorbax C_8 seems very high. Given the low accuracy of C determinations and the poor regression coefficients in Table VI, the $\gamma_s D_s/D_m$ values were not considered further.

All results of this work were obtained on the same densely grafted phase. In order to confirm these results, experiments on densely grafted octadecyl- (C_{18}), undecyl- (C_{11}) and cynodecylsilica are in progress in our laboratory.

REFERENCES

- 1 A. J. P. Martin and R. L. M. Synge, *Biochem. J.*, 35 (1941) 1358.
- 2 J. C. Giddings, *Dynamics of Chromatography*, Marcel Dekker, New York, 1965.
- 3 J. H. Knox and M. Saleem, *J. Chromatogr. Sci.*, 10 (1972) 80.
- 4 G. J. Kennedy and J. H. Knox, *J. Chromatogr. Sci.*, 10 (1972) 549.
- 5 J. N. Done and J. H. Knox, *J. Chromatogr. Sci.*, 10 (1972) 606.
- 6 J. H. Knox, *J. Chromatogr. Sci.*, 17 (1977) 352.

- 7 E. Grushka, L. R. Snyder and J. H. Knox, *J. Chromatogr. Sci.*, 13 (1975) 25.
- 8 L. R. Snyder, *J. Chromatogr. Sci.*, 7 (1969) 352.
- 9 J. F. K. Huber, *J. Chromatogr. Sci.*, 7 (1969) 86.
- 10 J. H. Knox and H. P. Scott, *J. Chromatogr.*, 282 (1983) 297.
- 11 A. Einstein, *Ann. Phys. (Leipzig)*, 17 (1905) 549.
- 12 J. F. Erard, L. Nagy and E. sz. Kováts, *Colloids Surf.*, 9 (1984) 263.
- 13 E. sz. Kováts, *Ger. Pat.*, 2 930 516, 1979.
- 14 D. Morel and J. Serpinet, *J. Chromatogr.*, 248 (1982) 231.
- 15 D. Morel, J. Serpinet, J. M. Letoffe and P. Claudy, *Chromatographia*, 22 (1986) 103.
- 16 A. Chartier, C. Gonnet, D. Morel, J. L. Rocca and J. Serpinet, *J. Chromatogr.*, 438 (1988) 263.
- 17 F. Gobet and E. sz. Kováts, *Adsorpt. Sci. Technol.*, 9 (1984) 77.
- 18 B. A. Bidlingmeyer and F. V. Warren, *Anal. Chem.*, 56 (1984) 1583A.
- 19 J. L. Rocca, J. W. Higgins and R. G. Brownlee, *J. Chromatogr. Sci.*, 23 (1985) 106.
- 20 G. I. Taylor, *Proc. R. Soc. London, Ser. A*, 223 (1954) 446.
- 21 R. Aris, *Proc. R. Soc. London, Ser. A*, 223 (1954) 538.
- 22 J. H. Knox and L. McLaren, *Anal. Chem.*, 36 (1964) 1477.
- 23 J. H. Knox and A. Pryde, *J. Chromatogr.*, 112 (1975) 171.
- 24 R. W. Stout, J. J. DeStephano and L. R. Snyder, *J. Chromatogr.*, 282 (1983) 263.
- 25 Cs. Horváth and H.-J. Lin, *J. Chromatogr.*, 149 (1978) 43.
- 26 J. P. Crombeen, H. Poppe and J. C. Kraak, *Chromatographia*, 22 (1986) 319.

CHROM. 21 372

DISCUSSION OF A CONTROVERSIAL CHIRAL RECOGNITION MODEL

WILLIAM H. PIRKLE* and JOHN E. McCUNE

School of Chemical Sciences, Box 44, Roger Adams Laboratory, University of Illinois, 1209 W. California Street, Urbana, IL 68108-3731 (U.S.A.)

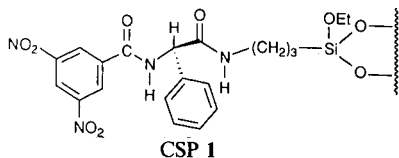
(First received November 17th, 1988; revised manuscript received February 1st, 1989)

SUMMARY

Wainer and Doyle and McDaniel and Snider have proposed a "head-to-head" chiral recognition model to rationalize the separation of the enantiomers of amide and anilide derivatives of chiral acids such as ibuprofen, naproxen and fenoprofen on a phenylglycine-derived chiral stationary phase. Pirkle and Reno and Nicoll-Griffith have proposed an alternative "head-to-tail" model. Evidence is presented which suggests that for a series of amide and anilide derivatives, both mechanisms are possible, additional structural features determining the contribution made by each to the observed time-averaged chiral recognition. For anilides, the head-to-head mechanism is less prevalent, its operation again requiring the presence of certain structural features in the analyte.

INTRODUCTION

Several groups have reported the chromatographic separation of the enantiomers of amide derivatives of α -arylpropionic and α -substituted arylacetic acids, compounds of pharmaceutical interest, on the chiral stationary phase (CSP) derived from (*R*)-*N*-(3,5-dinitrobenzoyl)phenylglycine. Conflicting proposals have been tendered as to the nature of the dominant chiral recognition mechanism(s) employed by this CSP toward these analytes. We now present new results which bear upon the nature of the chiral recognition processes.



Initially, Wainer and Doyle¹ described the separation of amide derivatives of ibuprofen, naproxen, fenoprofen and benoxaprofen on CSP 1. They rationalized their observations by means of a "face-to-face" approach of analyte to CSP promoted by "dipole stacking" of amide dipoles. Fig. 1 shows the arrangement of the components

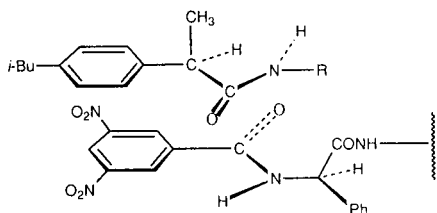


Fig. 1. The Wainer-Doyle model for the more stable diastereomeric adsorbate between ibuprofen derivatives and CSP 1 (representation of the chiral recognition mechanism published by the authors¹).

of the more stable diastereomeric adsorbate as proposed by Wainer and Doyle. Additionally, a π - π interaction between the dinitrobenzoyl group of the CSP and the aryl substituent of the acid-derived portion of the analyte was proposed, as were steric interactions between the CSP and the analyte enantiomers. This model, adapted from one proposed for a different type of amide analyte², we term a "head-to-head" arrangement. It was earlier noted that dipole stacking can occur in either a head-to-head arrangement, where the carboxylic acid components are oriented in the same direction, or a "head-to-tail" mode³. It has also been noted that when two competing chiral recognition processes are possible, additional structural features present in the analyte can be expected to determine the relative contribution made by each process to the overall time-averaged behavior ultimately observed⁴. In the Wainer-Doyle proposal (Fig. 1), the proposed π - π interaction makes the head-to-head approach plausible for amides prepared from amines lacking π -basic substituents. However, some of the amides utilized by these authors were prepared from amines containing π -basic aryl groups. Might this not alter the preferred mode of dipole stacking? This point was considered and dismissed by Wainer and Doyle, who suggested that, "If π - π interactions were the primary driving force in the formation of the CSP-solute complex, a reversal in elution order of the ibuprofen enantiomers would be expected with the addition of the 1-naphthalenemethyl group. This reversal would reflect the preferred π - π bonding between the naphthyl ring and the 3,5-dinitrobenzoyl ring". However, the reader will note that for the conformation having a 180° dihedral angle between the methine hydrogen and the carbonyl oxygen, 180° rotation of the analyte about the axis parallel to the C-O bond of the carbonyl group and a slight lateral displacement affords a "head-to-tail" arrangement which, in the case of derivatives prepared from amines containing π -basic aryl groups, would allow π - π interaction *without an inversion of elution order*. After such a rotation, the sterically large groups (*i.e.*, the phenyls) are still "external" to the stack. Hence, the observations that the separation factor for the enantiomers of ibuprofen 1-naphthalenemethylamide is not reduced (indeed, it is greater) relative to the methylamide and elution order is unchanged *cannot* be taken as evidence of an absence of head-to-tail stacking brought about by π - π bonding between the naphthyl and 3,5-dinitrobenzoyl moieties.

A reviewer raised the issue discussed by Wainer and Alembik⁵ concerning the "directionality" of amide dipoles. An instance was reported using (*R*)-CSP 1 in which "there is an inversion in the enantiomeric elution order for the amide derived from amines compared to those derived from carboxylic acids" ... "The major difference between these two compounds is the position of the chiral center relative to the amide moiety". The examples cited were N-benzoyl- α -methylbenzyl amine, $\alpha = 1.17$,

R elutes before *S*, and the anilide of α -phenylpropionic acid, $\alpha = 1.10$, *S* elutes before *R*. We disagree with the notion that “directionality” of the amide dipole determines the elution order of the analytes in question, believing rather that it is simply a matter of which group is preferentially used as the π -base (benzoyl < phenyl < anilide) during dipole stacking that determines the predominant sense of dipole stacking (*i.e.*, head-to-head or head-to-tail) and, in these instances, elution order.

McDaniel and Snider⁶ subsequently reported the separation of enantiomers of amide derivatives of ibuprofen, flurbiprofen and α -methoxyphenylacetic acid on the same CSP. They noted that amides derived from α -naphthylamine show greater enantioselectivity on CSP **1** than do the amides derived from any of the other amines used in the study and they proposed the chiral recognition model shown in Fig. 2, a model essentially that of Wainer and Doyle¹. They did not consider the likelihood that the enhanced enantioselectivity noted in this instance arises from a dominant π - π interaction between the 3,5-dinitrobenzoyl group of the CSP and the α -naphthylamido portion of the analyte, possibly because of the prior assertion that such π - π interaction (and the resultant head-to-tail arrangement) would lead to an elution order different than that actually observed¹.

Not all workers have agreed that head-to-tail arrangements would lead to “inverted” elution orders. Such head-to-tail stacking between N-(3,5-dinitrobenzoyl)-leucine derivatives and N-acylated- α -amino acid amides derived from aniline, *p*-tolidine, α -naphthylamine and β -naphthylamine has been invoked to explain enantioselectivity noted in both chromatography and asymmetric synthesis^{7,8}. Moreover, Nicoll-Griffith⁹ has also examined the chromatographic behavior of various ibuprofen anilides and amides on CSP **1**. Based on the observation that electron-withdrawing *para* substituents on the anilide moiety diminish selectivity whereas electron-donating substituents enhance selectivity, Nicoll-Griffith proposed the head-to-tail dipole stacking model shown in Fig. 3 and suggested that this model should also be valid for other α -methylarylacetic acid anilides, specifically citing naproxen, benoxaprofen and fenoprofen. Nicoll-Griffith inferred that “alternate substituents on the drug aromatic ring should not affect the chiral recognition mechanism, aromatic amide derivatives of these drugs should exhibit enhanced enantiomer separations and the same elution order”. Finally, the ibuprofen amides were proposed to resolve by the same head-to-tail dipole stacking model, with the π - π interaction between the anilide moiety and the 3,5-dinitrobenzoyl group of the CSP being replaced by a σ - π interaction.

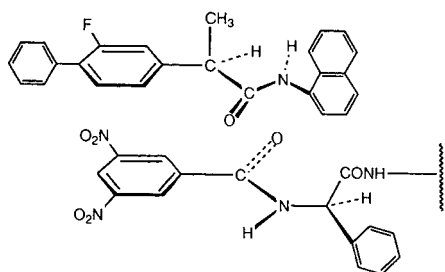


Fig. 2. The McDaniel-Snider model for the more stable diastereomeric adsorbate between ibuprofen derivatives and CSP **1** (representation of the chiral recognition mechanism published by the authors⁶).

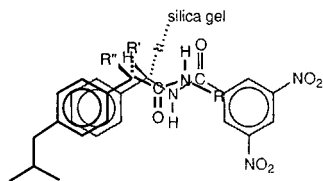


Fig. 3. The Nicoll-Griffith model for the more stable diastereomeric adsorbate between ibuprofen derivatives and CSP 1 (representation of the chiral recognition mechanism published by the author⁹).

EXPERIMENTAL

Apparatus

Chromatography was performed using a Bischoff isocratic pump, a Rheodyne injector, a Regis covalent Pirkle 1A column, two Milton Roy-LDC UV Monitor D[®] detectors (254 and 280 nm) in series and a Kipp-Zonen BD-41 dual-pen recorder.

Reagents

Racemic ibuprofen was isolated from a Motrin[®] tablet. Ibuprofen was partially resolved according to the procedure of Nicoll-Griffith⁹. Fenoprofen was a gift from Eli Lilly. Racemic and (*S*)-(+)-2-phenylbutyric acid, 2-ethoxy-1-ethoxycarbonyl-1,2-dihydroquinoline (EEDQ) and the various anilines and amines were obtained from Aldrich. The remaining acids were available from prior studies.

Derivatization

The anilides were made either via the acid chloride or through the agency of EEDQ. Acids **1** and **5** were converted to the acid chlorides using thionyl chloride. The remaining acids were converted to the mixed anhydrides with EEDQ. The former derivatization sequence has been described⁶. The amides of acids **1** and **2** were prepared from the corresponding acid chlorides by addition of the appropriate amine and using an extractive work-up as described below for the anilides.

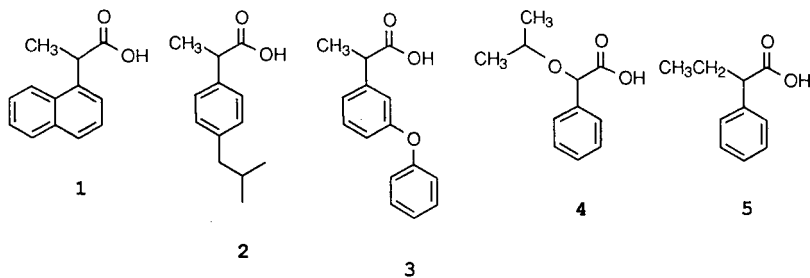
Anilide synthesis using EEDQ

Equal amounts (*ca.* 10 mg) of the acid and EEDQ were placed in a 5-ml screw-capped test-tube followed by two drops of the aniline and 0.5 ml of dichloromethane. After 30 min, 1.5 ml of dichloromethane and 1 ml of 1 *M* sodium hydroxide were added, the mixture shaken vigorously and the upper layer was removed with a pipet. The lower layer was similarly washed several times with water, then 1 ml of 1 *M* hydrochloric acid was added. The mixture was shaken vigorously, centrifuged if necessary to separate layers (the higher molecular weight *p*-alkylanilines form emulsions when acidified; excesses of these reagents were avoided) and the upper layer withdrawn. The lower layer was repeatedly washed with water. The resulting solutions were dried over anhydrous magnesium sulfate and analyzed directly. Early eluting impurities were noted in some instances, but did not interfere with the analyses¹⁰.

RESULTS AND DISCUSSION

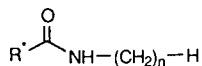
We recently described a variation of CSP **1** which usually affords enhanced enantioselectivity¹⁰. To evaluate this new CSP, we prepared and chromatographed a number of anilides of chiral acids¹¹. Some of these were prepared to distinguish head-to-head from head-to-tail alignments, alignments which cannot be distinguished by elution order as they are "same sense" mechanisms. These same analytes should also distinguish between the two stacking modes on CSP **1**. The basis for this distinction is simple. Note from Figs. 1 and 2 that were the head-to-head mechanism operative, amides made from *n*-alkylamines or from anilines having *para*-alkyl substituents would direct these alkyl groups toward the underlying silica support, the alkyl group being intercalated between adjacent strands of bonded phase. There is considerable precedent that, when such intercalation occurs, increasing the length of the alkyl substituent decreases, through steric interaction of the alkyl substituent with the flanking strands of the CSP and the underlying silica support, the stability of the diastereomeric adsorbate containing the enantiomer intercalating this group. This results in a reduced retention of this enantiomer relative to its antipode. Hence a change in the magnitude of α results. The shape of the resultant α vs. *n* plot (*n* is the number of carbons in the linear alkyl group) thus conveys considerable mechanistic information^{4,12}. We hasten to add that the mobile phase in these instances is normal, not reversed.

The chiral acids 2-(α -naphthyl)propionic acid (**1**) (a model for naproxen), ibuprofen (**2**), fenoprofen (**3**), 2-isopropoxyacetic acid (**4**) and 2-phenylbutyric acid (**5**) were used to prepare homologous series of amide derivatives using *n*-alkylamines and *p*-alkylanilines. These derivatives were chromatographed on CSP **1** and the effect of the length of the alkyl group on α , the separation factor for enantiomers, was noted.

*Amide derivatives*

Data pertinent to the separation of a series of *n*-alkylamine-derived amides of **1** and **2** appear in Table I. Note that, for the ibuprofen derivatives, α decreases as *n*, the number of carbons in the linear alkyl group, increases and no separations were observed with *n* > 6. This is in accord with the expectations generated by the Wainer-Doyle model. For the corresponding amides of **1**, the magnitude of α again decreases as *n* increases but enantiomer separation persists even when *n* = 18. Presumably, the greater π -basicity of the α -naphthyl substituent leads to a strong π - π interaction, one more difficult to disrupt in less favorable steric circumstances (*i.e.*,

TABLE I

CHROMATOGRAPHIC BEHAVIOR ON (*R*)-CSP 1 OF CHIRAL ACIDS 1 AND 2 AS THEIR *n*-ALKYLAMIDES

Acid (<i>n</i>)	1		2	
	α^a	$k'_1{}^b$	α^a	$k'_1{}^c$
18	1.12	2.80	1.00	1.73
14	1.16	3.14	1.00	1.87
10	1.19	3.42	1.00	2.13
8	1.20	3.57	1.00	2.37
6	1.21	4.05	1.06	2.40
4	1.28	4.85	1.08	2.83
3	1.33	5.44	1.11	3.07
2	1.31	6.60	1.13	4.37
1	1.27	8.57	1.14	6.33
0	1.14	7.96	1.00	7.13

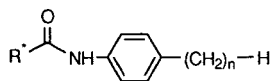
^a Chromatographic separation factor.^b Capacity factor for the first eluted enantiomer using 2-propanol-hexane (10:90, v/v) as the mobile phase; flow-rate, 2 ml/min.^c Capacity factor for the first eluted enantiomer using 2-propanol-hexane (5:95, v/v) as the mobile phase; flow-rate, 2 ml/min.

when a long alkyl group is involved). Note the significantly greater capacity ratios for derivatives of **1** relative to those of **2**. It also seems likely that the greater size of the naphthyl group permits a "shift" in the relative positions of the two π - π components which allows relaxation of some of the steric effects generated by the longer alkyl groups. The *R* enantiomers are preferentially retained on (*R*)-CSP 1, as expected from all the mechanisms advanced and from the elution orders reported for amides of ibuprofen and naproxen¹.

Anilide derivatives

Homologous series of *p*-(*n*-alkyl)anilides were prepared from acids **1-5** and examined chromatographically on CSP 1. The results are given in Table II. If the enantiomers of these anilides separate owing to a head-to-tail stacking model as shown in Fig. 3, the *p*-alkyl groups would be directed away from the silica and their length would be expected to have little effect on enantioselectivity. However, the absolute retention would be expected to decrease as *n* increases owing to increasing analyte solubility in the mobile phase. For the homologous series of anilides derived from ibuprofen, fenoprofen and 2-phenylbutyric acid, the length of the *p*-alkyl substituent affects the retention but, to a good approximation, not enantioselectivity. We consider this to be compelling evidence that the chromatographic behavior of these analytes is not significantly influenced by processes similar to the Wainer-Doyle and McDaniel-Snyder mechanisms. The observed lack of dependence of the selectivity on the length of the alkyl substituent is consistent with the mechanistic proposals offered by

TABLE II

CHROMATOGRAPHIC BEHAVIOUR ON (*R*)-CSP 1 OF CHIRAL ACIDS 1-5 AS THEIR *p*-ALKYLANILIDES

Acid (<i>n</i>)	1		2		3		4		5	
	α^a	$k'_1{}^b$	α^a	$k'_1{}^b$	α^a	$k'_1{}^b$	α^a	$k'_1{}^b$	α^a	$k'_1{}^b$
14	1.22	4.96	1.23	1.45	1.20	3.10	1.28	1.45	1.09	1.80
12	1.22	5.10	1.22	1.50	1.16	3.20	1.29	1.47	1.10	1.84
10	1.22	5.50	1.22	1.54	1.19	3.30	1.30	1.60	1.10	2.00
8	1.23	5.80	1.21	1.63	1.20	3.46	1.29	1.63	1.10	2.06
6	1.23	6.30	1.21	1.81	1.21	3.75	1.32	1.81	1.08	2.27
4	1.25	6.91	1.20	2.10	1.22	4.15	1.37	1.93	1.11	2.50
2	1.30	8.50	1.22	2.60	1.20	5.40	1.39	2.41	1.10	3.20
1	1.34	10.40	1.23	3.20	1.21	6.46	1.42	2.96	1.12	3.97
0	1.36	10.40	1.21	3.20	1.20	6.44	1.34	2.80	1.11	4.00

^a Chromatographic separation factor.^b Capacity factor for the first eluted enantiomer using 2-propanol-hexane (5:95, v/v) as the mobile phase; flow-rate, 2 ml/min.

Nicoll-Griffith⁹ and ourselves. The greater enantioselectivity noted for ibuprofen and fenoprofen anilides relative to those of 2-phenylbutyric acid can be explained by either stacking mode, as it is implicit in the models that differences in size between the alkyl and aryl groups on the stereogenic center are ultimately responsible for the observed enantioselectivity. Fig. 4 expresses this idea in a slightly different format than was used by Nicoll-Griffith, but the models are essentially the same.

The enantiomers of the anilides derived from **4** are separable on CSP **1**. Interestingly, the selectivity decreases as the length of the *p*-alkyl substituent increases, but never disappears. This suggests that chiral recognition is occurring by both head-to-head and head-to-tail arrangements. As the alkyl group becomes longer, the contribution of the head-to-head process lessens and the remaining enantioselectivity presumably stems from the head-to-tail process. Dipole stacking seems probable for the anilides of **1** and seemingly occurs by both head-to-head and head-to-tail arrangements. In this instance, the head-to-head contribution is rationalized by the greater π -basicity of the α -naphthyl substituent relative to the aryl substituents present in acids **2**, **3** and **5**. The two stacking modes lead to the same sense of enantioselectivity,

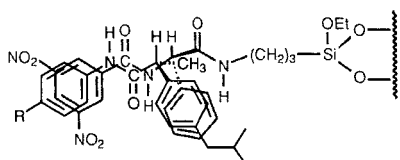


Fig. 4. Head-to-tail dipole stacking chiral recognition model.

the head-to-head contribution diminishing as the length of the *p*-alkyl substituent increases. With higher values of *n*, the remaining chiral recognition is considered to come principally from the head-to-tail contribution.

The elution orders for the enantiomers of the amides derived from acids **1** and **2** and of the anilides derived from acids **1–3** and **5** are known and conform to the chiral recognition mechanisms discussed. The elution order of the enantiomeric anilides derived from acid **4** is not yet established.

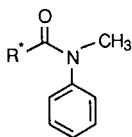
Dipole stacking

Similar to an approach used by Wainer and Doyle¹, tertiary amide derivatives of acids **1–5** were prepared to determine the effects of hydrogen bonding interactions between the anilide proton of the analyte and the CSP on α . If the anilide N–H participated in some essential hydrogen bonding interaction, its replacement by an alkyl substituent would seriously erode chiral recognition.

Chromatographic data for the separation of the N-methylanilide derivatives of acids **1–5** on CSP **1** are given in Table III. The chromatographic separation factors for the tertiary amide derivatives of acids **1–3** and **5** are comparable to those noted for the corresponding secondary amides in Table II. However, the capacity ratios are significantly reduced. These results indicate that hydrogen bonding of the anilide N–H proton is not essential to chiral recognition but, if present, may lead to achiral retention. These conclusions differ only slightly from those of Wainer and Doyle¹ who, noting chromatographic separation factors and capacity ratios of 1.11 and 15.5 for the enantiomers of ibuprofen benzylamide and 1.07 and 6.4 for those of the N-methylbenzylamide, suggest that hydrogen bonding increases the stability of the benzyl amide–CSP complex relative to that of the N-methylbenzylamide complex. The reduction in k'_1 which accompanies N-methylation clearly indicates a reduction in the energy of adsorption. However, multiple “complexes” are involved during chromatography and the added retention may not stem from the complex(es) which afford chiral recognition. Therefore, we do not consider the small changes in

TABLE III

CHROMATOGRAPHIC BEHAVIOUR ON (*R*)-CSP **1** OF CHIRAL ACIDS **1–5** AS THEIR N-METHYLANILIDES



Parameter	Acid				
	1	2	3	4	5
α^a	1.21	1.20	1.17	1.00	1.18
$k'_1{}^b$	3.47	1.67	3.57	4.27	1.36

^a Chromatographic separation factor.

^b Capacity factor for the first eluted enantiomer using 2-propanol–hexane (10:90, v/v) as the mobile phase; flow-rate, 2 ml/min.

separation factors to be compelling evidence for any hydrogen bonding *during the chiral recognition process*; the modest difference in separation factors may simply result from differences in conformational preferences which accompany N-methylation. Primary amides show substantial preference for population of the *Z* rotamer (about the carbonyl carbon–nitrogen bond) which will be markedly reduced upon N-methylation. Changes in conformational preferences might well influence both selectivity and retention, especially when the amide's nitrogen substituents intercalate between the strands of bonded phase.

Interestingly, the enantiomers of the tertiary amide of acid **4** do not separate on CSP **1** and the capacity ratio is much larger than that noted for the corresponding secondary amide. Apparently, hydrogen bonding of the anilide N–H proton is essential to the chiral recognition process for this analyte and we make no claim that dipole stacking is involved.

CONCLUSION

When chromatographing amide analytes on amide stationary phases, one should be aware that a variety of transient bonding interactions are possible. Hence, ascribing a retention mechanism or a chiral recognition mechanism is not as straightforward as might initially be thought. We have presented data demonstrating the occurrence of a head-to-tail chiral recognition mechanism for anilide derivatives when chromatographed on CSP **1**. Additionally, a head-to-head mechanism can contribute to chiral recognition for those analytes in which the acid component contains a substituent, suitably located and of adequate π -basicity, to compete with the aryl portion of the anilide for π - π interaction with the 3,5-dinitrobenzoyl group. Hence, alternate substituents on the drug aromatic ring *do* affect the partitioning between competing chiral recognition mechanisms but not, in these cases at least, the elution order. We have also presented evidence that is consistent with the operation of a head-to-head Wainer–Doyle type of mechanism in the separation of ibuprofen amides derived from *n*-alkylamines.

We emphasize that enantiodifferentiation is a time-weighted average of multiple processes and cannot be stringently ascribed to a single mechanism in all instances.

ACKNOWLEDGEMENTS

This work was partially supported by grants from the National Science Foundation and the Eli Lilly Company.

REFERENCES

- 1 I. W. Wainer and T. D. Doyle, *J. Chromatogr.*, 284 (1984) 117–124.
- 2 W. H. Pirkle, C. J. Welch and M. H. Hyun, *J. Org. Chem.*, 48 (1983) 5022–5026.
- 3 W. H. Pirkle, *Tetrahedron Lett.*, 24 (1983) 5707–5708.
- 4 W. H. Pirkle, M. H. Hyun and B. Bank, *J. Chromatogr.*, 316 (1984) 585–604.
- 5 I. W. Wainer and M. C. Alembik, *J. Chromatogr.*, 467 (1986) 59–68.
- 6 D. M. McDaniel and B. G. Snider, *J. Chromatogr.*, 404 (1987) 123–132.
- 7 W. H. Pirkle and D. S. Reno, *Tenth International Symposium on Column Liquid Chromatography, San Francisco, CA, May 18–23, 1986*, Paper No. 401.

- 8 D. S. Reno, *Ph.D. Dissertation*, University of Illinois, Champaign-Urbana, IL, 1987.
- 9 D. A. Nicoll-Griffith, *J. Chromatogr.*, 402 (1987) 179-187.
- 10 W. H. Pirkle and J. E. McCune, *J. Chromatogr.*, 441 (1988) 311-322.
- 11 W. H. Pirkle and J. E. McCune, *J. Chromatogr.*, 471 (1989) 271-281.
- 12 W. H. Pirkle and R. Däppen, *J. Chromatogr.*, 404 (1987) 107-115.

CHROM. 21 369

RESOLUTION OF A COELUTING CHROMATOGRAPHIC PAIR USING KALMAN FILTERING

TODD BARKER and STEVEN D. BROWN*

Department of Chemistry, University of Delaware, Newark, DE 19716 (U.S.A.)

(First received October 18th, 1988; revised manuscript received January 31st, 1989)

SUMMARY

A new approach is reported for enhancing resolution in chromatographic separations monitored by diode array spectroscopy. This approach uses a digital filter, known as the Kalman filter, to resolve coeluting chromatographic components by fitting the time-dependent spectral responses observed at the detector to the spectra of pure component models. The estimates of concentration as a function of time permit the creation of elution profiles for each chromatographic component included in the model.

The method is tested on synthetic three-dimensional chromatograms generated from Gaussian elution profiles, and it is demonstrated that, with adequate spectral models, the overlapped chromatographic components can be resolved. Arbitrarily poor chromatographic resolution, jitter in peak location, and high detector noise do not interfere. The method was applied to the separation of overlapped chromatographic peaks from dopamine and tyrosine, and it was demonstrated that accurate quantitation was possible, even when chromatographic resolution was less than ideal. The method fails when spectral responses occur that are not included in the filter model.

INTRODUCTION

Much of column chromatographic analysis is concerned with the resolution of overlapping peaks in the chromatogram. Quantitation of the components of the sample requires measurement of peak parameters that are not easily determined from most of the measurements made on poorly resolved chromatographic peaks.

Many techniques have been investigated for the enhancement of peak resolution. The straightforward approaches, such as dropping of perpendiculars to arbitrarily resolve peaks from location of peak valleys and tangential skimming of shoulder peaks^{1,2} have received much use because of their simplicity and their ability to produce resolved peaks as the chromatographic data are obtained. Depending on the degree of overlap, however, the use of these simple, fast methods has not always been successful³. More complex methods involving peak fitting of chromatograms to theoretical peak shapes (Gaussian-based functions and others) or empirical peak shapes^{4,5} have also been tried. Usually, these methods must be applied after the

chromatogram is obtained because of the fairly extensive calculations required, leading to delays between the collecting of data and the calculation of chromatographic parameters from the resolved peaks. Because small changes in peak shape and position can occur with changes in the sample matrix or in the composition of the analyte set, these methods are also affected by the nature of the separation used, as well as the nature of the sample separated. Other empirical methods have been suggested for use with the large amount of data available from diode-array detection. Methods include the calculation of absorbance ratios on the upslope and the downslope of peaks (to determine peak purity), derivative methods, and related approaches⁶⁻⁸. The simpler of these methods fail when similar spectra are obtained for coeluting species, while the more complex require constant operator interaction, a feature that is not practical for routine separations⁹.

Recently, however, two new approaches have been proposed. These address opposite ends of the problem of getting fast improvement of the resolution of overlapped chromatographic peaks by use of mathematical methods with minimal assumptions. In one approach, mathematical methods based on factor analysis are used to resolve partially overlapped peaks, by using information from diode array spectra collected across the chromatogram. Mathematical analysis of this three-dimensional data set requires few assumptions, but it requires considerable time. This method has been shown to be successful for obtaining spectra of overlapped mixtures, but somewhat less successful at quantitation of the mixtures unless some restrictions are met^{9,10}. The other approach uses a one-dimensional Kalman filter, run in real-time, to resolve partially overlapped chromatographic peaks using a one-dimensional empirical model based on prior measurements of peak shape and location¹¹⁻¹⁴. In essence, this Kalman filtering approach uses a peak-fitting method similar to others discussed above, but in this method, the calculations are performed in real-time, as are the less sophisticated tangential skimming and perpendicular drop methods often used. The assumptions made—the constancy of chromatographic peak shape and position over a range of separation conditions and the existence of moderate chromatographic resolution—are more substantial, but the calculations require little time. This approach works well when peak parameters remain fixed over a set of separations, but it fails when significant overlap occurs between peaks when overlapped components have similar spectra, when injection jitter occurs between runs of standards used for models and runs of mixtures, or when chromatographic peak-shape parameters vary slightly between runs¹⁴.

This paper introduces a novel Kalman filter for the resolution of column chromatographic peaks of arbitrary shape and position. The method is based on repetitive filtering of diode array spectra obtained across a chromatogram. Each filtering pass results in a set of state estimates for all modelled components, along with their associated error estimates. The concentration estimates obtained from filtering of diode array spectra are produced in real-time, as each spectrum is obtained, over the entire chromatogram; these estimates describe the elution behavior of all components included in the filter model. In the method, knowledge is assumed of the spectral properties of the components of the sample and the linearity of absorbance-concentration relations for the analyte species. Changes in chromatographic peak shape and position do not interfere, since the method is based on a spectral rather than a chromatographic model. Very highly overlapped (resolution <0.5) chromato-

graphic peaks may be resolved, identified, and quantitated in real-time. The pair of compounds selected for study, dopamine and tyrosine, elute near each other under many chromatographic conditions, and the components have similar ultraviolet spectra. The effects of chromatographic peak overlap, noise, and detector drift are evaluated on synthetic chromatograms generated from the spectra of these species, and the filtering method is used to enhance the chromatographic resolution of their mixtures.

THEORY

The Kalman filter and the systems approach used here have been previously reviewed^{15,16}. For clarity, a brief summary of Kalman filtering is provided below. The notation used here follows that used in most of the literature on Kalman filtering in chemistry.

The Kalman filter is used to estimate quantities in an n -dimensional vector, X , the state, based on a model relating the state to some measurement Z . That model, called the measurement model, is defined by the equation.

$$Z(k) = H^T(k)X(k) + v(k) \quad (1)$$

where $Z(k)$ is the measurement at point k , $H(k)$ is the measurement function vector at point k , $X(k)$ is the state vector at point k , and $v(k)$ represents noise in the measurement. It is possible to relate the state to an m -dimensional vector measurement using eqn. 1; in this case, $H^T(k)$ is an $m \times n$ matrix, and $v(k)$ is an m -dimensional vector. It may be that the state is not a constant vector; the state may change deterministically, randomly, or both, as described by the system dynamic equation

$$X(k) = F(k,k-1)X(k-1) + w(k-1) \quad (2)$$

where the matrix F describes deterministic changes in the state quantities, and where the vector w describes random changes in the state quantities, between point $k-1$ and point k .

The Kalman filter is simply a set of equations used to estimate the state at any point k , based on information obtained over the previous $k-1$ points. The work reported here used the Kalman and the Joseph algorithms for implementation of the Kalman filter. The Kalman algorithm is especially convenient for real-time use because it is computationally efficient. It is sensitive to round-off errors, however. The details of this algorithm have been extensively discussed¹⁵⁻¹⁷. Use of the Joseph algorithm reduces the effect of round-off error considerably, but at some cost in computation speed. The Joseph algorithm has also been discussed previously^{15,17}. In both the Kalman and the Joseph implementations of the Kalman filter, the calculation of the state vector is done recursively. Thus, the data storage is kept small, and changes to any part of the filter model (for example, to matrices F and vectors H and w) are possible as data processing proceeds. Recursive estimates of the error in the estimated states are also provided through propagation of the covariance matrix $P(k)$, another calculation that is part of all algorithms for the Kalman filter. An initial guess of the state X and covariance P is required to begin the Kalman filter, but the initial guess of

the state need not be accurate; if prior information is available on the state, that information can be included in the initial guess, and improved convergence will result.

It is possible to neglect part of the calculations involved in the propagation of state and covariance, provided the states are known to be unrelated. These reduced Kalman filters have previously been used with empirical chromatographic peak-shape models¹¹⁻¹⁴, but because spectra are usually somewhat correlated, their use is inappropriate here.

The data collected by using diode array spectroscopy to monitor the separation achieved in column chromatography can be described by a three-dimensional surface consisting of the spectral measurements made as a function of elution time. Each of the t diode-array spectra is an m -dimensional vector measurement. A typical example is shown in Fig. 1. Two approaches to processing this three-dimensional data are possible. In both, Kalman filtering is done first in wavelength, then in time. Both have as a goal the estimation of the n -dimensional state, which consists of the instantaneous concentrations of all species included in the filter model. The first has previously been called "three-dimensional" filtering¹⁸. With this approach, each vector measurement (a diode array spectrum) is processed by a vector Kalman filter, and an $m \times m$ matrix must be inverted for each spectrum. Estimates from filtering each spectral vector are used as initial guesses in filtering the next spectrum. In this way, the m -dimensional data obtained from the diode array spectrometer is compressed by the data analysis into an n -dimensional vector of concentration estimates. Since $m > n$ for this method, as well as other, regression-based methods, a considerable savings in storage results.

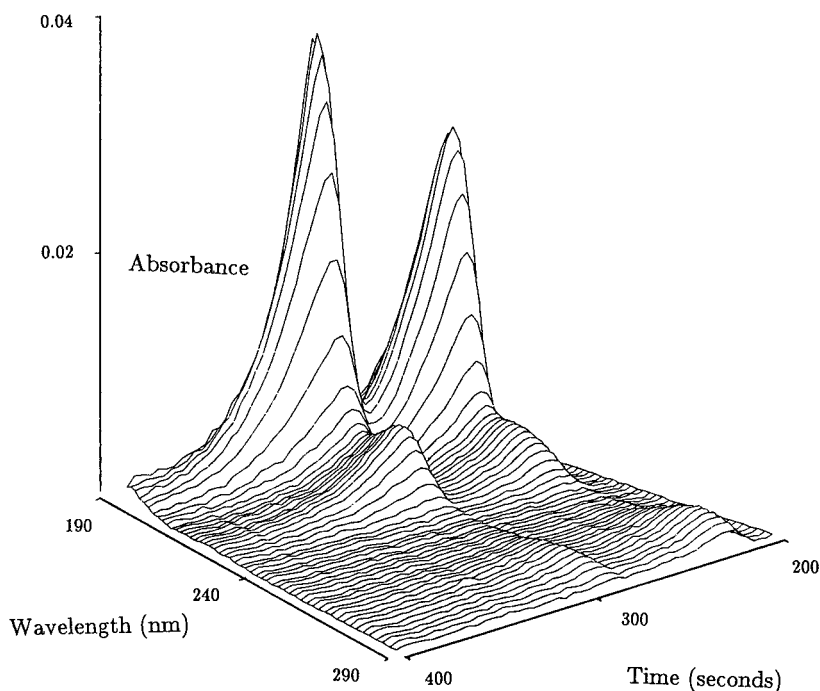


Fig. 1. Three-dimensional chromatogram of dopamine-tyrosine mixture.

The diode array spectrum can also be treated as a sequence of m independent scalar measurements, one from each diode, and these scalar measurements can be processed by a scalar Kalman filter. This is the second approach. As in the first approach, the n estimated states obtained from filtering one spectrum are used as initial guesses for filtering the next spectrum, but in this case these estimates are also changed from point to point as filtering proceeds through a single spectrum. With this approach, instead of a matrix inversion, $m \cdot n$ scalar divisions are required to process the m scalar measurements contained in the spectral vector. State estimates are available at every point of the three-dimensional data set, if needed, although in this study estimates were output only once per m -dimensional spectrum. As above, data compression results. Several advantages arise from the second approach, including the elimination of matrix inversions, the possibility of selecting data to be filtered from a spectral vector, and others. The elimination of the matrix inversion step increases precision in the calculations by reducing the effects of round-off error, and it may also lead to appreciable time savings as the number of states (here, components in the chromatogram) becomes large. Selective filtering of spectral data permits the elimination of poorly modelled data from the filter model.

Both of the methods outlined above require the coupling of the Kalman filter with a supervisory routine. This routine can be considered another Kalman filter, where the task of the "supervisory" filter is to make state estimates from filtering one spectrum available to the next pass of the "spectral" Kalman filter as the initial guess of the filter state. In the supervisory filter, the filter covariance matrix is also propagated as usual. For this work, however, the initial guess of the covariance matrix for the "spectral" filtering was set to the identity matrix prior to filtering each spectrum. The supervisory filter outputs the state estimates for each filter pass through a spectrum, giving a set of concentration estimates over time. In this way, the three-dimensional data set of time-based spectral measurements is effectively compressed to the usual format of chromatographic data, the elution profile. The elution profile described in this study differs from a typical chromatogram, consisting of a measurement of a zeroth-order sensor (*e.g.* absorbance) plotted with respect to time, however. Here, the profile is a *concentration* estimate for a single species, plotted with respect to time. Another difference lies in the number of elution profiles: in this work, there are as many profiles as species included in the filter model.

EXPERIMENTAL

Reagents

Reagent grade chemicals and deionized water were used to prepare all the solutions. A 0.05 M phosphate buffer prepared from potassium dihydrogenphosphate was adjusted to pH 4.0. With this solution, stock solutions of tyrosine were prepared by dissolving the solid in an 87:13 (v:v) mixture of the phosphate buffer and methanol. Stock solutions of dopamine were prepared in a similar fashion. Only freshly prepared solutions of dopamine were used, because dopamine is known to oxidize upon standing. The mobile phase, phosphate buffer (pH 4.0)–methanol (87:13, v:v), was selected to provide retention, but with minimal separation of the tyrosine and dopamine, all within moderate retention times, so that the full three-dimensional data set could be stored if desired. All chromatograms were obtained at mobile phase

flow-rates of 1.0 ml/min, with a measurement interval of 2.5 s. The flow conditions and mobile and stationary phases used here had previously been reported to provide only slight separation of dopamine and tyrosine in separations of amino acid mixtures⁷. Samples from the stock solutions were used to measure the ultraviolet-visible spectra used as models (H^T) in the Kalman filtering, and as the component spectra in the generation of synthetic chromatograms. Freshly prepared mixtures of tyrosine and dopamine prepared in methanol were used as the unknown samples in this study.

Instrumentation and software

An isocratic pumping system (LKB Model 2150) was used for all chromatographic runs. The chromatographic system employed a C_{18} column (250 × 4.6 mm I.D. Hypersil ODS, 5 μ m particle size), along with a sample injection valve (Model 50, Rheodyne), a 20- μ l injection loop, and a 24- μ l quartz flow-through cell (Type 75, Starna). The filled-loop injection technique was used for all chromatograms. Spectrophotometric detection was accomplished with a diode array spectrophotometer (HP8452, Hewlett-Packard), set for a wavelength range of 190–290 nm, with 2 nm resolution. The absorbance and variance in absorbance measured at each diode were passed to the filtering routine. The spectrometer was controlled via an IEEE-488 bus with a 10 MHz 80286-based microcomputer (SCSI) equipped with a 10 MHz 80287 math coprocessor, 72 MByte Winchester disk and EGA display. The computer ran under the MS-DOS operating system. The control microcomputer was used for data collection, transfer, and real-time filtering of data, and quantitation. A typical pass of the filter, including the time required for data transfer and format conversion, required *ca.* 2.5 s for a 50-point spectrum using a three-state, scalar Kalman filter with full calculation of covariances and filter innovations¹⁵. The time required for data transfer, conversion, filtering and display determined the temporal resolution obtained on the chromatogram. The elution profiles for all species chromatographed were displayed on the microcomputer monitor over the course of each chromatographic run, allowing the analyst to evaluate the performance of the chromatographic run. At the end of a run the analyst had the opportunity to store the three-dimensional data set on disk, for later off-line processing, or to proceed in using the results of filtering for immediate quantitation. Quantitation of each species was accomplished by calculating the area of the species' elution profiles with a multiple linear regression interpolation applied to the filter estimates.

Some off-line processing of stored data from earlier runs was performed on the control microcomputer. Additional off-line processing of data was performed on either a Celerity 1200 or a Pyramid superminicomputer under the Unix operating system. The control microcomputer was provided with serial interfaces to both systems. Data transfer was performed with the Kermit file transfer protocol.

Real-time control of the diode array detector and the IEEE-488 interface bus was accomplished using HPIB command software library obtained from Hewlett Packard, implemented in the C programming language. These functions were combined with other C language functions for filtering and display. Kalman filtering was accomplished by using C implementations of the Kalman and Joseph algorithms. Integration of elution profiles was accomplished by a polynomial least squares fit to a data window repetitively calculated as the data window was moved through the elution profile. In this study, a four-point data window was fit with a third-order

polynomial. The area calculated for the data window at each point was summed over the entire elution profile¹⁹. Real-time display of filtering results was accomplished using C functions from the GraphiC library (Scientific Endeavors). The Lattice-C compiler was used to obtain executable MS-DOS software from C sources.

RESULTS AND DISCUSSION

Dopamine and tyrosine were selected as model compounds for a study of digital filtering for the real-time enhancement of a chromatographic separation. As Fig. 2 illustrates, these compounds have similar spectra with low absorbances at 254 nm. To examine the feasibility of using filtering methods based on spectral differences for the enhancement of chromatographic separations, it was necessary to isolate aspects of the problem. Such isolation is easiest through use of synthetic data sets.

Synthetic data study

A series of synthetic, three-dimensional chromatograms was generated by coupling the experimentally measured absorption spectrum of tyrosine and dopamine with a Gaussian elution profile for each component. The time of elution and peak width for each of the two components could be changed arbitrarily, so that the data analysis methods could be evaluated under a wide range of chromatographic

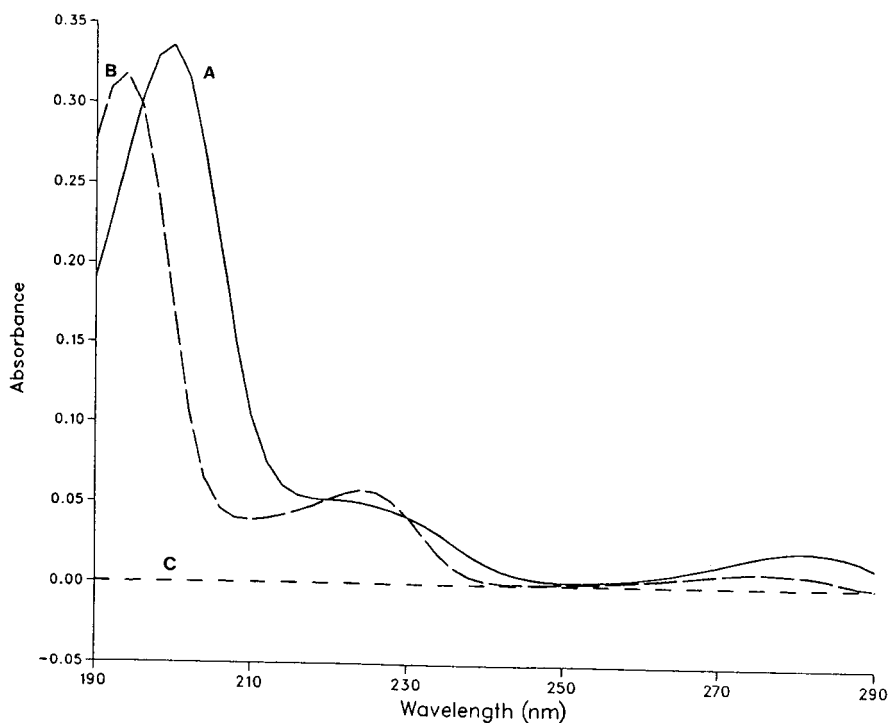


Fig. 2. Ultraviolet spectra of model components. (A) Tyrosine, concentration used was $8.373 \cdot 10^{-5} M$; (B) dopamine, concentration used was $7.599 \cdot 10^{-5} M$; (C) "Blank" component, collected on the mobile phase 200 s after injection: for an explanation of this component, see the text.

conditions. In this way, the contributions to the three-dimensional data could be tightly controlled, and the effects of each variable could be isolated and examined as a possible contributor to error in the data analysis step. The effects of several factors were studied in this manner. Data sets were generated with varying chromatographic resolution, with varying amounts of drift in the blank spectral response, and with varying amounts of random noise in the spectral response. Spectra for tyrosine and dopamine are shown in Fig. 2. A third spectrum used to represent a small, but unmodelled component was taken during the collection of spectral data from a chromatographic separation, at 200 s after injection of a tyrosine-dopamine mixture, the components of which eluted after 250 s. Only mobile phase was present in the detector at this time, but some small absorbance was observed, as is apparent from the Figure. Tables I and II further describe the synthetic data sets studied in this phase of the work. The noise levels used for the synthetic chromatograms were typical of those observed for spectral data collected on flowing samples, and the chromatographic resolution used permitted examination of data with fairly good resolution ($R = 1.1$), with low resolution (0.5), and with no resolution (0.0). One of the data sets with low resolution (number 6) also included the unmodelled component added as a Gaussian chromatographic response that overlapped that of the dopamine. The chromatographic resolution of the unmodelled response and the dopamine was zero, while the resolution of the tyrosine and the unmodelled response was 0.5. For these data sets, the Gaussian elution profile was taken as constant, as was the relation between area and injected concentration. Only known components were considered as involved in the separation, aside from set 6, and these components were taken as having known, unchanging spectra. Thus, except for data set 6, these sets represent "best-case" spectral data obtained over variable chromatographic conditions. Set 6 represents the case where an unknown chromatographic response, with unknown spectrum, interferes with the filtering. The small response of the unmodelled component represents either a small amount of a typical absorber, or it could represent strong, but momentary drift in the detection.

Table III summarizes the results obtained from application of the three-dimensional filtering methods discussed above to these data sets. In general, the results are good, even when no chromatographic resolution is present. Only when the

TABLE I
NOISE CHARACTERISTICS OF SYNTHETIC, THREE-DIMENSIONAL CHROMATOGRAPHIC DATA

<i>Data set^a</i>	<i>Measurement noise present</i>	<i>Modelled measurement noise</i>
1	$1.0 \cdot 10^{-8}$	$1.0 \cdot 10^{-8}$
2	$1.0 \cdot 10^{-8}$	$1.0 \cdot 10^{-8}$
3	$1.0 \cdot 10^{-8}$	$1.0 \cdot 10^{-8}$
4	$1.0 \cdot 10^{-7}$	$1.0 \cdot 10^{-8}$
5	$1.0 \cdot 10^{-8}$	$1.0 \cdot 10^{-7}$
6	$1.0 \cdot 10^{-8}$	$1.0 \cdot 10^{-8}$

^a The system noise Q was set at 0.0 for filtering all synthetic data.

TABLE II
CHROMATOGRAPHIC RESOLUTION AND RETENTION OF SYNTHETIC DATA SETS

Data set ^a	Dopamine retention time (s)	Tyrosine retention time (s)	Resolution
1	167	205	1.1
2	180	200	0.5
3	180	180	0.0
4	180	200	0.5
5	180	200	0.5
6 ^b	180	200	0.5

^a For each data set, the standard deviation of the Gaussian elution gradient was 12 s.

^b In this data set an unmodelled component with a retention time of 180 s and standard deviation of 12 s was added. Its spectral response is given in Fig. 2c.

measurement noise is underestimated by a considerable amount (set 4), or when an unanticipated (and unmodelled) component corrupts the spectral response of an eluting species (set 6) does error arise in estimating the components. Inclusion of the third component in the filter state model once again reduces the estimation error to zero, however. Because the models are exact, and because the linearity of the model response with concentration is perfect, varying the ratio of tyrosine and dopamine also does not lead to error from the data analysis, unless one or more components responses approaches the noise level. When relations between response and concentration deviate from linearity, however, estimated concentrations show error, although this error is small for peak ratios of 1:10 to 10:1. Similar behavior has been reported in other applications of digital filtering in peak resolution²⁰. Fluctuation of elution times for chromatographic components, as shown in Table II, also has no effect on the

TABLE III
RESULTS OF FILTERING SYNTHETIC DATA

Data set	Chemical species	Estimated area ^a	Error (%)
1	Dopamine	$9.462 \cdot 10^{-4}$	0.0
	Tyrosine	$8.562 \cdot 10^{-4}$	0.0
2	Dopamine	$9.462 \cdot 10^{-4}$	0.0
	Tyrosine	$8.558 \cdot 10^{-4}$	0.0
3	Dopamine	$9.462 \cdot 10^{-4}$	0.0
	Tyrosine	$8.556 \cdot 10^{-4}$	0.0
4	Dopamine	$9.511 \cdot 10^{-4}$	0.5
	Tyrosine	$8.542 \cdot 10^{-4}$	-0.2
5	Dopamine	$9.462 \cdot 10^{-4}$	0.0
	Tyrosine	$8.561 \cdot 10^{-4}$	0.0
6	Dopamine	$1.203 \cdot 10^{-4}$	27.0
	Tyrosine	$7.341 \cdot 10^{-4}$	-14.0
6 ^b	Dopamine	$9.462 \cdot 10^{-4}$	0.0
	Tyrosine	$8.562 \cdot 10^{-4}$	0.0

^a The results of integrating the plot of the time evolution of the concentration estimate.

^b Results obtained from use of a three-component model.

quality of the analytical results, so long as the linear relation between area and injected amount holds. Altering the peak shape, *e.g.* by using tailed peaks or non-Gaussian peaks of arbitrary profile²¹ also has no effect on the quality of the analytical results, so long as a linear relation between peak and injected amount remains known.

These results indicate that chromatographic resolution should have little effect on the accuracy of the filtering estimates, but errors in the spectral model used will propagate to the filtering results. Generally, these errors will be small, unless the spectral model is inadequate as a result of unanticipated contributors to the spectral response.

Tyrosine and dopamine calibration

Any mathematical method based on the assumption of a linear model is only as accurate as the linearity of the model used. The assumption of a linear model in real chromatographic and spectral data was checked by chromatographing a series of standard solutions containing either dopamine or tyrosine.

Serial dilutions of stock solutions of tyrosine and dopamine were prepared over a range of concentrations. Tyrosine is sparingly soluble in the water-methanol solutions used here. In contrast, dopamine is soluble, and higher concentrations are possible. The ultraviolet spectra of these solutions were measured over the 190–290 nm wavelength range. For dopamine and tyrosine, regions exist where the absorbance is linearly related to concentration, and these regions depend both on concentration and the wavelength selected. In general, peaks with smaller molar absorptivities gave rise to more linear absorbance *vs.* concentration relations. For this work, model concentrations were chosen from those falling on linear calibration curves at all wavelengths.

Once suitable spectral models are chosen from the linear region of absorbance *vs.* concentration for all wavelengths to be used in the filtering, an examination can be made of the relation of the filter estimates for the chromatographic peak height and area to the amount of analyte injected.

Real-time filtering was performed on single-component chromatograms, and the chromatographic peak height and area were measured. The chromatographic peak height was measured at the maximum of the elution profile produced from the real-time filtering. Results are given for the real-time filtering of chromatographic runs where the model included dopamine, tyrosine and a component representing detector drift. This component was a “blank” spectrum, taken just before elution of the first component of the mixture. For the data reported here, the blank model was obtained by measuring eluent absorbance at 200 s. This spectrum should be zero, since the detector reference was taken on the same mobile phase mixture prior to beginning the chromatogram. The existence of some response suggests drift in the detector response with time. By including this “drift” component as another component of the filter model, those small changes in the detector baseline as data collection proceeds can be accounted for without the need to alter the amounts assigned to the other model components. This component represents a small, but necessary correction to the spectral model.

In all cases, the maximum concentration observed for the component not present in the injection was not different from zero. In general, inclusion of additional components in the filter model is not harmful to filter estimates for those species actually present. Species included in the model but not observed in the data are

TABLE IV

DOPAMINE CALIBRATION

The data sets are single-component chromatograms of dopamine. Injected concentration = 0.0002 (± 0.0002) + 8.1 (± 0.5) (area), $r^2 = 0.991$. Injected concentration = 0.002 (± 0.003) + 197 (± 9) (absorbance), $r^2 = 0.994$.

Data set	Injected concentration ($\times 10^{-4}$)	Maximum absorbance ($\times 10^{-2}$)	Retention time (s)	Elution profile area ($\times 10^{-3}$)
1	1.006	1.60	250	0.886
2	2.012	3.87	247	1.860
3	3.018	6.01	252	2.821
4	4.024	7.99	255	3.478
5	5.030	9.46	257	4.159

estimated at zero concentration, the case here. However, if the filter model is expanded so that a linearly dependent set of spectra make up the model, failure of the filtering can result, since the filter states are no longer observable from the spectral data^{15,17}. Linear dependence arises only when spectra for model components do not differ within the spectral resolution of the detector, or when one of the model spectra can be produced from a combination of other model spectra, as might happen if a spectrum of a mixture is used as a model component along with the spectra of its constituents.

For a single-component chromatographic peak, the relation between peak height and amount injected is linear, as is the relation between injected amount and peak area calculated by direct integration of the elution profiles. Tables IV and V demonstrate these relations. The linearity results from the fact that the maximum absorbance observed as the chromatographic peak passes through the detector is well within the linear region of the absorbance vs. concentration relation at all wavelengths. Thus, strictly linear relations have been demonstrated for both the relation of absorbance to detected concentration, and for the relation of chromatographic peak parameters (area, peak height) to injected amounts.

Kalman filter-enhanced separation of dopamine-tyrosine mixtures

Several mixtures of dopamine and tyrosine were prepared in methanol. In this

TABLE V

TYROSINE CALIBRATION

The data sets are single-component chromatograms of tyrosine. Injected concentration = 0.002 (± 0.002) + 8.2 (± 0.5) (area), $r^2 = 0.991$. Injected concentration = 0.003 (± 0.002) + 204 (± 6) (absorbance), $r^2 = 0.997$.

Data set	Injected concentration ($\times 10^{-4}$)	Maximum absorbance ($\times 10^{-2}$)	Retention time (s)	Elution profile area ($\times 10^{-3}$)
1	0.998	2.462	297.5	0.886
2	1.996	4.252	300	1.860
3	2.993	6.206	302	2.821
4	3.991	8.233	307.5	3.478
5	4.989	10.630	304	4.159

TABLE VI
ANALYSIS OF CHROMATOGRAMS OF TYROSINE AND DOPAMINE

Mixture	Species	Injected concentration	Chromatographic resolution	Relative error (%) ^a	Relative error (%) ^b
1	Dopamine	$1.006 \cdot 10^{-4}$	1.7	3.1	3.2
	Tyrosine	$9.975 \cdot 10^{-5}$		5.2	5.7
2	Dopamine	$3.018 \cdot 10^{-4}$	1.7	0.3	0.8
	Tyrosine	$9.975 \cdot 10^{-5}$		0.5	-3.6
3	Dopamine	$1.006 \cdot 10^{-4}$	1.6	-1.2	4.2
	Tyrosine	$2.993 \cdot 10^{-4}$		2.5	0.4
4	Dopamine	$2.012 \cdot 10^{-4}$	1.2	1.8	1.9
	Tyrosine	$1.996 \cdot 10^{-4}$		2.1	2.2

^a Error from use of three-component model.

^b Error from use of two-component model.

study, approximately equimolar mixtures were used for simplicity. These mixtures were chromatographed under conditions similar to those where dopamine and tyrosine were reported to be retained, but poorly resolved⁷. We observed moderate resolution under these conditions, as indicated in Table VI. Results are given for the real-time filtering of chromatographic runs where the models contained only the spectra of dopamine and tyrosine, and where the model included these components and a component representing detector drift. As before, inclusion of the drift component in the filter model improves the quality of the analytical results. A typical set of elution profiles generated by the filtering is illustrated in Fig. 3.

The fluctuations observed in amounts of tyrosine and dopamine estimated by use of the real-time filtering seem attributable to small variations in injection and flow-rate, as judged from repetitive chromatograms obtained on a single mixture. Examination of evolution of filter states, such as those shown in Fig. 3, indicate that the drift component also fluctuates a small amount from run to run, as well as changing during a run. Thus, while including the drift component in the filter model is, in general, beneficial, the improvement in the accuracy of the filter results is variable. Often the improvement is small because the drift is small, a consequence of frequent measurement of reference spectra during data collection. Occasionally, however, the improvement upon including a drift component is fairly large, suggesting significant drift in the detector performance. Since the computational burden incurred by inclusion of the extra component is increased by only *ca.* 0.5 s per spectrum analysed, and since the use in the filter model of components not present in the data is not detrimental to estimates of species that are, in fact, present, inclusion of the drift component seems reasonable.

CONCLUSIONS

This study points out the advantages and disadvantages of three-dimensional Kalman filtering as applied to unresolved chromatographic systems detected by diode-array spectroscopy. Advantages include the method's insensitivity to variations in chromatographic conditions, peak shape, resolution, and noise. A disadvantage is the need to model all spectral responses well. If errors in the spectral model may be

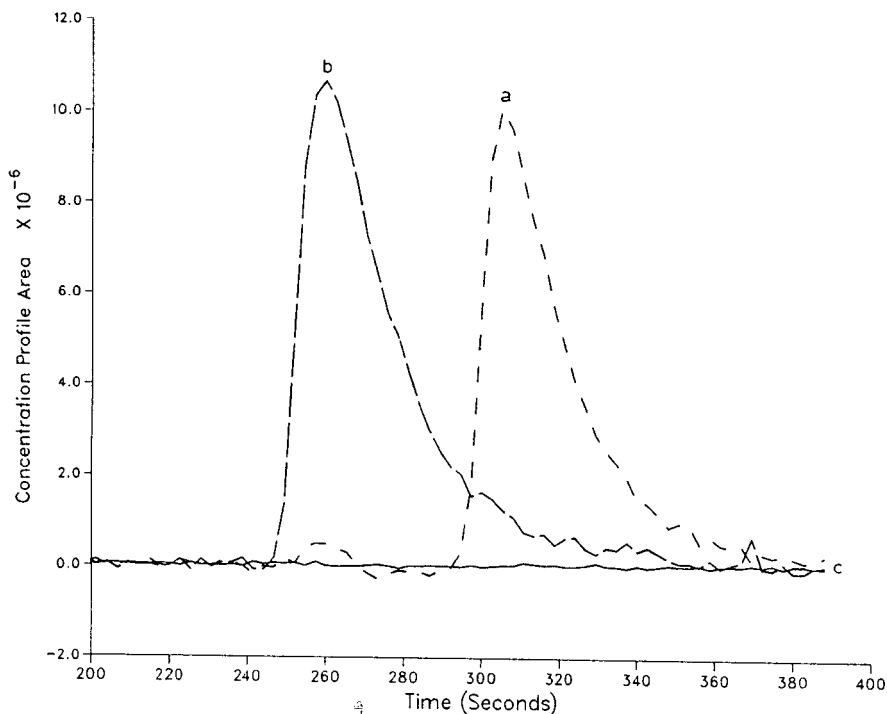


Fig. 3. Filter-generated elution profiles for dopamine-tyrosine chromatogram. (a) Elution profile for dopamine; (b) elution profile for tyrosine; (c) elution profile for "detector drift" component.

ignored or compensated, enhancement of the separation of known components in the presence of unknown components may be possible. Adaptive filters have already been used to compensate for model errors in some systems²². A second disadvantage of the method is the requirement of a strictly linear relation between area and injected amount. Small errors in spectral response can corrupt the relation, leading to errors in quantitation. Another paper in this series considers methods which can be used to reduce errors of this sort²³. Future work will investigate the application of dynamic models and adaptive filters to three-dimensional chromatographic systems.

ACKNOWLEDGEMENTS

The authors thank a reviewer for useful suggestions. Initial support for this research was provided by the University of Delaware Research Foundation. Additional funding was provided by the Division of Chemical Sciences, U.S. Department of Energy, under Grants DE-FG02-86ER13542 and DE-FG06-84ER13202.

REFERENCES

- 1 H. A. Hancock, L. A. Dahm and J. F. Muldoon, *J. Chromatogr. Sci.*, 8 (1970) 57.
- 2 A. W. Westerberg, *Anal. Chem.*, 41 (1969) 1770.
- 3 J. P. Foley, *J. Chromatogr.*, 384 (1987) 301.
- 4 S. D. Frans, M. L. McConnell and J. M. Harris, *Anal. Chem.*, 57 (1985) 1552.
- 5 R. A. Vaidya and R. D. Hester, *J. Chromatogr.*, 287 (1984) 231.
- 6 A. F. Fell, H. P. Scott, R. Gill and A. C. Moffat, *J. Chromatogr.*, 282 (1983) 123.
- 7 A. F. Fell, B. J. Clark and H. P. Scott, *J. Chromatogr.*, 297 (1984) 203.
- 8 A. F. Fell, H. P. Scott, R. Gill and A. C. Moffat, *J. Chromatogr.*, 273 (1983) 3.
- 9 P. J. Gemperline, *J. Comp. Sci. Inf. Sci.*, 24 (1984) 206.
- 10 R. F. Lacey, *Anal. Chem.*, 58 (1986) 1404.
- 11 Y. Hayashi, T. Shibasaki, R. Matsuda and M. Uchiyama, *J. Chromatogr.*, 407 (1987) 59.
- 12 Y. Hayashi, T. Shibasaki, R. Matsuda and M. Uchiyama, *Anal. Chim. Acta*, 202 (1987) 187.
- 13 Y. Hayashi, T. Shibasaki and M. Uchiyama, *J. Chromatogr.*, 411 (1987) 95.
- 14 Y. Hayashi, T. Shibasaki and M. Uchiyama, *Anal. Chim. Acta*, 201 (1987) 185.
- 15 S. D. Brown, *Anal. Chim. Acta*, 181 (1986) 1.
- 16 S. D. Brown, *Trends Anal. Chem.*, 6 (1987) 260.
- 17 A. Gelb (Editor), *Applied Optimal Estimation*, MIT Press, Cambridge, MA, 1974.
- 18 S. C. Rutan and S. D. Brown, *Anal. Chim. Acta*, 175 (1985) 219.
- 19 P. Bevington, *Data Reduction and Error Analysis for the Physical Sciences*, McGraw-Hill, New York, 1969.
- 20 C. A. Scolari and S. D. Brown, *Anal. Chim. Acta*, 166 (1984) 253.
- 21 J. P. Foley and J. G. Dorsey, *J. Chromatogr. Sci.*, 22 (1984) 40.
- 22 S. D. Brown and S. C. Rutan, *NBS J. Res.*, 90 (1985) 403.
- 23 T. Q. Barker and S. D. Brown, *Anal. Chim. Acta*, (1989) in press.

CHROM. 21 339

USE OF CENTRIFUGAL PARTITION CHROMATOGRAPHY FOR ASSESSING PARTITION COEFFICIENTS IN VARIOUS SOLVENT SYSTEMS

NABIL EL TAYAR

Institut de Chimie Thérapeutique, École de Pharmacie, Université de Lausanne, Place du Château, CH-1005 Lausanne (Switzerland)

ANDREW MARSTON

Institut de Pharmacognosie et Phytochimie, École de Pharmacie, Université de Lausanne, Place du Château, CH-1005 Lausanne (Switzerland)

ANTOINE BECHALANY

Institut de Chimie Thérapeutique, École de Pharmacie, Université de Lausanne, Place du Château, CH-1005 Lausanne (Switzerland)

KURT HOSTETTMANN

Institut de Pharmacognosie et Phytochimie, École de Pharmacie, Université de Lausanne, Place du Château, CH-1005 Lausanne (Switzerland)

and

BERNARD TESTA*

Institut de Chimie Thérapeutique, École de Pharmacie, Université de Lausanne, Place du Château, CH-1005 Lausanne (Switzerland)

(First received November 7th, 1988; revised manuscript received January 20th, 1989)

SUMMARY

Centrifugal partition chromatography (PC) was examined as a technique for measuring the partition coefficient of organic solutes. Two solvent systems of convenient viscosity were used, namely *n*-hexanol–water and cyclohexane–water. The partition coefficients thus determined (expressed as $\log P_{\text{CPC/ol}}$ and $\log P_{\text{CPC/ane}}$, respectively) were shown to be well correlated with literature partition coefficients obtained by the shake-flask (SF) method in the *n*-octanol–water and *n*-hexane–water systems, respectively. Hydrogen-bonding parameters, I_{H} , were calculated as $(\log P_{\text{CPC/ol}} - \log P_{\text{CPC/ane}})$ and $(\log P_{\text{oct}} - \log P_{\text{hex}})$; the good correlation between the I_{H} values derived from the CPC and SF methods indicates that the same partitioning mechanism is operative in both methods.

INTRODUCTION

Lipophilicity is an important molecular property of drugs and other xenobiotics often correlated with their biological activity. A number of experimental models have been developed to simulate partitioning processes in biological systems and to quantify lipophilicity. The shake-flask (SF) technique, using a biphasic liquid system

consisting of water and an organic solvent, remains the standard method for measuring the lipophilicity of chemical compounds; *n*-octanol is universally accepted as the reference organic solvent^{1–3}, but other solvents are of considerable value, for example in comparing the hydrogen-bonding ability of series of compounds^{4–6}. Thus, lipophilicity is often expressed as the logarithm of the partition coefficient ($\log P_{\text{oct}}$), defined as the equilibrium distribution of a single chemical species between the aqueous and the octanol phases. Yet despite its value, the SF method suffers a number of practical limitations and disadvantages due to various perturbing factors such as time consumption, solute stability, solute impurities, solute volatility, formation of microemulsions, concentration and salt effects, etc.^{7–9}.

Solid–liquid partition chromatography has been explored as an alternative means for measuring lipophilicity. Indeed, the use of chromatographic retention parameters, in particular those obtained from reversed-phase high-performance liquid chromatography (RP-HPLC), are becoming increasingly popular in replacing the *n*-octanol–water partition coefficient in quantitative structure–activity relationship (QSAR) studies^{10–13}. Unfortunately, the presence of a solid support with a non-negligible proportion of residual silanol groups on the surface of alkyl-bonded stationary phases dramatically influences the partitioning process of polar basic compounds due to an additional adsorption mechanism^{14–17}.

Recently, Terada *et al.*^{18,19} have used a new chromatographic technique known as centrifugal partition chromatography (CPC) to measure lipophilicity. CPC is a liquid–liquid chromatography technique resembling to some extent droplet counter-current chromatography (DCCC)^{20–22}. As in DCCC, two non-miscible liquids are used as the stationary and mobile phase, respectively. A centrifugal force maintains the liquid stationary phase in a set of interconnected columns (cartridges), while the mobile phase is pumped through the stationary phase in an ascending or descending mode depending on the respective densities of the two phases. General features of the CPC technique such as its efficiency and selectivity have been discussed in detail by Berthod and Armstrong^{23,24}. From their studies, Terada *et al.*^{18,19} concluded that CPC may be preferable to both the SF and RP-HPLC methods for measuring lipophilicity. Indeed, CPC has advantages over RP-HPLC or other chromatographic methods in that no solid support is present and no adsorption mechanism is involved. Consequently, as in the SF method, the retention mechanism is governed solely by partitioning processes. In addition, CPC can be performed over a very broad pH range since limitations imposed by a solid support such as silica do not apply. Moreover, CPC being a liquid–liquid chromatographic method opens promising possibilities for the precise and accurate assessment of partition coefficients in a large variety of solvent systems.

Exploring some of these possibilities constitutes the major objective of the present study. After optimizing the experimental conditions, the CPC technique was used to measure the partition coefficients of several organic compounds in an amphiprotic (*n*-hexanol) and an aprotic (cyclohexane) organic solvent.

EXPERIMENTAL

Materials

4-Pyridylalkanols were synthesized as previously described²⁵. Mono- and di-

substituted benzene derivatives were obtained from Fluka (Buchs, Switzerland); the buffer compound 3-morpholinopropanesulphonate (MPS), *n*-octanol, *n*-hexanol, *n*-hexane and cyclohexane were obtained from Merck (Darmstadt, F.R.G.). All compounds obtained were of analytical grade and used without further purification.

Centrifugal partition chromatography

Measurements were performed at 30°C using a centrifugal partition chromatograph (Model CPC-LLN; Sanki Engineering, Kyoto, Japan) connected to a 2238 Uvicord II detector operating at 254 nm (LKB, Bromma, Sweden) and a 600 chart recorder (W + W Scientific, Basle, Switzerland). Solvent delivery was by a Sanki constant flow pump (Model LBP-V; Sanki Engineering). The chromatograph was fitted with twelve Type 250W cartridges (total volume 250 ml) and samples were injected by means of a six-way valve and 3-ml sample loop. The apparatus was first packed with the stationary phase and then the mobile phase was pumped through. The sample was introduced when elution of the stationary phase was complete and the mobile phase had exited from the cartridges.

Two solvent systems were employed, namely *n*-hexanol–aqueous buffer (0.02 *M* MPS, pH 7.4) and cyclohexane–aqueous buffer (0.02 *M* MPS, pH 7.4). The aqueous and organic phases were mutually saturated. Preliminary studies using an *n*-octanol–aqueous buffer system and an *n*-hexane–aqueous buffer system were not successful. With the *n*-octanol–aqueous buffer system the pump pressure reached its upper limit due to the high viscosity of *n*-octanol. To overcome this problem, *n*-hexanol was chosen as the amphiprotic organic solvent. In the *n*-hexane–aqueous buffer system, inconsistent pump pressures and flow-rates of the mobile phase were observed probably due to the low density and/or low viscosity of *n*-hexane.

In the *n*-hexanol–aqueous buffer system, *n*-hexanol was used as the mobile phase and aqueous buffer as the stationary phase. The flow-rate was 1.8 ml/min and the pump pressure was 55 kg/cm² at a rotation rate of 500 rpm. In this solvent system the equilibrium partition coefficient is calculated from the following equation¹⁹

$$\log P_{\text{CPC/ol}} = \log [V_{\text{S}}/(V_{\text{R}} - V_{\text{M}})] \quad (1)$$

where V_{S} is the stationary phase volume, V_{R} is the retention volume of the solute and V_{M} is the dead volume (mobile phase volume in the cartridges).

In the cyclohexane–aqueous buffer system, water was used as the mobile phase and cyclohexane as the stationary phase. The flow-rate was 2.4 ml/min and the pump pressure was 50 kg/cm² at a rotation rate of 700 rpm. The equilibrium partition coefficients are calculated from the reverse of eqn. 1:

$$\log P_{\text{CPC/ane}} = \log [(V_{\text{R}} - V_{\text{M}})/V_{\text{S}}] \quad (2)$$

A systematic determination of the dead volume is very important in CPC due to the continuous decrease of the stationary phase volume. This phenomenon, known as column “bleeding”, occurs despite the presaturation of the phases and has been investigated in detail by Berthod and Armstrong²³. They have proposed the use of a dead volume tracer to take account of the variation in stationary phase volume. In the present study, sodium dichromate and biphenyl were used as the non-retained com-

pounds to assess the dead volumes in the cyclohexane–water system and the *n*-hexanol–water system, respectively.

RESULTS

n-Hexanol–water system

Typical V_R values of the compounds investigated are reported in Table I together with the partition coefficients expressed as $\log P_{CPC/ol}$ and calculated according to eqn. 1. Table I also reports literature partition coefficients obtained by the SF method in the *n*-octanol–water system and expressed as $\log P_{oct}$. The excellent reproducibility of $\log P_{CPC/ol}$ values should be noted (S.D. < 4%). The compounds investigated cover a $\log P_{oct}$ range of 2 units. A good linear relationship between $\log P_{CPC/ol}$ and $\log P_{oct}$ is revealed in eqn. 3 and depicted in Fig. 1

$$\log P_{oct} = 1.25(\pm 0.16) \log P_{CPC/ol} - 0.25(\pm 0.16) \quad (3)$$

$$n = 20, r = 0.968, s = 0.15, F = 269$$

where n is the number of compounds, r the correlation coefficient, s the standard deviation of the linear regression and F is the Fischer test of the statistical significance of the equation. The values in parentheses are the 95% confidence limits of the

TABLE I

PARTITION COEFFICIENTS OF VARIOUS ORGANIC COMPOUNDS MEASURED BY CPC IN AN *n*-HEXANOL–WATER SYSTEM, $\log P_{CPC/ol}$

Compound	V_R (ml) ^a	$\log P_{CPC/ol}$	$\log P_{oct}$ ^b
C ₆ H ₅ SO ₂ NH ₂	159.84	0.44	0.31
C ₆ H ₅ SOCH ₃	138.06	0.60	0.55
C ₆ H ₅ SO ₂ CH ₃	135.72	0.69	0.49
C ₆ H ₅ CONH ₂	129.60	0.74	0.64
C ₆ H ₅ NHCOCH ₃	118.80	0.99	1.16
C ₆ H ₅ NH ₂	119.34	1.03	0.90
C ₆ H ₅ CH ₂ OH	116.64	1.08	1.10
C ₆ H ₅ OH	110.16	1.34	1.47
C ₆ H ₅ OCOCH ₃	113.40	1.32	1.49
C ₆ H ₅ NO ₂	110.16	1.45	1.86
HO–C ₆ H ₄ –4–NH ₂	216.45	0.11	0.04
HO–C ₆ H ₄ –2–NH ₂	132.21	0.70	0.52
H ₂ N–C ₆ H ₄ –4–NO ₂	113.40	1.49	1.39
H ₂ N–C ₆ H ₄ –3–NO ₂	107.64	1.35	1.37
H ₂ N–C ₆ H ₄ –2–NO ₂	111.85	1.47	1.83
4–C ₅ H ₄ N–CH ₂ OH	192.24	0.22	0.06
4–C ₅ H ₄ N–(CH ₂) ₂ OH	179.28	0.30	0.10
4–C ₅ H ₄ N–(CH ₂) ₃ OH	130.57	0.80	0.58
4–C ₅ H ₄ N–(CH ₂) ₄ OH	120.96	1.01	0.90
4–C ₅ H ₄ N–(CH ₂) ₅ OH	112.32	1.47	1.39

^a V_M values in the range 100–108 ml.

^b Data taken from ref. 26 for the phenyl derivatives and from ref. 27 for the pyridyl derivatives.

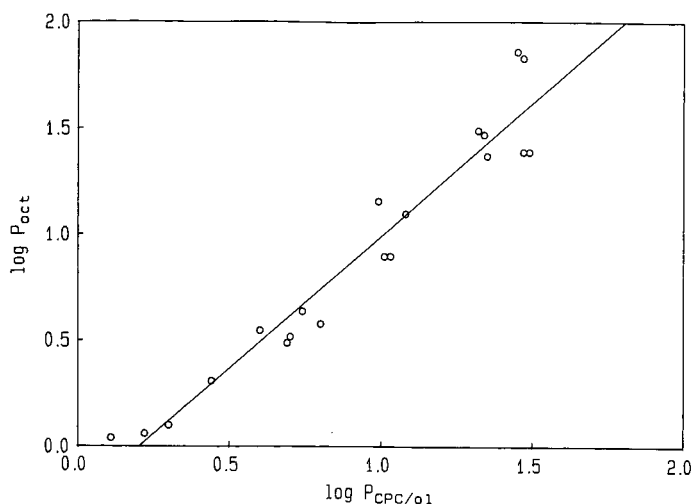


Fig. 1. Relationship between $\log P_{\text{CPC}/\text{ol}}$ and $\log P_{\text{oct}}$ for the 20 compounds in Table I.

regression coefficients. For the homologous series of 4-pyridylalkanols, the correlation is even better:

$$\begin{aligned} \log P_{\text{oct}} &= 1.08(\pm 0.15) \log P_{\text{CPC}/\text{ol}} - 0.22(\pm 0.13) \\ n &= 5, r = 0.997, s = 0.05, F = 526 \end{aligned} \quad (4)$$

This is presumably due to the good quality and single origin of the $\log P_{\text{oct}}$ values of these compounds, which were carefully measured under the same conditions in our laboratory²⁷.

Cyclohexane–water system

In Table II, partition coefficients of a series of mono- and disubstituted benzenes determined by CPC using the cyclohexane–aqueous buffer system were compared with those obtained by the SF method using *n*-hexane–water. The compounds investigated cover a $\log P_{\text{hex}}$ range of 2.5 units. Although only a limited number of $\log P_{\text{hex}}$ values are available ($n = 8$), a good linear relationship between $\log P_{\text{CPC}/\text{ane}}$ and $\log P_{\text{hex}}$ is revealed by eqn. 5 and shown in Fig. 2:

$$\begin{aligned} \log P_{\text{hex}} &= 1.05(\pm 0.31) \log P_{\text{CPC}/\text{ane}} - 0.21(\pm 0.29) \\ n &= 8, r = 0.959, s = 0.26, F = 69 \end{aligned} \quad (5)$$

Hydrogen bonding ability

It is well known that a linear relationship between partition coefficients obtained in different solvent systems is valid only when the organic solvents in the two systems are both either inert (*e.g.*, alkanes), hydrogen-bond acceptors (*e.g.*, ethers), hydrogen-bond donors (chloroform) or amphiprotic (*e.g.*, alkanols)^{28,29}. These restrictions have prompted Seiler⁴ to define a parameter, I_{H} , conceived as a measure of the hydrogen-bonding ability of a given solute. This parameter allows the intercon-

TABLE II

PARTITION COEFFICIENTS OF MONO- AND DISUBSTITUTED BENZENES MEASURED BY CPC IN A CYCLOHEXANE–WATER SYSTEM ($\log P_{\text{CPC/ane}}$), AND HYDROGEN-BONDING PARAMETERS, I_{H} , CALCULATED ACCORDING TO EQN. 6

Compound	V_R (ml) ^a	$\log P_{\text{CPC/ane}}$	$I_{\text{H(CPC)}}$	$\log P_{\text{hex}}$ ^b	$I_{\text{H(SF)}}$
$\text{C}_6\text{H}_5\text{SO}_2\text{NH}_2$	138.82	-2.28	2.72	–	–
$\text{C}_6\text{H}_5\text{SOCH}_3$	144.00	-1.29	1.89	–	–
$\text{C}_6\text{H}_5\text{SO}_2\text{CH}_3$	167.04	-0.59	1.28	–	–
$\text{C}_6\text{H}_5\text{CONH}_2$	132.48	-1.92	2.66	-2.35	2.99
$\text{C}_6\text{H}_5\text{NHCOCH}_3$	138.24	-1.31	2.30	-1.80	2.96
$\text{C}_6\text{H}_5\text{NH}_2$	289.44	0.12	0.91	-0.05	0.95
$\text{C}_6\text{H}_5\text{CH}_2\text{OH}$	169.97	-0.46	1.54	-0.76	1.86
$\text{C}_6\text{H}_5\text{CH}_2\text{CH}_2\text{OH}$	252.00	0.01	–	-0.39	1.75
$\text{C}_6\text{H}_5\text{OH}$	155.52	-0.69	2.03	-0.89	2.36
$\text{HO-C}_6\text{H}_4\text{-4-NH}_2$	132.48	-1.62	1.73	–	–
$\text{HO-C}_6\text{H}_4\text{-2-NH}_2$	141.12	-1.02	1.72	–	–
$\text{H}_2\text{N-C}_6\text{H}_4\text{-4-NO}_2$	145.44	-0.92	2.41	-0.62	2.01
$\text{H}_2\text{N-C}_6\text{H}_4\text{-2-NO}_2$	446.40	0.42	1.05	0.21	1.62

^a V_{M} values in the range 126–139 ml.

^b Data taken from ref. 26; blanks correspond to unavailable values.

version of partition coefficients from alkane–water systems to alkanol–water systems using the following general equation:

$$I_{\text{H}} = \log P_{\text{alkanol}} - \log P_{\text{alkane}} \quad (6)$$

The importance and the physicochemical interpretation of this parameter have been discussed at length in several recent papers^{5,6,30,31}. According to this concept, we

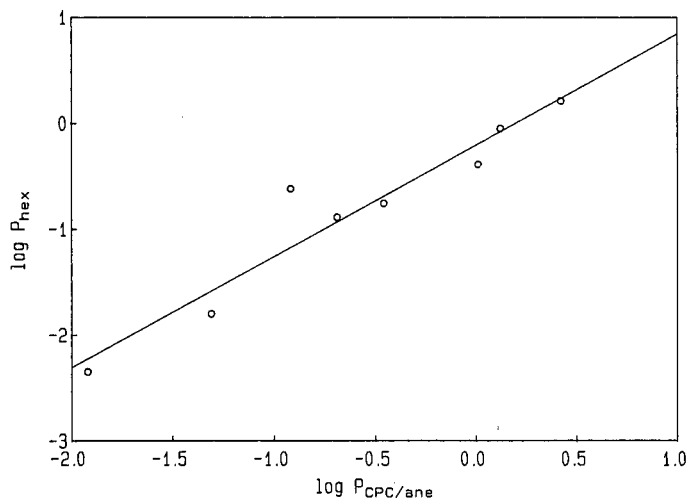


Fig. 2. Relationship between $\log P_{\text{CPC/ane}}$ and $\log P_{\text{hex}}$ for eight compounds in Table II.

have examined the relationship between I_H values obtained by the SF and CPC methods. A satisfactory correlation was found:

$$I_{H(\text{SF})} = 0.94(\pm 0.58) I_{H(\text{CPC})} + 0.38(\pm 1.15) \\ n = 7, r = 0.877, s = 0.38, F = 16.7 \quad (7)$$

In eqns. 3–5 and 7 the slopes are practically equal to one and the intercepts are close to zero. This leads to the important conclusion that both the SF and CPC methods are governed by the same partitioning mechanism and that the CPC method appears of value for assessing the hydrogen-bonding ability, I_H , of solutes, at least in the lipophilicity range investigated here.

DISCUSSION

In this study, we have examined the use of a CPC technique for the determination of partition coefficients of various compounds in two different solvent systems. The method appears suitable for a study of the partitioning behaviour of compounds in a variety of organic solvents. However, the range of partition coefficients which can be measured by this method was limited due to practical problems such as the long duration of elution and the band broadening characteristic of the more strongly retained compounds. Increasing the speed of rotation of the chromatograph improves the resolution but at same time leads to unacceptably high back pressures. To ensure good precision, the choice of solvent as either the stationary phase or mobile phase is very important. In the *n*-hexanol–aqueous buffer system, *n*-hexanol was chosen as the mobile phase and polar compounds tended to be more strongly retained in the stationary aqueous phase than less polar ones. This condition provided a maximum of selectivity and precision for the more polar compounds. It is clear that the relative error increases when the difference between V_R and V_M decreases. Thus, relatively lipophilic compounds ($\log P_{\text{oct}} > 2$) cannot be measured accurately under these conditions. Berthod and Armstrong³² have demonstrated that the retention volume of a given solute must be at least 5 ml higher than the dead volume to determine partition coefficients with less than 10% error. In contrast, polar compounds ($\log P_{\text{oct}} > -2$) can be accurately measured using *n*-hexanol as the mobile phase. In cyclohexane–aqueous buffer, water was used as the mobile phase, allowing a good selectivity and precision in the lipophilicity range investigated. However, the very long retention time of compounds with $\log P_{\text{hex}} > 0.5$ limits the usefulness of the conditions chosen. The lower limit which can be measured under these conditions is $\log P_{\text{hex}} > -2.5$.

Berthod *et al.*^{32,33} have also shown that CPC can be used directly to determine octanol–water partition coefficients over a $\log P_{\text{oct}}$ range of -2.5 to 2.5 . For accurate determination of the higher $\log P_{\text{oct}}$ values, they proposed to use water as the mobile phase and *n*-octanol as the stationary phase. In order to have reasonable retention times while retaining efficiency, they reduced the stationary phase volume using a procedure termed the “underloading mode”. Indeed, this method may extend the range of partition coefficients which can be measured by CPC using other amphiprotic organic solvents. However, further studies are needed to examine its utility.

Terada *et al.*^{18,19} have compared the *n*-octanol–water partition coefficients of

various organic compounds measured by the SF and CPC methods using two different solvent systems, *n*-hexane–acetonitrile and [*n*-octanol–*n*-hexane (20:80)]–water. A single linear relationship between $\log k_{\text{CPC}}$ and $\log P_{\text{oct}}$ was found in the latter but not in the former system, where the relationship was dependent on the chemical structures of the solutes. Terada *et al.*^{18,19} thus concluded that the (octanol–hexane)–water solvent system exhibits the same properties as the octanol–water system. Berthod *et al.*³³ have also used the [*n*-octanol–*n*-hexane (40:60)]–water system in order to expand the lipophilicity range which can be measured by the CPC method. The reason for using octanol–hexane mixtures as the organic phase is to reduce the retention time, *i.e.*, to increase the lipophilicity range, and also to decrease the high viscosity of *n*-octanol which causes pressure problems. In these studies^{19,33} however, the dramatic decrease in polarity of the organic phase caused by the addition of *n*-hexane was not taken into consideration, particularly at such high proportions of *n*-hexane.

That this neglect may be misleading is shown by the work of Okada *et al.*³⁴, who investigated the effect of mixed organic solvents on the partition coefficient of procaine and *p*-aminobenzoic acid, demonstrating that partition coefficients in (pentanol–cyclohexane)–water systems gradually increase with increasing proportions of pentanol. They interpreted this behaviour as a polarity-dependent change in the ability of the organic phase to solvate a given solute. As a consequence, the partition behaviour of various solutes, in particular polar compounds, will be quite different in an (octanol–hexane)–water or an octanol–water system. The conclusion to draw from such studies is that (octanol–hexane)–water partition coefficients cannot be used to predict octanol–water partition coefficients in a classical Collander approach^{28,29}.

It should also be noted that biphasic organic–organic systems such as hexane–acetonitrile or hexane–methanol cannot be used to determine the hydrophobicity of compounds. Indeed, the hydrophobic effect is determined mainly by the hydrogen-bonding network structure of water molecules which cannot be simulated by either acetonitrile or by methanol.

We thus conclude that CPC is a useful tool for measuring partition coefficients in different solvent systems. However, the range of measurable lipophilicities cannot be expanded very far due to the solvent limitations discussed above. Technical improvements of the CPC apparatus, *e.g.*, higher pump pressures, and better stability with low viscosity solvents should alleviate these limitations.

ACKNOWLEDGEMENTS

B.T., N.E.T. and A.B. are indebted to the Swiss National Science Foundation for grant 3.508-86.

REFERENCES

- 1 A. Leo, C. Hansch and D. Elkins, *Chem. Rev.*, 71 (1971) 525.
- 2 T. Fujita, J. Iwasa and C. Hansch, *J. Am. Chem. Soc.*, 86 (1964) 5175.
- 3 J. C. Dearden and J. H. O'Hara, *Eur. J. Med. Chem.*, 13 (1978) 415.
- 4 P. Seiler, *Eur. J. Med. Chem.*, 9 (1974) 473.
- 5 T. Fujita, T. Nishioka and M. Nakajima, *J. Med. Chem.*, 20 (1977) 1071.
- 6 M. Gryllaki, H. van de Waterbeemd, B. Testa, N. El Tayar, J. M. Mayer and P. A. Carrupt, *Int. J. Pharm.*, in press.

- 7 H. Könemann, R. Zelle, F. Busser and W. E. Hammers, *J. Chromatogr.*, 178 (1979) 559.
- 8 N. El Tayar, H. van de Waterbeemd, M. Gryllaki, B. Testa and W. F. Trager, *Int. J. Pharm.*, 19 (1984) 271.
- 9 N. El Tayar, H. van de Waterbeemd and B. Testa, *J. Chromatogr.*, 320 (1985) 305.
- 10 T. L. Hafkenschied and E. Tomlinson, *Int. J. Pharm.*, 16 (1983) 225.
- 11 Th. Braumann, *J. Chromatogr.*, 373 (1987) 191.
- 12 N. El Tayar, G. J. Kilpatrick, H. van de Waterbeemd, B. Testa, P. Jenner and C. D. Marsden, *Eur. J. Med. Chem.*, 23 (1988) 173.
- 13 D. J. Minick, J. J. Sabatka and D. A. Brent, *J. Liq. Chromatogr.*, 10 (1987) 2565.
- 14 A. Nahum and Cs. Horváth, *J. Chromatogr.*, 203 (1981) 53.
- 15 H. Colin, A. Krstulović, G. Guiochon and Z. Yun, *J. Chromatogr.*, 255 (1983) 295.
- 16 E. Bayer and A. Paulus, *J. Chromatogr.*, 400 (1987) 1.
- 17 N. El Tayar, A. Tsantili-Kakoulidou, T. Ræthlisberger, B. Testa and J. Gal, *J. Chromatogr.*, 439 (1988) 237.
- 18 H. Terada, Y. Kosuge, N. Nakaya, W. Murayama, Y. Nunogaki and K.-I. Nunogaki, *Chem. Pharm. Bull.*, 35 (1987) 5010.
- 19 H. Terada, Y. Kosuge, W. Murayama, N. Nakaya, Y. Nunogaki and K.-I. Nunogaki, *J. Chromatogr.*, 400 (1987) 343.
- 20 W. Murayama, T. Kobayashi, Y. Kosuge, H. Yano, Y. Nunogaki and K.-I. Nunogaki, *J. Chromatogr.*, 239 (1982) 643.
- 21 K. Hostettmann, M. Hostettmann and A. Marston, *Preparative Chromatographic Techniques*, Springer, Berlin, 1986.
- 22 A. Marston, C. Borel and K. Hostettmann, *J. Chromatogr.*, 450 (1988) 91.
- 23 A. Berthod and D. W. Armstrong, *J. Liq. Chromatogr.*, 11 (1988) 547.
- 24 A. Berthod and D. W. Armstrong, *J. Liq. Chromatogr.*, 11 (1988) 567.
- 25 J. M. Mayer and B. Testa, *Helv. Chim. Acta*, 65 (1982) 1868.
- 26 *Log P and Parameter Database: a Tool for the Quantitative Prediction of Bio-activity*, Pomona College Medicinal Project, Comtex Scientific Corporation, New York, 1983.
- 27 J. M. Mayer, B. Testa, H. van de Waterbeemd and A. Bornand-Crausaz, *Eur. J. Med. Chem.*, 17 (1982) 453.
- 28 R. Collander, *Acta Chem. Scand.*, 4 (1950) 1085.
- 29 R. Collander, *Acta Chem. Scand.*, 5 (1951) 774.
- 30 R. C. Young, R. C. Mitchell, T. H. Brown, R. Ganellin, C. R. Griffiths, M. Jones, K. K. Rana, D. Saunders, I. R. Smith, N. E. Sore and T. J. Wilks, *J. Med. Chem.*, 31 (1988) 656.
- 31 H. van de Waterbeemd and B. Testa, *Adv. Drug Res.*, 16 (1987) 85-225.
- 32 A. Berthod and D. W. Armstrong, *J. Liq. Chromatogr.*, 11 (1988) 1187.
- 33 A. Berthod, Y. Han and D. W. Armstrong, *J. Liq. Chromatogr.*, 11 (1988) 1441.
- 34 S. Okada, H. Nakahara, C. Yomota and K. Mochida, *Chem. Pharm. Bull.*, 33 (1985) 4916.

CHROM. 21 312

π -ACCEPTOR AMIDE GROUP FOR LIQUID CHROMATOGRAPHIC CHIRAL SEPARATIONS WITH SPECIAL EMPHASIS ON THE 3,5-DINITRO-BENZOYL AMIDE^a

RICHARD DÄPPEN*

Central Research Laboratories, Ciba-Geigy Ltd., R-1060.2.14, CH-4002 Basle (Switzerland)
and

HEINRICH R. KARFUNKEL and FRANK J. J. LEUSEN

Central Research CAMM, Ciba-Geigy Ltd., CH-4002 Basle (Switzerland)

(First received July 21st, 1988; revised manuscript received January 12th, 1989)

SUMMARY

A series of achiral π -acceptor benzene derivatives and of achiral benzamide derivatives were chromatographed on a chiral and an achiral stationary phase to study the specific interactions of π -acceptor samples with a chiral π -donor stationary phase. The specific interactions with the chiral moiety of the stationary phase are expressed by the relative selectivity k'^* [$k'^* = k'$ (chiral phase)/ k' (achiral phase)]. To study the chiral recognition, a series of chiral phenylethylamine derivatives were chromatographed on the same two phases to determine the influence of the π -acceptor amide group on the chiral separation. The separation factor α does not correlate with the capacity factor k_2' but it correlates with the relative selectivity $k_2'^*$. If the aromatic moiety of the π -acceptor is flat, there is a correlation of the AMPAC-calculated LUMO (lowest unoccupied molecular orbital) with the relative selectivity k'^* . The 3,5-dinitrobenzoyl group ideally combines flatness with a low LUMO.

INTRODUCTION

The 3,5-dinitrobenzoyl (3,5-DNB) group was first incorporated into many solutes to extend the scope of a π -donor (chiral 9-anthryl-1,1,1-trifluoroethanol grafted to silica) chiral stationary phase¹. This led to the synthesis of the first chiral stationary phase (CSP) containing the 3,5-DNB group^{2,3} (e.g., 3,5-dinitrobenzoylphenylglycine phase). Many more chiral separations using such a π - π interaction have since been reported.

Pirkle and co-workers made substantial investigations of the chiral recognition mechanisms in which π - π interactions are involved. Based on the fact that the elution

^a Presented in part as a poster at the *1st International Symposium on the Separation of Chiral Molecules, Paris, May 31-June 2, 1988*. The proceedings of this symposium were published in *J. Chromatogr.*, Vol. 450, No. 2 (1988).

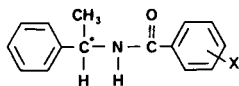


Fig. 1. General structure of the chiral phenylethylamine (PEA) derivatives investigated.

order can change within a series of homologous compounds, the concept of two competing chiral recognition processes was proposed⁴. Such processes ("dipole-stacking" and "hydrogen-bonded" mechanisms) have been found in many related separations⁵⁻¹¹. These processes include the interaction of amide groups of the CSP and the analyte combined with a parallel arrangement of the aromatic systems and steric interactions. One of these systems was investigated also by spectroscopic methods^{12,13}, confirming the importance of π - π interactions. In this paper we introduce an alternative method for studying π - π interactions in chiral chromatography.

To investigate the chiral separation mechanism of 3,5-DNB compounds on π -donor phase, we synthesized a series of π -acceptor compounds. The general structure of the chiral phenylethylamine (PEA) derivatives is shown in Fig. 1. These PEA compounds were chromatographed on (*R*)-*N*-pivaloylnaphthylethylamide [(*R*)-PNEA], a π -donor stationary phase considered previously¹⁴ (see Fig. 2).

Despite the structural similarity of the compounds, the capacity factors varied considerably. To study the chiral recognition, it was necessary to separate non-specific achiral effects due to the general polarity of the compounds from specific chiral effects due to complexation of the sample with the chiral moiety. We therefore use the relative selectivity k'^* [$k'^* = k'(\text{chiral phase})/k'(\text{achiral phase})$] to determine the tendency for each enantiomer to complex with the chiral stationary phase. An achiral phase is used as a reference phase to measure the polarity of a compound. Of course, the k'^* values depend on the choice of the reference phase. However, within a series of compounds, one can expect low k'^* values for compounds that are retained non-specifically and high k'^* values for compounds that are retained specifically on the chiral columns. On chiral π -donor columns, the latter should apply for compounds with a good π -acceptor group being retained by π - π interactions. For the other compounds, k'^* should be small and constant. If π - π interactions are important, there should be a correlation of the k'^* values with the electron affinity of the π -acceptor group¹⁵. As a measure of the electron affinity we use the LUMO (lowest unoccupied molecular orbital¹⁶) of the π -acceptor group. The concept of relative selectivity can also be used for a detailed discussion of the separation of a homologous series of 3,5-dinitrobenzoylamides on structurally related π -donor chiral stationary phases¹⁷.

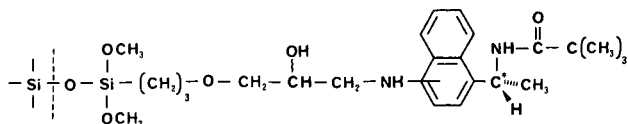


Fig. 2. Structure of the chiral π -donor phase (*R*)-*N*-pivaloylnaphthylethylamide [(*R*)-PNEA] used (mixture of positional isomers).

EXPERIMENTAL

The compounds were synthesized according to literature methods. Their identities were checked by NMR and mass spectrometry and elemental analysis.

Chromatography was performed on a Shimadzu LC-6A system at room temperature with *n*-hexane–isopropanol (4:1) as eluent. The dead volume was determined with toluene. The chiral phase (*R*)-PNEA was synthesized according to the literature¹⁴ based on Daltosil (4 μ m) (Serva, Heidelberg, F.R.G.). The achiral phase was aminopropyl-Si100 polyol (5 μ m) (Serva). Columns of 250 \times 4.6 mm I.D. were used at a flow-rate of 2 ml/min.

Structures were minimized by the semi-empirical quantum mechanical AMPAC program (QCPE Program No. 506) on a VAX-8650 and a FPS-164 computer using the AM1 and precise options. Conformational analysis was performed utilizing the molecular modelling package Chem-X (Molecular Modelling Systems, Chemical Design, Oxford, U.K.) and the local minima so found were reoptimized with AMPAC.

RESULTS AND DISCUSSION

Table I gives the chromatographic data for some achiral benzene derivatives on the chiral phase (*R*)-PNEA and on an aminopropyl phase, using the same eluent. The choice of the achiral reference column is arbitrary. An aminopropyl phase was chosen because there is a secondary amine present in the chiral phase. Without doing quantitative correlations, it can be seen that the k' values in Table I (on the chiral and achiral phases) do not correlate with the calculated molecular parameter LUMO. To do this, additional parameters for the general polarity of the compounds need to be considered, *e.g.*, the logarithm of the octanol–water partition coefficient^{18,19}. This would include hydrophobicity effects.

With the exception of 1,4-dinitrobenzene, the relative selectivity k'^* generally increases with decreasing LUMO. This means that the chiral phase with the π -donor moiety shows a greater tendency than the achiral phase to retain the π -acceptor

TABLE I

π - π -EFFECTS FOR ACHIRAL BENZENE DERIVATIVES ON (*R*)-PNEA RELATIVE TO AN AMINOPROPYL PHASE

The capacity factors were measured with *n*-hexane–isopropanol (4:1). Each LUMO was calculated with AMPAC. The relative selectivity k'^* is the ratio k' (PNEA)/ k' (aminopropyl).

Compound	k' (PNEA)	k' (amino)	k'^*	LUMO
Benzene	0	0	—	0
Nitrobenzene	0.49	0.20	2.5	-1.06
1,4-Dinitrobenzene	0.93	0.37	2.5	-2.21
1,2-Dinitrobenzene	4.15	1.44	2.9	-1.84
1,3-Dinitrobenzene	1.62	0.54	3.0	-2.08
1,3-Dinitro-5-cyanobenzene	2.59	0.83	3.1	-2.26
1,3,5-Trinitrobenzene	2.81	0.82	3.4	-2.53

samples in Table I. For a series of structurally related compounds the empirical k'^* value can therefore be used as an indicator of π - π interactions in retention processes.

Table II shows similar chromatographic data for some substituted achiral benzamide derivatives. There is no correlation between the relative selectivity k'^* and the LUMO. With the exception of 3-nitrobenzamide, k'^* correlates with the LUMO for those benzamides whose substituents are in the plane of the aromatic ring. As in Table I, k'^* generally increases with decreasing LUMO. 3,5-Diaminobenzoylamide, a π -donor compound, also has a low relative selectivity.

Of course, the relative selectivity of a compound does not depend exclusively on the π -acceptor group. The effects of the N-substituent is shown in Table III for 3,5-dinitrobenzamides. Relative to the unsubstituted 3,5-dinitrobenzamide, the substituted test compounds have smaller capacity factors on the aminopropyl phase, which reflects the general polarity of these compounds. However, on the chiral phase, not all capacity factors are smaller. This shows that the complexation of the samples with the chiral phase can be very tight owing to additional interactions. Therefore, in order to rationalize the retention mechanism of 3,5-dinitrobenzoyl amides on PNEA, attractive interactions between the N-substituents and the phase must be considered.

The data in Tables I-III show that the chiral phase is on average 2.5 times more polar than the aminopropyl phase used in our investigation. A relative selectivity k'^* between 2 and 3 corresponds to non-specific complexation of the sample due to some sort of hydrophobic effects on the chiral and the achiral phases. Compounds with a relative selectivity higher than 3 are retained on the chiral phase due to specific interactions. Only for such compounds can one expect a large chiral separation to occur. On the other hand, small α -values can be due to interactions that are less specific or due to various specific interactions that cancel the effect of each other. These aspects were studied with the chiral PEA derivatives in Fig. 1.

TABLE II

π - π EFFECTS FOR ACHIRAL BENZAMIDE DERIVATIVES ON (R)-PNEA RELATIVE TO AN AMINOPROPYL PHASE

Details as in Table I. In each instance the LUMO of the N-methyl compound was calculated.

Substituent	k' (PNEA)	k' (amino)	k'^*	LUMO
None	3.31	1.71	1.9	-0.19
3,5-Diamino	31.5	11.2	2.8	+0.18
3-Cyano	7.23	2.85	2.5	-0.74
4-Cyano	7.76	3.09	2.5	-0.89
2-Nitro ^a	21.3	6.06	3.5	-1.33
3-Nitro	9.04	2.69	3.4	-1.31
4-Nitro	7.70	2.48	3.1	-1.51
3-Nitro-5-methoxycarbonyl	7.80	2.57	3.0	-1.57
2,6-Dinitro ^a	25.4	12.1	2.1	-1.87
3,4-Dinitro ^a	22.1	7.12	3.1	-2.14
3,5-Dinitro-2-methyl ^a	7.22	2.79	2.6	-2.11
3,5-Dinitro	9.78	2.82	3.5	-2.23

^a Flat arrangement of the molecule very unfavourable according to AMPAC.

TABLE III

RELATIVE SELECTIVITIES, k'^* , FOR SOME N-SUBSTITUTED 3,5-DINITROBENZOYL AMIDES ON (R)-PNEA RELATIVE TO AN AMINOPROPYL PHASE

Details as in Table I.

Substituent	k' (PNEA)	k' (amino)	k'^*
None	9.78	2.82	3.5
CH ₃	7.51	2.13	3.5
C ₆ H ₅ ^a	7.58	2.22	3.4
cyclo-C ₆ H ₁₁	4.08	1.01	4.0
CH ₂ -C ₆ H ₅	7.92	1.60	5.0
CH ₂ -1-naphthyl ^b	15.7	2.06	7.6
CH ₂ -C ₆ H ₅ and CH ₃	2.16	0.82	2.6
CH ₂ -C ₆ H ₄ - <i>o</i> -F	7.42	1.60	4.6
CH ₂ -C ₆ H ₄ - <i>o</i> -OCH ₃	8.94	1.87	4.8
CH ₂ -C ₆ H ₃ - <i>m,p</i> -Cl ₂	9.22	2.53	3.6
CH ₂ -C ₆ H ₃ - <i>o,p</i> -Cl ₂	6.98	1.63	4.3

^a Significantly different LUMO owing to conjugation with the N-substituent.^b Highest k' (PNEA), although the compound is less polar than many of the other compounds within this series.

Table IV gives the chromatographic and calculated data for the chiral test compounds. The changes in the k' and α -values must be attributed to the benzamide moiety, the only part varied. It is obvious that the k_1' and k_2' do not correlate with the separation factor α . The capacity factors are very high if the amide group is far out of the plane of the aromatic ring (2-nitro- and 2,6-dinitro compounds). The corresponding retention process does not give a large chiral separation. The specific retention of the test compounds on (R)-PNEA, expressed as k'^* , is high if the amide group is almost coplanar with the aromatic group and if the compound has a low LUMO (3-nitro-5-methoxycarbonyl-, 3,5-dicyano-, 3-nitro-5-cyano- and 3,5-dinitro-compounds). For these compounds without any substituents *ortho* to the amide and with planar substituents, the chiral separation factor α increases with decreasing LUMO. Additionally, both $k_1'^*$ and $k_2'^*$ increase with decreasing LUMO. One can therefore conclude that the first and second eluted enantiomers of these compounds are retained by similar retention processes, both involving π - π interactions. For the other compounds in Table IV alternative retention processes are probable.

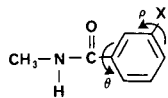
As is to be expected, the separation factor α correlates generally with the relative selectivity k'^* . Within the series, $k_1'^*$ is not constant and can reach significant values, e.g., the relative selectivity $k_1'^*$ of the 3,5-DNB compound is higher than most of the $k_2'^*$ values in Table IV. Therefore, a proper discussion of retention mechanisms for a series of compounds should include the specific complexation of the first and second eluted enantiomers. In our series of compounds we did not find a derivative of PEA with high $k_1'^*$ and $k_2'^*$ (greater than 3) and a small α -value. No competing chiral processes are operating in our system of PEA-benzamides of (R)-PNEA.

The naphthoyl derivatives have a very low LUMO. Unfortunately, the nitro groups are not in the plane of the aromatic system. The chiral recognition is not better than that for the 3,5-DNB derivative. The naphthoyl compounds were not eluted

TABLE IV

CHROMATOGRAPHIC RESULTS OF THE CHIRAL PEA COMPOUNDS ON (*R*)-PNEA AND ON AN AMI-NOPROPYL PHASE, AND CALCULATED DATA

k_1' = capacity factor of the first eluted enantiomer; k_2' = capacity factor of the second eluted enantiomer; α = separation factor; $k'(a)$ = k' (amino); k'^* and LUMO, see Tables I and II. AC, absolute configuration of the better retained enantiomer. The naphthoyl derivatives were chromatographed with *n*-hexane-isopropanol (3:2); ne = not eluted. R according to Fig. 1. The net atomic charges on the amide hydrogens were virtually constant throughout the series. Definition of angle θ , ρ_1 , ρ_2 and ρ_3 as illustrated.



Structure	k_1'	k_2'	α	$k'(a)$	$k_1'^*$	$k_2'^*$	AC	LUMO	θ	ρ_1	ρ_2	ρ_3
	1.88	1.97	1.04	0.91	2.07	2.16	R	-0.11	37 ^{a,b}			
	8.57	8.91	1.04	2.96	2.90	3.01		-1.27	70	33		
	3.75	4.48	1.14	1.52	2.47	2.82	R	-1.31	34	0		
	2.89	3.20	1.11	1.43	2.02	2.24		-1.46	40	0		
	4.36	5.98	1.37	1.22	3.57	4.90	R	-1.57	39	0	0	
	4.34	6.52	1.50	1.81	2.36	3.54		-1.20	37			
	5.58	9.15	1.70	1.71	3.15	5.35		-1.73	38	0		
	2.40	2.60	1.08	1.29	1.86	2.02	R	-2.11	74	20	0	
	5.53	6.78	1.23	3.12	1.77	2.17		-2.11	37	38	38	
	17.2	17.9	1.04	7.07	2.43	2.53		-1.93	80	35	15	

TABLE IV (continued)

Structure	k_1'	k_2'	α	$k' (a)$	$k_1'^*$	$k_2'^*$	AC	LUMO	θ	ρ_1	ρ_2	ρ_3
	7.09	13.3	1.88	1.52	4.66	8.75	R	-2.23	37	0	0	
	8.30	14.5	1.75	ne	-	-		-2.71	35	40	40	0
	6.4	11.5	1.80	ne	-	-		-2.85	35	40	40	35

^a In good agreement with X-ray data (26.1° for benzamide²⁰).

^b Planar conformation less stable by 1.05 kcal/mol.

from the aminopropyl column with *n*-hexane-isopropanol. Therefore, the relative selectivity was not accessible.

The relative selectivities of the chiral compounds correlate well with the relative selectivities of the corresponding achiral compounds in Table II. This indicates that the π -acceptor amide group controls the retention in both instances. To study further the retention mechanism of 3,5-dinitrobenzoyl compounds with π -donors, we calculated the most favourable conformations of simplified PNEA and the chiral PEA-3,5-DNB as shown in Fig. 3. The chosen 3,5-DNB sample is a simple case with only two conformational minima. (*R*)-PNEA is more complicated, with three minima. The corresponding data are given in Table V. Fig. 4 shows stereo views of PEA-3,5-DNB and (*R*)-PNEA in their minimum energy conformations. Using these conformations, diastereomeric adsorption complexes according the "hydrogen-bonded" or the "dipole-stacking" process⁴ cannot be formed without considerable conformational changes. This was studied using computer assisted molecular modeling; the results will be published elsewhere²¹. Although we do not propose any structure for the diastereomeric adsorption complexes in this paper, we would point out that the relative selectivity (and the capacity factor) for the achiral benzyl-3,5-DNB (see Ta-

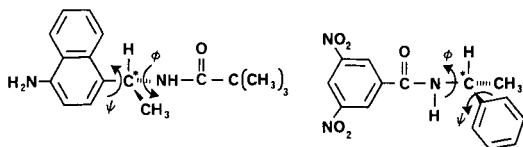


Fig. 3. Structure of the compound used to simulate (*R*)-PNEA with the computer and the chiral test compound (*R*)-PEA-3,5-DNB. For (*R*)-PNEA $\phi = C_1-C^*-N-C$ and for $\psi = C_2-C_1-C^*-N$ [analogously for (*R*)-PEA-3,5-DNB].

TABLE V

COMPUTED AMPAC ENERGETIC MINIMA, E (kcal/mol), OF (*R*)-PNEA AND THE 3,5-DI-NITROBENZOYLAMIDE OF (*R*)-PEA

The torsion angles Φ and Ψ are defined as shown in Fig. 3.

Parameter	(<i>R</i>)-PNEA (min. 1)	(<i>R</i>)-PNEA (min. 2)	(<i>R</i>)-PNEA (min. 3)	(<i>R</i>)-PEA- 3,5-DNB (min. 1)	(<i>R</i>)-PEA- 3,5-DNB (min. 2)
Φ	114.4°	120.8°	-82.1°	102.8°	-79.1°
Ψ	91.4°	-118.8°	68.9°	24.2°	68.7°
E	-17.00	-15.32	-14.09	24.17	26.17

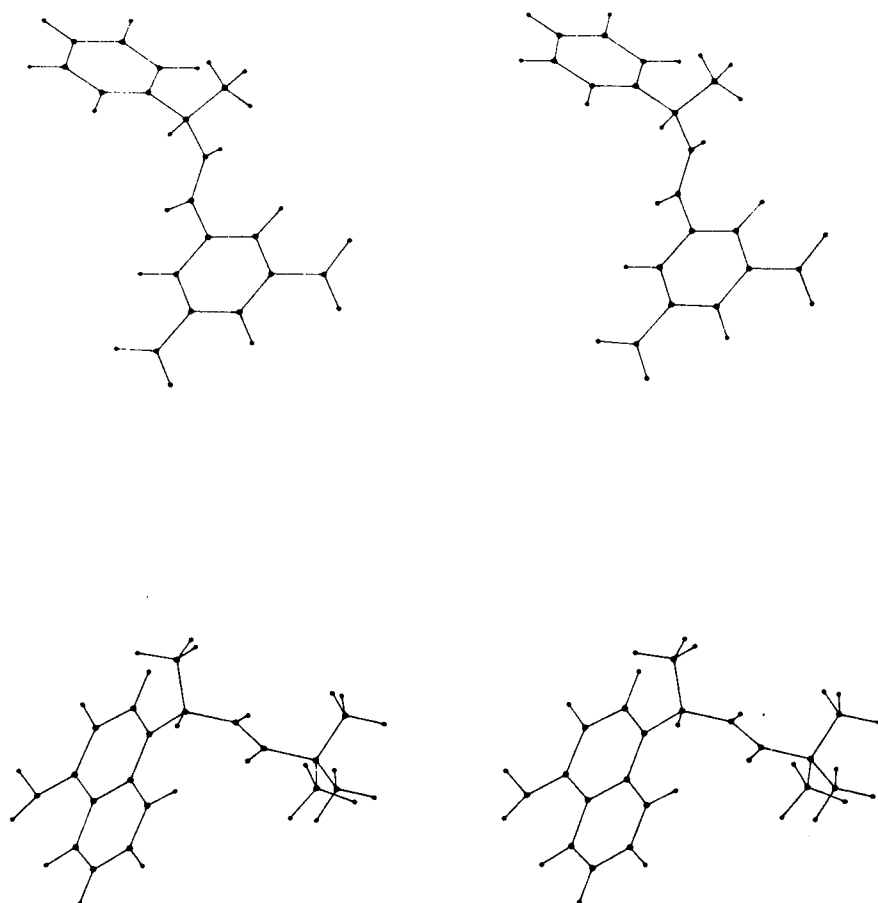


Fig. 4. Stereo view of the energetically most favourable conformations of (*R*)-PNEA and (*R*)-PEA-3,5-DNB, as calculated with AMPAC.

ble III) is closer to the relative selectivity of the first eluted (*S*)-PEA-3,5-DNB (see Table IV) than the last eluted (*R*)-PEA-3,5-DNB. This is not easily rationalized using the concept of attractive interactions of the π - and amide groups combined with steric repulsion of alkyl and aryl groups. To rationalize this elution order we therefore propose to consider several attractive interactions of (*R*)-PEA-3,5-DNB with (*R*)-PNEA (interaction of the benzamide group and interactions of the phenyl and the methyl group). For the (*S*)-PEA-DNB less attractive interactions (interaction of the benzamide group and interaction of the phenyl or methyl group) would be possible. The achiral benzyl-3,5-DNB also has less possibility of interacting with (*R*)-PNEA than the (*R*)-PEA-3,5-DNB (interaction of the benzamide group and interaction of the phenyl group), resulting in a similar retention to that of the (*S*)-PEA-3,5-DNB.

CONCLUSIONS

For the series of phenylethylamine- π -acceptor amides on the π -donor stationary phase (*R*)-PNEA, the separation factor α generally increases with increasing relative selectivity k_2' . There was no case with high k_2' and small α . However, the relative selectivities k_1' are neither constant nor negligible. The 3,5-dinitrobenzoyl-amide group has a great tendency to complex with the chiral phase. This seems to be possible owing to lack of *ortho* substituents (favouring a flat arrangement of the benzamide moiety) and a low LUMO. The π - π interaction and the interaction of the amide groups bring the sample into very close proximity with the phase, so that the other groups at the chiral centre can interact with the phase. More investigations are necessary to decide whether the concept of steric repulsion or a concept based on Van der Waals attractions must be used to discuss the chiral recognition processes.

ACKNOWLEDGEMENT

We thank Dr. Romain Wolf for valuable discussions.

REFERENCES

- 1 W. H. Pirkle and D. W. House, *J. Org. Chem.*, 44 (1979) 1957.
- 2 W. H. Pirkle, D. W. House and J. M. Finn, *J. Chromatogr.*, 192 (1980) 143.
- 3 W. H. Pirkle and J. M. Finn, *J. Org. Chem.*, 46 (1981) 2935.
- 4 W. H. Pirkle, M. H. Hyun and B. Bank, *J. Chromatogr.*, 316 (1984) 585.
- 5 W. H. Pirkle and M. H. Hyun, *J. Chromatogr.*, 322 (1985) 309.
- 6 W. H. Pirkle and M. H. Hyun, *J. Chromatogr.*, 328 (1985) 1.
- 7 W. H. Pirkle, T. C. Pochapsky, G. S. Mahler and R. E. Field, *J. Chromatogr.*, 348 (1985) 89.
- 8 W. H. Pirkle, G. S. Mahler, T. C. Pochapsky and M. H. Hyun, *J. Chromatogr.*, 388 (1987) 307.
- 9 W. H. Pirkle and R. Däppen, *J. Chromatogr.*, 404 (1987) 107.
- 10 I. W. Wainer, T. O. Doyle, F. S. Fry Jr., and Z. Hamidzadeh, *J. Chromatogr.*, 355 (1986) 149.
- 11 G. Krüger, J. Grötzinger and H. Berndt, *J. Chromatogr.*, 397 (1987) 223.
- 12 W. H. Pirkle and T. C. Pochapsky, *J. Am. Chem. Soc.*, 108 (1986) 5627.
- 13 W. H. Pirkle and T. C. Pochapsky, *J. Am. Chem. Soc.*, 109 (1987) 5975.
- 14 R. Däppen, V. R. Meyer and H. Arm, *J. Chromatogr.*, 361 (1986) 93.
- 15 A. Streitwieser, *Molecular Orbital Theory for Organic Chemists*, Wiley, New York, 1961, p. 199.
- 16 I. Fleming, *Frontier Orbitals and Organic Chemical Reactions*, Wiley, New York, 1976 (reprinted 1978), p. 19.
- 17 R. Däppen, V. R. Meyer and H. Arm, *J. Chromatogr.*, 464 (1989) 39.

- 18 C. Hansch and A. J. Leo, *Substituent Constants for Correlation Analysis in Chemistry and Biology*, Wiley, New York, 1979, pp. 1-339.
- 19 R. L. Lopez de Compadre, A. J. Shusterman and C. Hansch, *Int. J. Quantum Chem.*, 34 (1988) 91.
- 20 C. C. F. Blake and R. W. H. Small, *Acta Crystallogr., Sect. B.*, 28 (1972) 2201.
- 21 R. Däppen, H. R. Karfunkel and F. J. J. Leusen, *J. Am. Chem. Soc.*, submitted for publication.

CHROM. 21 316

IONIZATION OF DEAE-CELLULOSE

DEPENDENCE OF pK ON IONIC STRENGTH

MARVIN A. SMITH* and PAUL C. GILLESPIE

Graduate Section of Biochemistry, 226 Eyring Science Center, Brigham Young University, Provo, UT 84602 (U.S.A.)

(Received January 5th, 1989)

SUMMARY

The salt dependence of the ionization of DEAE-cellulose has been investigated using potentiometric acid–base titrations. Two ionizable groups were identified. The pK of the major group was exponentially related to ionic strength. However, the minor group was very much less sensitive to changes in ionic strength. The fraction of total ion-exchange sites represented by the minor group decreased with increasing salt concentrations and was insignificant in back titrations with sodium hydroxide, suggesting the elimination of structural or electrostatic barriers which otherwise sequester a significant fraction of potential ion-exchange sites which resist ionization.

INTRODUCTION

Ion-exchange chromatography continues to be one of the most useful and powerful methods for isolation and purification of polyelectrolytes. The development of recombinant DNA techniques, and commercial exploitation of these techniques for large scale production of biologically important proteins and peptides, has become an important driving force behind technical development of chromatographic separations¹. This renewed emphasis has led to modifications of previously well established methods². Since the initial introduction of substituted celluloses³ other materials such as dextrans, polyacrylamide⁴ and more recently polyethyleneimine coated silica⁵ have been successfully applied to the purification of proteins by gel and high-performance ion-exchange chromatography. It is significant that pellicular supports have the same general mobile phase elution characteristics as conventional gel-type ion exchangers, and that ionic and pH conditions that work well for the latter are usually suitable for high-performance columns^{2,6}. Although there has been a significant shift from classical gel-type to high-performance media⁶ the former is still commonly used in large scale and preparative procedures. Despite the availability of many types of ion exchangers, diethylaminoethyl and carboxymethyl modified exchangers are perhaps the most commonly used. This is a consequence of improvements in physical and chemical characteristics of these exchangers. In a previous communication⁷ we have tested a model, based essentially on the law of mass action as applied by Langmuir to

surface phenomena, to the ion-exchange elution characteristics of a homologous polylysine series. Although the validity of the model is limited by simplifying assumptions, it does explain many characteristics observed in the ion exchange of polyelectrolytes, such as proteins. The relationship of various process parameters on resolution has also been investigated^{2,8,9}, and the effect of salt on the capacity¹⁰ of some ion exchangers has been demonstrated, *i.e.*, the salt dependence of the $pK^{2,11,12}$. The importance of local charge distribution on chromatographic behavior of proteins has also been superbly documented¹³, as has the observation that very small ionic strength changes can result in large elution volume differences of polyelectrolytes^{7,14}. As a correlary to the latter, in this communication we describe changes in the ionic structure of DEAE-cellulose that are exponentially related to salt concentration, and putative changes in local charge distribution, as observed by potentiometric acid-base titrations.

EXPERIMENTAL

Buffers

The following reference buffers were prepared as described¹⁵: phosphate (0.025 *M* KH_2PO_4 , 0.025 *M* Na_2HPO_4) pH 6.87 at 23°C, borate buffer (0.01 *M* $Na_2B_4O_7$) pH 9.205 at 23°C. These buffers were prepared in double distilled, boiled water and stored under argon or nitrogen.

Solutions

Sodium chloride (Mallinckrodt, Analytical Reagent) solutions were prepared in double distilled, boiled water and stored under argon or nitrogen. After bubbling nitrogen, to remove CO_2 , solutions of higher salt concentration remained basic and were titrated dropwise to neutrality (pH 6.8–7.2) with 0.001 *M* HCl.

Titants

HCl (Baker, Reagent) and NaOH (Mallinckrodt, Anal. Reagent) were prepared in double distilled boiled water, standardized against Tris [tris(hydroxymethyl)amino-methane] (Fisher Scientific) and against potassium biphthalate (Baker, Reagent) respectively, and stored under argon or nitrogen. During titration, titrants were protected with Ascarite-filled caps. NaOH was passed through a Dowex-1 column to remove carbonates.

DEAE-cellulose

Whatman (DE-52 microgranular, preswollen, 1.0 mequiv./g); BioRad (Cellex-D, 0.66 mequiv./g); Mann Research (Mannex-DEAE, 1.1 mequiv./g; Sigma (DEAE-cellulose, 0.89 mequiv./g). Celluloses were processed by washing with 0.5 *M* HCl (30 min), with water, then 0.5 *M* NaOH (30 min), then water until effluent was neutral.

Titration procedure

All titrations were carried out with a Radiometer automatic titrator (pHM26, ABU12, TTT11, SBR2c) and electrode (GK2301c). The pH meter was accurate to ± 0.007 pH units from pH 0 to 12. The buret capacity was 2.5 ± 0.0025 ml. Titration rates were from 0.03125 to 0.125 ml/min. Results from faster titration rates were not

significantly different from those obtained at slower rates. The pH meter was standardized with phosphate and borate buffers and rechecked before and after each titration. Titrations were carried out in 20.0 ml of water or salt. Nitrogen, scrubbed with Ascarite and washed with sulfuric acid and then water, was bubbled through the solutions, which were adjusted if necessary to neutrality (pH 6.8–7.2) with 0.001 *M* HCl and the normality of initial salt solutions corrected accordingly. Similar corrections were made following addition of DEAE-cellulose (about 0.6 mequiv.). No precipitates were obtained from alkaline extracts of cellulose upon addition of BaCl₂. Base titrations were carried out following acid titrations using the resulting hydrochloride form of the exchangers.

Determination of pK values

Equivalence points and *pK* values were determined graphically from tangential lines drawn through inflection points using standard procedures¹² as shown for a typical acid titration curve (Fig. 1). Inflection points of steep portions of the curves were assumed to represent equivalence points. *pK* values at each salt concentration were calculated from several (2–4) independent titrations and uncertainties calculated for a 0.95 probability.

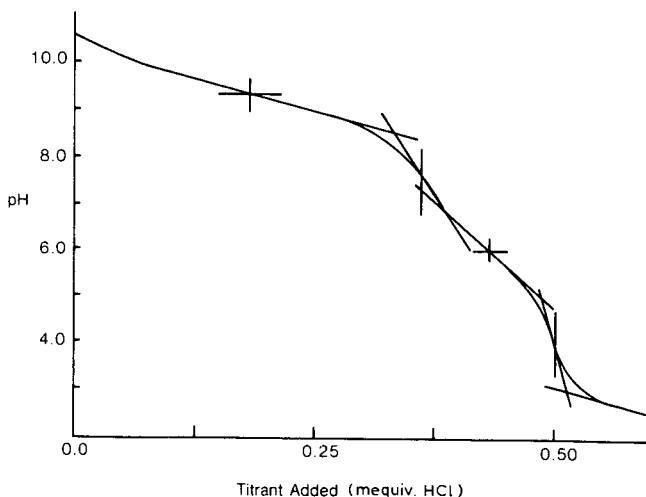


Fig. 1. Typical acid titration curve of DEAE-cellulose. Preswollen DEAE-cellulose (2.0 g, Whatman DE-52) was titrated with HCl (0.241 *M*) in NaCl (0.20 *M*). Standard graphical methods were used to calculate *pK* values and end points, as shown.

Kjeldahl determinations for total nitrogen content were run by standard procedures by the Department of Agronomy and Horticulture of this university.

Calorimetric titrations were run on a Tronac Model 450 isoperibol titration calorimeter using standard procedures²⁰, in cooperation with Dr. Lee D. Hansen.

RESULTS

In the present study microgranular DEAE-cellulose was chosen because of its improved matrix and distribution of charged groups¹⁶. Such ion exchangers purportedly are structurally more reproducible, have faster kinetics, higher capacity, and give maximum resolution (see Whatman Technical Bulletin). Since precycling is necessary to release full capacity and provide optimum interaction with large molecules, all exchangers used in this study were precycled as described in Experimental. Care was also taken to remove CO₂ in order to avoid artifacts caused by the high affinity of carbonate and bicarbonate for DEAE-cellulose.

When determined directly from acid-base titration curves, the *pK* values of DEAE-cellulose³ and various polyethyleneimine-coated silica exchangers² are known to be dependent on salt concentration. The *pK* of DEAE-cellulose is about 8.0 in water and 9.5 in NaCl (0.5–1.0 *M*)¹². PEI6-LiChrosorb Si 100 anion exchanger used in high-performance ion-exchange chromatography (HPIEC)⁵ is similar in this respect. During the last 25 years ionic-strength gradients, at fixed pH values, have been widely used to purify specific components from complex mixtures of proteins and other electrolytes using ion-exchange chromatography². Since the ionic structure or configuration, as expressed by the *pK*, of numerous ion exchangers is subject to change under such conditions, a more detailed investigation of the characteristics of such salt dependent *pK* changes is warranted in order to optimize column performance. DEAE-cellulose was specifically selected for a more detailed investigation of the dependence of *pK* on salt concentration, because of its wide use in large scale purification of proteins and enzymes².

Aqueous slurries containing about 0.6 mequiv. of the free amine (of DEAE-cellulose) in 20.0 ml of water, or various concentrations of NaCl, were titrated with HCl (0.24 *M*). A typical titration curve, obtained in 0.20 *M* NaCl, is shown in Fig. 1. Two apparent buffering regions are observed, a major one at about pH 9.3 and a minor one at about 6.0. The graphic method used for calculating end points and *pK* values is also illustrated. Similar titrations were carried out under other ionic conditions, and *pK* values and end point determined as described above. The major acid titratable group (about 70%) has a salt-dependent *pK* ranging from 6.92 in water to 9.70 in 2.0 *M* NaCl, Table I. The *pK* increased dramatically in dilute salt (0.0–0.2 *M* NaCl) after

TABLE I

EFFECT OF SODIUM CHLORIDE CONCENTRATION ON THE OBSERVED *pK* OF THE MAJOR ACID-TITRATABLE GROUP OF DEAE-CELLULOSE (WHATMAN DE-52)

<i>NaCl</i> (<i>M</i>)	Corrected Cl ⁻ (<i>M</i>)	Ave. <i>pK</i>
0.00	0.00	6.92 ± 0.06
0.01	0.0095	8.35 ± 0.24
0.05	0.048	8.98 ± 0.06
0.10	0.095	9.15 ± 0.09
0.20	0.19	9.28 ± 0.09
0.30	0.29	9.43 ± 0.1
0.50	0.47	9.47 ± 0.1
1.00	0.93	9.59 ± 0.03
2.00	1.82	9.70 ± 0.02
6.24 (satd.)	6.24	9.83 ± 1.0

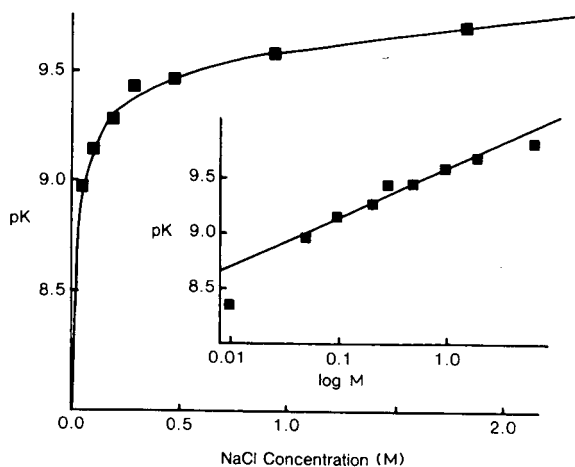


Fig. 2. Effect of increasing salt concentration on the pK of DEAE-cellulose. pK values were determined by acid titration of the free amine in various concentrations of NaCl, as shown in Fig. 1. Values were averaged from 2-4 titrations. Normalities were corrected for volume changes resulting from added titrant.

which it asymptotically approached the putative limiting value of aqueous solutions of diethylaminoethanol³. As shown in Fig. 2, the pK of this group is, as a first approximation, exponentially related to sodium chloride concentration. A departure from this logarithmic relationship was observed in salt concentrations of 0.01 M or less, where continual pH drifts were encountered and reproducible results were difficult to obtain. This difficulty has previously been reported^{3,5}, and may be a consequence of poor access of the titrant to the hydrated but insoluble cellulose matrix under these conditions. Reproducible results were also difficult to obtain in saturated NaCl titrations.

The pK of the minor group (about 30%) is relatively insensitive to change in salt concentration and has a value of about 6, Table II. However the percent of this minor

TABLE II

EFFECTS OF SODIUM CHLORIDE CONCENTRATION ON THE OBSERVED pK AND THE AMOUNT OF THE MINOR ACID-TITRATABLE GROUP OF DEAE-CELLULOSE (WHATMAN DE-52)

NaCl (M)	pK		Ave. pK	Ave. % ^a
	Run 1	Run 2		
0.01	5.98	—	5.98	43
0.05	5.86	5.87	5.87	34
0.1	6.01	5.93	5.97	27
0.2	6.04	6.05	6.04	27
0.3	6.03	6.14	6.09	26
0.5	5.96	6.18	6.07	24
1.0	6.00	6.17	6.08	23

^a Calculated as percent of total mequiv. titrated.

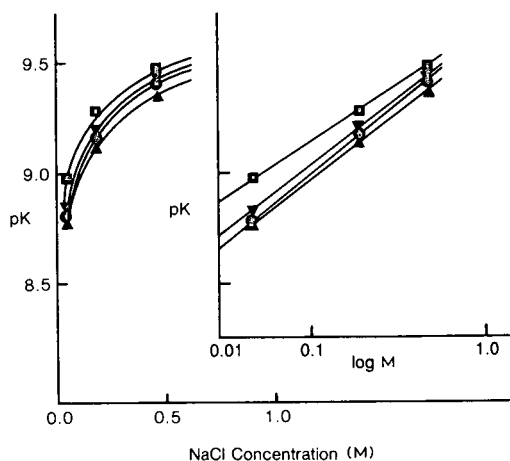


Fig. 3. Effect of increasing salt concentration on the pK values of various commercially available DEAE-celluloses. Values were determined as described in Figs. 1 and 2. pK values were averaged from 2 or 3 titrations. (▲) Sigma; (●) Mannex; (▼) Bio-Rad; (■) Whatman.

group, relative to total acid titratable groups, decreases from about 43% in dilute salt (0.01 M) to 23% in 1.0 M NaCl.

Several commercially available DEAE-cellulose preparations were similarly titrated and compared over a limited range of salt concentrations (Fig. 3). BioRad, Cellex-D, Mannex-DEAE, and Sigma DEAE-celluloses gave similar results. The difference in the slope (log plot) of DE-52 (Whatman) may represent differences in the preparation of this microgranular ion exchanger.

Because of differences in the ionic structure or local charge distribution of the hydrochloride form of DEAE-cellulose relative to the free tertiary amine, basic titrations were also carried out. Calculated pK values at various salt concentrations were very similar to those obtained with acid titrations, Table III. In fact, the relationship between these titration parameters in acid and base, for the major titratable group, was identical, *i.e.*, alkaline titration data were super imposable with those shown in Fig. 2. However the minor buffering group observed in acid titrations, which decreased dramatically with increasing salt concentration, was much less pronounced in basic titrations and disappeared entirely with increasing salt concentrations (data not shown).

TABLE III
EFFECT OF SODIUM CHLORIDE CONCENTRATION ON THE OBSERVED pK OF THE BASE TITRATABLE GROUP OF DEAE CELLULOSE (WHATMAN DE-52)

NaCl (M)	Corrected Cl^- (M)	Ave. pK
0.05	0.047	9.00 ± 0.25
0.20	0.18	9.25 ± 0.06
0.50	0.44	9.44 ± 0.04

DISCUSSION

Acid–base titration has been used to characterize changes in charge distribution of DEAE-cellulose, as expressed by pK changes with increasing salt concentration. Although this salt dependence is well known^{11,12} it has never really been studied in detail. In the majority of experiments described in this communication, Whatman DE-52 microgranular, preswollen ion exchanger (1.0 mequiv./g) was used. The ion exchange capacity calculated from potentiometric (0.96 ± 0.01 mequiv./g) and calorimetric acid titrations (0.99 ± 0.09 mequiv./g) agreed with the manufacturer's value (1.00 mequiv./g), while Kjeldahl total nitrogen values (average of five separate determinations) were somewhat lower (0.90 ± 0.03 mequiv./g dry weight). We have consistently observed that the first of a repeated series of potentiometric acid titrations (using prewashing conditions described in Experimental) gives an exchange capacity significantly higher (10–15%) than subsequent titrations (e.g. 0.01 *M* NaCl: 0.472, 0.404, 0.415, 0.405, 0.418 mequiv.; 0.10 *M* NaCl: 0.530, 0.467, 0.471, 0.456 mequiv.). This phenomenon was observed for all concentrations of NaCl. It might simply be a consequence of residual NaOH contaminating DEAE-cellulose preparations after the final water wash (see Experimental), or perhaps an artifact caused by contaminating quaternary ammonium groups in the hydroxide form.

Several explanations have been given for the observed salt dependence of various ion exchanger materials, including the putative requirement for “bound” counter ions by “insoluble resins”¹¹. If this explanation is correct, at pH values near the pK added salt would shift the equilibrium toward ionization, stabilizing the protonated form of the tertiary amine and shifting the pK to higher values. Another explanation is the putative “inaccessibility” of interior groups because of “electrostatic shielding” at low ionic strength^{3,12}. The contribution of electrostatic interaction can be estimated using the semi-empirical equation of Kern¹⁷, $pH = pK + n \log (1 - \alpha)/\alpha$, where α is the degree of ionization and n the putative extent of electrostatic interaction, which should approach unity in dilute aqueous solutions. The potentiometric acid titration data for the major salt dependent ionic group does give a series of straight lines, as predicted by the Kern equation (Fig. 4). Values of n calculated from the slope at each salt concentration are shown in Table IV. This data suggests that in 0.2 *M* NaCl or above, where n is nearly unity, the DEAE-groups behave much like “soluble” amines with negligible electrostatic interaction. At lower salt concentrations, however, the value of n increases proportionally from 1.0 to about 1.3 or 1.4 in distilled water, suggesting a moderate dependence of pK on the degree of ionization.

Of practical importance is the exponential relationship between salt concentration and pK (Fig. 2). Salt gradient elution techniques common in ion exchange chromatography of proteins, have the potential of generating such pK changes and subsequent ionic strength or pH shifts^{12,18,19}. The latter are easily observed in batch experiments by addition of salt to aqueous slurries of DEAE-cellulose at pH values near the pK . With increasing salt the limiting value of the pK is expected to approach that of soluble diethylaminoethanol (9.9) (ref. 3) as observed in Table I. Since elution characteristics of polyelectrolytes, such as many proteins, are very sensitive to small pH or ionic strength changes^{7,14}, salt dependent increases in pK could generate elution artifacts.

The pK of the minor titratable group (about 6.0, Fig. 1) varied little (less than

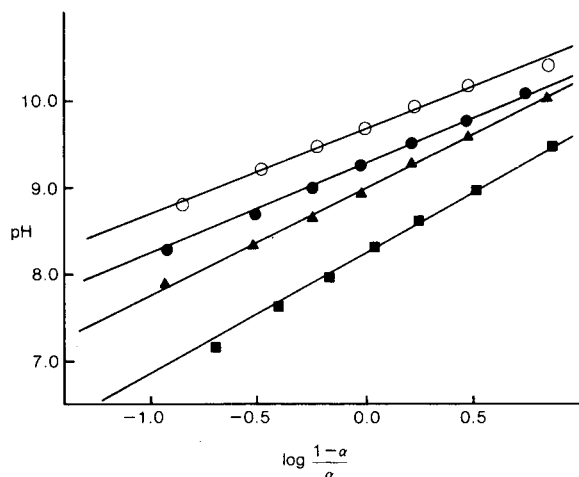


Fig. 4. The relationship between pH and the ionization of DEAE-cellulose, at various concentrations of sodium chloride. The degree of ionization (α) was assumed to be equal to the degree of neutralization or the fraction titrated. The extent of electrostatic interaction (n) was calculated from the slopes at various concentrations of NaCl, and is shown in Table IV¹⁷. (○) 2.00; (●) 0.20; (▲) 0.05; (■) 0.01 *M* NaCl.

4%) with increasing salt concentration, Table II. Although its fraction of the total potential ion exchange groups is significant in water or dilute salt (43%), this fraction decreases significantly with increasing salt concentration, Table II, and is hardly detectable in alkaline back titrations. This apparent minor group may be an artifact generated by non-equilibrium conditions in low salt. Continuous pH drifts observed with manual titrations at extremely slow flow-rates (one drop at a time), are consistent with this possibility. Such pH drifts were not observed in the absence of DEAE-cellulose. These observations suggest that a significant fraction of potential ion exchange

TABLE IV
EFFECT OF SODIUM CHLORIDE CONCENTRATION ON THE ELECTROSTATIC INTERACTION (n) OF DEAE-CELLULOSE

Values were determined from acid titration data as shown in Fig. 4.

NaCl (<i>M</i>)	<i>pK</i>	<i>n</i>	r^{2a}
0.00	7.01	1.28	0.98
0.01	8.25	1.39	1.00
0.05	9.00	1.25	1.00
0.10	9.14	1.13	1.00
0.20	9.28	1.03	1.00
0.30	9.40	1.01	1.00
0.50	9.47	1.04	1.00
1.00	9.58	1.02	0.99
2.00	9.68	0.96	1.00
6.24 (satd.)	9.77	1.14	0.99

^a r = simple correlation coefficient.

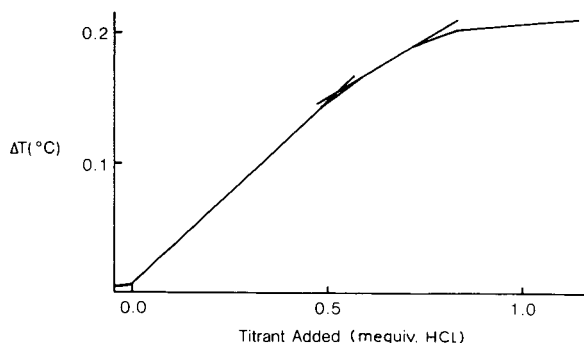


Fig. 5. Thermogram of the acid titration of DEAE-cellulose. DEAE-cellulose (0.84 g, Whatman DE-52) was titrated in water (35 ml) with HCl (0.531 *M*).

groups are sequestered in the cellulose matrix while in the neutral unprotonated form, perhaps stabilized by hydrogen bonding to neighboring glucose residues, and that optimum column performance can only be expected following ionization by an initial acid wash.

Thermograms obtained from preliminary calorimetric acid titration experiments (Fig. 5), also demonstrate the existence of two distinct groups, a major and a minor. However, in contrast to the results described above, sharp end points suggest rapid and complete reaction²⁰ of all acid titratable groups. The significance of this apparent contradiction is not obvious.

The existence, in some batches of DEAE-cellulose, of a minor ionizable group containing two closely spaced nitrogen atoms has been suggested¹². The charge resulting from the addition of a proton to the first nitrogen would "oppose" proton addition to the second nitrogen. Such groups purportedly have salt dependent *pK* values¹¹, whereas the minor group in the titrations described above is relatively salt independent (Table II). It is significant that *pK* values calculated from base titration data are practically super-imposable with those from acid titrations shown in Fig. 2, and that the minor titratable group is hardly detectable in base titration curves, especially at higher ionic strengths (data not shown). This suggests that once protonated the putative sequestered groups tend to lose their identity and become indistinguishable from major ionic groups. Perhaps the ionic strength related improved resolution obtained during the first few hours with pellicular exchange packings⁵ is also a consequence of unmasking sequestered groups. The disappearance of the minor group with increasing salt suggests structural changes of the ion exchange matrix, and resulting charge distribution changes. This might result in altered chromatographic behavior, as has been observed with changes in protein structure¹³.

Preliminary titration experiments in aqueous solutions of multivalent salts (MgCl_2 , Na_2SO_4) demonstrated that the salt dependence of *pK* is not a simple function of ionic strength (data not shown). Data was not superimposable with those obtained in NaCl when expressed either as ionic strength or molarity, except in the case of MgCl_2 when only chloride concentration was considered in relating *pK* to salt concentration.

In conclusion, several commercially available batches of DEAE-cellulose were

titrated with acid and base, in solutions containing increasing concentrations of NaCl. A near exponential relationship was found between the pK and the normality of sodium chloride. A major and a minor titratable group was found. The first group accounted for the observed salt dependent pK . The pK of the second group was relatively salt independent and its fraction of the total ionizable groups decreased with increasing concentration (from 43 to 0%). Potentiometric titrations in low salt concentration (0–0.01 M NaCl), and near the pK of the minor ionizable group, were characterized by a gradual pH drift, suggesting sequestered groups and lack of equilibrium. This is however inconsistent with preliminary calorimetric titrations which were characterized by thermograms having sharp end points.

ACKNOWLEDGEMENTS

This research was supported by Brigham Young University through the Chemistry Department.

REFERENCES

- 1 D. McCormick, *BioTechnology*, 6 (1988) 158.
- 2 F. E. Regnier, *Methods Enzymol.*, 104 (1984) 170.
- 3 E. A. Peterson and H. A. Sober, *J. Am. Chem. Soc.*, 78 (1956) 751.
- 4 J. X. Khym, *Analytical Ion-Exchange Procedures in Chemistry and Biology*, Prentice-Hall, Englewood Cliffs, NJ, 1974, p. 76.
- 5 A. J. Alpert and F. E. Regnier, *J. Chromatogr.*, 185 (1979) 375.
- 6 H. G. Barth, W. E. Barber, C. H. Lochmuller, R. E. Majors and F. E. Regnier, *Anal. Chem.*, 58 (1986) 211R.
- 7 M. A. Smith, M. A. Stahmann and G. Semenza, *J. Chromatogr.*, 18 (1965) 366.
- 8 G. Sofer and C. Mason, *BioTechnology*, 5 (1987) 239.
- 9 M. A. Smith and M. A. Stahmann, *J. Chromatogr.*, 41 (1969) 228.
- 10 F. Helfferich, *Ion Exchange*, McGraw-Hill, New York, 1962.
- 11 J. A. Kitchener, *Ion Exchange Resins*, Wiley, New York, 1958, p. 42.
- 12 E. Peterson, in T. S. Work and E. Work (Editors), *Laboratory Techniques in Biochemistry and Molecular Biology*, Vol. 2, North-Holland, Amsterdam, 1970, p. 235.
- 13 F. E. Regnier, *Science (Washington, D.C.)*, 238 (1987) 319.
- 14 B. Ekstroem, *Anal. Chem.*, 142 (1984) 134.
- 15 H. H. Willard, L. L. Merritt Jr. and J. A. Dean, *Instrumental Methods of Analysis*, Van Nostrand, NJ, 4th ed., 1965, p. 585.
- 16 C. S. Knight, *Adv. Chromatogr.*, 4 (1967) 61.
- 17 W. Kern, *Biochem. Z.*, 301 (1939) 338.
- 18 J. W. Clayton and W. Bushuk, *J. Chromatogr.*, 21 (1966) 67.
- 19 C. C. Nimmo, M. T. O'Sullivan, A. Mohammad and J. W. Pence, *Cereal Chem.*, 40 (1963) 390.
- 20 G. A. Vaughan, *Thermometric and Enthalpimetric Titrimetry*, Van Nostrand Reinhold, London, 1973, pp. 7, 13.

CHROM. 21 366

STUDY OF THE LIPOPHILIC CHARACTER OF A SERIES OF β -CARBOLINES

G.L. BIAGI*

Istituto di Farmacologia, Università di Bologna, Via Irnerio 48, 40126 Bologna (Italy)

M. C. PIETROGRANDE

Dipartimento di Chimica, Università di Ferrara, Ferrara (Italy)

A.M. BARBARO and M. C. GUERRA

Istituto di Farmacologia, Università di Bologna, Bologna (Italy)

P. A. BOREA

Istituto di Farmacologia, Università di Ferrara, Ferrara (Italy)

and

G. CANTELLI FORTI

Istituto di Farmacologia, Università di Bologna, Bologna (Italy)

(First received October 17th, 1988; revised manuscript received January 31st, 1989)

SUMMARY

The lipophilic character of a series of β -carbolines has been studied. The R_M values were measured by means of a reversed-phase thin-layer chromatographic (TLC) technique and compared with the R_M values obtained by high-performance TLC (HPTLC), the $\log k'$ obtained by high-performance liquid chromatography (HPLC), and the $\log P$ values. The best equation shows a very good linear relationship between our R_M values and the classical $\log P$ values obtained using an octanol-water system. The choice of a pH of 13.0 for the TLC system allowed the measurement of the R_M values of molecules in their non-ionized form. The deviations from the linear relationship shown by the R_M (HPTLC) and $\log k'$ values of two compounds were due to the fact that both compounds were at least partially ionized at the pH of 7.0 at which the HPTLC and HPLC determinations were carried out.

INTRODUCTION

β -Carboline derivatives are new drugs which exert their pharmacological action by interacting with the benzodiazepine receptor in the mammalian central nervous system (CNS)¹. Chemically unrelated to the benzodiazepines, they have been classified according to their spectrum of biological activity as (a) agonists (anxiolytic), (b) inverse agonists (anxiogenic) or (c) antagonists (without any biological effect but preventing the interaction of agonists and inverse agonists with the receptor)². Qualitative studies have recently been devoted to structure-activity relationships for this

layer with silicone DC 200 (350 cSt) (Applied Science Labs., State College, PA, U.S.A.). The impregnation was carried out by developing the plates in a 5% silicone solution in diethyl ether. The mobile phase, saturated with silicone, was an aqueous buffer (glycine at pH 13.0), alone or mixed with various amounts of acetone.

Two plates were developed simultaneously in a chromatographic chamber containing 200 ml of mobile phase. The β -carbolines were dissolved in methanol (1–2 mg/ml) and 1 μ l of solution was spotted randomly on the plates in order to avoid any systematic error. The developed plates were dried and the spots detected under UV light (254 nm). The R_M values were calculated by means of equation $R_M = \log [(1/R_F) - 1]$.

The HPTLC determinations were previously carried out on Whatman KC 18F plates¹¹. A Camag Nanomat (Camag, Berlin, F.R.G.) was used to spot the compounds on the plates (about 100 nl of each β -carboline solution in methanol). The solutes were detected under UV light (254 nm). Solvent mixtures of methanol–phosphate buffer (pH 7.0) in the concentration range 45–80% were used as mobile phases.

Determination of HPLC retention times

The HPLC measurements were previously performed on a Spectra-Physics chromatograph consisting of an SP 8700 solvent delivery system and an SP 8750 organizer module. A Varian Aerograph UV detector was operated at 254 nm. A μ Bondapak C₁₈ column (30 cm \times 3.9 mm I.D.) from Waters (Milford, MA, U.S.A.) was used. The mobile phase was methanol in various mixtures with phosphate buffer (pH 7.0; ionic strength = 0.05 M) at a flow-rate of 1 ml/min. The β -carboline solutions in methanol were injected into the column by a 10- μ l loop.

The experiments were performed at room temperature. The retention time of potassium nitrate was taken as t_0 . The capacity factor, k' , was evaluated from the t_0 value and the retention time of the solute, t_R , by the equation $k' = (t_R - t_0)/t_0$. For each compound the retention data were measured at different methanol concentrations (20–80%) in the mobile phase.

Measurement and calculation of log P values

The log P values for three compounds (harman, harmine and nor-harman) were determined at pH 13.0 in octanol–water. The log P values of the other β -carboline derivatives were calculated from the experimental log P value for nor-harman, by taking advantage of the additive property of the Hansch π values¹³.

RESULTS

The reversed-phase TLC of the β -carboline derivatives showed that increasing acetone concentrations in the mobile phase resulted in decreasing R_M values. The equations describing the linear relationship between R_M values and acetone concentrations allowed the calculation of extrapolated R_M values at 0% acetone in the mobile phase (Table II). The R_M values, as measured in the chromatographic system at pH 13.0, should be an expression of the lipophilic character of the β -carbolines in their non-ionized form. The R_M (HPTLC) and log k' values reported in Table II were obtained in a similar way by extrapolation from the linear relationship between partition data and organic solvent concentrations in the mobile phase. However, the

TABLE II
LIPOPHILIC PARAMETERS OF β -CARBOLINES

Compound	R_M	$R_M(\text{HPTLC})$	$\log k'$	$\log P$
1	2.06	3.35	2.54	3.50
2	2.02	3.10	2.73	3.56
3	1.75	2.82	2.10	3.06
4	1.42	2.62	2.01	2.55
5	1.97	2.92	2.83	3.16
6	2.08	3.50	2.65	3.68
7	2.36	3.54	3.15	4.24
8	2.16	3.70	2.98	4.14
9	2.74	4.60	3.86	4.56
10	2.83	4.76	3.89	5.18
11	1.24	2.71	2.11	2.75
12	2.18	1.92	1.71	3.71
13	1.44	2.04	1.10	3.06
14	2.56	3.93	3.98	4.56
15	1.82	3.12	2.51	3.17

R_M (HPTLC) and $\log k'$ values of harmaline and harmalol in those systems should reflect the partial ionization of both compounds at pH 7.0 (Table II). Finally, the $\log P$ values reported in Table II were calculated from the experimental $\log P$ value for nor-harman at pH 13.0 and therefore they should refer to their non-ionized form.

The relationship between R_M and $\log P$ values is described by eqn. 1, which shows a very good correlation coefficient.

$$R_M = -0.133(\pm 0.198) + 0.594(\pm 0.053)\log P \quad (1)$$

$(n=15; r=0.952; s=0.148; F=125.9; P<0.005)$

The $\log P$ values explain 90% of the variance in the R_M values ($R^2=0.906$). The equation holds over a range of R_M values, showing a 38.9-fold difference in lipophilicity. However, the slope of eqn. 1 is lower than 1 and indicates the wider range of the $\log P$ values. An intercept different from zero indicates a systematic difference between the two systems.

On the other hand, eqns. 2 and 3, describing the relationship between the R_M values and the $R_M(\text{HPTLC})$ and $\log k'$ values, respectively, are not as good as eqn. 1.

$$R_M = 0.561(\pm 0.324) + 0.457(\pm 0.097)R_M(\text{HPTLC}) \quad (2)$$

$(n=15; r=0.793; s=0.295; F=22.03; P<0.005)$

$$R_M = 0.766(\pm 0.237) + 0.477(\pm 0.085)\log k' \quad (3)$$

$(n=15; r=0.841; s=0.262; F=31.40; P<0.005)$

This is mainly due to the $R_M(\text{HPTLC})$ and $\log k'$ values of harmaline and harmalol, which had been measured at pH 7.0. In fact, eqns. 4 and 5, calculated without these two compounds, were found to be much better. In particular, their slopes are very close to that of eqn. 1.

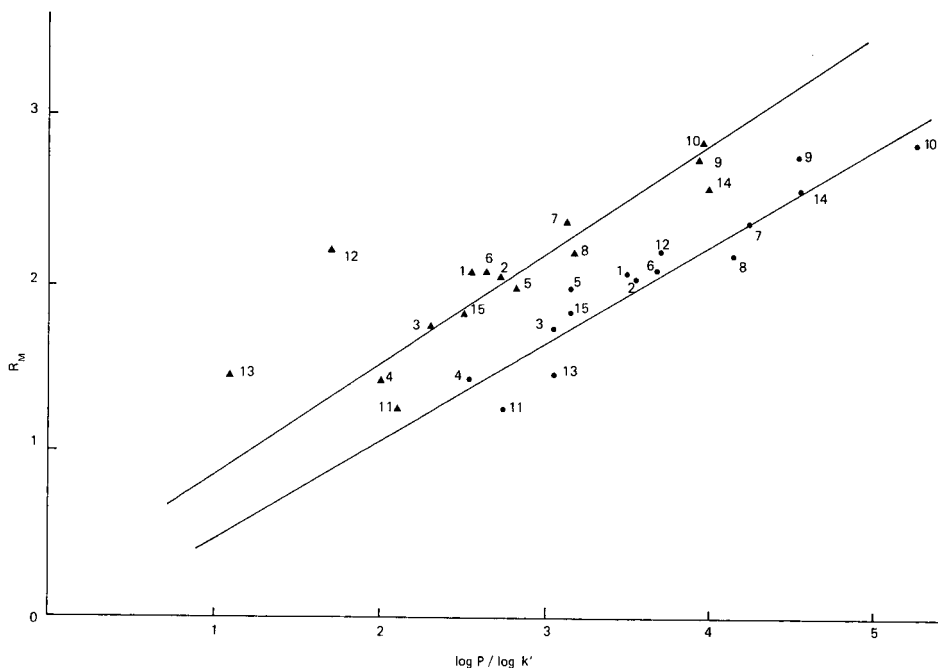


Fig. 1. Plots of R_M vs. $\log P$ (●) and $\log k'$ (▲) values. The straight lines were calculated from eqns. 1 and 5, respectively. For identification of compounds, see Table I.

$$R_M = -0.149(\pm 0.262) + 0.648(\pm 0.075)R_M(\text{HPTLC}) \quad (4)$$

$(n = 13; r = 0.934; s = 0.176; F = 74.80; P < 0.005)$

$$R_M = 0.212(\pm 0.207) + 0.649(\pm 0.070)\log k' \quad (5)$$

$(n = 13; r = 0.941; s = 0.165; F = 85.54; P < 0.005)$

As mentioned in the Introduction, in a previous study¹¹ a significant correlation had been found between $R_M(\text{HPTLC})$, $\log k'$ or $\log P$ values and receptor binding affinity. This was due to the fact that both lipophilicity indexes and binding assay had been measured at the same pH 7.0.

DISCUSSION

Eqn. 1 shows a very good linear relationship between R_M and $\log P$ values. The correlation coefficient is 0.954, indicating that only about 9% of the inaccuracies are not accounted for. This may be due to the fact that most of the $\log P$ values were calculated by taking advantage of the Hansch π values¹³. In any event, the R_M values, despite their narrower range as shown by the slope of eqn. 1, seem to be a reliable alternative to the $\log P$ values. The experimental determination of the octanol-water partition coefficient is likely to give more accurate and unequivocal data. However, the chromatographic method has several advantages¹⁴: (a) it is simple and rapid; (b) it requires little material; (c) the material does not need to be very pure because

impurities are separated during the determination; (d) the detection of spots by un-specific methods avoids the need for specific quantitative analytical methods; (e) the determination of the partition coefficient of slightly water-soluble compounds requires a long period of equilibration to achieve thorough partitioning between the phases; and (f) the range of linearity between the R_M values and the mobile phase composition allows the calculation of a theoretical R_M value at 0% acetone in the mobile phase, *i.e.*, in a standard system where all the compounds could be compared. However, this procedure has another great advantage over the determination of the R_M values at only one organic solvent concentration in the mobile phase. In fact, in this way one can avoid the error that might arise because of the different slopes of the straight lines describing the relationship between R_M values and organic solvent concentration in the mobile phase. Two compounds might have the same R_M value at a given organic solvent concentration and different extrapolated R_M values.

On the other hand the TLC technique has another important advantage over the HPLC method, which is similarly suggested as an alternative to the classical determination of the partition coefficients. All bonded-phase packing materials based on silica gel are alkali-labile. Therefore, in HPLC one has to work in the pH range 2–8 in order to avoid any alteration of the column. Particularly with basic compounds, it may be difficult to have them in the non-ionized form. In reversed-phase TLC using silicone-impregnated layers or KC 18F plates, one does not face such a problem, as it is possible to choose pH values at which any compound can be considered to be in the non-ionized form. In this way it should be possible to avoid the discrepancies resulting from eqn. 3.

In a previous paper¹⁵ we reported $R_{M_0} = 1.82$ as the optimum lipophilic character for the activity of a series of benzodiazepines in the CNS. As the β -carbolines are assumed to interact with the same receptor, they could have a similar lipophilic character. However, as reported previously¹¹, the lack of a parabolic relationship between R_M values and biological activity does not allow any definite conclusion.

REFERENCES

- 1 C. Braestrup, M. Nielsen, T. Honore, L. H. Jensen and E. N. Petersen, *Neuropharmacology*, 22 (1983) 1451.
- 2 C. Braestrup, T. Honore, M. Nielsen, E. N. Petersen and L. H. Jensen, *Biochem. Pharmacol.*, 33 (1984) 859.
- 3 C. Braestrup and M. Nielsen, in L. L. Iversen, S. D. Iversen and S. H. Snyder (Editors), *Handbook of Psychopharmacology*, Plenum Press, New York, 1983, p. 285.
- 4 P. A. Borea, V. Ferretti and G. Gilli, *Br. J. Pharmacol.*, 86 (1985) 666P.
- 5 G. Loew, J. Nienow, J. A. Lawson, L. Toll and E. T. Uyeno, *Mol. Pharmacol.*, 28 (1985) 17.
- 6 P. A. Borea, V. Bertolasi, V. Ferretti and G. Gilli, *Mol. Pharmacol.*, 31 (1987) 334.
- 7 W. Haefely, E. Kyburz, M. Gerecke and H. Mohler, *Adv. Drug Res.*, 14 (1985) 165.
- 8 P. W. Coddling, *Can. J. Chem.*, 61 (1983) 529.
- 9 H. G. Schauzu and P. P. Mager, *Pharmazie*, 38 (1983) 490.
- 10 P. A. Borea and V. Ferretti, *Biochem. Pharmacol.*, 35 (1986) 2836.
- 11 P. A. Borea, M. C. Pietrogrande and G. L. Biagi, *Biochem. Pharmacol.*, 37 (1988) 3953.
- 12 G. L. Biagi, A. M. Barbaro, M. F. Gamba and M. C. Guerra, *J. Chromatogr.*, 41 (1969) 371.
- 13 C. Hansch and A. J. Leo, *Substituent Constants for Correlation Analysis in Chemistry and Biology*, Wiley, New York, 1969.
- 14 G. L. Biagi, A. M. Barbaro and M. C. Guerra, *Adv. Chem. Ser.*, 114 (1973) 61.
- 15 G. L. Biagi, A. M. Barbaro, M. C. Guerra, M. Babbini, M. Gaiardi and M. Bartoletti, *J. Med. Chem.*, 23 (1980) 193.

CHROM. 21 342

NORMALISATION OF HIGH-PERFORMANCE LIQUID CHROMATOGRAPHY PEAK RETENTION TIMES FOR COMPUTERISED COMPARISON OF WHEAT PROLAMIN CHROMATOGRAMS^a

HARRY D. SAPIRSTEIN, MARTIN G. SCANLON* and WALTER BUSHUK

Grain Industry Research Group, Food Science Department, University of Manitoba, Winnipeg, Manitoba, R3T 2N2 (Canada)

(First received November 1st, 1988; revised manuscript received January 24th, 1989)

SUMMARY

To improve the reproducibility of wheat protein separations, reversed-phase high-performance liquid chromatography peak retention times were normalised relative to an external reference chromatogram run interveningly as part of a standardised experimental procedure. The computer program functions, without operator intervention, to identify five designated calibration peaks in the chromatogram of ethanol-soluble proteins (wheat prolamins or gliadins) from the standard hard red spring wheat variety Neepawa. The retention times of these peaks are then used as anchor points in a piecewise calibration algorithm to normalise chromatograms of samples run in the interval between two of the standards. For chromatograms acquired over a two-month period, this procedure decreased the average experimental error in peak retention times five-fold to a level of precision comparable to that of short-term analyses.

INTRODUCTION

Wheat prolamins (gliadins), the proteins extractable with 70% aqueous ethanol from wheat endosperm, can be separated by reversed-phase high-performance liquid chromatography (RP-HPLC)¹. In most cases extracts of grain of a given variety (or genotype) will produce a unique chromatogram². Chromatograms can be automatically integrated and thus reduced to a set of peak retention times and associated peak heights or areas. By analysing certified genotypes in this way, a library of reference chromatographic data can be built up and, similar to electrophoretic patterns^{3,4}, the data can be used to identify unknown grain samples or for estimation of homology with reference genotypes.

As in electrophoresis, the reliability of the HPLC methodology depends on the precision of the data. Sample and solvent preparation and machine performance can,

^a Publication no. 146, Food Science Department.

and do, contribute to systematic and random errors, causing retention time variation⁵. Incomplete resolution of peaks, even after method optimisation⁶, can also result in erroneous peak assignments due to integrator artefacts⁷. A major source of systematic errors, however, can arise from variability between nominally identical columns⁸ and from progressive changes in column properties with time⁹. While many of these factors can be controlled by adhering to rigorously controlled experimental procedures, appropriate correction (or normalisation) of peak retention times is required to obtain the precision necessary for accurate comparison of chromatographic data¹⁰.

Chromatogram normalisation typically requires definition of peak retention time on a column as an index relative to the retention of reference compounds¹¹. However, no similar quantitative approach has been reported in cereal protein analyses. The complex heterogeneity of wheat endosperm proteins results in complex chromatograms of numerous components with a broad range of hydrophobicities. Hence, sample and standard peaks are likely to be confounded, as Bietz and Cobb¹² found when they added alkyl aryl ketones to an ethanolic extract of the wheat variety Chinese Spring.

This paper describes a computer-based procedure for normalising peak retention times of gliadin components separated by RP-HPLC, relative to the retention times of five gliadin calibration peaks of a standard wheat variety. Any changes in operating conditions and column properties which affect retention times will thus be corrected by standards that interact with the stationary phase in a manner similar to the interactions between samples and the stationary phase^{13,14}. The normalisation is essential to achieve the precision required for computerised wheat variety identification and calculation of inter-genotype homologies.

EXPERIMENTAL

Materials

HPLC grade acetonitrile and ethanol were obtained from Fisher Scientific (Fair Lawn, NJ, U.S.A.). Sequanal grade trifluoroacetic acid (TFA) was purchased from Pierce (Rockford, IL, U.S.A.). Water was distilled and then purified with a Millipore Milli-Q system (Bedford, MA, U.S.A.). Grain of the Canadian bread wheat variety Neepawa, verified as authentic and pure by polyacrylamide gel electrophoresis¹⁵, was used to prepare extracts of the standard for the calibration chromatogram.

Chromatography and sample preparation

Preparation of gliadin extracts and the relevant experimental procedures have been described previously¹⁶. RP-HPLC was performed with a 1090M Hewlett-Packard Liquid Chromatograph using a wide pore (300Å), C₈ Supelcosil column. Solutions of water and acetonitrile (both containing 0.1% TFA)¹ were made fresh for each, or every second, set of analyses (see below). Optimization of gradient elution and data acquisition conditions ensured that peaks were reproducibly integrated for any given separation¹⁶.

A chromatogram set was arbitrarily defined as comprising no more than eight experimental samples plus two extracts of the standard. One standard was run at the beginning and one at the end of each set. This provided a relatively low (maximum

4:1) ratio of experimental to standard analyses. For successive runs involving more than eight samples, the last standard of the previous set became the first of the next set. Column clean-up¹⁷ was performed, on average, after nine samples were run. To obtain the results reported in this paper, the sets were run intensively for 2 months.

Protein elution profiles recorded at 210 nm were integrated on the chromatograph's HP-310 computer using Hewlett-Packard software (HP 79994A) to obtain data on peak retention times and quantitation parameters for statistical analysis.

RESULTS AND DISCUSSION

Selection of the variety Neepawa as an RP-HPLC standard

Five peaks in the chromatogram of the standard (Fig. 1) were selected as retention time calibration peaks on the basis of their positions across the chromatogram and their reliability for automated detection. The distinctive heights of these peaks, within defined regions of the chromatogram (Fig. 1), made them easily identifiable by computer (see below). For 2 months, during which there were changes in the selectivity of some of the other peaks, the sizes and shapes of the calibration peaks did not change. Furthermore, location effects and other common environmental factors during the growing season¹⁸ do not affect peak retention times. The variety Neepawa is homogeneous in genetic composition¹⁵, and its grain is readily available. Neepawa was adopted in 1987 as the standard variety for the Canada Western Red Spring class of wheat¹⁹ and has been used as a reference variety in electrophoretic studies^{15,20}. Accordingly, the variety Neepawa appears to be an excellent standard.

Specification and identification of standard peaks

In order to use the selected calibration peaks as standards for automated chromatogram normalisation, prior knowledge of peak retention times is required. Integrated report files provided the source data for all analyses, including identification of the five calibration peak retention times. For assessing the variation of peak reten-

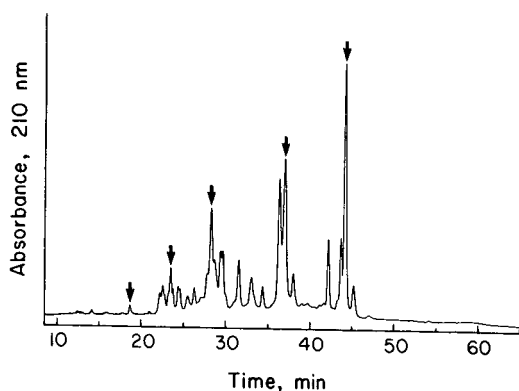


Fig. 1. Chromatogram of an extract of the variety Neepawa showing the five calibration peaks ($S_1 - S_5$, left to right, respectively). Column, C_8 Supelcosil (25 cm \times 4.6 mm I.D.); elution conditions, acetonitrile-water (25:75) containing 0.1% TFA for 5 min at 1 ml/min followed by a linear gradient (0.5%/min) to acetonitrile-water (55:45) containing 0.1% TFA at 1 ml/min.

tion times before and after normalisation a set of 30 peaks was chosen in the time range 18–50 min in 25 Neepawa chromatograms (Fig. 1). These 30 peaks were rigorously identified as matching components in the 25 replicates sampled during the 2-month experimental period on the basis of direct visual inspection of the peaks and collation with peak integration results.

Computer identification of the calibration peaks was based on finding the largest peak in each of five narrow retention time windows. Calibration peaks were selected so that no other peak maxima could exist in their neighbourhood given the retention-time drifts that could normally occur. The five calibration peaks (S_1 – S_5) were always correctly identified by this approach in 48 Neepawa samples analysed in the 2-month period, during which more than 250 separations were performed. The population mean retention times for the five calibration peaks S_1 – S_5 were 19.61 min, 24.54 min, 29.01 min, 37.82 min and 44.78 min, respectively. These values served as anchor points (k_1 – k_5) in the algorithm described below for correction of observed retention times relative to the calibration peaks. Alternatively, k_1 – k_5 might be defined as the observed retention times (t_{S_1} – t_{S_5}) for a standard run when a new column is installed. That is, all chromatograms are normalised relative to the calibration peaks in the first chromatogram of the standard.

Application of external calibration peaks for determination of relative retention times

Normalisation of observed peak retention times was implemented by an algorithm comprising three steps (*cf.* Table I):

(1) Correction of observed sample peak retention time (t_e) to a corrected retention time (t_R), relative to the observed retention time for each of the five calibration peaks (t_{S_1} – t_{S_5});

(2) Determination of the “weighing function” (w_i) for the four internal chromatogram ranges (t_{S_1} to t_{S_2} , t_{S_2} to t_{S_3} , etc.) to correct calibration peak retention times (t_{S_1} – t_{S_5}) to the anchor points (k_1 – k_5);

(3) Computation of relative retention times (t') for sample peaks according to the positions of their observed retention times relative to the calibration peaks.

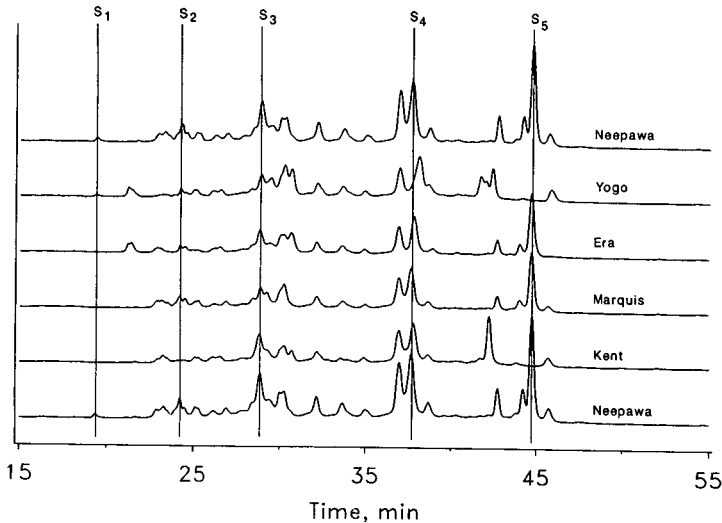
The formulae which are implemented in the computer program to determine relative peak retention times are given in Table I. Equations 1–5, 6–9, and 10–15 correspond to steps 1, 2 and 3, respectively. The expression invoked (eqns. 10–15) to determine the relative peak retention time for a sample is contingent upon the position of a given protein peak within the chromatogram (Fig. 2). For example, if the observed retention time (t_e) for a sample peak is less than the value (t_{S_1}) for the first calibration peak (S_1) the retention time is corrected relative to S_1 alone using eqn. 10. Similarly if a peak elutes with a retention time greater than the observed value for calibration peak S_5 , eqn. 15 is invoked to make the correction. On the other hand, if a peak elutes in the interval between two calibration peaks, its relative retention time is determined relative to the retention times of the two flanking calibration peaks, but weighted according to the proximity of the peak to each of the two calibration peaks (eqns. 11–14).

The task of identifying sample and calibration peaks, along with related retention-time peak corrections, was carried out by a computer program developed in FORTRAN 77. Program implementation was on the HP-310 computer of the HPLC HP-1090M workstation. Because peak identification was based on integration report

TABLE I

RELATIONSHIPS USED TO CORRECT OBSERVED PEAK RETENTION TIMES TO RELATIVE BASIS BY MULTIPLE CALIBRATION PEAKS

Parameter	Definition	Eqn. No.
Retention time relative to calibration peak: ^a		
S_1	$t_{R1} = k_1(t_c/t_{S1})$	(1)
S_2	$t_{R2} = k_2(t_c/t_{S2})$	(2)
S_3	$t_{R3} = k_3(t_c/t_{S3})$	(3)
S_4	$t_{R4} = k_4(t_c/t_{S4})$	(4)
S_5	$t_{R5} = k_5(t_c/t_{S5})$	(5)
Weight function for chromatogram range: ^a		
t_{S1} to t_{S2}	$w_1 = (t_{S2} - k_1)/(k_2 - k_1)$	(6)
t_{S2} to t_{S3}	$w_2 = (t_{S3} - k_2)/(k_3 - k_2)$	(7)
t_{S3} to t_{S4}	$w_3 = (t_{S4} - k_3)/(k_4 - k_3)$	(8)
t_{S4} to t_{S5}	$w_4 = (t_{S5} - k_4)/(k_5 - k_4)$	(9)
Relative peak retention time (t'):		
$t_c < t_{S1}$	$t' = t_{R1}$	(10)
$t_{S1} < t_c < t_{S2}$	$t' = (1 - w_1)t_{R1} + (w_1)t_{R2}$	(11)
$t_{S2} < t_c < t_{S3}$	$t' = (1 - w_2)t_{R2} + (w_2)t_{R3}$	(12)
$t_{S3} < t_c < t_{S4}$	$t' = (1 - w_3)t_{R3} + (w_3)t_{R4}$	(13)
$t_{S4} < t_c < t_{S5}$	$t' = (1 - w_4)t_{R4} + (w_4)t_{R5}$	(14)
$t_c > t_{S5}$	$t' = t_{R5}$	(15)

^a Refer to Fig. 2; see text for additional details.Fig. 2. Set of chromatograms from four sample wheat varieties and two standards to show peak normalisation relative to the calibration peaks. Lines drawn across the chromatograms denote the equivalent retention times of calibration peaks $S_1 - S_5$ in sample chromatograms.

files, and the process described above is not complex, program implementation using a low-cost personal computer should be satisfactory.

Retention time precision

The coefficients of variation (C.V.) and the standard deviations (S.D.) shown in Table II attest that the precision of uncorrected retention times for standardised analyses of gliadins carried out over a short period (2 weeks), was substantially better than that for the same analyses performed over a prolonged period (2 months). The mean S.D. of uncorrected retention times for chromatograms acquired over a short term was 0.06 min, compared with 0.53 min for the long-term data. Underlying this result was a significant difference in the pattern of variation of uncorrected retention times (Fig. 3). For analyses carried out over the long-term period, retention time variation was substantially greater for the early eluting proteins than for the later eluting counterparts. Possible factors contributing to this result have been discussed previously¹⁶. Even so, the uncorrected long-term variation in wheat protein retention times compares well with the reported capacity factors for column test compounds and barbiturates (mean C.V. of 2.67% and 3.95% respectively)²¹, thiazide diuretics (mean C.V. = 1.93%)²², and the retention times of seven drugs (mean C.V. = 1.78%)²³, analysed over short periods.

Normalised retention times are significantly more precise than the observed retention times over the long-term period (Fig. 3). On average, the uncertainty in the data was reduced more than five-fold (Table II). The magnitude of normalisation was significantly greater for early eluting proteins, *i.e.* for peaks with retention times less than 35 min, where an eight-fold improvement in experimental error was realised; the C.V. being reduced from 2.5% to 0.3%.

A characteristic feature of the normalisation procedure is the increasing influence of the magnitude of correction for peaks that elute closer to the calibration peaks. The effect is clearly illustrated in Fig. 3, as distinct S.D. minima are reached in the neighbourhood of calibration peak positions. This indicates that peaks of both experimental and standard samples which have retention times close to those of the calibration peaks are essentially free of experimental error.

Overall, the corrected long-term retention time precision (C.V. = 0.31%,

TABLE II

COMPARISON OF MEAN PRECISION PARAMETERS FOR OBSERVED AND CORRECTED RP-HPLC PEAK RETENTION TIMES

Experimental conditions as in Fig. 1.

	<i>Retention time range (min)</i>	<i>C.V. (%)^a</i>	<i>S.D. (min)</i>	<i>L.S.D. (min)^b</i>
Long-term (uncorrected)	19.6–47.4	1.82	0.53	2.12
Short-term (uncorrected)	18.1–47.5	0.20	0.06	0.24
Long-term (corrected)	19.6–47.4	0.31	0.10	0.40

^a Number of replicate analyses > 15.

^b Least significant difference, $p = 0.05$.

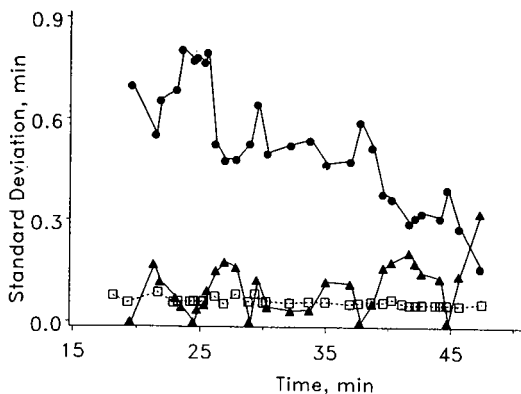


Fig. 3. Standard deviations of retention times for gliadin peaks from Neepawa extracts: (□) short-term (2 weeks) retention times; (●) long-term (2 months) retention times; and (▲) long-term retention times corrected by the normalisation procedure. Experimental conditions as in Fig. 1.

S.D. = 0.10 min) compared favourably with the reproducibility of short-term analyses (C.V. = 0.20%, S.D. = 0.06 min). This represents a satisfactory level of performance for RP-HPLC of wheat proteins. The long-term corrected retention times also compare well with the results for indexation to standard compounds such as alkyl aryl ketones¹¹ and 2-keto alkanes²³ obtained over short periods of analysis, where mean C.V. of 0.99%, 0.24% and 0.21% were obtained for drugs²³, barbiturates²¹ and thiazide diuretics²², respectively.

Applications

In practical terms, the normalisation procedure should result in a significant improvement in precision for comparing chromatographic data, especially data obtained with one column over a long period. Since the prime characteristic of a chromatogram is peak positioning²⁴, changes in retention characteristics of the column with loss of binding capacity⁹ should be monitored by molecules that have functional groups of similar retention characteristics as the compounds of interest, especially for molecules with strong hydrogen-bonding capacities²⁵ (such as wheat proteins²⁶). Using Neepawa as the source of standards has the disadvantage that results are standardised with reference compounds which another laboratory may decide is inappropriate for their purposes, and hence the potential exists for an undesirable proliferation of standards (as pointed out by Smith *et al.*²⁷). However, since the mechanism of retention and elution of proteins is substantially different from that of small molecules¹⁷, such a proliferation may be justified in order to adequately correct retention time variations in order to carry out comparative analyses¹⁴.

Inferences on component identity are mainly based on comparisons of peak retention times. Accordingly, residual variation in retention times that occurs must be accounted for²⁸ by allowing a retention time threshold (or window) when comparing peaks. As in the case of electrophoretic separations of gliadins¹⁵, this threshold must be sufficiently large to accept "truly" identical protein components, but not so large that mismatches result on account of real differences. The problem is a classical one of minimising the so-called type I (rejection of true peak identity) and type II (accept-

ance of false peak identity) errors. In electrophoretic and RP-HPLC analyses of gliadins, type II errors dominate owing to the complex heterogeneity of the protein separations. For example, the mean separation distance between adjacent peaks is small (less than 45 s). Direct comparison of chromatograms indicates that *ca.* 20 s represents the smallest detectable difference in retention time for visually different peaks. Left uncorrected, the least significant difference (L.S.D.) in peak retention times with prolonged column use is greater than 2 min (Table II). Therefore, the experimental error in long-term data will undermine comparative analyses because of false matches.

In contrast, data normalised by this procedure will be sufficiently precise that differences of *ca.* 0.4 min (24 s) in peak retention times would be detected (Table II). This is close to the smallest difference detectable visually. It is interesting to note that for data acquired over a 2-week period, the L.S.D. in peak retention time was *ca.* 15 s. To achieve this high level of statistical performance, incorporation of additional calibration peaks in the normalisation algorithm would be required. Nevertheless, the procedure as it stands should result in a substantial reduction in the number of peak mismatches that would otherwise occur, and allow significantly higher degrees of confidence in the computerised comparative analysis of chromatographic data acquired over long periods.

CONCLUSIONS

Despite rigorously standardised chromatographic conditions and efforts to prevent column deterioration with use, random and systematic variations in peak retention times do occur. For separations of complex mixtures, where complete resolution of components is not always possible, retention time normalisation is essential if chromatograms run at different times are to be compared. The described normalisation procedure, based on five calibration peaks, stabilises variability in retention time at a low level across the entire chromatogram. The average uncertainty in the retention time of gliadin peaks was reduced more than five-fold. The advantage of this procedure for gliadins, over the alkyl aryl ketone retention index scale, is that normalisation is performed relative to standards that have essentially the same retention properties and span almost the full range of gliadin retention times. The normalised chromatograms can then be directly compared by computer with a previously acquired library of similarly normalised chromatograms, for wheat variety identification and for calculation of the degree of homology between genotypes.

ACKNOWLEDGEMENTS

We are grateful for financial assistance for this project from the Natural Sciences and Engineering Research Council of Canada, and to Denise Lawless for performing some of the chromatographic analyses.

REFERENCES

- 1 J. A. Bietz, *J. Chromatogr.*, 255 (1983) 219.
- 2 B. A. Marchylo, D. W. Hatcher and J. E. Kruger, *Cereal Chem.*, 65 (1988) 28.

- 3 G. L. Lookhart, B. L. Jones, D. E. Walker, S. B. Hall and D. B. Cooper, *Cereal Chem.*, 60 (1983) 111.
- 4 H. D. Sapirstein and W. Bushuk, *Seed Sci. Technol.*, 14 (1986) 489.
- 5 J. N. Brown, M. Hewins, J. H. M. van der Linden and R. J. Lynch, *J. Chromatogr.*, 204 (1981) 115.
- 6 T. Hoshino, M. Senda, T. Hondo, M. Saito and S. Tohei, *J. Chromatogr.*, 316 (1984) 473.
- 7 A. C. Brown III, D. L. Wallace, G. L. Burce and S. Mathes, in T. M. Vickrey (Editor), *Liquid Chromatography Detectors*, Marcel Dekker, New York, 1983, Ch. 9, p. 355.
- 8 A. P. Goldberg, *Anal. Chem.*, 54 (1982) 342.
- 9 J. L. Glajch, J. J. Kirkland and J. Köhler, *J. Chromatogr.*, 384 (1987) 81.
- 10 R. M. Smith, T. G. Hurdley, R. Gill and A. C. Moffat, *Anal. Proc.*, 22 (1985) 331.
- 11 R. M. Smith, *J. Chromatogr.*, 236 (1982) 313.
- 12 J. A. Bietz and L. A. Cobb, *Cereal Chem.*, 62 (1985) 332.
- 13 J.-C. Chen and S. G. Weber, *J. Chromatogr.*, 248 (1982) 434.
- 14 C. T. Mant and R. S. Hodges, *LC, Liq. Chromatogr. HPLC Mag.*, 4 (1986) 250.
- 15 H. D. Sapirstein and W. Bushuk, *Cereal Chem.*, 62 (1985) 372.
- 16 M. G. Scanlon, H. D. Sapirstein and W. Bushuk, *Cereal Chem.*, 66 (1989) 112.
- 17 C. T. Wehr, *J. Chromatogr.*, 418 (1987) 27.
- 18 F. R. Huebner and J. A. Bietz, *Cereal Chem.*, 65 (1988) 362.
- 19 Canadian Grain Commission, *Official Grain Grading Guide*, Canadian Grain Commission, Winnipeg, 1987 ed., 1987.
- 20 P. K. W. Ng and W. Bushuk, *J. Cereal Sci.*, 9 (1989) 53.
- 21 R. M. Smith, T. G. Hurdley, R. Gill and A. C. Moffat, *Chromatographia*, 19 (1984) 401.
- 22 R. M. Smith, G. A. Murilla, T. G. Hurdley, R. Gill and A.C. Moffat, *J. Chromatogr.*, 384 (1987) 259.
- 23 J. K. Baker, L. A. Cates, M. D. Corbett, J. W. Huber and D. L. Lattin, *J. Liq. Chromatogr.*, 5 (1982) 829.
- 24 R. J. Marshall, A. J. Bleasby, R. Turner and E. H. Cooper, *Chemomet. Intell. Lab. Syst.*, 1 (1987) 285.
- 25 N. El Tayar, A. Tsantili-Kakoulidou, T. Roethlisberger, B. Testa and J. Gal, *J. Chromatogr.*, 439 (1988) 237.
- 26 J. D. Schofield and M. R. Booth, in B. J. F. Hudson (Editor), *Developments in Food Proteins—2*, Applied Science Publishers, Barking, 1983, Ch. 1, p. 1.
- 27 R. M. Smith, G. A. Murilla and C. M. Burr, *J. Chromatogr.*, 388 (1987) 37.
- 28 F. N. Konstantinides, L. Garr, J. C. Li and F. B. Cerra, *J. Chromatogr. Sci.*, 25 (1987) 158.

CHROM. 21 329

ANALYTICAL RESOLUTION OF 4(5)-ALKYLATED $\gamma(\delta)$ -LACTONES BY HIGH-PERFORMANCE LIQUID CHROMATOGRAPHY ON A SILICA-BONDED CHIRAL POLYACRYLAMIDE SORBENT

CHROMATOGRAPHIC CHARACTERIZATION OF A STATIONARY PHASE

MANFRED HUFFER and PETER SCHREIER*

Lehrstuhl für Lebensmittelchemie, Universität Würzburg, Am Hubland, D-8700 Würzburg (F.R.G.)

(First received November 17th, 1988; revised manuscript received January 13th, 1989)

SUMMARY

A silica bonded chiral polyacrylamide phase (Merck Hibar ChiraSpher column, RT 250-4) was used for high-performance liquid chromatographic separation of homologous chiral 4(5)-alkylated $\gamma(\delta)$ -lactones (alkyl chain lengths from C₁ to C₈). For all compounds, the order of elution was (*S*)- before (*R*)-enantiomer. Column characteristics, such as the capacity factor, k' , number of theoretical plates, N , resolution, R , and $H-u$ curve were evaluated. Furthermore, a correlation between the selectivity, α , and the alkyl chain length of the lactones with the separation mechanism of the system used was attempted.

INTRODUCTION

4(5)-Substituted $\gamma(\delta)$ -lactones are widely used as intermediates in the synthesis of natural products and are important, widespread flavour compounds^{1,2}. Most of these lactones are chiral compounds and their potential physiological activity, such as, *e.g.*, odour or taste depends on the absolute configuration³. Due to the importance of this class of chemicals there have been a number of publications dealing with their chiral analysis. Additionally to gas and liquid chromatographic analysis using achiral phases after derivatization with optically pure reagents⁴⁻⁸, increasing information about direct enantiomer separation on chiral stationary phases is available. Thus, complexation gas chromatography^{9,10} as well as gas chromatography on chiral amide¹¹ and modified α -cyclodextrin phases¹⁰ have been described. Direct liquid chromatographic separation of lactone enantiomers has been recently achieved using cellulose triacetate¹². However, this study was carried out with the aim of preparative isolation of lactone enantiomers and, consequently, low pressure and large columns were used, resulting in extremely high retention times.

This paper concerns the direct liquid chromatographic separation of chiral 4(5)-alkylated $\gamma(\delta)$ -lactones using a silica-bonded chiral polyacrylamide phase as well as the characterization of the stationary phase.

EXPERIMENTAL

A Hibar ChiraSpher column (RT 250-4, 250 mm \times 4 mm, $d_p = 5 \mu\text{m}$; Merck, Darmstadt, F.R.G.) was used. With the LC pump 410 (Kontron, London, U.K.), injection valve 7125 (Rheodyne, Cotati, CA, U.S.A.) with a 20- μl sample loop and a variable wavelength UV detector (Knauer, Berlin, F.R.G.), a pressure of 20 bar was found at a flow-rate of 1.2 ml/min at 22°C [eluent composition: *n*-hexane-*tert*-butyl methyl ether (95:5)]. The wavelength used was 220 nm.

Before use, distilled eluents (*n*-hexane, *tert*-butyl methyl ether, ethanol, tetrahydrofuran, dioxane) were degassed in an ultrasonic bath. To all eluent compositions, 0.2 ml ethanol/l were added to coat free OH groups of the silica gel in order to avoid undesired adsorptive interactions of the solutes with the sorbent. Furthermore, the samples dissolved more easily in an ethanol-containing solvent.

The solutes were the homologous 4(5)-alkylated $\gamma(\delta)$ -lactones with alkyl chain lengths from C₁ to C₈ (γ -penta- and δ -hexalactone to γ -dodeca- and δ -tridecalactone; Roth, Karlsruhe, F.R.G.).

The determination of the order of elution was performed by multiple injection of the solutes. With approximately 1.5 mg of separated enantiomers obtained by this repeated procedure, the optical rotations were determined. This was achieved using a 241 MC polarimeter and a 1-ml cell (length 10 cm; Perkin-Elmer, Überlingen, F.R.G.) at 546 nm (21°C). By use of knowledge of the correlation between optical rotation and absolute configuration, the order of elution was determined [(*S*)- before (*R*)-enantiomer].

RESULTS AND DISCUSSION

The stationary phase studied consisted of a polar silica, the surface of which had been modified by radical polymerization of optically active acrylamides with (*S*)-phenylalanine ethyl ester residues. For the characterization of such a chiral high-performance liquid chromatographic (HPLC) phase its retention behaviour and selectivity are of particular importance. The quality of the column is determined by analytically non-variable parameters, such as the form and size of the particles, and

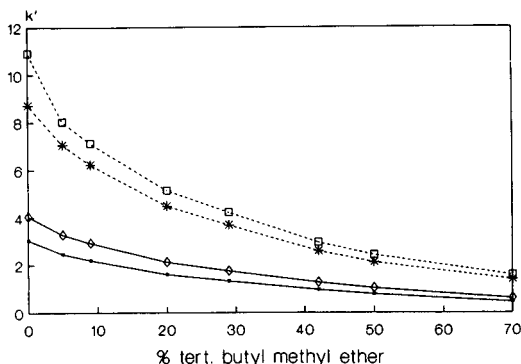


Fig. 1. Dependence of k' on the eluent composition. Flow-rate: 1.2 ml/min. ● = (*S*)- γ -Undecalactone; ◇ = (*R*)- γ -undecalactone; * = (*S*)- γ -pentalactone; □ = (*R*)- γ -pentalactone.

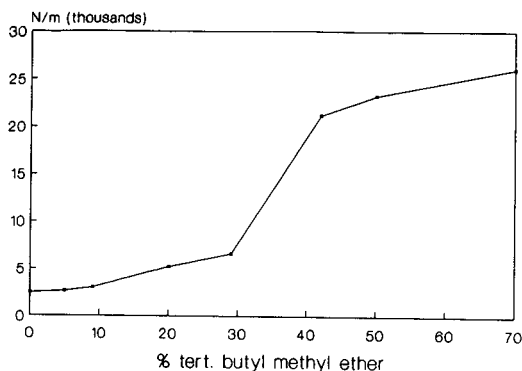


Fig. 2. Dependence of N on the eluent composition. Flow-rate: 1.2 ml/min. Example: (*R*)- γ -undecalactone.

can only be slightly optimized by the composition and flow of the mobile phase as well as the column length.

Since the capacity factor, k' , represents the weight ratio of components in the stationary and mobile phases, it depends on the eluent composition. Fig. 1 shows this dependence using an increasing amount of *tert.*-butyl methyl ether (0–70%) in the eluent. For the example of γ -undecalactone enantiomers, amounts of *tert.*-butyl ether up to 10% were necessary to obtain the desired k' values of 2–5¹³. Due to the higher polarity of γ -pentalactone, for this lactone, optimum k' values were found using 10–50% ether in the eluent. Since longer-chain lactones are especially important as flavour components, in the following experiments, based on the k' values determined, 5% ether in the eluent was used.

The dependence of the number of theoretical plates, N , on the eluent composition is outlined in Fig. 2 for the example of (*R*)- γ -undecalactone. Up to 30% ether in the eluent approximately 6500 theoretical plates/m were determined, corresponding to one fourth of the value evaluated for mesitylene ($N = 33\,813/m$), a compound practically not retarded by the column. According to the theory, with increasing eluent polarity N approaches the value for mesitylene. In general, an increase in the

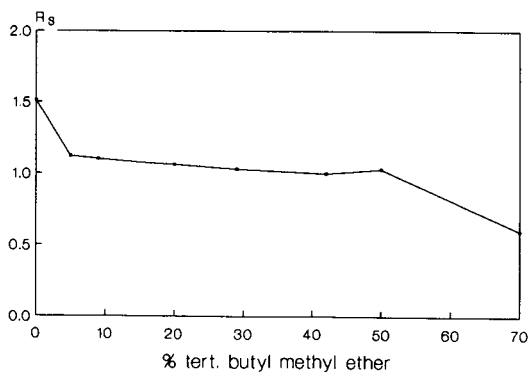


Fig. 3. Dependence of R_s on the eluent composition. Flow-rate: 1.2 ml/min. Example: (*R,S*)- γ -pentalactone.

amount of polar solvent in the mobile phase leads to a shortening of retention times and an improvement in the number of plates. However, parallel to this, k' decreases resulting in a loss of separation capacity. Also in this case, the optimum values were 5–20% ether in the mobile phase (Fig. 2).

The resolution, R_s , comprises parameters such as the column selectivity and capacity factors as criteria of analysis time and the theoretical number of plates. The selectivity, α , is independent of the eluent composition. Thus, the development of the curve in Fig. 3 can be discussed by means of k' and N . The strong increase of R_s using eluents containing 0–5% ether can be explained by the great differences of k' found in this region. With eluents containing 5–50% ether, the decrease in capacity factors and increase in the number of plates are approximately equivalent. In this region, a nearly constant resolution was found; the values of $R_s = 1.2$ – 1.3 determined are optimal for practical purposes¹³. Exchange of *tert.*-butyl methyl ether by tetrahydrofuran and dioxane resulted (at the same polarity) in a loss in resolution in spite of comparable α values. This phenomenon can be explained by the higher viscosity and, thus, lower diffusion coefficient of the sample as well as a potentially changed swelling behaviour of the polymer film resulting in variation of mass transport in the stationary phase.

In addition to selectivity and retentivity, the efficiency of a chromatographic column is important in order to obtain short analysis times with sufficient resolution. The efficiency of the column studied was checked by measurement of the plate height, H , of retarded peaks as a function of the linear velocity of mobile phase, u . The H - u curve evaluated for (*R*)- γ -decalactone is presented in Fig. 4. The broad minimum observed allows a wide range of application. As a compromise between the least possible plate height, H , and the analysis time, a flow-rate of 0.17 cm/s (= 1.2 ml/min) was selected.

The selectivity of a chromatographic column is determined by the relative retention, α . In order to study the dependence of α on the molecular structure of the sample, the α values for the enantioresolution of homologous γ - and δ -lactones were evaluated as a function of the alkyl chain length, n . As outlined in Fig. 5, an increase in selectivity with increasing chain length was observed, exhibiting a slight minimum for $n = 3$ – 5 . With $n > 3$, γ -lactones showed higher relative retention than δ -lactones. Similar α values were found in both series of lactones for $n = 1$ – 4 .

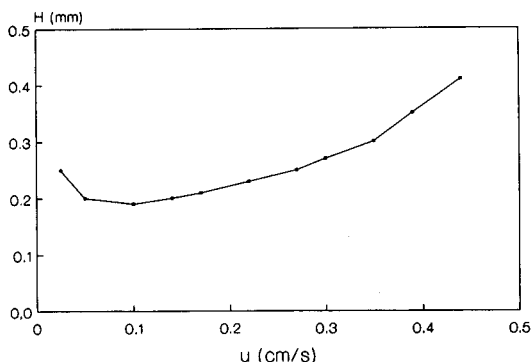


Fig. 4. Plate height, H vs. the linear velocity, u . Eluent: 5% *tert.*-butyl methyl ether-*n*-hexane. Flow-rate: 1.2 ml/min. Example: (*R*)- γ -decalactone.

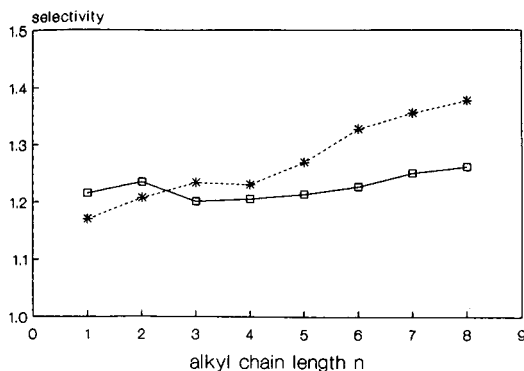


Fig. 5. Selectivity, α , vs. the alkyl chain length, n . Eluent: 5% *tert.*-butyl methyl ether-*n*-hexane. Flow-rate: 1.2 ml/min. * = γ -lactones; \square = δ -lactones.

These phenomena can be explained by the particular separation mechanism of the column used. The silica-bonded polymer forms a three-dimensional network, in which the molecules of the sample diffuse. Interaction forces, such as dipole-dipole and hydrogen bonding can play an additional role in the interior of the cavities, but in particular the sizes and structures of the sample molecules are essential for the selectivity. The increased selectivity observed for γ -lactones is likely dependent on the half-planar structure of the five-membered ring and, thus, the higher steric differentiation of both enantiomers. With short alkyl chains, this effect is less distinct, resulting in similar α values for the lower homologues of the γ - and δ -lactones. In comparison to cellulose triacetate^{1,2}, the phase studied exhibits contrary selectivity.

The limits for detection (signal-to-noise ratio = 2:1) and resolution, ($R_s = 0.9$) ranged from 0.1 to 50 mg/ml for 20 μ l injected. Thus, semipreparative use of the column is also possible (*cf.* Experimental).

REFERENCES

- 1 J. A. Maga, *Crit. Rev. Food Sci. Nutr.*, 8 (1976) 1.
- 2 G. Ohloff, *Fortschr. Chem. Org. Naturst.*, 35 (1978) 431.
- 3 C. Günther, *Dissertation*, Würzburg, 1988.
- 4 R. Tressl, and K.-H. Engel, in P. Schreier (Editor), *Analysis of Volatiles*, Walter de Gruyter, Berlin, New York, 1984, p. 339.
- 5 A. Mosandl, M. Gessner, C. Günther, W. Deger and G. Singer, *J. High Resolut. Chromatogr. Chromatogr. Commun.*, 10 (1987) 67.
- 6 C. Günther and A. Mosandl, *Z. Lebensm.-Unters.-Forsch.*, 185 (1987) 1.
- 7 A. Mosandl, *Food Rev. Int.*, 4 (1988) 1.
- 8 M. Gessner, W. Deger and A. Mosandl, *Z. Lebensm.-Unters.-Forsch.*, 186 (1988) 417.
- 9 V. Schurig, in P. Schreier (Editor), *Bioflavour '87*, Walter de Gruyter, Berlin, New York, 1988, p. 35.
- 10 A. Mosandl, U. Palm, C. Günther and A. Kustermann, *Z. Lebensm.-Unters.-Forsch.*, 188 (1989) 148.
- 11 J. Bricout, in M. Martens, G. A. Dalen and H. Russwurm Jr. (Editors), *Flavour Science and Technology*, Wiley, Chichester, New York, 1987, p. 187.
- 12 E. Francotte, D. Lohmann, *Helv. Chim. Acta*, 70 (1987) 1569.
- 13 V. Meyer, *Praxis der Hochleistungs-Flüssigchromatographie*. Sauerländer, Aarau, 1979, p. 23.

CHROM. 21 358

GAS CHROMATOGRAPHIC AND SORPTION PROPERTIES OF MACRO-POROUS METHACRYLATE COPOLYMERS

J. HRADIL* and F. ŠVEC

Institute of Macromolecular Chemistry, Czechoslovak Academy of Sciences, 162 06 Prague (Czechoslovakia)

N. P. PLATONOVA and L. D. BELYAKOVA

Institute of Physical Chemistry of the U.S.S.R. Academy of Sciences, Moscow 117971 (U.S.S.R.)

and

V. MAROUŠEK

Institute of Chemical Technology, 166 28 Prague 6 (Czechoslovakia)

(First received November 2nd, 1988; revised manuscript received January 27th, 1989)

SUMMARY

The chromatographic properties of copolymers of 2,3-epoxypropyl methacrylate and 2,3-epithiopropyl methacrylate with ethylene dimethacrylate and of their derivatives modified with amines were investigated by means of gas chromatography and by the sorption of sulphur and carbon dioxides. The relative retention volumes and the changes in the free energy of adsorption of various compounds depend on the extent of the specific surface area of copolymers and on the content of functional groups. A study of the sorption of different compounds revealed that with increasing specific surface area the non-specific interactions increase while specific interactions decrease. This suggests that the accessibility of functional groups decreases with increasing extent of cross-linking of the sorbent.

INTRODUCTION

In recent years, porous polymers have become widely used as supports in the size-exclusion chromatography of oligomers and polymers, in affinity and gas and liquid adsorption chromatography and also as sorbents of gases and vapours^{1,2}. Numerous applications of such polymers have been made possible by the easy chemical modification of some polymer surfaces, by means of which various functional groups can be introduced. Some years ago the chromatographic properties of methacrylate copolymers were investigated³⁻⁵. This paper describes the sorption and chromatographic properties of methacrylate copolymers with various degrees of cross-linking containing epoxy and epithio groups.

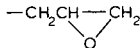
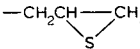
EXPERIMENTAL

Materials

Copolymers based on 2,3-epoxypropyl methacrylate (EPMA) and 2,3-epithiopropyl methacrylate (ETPMA) cross-linked with ethylene dimethacrylate (EDMA) were prepared by suspension radical copolymerization in the presence of inert solvents, as described elsewhere^{6,7}. Table I summarizes the chemical compositions and pore characteristics of the synthesized macroporous copolymers.

TABLE I

PROPERTIES OF SORBENTS BASED ON COPOLYMERS OF EPMA AND ETPMA WITH EDMA PREPARED IN THE PRESENCE OF CYCLOHEXANOL-DODECANOL AS A POROGENIC AGENT

Sorbent No.	Functional groups	Content of groups (mmol/g) ^a	EDMA ^b (%)	Cyclohexanol ^c (%)	S _g ^d (m ² /g)	V _p ^e (ml/g)
1		5.52	20	100	18.5	0.22
2		4.83	30	85	30	1.13
3		4.14	40	91	56	1.47
4		2.76	60	85	94	1.21
5		3.76	38	85	51	1.25
6		3.50	38	91	66	1.10
7		2.20	60	91	109	1.66
8		1.20	80	91	224	1.87
9 ^f	-CH ₂ CH(OH)CH ₂ NH ₂	1.40			42	
10 ^g	-CH ₂ CH(OH)CH ₂ NH(CH ₂) ₂ NH ₂	2.45			53	
11 ^h	-CH ₂ CH(SH)CH ₂ NH ₂	1.20			66	
12 ⁱ	-CH ₂ CH(SH)CH ₂ NH(CH ₂) ₂ NH ₂	1.20			224	

^a Calculated from elemental analysis of oxygen, sulphur and nitrogen.

^b Percentage of EDMA in monomer mixtures.

^c Percentage of cyclohexanol in porogen mixture.

^d Specific surface area measured by thermal desorption of nitrogen.

^e Pore volume calculated from cyclohexane regain.

^f With ammonia-modified sorbent 3.

^g With ethylenediamine-modified sorbent 3.

^h With ammonia-modified sorbent 6.

ⁱ With ethylenediamine-modified sorbent 6.

Chromatographic measurements

Chromatographic measurements were carried out using a chromatograph provided with flame ionization detection. The copolymers were packed into a glass column (0.8 m × 0.3 cm I.D.) with a flow-rate of nitrogen in the column of 10–20 ml/min.

For chromatographic standards chosen from alkanes, aromatic hydrocarbons, alcohols, ketones and esters of carboxylic acids, specific retention volumes (V_g) were determined and used to determine the relative retention volumes (V_{rel}) with respect to

hexane, Henry adsorption constants (K_1 ml/m²)⁸ using eqn. 1 and changes in the free energy of adsorption ($-\Delta F$) according to eqn. 2.

$$K_1 = V_g/S_g \quad (1)$$

$$-\Delta F = RT \ln K_1 + \text{constant} \quad (2)$$

where S_g is the specific surface area of the sorbent. The retention data were corrected to non-ideality.

The extent of specific interactions was determined from the retention volumes in relation to alkanes or from the difference in changes in the free energy of adsorption:

$$-\Delta F = \Delta F_{\text{spec}} - \Delta F_{\text{alk}} \quad (3)$$

for alkanes (alk) and other sorbates (spec) having the same number of carbon atoms.

It should be borne in mind, however, that in addition to the sorption of organic compounds on polymeric sorbents at 150°C, dissolution of the compounds occurs together with adsorption. In this case changes in the partial molar free energy of the methylene group, $\Delta G^E(\text{CH}_2)$, are usually determined⁹.

The specific surface area was determined in the dry state by the three-point BET method using a Quantasorb apparatus (Quantachrome, Greenvale, NY, U.S.A.) and nitrogen as the sorbate with an experimental error of 5%.

The sorption of gases (sulphur and carbon dioxides) was investigated by using the static method and a vacuum apparatus.

RESULTS AND DISCUSSION

The EPMA-EDMA and ETPMA-EDMA polymers investigated are characterized by the monomer composition in the polymerization mixture, by the content of functional groups in the polymer, by the specific surface area (S_g) and by the specific pore volume (V_p) summarized in Table I. Fig. 1 shows the dependences of the specific

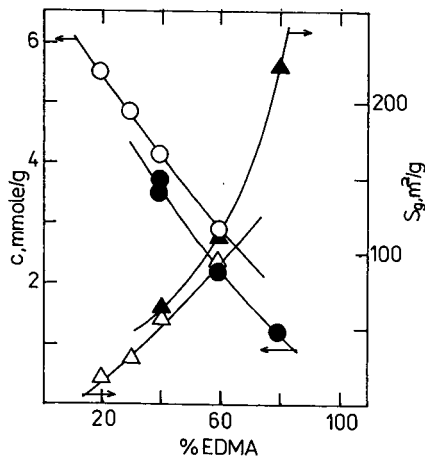


Fig. 1. Dependence of the content of (○) epoxy and (●) epithio groups and of the specific surface area (S_g) of (△) EPMA and (▲) ETPMA copolymers on the content of the cross-linking agent (EDMA) in the mixture of monomers.

TABLE II

RELATIVE RETENTIONS (V_{rel}) AND HENRY CONSTANTS (K_1) OF VARIOUS COMPOUNDS ON COLUMNS PACKED WITH SORBENTS 3 AND 5 AT 150°C

Sorbate	EDPMA-EDMA		ETPMA-EDMA	
	K_1	V_{rel}	K_1	V_{rel}
<i>n</i> -C ₆ H ₁₄	0.1	1.0	0.2	1.0
<i>n</i> -C ₇ H ₁₆	0.2	1.8	0.4	1.9
<i>n</i> -C ₈ H ₁₈	0.4	3.5	0.7	3.7
<i>n</i> -C ₉ H ₂₀	0.7	6.4	1.3	7.1
<i>n</i> -C ₁₀ H ₂₂	1.3	11.5	2.5	13.1
C ₆ H ₆	0.3	2.7	0.7	3.4
C ₆ H ₅ CH ₃	0.7	6.4	1.4	7.1
C ₆ H ₅ C ₂ H ₅	1.2	10.5	2.5	13.2
CH ₃ OH	0.1	1.3	0.3	1.6
C ₂ H ₅ OH	0.2	1.7	0.5	2.4
C ₃ H ₇ OH	0.4	3.2	1.0	5.2
C ₄ H ₉ OH	0.7	6.3	2.1	11.2
C ₅ H ₁₁ OH	1.3	11.6	—	—
CH ₃ COCH ₃	0.2	1.9	0.4	2.1
CH ₃ COC ₂ H ₅	0.4	3.2	0.8	4.0
CH ₃ COC ₃ H ₇	0.8	7.1	1.4	7.6
CH ₃ COC ₄ H ₉	1.1	10.4	2.9	15.2
CH ₃ COOCH ₃	0.2	1.7	0.3	1.7
CH ₃ COOC ₂ H ₅	0.3	2.6	0.6	3.2
CH ₃ COOC ₃ H ₇	0.5	4.8	1.2	6.4
CH ₃ COOC ₄ H ₉	1.0	9.4	2.4	12.8
CH ₃ NO ₂	0.6	5.6	0.8	4.3

surface area and of the concentration of functional groups on the amount of cross-linking agent for both polymer groups. With increasing EDMA content in the polymerization mixture the specific surface area of the polymers increases, but the concentration of functional groups decreases. These values are close for both types of polymers, and the dependences are parallel.

Chromatographic properties

Gas chromatography allows the properties of the sorbents to be investigated at a low surface coverage, under conditions where the sorbate-sorbate interactions are minimal. Table II summarizes the Henry adsorption constants (K_1) and relative retentions (V_{rel}) of various groups of compounds on sorbents 3 and 5, which have approximately the same concentrations of epithio and epoxy groups and similar geometries of the porous structure. As shown in Table II and Fig. 2, K_1 , V_{rel} , ΔF and Kováts retention indices (I) for all sorbates, except for nitromethane in the case of V_{rel} and for aromatic hydrocarbons in the case of ΔF , are higher on the sulphur-containing polymer than on that with epoxide groups. This suggests that stronger specific

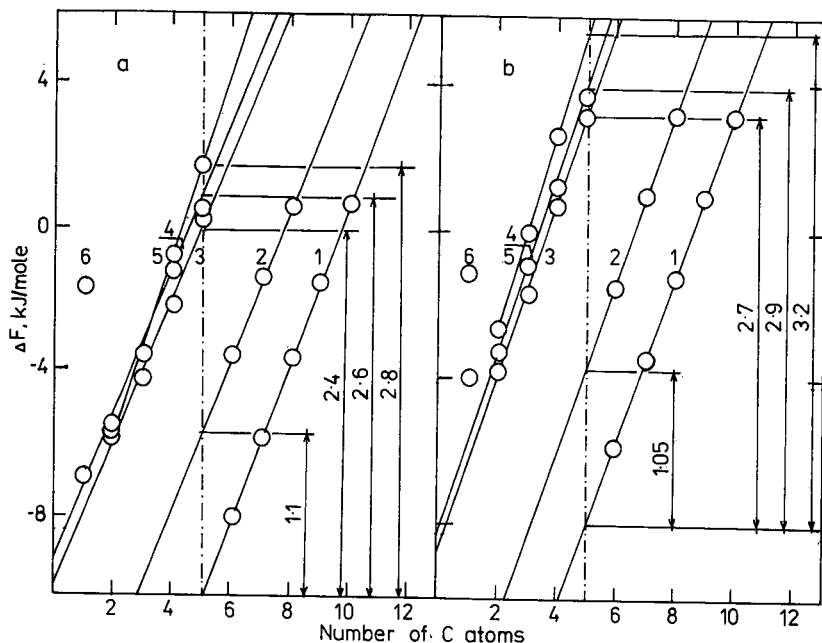


Fig. 2. Dependence of free energy of adsorption (ΔF , kJ/mol) of various compounds on the number of carbon atoms for EPMA-EDMA (a, sorbent 3) and ETPMA-EDMA copolymers (b, sorbent 5). 1, alkanes; 2, aromatic hydrocarbons; 3, acetates; 4, ketones; 5, alcohols; 6, nitromethane.

interactions occur between sorbed molecules and sulphur-containing groups. The largest contribution of specific interactions was found with nitromethane ($\mu = 3.6$ D), corresponding to the orientational forces.

Table III gives values of the constants a and b in the equation

$$-\Delta F = a + bn \quad (4)$$

TABLE III

COEFFICIENTS OF THE EQUATION $-\Delta F = a + bn$ (kJ/mol) DETERMINED USING RETENTIONS OF HOMOLOGOUS SERIES OF VARIOUS COMPOUNDS ON METHACRYLATE COPOLYMERS AT 150°C

Sorbent No.	Alkanes		Aromatic hydrocarbons		Alcohols		Ketones		Acetates	
	a	b	Δa^a	b	Δa^a	b	Δa^a	b	Δa^a	b
1	4.6	0.37	2.2	0.27	2.8	0.36	2.9	0.29	2.8	0.28
2	4.7	0.41	1.7	0.39	2.7	0.45	2.8	0.41	2.7	0.37
3	5.0	0.52	1.2	0.49	2.7	0.50	2.7	0.50	2.1	0.70
4	5.5	0.73	1.1	0.67	3.2	0.53	3.2	0.64	3.1	0.67
5	4.0	0.46	0.5	0.57	1.0	0.61	2.2	0.58	2.1	0.57
6	4.7	0.54	1.0	0.56	2.8	0.64	2.7	0.61	2.6	0.56
7	5.0	0.66	0.6	0.67	2.3	0.70	2.6	0.64	2.6	0.62
8	5.7	0.80	0.40	0.79	2.5	0.83	2.9	0.75	2.7	0.81

^a Δa denotes differences from values for alkanes.

where n is the number of methylene groups for various types of compounds relative to alkanes. The b values are a measure of changes in the free energy of the methylene group, *i.e.*, a measure of dispersion interactions, and characterize the selectivity with respect to the individual homologues. Changes in a for various types of compounds characterize the specific interactions of compounds containing the same number of methylene groups but having functional groups of different types.

Table III indicates that for the same sorbent the b values of the compounds investigated vary only slightly, *i.e.*, the character of the functional groups has only a weak influence on the contribution of dispersion forces. With increasing specific surface area, the contribution of non-specific interactions increases for both types of sorbent. The contribution of specific interactions is also affected by the number of accessible functional groups of the sorbent.

Fig. 3 shows the dependences of $\ln K_1$ for various sorbates on the content of groups localized on the sorbent surfaces. The functional groups accessible on the inner surface (c_p) were determined from the ratio of the total content of groups (c_0) to the specific surface area (S_g). This value was corrected for the size of the globules (R) forming the sorbent bead ($R = 3000/\rho S_g$, nm) and by the size of the structural unit of EPMA or ETPMA, $l = 1.0$ nm. The correction factor for the monomer EPMA (or ETPMA) distribution in the globule is then given by

$$A = 1 - \left(\frac{3000}{\rho S_g} - 1 \right)^3 \left(\frac{\rho S_g}{3000} \right)^3 \quad (5)$$

where ρ is the copolymer density (1.3 g/ml).

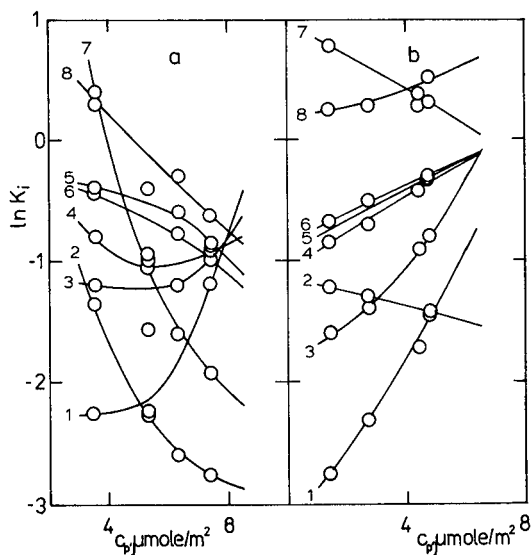


Fig. 3. Henry adsorption constant ($\ln K_1$) as a function of the specific surface concentration of oxirane and epithio groups (c_p) in (a) EPMA-EDMA and (b) ETPMA-EDMA copolymers. Sorbates: 1 = methanol; 2 = hexane; 3 = acetone; 4 = propanol; 5 = ethyl acetate; 6 = benzene; 7 = *n*-octane; 8 = toluene.

The content of surface groups (c_p) is given by

$$c_p = \frac{c_0}{S_g} \cdot A \quad (6)$$

As follows from the calculations, there are no differences in proportionality between surface concentration and total content of groups.

The dependences in Fig. 3 confirm the preceding observations regarding the polar character of both types of sorbent. The non-linearity of the $\ln K_i$ vs. c_p dependence can be interpreted as a deviation from the regular distribution of functional groups of the polymers prepared. With increasing content of surface glycidyl or epithio groups, the distribution coefficients of alkanes decrease, whereas those of methanol and acetone increase.

The retentions of medium-polarity compounds and aromatic hydrocarbons increase with increasing concentration of surface groups with the copolymer ETPMA, but decrease with EPMA.

The retentions of alkanes decrease more with increasing concentration of surface groups the longer is the hydrocarbon chain. The retention of molecules that are sorbed specifically increases more markedly with increasing content of groups the shorter is the hydrocarbon portion of the molecule. With epoxy copolymers the effect of the hydrocarbon part of the sorbate molecules on their retention is stronger than that with epithio copolymers, which indicates a weaker polarity of the epoxy groups.

Table IV gives the Kováts retention indices of various types of compounds on EPMA-EDMA and ETPMA-EDMA copolymers. A comparison of copolymers with similar compositions (Table I, copolymers 3 and 6) shows that the Kováts retention indices on ETPMA-EDMA copolymers are higher than those on EPMA-EDMA copolymers, which suggests that the specific interactions of sulphur-containing polymers may be stronger than those of copolymers which contain only oxygen.

Sorption of sulphur dioxide and carbon dioxide

Unlike chromatographic methods, sorption methods applied under static conditions make possible measurements with saturated surfaces of the sorbent. Fig. 4 shows the sorption isotherms of sulphur dioxide on EPMA-EDMA and ETPMA-EDMA copolymers. For polymers 5-7 the absorption (a , mmol/g) decreases with increasing S_g from 51 to 109 m²/g and with decreasing sulphur content from 12 to 7%. The sorbent having the lowest sulphur content and the largest specific surface area (224 m²/g) usually exhibits a high sorption of sulphur dioxide.

Fig. 5 shows the dependence of the sulphur dioxide sorption relative to unit surface area on the amount of sulphur in epithio groups of the ETPMA copolymer. The increase in the adsorption of sulphur dioxide in polymers with a sulphur content above 7% can be related to an increasing amount of epithio groups contributing to specific interactions with sulphur dioxide, particularly due to orientational forces ($\mu = 1.6$ D). The ascending part of the dependence on the left (content of sulphur below 7%) can be explained by increasing dispersion interactions with the surface of the adsorbent proportional to the specific surface area.

The dependence of the sorption of sulphur dioxide on the content of functional groups in polymers, and on the specific surface area (Fig. 5), is caused by the varying

TABLE IV

KOVÁTS RETENTION INDEXES OF EPMA-EDMA AND ETPMA-EDMA COPOLYMERS AT 150°C

Solute	Sorbent No.							
	1	2	3	4	5	6	7	8
C ₆ H ₆	1042	956	766	709	816	781	702	653
C ₆ H ₅ CH ₃	1119	1051	903	795	964	901	802	749
C ₆ H ₅ C ₂ H ₅	1199	1136	984	—	1070	998	—	—
C ₆ H ₅ C ₃ H ₇	1256	—	—	—	—	—	—	—
CH ₃ COCH ₃	944	863	710	621	711	707	587	562
CH ₃ COC ₂ H ₅	1044	950	792	713	830	812	687	649
CH ₃ COC ₃ H ₇	—	1069	924	—	969	912	781	740
CH ₃ COC ₄ H ₉	1085	1116	992	—	1095	1019	—	843
CH ₃ COOCH ₃	901	817	690	621	697	684	588	555
CH ₃ COOC ₂ H ₅	975	884	761	704	794	778	674	650
CH ₃ COOC ₃ H ₇	1054	979	860	801	932	885	775	741
CH ₃ COOC ₄ H ₇	1137	1080	968	—	1065	997	—	852
CH ₃ OH	964	809	639	514	604	676	468	432
C ₂ H ₅ OH	976	846	693	588	690	735	566	524
C ₃ H ₇ OH	1046	951	790	625	822	851	677	631
C ₄ H ₉ OH	1166	1083	900	—	989	975	—	742
C ₅ H ₁₁ OH	1251	1169	1001	—	1113	—	—	—
CH ₃ NO ₂	1269	1095	793	—	853	822	681	624
CH ₃ CN	1148	1002	889	642	—	—	—	—

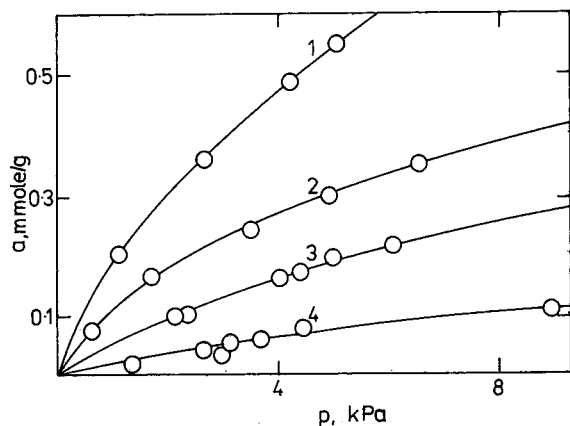


Fig. 4. Sorption isotherms of sulphur dioxide on ETPMA-EDMA copolymers measured at 30°C. 1 = sorbent 8; 2 = sorbent 5; 3 = sorbent 6; 4 = sorbent 7.

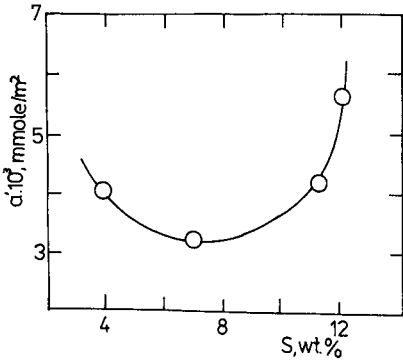


Fig. 5. Dependence of the amount of sulphur dioxide sorbed by unit surface area (a') of ETPMA-EDMA polymers as a function of the content of sulphur in epithio groups.

contributions of non-specific and specific interactions; in other words, it shows the role of the chemical nature of the surface, which is also reflected in the case of considerable saturation of the surface with the adsorbate.

Similarly to EPMA-EDMA copolymers, the ETPMA-EDMA copolymers modified with amines or with ethylenediamine¹⁰ also adsorb more sulphur dioxide than the starting polymers (Fig. 6), but the sorption of sulphur dioxide and carbon dioxide on copolymers based on EPMA is several times higher. Different roles of the SH and OH groups of the polymer in the sorption of sulphur dioxide and carbon dioxide seem to be operative in this instance.

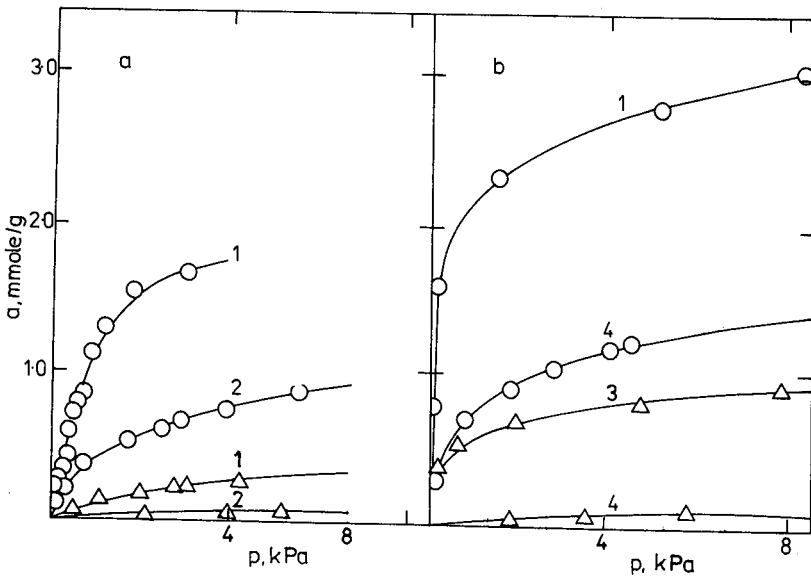


Fig. 6. Sorption isotherms of (O) sulphur dioxide and (Δ) carbon dioxide at 30°C on copolymers modified by (a) ammonia and (b) ethylenediamine; 1 = copolymer 9; 2 = copolymer 11; 3 = copolymer 10; 4 = copolymer 12.

CONCLUSIONS

This chromatographic study of macroporous methacrylate copolymers has shown that with increasing specific surface area the non-specific interactions increase while specific interactions decrease. This confirms the suggestion that the accessibility of functional groups decreases with increasing amount of cross-linking agent in the sorbent.

The polar adsorbates are bound more strongly to the polymers with epithio groups than to those containing epoxy groups. The non-linearity or extremes of the dependences follow the changes in the ratio of specific and non-specific interactions caused by the irregular group distribution in the polymer globules.

REFERENCES

- 1 L. D. Glazunova, L. I. Panina and K. I. Sakodynskii, *Usp. Khim.*, 52 (1983) 1223.
- 2 L. D. Belyakova, A. V. Kiselev, N. P. Platonova and T. I. Shevchenko, *Adv. Colloid Interface Sci.*, 21 (1984) 55.
- 3 J. Hradil, *J. Chromatogr.*, 144 (1977) 63.
- 4 J. Lukáš, F. Švec and J. Kálal, *J. Chromatogr.*, 153 (1978) 15.
- 5 J. Lukáš, F. Švec, E. Votavová and J. Kálal, *J. Chromatogr.*, 153 (1976) 373.
- 6 F. Švec, J. Hradil, J. Čoupek and J. Kálal, *Angew. Makromol. Chem.*, 48 (1975) 135.
- 7 V. Maroušek, M. Bleha, E. Votavová and J. Kálal, *Sci. Pap. Prague Inst. Chem. Technol.*, S3 (1980) 269.
- 8 A. V. Kiselev, Ya. I. Yashin, *Gazo-adsorptsiionnaya Khromatografiya*, Nauka, Moscow, 1967, p. 116.
- 9 J. Novák, J. Růžičková, S. Wičar and J. Janák, *Anal. Chem.*, 45 (1973) 1365.
- 10 J. Hradil, F. Šec, J. Kálal, L. D. Belyakova, A. V. Kiselev, N. P. Platonova and T. I. Shevchenko, *React. Polym.*, 1 (1982) 59.

CHROM. 21 331

USE OF CROWN ETHERS IN GAS CHROMATOGRAPHY

YONGHAO JIN and RUONONG FU*

Department of Chemical Engineering, Beijing Institute of Technology, P.O. Box 327, Beijing (China)
and

ZAIFU HUANG

Department of Environmental Science, Wuhan University, Wuhan (China)

(First received July 28th, 1988; revised manuscript received January 13th, 1989)

SUMMARY

Two new kinds of crown ethers, 4,4-dipentadecyl- or 4,3'-dipentadecyldibenzo-30-crown-10 and 3-pentadecylbenzo-15-crown-5, were coated on glass capillary columns and fused-silica capillary columns, and their chromatographic characteristics studied. The polarity, selectivity and stability of the crown ethers were characterized. The rôle of the crown ether ring in separating solutes is also mentioned.

INTRODUCTION

Crown ethers or macrocyclic polyethers, which were first introduced by Pedersen¹, have the ability to form stable complexes with metal-cations. They are interesting organic compounds and have found wide applications in chemistry, especially in analytical chemistry. They can be used as solvent extraction reagents for the separation and isolation of metal ions, as components in membranes for ion-selective electrodes and as a component of the stationary and mobile phases in liquid chromatography. A very important review on the applications of crown ethers in analytical chemistry has been written by Kolthoff².

Blasius *et al.*³ and Cram and co-workers⁴ first reported the use of crown ethers in chromatography. Since then this usage has developed greatly, especially in liquid chromatography. Chromatographers have just began to pay attention to them in gas chromatography (GC) and there have been a few articles⁵⁻⁹ concerning the application of crown ethers in GC. Li^{5,6} used packed columns coated with dibenzo-24-crown-8, dibenzo-18-crown-6 and other crown ethers to separate hydrocarbons, alcohols, amines and other compounds. Graphitized thermal carbon blacks modified with crown ethers can also be used to separate hydrocarbons, aromatic compounds and halides, etc.⁷. Fine *et al.*⁸ coated crown ethers including polymers with crown ether groups on glass capillary columns and characterized their chromatographic properties. 18-Crown-6-substituted polysiloxane was synthesized and used as a stationary phase by Lee and co-workers⁹.

Two new kinds of crown ethers indicated in Fig. 1 have similar structure and

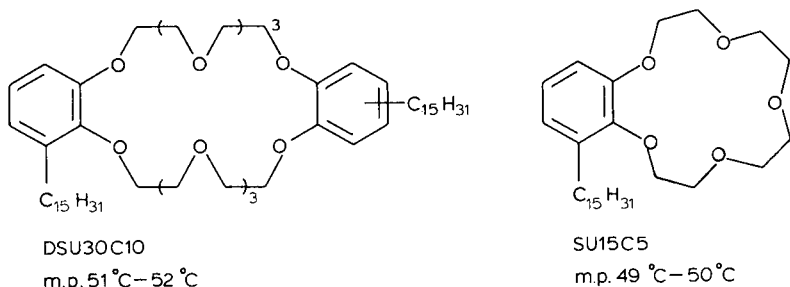


Fig. 1. Structures of crown ethers used in this study.

each has three different functional groups: long apolar alkyl, easily polarizable benzene ring and polar polyether ring. Thereby they were expected to have strong abilities in separating different classes of organic compounds. They were both coated on glass and fused-silica capillary columns and their chromatographic characteristics were studied.

EXPERIMENTAL

A Model SP-2305 gas chromatograph (Beijing Analytical Instrument Factory, China) equipped with a capillary split injection system, flame ionization detector and integrator was used. Glass tubing with 7 mm O.D. and 3 mm I.D. (Beijing Glass Experimental Factory, China) was drawn into capillary columns (0.29 mm I.D.) by using a Model GDM-1B glass drawing machine (Shimadzu, Japan). Prior to drawing, the tubes were rinsed with chromic acid, water, methanol and acetone and then dried. Glass capillaries were filled to 80–90% of their lengths with 20% hydrochloric acid, sealed at both ends and then heated at 170°C overnight. The ends were opened and the columns were rinsed with diluted hydrochloric acid (pH 3), methanol and acetone, and then dried at 200°C under a stream of nitrogen. The columns were coated dynamically with hexamethyldisilazane. Then the ends were sealed and the columns were heated at 400°C for 4 h. The ends were opened and the columns were rinsed with dichloromethane, methanol and acetone. The columns were dried at 150°C for 2 h. Fused-silica columns (0.22 mm I.D.; Yongnian Optical Fibre Factory, China) were purged with nitrogen at 170°C for 6 h before coating. Glass and fused-silica capillary columns were then statically coated at room temperature with stationary phase solutions in pentane. Each column was conditioned at 100, 150 and 190°C for 1 h, respectively.

The crown ethers were obtained from the Department of Environmental Science, Wuhan University, China. All other chemicals used for characterization were analytical reagent grade.

RESULTS AND DISCUSSION

Table I shows the characteristics of the crown ether capillary columns. It indicates that fused-silica columns have higher column efficiencies than glass capillary columns though the former were not deactivated.

The selectivity and polarity of the crown ethers are expressed by McReynolds

TABLE I
CHARACTERISTICS OF CROWN ETHER CAPILLARY COLUMNS USED IN THIS WORK
Test compound: 1-octanol.

Column No.	Column size (L × I.D.)	Type of capillary	Stationary phase	Column efficiency (n/m)
1	17 m × 0.29 mm	Glass	DSU30C10	1860
2	10 m × 0.22 mm	Silica	DSU30C10	2750
3	20 m × 0.22 mm	Silica	DSU30C10	2680
4	16 m × 0.29 mm	Glass	SU15C5	1580
5	10 m × 0.22 mm	Silica	SU15C5	2550
6	20 m × 0.22 mm	Silica	SU15C5	2770

constants, b (the slope of the curve obtained when the logarithm of the adjusted retention times of n -alkanes are plotted as a function of the number of carbon atoms and $r = t'_R(n+1)/t'_R(n)$). These parameters and the average polarity shown in Table I were obtained at 120°C.

The average polarity for the crown ethers is much lower than that of PEG-20M, owing to their long apolar alkyl groups and benzene. However, the b value for the crown ethers is higher than that of SE-30, indicating that the crown ethers are very convenient for separating apolar compounds. As Fig. 2 shows, the slope of the plot of $\log t'_R$ vs. carbon number of homologous alcohols on DSU30C10 is higher than on PEG-20M, implying that DSU30C10 has higher selectivity for alcohol than PEG-20M does. 18-C-6 substituted polysiloxane has a higher selectivity for nitrogen-containing polycyclic aromatic compounds than has a polar stationary phase⁹, but there is no appreciable difference in the interaction of biphenyl with the crown and Carbowax 20M because biphenyl is too large to fit in the cavity of the crown ether ring. The selectivity of crown ethers depends mainly on the relative size of the solute and the crown ether cavity, the type, number and placement of hetero atoms and the conformational flexibility of the crown ether ring.

Crown ethers have special selectivity, especially for aromatic compounds and their derivatives, amines, anilines, etc.⁷. The two crown ethers are versatile gas chromatographic stationary liquids. They give excellent separations of organic

TABLE II
SELECTIVITY AND POLARITY OF THE CROWN ETHERS USED

X' = Benzene, Y' = butanol, Z' = 2-pentanone, U' = nitropropane, S' = pyridine.

Stationary phase	McReynolds constants (I)					Mean	b	r
	X'	Y'	Z'	U'	S'			
DSU30C10	82	116	128	213	166	141.0	0.272	1.903
SU15C5	121	218	165	242	195	188.2	0.273	1.877
SE-30 ¹⁰	15	44	53	64	41	432.4	0.2495	1.766
PEG-20M ¹⁰	322	536	368	572	510	461.2	0.2235	1.673

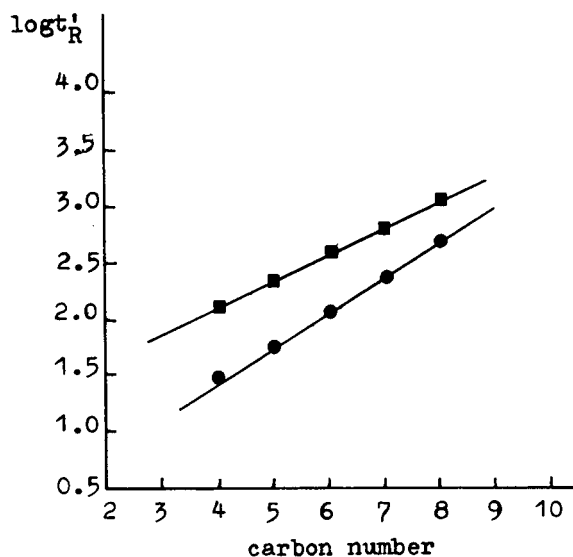


Fig. 2. Plot of log (adjusted retention time) against carbon number for homologous alcohols. (■) PEG-20M; (●) DSU30C10. Column temperature: 104°C.

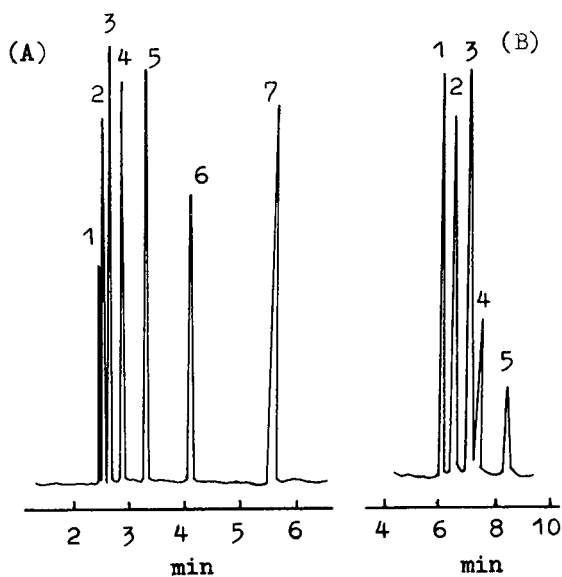


Fig. 3. Chromatogram of organic compounds with hydroxyl groups. (A) On column 1, carrier gas (nitrogen) flow-rate 13 cm/s, splitting ratio 1/100, at 132°C. Peaks: 1 = C_2H_5OH ; 2 = $n-C_3H_7OH$; 3 = $n-C_4H_9OH$; 4 = $n-C_5H_{11}OH$; 5 = $n-C_6H_{13}OH$; 6 = $n-C_7H_{15}OH$; 7 = $n-C_8H_{17}OH$. (B) On column 6, carrier gas (nitrogen) flow-rate 15 cm/s, splitting ratio 1/100, at 194°C. Peaks: 1 = 2,6-; 2 = 2,4- and 2,5-; 3 = 3,5-; 4 = 3,4-; 5 = 2,3-dihydroxytoluene.

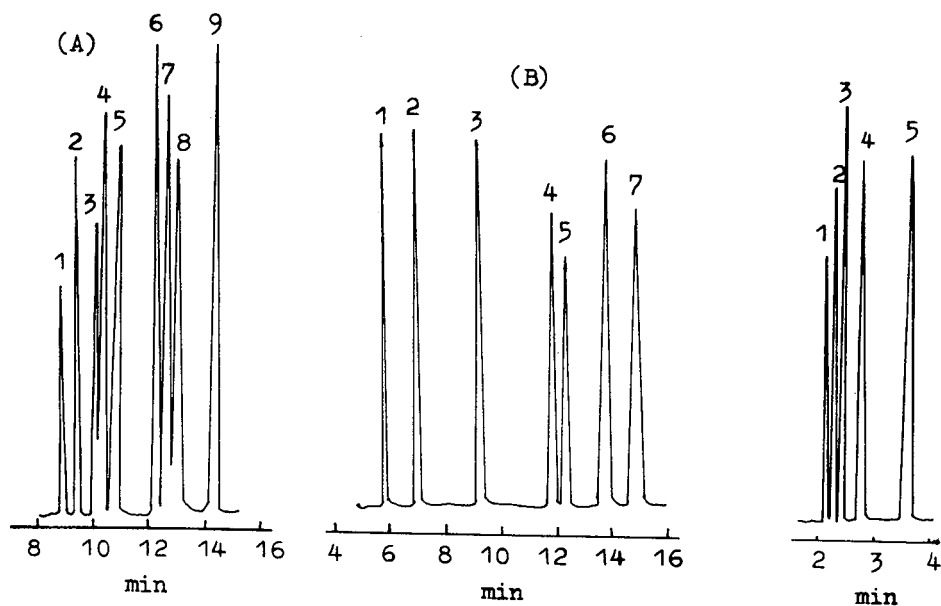


Fig. 4. Chromatogram of aromatic hydrocarbons (A) and their derivatives (B). (A) On column 5, carrier gas (nitrogen) flow-rate 13 cm/s, at 133°C. (B) On column 3, carrier gas (nitrogen) flow-rate 13 cm/s, at 128°C. Peaks: 1 = toluene; 2 = chlorobenzene; 3 = bromobenzene; 4 = *m*-dichlorobenzene; 5 = *p*-dichlorobenzene; 6 = *o*-dichlorobenzene; 7 = iodobenzene.

Fig. 5. Chromatogram of halohydrocarbons on column 4 at 132°C, carrier gas (nitrogen) flow-rate 13 cm/s, splitting ratio 1/100. Peaks: 1 = ethyl bromide; 2 = *n*-butyl chloride; 3 = *n*-butyl bromide; 4 = 1,3-dichloropropane; 5 = 1,4-dichlorobutane.

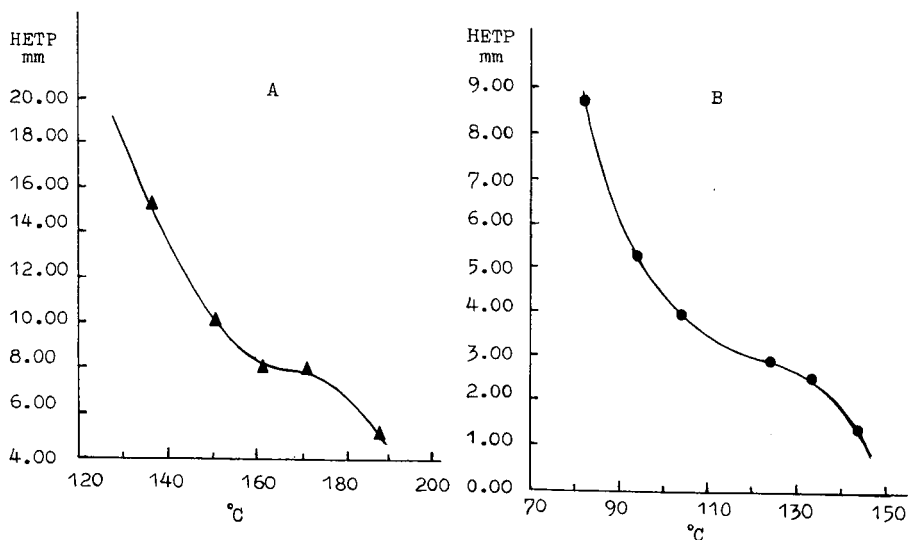


Fig. 6. Plot of HETP against temperature for *n*-octanol on column 5 (A) and *n*-tridecane on column 1 (B).

compounds with hydroxyl groups, without tailing (Fig. 3). This is due to the high efficiency and the deactivation of the residual silanol groups on the surface of the column walls by crown ethers rings. Apolar compounds such as alkanes, easily polarizable compounds such as aromatic hydrocarbons and their derivatives (Fig. 4) and moderately polar compounds such as halohydrocarbons (Fig. 5) were separated.

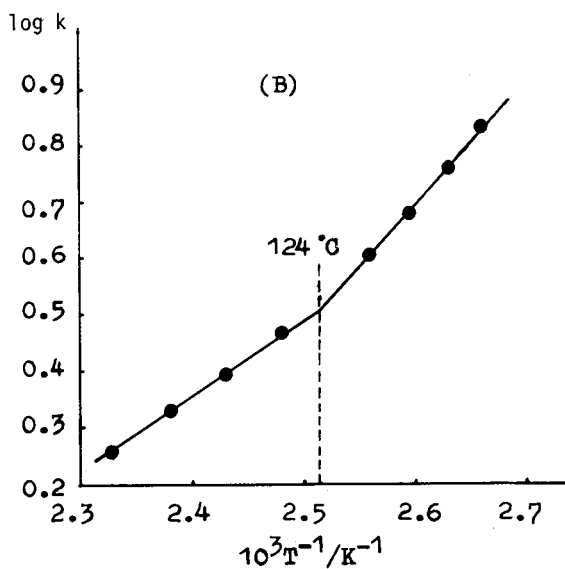
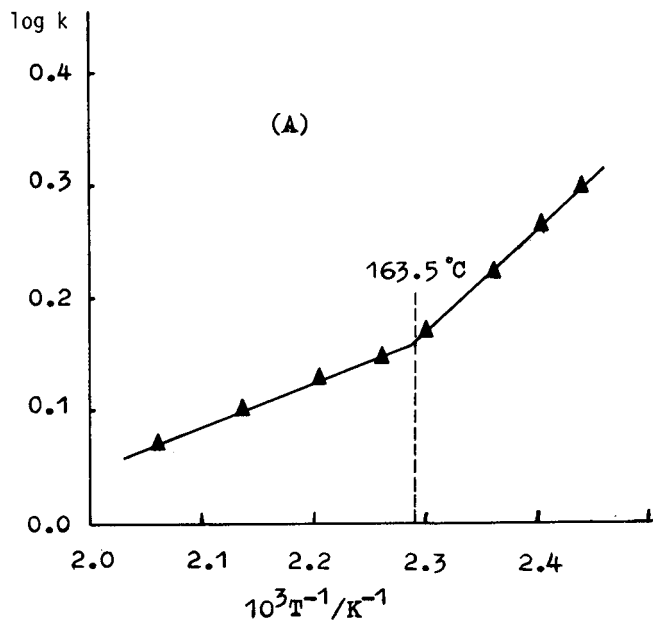


Fig. 7. Plots of $\log k$ against reciprocal absolute temperature for $n\text{-C}_{12}\text{H}_{26}$ with SU15C5 (A) and DSU30C10 (B) as the stationary phase. The transition temperature is indicated by the vertical dashed line.

To determine the effect of temperature on column efficiency, the height equivalent to a theoretical plate (HETP) was measured at different temperatures. Fig. 6 shows a plot of HETP vs. T for octanol and n -tridecane on the two crown ether columns. It is apparent that column efficiency increases with increasing temperature up to the temperature at which crown ethers begin to bleed obviously. Each curve has a turning point which implies that there is a liquid-liquid transition (see Fig. 7).

The maximum allowable operating temperature of the crown ether columns is relatively high, if their molecular weights are taken into account. The baseline is even when the column temperature is lower than 200°C. The capillary columns were used at about 200°C for 2 months without losses in column efficiency and capacity.

The minimum allowable operating temperature is low (about 50°C) as the crown ethers have low melting points. However, the column efficiency is rather low at this temperature.

REFERENCES

- 1 C. J. Pedersen, *J. Am. Chem. Soc.*, 89 (1967) 2495.
- 2 I. M. Kolthoff, *Anal. Chem.*, 51 (1979) 1R.
- 3 E. Blasius, W. Adrian, K.-P. Janzen and G. Klautke, *J. Chromatogr.*, 96 (1974) 89.
- 4 L. R. Sousa, D. H. Hoffman, L. Kaplan and D. J. Cram, *J. Am. Chem. Soc.*, 96 (1974) 7100.
- 5 R. Li, *Wuhan Daxue Xuebao, Ziran Kexueban*, 4 (1985) 121.
- 6 R. Li, *Sepu*, 4 (1986) 304.
- 7 E. V. Zagorevskaya and N. Y. Kovaleva, *J. Chromatogr.*, 365 (1986) 7.
- 8 D. D. Fine, H. L. Gearhart, II, and H. A. Mottola, *Talanta*, 32 (1985) 751.
- 9 C. A. Rouse, A. C. Finlinson, B. J. Tarbet, J. C. Pixton, N. M. Djordjevic, K. E. Markides and M. L. Lee, *Anal. Chem.*, 60 (1988) 901.
- 10 W. O. McReynolds, *J. Chromatogr. Sci.*, 8 (1970) 685.

CHROM. 21 406

ANALYSIS OF SOLVENT RESIDUES IN PHARMACEUTICAL BULK DRUGS BY WALL-COATED OPEN TUBULAR GAS CHROMATOGRAPHY

DAVID W. FOUST and MICHAEL S. BERGREN*

The Upjohn Company, Control Division, Kalamazoo, MI 49001 (U.S.A.)

(First received June 9th, 1988; revised manuscript received February 10th, 1989)

SUMMARY

A simple general method for the determination of solvent residues in drugs is described. The procedure is based on wide-bore wall coated open tubular (WCOT) gas chromatographic analysis of bulk drug solutions. The use of wide-bore WCOT columns with chemically crosslinked methyl silicone stationary phases offers improvements in specificity and sensitivity over earlier packed-column methods. The factors that influence method accuracy are discussed, including a consideration of instrumental and matrix contributions to the linearity and bias of the method. Some problems with interferences peculiar to benzyl alcohol are reported.

INTRODUCTION

The analysis of solvent residues is receiving greater emphasis in the evaluation of bulk pharmaceuticals. High-purity bulk drugs are produced by the pharmaceutical manufacturer using carefully tailored final process recrystallizations. As a result, solvents are a minor but ubiquitous component of these materials. The role of solvent residues in the toxicology, stability, and pharmaceutical properties of the finished dosage form is insignificant if the solvent content is controlled in the bulk drug, raw materials, packaging components and production systems. A general method applicable to all of the possible solvents and bulk drugs is attractive. The reliance on a single method would eliminate the confusion and inefficiencies that result from using a number of comparable, but instrumentally distinct, methods in routine application.

Several procedures based on packed-column separations have been reported¹⁻⁴. Most of these employ porous polymer packings or packings based on graphitised carbon supports. The procedure of Haky and Stickney³ is notable because of the simplicity of sample preparation and ease of adaptability to standard sampling equipment. The need for a general organic volatiles procedure in the U.S. Pharmacopeia has been noted⁵, and recently, a procedure based on the Haky and Stickney method³ has been proposed for adoption in that compendium⁶.

The importance of evaluating solvent residues in research pharmaceuticals, as distinct from marketed pharmaceuticals, should not be underemphasized. Because of the high attrition rate for research compounds in the pharmaceutical industry, mar-

keted pharmaceuticals represent only a fraction of the compounds that require analytical evaluation. Large numbers of experimental drugs are continually being introduced. These drugs are the objects of laboratory study as well as clinical study. Modifications to the process chemistry may result in changes in the types or amounts of solvents retained in the bulk drug. The need exists for a quantitative solvent screen, which is capable of providing reliable information on the type and quantity of solvent residue present. In this application, the selectivity, peak capacity, and reproducibility of retention times have increased importance. The ability to interface the method to structurally informative detection schemes, such as mass spectrometry (MS) or infrared spectroscopy, is an important advantage.

Unfortunately, the variety of available solvents and bulk drug matrices is so diverse that a truly general method would probably be complex and expensive to implement on a routine basis. Headspace sampling, high-efficiency capillary gas chromatography (GC), and selective detection schemes are needed in the widest variety of potential applications. Our experience in pharmaceutical analysis, however, suggests that the complexity of the most general method is dictated by a small percentage of cases. The solvents in most of the current market or research pharmaceuticals are amenable to analysis on a much simpler and less expensive system. Our goal has been the development of a procedure suitable for the analysis of solvent residues in 80–90% of the available bulk drugs. Our approach reflects an attempt to provide optimum performance in terms of separation power, precision, dynamic range and simplicity for the largest number of compounds.

Recent advances in GC have provided the basis for improvements in the routine GC evaluation of solvent residues. In particular, the availability and ease of use of wide-bore (0.53 mm) fused-silica wall-coated open tubular (WCOT) columns with thick chemically bonded phases has provided a bridge between packed-column GC and high-resolution capillary methods. These columns yield improvements in separation efficiency by a factor of 3–10 over packed columns. They have a large sample capacity, which eliminates the need for split injection techniques required by narrower-bore capillary columns. The difficulty of coupling autosampler systems with capillary methods has been cited by other investigators³. These problems are not significant for wide-bore column systems if direct injection methods are employed on commercially available instruments.

EXPERIMENTAL

Equipment and materials

The method was developed on a Hewlett-Packard 5890 gas chromatograph equipped with a Hewlett-Packard 7673A robotic autosampler (Hewlett-Packard, Avondale, PA, U.S.A.). The Hewlett-Packard split/splitless injector port was used in splitless mode with the standard splitless insert. Samples were injected in the direct mode. A continuous inlet purge of 140 ml/min of carrier gas was maintained, except for a 30-s sampling time during the injection. A Hewlett-Packard flame ionization detector was used with a capillary jet and 30 ml/min of nitrogen make-up gas. Signals were digitised with a Hewlett-Packard 3392A integrator, and the digital data was processed on an in-house VAX computer based chromatography analysis system.

The columns were 30 m × 0.53 mm I.D. fused-silica columns with a 5- μ m thick

chemically crosslinked methyl silicone stationary phase. RTx-1 halfmil columns (Restek, Port Matilda, PA, U.S.A.) or DB-1 Megabore columns (J&W Scientific, Rancho Cordova, CA, U.S.A.) were used interchangeably. The analytical columns were coupled to a 5 m × 0.53 mm I.D. phenyl methyl silicone deactivated retention gap (Restek Corp.) acting as a guard column. The columns were coupled with a butt connector with Vespel SP-211 ferrules (Supelco, Bellefonte, PA, U.S.A.). Carrier gas was purified with a heated scrubber (Supelco) to remove oxygen.

Benzyl alcohol was obtained from Aldrich (Milwaukee, WI, U.S.A.) as a 99% purity grade or as puriss grade from Fluka (Ronkonkoma, NY, U.S.A.). All other solvents were obtained from the Aldrich, Burdick & Jackson Labs. (Muskegon, MI, U.S.A.), Eastman Kodak (Rochester, NY, U.S.A.), and U.S. Industrial Chemicals (Houston, TX, U.S.A.) in high purity (98 + %) grades and used without further purification. Drug samples were obtained from in house sources at the Upjohn Co.

Sample preparation and analysis

Samples were prepared by dissolving about 10 mg of the drug, accurately weighed, per gram of benzyl alcohol and shaking to effect dissolution. Standards consisted of accurately prepared solutions of the appropriate solvents in benzyl alcohol. Where necessary, dilutions of concentrated standard solutions were calculated by weight. Typical concentrations for standard solutions were 0.02–0.05 mg solvent per gram of benzyl alcohol. These values correspond to solvent levels of 0.2–0.5% by weight in bulk drug for bulk drug samples of nominal 10 mg/g concentration. To avoid the loss of volatile components, headspace exchanges were minimized during the preparation of samples and standards.

Volumes of 0.5 μ l of sample and standard preparations were alternately injected onto the GC system. Helium was used as the carrier gas, back-pressure regulated at 3 p.s.i. and with a linear velocity of *ca.* 35 cm/s. The injector and detector temperature were 180 and 260°C, respectively. The oven program was: 35°C (5 min hold); 8°C/min ramp to 175°C (0 min hold); ballistic ramp to 260°C (16 min hold). Quantitative determinations were accomplished by the external standard method.

RESULTS

Specificity

The chromatographic specificity is illustrated by the separation of 27 different process solvents shown in Fig. 1. With the exception of a few co-eluting solvents, the solvents of interest are distributed uniformly throughout the chromatographic profile. The time available for analysis, prior to the elution of benzaldehyde, is about 20 min. The peaks are symmetric with uniform widths of about 0.1 min throughout the chromatogram under the conditions employed. If Gaussian peaks are assumed, and a separation of 4σ is used as a criterion for resolution, a rough estimate of the peak capacity of the system is 110–120.

The reproducibility of retention times is illustrated in Table I, where representative results were taken from the ten injections of a fourteen-component standard. These injections were interspersed with drug samples in a sequence of chromatographic runs that spanned 55 h. The standard deviations (S.D.) are limited by the two significant digits in retention times for the data reported in the table. The repro-

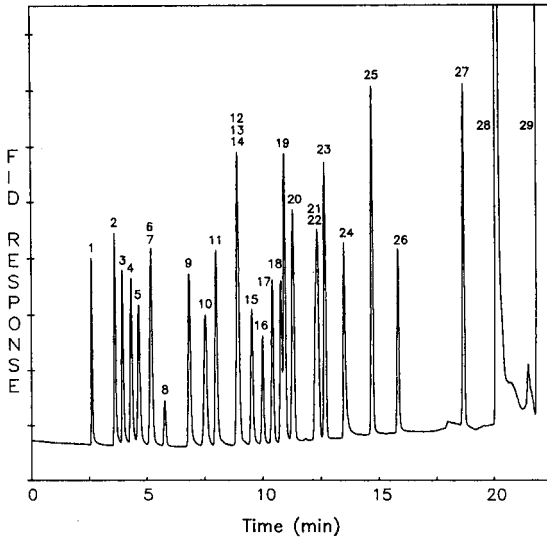


Fig. 1. Separation of a mixture of 27 different common process solvents. FID = Flame ionization detection. Peaks: 1 = methanol; 2 = ethanol; 3 = acetonitrile; 4 = acetone; 5 = isopropanol; 6 = diethyl ether; 7 = pentane; 8 = dichloromethane; 9 = *n*-propanol; 10 = methyl *tert.*-butyl ether; 11 = methyl ethyl ketone; 12 = ethyl acetate; 13 = hexane; 14 = chloroform; 15 = tetrahydrofuran; 16 = ethylene dichloride; 17 = *n*-butyl chloride; 18 = *n*-butanol; 19 = benzene; 20 = cyclohexane; 21 = isooctane; 22 = dioxane; 23 = heptane; 24 = pyridine; 25 = toluene; 26 = *n*-butyl acetate; 27 = *o*-xylene; 28 = benzaldehyde; 29 = benzyl alcohol.

ducibility of retention times between injections permits reliable identification of most components.

The slight variations in retention times from column to column and run to run are due to small differences in carrier flow and phase ratio. These variations can be

TABLE I
REPRODUCIBILITY OF RETENTION TIMES FOR SELECTED SOLVENTS

Results represent the average of ten determinations.

Solvent	Retention time (min)	S.D. (min)
Methanol	2.29	0.005
Ethanol	3.15	0.005
Acetone	3.75	0.005
Dichloromethane	5.02	0.005
Methyl <i>tert.</i> -butyl ether	6.71	0.005
Ethyl acetate	8.08	0.005
Tetrahydrofuran	8.69	0.005
<i>n</i> -Butyl chloride	9.58	0.004
Benzene	10.08	0.004
Dioxane	11.40	0.003
Pyridine	12.63	0.008
Toluene	13.82	0.000
<i>n</i> -Butyl acetate	14.96	0.000
<i>o</i> -Xylene	17.73	0.003

reduced by calculating the capacity factor of the solvent relative to the capacity factor of an arbitrarily chosen standard. The resulting relative capacity factors are reported in Table II for a number of solvents with toluene as a retention standard. Toluene is a convenient choice, because it is a common minor constituent of benzyl alcohol. Within our limited experience, the numbers in Table II usually agree with the measured values in a specific experimental configuration within ± 0.04 .

Accuracy

The accuracy of the method cannot be assessed for general combinations of drugs and solvents. In any given case, the chromatographic system and the specific analytical matrix influence the signal for a specific solvent. In evaluating the limitations on experimental accuracy however, a number of practical points can be considered independently; the linearity and the bias of the method can be assessed at various levels of generality. In particular, the instrumental contributions to non-linearity and bias are important determinants of method performance.

A method that is linear over several decades of dynamic range is useful for quantitative solvent screening, because a complete standard curve is not essential for reasonably accurate assessment of solvent content at low (0.001–0.05%) as well as high (0.05–5.0%) levels. In practice, the most accurate determinations are necessary at levels where general quantitative limits on solvents are set. The typical levels of interest for most of the less toxic solvents are in the 0.05–1.0% range. Linearity has been examined for each of the 27 solvents shown in Fig. 1 over the range of 0.01–5.0%. Solutions were prepared for several nominal percentages of solvent in bulk drug: 0.01, 0.02, 0.05, 0.1, 0.2, 0.4, 0.6, 0.8, 1.0, 2.0 and 5.0%. These standards were prepared by dilution of the most concentrated sample containing the equivalent of 5% solvent in bulk drug. Dilutions were calculated by weight, and care was taken to

TABLE II
RETENTION OF SEVERAL SOLVENTS EXPRESSED AS THE CAPACITY FACTOR RELATIVE TO TOLUENE

Results represent an average over two separate determinations on different columns.

<i>Solvent</i>	<i>Capacity factor (relative to toluene)</i>	<i>Solvent</i>	<i>Capacity factor (relative to toluene)</i>
Methanol	0.062	Tetrahydrofuran	0.588
Ethanol	0.134	Dichloroethane	0.626
Acetonitrile	0.158	Butyl chloride	0.659
Acetone	0.185	<i>n</i> -Butanol	0.688
2-Propanol	0.208	Benzene	0.700
Diethyl ether	0.248	Cyclohexane	0.730
Pentane	0.248	Dioxane	0.806
Dichloromethane	0.294	Isooctane	0.813
<i>n</i> -Propanol	0.374	Heptane	0.839
Methyl <i>tert.</i> -butyl ether	0.429	Pyridine	0.904
Methyl ethyl ketone	0.464	Toluene	1.000
Ethyl acetate	0.539	<i>n</i> -Butyl acetate	1.091
Hexane	0.540	Dimethylsulfoxide	1.288
Chloroform	0.548	<i>o</i> -Xylene	1.317

avoid headspace losses. (In our first attempts, failure to minimize headspace exchanges during preparation resulted in significant curvature in the response plots. The problem was most pronounced for the volatile non-polar solvents like pentane and hexane.) Solvents were divided into three groups to avoid mutual interferences to peak integration within groups. Samples were injected in duplicate.

Linear regression was used to evaluate linearity throughout the 0.2–1.0% range, a range of concentrations used routinely for external standards. Five points between 0.2 and 1.0% inclusive were included. For each solvent, the linear fit to the data has a correlation coefficient of 0.999 or greater, and the absolute value of the intercept corresponds to the signal produced by 0.01% of the solvent or less.

Response linearity over the full range of concentrations from 0.01 to 5.0% cannot be evaluated adequately by simple linear regression. A plot of the specific response (area response per unit weight) as a function of concentration is given in Fig. 2. The response for each solvent is scaled relative to the value at the 5% level. The specific response at the 5.0% concentration has been set to 1.00 for each solvent to present the data on a single plot. The contribution of limited experimental precision to the spread of data points in Fig. 2 has not been determined. Pyridine has a concentration dependent peakshape, which is not typical of the other solvents investigated. Peaks for pyridine at concentrations below 0.05% were difficult to integrate, and the corresponding data are not included in the plot. For the remainder of the solvents, if standards at the high end of the response range are employed, the instrumental contribution to the inaccuracy of estimates at the low end is not worse than about 25% of the actual value. At the 0.1% level, the deviations are less than 10% of the actual

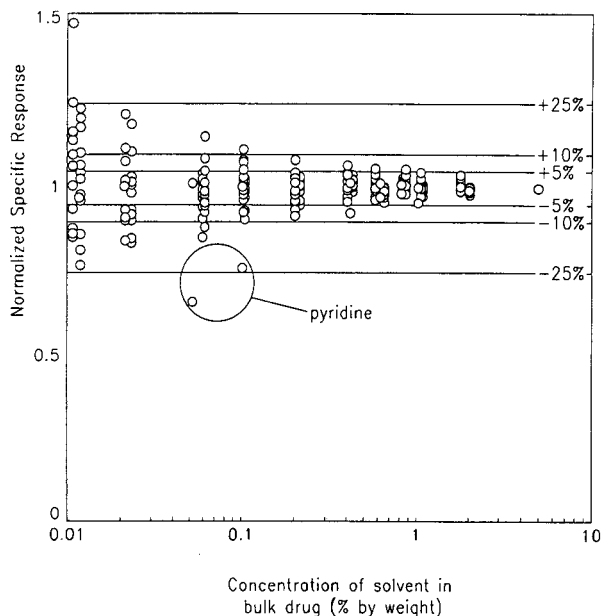


Fig. 2. Specific response for the 27 solvents of Fig. 1 as a function of solution concentration. Responses for each solvent are normalized to the response observed for that solvent at the 5% concentration. Data for pyridine are not included below 0.05%.

value. This performance is satisfactory for most applications. Instrumental contributions to inaccuracy can be reduced at low levels by preparation of standards appropriate to the concentration range.

In addition to instrumental non-linearities, sample dependent bias can also contribute to the loss of accuracy. Two major sources of bias can be identified. The first of these is bias from matrix contributions to the solvent profile. The matrix contributions include non-solvent organic volatiles, volatile thermal decomposition products, and volatile products arising from the interaction between components of the bulk drug and the benzyl alcohol in the injection port. Peaks that originate from these matrix components make a positive contribution to the solvent profile. The bias from these peaks can be particularly important if they are interpreted as true solvent peaks in a general solvent screen.

The absence of this positive matrix bias can be demonstrated for a given compound by verifying the absence of solvent peaks in the presence of the remaining matrix components. In many cases a simple sequence of experiments will suffice to establish the absence of this type of bias. First the residual solvent profile of the bulk drug is determined. A number of solvent responses may be observed. A sample of the drug is dissolved in a solvent that was not observed in the initial screen. The sample is dried under a stream of nitrogen or under vacuum, and the solvent profile of the sample is redetermined. If the solvents observed in the original determination are not present, or if the levels of these solvents are insignificant, they are probably not derived from matrix interferences.

This approach may not be effective if there are significant changes in the matrix composition during the dissolution and drying steps. Nevertheless, it is a simple scheme for establishing an additional measure of confidence in the ability to screen a given compound for a wide variety of solvents. An example of the chromatography from a typical initial screen is shown in Fig. 3a, where acetone is observed at 1.2% in an antibiotic drug. After dissolving the drug in methanol and drying under vacuum, the sample was reanalyzed. The results, shown in Fig. 3b, show that the methanol is observed, but the acetone in the original sample is now absent. Acetone is a true solvent response and not an interference from matrix decomposition products. More importantly, the major components of the matrix do not produce chromatographic peaks that interfere with the analysis for any solvents.

Bias can also result from the interaction between solvents and other components of the sample solution in the injection port. This interaction will decrease the response for the solvent and result in reduced recovery. If the solvent is converted to other volatile products, a positive bias for other volatiles may result. The hydrolysis of ethyl acetate, for example, would yield ethanol and acetic acid peaks. The injection port temperature (180°C) is high enough to preclude most of the physical losses, such as occlusion or adsorption of volatile solvents on a solid matrix, but low enough to suppress many problems with chemical reactivity. Our experience with an earlier packed column method at injection port temperatures greater than 250°C revealed a higher incidence of problems with volatile drug decomposition products.

In specific instances, however, solvents may be partially consumed by reactions within the injection port, or otherwise retained by matrix residue. If the solvent and bulk drug are specified, the bias can be evaluated from standard recovery experiments in the range of interest. Haky and Stickney³ have adopted a standard additions

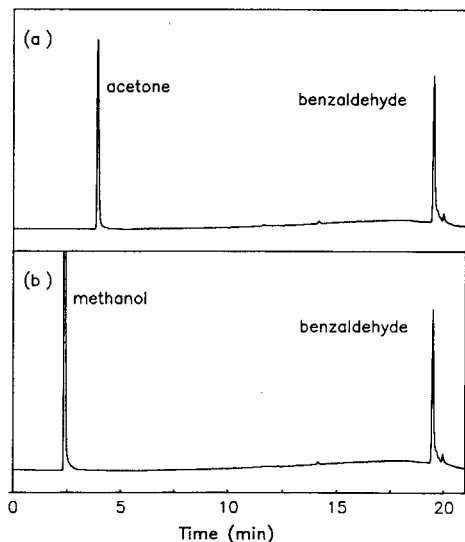


Fig. 3. Results of a typical experiment to evaluate matrix contributions to the solvent profile. (a) Acetone is observed at a level of 1.2% in an antibiotic. (b) The acetone response is eliminated after the drug is dissolved in methanol and taken to dryness.

approach to the analysis of solvent residues to account for proportional bias. For a number of specific examples they conclude that, even in the instances where statistically significant bias can be demonstrated, the bias is unimportant relative to the magnitude of the result.

Benzyl alcohol may contain contaminants that contribute to the solvent response in samples and standards, making blank corrections essential. Fortunately, benzyl alcohol is routinely available in high-purity grades. Aside from benzaldehyde and other oxidation products, the most common impurities observed in commercial high-purity benzyl alcohol are toluene and methanol at levels corresponding to about 0.01% of these solvents in bulk drug for the nominal sample preparation. Blank runs are made routinely to evaluate the contribution of contaminants. Fig. 4 is a typical example.

A small but significant matrix bias that is peculiar to benzyl alcohol has been observed for several drugs. A response for benzene is obtained for a number of salts, including some sodium salts, hydrochlorides, and mesylates that do not contain benzene. Benzene has been confirmed by GC-MS for these materials, and the absence of benzene in the benzyl alcohol diluent has been confirmed. The maximum quantity observed in any particular instance is as high as 0.07% of benzene in drug. A worst case example is shown in Fig. 5. Benzene is not observed when alternate diluents, such as dimethyl formamide, are used, and the benzene response is reduced at lower injection port temperatures. The benzene peak can be eliminated by using benzyl alcohol with very low levels ($< 0.005\%$) of benzaldehyde and associated air oxidation products such as perbenzoic acid and benzoic acid. Commercial benzyl alcohol with these specifications is suitable for routine use. As an alternative, the treatment of benzyl alcohol with a small amount of sodium borohydride followed by reduced

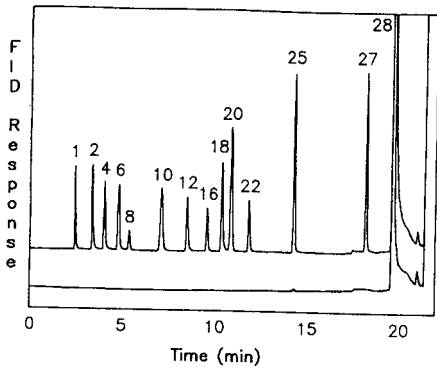


Fig. 4. Lower trace: typical chromatographic trace of benzyl alcohol blank. Upper trace: chromatography of several solvent standards at a level equivalent to 0.20% in bulk drug. Numbers as in Fig. 1.

pressure distillation is a satisfactory means of preparing benzyl alcohol with a low concentration of oxidation products.

Precision and limits of detection

The incompatibility of autosampling equipment with high-precision modes of sample introduction in capillary systems has been viewed as a major obstacle to the use of open-tubular chromatography in solvent residue analysis. With the wide-bore

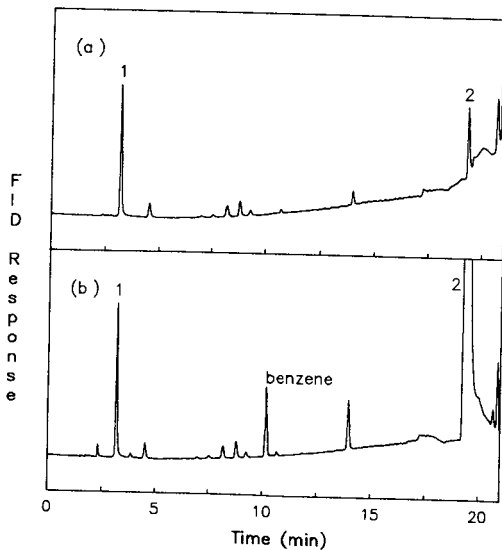


Fig. 5. Chromatography from the residual solvent determination of a bulk drug (hydrochloride salt) that interacts with benzyl alcohol contaminants to form benzene. (a) Sample prepared with benzyl alcohol that has been treated to eliminate benzaldehyde and other air oxidation products. (b) Sample prepared with commercial benzyl alcohol containing typical levels of benzaldehyde and other air oxidation products. Peaks: 1 = ethanol (0.24%); 2 = benzaldehyde.

thick film columns, injections can be made in the direct mode, and acceptable precision can be obtained with autosamplers for injections as small as 0.5 μ l. The results in Table III were obtained from multiple injections of standard solutions prepared at levels of 0.02, 0.2 and 2.0% of solvent in drug. Based on the 2.0% data, the sampling precision is better than about 0.5%. The poorest precision is observed at the 0.02% level for components with low specific responses, such as chloroform. Signal-to-noise limitations become important at this level. The precision is not improved by extending the sampling time from 30 to 60 s.

Examples of the reproducibility of typical evaluations based on multiple sample preparations are given in Table IV. The reproducibility between preparations is as good as the precision between injections as long as the sample homogeneity is not a limiting factor.

Approximate limits of detection have been determined for our experimental configuration based on a signal-to-noise ratio of six. Results of this determination are given in Table V. The solvents in the table have been chosen to represent a wide range of elution times and specific responses. The chromatography of some representative solvents at the 100-ppm level and at the 5-ppm level is shown in Fig. 6. Acceptable integration of the peaks at the 5-ppm level is possible. The achievement of trace level limits of detection was not, however, an objective of this study. Lower limits can be achieved, if necessary, by injecting larger volumes of more concentrated drug solutions.

Ruggedness

Potential problems with system ruggedness have prompted some workers to develop methods based on headspace analysis. Specifically, Guimbard *et al.*⁴, cite the

TABLE III

PRECISION [R.S.D. (%)] OF PEAK AREA DETERMINATION AT THE 0.02, 0.2 AND 2.0% LEVELS AVERAGED OVER SIX INJECTIONS

Solvent	Standard concentration			Solvent	Standard concentration		
	0.02%	0.2%	2.0%		0.02%	0.2%	2.0%
Acetone	1.3	1.0	0.4	Heptane	4.2	1.0	0.8
Acetonitrile	0.9	0.4	1.3	Hexane	1.4	0.4	0.2
Benzene	0.3	0.3	0.2	Isooctane	3.6	0.8	0.9
<i>n</i> -Butanol	2.7	1.3	0.5	Methanol	1.7	0.8	0.7
<i>n</i> -Butyl acetate	4.5	2.5	0.3	Methyl <i>tert.</i> -butyl ether	0.6	0.7	0.2
Butyl chloride	4.9	0.7	0.3	Methyl ethyl ketone	0.8	0.7	0.3
Chloroform	9.8	1.8	2.4	Pentane	0.7	0.4	0.2
Cyclohexane	4.0	0.5	0.2	2-Propanol	0.4	0.2	0.9
Dichloroethane	5.2	1.6	0.2	<i>n</i> -Propanol	0.8	0.5	0.2
Dichloromethane	1.3	1.0	0.3	Pyridine	10.5	1.9	0.9
Diethyl ether	0.6	0.3	0.5	Tetrahydrofuran	1.3	0.5	0.2
Dioxane	2.9	1.8	0.6	Toluene	3.7	0.8	0.2
Ethanol	0.4	1.2	0.9	<i>o</i> -Xylene	4.5	0.5	0.2
Ethyl acetate	2.4	1.1	0.3				

TABLE IV

REPRODUCIBILITY FOR DETERMINATIONS OF RESIDUAL SOLVENTS IN BULK DRUGS

Statistics are calculated for single injections of each of six sample preparations for each drug. The mean and standard deviation (S.D.) are given as percent by weight of the drug. ST1, ST2 = Steroids; CNS1, CNS2 = CNS agents; AB1, AB2 = antibiotics.

<i>Drug</i>	<i>Solvent</i>	<i>Mean</i> (%)	<i>S.D.</i> (%)
ST1	Acetone	0.105	0.001
	Isooctane	0.033	0.001
AB1	Acetone	1.076	0.06
ST2	<i>n</i> -Butanol	0.080	0.014
AB2	Acetone	0.021	0.002
	Diethyl ether	0.070	0.001
	Ethyl acetate	0.517	0.003
CNS1	Methanol	0.085	0.003
	Diethyl ether	0.0479	0.0004
CNS2	<i>n</i> -Butyl acetate	0.011	0.001

contamination of the column with drug as a major deterrent to the direct analysis of drug solutions. There are four factors which lessen the severity of this problem on our system: (1) most of the contamination is confined to the inlet liner where its influence on column performance is reduced, (2) a 5-m retention gap acts as a guard column to protect the analytical column from the build-up of non-volatile residue, (3) the injected drug load is small (*ca.* 5 μ g), and (4) the inlet purge vents most of the products that slowly vaporize in the injection port. The injection volume is typically lower by a factor of ten than the volumes recommended for packed-column procedures with the same drug concentration³. The higher sensitivity of open-tubular column chromatography relative to packed-column systems permits smaller sample sizes to be employed without sacrificing detection limits.

Overall, we have experienced very few problems with system contamination over several months of operation. Single-run sequences as long as 55 h have included as many as ten different drug samples. No significant changes in retention times, peak shapes or peak areas have been observed for injections of multicomponent standards spaced throughout these runs. The data in Table I were taken from one of these

TABLE V

LIMITS OF DETECTION FOR REPRESENTATIVE SOLVENTS AT A NOMINAL DRUG CONCENTRATION OF 10 mg BULK DRUG PER GRAM OF BENZYL ALCOHOL

<i>Solvent</i>	<i>Detection limit</i> (ppm in bulk drug)	<i>Solvent</i>	<i>Detection limit</i> (ppm in bulk drug)
Methanol	3	Ethyl acetate	5
Ethanol	3	Tetrahydrofuran	4
Acetone	4	<i>n</i> -Butanol	3
2-Propanol	4	Isooctane	4
Dichloromethane	11		

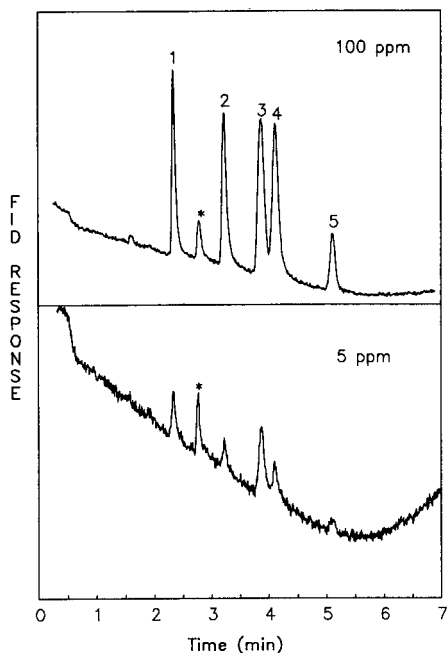


Fig. 6. Chromatography of several solvents near the limit of detection. Peaks: 1 = methanol; 2 = ethanol; 3 = acetone; 4 = isopropanol; 5 = dichloromethane. The asterisk indicates blank interference.

sequences. The inlet liners are changed regularly, but the guard column has not shown evidence of contamination after analyzing over 200 drug samples. (The guard column is shortened occasionally when columns are removed and replaced in the oven, so it is difficult to determine how long it will last before the contamination becomes severe enough to influence the chromatography.)

CONCLUSIONS

Wide-bore WCOT column GC can be coupled with the generalized sample preparation procedure proposed by Haky and Stickney³ to provide an effective method for the analysis of solvent residues in drugs. If the direct mode of injection is employed, automation of the procedure yields analytical precision that is comparable to that obtained from automated packed-column methods. The efficiency of the chromatographic system provides a high usable peak capacity for a short analysis time relative to packed-column alternatives. The method is particularly useful for screening a variety of common solvents in bulk drugs.

We have not encountered any instrumental limitations to method accuracy under normal use over the range of 0.01 to 5.0% of solvent in drug. Levels as low as 10 ppm have been determined reliably without modifications to the procedure. The contribution of non-solvent components of the matrix can usually be assessed for each drug by a straightforward sequence of experiments. In our laboratories, this sequence provides the minimal validation data necessary prior to implementing the

method for routine analysis. Recovery experiments are used to provide additional validation data if poor recovery is suspected. Benzene can be produced in the injection port by the interaction between some drugs and common contaminants of benzyl alcohol. Because benzene is rarely used as a process solvent in the pharmaceutical industry, a positive response for benzene should always be evaluated carefully to determine whether the appearance of benzene is an artifact of the procedure.

ACKNOWLEDGEMENTS

The authors have benefitted from the contributions of Dennis Hassing and Phil Bowman to the problem of solvent residue analysis at the Upjohn Co. Steve MacLeod is acknowledged for his technical assistance with gas chromatography.

REFERENCES

- 1 C. Bicchi and A. Bertolino, *Farmaco, Ed. Prat.*, 37 (1982) 88-97.
- 2 F. Matsui, E. G. Lovering, J. R. Watson, D. B. Black and R. W. Sears, *J. Pharm. Sci.*, 73 (1984) 1664-1666.
- 3 J. E. Haky and T. M. Stickney, *J. Chromatogr.*, 321 (1985) 137-144.
- 4 J. P. Guimbard, M. Person and J. P. Vergnaud, *J. Chromatogr.*, 403 (1987) 109-121.
- 5 J. C. Sheridan, J. P. Hetcher, D. W. Hughes and B. B. Hubert, *Pharmacopoeial Forum*, July-August (1986) 1635-1636.
- 6 *Pharmacopoeial Forum*, March-April (1988) 3600-3604.

CHROM. 21 374

SEPARATION OF 4-(2-PYRIDYLAZO)RESORCINOLATO METAL CHELATES BY MICELLAR ELECTROKINETIC CAPILLARY CHROMATOGRAPHY

TOHRU SAITOH^a, HITOSHI HOSHINO* and TAKAO YOTSUYANAGI

Department of Molecular Chemistry and Engineering, Tohoku University, Aramaki, Aoba, Sendai 980 (Japan)

(First received December 28th, 1988; revised manuscript received January 30th, 1989)

SUMMARY

The first application of micellar electrokinetic capillary chromatography to the separation of metal chelate compounds is demonstrated. The resolution of the peaks of 4-(2-pyridylazo)resorcinolato (par) chelates is excellent on a 60 cm × 0.05 mm I.D. silica capillary filled with a 0.02 mol dm⁻³ sodium dodecylsulphate micellar eluent at an applied voltage of 16.5 kV (driving current 12 μA). The theoretical plate number for the chelates reaches to more than 1 · 10⁵ per 60 cm. The elution behaviour is discussed in terms of electrokinetic and micellar partition characteristics of the metal-par chelates. The chromatographic system is highly promising for the ultratrace determination of metals at the femtomole level in a very small sample injection volume (*ca.* 6 nl).

INTRODUCTION

Recently, micellar electrokinetic capillary chromatography (MECC) has been developed^{1,2} and as found applications in the determination of phenols,^{1,2} amino acids,^{3,4} B-6 vitamers⁵ and oligonucleotides⁶ in very small samples. The separation principle and the theoretical basis have been given by Terabe *et al.*² and Sepaniak and co-workers^{7,8}. When a high voltage is applied across a capillary, an aqueous solution is forced to flow toward the negative end by electroosmosis, while anionic micelles, *e.g.*, of sodium dodecylsulphate, in the solution are considerably retarded by the electrophoretic migration, thus acting as a dynamic stationary phase of colloidal dimensions. As this chromatography has very high efficiency, multi-element simultaneous detection was thought to be achievable. Of practical importance is the minimization of the contamination from metal contacts encountered in ordinary high-performance liquid chromatography (HPLC) (pump, column and tubing), because this capillary chromatography can be performed out of contact with metals except inert platinum electrodes. In addition, as the sample volume necessary for

^a Present address; Laboratory of Analytical Chemistry, Faculty of Engineering, Hokkaido University, Sapporo 060, Japan.

injection is very small (a few nanolitres)², the system is suitable for monitoring metal ions in clinical testing or quality control of electronics materials, where only limited amounts of samples are available.

In this paper, the MECC of metal chelates of the well known chromogenic reagent 4-(2-pyridylazo)resorcinol (par, H₂L) is described and the separation behaviour is discussed.

EXPERIMENTAL

Apparatus and reagents

A Horiba M-5 pH meter and a Hitachi Model 124 double-beam recording spectrophotometer were used. The chromatographic system consisted of a Shimadzu Isotachophoresis IP-2A constant-current supply with platinum electrodes and a JASCO Uvidec 100-IV visible spectrophotometric detector. A fused-silica glass capillary (850 mm × 0.05 mm I.D.) was obtained from Scientific Glass Engineering. On-column absorbance detection was employed; the width of the slit made of aluminium foil was matched to the inner diameter of the capillary, and the height of the slit was 1 mm. This slit was attached 150 mm from the negative end of the tube. The chromatographic data were processed with a Shimadzu Chromopak C-R3A LC data processor.

Sodium dodecylsulphate (SDS) was obtained from Wako and par from Dojindo Labs. was dissolved in a slightly alkaline solution. All other reagents were of analytical-reagent grade.

Procedures

The sample solutions were prepared by mixing the appropriate solutions of metal ions with the par solution, followed by additions of SDS and buffer solutions to give the same bulk composition as that of the eluent to be used. A stock chromium (III)-par chelate solution was prepared as reported previously⁹.

All procedures in the MECC were carried out in a similar manner to those reported by Terabe and co-workers^{1,2}. The capillary tube was filled with a buffered SDS eluent and each end was immersed in the same eluent solution. A small amount of par ($1 \cdot 10^{-4}$ mol dm⁻³) was added to the eluent to prevent the dissociation of relatively unstable chelates such as those of Zn(II), Cd(II) and Cu(II) during the separation. The applied voltage and the driving current are given in the captions of the figures. The sample solution was injected into the capillary by syphonic action. The sample solution was introduced 3 mm from the positive end (*ca.* 6 nl). The temperature of the system was kept at $25 \pm 1^\circ\text{C}$ in a safety box with an interlock system.

RESULTS AND DISCUSSION

A typical chromatogram of Co(III), Cr(III), Fe(III) and Ni(II) chelates and the retention data are shown in Fig. 1 and Table I, respectively. The concentration of each metal ion was $1 \cdot 10^{-5}$ mol dm⁻³. As can be seen from Fig. 1, very sharp peaks are produced within an acceptable total elution time. The theoretical plate numbers of the chelates were in the range 105 000–120 000 per 60 cm. The surprisingly high efficiency of the MECC was also confirmed for the chelate compounds. The elution order of the

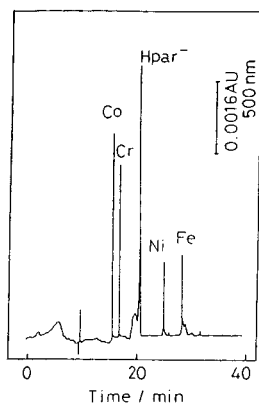
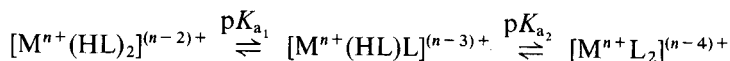


Fig. 1. MECC separation of metal-par chelates. Eluent: [SDS] = 0.02 mol dm⁻³, [NaH₂PO₄] = 0.05 mol dm⁻³, [Na₂B₄O₇] = 0.0125 mol dm⁻³, [par] = 1.0 · 10⁻⁴ mol dm⁻³. Applied voltage: 16.5 kV (25 μA). Complexation conditions; [par] = 1.0 · 10⁻³ mol dm⁻³; [metal ion]/(10⁻⁵ mol dm⁻³), Co(II) 0.995, Cr(III) 1.23, Fe(III) 1.00, Ni(II) 1.01; [triethanolamine] = 0.025 mol dm⁻³ (pH = 8.8 with HCl), heated at 98°C for 30 min.

chelates is [CoL₂]⁻, [CrL₂]⁻, [NiL₂]²⁻ and [FeL₂]⁻ under the conditions used. It should be noted that the complete separation of Co(III) and Cr(III) chelates is readily achieved, whereas this was a serious problem in ion-pair HPLC on an ODS stationary phase⁹. Other cations that form unstable par chelates, such as Mn(II)¹⁰ and alkaline earth metal ions, gave no peaks under the conditions employed.

The retention of the chelates varies with the eluent pH, as shown in Fig. 2, owing to the acid dissociation equilibria of the par chelates (1-hydroxy groups of par ligands):



Under the pH conditions tested, the Co(III) and Cr(III) chelates are fully deprotonated species, [ML₂]⁻ [the pK_{a2} values are 4.41 and 4.35 for the Co(III)¹¹ and Cr(III)⁹ chelates, respectively]. The acid dissociation equilibria of the Ni(II) chelate (pK_{a1} = 6.2 and pK_{a2} = 7.1)¹² obviously cause a decrease in the *k'* value in the pH range 5–8. The

TABLE I
CAPACITY FACTORS (*k'*) AND THEORETICAL PLATE NUMBERS (*N*) OF par (HL⁻ FORM) AND THE METAL CHELATES ([ML₂]ⁿ⁻)^a

Solute	<i>k'</i>	<i>N</i> (per 60 cm)
[Co(III)L ₂] ⁻	0.79	114 000
[Cr(III)L ₂] ⁻	0.99	108 000
HL ⁻	1.61	65 000
[Ni(II)L ₂] ²⁻	2.54	120 000
[Fe(III)L ₂] ^{-b}	3.38	105 000

^a Chromatographic conditions as in Fig. 1.

^b Injected form. Possibly reduced to [Fe(II)L₂]²⁻.

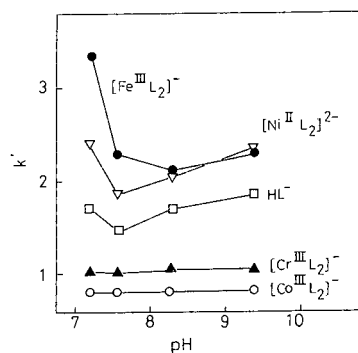


Fig. 2. Capacity factor vs. eluent pH plots for par and the chelates. The eluent pH was adjusted by mixing appropriate phosphate and borate buffer solutions to give a constant ionic strength. Other conditions as in Fig. 1. Temperature: $25 \pm 1^\circ\text{C}$.

possibility of reduction of the Fe(III)–par chelates to the Fe(II) form, $[\text{FeL}_2]^{2-}$, during the electrokinetic separation was suggested as the elution time of the iron chelate is very close to those of the other divalent metal chelates (Ni, Cu and Zn) (see Fig. 3 and Table I). In this work, slightly alkaline conditions ($\text{pH} = 9.2$, 0.05 mol dm^{-3} sodium acetate, 0.01 mol dm^{-3} disodium tetraborate), where the 1-hydroxy groups of the chelates are fully dissociated,¹² were employed for the quantitative elution studies.

Several chromatograms of metal–par chelates at different concentrations of SDS ($0, 0.05, 0.10$ and 0.15 mol dm^{-3}) in the eluent are shown in Fig. 3. Under these conditions, the peaks of the Co(III), Fe(III), Ni(II), Zn(II) and Cd(II) chelates are detected. As shown in Fig. 3, the SDS micellar concentration in the eluent significantly influences the order of elution of the chelates. With no added SDS, *i.e.*, running the system in the electrophoresis mode, the resolution of the chelates is unsatisfactory. These observations clearly indicate that a partition process of the chelates between the bulk aqueous eluent and the micellar pseudo-stationary phase is vital for the separation. It is interesting that the separation of the anions can be accomplished very effectively using the SDS micelles of the same charge type. This may indicate that

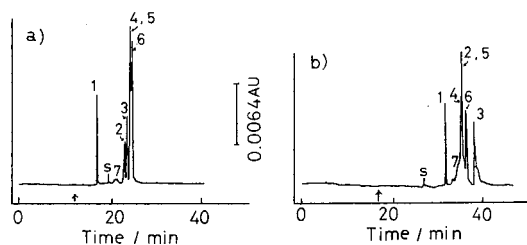


Fig. 3. Chromatograms of metal–par chelates at various concentrations of SDS present in the eluent. Peaks: (1) Co(III); (2) Cu(II); (3) Cd(II); (4) Ni(II); (5) Fe(III); (6) Zn(II); (7) HL^- ; (s) system peak; arrow indicates solvent front position. Eluent: $[\text{NaOOCCH}_3] = 0.05 \text{ mol dm}^{-3}$, $[\text{Na}_2\text{B}_4\text{O}_7] = 0.01 \text{ mol dm}^{-3}$, $[\text{par}] = 1 \cdot 10^{-4} \text{ mol dm}^{-3}$; [SDS], (a) none at 14.5 kV ($25 \mu\text{A}$), (b) 0.05 mol dm^{-3} at 12.6 kV ($25 \mu\text{A}$), (c) 0.10 mol dm^{-3} at 12.2 kV ($30 \mu\text{A}$), (d) 0.15 mol dm^{-3} at 13.0 kV ($40 \mu\text{A}$). Temperature: $25 \pm 1^\circ\text{C}$. Complexation conditions: $[\text{par}] = 1 \cdot 10^{-3} \text{ mol dm}^{-3}$, $[\text{metal ion}] = (3.6\text{--}4.4) \cdot 10^{-5} \text{ mol dm}^{-3}$, $[\text{NaOOCCH}_3] = 0.05 \text{ mol dm}^{-3}$, $[\text{Na}_2\text{B}_4\text{O}_7] = 0.01 \text{ mol dm}^{-3}$; $\text{pH} = 9.2$.

a relatively weak interaction of the solutes with the SDS micellar pseudo-phase is operative in the delicate MECC resolution. Presumably, the tight binding of solutes to the micelles via strong hydrophobic or electrostatic interactions, although it provides a greater retention, is unfavourable for the mutual resolution. The results in Fig. 3 suggest that in addition to the chromatographic partitioning into the pseudo-stationary phase, the concomitant electrophoretic retardation of the anions possibly plays a subtle role in the peak resolution.

The capacity factors (k'), a measure of the partition of the solutes into the micellar phase, are derived from the retention data as follows²: for neutral species,

$$k' = \frac{t_R - t_0}{t_0(1 - t_R/t_{mc})} = \frac{(1/v_R - 1/v_0)v_0}{(1 - v_{mc}/v_R)} \quad (1)$$

where t_0 , t_R and t_{mc} are the elution times of the solvent, the solute and the micelle-bound reference solute (orange OT dye was employed), respectively, and v_0 , v_R and v_{mc} are the electroosmotic flow velocity of the bulk eluent and the elution velocity of the solute and of the micelles, respectively. For anionic species, the electrophoretic velocity, v_{ep} , must be considered. Using the apparent elution velocity, v_{app} , eqn. 1 is rewritten as

$$k' = \frac{[1/(v_{app} - v_{ep}) - 1/v_0]v_0}{1 - v_{mc}/(v_{app} - v_{ep})} \quad (2)$$

As the values of v_{ep} are dependent on the potential gradient, the approximate values are estimated from the calibration graphs of applied voltage *versus* v_{ep} in the absence of SDS.

The k' values can be related to the aqueous-SDS micellar partition constant (K_d) via

$$k' = K_d V(C - cmc) \quad (3)$$

where V is the partial molar volume of the SDS micelle ($0.26 \text{ dm}^3 \text{ mol}^{-1}$)¹³, C is the total concentrations of SDS and cmc is the critical micellar concentration of SDS ($= 0.003 \text{ mol dm}^{-3}$) under the conditions used¹⁴. The values for k' and K_d of $[\text{CoL}_2]^-$, $[\text{FeL}_2]^-$, $[\text{NiL}_2]^{2-}$ and HL^- at eluent SDS concentrations of 0.10 and 0.15 mol dm^{-3} are shown in Table II. The K_d values in Table II for each compound at the two SDS concentrations are considered to be substantially equal because of some errors involved in the v_{ep} values. In addition, a rise in temperature due to Joule heating possibly affects the results unless the voltage-current conditions are identical.

The line-shaped peaks shown in Fig. 1 provide a remarkably increased sensitivity on a mass basis. The noise level of the detection system is about $2 \cdot 10^{-4}$ absorbance at 500 nm. From the peak height of the Cr-par chelates in Fig. 1, the concentration that gives a signal three times the noise level is calculated to be $2.3 \cdot 10^{-7} \text{ mol dm}^{-3}$. This molar concentration corresponds to an absolute amount of $1.4 \cdot 10^{-15} \text{ mol}$ ($7.2 \cdot 10^{-14} \text{ g Cr}$) in a 6-nl injection. This absolute detection limit (calculated) is about 700 times lower than that obtained in ion-pair HPLC (1.0 pmol in a $100\text{-}\mu\text{l}$ injection)⁹.

TABLE II
CAPACITY FACTORS (k') AND PARTITION CONSTANTS (K_d) OF METAL-par CHELATES^a

Solute	[SDS] (mol dm ⁻³)			
	0.10 (30 μ A, 12.2 kV)		0.15 (40 μ A, 13.0 kV)	
	k'	Log K_d	k'	Log K_d
[Co(III)L ₂] ⁻	0.555	1.34	0.919	1.38
[Fe(III)L ₂] ^{-b}	0.088	0.55	0.183	0.68
[Ni(II)L ₂] ²⁻	0.072	0.45	0.150	0.59
HL ⁻	0.190	0.88	0.361	0.98

^a Other chromatographic conditions as in Fig. 3.

^b Injected form. Possibly reduced to [Fe(II)L₂]²⁻.

TABLE III
ELUTION TIMES (min) OF par AND THE CHELATE SPECIES IN MECC^a

Species	[SDS] (mol dm ⁻³)			
	0 (14.5 kV, 25 μ A)	0.05 (12.6 kV, 25 μ A)	0.10 (12.2 kV, 30 μ A)	0.15 (13.0 kV, 40 μ A)
[Co(III)L ₂] ⁻	17.2	32.3	44.0	57.7
[Fe(III)L ₂] ^{-b}	24.5	35.7	39.9	40.8
[Ni(II)L ₂] ²⁻	24.7	35.1	39.5	39.5
[Cu(II)L ₂] ²⁻	23.7	35.7	42.0	43.5
[Zn(II)L ₂] ²⁻	25.0	36.5	41.4	42.8
[Cd(II)L ₂] ²⁻	24.4	39.4	47.8	52.0
HL ⁻	21.9	34.2	42.6	45.3
Orange OT		111.3	169.0	216.6

^a Other conditions as in Fig. 3.

^b Injected form. Possibly reduced to [Fe(II)L₂]²⁻.

MECC seems a fairly promising approach for monitoring metal ions *in vivo* and *in vitro* and in sophisticated industrial analyses where the absolutely small amounts rather than the low concentrations are to be determined. Investigations are in progress on the application of MECC using chelating reagents such as azo dyes, hydrazones and porphyrins.

ACKNOWLEDGEMENTS

This work was financially supported in part by a Grant-in-Aid for Science Research (No. 62850137) from the Ministry of Education, Science and Culture, Japan (1987/1988).

REFERENCES

- 1 S. Terabe, K. Otsuka, K. Ichikawa, A. Tsuchiya and T. Ando, *Anal. Chem.*, 56 (1984) 111.
- 2 S. Terabe, K. Otsuka and T. Ando, *Anal. Chem.*, 57 (1985) 834.
- 3 S. Terabe, H. Ozaki, K. Otsuka and T. Ando, *J. Chromatogr.*, 332 (1985) 211.
- 4 K. Otsuka, S. Terabe and T. Ando, *J. Chromatogr.*, 332 (1985) 219.
- 5 D. E. Burton, M. J. Sepaniak and M. P. Maskarinec, *J. Chromatogr. Sci.*, 24 (1986) 347.
- 6 A. S. Cohen, S. Terabe, J. A. Smith and B. L. Karger, *Anal. Chem.*, 59(1987) 1021.
- 7 M. J. Sepaniak and R. O. Cole, *Anal. Chem.*, 59 (1987) 472.
- 8 A. T. Balchunas and M. J. Sepaniak, *Anal. Chem.*, 59 (1987) 1466.
- 9 H. Hoshino and T. Yotsuyanagi, *Anal. Chem.*, 57 (1985) 625.
- 10 D. Nonova and B. Evtimova, *Talanta*, 20 (1973) 1347.
- 11 H. Hoshino and T. Yotsuyanagi, *Talanta*, 31 (1984) 525.
- 12 H. Hoshino and T. Yotsuyanagi, *Bull. Chem. Soc. Jpn.*, 58 (1985) 1037.
- 13 C. Tanford, *The Hydrophobic Effect. Formation of Micelles and Biological Membranes*, Wiley, New York, 2nd ed., 1980.
- 14 J. M. Corkill, J. F. Goodman and T. Walker, *J. Chem. Soc., Faraday Trans. 1*, 63 (1967) 768.

CHROM. 21 420

CHROMATOGRAPHIC APPROACHES TO THE QUALITY CONTROL OF CHIRAL PROPRIONATE ANTI-INFLAMMATORY DRUGS AND HERBICIDES

B. BLESSINGTON*, N. CRABB and S. KARKEE

Department of Pharmaceutical Chemistry, School of Pharmacy, University of Bradford, Bradford, West Yorkshire BD7 1DP (U.K.)

and

A. NORTHAGE

Perkin Elmer Demonstration Unit, Phoenix Building, University of Bradford, Bradford, West Yorkshire BD7 1DP (U.K.)

(First received November 24th, 1988; revised manuscript received February 14th, 1989)

SUMMARY

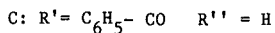
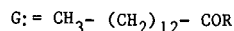
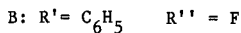
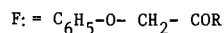
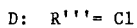
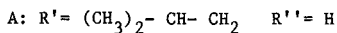
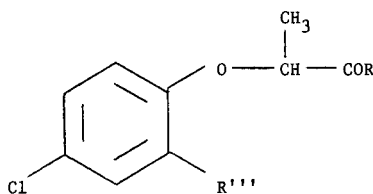
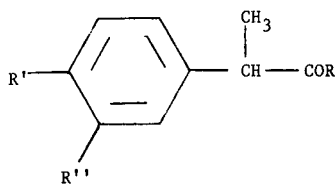
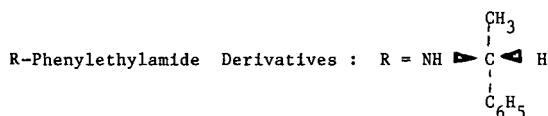
The chiral analysis of a range of propionate anti-inflammatory drugs and herbicides was accomplished by gas chromatographic separation of their *R*- α -phenylethylamide diastereomeric derivatives. Using a packed column (3% OV-1 on Chromosorb G) good separations were obtained but analysis times were rather long. Examination of the same crystalline derivatives using a capillary column (bonded methylsilicone) resulted in good separations together with much reduced total analysis times. The technique was validated through the analysis of several derivatives prepared on a micro scale and examined directly by gas chromatography without any crystallisation step. Racemic materials all gave virtually 50:50 response ratios while the analysis of optically pure samples produced no evidence of significant racemisation. Derivatives of phenoxyacetic acid and myristic acid were also prepared and chromatographed as potential internal standards.

INTRODUCTION

Marked differences in the activities of different enantiomers have been reported for chiral propionate anti-inflammatory drugs¹ and phenoxypropionate herbicides². In some cases this has led to the commercial production and marketing of single active enantiomers². Such developments have stimulated the search for analytical methods which will form the basis of legally enforceable statutes. We have already reported on the role of the two chiral stationary phases (CSPs), the α_1 -acid glycoprotein and "Ionic Pirkle" phases for the high-performance liquid chromatographic (HPLC) analysis of such materials^{3,4}. The translation of such methods to routine quality control, statutory evaluation laboratories and laboratories analyzing biological matrices produces some problems. The sheer volume of samples for analysis and their chemical complexity means that methods must not only work but they should be

robust. Their speed and reproducibility are as important as their capacity to separate. Using these criteria CSPs have serious limitations since they are all rather "delicate". In this paper we wish to report a method for the chiral analysis of such compounds which is based on the gas chromatographic (GC) method of Vangiessen and Kaiser⁵, involving the preparation of diastereomeric *R*-phenylethylamide derivatives with subsequent separation by GC (both packed and capillary columns). The samples examined were the (\pm), (+) and (-) forms of ibuprofen (A), flurbiprofen (B), ketoprofen (C), 2-(2,4-dichlorophenoxy)-propanoic acid (2,4-DP) (D) and 2-(4-chloro-2-methylphenoxy)-propanoic acid (CMPP) (E). Phenoxyacetic acid (F) and myristic acid (G) were also examined as potential internal standards.

Free Acids: R = OH



EXPERIMENTAL

Materials

All CMPP samples and (*R*)-(+)-phenylethylamine were obtained as gifts from A.H. Marks & Co. (Bradford, U.K.) or May & Baker (Dagenham, U.K.). Ibuprofen and flurbiprofen samples were obtained as gifts from Boots plc. (Nottingham, U.K.) or Approved Prescription Services (Bradford, U.K.). Ketoprofen samples were gifts from May & Baker. All solvents used were HPLC grade, other materials were of laboratory grade.

Packed-column GC

The instrument used was a dual-column Pye Series 104 chromatograph, equipped with a flame ionization detector. A 5 ft. \times $\frac{1}{4}$ in. glass column packed with 3% OV-1 on Chromosorb G was used. The carrier gas was nitrogen at a flow-rate of 30 ml/min. The detector temperature was 336°C. A Hewlett-Packard 3388A integrator/printer terminal was used for recording and data processing.

Capillary-column GC

A Perkin-Elmer 8420 capillary chromatograph, connected to a Perkin-Elmer GP-100 graphics printer was used. A 12 m \times 0.22 mm I.D. bonded methylsilicone (SGE BP-1) column was used. The carrier gas (flow-rate *ca.* 0.5 ml/min) was either nitrogen or helium used at an inlet pressure of 8.0 p.s.i. The line was fitted with a Supelco high-capacity carrier gas purifier. The oven temperature was 250°C for 1 min, then rising at 5°C/min to 270°C. The sample was introduced via split injection with split ratio 200:1. The injector temperature was 200°C. A high-sensitivity flame ionization detector was used at 350°C.

Identification of compounds

All samples were examined as KBr discs on a Perkin-Elmer Model 297 infrared spectrophotometer. UV spectra were recorded on a Pye Unicam SP 800 UV spectrophotometer. Ethanol (95%) was used as solvent and reference sample. Mass spectra were run, using a direct-insertion probe, on an AEI MS-902 instrument (source 250°C; 70 eV ionising energy; 100 μ A emission) equipped with a Mass Spectrometry Services data system. Melting points were determined in capillary tubes on a Galenkamp melting point apparatus.

Preparation and characterisation of R-phenylethylamide derivatives

Macro reaction. The required acid (1 g) was weighed into a 250-ml quickfit round bottomed flask. Thionyl chloride (0.4 ml) was added and the mixture was refluxed on a steam bath for 1 h. Excess thionyl chloride was removed under vacuum. The viscous residue was dissolved in dichloromethane (10 ml) and *R*-phenylethylamine (0.7 ml) was added dropwise, shaking the flask after each addition. The solution was frequently shaken for 20 min before being washed twice with hydrochloric acid (4 *M*; 5 ml) and finally with distilled water (5 ml). The organic layer was dried over anhydrous sodium sulphate, filtered and the solvent removed under reduced pressure. The residue was dissolved in aqueous ethanol (65%, v/v; 5 ml) by warming on a steam bath. The hot solution was filtered and then allowed to cool slowly. Crystals were collected after 1 h. A further crop of crystals were collected after keeping the mother liquor overnight at room temperature.

The crystalline derivatives were all characterised by their melting points, mass, IR and UV spectra. The principal spectroscopic peaks and melting points are shown for each derivative in Table I.

Micro reaction. The required acid (2 mg) was weighed into a quickfit centrifuge tube. Thionyl chloride (1 drop) was added and the tube was stoppered and heated on a steam bath for 10 min. The contents were then evaporated to dryness under reduced pressure and chloroform (0.5 ml) was added. *R*-phenylethylamide (1 drop) was added and the tube was shaken regularly over a period of 10 min. The solution was examined directly by GC.

TABLE I

CHARACTERISATION OF *R*-PHENYLETHYLAMIDE DERIVATIVES OF SOME CHIRAL PROPRIONATE ANTI-INFLAMMATORY DRUGS AND HERBICIDES, AND POTENTIAL INTERNAL STANDARDS

<i>R</i> -Phenylethylamide of	Melting point (°C)	Principal spectroscopic data			
		MS		IR (cm ⁻¹) (functional group region)	UV _{max} (nm)
		Molecular peak(s)	Base peak		
(±)-CMPP	115–118	319, 317	105	3260, 1650	218, 320, 282
(-)-CMPP	124–126	319, 317	105	3250, 1650	213, 229, 280
(+)-Ibuprofen	94–96	309	161	3300, 1640	212, 258, 264
(-)-Ibuprofen	109–111	309	161	3300, 1640	212, 258, 265
(±)-Ibuprofen	73–75	309	161	3300, 1640	213, 259, 264
(+)-Flurbiprofen	144–146	347	199	3310, 1640	210, 249
(-)-Flurbiprofen	139–141	347	199	3375, 1640	210, 249
(±)-Flurbiprofen	124–130	347	199	3325, 1640	210, 249
(±)-Ketoprofen	84–86	357	105	3290, 1640	217, 255
Phenoxyacetic acid	73–74	256	105	3350, 1660	213, 270
Myristic acid	68–70	331	105	3320, 1640	213, 258

RESULTS AND DISCUSSION

A good analytical method should be applicable to the analysis of a group of structurally related compounds. We have found that a wide range of racemic organic herbicides (CMPP, 2,4-DP) and anti-inflammatory drugs (ibuprofen, flurbiprofen and ketoprofen) can all be separated by GC as their *R*-phenylethylamide diastereomeric derivatives. This contrasted with our experiences with ODS reversed-phase HPLC analysis of the same compounds.

Initially these separations were carried out on packed GC columns (3% OV-1). Table II shows the results of these separations. Where the individual enantiomers of the organic acids were available, these were derivatised as their *R*-phenylethylamides and chromatographed. Their retention times, along with those for the *R*-phenylethylamides of phenoxyacetic acid and myristic acid (potential internal standards) are also shown in Table II. Usable separations were obtained but rather high temperatures were required for the higher-molecular-mass compounds. Inevitably retention times were long.

Vast improvements, however, were found when the same compounds were analysed using a bonded methylsilicone (BP-1) capillary GC column. Initially helium was used as the carrier gas since its low viscosity allows the use of high flow-rates with only modest reductions in column efficiency. In contrast, where nitrogen is used as the carrier gas, sharp reductions in efficiency are observed when flow-rates are altered from the optimum. In these investigations, however, good results were obtainable using helium or nitrogen; nitrogen was therefore selected on the grounds of economy. The results of the separations obtained using nitrogen as the carrier gas are also shown in Table II. Comparative chromatograms for the diastereomeric amides of (±) CMPP and (±) flurbiprofen run on the packed-column and capillary GC sys-

TABLE II

GC EXAMINATION OF R-PHENYLETHYLAMIDE DERIVATIVES OF SOME CHIRAL PROPRIONATE ANTI-INFLAMMATORY DRUGS AND HERBICIDES, AND POTENTIAL INTERNAL STANDARDS

t_R = Retention time (min) from injection. R_s = Resolution = $(t_{R2} - t_{R1})[2/(W_1 + W_2)]$, where W = peak width at the base.

<i>R</i> -Phenylethylamide of	Packed column (3% OV-1) ^a				Capillary column (BP-1)		
	Column temperature (°C)	t_R 1st Isomer	t_R 2nd Isomer	R_s	t_R 1st Isomer	t_R 2nd Isomer	R_s
(±)-CMPP	210	21.2	24.5	1.33	2.82	3.00	1.78
(+)-CMPP	210	21.1	—	—	2.83	—	—
(-)-CMPP	210	—	24.6	—	—	3.02	—
(±)-2,4-DP	210	24.2	28.1	1.10	3.17	3.40	2.30
(+)-2,4-DP	210	24.4	—	—	3.21	—	—
(±)-Ibuprofen	200	28.7	31.7	1.20	2.89	3.03	1.42
(+)-Ibuprofen	200	—	31.7	—	—	3.04	—
(-)-Ibuprofen	200	28.5	—	—	2.91	—	—
(±)-Flurbiprofen	220	52.8	60.5	1.60	5.54	5.88	2.30
(+)-Flurbiprofen	220	—	60.7	—	—	5.86	—
(-)-Flurbiprofen	220	53.1	—	—	5.56	—	—
(±)-Ketoprofen	234	51.5	58.0	1.30	7.60	8.10	2.00
(+)-Ketoprofen	234	—	58.2	—	—	8.21	—
(-)-Ketoprofen	234	51.3	—	—	7.56	—	—
Phenoxyacetic acid	200	16.0	—	—	1.93	—	—
Phenoxyacetic acid	210	11.5	—	—	—	—	—
Mysteric acid	220	43.5	—	—	4.39	—	—

^a Some of the packed-column data were previously published as a poster at the *Chromatographic Society International Symposium on Chiral Separations, Guilford, September, 1987*.

tems are shown in Figs. 1 and 2. Phenoxyacetic acid was found to be a suitable internal standard for CMPP, 2,4-DP and ibuprofen on both the packed and capillary systems. Myristic acid was found to be a more suitable GC internal standard for ketoprofen and flurbiprofen.

The analysis of crystalline diastereomeric derivatives (*i.e.*, those produced by the macro reactions) is inappropriate for determining the optical constitution of a sample since the crystallisation process leads to the preferential crystallisation of one diastereomer. It is therefore essential that all diastereomeric product formed remains in solution. To ensure that this occurred we developed the micro derivatisation procedure.

Strict validation is required because of potential problems associated with chiral analysis based on the separation of diastereomeric derivatives. Theoretically the enantiomers of a pair may react at different rates with the chiral derivatising agent and/or the chiral reagent may be of insufficient optical purity and/or the two diastereomers may give different detector responses and/or the derivatisation reaction could result in some racemisation (although the possibility of racemisation applies equally to the chiral separation of enantiomeric derivatives).

R-phenylethylamide derivatives of several of the herbicide and anti-inflammatory samples were prepared using the micro method. Using the capillary GC system,

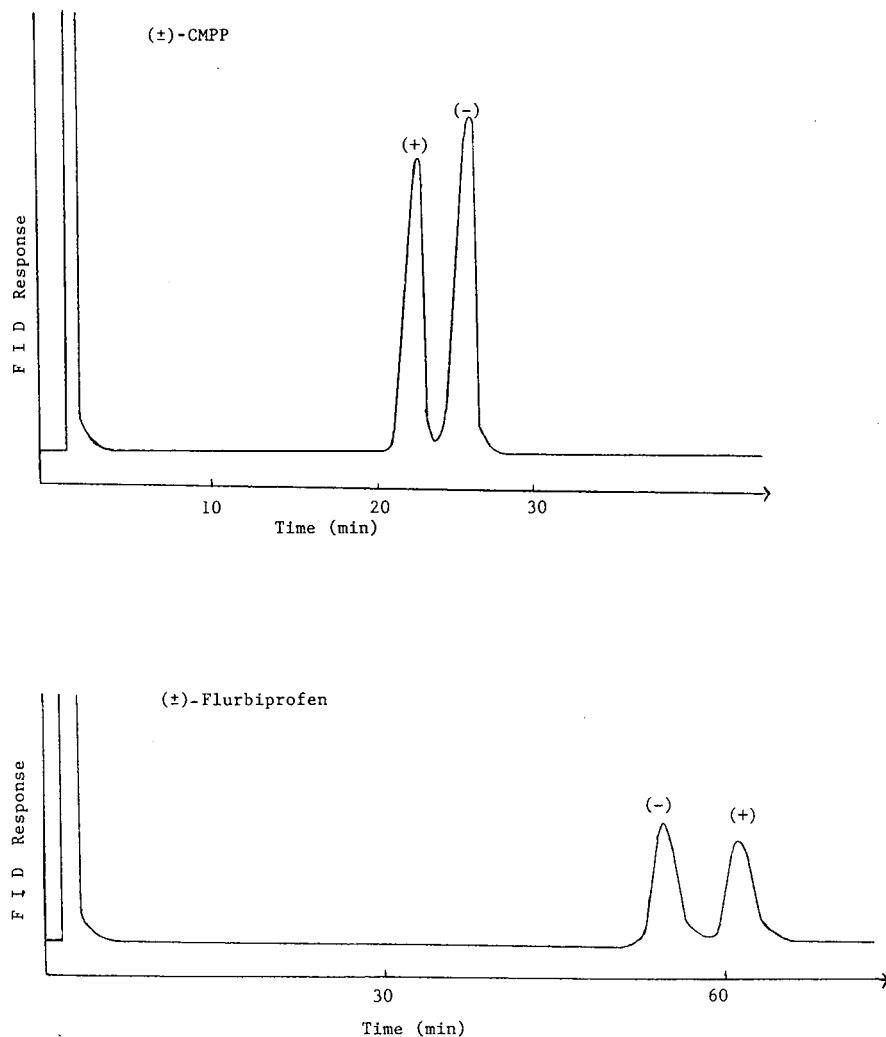


Fig. 1. Packed-column-analysis of (±)-CMPP (210°C) and (±)-flurbiprofen (220°C) as their diastereomeric *R*-phenylethylamide derivatives. FID = flame ionization detection.

each sample was chromatographed five times and the diastereomeric ratios were calculated from the integrated peak areas. For each sample the mean and standard deviation (S.D.) are shown in Table III. The racemic acids all gave virtually 50:50 response ratios for the diastereomeric amides while the optically pure samples gave between 2.9 and 5.3% of the unwanted isomer. These minor discrepancies may arise from reaction influences as discussed above. However we believe they are more likely to arise from small amounts of optical impurities present in the starting materials. We base this claim on our earlier CMPP studies, using a non-derivatising HPLC method³. It was therefore concluded that the method could be used to assess chiral purity.

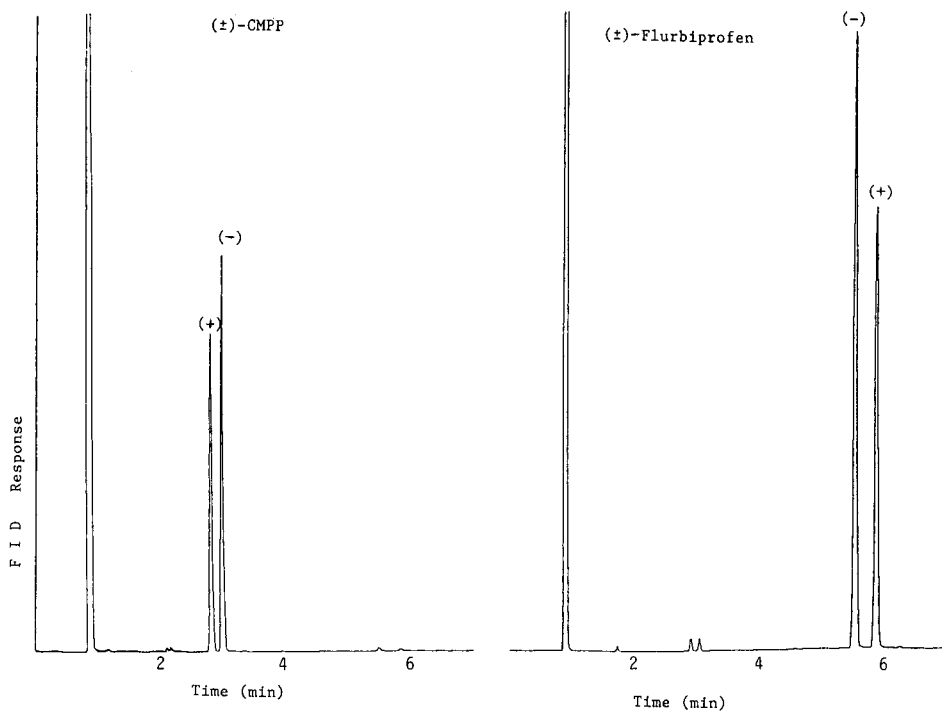


Fig. 2. Analysis of (\pm)-CMPP and (\pm)-flurbiprofen as their diastereomeric *R*-phenylethylamide derivatives using the capillary-column (BP-1) system.

TABLE III

ANALYSIS OF SAMPLES DERIVATISED USING THE MICRO METHOD

(+) and (-) designations refer to the starting enantiomeric acids, not their diastereomeric amides.

<i>R</i> -Phenylethylamide of	% (+)- and (-)-isomers (Mean of 5 injections)		<i>S.D.</i>
	(+)	(-)	
(\pm)-Ibuprofen	50.8	49.2	0.083
(+)-Ibuprofen	96.1	3.9	0.089
(-)-Ibuprofen	4.2	95.8	0.25
(\pm)-Flurbiprofen	48.8	51.2	0.24
(+)-Flurbiprofen	94.7	5.3	0.27
(-)-Flurbiprofen	4.5	95.5	0.32
(\pm)-Ketoprofen	48.4	51.6	0.31
(\pm)-CMPP	49.4	50.6	0.24
(+)-CMPP	97.1	2.9	0.65
(-)-CMPP	3.8	96.2	0.08
(\pm)-2,4-DP	51.0	49.0	0.16

Further work is in hand to optimize the reaction conditions and to determine and minimize the extent of racemisation. Comparative studies using chiral HPLC are also in hand.

To our knowledge no chromatographic methods have been reported for the direct chiral analysis (*i.e.*, without any form of derivatisation) of such a range of acids. If derivatisation is required for indirect methods then distereomer formation followed by separation on conventional GC phases offers a rapid and robust analysis suitable for quality control and statutory purposes.

REFERENCES

- 1 A. Hutt and J. Caldwell, *J. Pharm. Pharmacol.*, 35 (1983) 693–704.
- 2 H. Luers, *The Agronomist*, No. 1, BASF, Hadleigh, 1988, pp. 6–7.
- 3 B. Blessington, N. Crabb and J. O'Sullivan, *J. Chromatogr.*, 396 (1987) 177–182.
- 4 B. Blessington and N. Crabb, *J. Chromatogr.*, 454 (1988) 450–454.
- 5 G. Vangiessen and D. Kaiser, *J. Pharm. Sci.*, 64 (1975) 798–801.

CHROM. 21 336

DERIVATIZATION OF N-METHYL AND CYCLIC AMINO ACIDS WITH DIMETHYLFORMAMIDE DIMETHYL ACETAL

MARY F. GRUBB and PATRICK S. CALLERY*

Department of Medicinal Chemistry/Pharmacognosy, University of Maryland, 20 N. Pine Street, Baltimore, MD 21201 (U.S.A.)

(First received September 5th, 1988; revised manuscript received January 20th, 1989)

SUMMARY

Six amino acids containing either an N-methyl or a cyclic secondary amine were converted to volatile derivatives by reaction with dimethylformamide dimethyl acetal. The amine functionalities were formylated by way of an amide acetal intermediate while the carboxylic acid groups were esterified directly. The resulting N-formyl esters were stable to solvent extraction and exhibited gas chromatography–mass spectrometry properties suitable for assay development.

INTRODUCTION

The reaction of primary amines¹, secondary amines^{2,3}, and primary amino acids^{4,5} with dimethylformamide dimethyl acetal (DMF–DMA) has served as a derivatization step in a variety of analytical methods for biologically important substances. The derivatives are more volatile than the parent compounds and are thus more amenable to gas chromatography (GC–MS) analysis.

A number of derivatization methods for cyclic amino acids, such as proline, have been described in the literature. Representative reactions include formation of phenylthiohydantoins⁶, N-dinitrophenyl esters⁷, N-trifluoroacetyl *n*-butyl esters⁸, and other acyl esters⁹. While these derivatives serve well for proline, the reaction conditions required may induce thermal cyclization of N-monosubstituted γ -amino carboxylic acids, yielding a lactam by-product¹⁰.

Since DMF–DMA reacts with both secondary amines and carboxylic acids to form stable derivatives, an evaluation of this reagent for the derivatization of cyclic and N-methyl acyclic secondary amino acids was undertaken.

EXPERIMENTAL

Materials and methods

Dimethylformamide dialkyl acetals, 4-methylaminobutanoic acid hydrochloride, H₂¹⁸O, and NMR solvents were purchased from Aldrich (Milwaukee, WI, U.S.A.). 1-Methyl-2-pyrrolidinone was obtained from J. T. Baker (Phillipsburg, NJ,

U.S.A.). 3-Piperidinecarboxylic acid (nipecotic acid) and 2-piperidinecarboxylic acid (isonipecotic acid) were provided by Dr. Alex Chang and N-methyl-D-aspartic acid by Dr. J. Edward Moreton. ^1H NMR spectra were recorded on a General Electric QE-300 magnetic resonance spectrometer using tetramethylsilane as reference standard. IR analysis was conducted with an Analect Instruments Model fx-6160 Fourier Transform spectrophotometer. Elemental analyses were performed by Galbraith Laboratories, Knoxville, TN, U.S.A.

Typical derivatization procedure

Solid secondary amino acid (10–50 μg) was dissolved in DMF–DMA (100 μl) in a 1-ml reaction vial and the resulting solution heated at 100°C for 15 min. On cooling, 200 μl of water were added and the mixture was then extracted with chloroform (500 μl). The chloroform layer was concentrated prior to GC–MS analysis.

Synthesis of methyl N-formyl-4-methylaminobutanoate (1b)

DMF–DMA (2.0 ml, 15 mmol) was added to 4-methylaminobutanoic acid hydrochloride (1.0 g, 6.8 mmol) in an acylating vessel which was then capped with a PTFE-lined screwtop. The mixture was agitated briefly, and heated for 10 min at 110°C. Water (4.0 ml) was added to the mixture when cool, and the resulting mixture was extracted with chloroform (2×10 ml). The combined chloroform layers were evaporated and the residue (crude yield 91%) was distilled to give the desired product in 25% yield: b.p. 100°C at 0.45 Torr; ^1H NMR (C^2HCl_3), δ 2.89 and 2.90 ppm (3 H, singlet, N-CH₃, reflecting approximately equal populations of the *E* and *Z* isomers), 3.70 (3 H, singlet, ester CH₃), 8.00 (1 H, singlet, formyl); IR (neat), 1739, 1671 cm^{-1} ; C H N analysis of the partially hydrated product was consistent with $\text{C}_7\text{H}_{13}\text{NO}_3 \cdot 1/2\text{H}_2\text{O}$.

GC–MS

Electron impact (EI) mass spectra were acquired on a Hewlett-Packard mass-selective detector Model 5970 interfaced with a Model 5890 gas chromatograph. An Extrel Simulscan mass spectrometer, interfaced with a Carlo-Erba gas chromatograph, was used to obtain methane positive ion chemical ionization (CI) spectra. Both GC–MS instruments were equipped with a capillary column (HP-1, 12 m \times 0.20 mm I.D.) (Hewlett-Packard, Avondale, PA, U.S.A.) and were operated in the splitless injection mode. The column ovens were programmed from 130 to 180°C at 15°C/min following a 1-min solvent delay.

RESULTS AND DISCUSSION

Six secondary amino acids were converted to their N-formyl methyl ester derivatives by reaction with DMF–DMA (Fig. 1 and Table I). Since lactam by-products were not observed for compounds **1** and **2**, it was concluded that thermal cyclization of these γ -amino acids was avoided under the reaction conditions employed.

4-Methylaminobutanoic acid (**1**) was studied as a model N-substituted γ -amino acid. Esterification of the carboxyl group with DMF–DMA provided the methyl ester. This reaction involves an electrophilic alkoxyiminium intermediate derived from

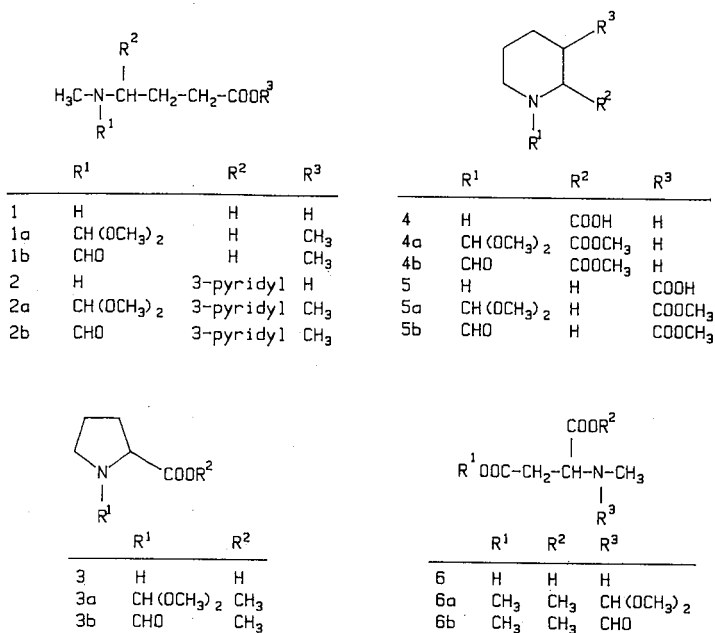


Fig. 1. Structures of secondary amino acids and the corresponding amide acetal and N-formyl methyl ester derivatives.

dissociation of an alkoxy unit from the reagent^{11,12}. The weakly nucleophilic carboxylate moiety displaces an alkyl group from this reactive intermediate by an S_N2 mechanism producing the ester along with methanol and dimethylformamide. In contrast, esterification methods based on acid catalysis¹³ or mixed anhydride formation¹⁴ activate the carboxyl function of the analyte, promoting susceptibility to

TABLE I

GC-MS CHARACTERISTICS OF N-FORMYL METHYL ESTER DERIVATIVES OF SOME N-SUBSTITUTED AMINO ACIDS

Derivative	Retention time (min)	Ions (relative intensity, %) ^a					
		CI		EI			
		MH ⁺	M ⁺	[M-28] ⁺	[M-59] ⁺	[M-87] ⁺	Other ions
1b	2.2	160 (100)	159 (10)	131 (26)	100 (68)	72 (100)	130 (18), 86 (68)
2b	7.1	237 (100)	236 (29)	n.d.	177 (8)	149 (53)	207 (45), 175 (37), 163 (100), 121 (100)
3b	2.5	158 (100)	157 (10)	129 (13)	98 (100)	70 (75)	
4b	3.5	172 (100)	171 (100)	143 (6)	112 (79)	84 (32)	142 (66, 82 (84), 56 (94)
5b	3.4	172 (100)	171 (27)	143 (5)	112 (100)	84 (25)	56 (43)
6b	4.3	204 (83)	n.d.	n.d.	n.d.	n.d.	102 (100), 58 (32)

^a n.d. = not detected.

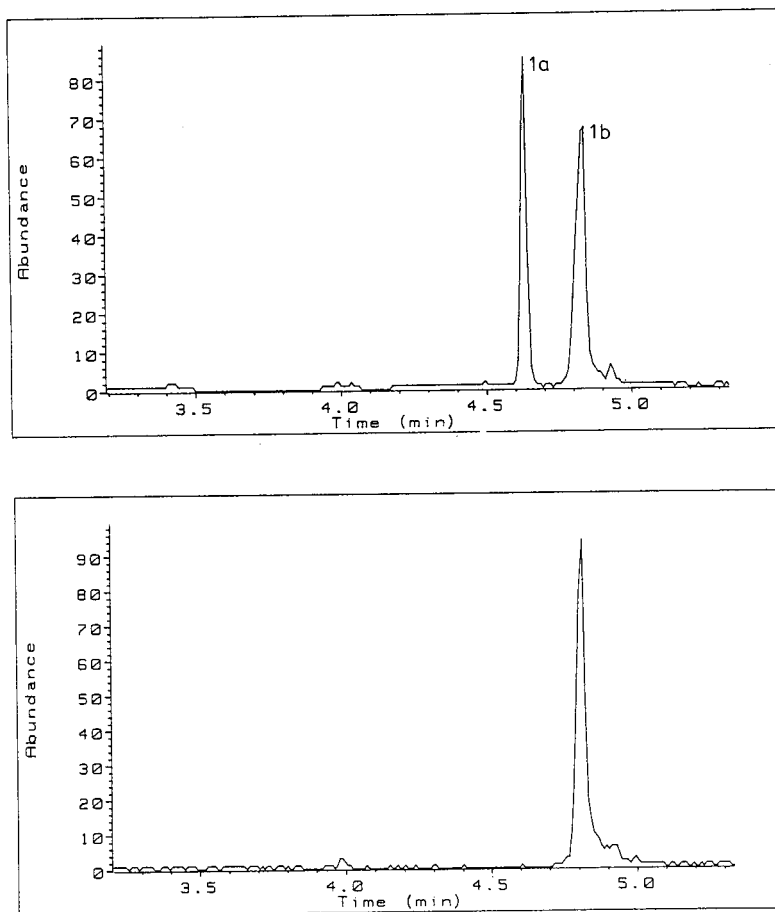


Fig. 2. Total ion current mass chromatograms of the products of the reaction of 4-methylaminobutanoic acid (10 mg) with DMF-DMA (100 μ l) before (top) and after (bottom) addition of water (20 μ l).

reaction with a wide variety of nucleophiles and thus leading to the formation of multiple products.

Derivatization of the secondary amine moiety with DMF-DMA was less straightforward. Dissolution of 4-methylaminobutanoic acid in DMF-DMA yielded two products on GC-MS analysis (Fig. 2), neither of which was the cyclized product, N-methyl-2-pyrrolidinone. The mass spectrum of the later eluting substance provided evidence for the assignment of an N-formyl methyl ester structure (**1b**) consistent with the properties of an N-formyl derivative previously identified for another secondary amine, desipramine^{2,3}. The identity of the earlier eluting peak was assigned as the transamination product, methyl N-dimethoxymethyl-N-methyl-4-aminobutanoate (**1a**). Following addition of water to the reaction mixture, the first peak disappeared while the second peak increased in area (Fig. 2, bottom). This suggested that the N-formyl product was the result of the hydrolysis of the transaminated intermediate.

Consistent with the reactivity of DMF-DMA^{11,12,15}, Fig. 3 presents a proposed

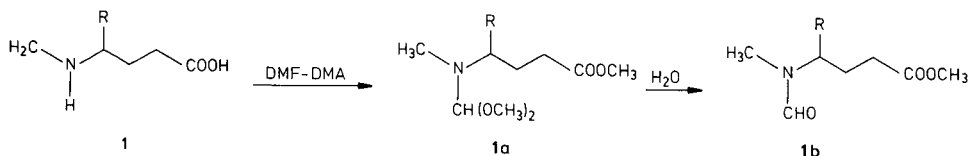


Fig. 3. Formation of the N-formyl methyl ester derivative of 4-methylaminobutanoic acid.

reaction pathway for the derivatization of 4-methylaminobutanoic acid with DMF-DMA. In a study of the reaction of dimethylformamide dialkyl acetals with secondary amines, Wawer and Osek found that the predominant product was an amide acetal resulting from nucleophilic attack of the amine on the acetal carbon with elimination of dimethylamine¹⁵. The reaction between substituted anilines and various dimethylformamide dialkyl acetals followed second order kinetics¹⁶.

The hydrolysis step in the formation of the N-formyl derivative from the amide acetal intermediate was further verified by an experiment in which ¹⁸O-labeled water was used in the hydrolysis step. The observed molecular ion in the mass spectrum of the N-formyl methyl ester indicated the presence of one ¹⁸O atom (Fig. 4). Since the formyl and ester oxygens do not exchange readily with water, and in that addition of H₂¹⁸O to DMF-DMA afforded [¹⁸O]dimethylformamide, the most probable source of oxygen in the N-formyl grouping is water and not the reagent.

The ¹⁸O-labeling experiment was also useful in assigning the identity of the EI mass spectral fragments. As was the case with the mass spectra of ester derivatives of primary amino acids⁵, a characteristic [M - 59]⁺ fragment in the spectra of most of the secondary amino acid derivatives was observed (Table I). At first, this fragment was assigned as loss of a carbomethoxy radical from the methyl ester functionality. However, the mass spectrum of ¹⁸O-labeled **1b** (Fig. 4) yielded [M - 30]⁺ and [M - 61]⁺ ions rather than the expected [M - 28]⁺ and [M - 59]⁺ ions, indicating that these fragments arise from cleavage at the ¹⁸O-containing formyl terminus.

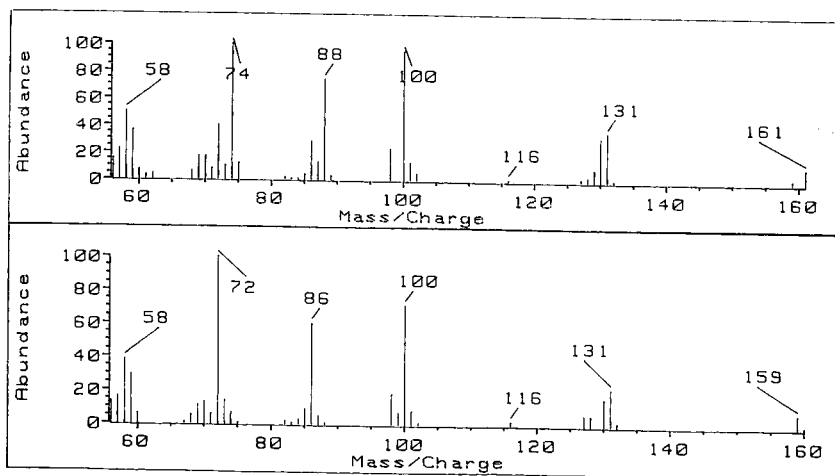


Fig. 4. Mass spectra of 4-methylaminobutanoic acid N-formyl methyl ester derivatives formed in the presence of H₂¹⁸O (top) and H₂¹⁶O (bottom).

TABLE II

GC-MS CHARACTERISTICS OF N-DIMETHOXYMETHYL METHYL ESTER INTERMEDIATES IN THE DERIVATIZATION OF SOME N-SUBSTITUTED AMINO ACIDS

Derivative	Retention time (min)	Ions (relative intensity, %) ^a			
		CI		EI	
		[M-1] ⁺	[M-31] ⁺	[M-31] ⁺	Other ions
1a	2.1	204 (7)	174 (100)	174 (34)	101 (36), 75 (100), 59 (38)
2a	6.9	—	—	n.d.	87 (61), 74 (100)
3a	2.0	202 (6)	172 (100)	172 (30)	75 (100)
4a	3.2	216 (6)	186 (100)	186 (76)	75 (100)
5a	3.0	216 (5)	186 (100)	186 (71)	75 (100)
6a	3.3	—	—	218 (27)	75 (80)

^a n.d. = not detected; — = not determined.

Molecular ions were not recorded in EI mass spectra of the amide acetals, although there were strong $[M-31]^+$ peaks, accounted for by loss of a methoxy radical.

Methane positive ion CI mass spectra of the N-formyl methyl ester derivatives were characterized by abundant protonated molecular species (MH^+ ions). Ions of $[MH-32]^+$ appeared in the CI mass spectra of the amide acetals, consistent with loss of methanol¹⁷ (Table II). Present also were $[M-1]^+$ ions of low abundance, accounted for as the resonance-stabilized acetal carbocations.

In summary, reaction between DMF-DMA and N-substituted amino acids yields, in the first step, methyl esters of unstable amide acetal intermediates. Addition of water to these intermediates results in the hydrolysis of the amide acetals yielding stable N-formyl methyl ester derivatives. The derivatization is easy to perform since it is a one-pot reaction with a single reagent. The product is stable to isolation procedures, such as solvent extraction, and GC analysis.

REFERENCES

- 1 M. W. Scoggins, *J. Chromatogr. Sci.*, 13 (1975) 146.
- 2 M. S. B. Nayar and P. S. Callery, *Anal. Lett.*, 13 (1980) 625.
- 3 J.-P. Thenot, T. I. Ruo and O. J. Bouwsma, *Anal. Lett.*, 13 (1980) 759.
- 4 I. Horman and F. J. Hesford, *Biomed. Mass Spectrom.*, 1 (1974) 115-119.
- 5 J.-P. Thenot and E. C. Horning, *Anal. Lett.*, 5 (1972) 519.
- 6 J. J. Pisano, W. J. A. Van den Heuvel and E. C. Horning, *Biochem. Biophys. Res. Commun.*, 7 (1962) 82-86.
- 7 N. Ikekawa, O. Hoshino, R. Watanuki, H. Orimo, T. Fujita and M. Yoshikawa, *Anal. Biochem.*, 17 (1966) 16.
- 8 D. Roach and C. W. Gehrke, *J. Chromatogr.*, 44 (1969) 269.
- 9 H. Iwase and A. Murai, *Anal. Biochem.*, 78 (1978) 340.
- 10 G. Losse, A. Losse and J. Stock, *Z. Naturforsch.*, 17 (1962) 785.
- 11 R. F. Abdulla and R. S. Brinkmeyer, *Tetrahedron*, 35 (1979) 1675.
- 12 H. Brechbuhler, H. Buchi, E. Hatz, J. Schreiber and A. Eschenmoser, *Helv. Chim. Acta*, 48 (1965) 1746.
- 13 W. Stoffel, F. Chu and E. H. Ahrens, Jr., *Anal. Chem.*, 31 (1959) 307.
- 14 E. J. Bourne, M. Stacey, J. C. Tatlow and J. M. Tedder, *J. Chem. Soc.*, (1949) 2976.
- 15 I. Wawer and J. Osek, *J. Chem. Soc. Perkin Trans. 2*, (1985) 1669.
- 16 J. Osek, J. Oszczapowicz and W. Drzewinski, *J. Chem. Soc. Perkin Trans. 2*, (1986) 1961.
- 17 A. G. Harrison, *Chemical Ionization Mass Spectrometry*, CRC Press, Boca Raton, FL, 1983, p. 99.

CHROM. 21 332

DEGRADATION AND ANALYSIS OF POLYOXYETHYLENE MONOALKYL ETHERS IN THE PRESENCE OF ACETYL CHLORIDE AND FERRIC CHLORIDE

J. SZYMANOWSKI*

Technical University of Poznań, Institute of Chemical Technology and Engineering, Pl. Skłodowskiej-Curie 2, 60-965 Poznań (Poland)

and

P. KUSZ, E. DZIWIŃSKI, H. SZEWCZYK and K. PYŻAŁSKI

Institute of Heavy Organic Synthesis "Blachownia", 47-225 Kedzierzyn-Koźle 7 (Poland)

(First received July 11th, 1988; revised manuscript received January 16th, 1989)

SUMMARY

Degradation of model and commercial polyoxyethylene glycol monoalkyl ethers in the presence of anhydrous ferric chloride and an excess of acetyl chloride was studied. It was found that 2-chloroethyl acetate is the main product of the polyoxyethylene chain degradation. Hydrophobic alkyls form mainly unidentified resins. 2,6-Dimethyl- γ -pyrone and its derivatives are by-products formed from acetyl chloride and acetic acid. Using an internal standard method, the composition of the products obtained by degradation of polyoxyethylene chains can be determined and used to calculate the average degree of ethoxylation. However, this method is limited to preparations for which the hydrophobes can be identified and their contents determined.

INTRODUCTION

In our previous papers^{1,2} the degradation of polyoxyethylene glycols, block copolymers of ethylene oxide-butylene oxide and polyoxyethylene monoalkyl ethers in the presence of an excess of acetyl chloride was reported. The degradation is complete after 2 h at 250°C. 2-Chloroethyl acetate formed from the polyoxyethylene chain and alkyl chlorides obtained from the hydrophobic alkyls are the main products. However, other products are also formed during the degradation. As a result, several components must be identified and their contents determined by taking into account correction factors. This is troublesome even for model pure compounds or poly-disperse polyoxyethylene glycol monoalkyl ethers obtained by ethoxylation of a single alcohol.

Commercial products are obtained from mixtures of different alcohols and their compositions are usually very complex. Therefore, the composition of the degradation products is also very complex and it is a very difficult task to separate and identify all

components formed during degradation. This complexity decreases the precision and accuracy of the qualitative analysis.

The aim of this work is to study the degradation of some model and commercial polyoxyethylene glycol monoalkyl ethers in the presence of acetyl chloride and ferric chloride and the application of this method, proposed for the first time by Waszeciak and Nadeau³, for determining the average degree of alcohol ethoxylation and the composition of the hydrophobic constituent in some commercial products.

EXPERIMENTAL

The following reagents were used for degradation studies: model trioxyethylene glycol monoalkyl ether (E-3), $\text{H}(\text{OCH}_2\text{CH}_2)_3\text{OC}_{10}\text{H}_{21}$, of purity >94% as determined by gas chromatography (GC); commercial oleyl alcohol fraction treated with ethylene oxide (O-5); commercial Rokanol K-3 (NZPO Rokita, Brzeg Dolny, Poland), a product of the reaction of alcohols obtained from rape seed oil with ethylene oxide; commercial Rokanol K-20 (NZPO Rokita), a product of the reaction of alcohols obtained from rape seed oil with ethylene oxide; commercial Rokanol L-3 (NZPO Rokita), a product of the reaction of a mixture of saturated alcohols $\text{C}_{12}\text{--}\text{C}_{18}$ with ethylene oxide; acetyl chloride, pure for analysis (Fluka, Buchs, Switzerland); anhydrous ferric chloride (POCh Gliwice, Poland).

A sample (0.05 g) of polyoxyethylene glycol monoalkyl ethers, 0.005–0.02 g of hexadecane used as an internal standard and 0.05 g of anhydrous ferric chloride were weighed into a reaction vial of capacity 5 cm^3 (Supelco, Bellefonte, PA, U.S.A.). Acetyl chloride (0.8 cm^3) was added by means of a syringe and the reaction mixture was shaken to obtain a clear solution. It was heated at 150°C for 30 min. The cooled post-reaction mixture was diluted 1:1 in dichloromethane and analyzed by means of GC.

A gas chromatograph (Perkin-Elmer Model 900) with a flame ionization detector was used. The separation was carried out in stainless-steel columns: I, $0.9\text{ m} \times 2.7\text{ mm}$ I.D. packed with 3% OV-101 on Chromosorb G AW DMCS, 60–80 mesh; II, $0.9\text{ m} \times 2.7\text{ mm}$ I.D. packed with 3% OV-17 on Chromosorb G AW DMCS, 60–80 mesh; III, $1.6\text{ m} \times 2.7\text{ mm}$ I.D. packed with 12% Carbowax 20 M-TPA on Chromosorb W AW DMCS, 80–100 mesh. Argon was used as the carrier gas and its flow-rate was $30\text{ cm}^3\text{ min}^{-1}$. The temperature of column I was 100°C for 1 min, and then raised to 300°C at 8°C min^{-1} . The temperatures of the injector and the detector were 300 and 320°C , respectively. The temperature of column II was 80°C for 1 min, and then raised to 290°C at 6°C min^{-1} . The temperatures of the injector and the detector were 300°C . The temperature of column III was 100°C for 1 min, and then raised to 220°C at 5°C min^{-1} . The temperatures of the injector and the detector were 250°C .

The average degree of ethoxylation was calculated in a similar way as in our previous work². Correction factors were calculated according to the method of Stenberg *et al.*⁴ using the concept of the effective number of carbon atoms.

For comparison the ethoxylation degrees of polyoxyethylene monoalkyl ethers were also determined by the standard ISO 2270-1972(E) method.

In a direct analysis, polyoxyethylene glycol monoalkyl ethers were analyzed in the form of their acetates prepared in the standard way. Polyoxyethylene glycols were determined according to the Weibull method⁵.

The identification of the separated components was carried out by means of a mass spectrometer coupled to a gas chromatograph (GC-MS 2091; LKB, Bromma, Sweden). The chromatographic columns and separation conditions were the same as in the GC analysis: columns II and III were used. An ionization energy of 70 eV and an ion-source temperature of 250°C were employed.

RESULTS AND DISCUSSION

In the previous paper² model E-3 and E-7 products were used only for degradation studies. E-3 contains mainly the homologue having three oxyethylene groups and its content is above 94%. E-7 is a polydisperse mixture obtained from pure dodecyl alcohol and contains succeeding homologues up to the compound having seventeen oxyethylene groups. O-5 contains homologues only up to compounds having six oxyethylene groups. However, in this case three different hydrophobic alkyls are present; the main components are appropriate derivatives of oleyl alcohol. L-3 contains homologues up to compounds having seven to eight oxyethylene groups and four different saturated alcohols (C_{12} - C_{18}) are present in this product (Fig. 1).

Chromatograms of these four products are relatively simple and all components can be separated. They can easily be identified by means of their retention indices⁶ and their contents can be determined by the normalization method (Table I). These results can be further used to calculate the average degree of ethoxylation.

The chromatogram obtained for Rokanol K-3 is much more complex as a result of the presence of different saturated and unsaturated alcohols C_{12} - C_{22} present in this product (Fig. 2). Therefore, it is impossible to separate all the components present and

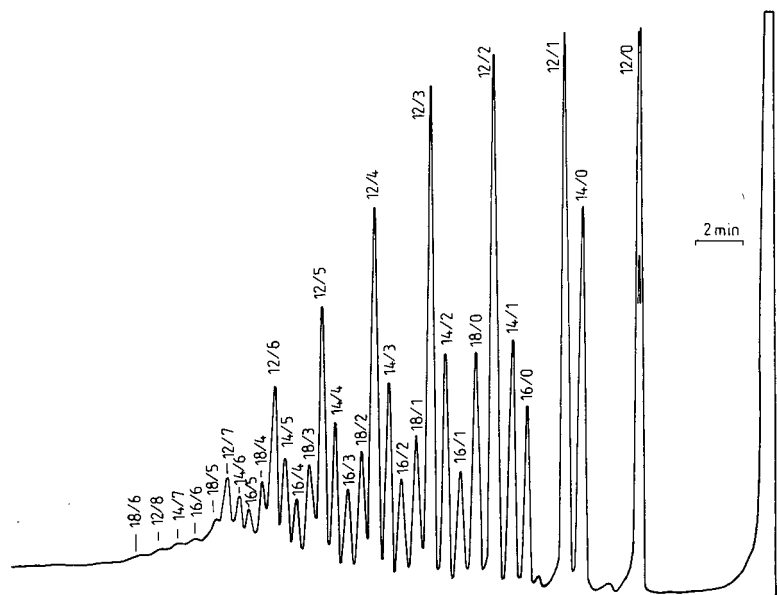


Fig. 1. Chromatogram of Rokanol L-3 on column I. Peak labelling: number of carbon atoms/degree of ethoxylation.

TABLE I
COMPOSITIONS OF THE POLYOXYETHYLENE GLYCOL MONOALKYL ETHERS
EO = Ethylene oxide.

<i>E-7</i>			<i>O-5</i>			<i>Rokanol L-3</i>		
<i>Formula</i>	<i>n</i>	<i>Content</i> (%, w/w)	<i>Formula</i>	<i>n</i>	<i>Content</i> (%, w/w)	<i>Formula</i>	<i>n</i>	<i>Content</i> (%, w/w)
$C_{12}H_{25}O(EO)_nH$	0	5.51	$C_{16}H_{33}O(EO)_nH$	0	0.00	$C_{12}H_{25}O(EO)_nH$	0	11.73
	1	3.15		1	0.00		1	10.85
	2	4.45		2	0.21		2	9.78
	3	5.95		3	0.83		3	8.77
	4	7.53		4	2.39		4	6.54
	5	8.69		5	1.68		5	4.10
	6	9.01	$C_{18}H_{37}O(EO)_nH$	6	0.92	6	2.32	
	7	9.56		0	0.00	7	1.13	
	8	9.35		1	0.46	8	0.11	
	9	9.01		2	1.01	$C_{14}H_{29}O(EO)_nH$	0	6.84
	10	8.03		3	6.01		1	4.46
	11	6.75		4	5.17		2	3.73
	12	5.30	5	1.58	3		3.09	
	13	3.64	$C_{18}H_{35}O(EO)_nH$	0	0.46		4	2.34
	14	2.33		1	0.97		5	1.34
	15	1.20		2	2.98	6	0.80	
	16	0.46		3	26.62	7	0.28	
17	0.08	4		34.39	$C_{16}H_{33}O(EO)_nH$	0	3.30	
		5		13.02		1	1.89	
		6	1.32	2		1.57		
		3	1.26	4		0.67		
4	0.67	5	0.54					
5	0.54	6	0.34	$C_{18}H_{37}O(EO)_nH$		0	4.00	
6	0.34	1	2.32		1	2.32		
		2	2.15		2	2.15		
		3	1.65		3	1.65		
		4	1.07		4	1.07		
		5	0.85		5	0.85		
		6	0.19	6	0.19			

some of them are coeluted (Table II). Thus, the contents of all components cannot be determined and the average degree of ethoxylation cannot be correctly calculated.

Rokanol K-20 contains much higher analogues having more oxyethylene groups and it cannot be analyzed by GC. As a result, its average degree of ethoxylation cannot be determined.

Polyoxyethylene glycols are also present in these products, but their contents, as determined by the Weibull method⁵, are relatively low and equal to 0.0, 1.5, 0.96, 0.41, 1.17 and 2.19% for E-3, E-7, O-5, L-3, K-3 and K-20, respectively.

Degradation products were analyzed using columns containing silicone resins OV-101 and OV-17 and Carbowax 20 M-TPA as the liquid phases in columns I, II and III, respectively. Columns I and II were used to check the degree of degradation, while

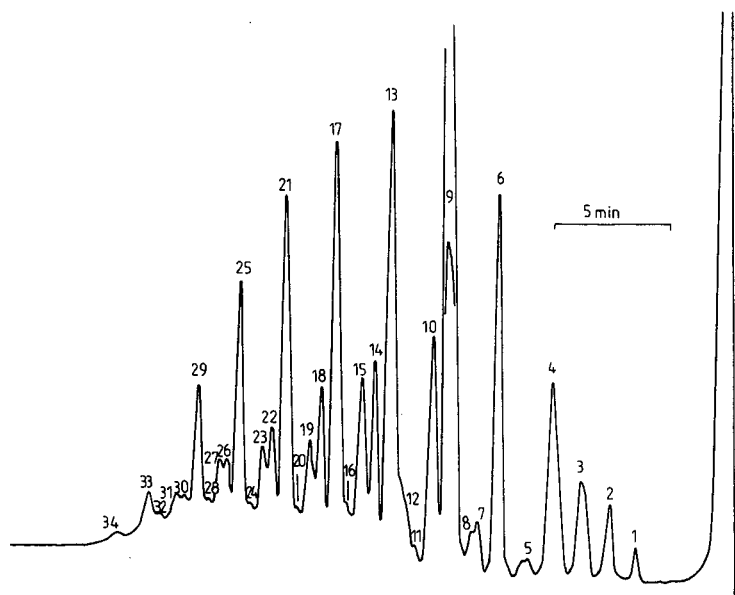


Fig. 2. Chromatogram of Rokanol K-3 on column I.

column III was used to separate all components after degradation and to determine their contents.

It was found that the degradation is complete at 150°C after 30 min (Fig. 3b). At 100°C, chromatograms are more complex and several peaks are observed (Fig. 3a). Most of these peaks are formed by the degradation of the hydrophobic alkyls (Table III). Their mass spectra have parent ions and show characteristic lines at m/z differing by 14 units, *i.e.*, the value characteristic for the methylene group. Thus, they are formed by splitting of methylene groups from the hydrophobic alkyls. These peaks largely disappear as the degradation is carried out at 150°C. Some high boiling resins are formed and they are not eluted from the column. However, small peaks of the products formed by degradation of the hydrophobic alkyls are still observed, and they can be used to identify hydrophobes in the initial polyoxyethylene glycol monoalkyl ethers.

Exemplary chromatograms of the degradation products are shown in Figs. 4 and 5. Hexane was used as an internal standard. The separated components were identified by gas chromatography–mass spectrometry (GC–MS) and by comparison of their retention indices with those determined for chromatographic standards (Tables IV and V). Also reported are the contents of the separated components as determined by the internal standard method.

Polyoxyethylene chains degrade in the same way as was reported previously for polyoxyethylene glycols¹. Four different components were found with retention indices of 1065, 1318, 1536 and 1757 on Carbowax 20M-TPA, corresponding to 1,2-dichloroethane, 2-chloroethyl acetate, bis(2-chloroethyl) ether and 5-chloro-3-oxapentyl acetate. 2-Chloroethyl acetate is the main product of degradation. Acetic acid ($I_p = 1427$) is formed from an excess of acetyl chloride and can be neglected. Under the degradation conditions in the presence of ferric chloride, acetyl chloride and

TABLE II
 COMPOSITION OF ROKANOL K-3

Peak No.	Component	Content (% w/w)
1	Unknown	0.62
2	C ₁₂ H ₂₅ OH	1.57
3	Unknown	2.98
4	C ₁₄ H ₂₉ OH + C ₁₂ H ₂₅ O(EO)H	5.82
5	Unknown	0.54
6	C ₁₆ H ₃₃ OH	6.94
7	C ₁₄ H ₂₉ O(EO)H	0.85
8	C ₁₂ H ₂₅ O(EO) ₂ H	0.70
9	C ₁₈ H ₃₇ OH + C ₁₈ H ₃₅ OH	22.44
10	C ₁₆ H ₃₃ (EO)H	4.17
11	C ₁₄ H ₂₉ O(EO) ₂ H	0.22
12	C ₁₂ H ₂₅ O(EO) ₃ H + C ₂₀ H ₄₁ OH	1.31
13	C ₁₈ H ₃₇ O(EO)H + C ₁₈ H ₃₅ O(EO)H	11.80
14	C ₁₆ H ₃₃ O(EO) ₂ H	2.64
15	C ₂₀ H ₄₁ O(EO)H + C ₂₂ H ₄₅ OH + C ₁₄ H ₂₉ O(EO) ₃ H	3.27
16	C ₁₂ H ₂₅ O(EO) ₄ H	0.12
17	C ₁₈ H ₃₇ (EO) ₂ H + C ₁₈ H ₃₅ (EO) ₂ H	9.18
18	C ₁₆ H ₃₃ O(EO) ₃ H	2.00
19	C ₂₀ H ₄₁ O(EO) ₂ H + C ₂₂ H ₄₅ O(EO)H + C ₁₄ H ₂₉ O(EO) ₄ H	1.38
20	C ₁₂ H ₂₅ O(EO) ₅ H	0.15
21	C ₁₈ H ₃₇ O(EO) ₃ H + C ₁₈ H ₃₅ O(EO) ₃ H	6.96
22	C ₁₆ H ₃₃ O(EO) ₄ H	1.42
23	C ₂₀ H ₄₁ O(EO) ₃ H + C ₂₂ H ₄₃ O(EO) ₂ H + C ₁₄ H ₂₉ O(EO) ₅ H	1.16
24	C ₁₂ H ₂₅ O(EO) ₆ H	0.16
25	C ₁₈ H ₃₇ O(EO) ₄ H + C ₁₈ H ₃₅ O(EO) ₄ H	4.60
26	C ₁₆ H ₃₃ O(EO) ₅ H	1.17
27	C ₂₀ H ₄₁ O(EO) ₄ H + C ₂₂ H ₄₃ O(EO) ₃ H + C ₁₄ H ₂₉ O(EO) ₆ H	1.01
28	C ₁₂ H ₂₅ O(EO) ₇ H	0.18
29	C ₁₈ H ₃₇ O(EO) ₅ H + C ₁₈ H ₃₅ O(EO) ₅ H	2.66
30	C ₁₆ H ₃₃ O(EO) ₆ H	0.49
31	C ₂₀ H ₄₁ O(EO) ₅ H + C ₂₂ H ₄₃ O(EO) ₄ H + C ₁₄ H ₂₉ O(EO) ₇ H	0.31
32	C ₁₂ H ₂₅ O(EO) ₈ H	0.19
33	C ₁₈ H ₃₇ O(EO) ₆ H + C ₁₈ H ₃₅ O(EO) ₆ H	0.86
34	C ₁₆ H ₃₃ O(EO) ₇ H	0.13

acetic acid can form γ -pyrone derivatives which were identified in our previous work¹. As they are not formed in the absence of ferric chloride, the appropriate peaks ($I_p = 2035, 2107, 2227$ and 2405) can also be ignored. Other small peaks having the retention indices $1470, 1684, 1873, 1893, 2078, 2241, 2288, 2480, 2692$ and 2898 were the products formed by the degradation of hydrophobic alkyls. They can be used only to identify the alkyl structures in the initial polyoxyethylene glycol monoalkyl ethers because these alkyl groups formed mainly unidentified resins.

Due to this, the normalization method cannot be used to determine the composition of the degradation products. Thus, the internal standard method was

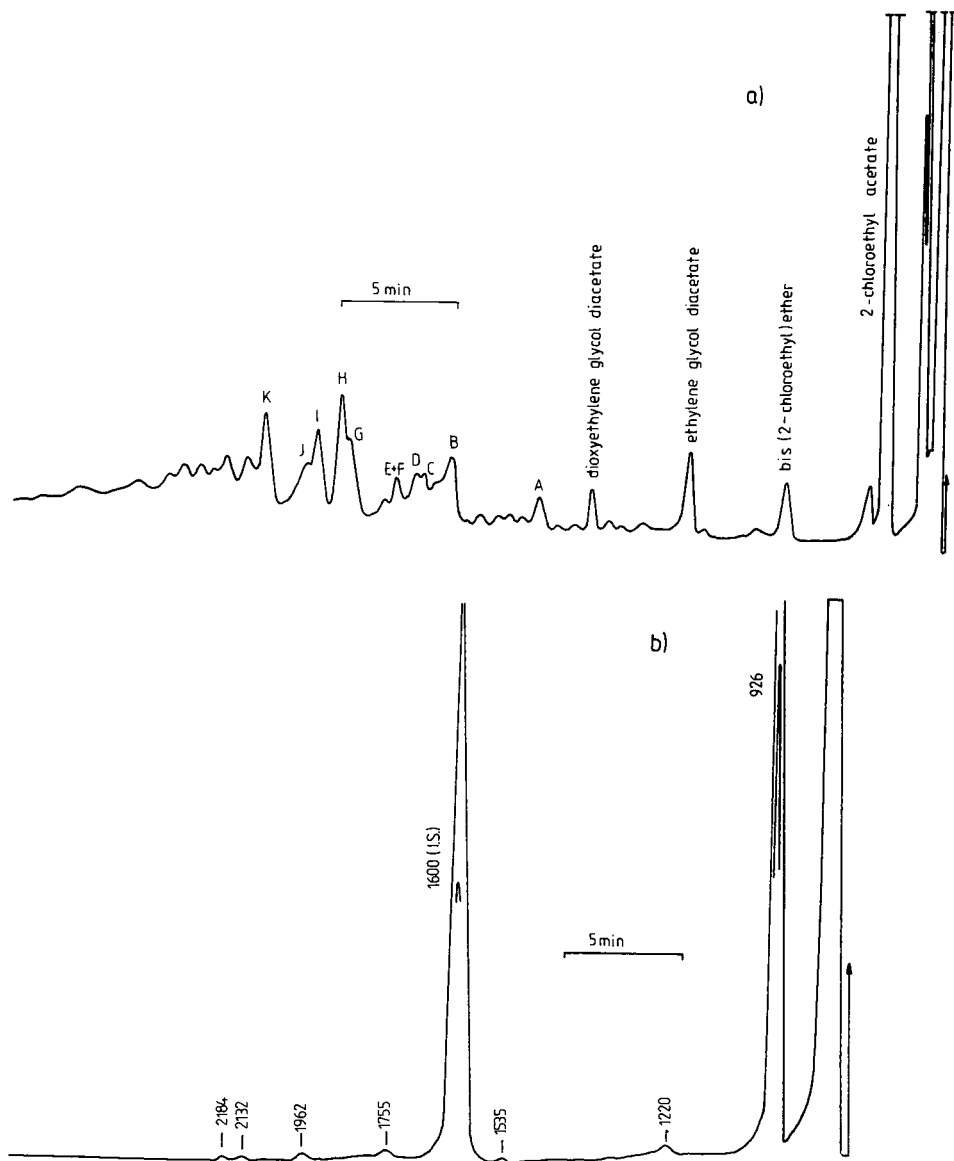


Fig. 3. Chromatograms of O-5 after degradation at (a) 100, (b) 150°C, on column II.

used. The small peaks of chlorohydrocarbons can be neglected and the average degrees of ethoxylation calculated from the masses of polyoxyethylene glycol monoalkyl ethers taken for analyses and from the contents of 1,2-dichloroethane, 2-chloroethyl acetate, bis(2-chloroethyl) ether and 5-chloro-3-oxapentyl acetate formed from the polyoxyethylene chains during their degradation.

The values of the degree of ethoxylation together with some statistical

TABLE III
COMPONENTS IDENTIFIED IN THE DEGRADATION OF HYDROPHOBIC ALKYL
O-5, silicone resin OV-17, $T = 100^{\circ}\text{C}$.

Peak	Molecular mass	Component
A	224	$\text{C}_{16}\text{H}_{32}$
B	250 + 252	$\text{C}_{18}\text{H}_{34} + \text{C}_{18}\text{H}_{36}$
C	250 + 224	$\text{C}_{18}\text{H}_{34} + \text{C}_{16}\text{H}_{32}$
D	250 + 224	$\text{C}_{18}\text{H}_{34} + \text{C}_{16}\text{H}_{32}$
E	260	$\text{C}_{16}\text{H}_{33}\text{Cl}$
F	238	$\text{C}_{17}\text{H}_{34}$
G	286 + 250	$\text{C}_{18}\text{H}_{35}\text{Cl} + \text{C}_{18}\text{H}_{34}$
H	286 + 250	$\text{C}_{18}\text{H}_{35}\text{Cl} + \text{C}_{18}\text{H}_{34}$
I	286 + 250	$\text{C}_{18}\text{H}_{35}\text{Cl} + \text{C}_{18}\text{H}_{34}$
J	250	$\text{C}_{18}\text{H}_{34}$
K	316	$\text{C}_{20}\text{H}_{41}\text{Cl}$

assessment are presented in Table VI. Much higher values were obtained after degradation as a result of incomplete elution in the direct analysis of homologues containing long polyoxyethylene chains. Similar results were obtained from both methods for the model trioxyethylene glycol monodecyl ether.

Thus, the direct analysis cannot be used to determine the average degree of ethoxylation for commercial non-ionic surfactants. In this case the surfactants must first be degraded and the average degrees of ethoxylation can be calculated from the contents of components formed by degradation of the polyoxyethylene chains.

The contents of the oxyethylene groups present in the surfactants studied and/or the average degrees of ethoxylation obtained by means of the method discussed are

TABLE IV
CONTENTS OF THE COMPONENTS FORMED BY DEGRADATION OF HYDROPHOBIC ALKYL

Compound	Retention index		Content (% w/w)					
	Carbowax 20M-TPA	OV-17	E-3	E-7	O-5	L-3	K-3	K-20
1-Chlorodecane	1470	1335	5.50	—	—	—	—	—
1-Chlorododecane	1684	1535	—	8.42	0.18	7.29	0.25	0.10
Dodecyl acetate	1893	<i>a</i>	—	0.30	—	—	—	—
1-Chlorotetradecane	1873	1755	—	—	0.20	5.52	0.20	0.15
1-Chlorohexadecane	2078	1962	—	—	0.74	3.13	1.99	0.56
1-Chloro-9-octadecene	2241	2132	—	—	0.96	—	—	—
1-Chlorooctadecane	2288	2184	—	—	0.37	1.17	6.22	0.50
1-Chloroeicosane	2480	2398	—	—	—	0.62	6.09	0.28
1-Chlorodocosane	2692	2610	—	—	—	—	0.50	—
1-Chlorotetracosane	2898	2818	—	—	—	—	0.50	—
High-boiling resins	<i>b</i>	<i>b</i>	51.42	29.70	52.56	52.06	50.65	26.07

^a Not determined.

^b Not eluted.

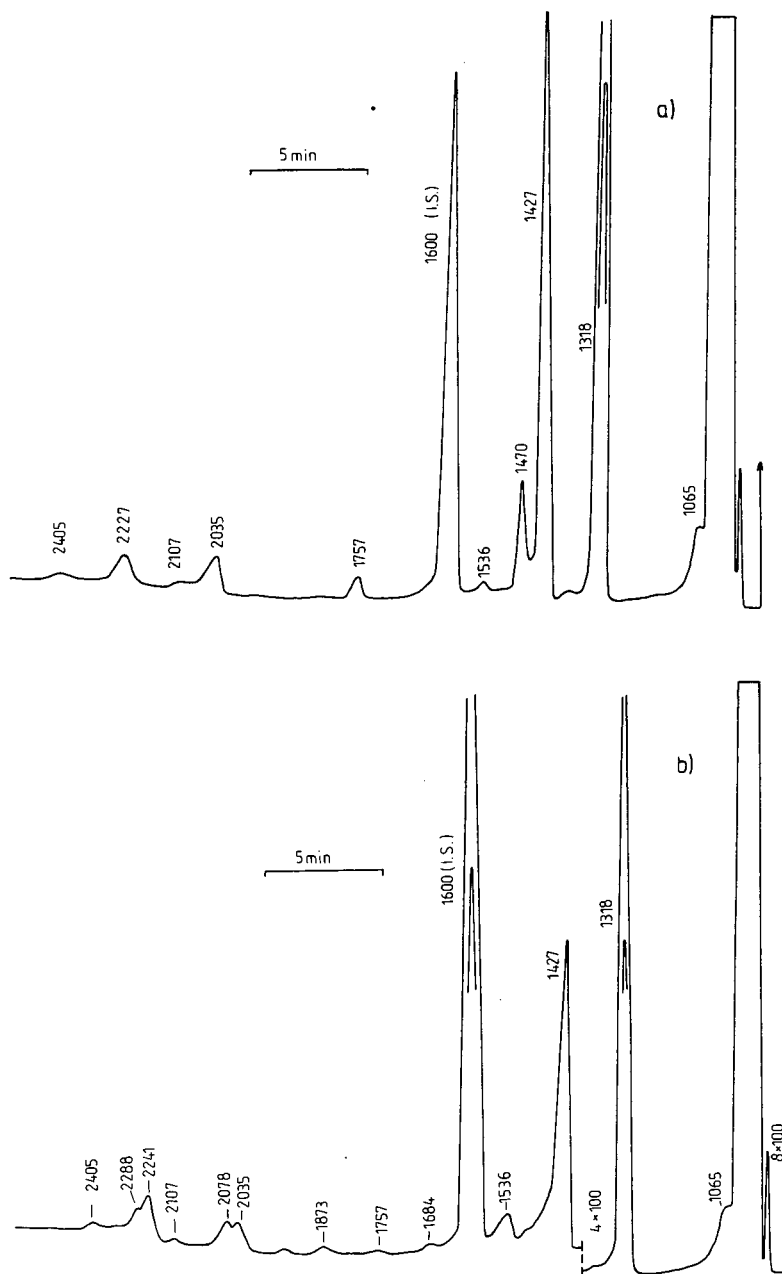


Fig. 4. Chromatograms of the degradation products of (a) E-3, (b) O-5 at 150°C, on column III.

somewhat lower than the values obtained according to the standard method ISO 2270-1972(E). The ratios of the contents determined by the standard method to those determined by GC after degradation are equal to 1.06, 1.04, 1.11, 1.10, 1.16 and 1.17 for E-3, E-7, O-5, L-3, K-3 and K-20, respectively. Thus, for surfactants having well

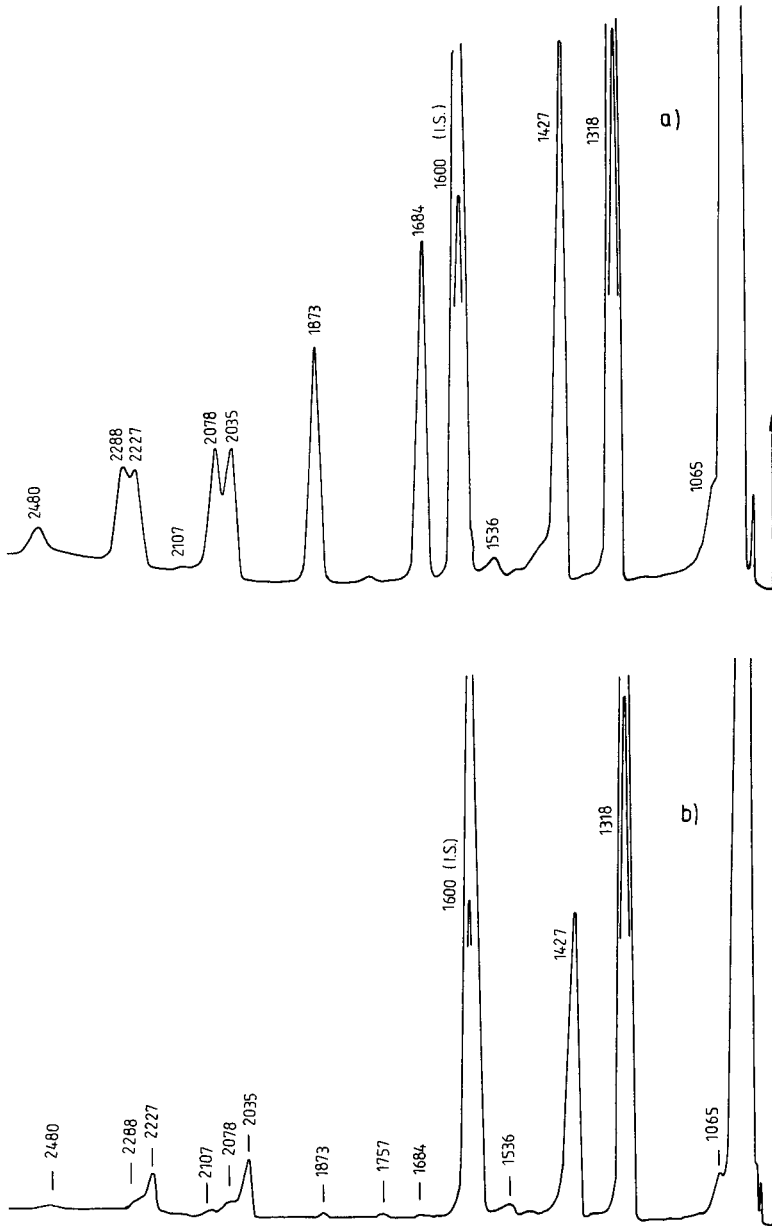


Fig. 5. Chromatograms of the degradation products of (a) Rokanol L-3, (b) Rokanol K-20 at 150°C, on column III.

defined hydrophobic constituents the differences are small but statistically significant; they are equal to 5–10%. Lower deviations are expected when the experimentally determined correlation coefficients are used.

However, in the case of preparations K-3 and K-20 having more complex

TABLE V

CONTENTS OF THE COMPONENTS FORMED BY DEGRADATION OF POLYOXYETHYLENE CHAINS

Compound	Retention index		Content (% w/w)					
	Carbowax 20M-TPA	OV-17	E-3	E-7	O-5	L-3	K-3	K-20
1,2-Dichloroethane	1065	<i>a</i>	2.45	5.08	2.12	2.43	2.68	10.35
2-Chloroethyl acetate	1318	926	38.57	54.33	42.02	26.10	29.37	60.44
Bis(2-chloroethyl) ether	1536	1220	0.74	1.34	0.85	0.95	0.56	0.88
5-Chloro-3-oxapentyl acetate	1757	<i>b</i>	1.32	0.84	0.00	0.73	0.99	0.67

^a Eluted with the solvent.^b Not determined.

TABLE VI

AVERAGE DEGREE OF ETHOXYLATION OF ALIPHATIC ALCOHOLS

Polyoxyethylene glycol monoalkyl ethers	Direct analysis	Analysis after degradation	Relative difference (%)
E-3	2.70 ± 0.11	2.72 ± 0.18	0.7
E-7	5.43 ± 0.23	6.78 ± 0.29	24.9
O-5	3.46 ± 0.29	4.95 ± 0.19	43.1
Rokanol L-3	1.67 ± 0.08	2.06 ± 0.20	23.3
Rokanol K-3	1.39 ± 0.02	3.00 ± 0.04	115.8
Rokanol K-20	<i>a</i>	15.50 ± 0.46	—

^a Direct analysis is impossible.

compositions of the hydrophobic part, these differences are near 20%. This is caused by the errors in the average molecular mass determination of the hydrophobic part. Thus, the use of the chromatographic technique proposed is limited to products having well defined hydrophobic constituents or to those for which the hydrophobic constituents can be identified and their contents precisely determined. The positive feature of this method is the possibility of identifying the composition, of alcohols used to prepare non-ionic surfactants. This parameter must be always taken into consideration when non-ionic surfactants are analyzed, and it cannot be determined by the traditional standard method ISO 2270-1972 (E).

CONCLUSIONS

Degradation of polyoxyethylene glycol monoalkyl ethers in the presence of anhydrous ferric chloride and an excess of acetyl chloride is complete at 150°C after 30 min. 2-Chloroethyl acetate is the main product of the polyoxyethylene chain degradation. 1,2-Dichloroethane, bis(2-chloroethyl) ether and 5-chloro-3-oxapentyl acetate are also formed but only in small amounts. 2,6-Dimethyl- γ -pyrone and its

derivatives are by-products formed from acetyl chloride and acetic acid. Hydrophobic alkyls form mainly unidentified resins.

This method of degradation can be used for commercial products, even with quite an high degree of ethoxylation. Using an internal standard method, the composition of the products obtained by degradation of polyoxyethylene chains can be determined and used to calculate the average degree of ethoxylation. The components of the hydrophobic constituents in commercial products can also be identified. However, in the case of surfactants having very complex compositions of the hydrophobic part, some significant deviation of the polyoxyethylene chain content and/or of the degree of ethoxylation can be observed.

REFERENCES

- 1 J. Szymanowski, P. Kusz and E. Dziwiński, *J. Chromatogr.*, 455 (1988) 131.
- 2 J. Szymanowski, P. Kusz, E. Dziwiński and Cs. Latocha, *J. Chromatogr.*, 455 (1988) 119.
- 3 P. Waszeczak and H. G. Nadeau, *Anal. Chem.*, 36 (1964) 764.
- 4 J. C. Stenberg, W. S. Gallaway and D. T. L. Jones, in N. Brenner, J. E. Callen and H. D. Weiss (Editors), *Gas Chromatography*, Academic Press, New York, 1962, p. 231.
- 5 B. Weibull, *Proc. 3rd Int. Congr. Surface Activity, Cologne*, 1960, Vol. 3, p. 121.
- 6 E. A. Taylor, *J. Chromatogr.*, 64 (1972) 71.

MASS SPECTRAL INVESTIGATIONS ON TRICHOHECENE MYCOTOXINS

VII. LIQUID CHROMATOGRAPHIC-THERMOSPRAY MASS SPECTROMETRIC ANALYSIS OF MACROCYCLIC TRICHOHECENES

THAIYA KRISHNAMURTHY*

Research Directorate, U.S. Army Chemical Research, Development and Engineering Center, Aberdeen Proving Ground, MD 21010-5423 (U.S.A.)

DEBRA J. BECK and ROBERT K. ISENSEE

Oneida Research Services, One Halsey Road, Whitesboro, NY 13492 (U.S.A.)

and

BRUCE B. JARVIS

Department of Chemistry, University of Maryland, College Park, MD (U.S.A.)

(First received May 2nd, 1988; revised manuscript received January 6th, 1989)

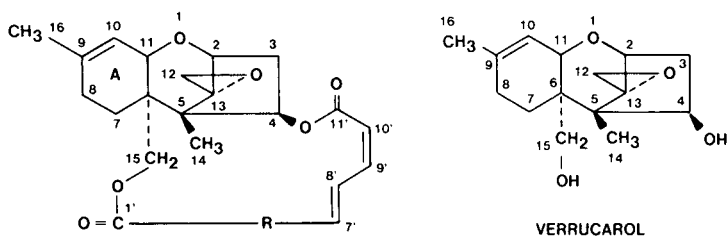
SUMMARY

Thermally labile, polar toxic roridins and biologically active, isomeric baccharinoids were separated on a reversed-phase high-performance liquid chromatography column and effectively ionized under thermospray ionization conditions. The mass spectra indicated the formation of corresponding molecular ion-ammonium adducts in great abundance. Experiments designed for monitoring specific ions of these analytes at predesignated intervals were utilized for the accurate analysis of these macrocyclic trichothecenes in real, crude samples. A synthetically modified macrocyclic trichothecene, 8-ketoverrucarin A, was used as the internal standard for the detection and quantification of these compounds. Minimum detectable limits, during this first reported method for the unambiguous analysis of these structurally related macrocyclic trichothecenes, were determined to be 2–5 ng.

INTRODUCTION

Trichothecenes are toxic fungal metabolites, which have been associated with human health hazards, loss of farm products, live stock and other animals for decades^{1–5}. They were also alleged to have been used as chemical warfare agents^{6–9}. Recently, the growth of trichothecene producing fungi has been also detected in the U.S. urban environments¹⁰. Thus, the development of rapid, specific, sensitive, and accurate methods for the analysis of these toxins in environmental, agricultural, and biological samples has become vital. The large number of trichothecenes present and their polar and labile properties pose a great challenge in developing one common methodology to analyze all the derivatives of interest^{11,12}.

Recently, several mass spectrometric (MS) and direct tandem MS methods have been developed for the analysis of simple trichothecenes¹³⁻²³. We have previously reported several such methods having excellent speed, selectivity, and sensitivity with minimal sample clean-up¹⁷⁻²³. Some of these procedures were the first ever methods reported for the analysis of macrocyclic trichothecenes (Fig. 1), the most toxic variety^{1,2,24-26}. However, none of them were direct and could be used for the unambiguous detection of the isomeric macrocyclics. Development of one single MS



COMPOUND	MOL. WT.	R	OTHER
RORIDIN A	532	$\begin{array}{ccccccc} 2' & 3' & 4' & 5' & 6' & & \\ -\text{CHOH} & \text{CH} & \text{CH}_3 & \text{CH}_2 & \text{CH}_2 & \text{OCH} & \text{CHOH} & \text{CH}_3 \\ & & 12' & & & 13' & 14' & \end{array}$	—
RORIDIN D	530	$\begin{array}{ccccccc} 2' & 3' & 4' & 5' & 6' & & \\ -\text{CH} & -\text{CH} & \text{CH}_3 & \text{CH}_2 & \text{CH}_2 & \text{OCH} & \text{CHOH} & \text{CH}_3 \\ & & 12' & & & 13' & 14' & \end{array}$	—
RORIDIN E	514	$\begin{array}{ccccccc} 2' & 3' & 4' & 5' & 6' & & \\ -\text{CH} = & \text{CH} & \text{CH}_3 & \text{CH}_2 & \text{CH}_2 & \text{OCH} & \text{CHOH} & \text{CH}_3 \\ & & 12' & & & 13' & 14' & \end{array}$	—
RORIDIN H	512	$\begin{array}{ccccccc} 2' & 3' & 4' & 5' & 6' & & \\ -\text{CH} = & \text{CH} & \text{CH}_3 & \text{CH}_2 & \text{CH} & & \text{CH} - \\ & & 12' & & & & & \\ & & & & & & \text{O} & \\ & & & & & & & \\ & & & & & & \text{CH} & \text{CH}_3 \\ & & & & & & 13' & 14' \end{array}$	—
BACCHARINOID-1 AND 2	548	$\begin{array}{cccccccc} 2' & 3' & 12' & 4' & 5' & 6' / 13' & 14' \\ -\text{CH}_2 & \text{CH} & \text{CH}_3 & \text{CHO} & \text{HCH}_2 & \text{O} & \text{CH} & \text{CHOH} & \text{CH}_3 \end{array}$	8 β -OH
BACCHARINOID-3 AND 7	548	$\begin{array}{ccccccc} 2' & 3' & 12' & 4' & 5' & / 13' & 14' \\ -\text{CHO} & \text{HCH} & \text{CH}_3 & \text{CH}_2 & \text{CH}_2 & \text{O} & \text{CH} & \text{CHOH} & \text{CH}_3 \\ & & & & & & 6' & & \end{array}$	8 β -OH
BACCHARINOID-4	562	$\begin{array}{ccccccc} 2' & 3' & 4' & 5' & 6' / * & & \\ -\text{CH} & -\text{CH} & \text{CH}_3 & \text{CHOH} & \text{CH}_2 & \text{O} & \text{CH} & \text{CHOH} & \text{CH}_3 \\ & & 12' & & & & 13' & 14' & \end{array}$	8 β -OH
BACCHARINOID-5	562	$\begin{array}{ccccccc} 2' & 3' & 4' & 5' & 6' / * & & \\ -\text{CH} & -\text{CH} & \text{CH}_3 & \text{CHOH} & \text{CH}_2 & \text{O} & \text{CH} & \text{CHOH} & \text{CH}_3 \\ & & 12' & & & & 13' & 14' & \end{array}$	9,10-EPOXY
8-KETOVERRUCARIN A (KVA)	516	$\begin{array}{ccccccc} 2' & 3' & 4' & 5' & 6' & & \\ -\text{CHOH} & \text{CH} & \text{CH}_3 & \text{CH}_2 & \text{CH}_2 & \text{O} & \text{C} - \\ & & 12' & & & & \\ & & & & & & \text{O} \end{array}$	8-KETO

* CENTER OF EPIMERIZATION

Fig. 1. Structures of roridins and baccharinoids.

methodology for the accurate and unambiguous detection of all known types of trichothecenes including the isomers present in complex, aqueous matrices is highly desirable.

Hence, we have recently investigated the thermospray ionization²⁷ of some of the most toxic (roridins) and few known benevolent (baccharinoids) and isomeric macrocyclic trichothecenes and developed a simple liquid chromatography–mass spectrometry (LC–MS) procedure for their analysis. It was applied to the analysis of these compounds in crude, aqueous extracts from Brazilian *Baccharis megapotamica* and *B. coridifolia* plants. A semi-synthetic macrocyclic trichothecene, 8-ketoverrucarin A (KVA)²⁸, which was used earlier as an internal standard for the analysis of macrocyclic trichothecenes by direct, chemical ionization tandem MS methods^{20–22}, was found to be an adequate internal standard under these conditions as well. The unambiguous identification of the isomeric baccharinoids, which was not possible by earlier methods, and their quantification were possible during this newly developed procedure.

EXPERIMENTAL

A Finnigan-MAT TSQ tandem mass spectrometer, Waters Assoc. standard high-performance liquid chromatograph with dual pumps, automatic gradient controller (680), Waters 600 multisolvent delivery system, Rheodyne injector (1125), Waters universal U6K injector and Vestec thermospray LC–MS interface were used throughout this investigation.

All methanolic standard solutions were stored in reactivials fitted with mininert valves (Supelco) at 2°C. Glass distilled HPLC grade solvents, purchased from Burdick & Jackson Labs., were used as received. The reversed-phase C₈ LC column (25 cm × 4.6 mm, 5 μm) manufactured by Waters Assoc. was used for all measurements.

Standard or sample solutions (20 μl or less) were injected onto the LC column and separated using 0.1 M aqueous ammonium acetate–methanol (50:50) at a flow-rate of 1.2 ml/min. The effluent from the column was introduced into the mass spectrometer via the thermospray LC–MS interface. The probe tip and the source block temperatures were maintained at 205°C and 265°C, respectively. The aerosol temperature was kept at 255°C. The source pressure was kept at 3.3 Torr. The ionized molecules were analyzed by scanning quadrupole 3 from 100 to 600 a.m.u. in 0.5 s. Alternatively, specific programs were used for monitoring only selected ions at predesignated intervals using quadrupole 3. Each sample analysis was preceded by a blank run regardless of the mode of analysis.

Extraction of baccharis plants

A 5-g sample of dried plant material was crushed in small pieces and soaked overnight in 40 ml of 90% aqueous methanol. The solvent was decanted and the residue was treated again with 40 ml of 90% aqueous methanol and left to extract overnight. The combined extracts were filtered and washed twice with 50 ml of hexane. The methanol solution was concentrated on a rotary evaporator and the resulting solution was extracted three times with 20 ml of methylene chloride. The combined methylene chloride solution was dried over anhydrous sodium sulfate and decanted; and the solvent was removed on a rotary evaporator. The residue was dissolved in

a minimum amount of methylene chloride and loaded on a silica gel column, packed in a pasteur pipette and washed with methylene chloride (5 ml), methanol–methylene chloride (10:90) (5 ml) and methanol–methylene chloride (25:75) (5 ml). The combined effluent was concentrated under vacuum, dissolved in methanol (1 ml) and stored in a vial (2 ml) at 2°C prior to analysis.

RESULTS AND DISCUSSION

The optimum conditions for the thermospray ionization of the individual macrocyclic trichothecenes were determined by introducing them (500 ng) directly into the mass spectrometer via a blank column and the thermospray interface and a methanol–0.1 *M* ammonium acetate buffer (50:50). This solvent system, a midpoint of the possible solvent mixture to be used during the LC separation, was chosen for the measurements. Hence, the experimentally determined optimum ionization conditions could be modified slightly, if required, during the LC–MS analysis of the mixtures. The individual temperatures of the source block, probe tip, and aerosol jet were varied step-wise, keeping two out of three constant, and acquiring the positive ion MS data. The recorded total ion counts and that of the ammonium adducts provided the required information. In like manner, the optimum conditions for the ionization of the mixture containing all of the analytes were determined.

The analytes were ionized most efficiently when the probe tip and the source block temperatures were kept at 205°C and 265°C, respectively. Optimum aerosol temperature was determined to be 255°C. The ionization efficiency of the analytes were comparable, when the above temperatures were maintained which required occasional manual adjustment of the temperature, regardless of the variation in the composition of the eluting solvent (buffer–methanol) during the HPLC separation of the components. Optimum thermospray temperatures were checked everyday prior to measurements. Only slight modifications if any was required throughout this investigation. The source pressure was maintained at 3.3 Torr. Similarly, the optimum flow-rates (1.2 ml/min) of the solvents and minimum concentration of ammonium acetate (20%) required for maximizing the ionization were determined.

Optimum conditions for the LC separation of the roridins and baccharinoids were determined after a series of controlled experiments. The eluted compounds were ionized and their full-scan mass spectra (m/z 100–600) were acquired. The corresponding mass chromatograms of the ammonium adducts were traced to determine the resolution of compounds. The mass spectra of all resolved components were obtained. Conditions where a base line separation was achieved with well defined mass spectra of the components were sought after during these experiments. Isocratic conditions involving solvent mixtures ranging from 20 to 50% methanol were tried. Alternatively, we used gradient programming (curve 6) from the initial concentration (20–60% methanol) maintained for 2 min and increased to final concentration (60–80% methanol) in 4 min and maintained until all components were eluted. Most of the components except baccharinoids-2 and -3 were well resolved in a shorter duration under isocratic elution using 0.1 *M* ammonium acetate–methanol (35:65) or when the initial concentration of 50% methanol was maintained for 2 min and increased to 70% methanol in 4 min using the gradient curve 6 (Fig. 2).

Alternatively, solvent mixtures of different ratios were introduced, as specified

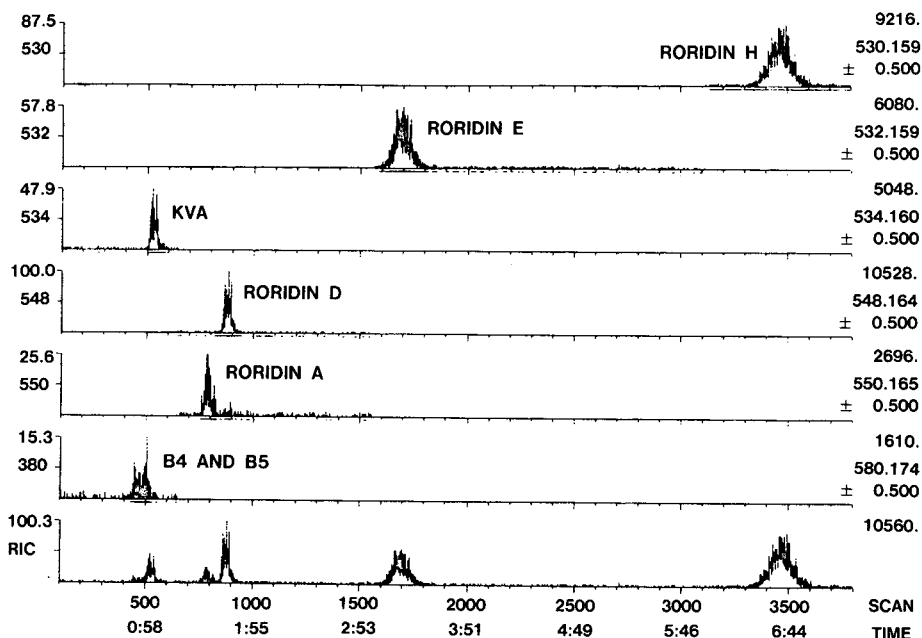


Fig. 2. Mass chromatograms of roridins and baccharinoids standards. Initial concentration of methanol-0.1 *M* ammonium acetate (50:50) maintained for 2 min and increased to 70% methanol in 4 min and maintained during rest of the period.

below, into the column at predesignated intervals using the Waters 600 multisolvent delivery system. The initial concentration ratio of buffer-methanol (59:41) was maintained for 1 min and changed to 56:44 and maintained for 19 min. Then the ratio was rapidly changed to 20:80 and maintained until the end of the run. All components including baccharinoids were resolved and unambiguously detected under these following conditions (Fig. 3) and hence used throughout the investigation.

A mixture containing 1 μg of all the roridin and baccharinoid standards was analyzed under the above experimentally determined optimum conditions. The list of observed positive ions in the mass spectra and their relative abundances are listed in Table I. Most of the analytes formed fewer ions under these softer thermospray ionization conditions and invariably the molecular ion-ammonium adduct ions were the most abundant ones.

Two Brazilian *Baccharis* plant extracts, labelled as "meg10" and "cor3", were analyzed under the same conditions. They were obtained from *B. megapotamica* and *B. coridifolia* plants, respectively. Roridins A, D, and E were detected in "cor3" sample. The presence of roridins A (traces), D, E and baccharinoids 1-5, and 7 was observed in "meg10" sample. The observed relative retention times of the compounds in standard and sample solutions are listed in Table II. The standard spectrum of roridin A along with the sample spectrum (cor3) are shown in Fig. 4. The spectra of baccharinoid 5 in the standard and "meg10" sample are indicated in Fig. 5. The characteristic ions with their relative abundances, in comparison with abundances observed for the standards, are noted in the sample spectra. The relative retention times observed for compounds in samples were comparable to those of standards. These are sufficient for the

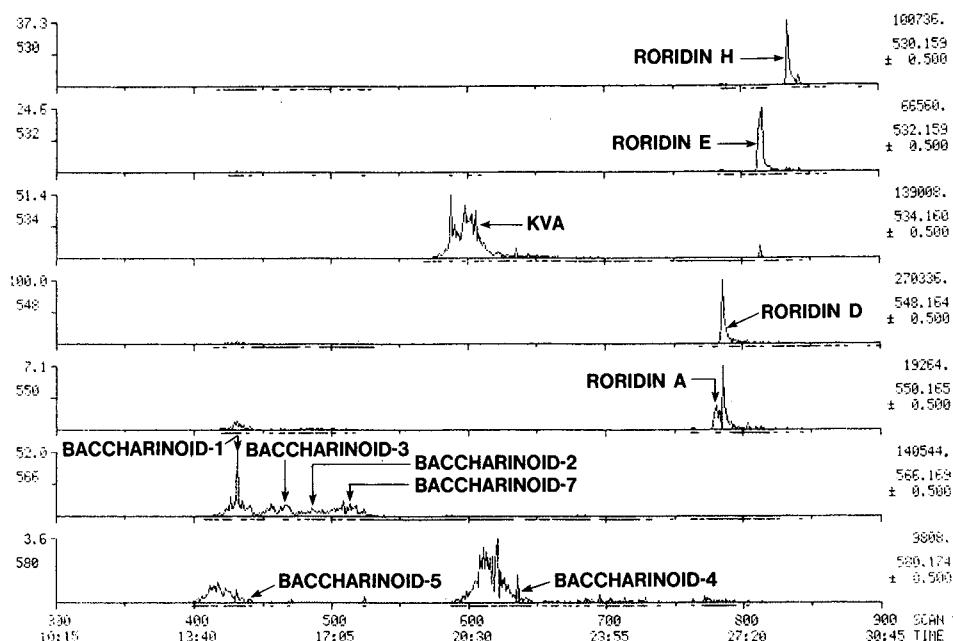


Fig. 3. Reconstructed ion chromatogram of resolved baccharinoids and roridins. Initial concentration of methanol-0.1 *M* ammonium acetate (59:41) was maintained for 1 min and changed to 56% methanol and kept for 19 min and then changed to 20% methanol and maintained until the end of the run.

TABLE I

MASS SPECTRA OF AMMONIUM ADDUCTS (THERMOSPRAY IONIZATION) OF MACROCYCLIC TRICHOHECENES

Only 10 most abundant ions are tabulated.

<i>Trichothecenes</i>	<i>m/z</i> (relative abundances)				
Roridin D	548 (100)	504 (68)	394 (2)	318 (1)	266 (16)
	249 (22)	231 (3)	182 (3)	148 (2)	106 (6)
Roridin E	532 (100)	489 (12)	488 (56)	378 (2)	249 (3)
	150 (3)	124 (5)	120 (3)	109 (1)	
Roridin H	530 (100)	513 (5)	266 (5)	249 (4)	209 (1)
	124 (2)	106 (1)			
Baccharinoid-1	566 (85)	548 (4)	530 (8)	504 (3)	282 (94)
	265 (100)	257 (43)	247 (12)	229 (4)	110 (11)
Baccharinoid-2	566 (100)	548 (6)	530 (5)	522 (7)	504 (9)
	282 (36)	265 (73)	247 (12)	229 (6)	150 (9)
Baccharinoid-3	566 (100)	549 (37)	531 (2)	419 (9)	401 (15)
	349 (24)	265 (28)	247 (66)	229 (25)	155 (13)
Baccharinoid-4	580 (20)	534 (100)	298 (2)	282 (4)	265 (12)
	263 (10)	245 (24)	227 (2)	150 (12)	148 (32)
Baccharinoid-7	566 (100)	548 (5)	522 (29)	505 (3)	282 (4)
	265 (5)	247 (3)	229 (1)	217 (1)	110 (3)
KVA	534 (100)	392 (2)	298 (3)	280 (6)	263 (6)
	245 (7)	228 (2)	148 (28)		

TABLE II

RELATIVE RETENTION DATA

Retention time for the internal standard, KVA, is 19:59 minutes.

Compound	Standard	Sample	
		Cor3	Meg10
Roridin A	1.30	1.30	—
Roridin D	1.31	1.31	1.30
Roridin E	1.36	1.36	1.35
Roridin H	1.40	—	—
Baccharinoid-1	0.72	—	0.73
Baccharinoid-2	0.82	—	0.82
Baccharinoid-3	0.77	—	0.78
Baccharinoid-4	1.03	—	1.03
Baccharinoid-5	0.69	—	0.70
Baccharinoid-7	0.86	—	0.86
KVA	1.00	1.00	1.00

identification of these trichothecenes and possibly for their analysis in samples. They are in agreement with earlier results observed during the isolation of these compounds from several kilogram quantities of the plant materials and their characterization by spectrometric methods²⁹.

However, the high noise levels observed in the sample spectra cannot be ignored. Either more rigorous sample clean-up procedures prior to analysis or careful analysis of sample and standard spectra with respect to the relative abundances of the characteristic ions should be performed for their unambiguous identification and quantification in unknown samples.

Alternate methods for the detection and confirmation of these compounds with increased sensitivities were developed. Two procedures (Table III) were devised by programming the data system to monitor the one or more selected ions (Table I) for each analyte at predesignated intervals. These intervals were based on the retention times of the compounds. These procedures are more efficient than detecting the specific ions of all compounds during the entire analysis. The added advantage of such procedures is that the detected analytes could be confirmed by selectively monitoring only the characteristic ions and not the background noise during the LC-MS sample runs. Such approaches were successful during the accurate analysis of several simple trichothecenes by gas chromatography (GC)-MS methods¹⁷⁻¹⁹.

Analysis of a mixture containing 5 ng of each of the standards was performed by procedure L₁, described in Table III. Each analyte was detected with good resolution and signal to noise ratio of 1/5 or better. The mass chromatogram observed while analyzing the *B. megapotamica* sample under the same condition is shown in Fig. 6. A simple experiment for the confirmation of baccharinoid-4 by monitoring the six most characteristic ions was devised (Table IV). The less abundant ions were monitored with longer dwell times for higher sensitivity. Ions specific to the internal standards were also monitored at appropriate intervals during the same run (Table IV). The compounds were eluted isocratically using acetonitrile-0.1 M aqueous

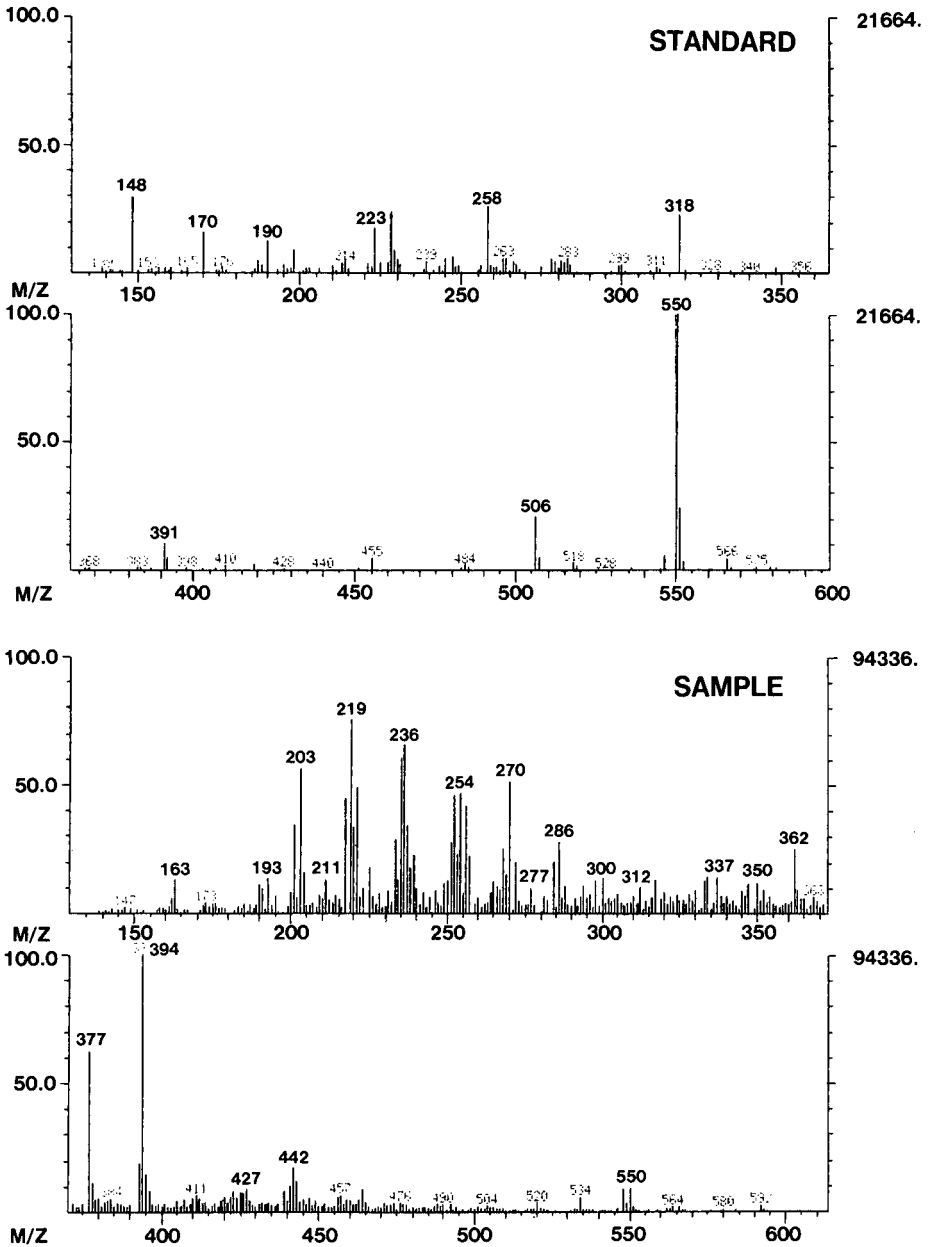


Fig. 4. Mass spectra of roridin A in standard and *B. coridifolia* ("cor3") sample.

ammonium acetate (60:40), in order to reduce the analysis time. Results observed during the standard and sample ("meg10") analyses are shown in Fig. 7. The relative abundance values observed for the standard and the sample are quite adequate for the unambiguous detection of baccharinoid-5 in the sample. Analysis of crude samples by

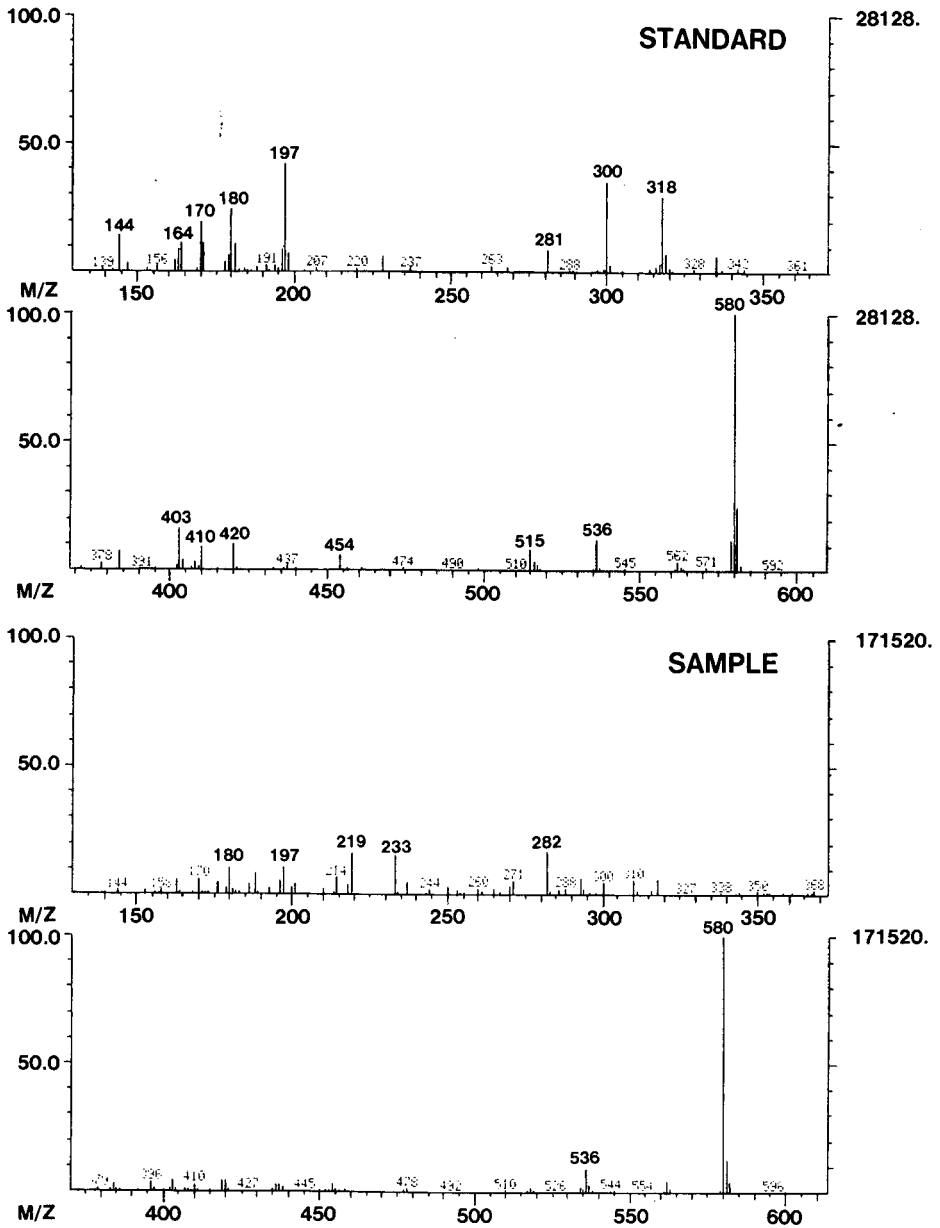


Fig. 5. Mass spectra of baccharinoid-5 in standard and *B. megapotamica* ("meg10") sample.

such selected ion monitoring procedures (L_1 in Tables III and IV) for the detection and confirmation of analytes is highly effective and applicable to the analysis of unknowns.

The procedure such as L_3 (Table III) could be used for the simultaneous detection and confirmation of analytes, during a single analysis, in an unknown sample

TABLE III
SELECTED ION MONITORING AT SPECIFIC INTERVALS

Compounds	Monitored ions (m/z)		Monitoring time (min)		
	L_1	L_3	Start	Run	End
KVA	534, 566, 580	245, 263, 534	0	24.00	24.00
Baccharinoids		247, 566, 580			
Roridin A	548, 550	249, 504, 506	24.00	3.00	27.00
Roridin D		548, 550			
Roridin E	530, 532	249, 488, 513	27.00	5.00	32.00
Roridin H		530, 532			

of limited quantity. A standard mixture containing 20 ng of all the roridins and baccharinoids was analyzed with good sensitivity.

The minimum detectable limits under the conditions expressed in experiments L_1 for roridins (and KVA) and baccharinoids were 2 and 5 ng, respectively. Under L_3 experimental conditions, 20 ng of each of the analytes could be detected. The signal-to-noise ratio observed under both conditions was at least 10/1. Full-scan (m/z 100–600) mass spectra of the roridins and baccharinoids could be obtained from 100 ng of the standards.

A procedure such as L_1 (Table III) can be utilized for the quantification of the detected analytes as well. Mixtures containing each of the analytes (5–100 ng) and KVA (10 ng) were analyzed under these conditions. The relative amounts of the analytes with respect to the internal standard were plotted against their corresponding

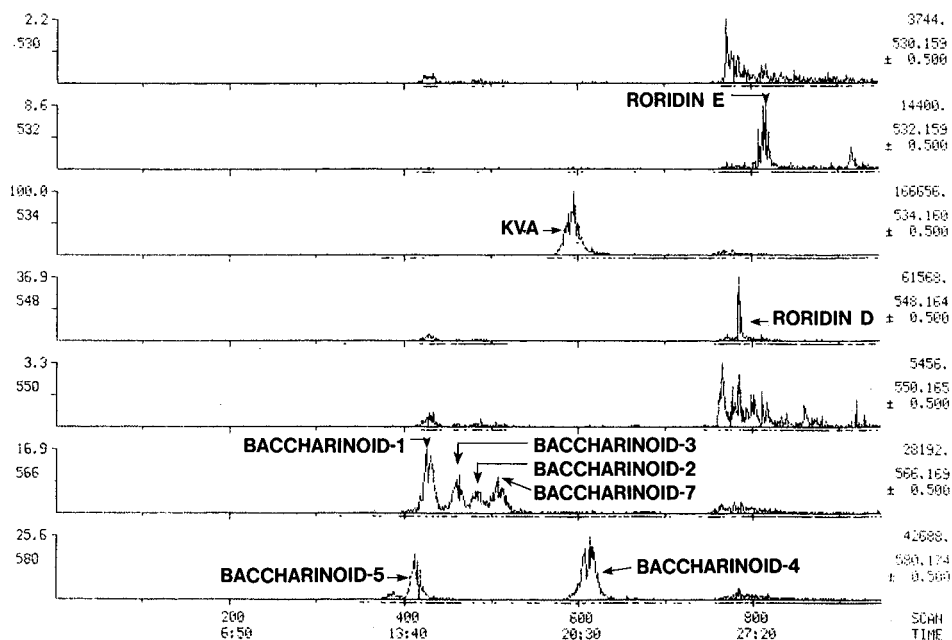


Fig. 6. Selected reaction monitoring of *B. megapota mica* sample.

TABLE IV
CONFIRMATION OF ANALYTES IN SAMPLE

Compound	Ions (m/z) ^a					
Baccharinoid-4	580 (0.03)	536 (0.06)	282 (0.06)	265 (0.06)	263 (0.12)	245 (0.06)
KVA	534 (0.03)	517 (0.12)	280 (0.12)	263 (0.12)	245 (0.06)	148 (0.06)
Roridin A	550 (0.03)	533 (0.12)	506 (0.12)	284 (0.03)	266 (0.03)	249 (0.03)

^a Monitoring time (s) for each ion is mentioned in the parenthesis.

TABLE V
CALIBRATION DATA

Internal standard (8-ketoverrucarin A), 25 ng.

Compound	Response factor	Linear regression constants		
		Correlation coefficient	Slope	Intercept
Roridin A	0.37 ± 0.03	0.999	0.449	-0.082
Roridin D	5.93 ± 1.83	0.961	7.884	-1.032
Roridin E	1.30 ± 0.53	0.931	1.256	0.523
Roridin H	1.03 ± 0.15	0.978	0.851	0.280
Baccharinoid-1	1.42 ± 0.33	0.999	1.084	1.564
Baccharinoid-2	0.35 ± 0.08	0.993	0.265	0.140
Baccharinoid-3	0.68 ± 0.17	0.993	0.895	0.413
Baccharinoid-4	0.22 ± 0.05	0.996	0.289	0.136
Baccharinoid-5	0.26 ± 0.06	0.990	0.305	-0.069
Baccharinoid-7	0.55 ± 0.02	0.999	0.525	0.089

TABLE VI
SAMPLE ANALYSIS DATA*

KVA, 25 ng; spiked amounts, 25-50 ng.

Compound	Amount detected ^a		Recovery Meg10 (%)
	Cor3	Meg10	
Roridin A	21.75	-	22.5
Roridin D	14.38	9.68	59 ± 15
Roridin E	4.35	5.4	79 ± 13
Roridin H	-	-	60 ± 23
Baccharinoid-1	-	0.11	71 ± 18
Baccharinoid-2	-	3.38	73 ± 9
Baccharinoid-3	-	1.20	113 ± 11
Baccharinoid-4	-	195.9	53 ± 4
Baccharinoid-5	-	105.9	60 ± 8
Baccharinoid-7	-	1.27	69 ± 11

^a Amount (ng) of analyte detected in the analyzed volume.

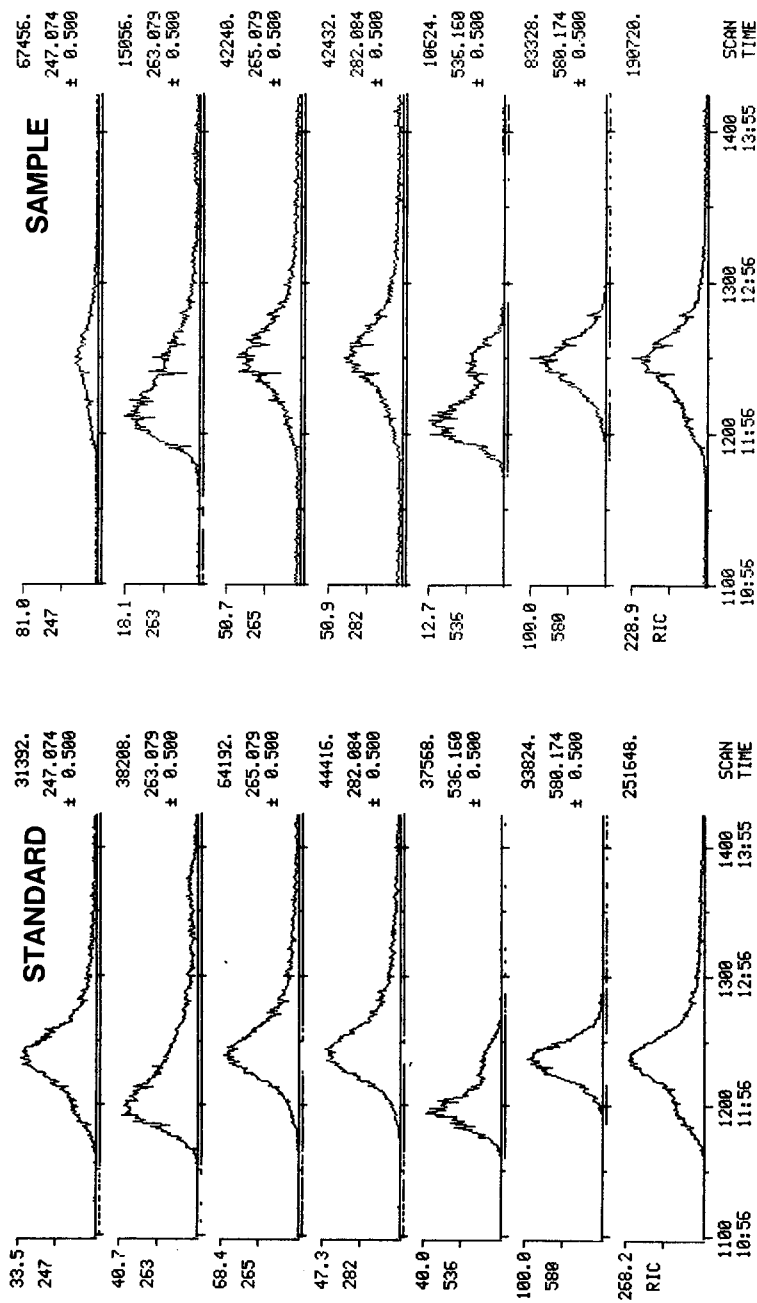


Fig. 7. Confirmation of baccharinoid-4 in *B. megapotamica* by selected ion monitoring.

relative ion abundances. A linear correlation between these two measured factors was observed for all analytes (Table V). Samples "cor3" and "meg10" and spiked solutions were also analyzed under the same conditions. The observed quantification data of the samples are listed in Table VI. It was clearly demonstrated that 5-ng quantities of these macrocyclic trichothecenes could be accurately analyzed in real samples via carefully designed experiments for monitoring selected ions at specific intervals.

In summary, the thermospray ionization of toxic roridins and biologically active baccharinoids, followed by MS analysis appears to be adequate for analyzing a number (10) of macrocyclic trichothecenes (including some isomeric compounds). KVA appears to be a suitable internal standard for the LC-MS analysis of these compounds. Selective ion monitoring procedures for the specific and sensitive analysis of roridins and baccharinoids are preferred to obtaining full-scan mass spectra. The high noise levels observed during the analysis of crude samples are thereby avoided.

ACKNOWLEDGEMENTS

The authors gratefully acknowledge Mrs. Marguerite E. Brooks, and Dr. Richard Smardzewski of U.S. Army Chemical Research, Development, and Engineering Center, Aberdeen Proving Ground, MD, U.S.A. for their interest and valuable suggestions rendered throughout this investigation.

REFERENCES

- 1 Y. Ueno, in Y. Ueno (Editor), *Developments in Food Science. 4-Trichothecenes, Chemical, Biological and Toxicological Aspects*, Elsevier, Amsterdam, 1983, pp. 1-6.
- 2 H. Kurata and Y. Ueno (Editors), *Toxigenic Fungi—Their Toxins and Health hazards*, Elsevier, Amsterdam, 1984.
- 3 J. V. Rodrick, C. W. Hesseltine and M. A. Mehlman, *Mycotoxin in Human and Animal health*, Pathotox Publishers, Park Forest, IL, 1st ed., 1977, pp. 189-340.
- 4 J. Palti, *Toxigenic Fusaria, Their Distribution and Significance Causes of Disease in Animals and Men*, Paul Parey, Berlin, 1978.
- 5 D. Eaker and T. Wadstrom (Editors), *Natural Toxins*, Plenum, New York, 1980.
- 6 A. M. Haig, *Chemical Warfare in Southeast Asia and Afganistan*, U.S. Department of State Special Report Number 98, Washington, DC, March 1982.
- 7 G. P. Shultz, *Chemical Warfare in Southeast Asia and Afganistan: An Update*, U.S. Department of State Special Report Number 104, Washington, DC, November 1982.
- 8 R. T. Rosen and J. D. Rosen, *Biomed. Mass Spectrom.*, 9 (1982) 443.
- 9 C. J. Mirocha, R. A. Pawlosky, K. Chatterjee, S. Watson, W. Hayes, *J. Assoc. Off. Anal. Chem.*, 66 (1983) 1485.
- 10 W. A. Croft, B. B. Jarvis and C. S. Yatawara, *Atmos. Environ.*, 20 (1986) 549.
- 11 K. Ishi, in Y. Ueno (Editor), *Developments in Food Science. 4-Trichothecenes, Chemical, Biological and Toxicological Aspects*, Elsevier, Amsterdam, 1983, pp. 7-19.
- 12 B. B. Jarvis in Y. Ueno (Editor), *Development in Food Science. 4-Trichothecenes, Chemical, Biological and Toxicological Aspects*, Elsevier, Amsterdam, 1983, 20-38.
- 13 P. M. Scott, P. Lau, S. R. Kanhue, *J. Assoc. Off. Anal. Chem.*, 64 (1981) 1364.
- 14 J. M. Rothberg, J. L. McDonald and J. C. Swims, *ACS Symp. Ser.*, 234 (1983) 272.
- 15 R. D. Voyksner, W. M. Hagler, Jr., K. Tyczkowska and C. A. Haney, *J. High Resolut. Chromatogr. Chromatogr. Comm.*, 8 (1985) 119.
- 16 R. D. Plattner, G. A. Bennett, *J. Assoc. Off. Anal. Chem.*, 66 (1983) 1470.
- 17 T. Krishnamurthy, M. B. Wasserman and E. W. Sarver, *Biomed. Mass Spectrom.*, 13 (1986) 503.
- 18 T. Krishnamurthy, E. W. Sarver, B. B. Jarvis and S. L. Greene, *J. Assoc. Off. Anal. Chem.*, 70 (1987) 132.
- 19 T. Krishnamurthy and E. W. Sarver, *J. Chromatogr.*, 355 (1986) 253.

- 20 T. Krishnamurthy and E. W. Sarver, *Biomed. Environ. Mass Spectrom.*, 15 (1988) 13.
- 21 T. Krishnamurthy and E. W. Sarver, *Biomed. Environ. Mass Spectrom.*, 13 (1987) 185.
- 22 T. Krishnamurthy and E. W. Sarver, *Anal. Chem.*, 59 (1987) 1272.
- 23 T. Krishnamurthy, E. W. Sarver and B. B. Jarvis, in J. F. J. Todd (Editor), *Adv. Mass Spectrometry*, Wiley, New York, NY, 1986, pp. 595–596.
- 24 B. B. Jarvis, N. B. Pena, M. M. Rao, N. S. Comezoglu, T. F. Comezoglu and N. B. Mandava, in A. C. Thompson (Editor), *The Chemistry of Allelopathy*, *Am. Chem. Soc. Symp. Ser.*, 268, 1984, p. 149.
- 25 G. G. Habermehl and L. Busam, *Liebigs. Ann. Chem.*, (1984) 1746.
- 26 B. B. Jarvis and E. P. Mazzola, *Acc. Chem. Res.*, 15 (1983) 388.
- 27 M. L. Vestal, *Int. J. Mass Spectrom. Ion Phys.*, 15 (1982) 388.
- 28 B. B. Jarvis, G. P. Stahly, G. Pavanadasivam, E. P. Mazzola, *J. Med. Chem.*, 23 (1980) 1054.
- 29 B. B. Jarvis, Department of Chemistry, University of Maryland, College Park, MD, 1984, unpublished results.

CHROM. 21 407

SAMPLE-INDUCED INTERNAL GRADIENT OF IONIC STRENGTH IN ION-EXCLUSION MICROCOLUMN LIQUID CHROMATOGRAPHY

K. ŠLAIS

Institute of Analytical Chemistry, Czechoslovak Academy of Sciences, Leninova 82, CS-611 42 Brno (Czechoslovakia)

(First received December 29th, 1988; revised manuscript received February 10th, 1989)

SUMMARY

A simple method for the generation of a variable internal gradient of decreasing ionic strength is described. The principle permits the gradient elution of organic ions under the conditions of ion-exclusion chromatography, *i.e.*, with the signs of the solute and sorbent charges being the same. The method allows the gradient to be induced simultaneously with sample introduction on to the separation column. Such conditions are useful for trace analysis based on on-column preconcentration from a large sample volume and subsequent gradient elution. The method was applied to the separation of UV-absorbing organic anions on a microcolumn packed with a reversed-phase sorbent with fixed anionic groups.

INTRODUCTION

Column liquid chromatography (LC) is often used to determine trace concentrations of solutes in complex matrices. The analytical sensitivity can be improved and the “general elution problem” can be solved by the use of a continuous gradient of the mobile phase composition which leads to a continuous decrease in solute retention on the separation column¹. The retention of ionized solutes can be controlled by adjusting the mobile phase pH, ionic strength and contents of organic solvent and ion-interacting compounds. In conventional LC, a mobile phase gradient is generated by time-programmed addition of the streams of components in the solvent delivery device. In microcolumn LC, this method of gradient generation is difficult. Therefore, gradient mixers have been suggested, *e.g.*, tubular mixers^{2,3} can generate a gradient of variable profile for microcolumns of 1 mm I.D..

The ultimate independence of pre-column gradient instrumentation can be achieved if a gradient is generated in the separation column. Internal gradients of pH⁴ and counter-ion⁵ and co-ion⁶ concentration have been suggested for microcolumn LC.

The control of ionic strength is a powerful technique in ionic solute gradient elution⁷. If the signs of the charges of the solute and the stationary phase are opposite, an increase in ionic strength decreases the solute retention. Organic ionic com-

pounds can also be effectively separated on a stationary phase that has a charge of the same sign as the solute; this is the principle of ion-exclusion chromatography⁸. It has been shown both theoretically⁹ and practically^{9,10} that the solute retention decreases with decreasing mobile phase ionic strength in this type of chromatography.

In this work, the generation of an internal gradient of decreasing ionic strength is described. Such a gradient permits the gradient elution of organic anions under the conditions of ion-exclusion chromatography. Aromatic sulphonic and carboxylic acids were chosen as model solutes because of their good detectability with a UV photometric detector. The suitability of the method for solute on-column preconcentration and trace analysis by microcolumn LC is discussed.

EXPERIMENTAL

Apparatus

The chromatograph used included an MC 300 micropump (Mikrotechna, Prague, Czechoslovakia), a laboratory-made six-port valve with external loops (1 or 60 μl), an SF 769 Z UV detector (Kratos, Ramsey, NJ, U.S.A.) equipped with a 0.5- μl flow cell and a CDLC 1 conductivity detector (Laboratory Instruments, Prague, Czechoslovakia) with a 1- μl capillary flow cell. An OP 208/1 pH meter (Radelkis, Budapest, Hungary) equipped with a 100- μl flow electrode was connected to the outlet of the chromatograph to monitor the pH of the column effluent. Chromatograms were recorded on a TZ 4200 dual recorder (Laboratory Instruments). Conductivities of the water used and of the solutions prepared were checked with an OK 102/1 bath conductimeter (Radelkis).

Chemicals

Salts used for the mobile phase preparation were of analytical-reagent grade (Lachema, Brno, Czechoslovakia). Model mixtures of organic anions were prepared from deionized water and free organic acids or their sodium salts and adjusted to pH 7 with ammonia solution. Sodium benzenesulphonate, toluenesulphonic acid, benzoic acid, 1-naphthylacetic acid, 2,4-dichlorophenoxyacetic acid and sodium dodecyl sulphate (SDS) were from Lachema, 2-naphthalenesulphonic acid, toluic acid and 3,4-dimethylbenzoic acid from Aldrich (Milwaukee, WI, U.S.A.), indole-3-acetic acid, indole-3-butyric acid and 2-(2,4-dichlorophenoxy)propanoic acid from Sigma (St. Louis, MO, U.S.A.), 1-naphthalenesulphonic acid from Fluka (Buchs, Switzerland) and 1-naphtoic acid from BDH (Poole, U.K.). Sodium 3,4-dimethylbenzenesulphonate was prepared by sulphonation of *o*-xylene and recrystallized. The deionized water used had a conductivity of 2 $\mu\text{S cm}^{-1}$.

Microcolumn preparation

The microcolumn used was a CGC (150 \times 1 mm I.D.) glass cartridge (Tessek, Prague, Czechoslovakia) packed with Separon SGX C₁₈ (5 μm) reversed-phase silica-based sorbent. The microcolumn was fitted directly to the six-port sampling valve. The packing was dynamically modified with SDS by injection of 5 \times 60 μl of 0.1 mol l⁻¹ SDS solution. The microcolumn was then washed with about 10 ml of deionized water. The retentions of solutes were stable enough to demonstrate the influence of the salt concentration in the mobile phase. The void volume (90 μl) of the micro-

column was determined as the retention volume of glycerine measured as the deflection of the UV detector baseline caused by the change in the refractive index of the mobile phase.

RESULTS AND DISCUSSION

Isocratic elution

An earlier study¹⁰ showed that the nature of the salt dissolved in the mobile phase has only a small influence on the retention of organic anions separated by ion-exclusion chromatography. On the basis of this finding, our preliminary experiments and the UV transparency and corrosivity of the salt, ammonium sulphate was chosen to adjust the mobile phase ionic strength in the isocratic measurements.

In order to investigate the influence of the salt concentration on solute retention, sodium salts of selected sulphonic and carboxylic acids were chromatographed using mobile phases containing several concentrations of ammonium sulphate. The mobile phase pH was adjusted to pH 7 with ammonia solution. The volume of sample solution injected was 3 μl , which was calculated as the sum of the valve internal and external loops. Examples of chromatograms obtained after the injection of some model mixtures are shown in Fig. 1. The conductivity trace is corrected for the volume between the cells of the UV and conductivity detectors. Simultaneous conductivity and UV photometric detection not only permits the detection of organic anions, but also enables the elution of Na^+ ion to be followed.

Fig. 2 shows that the retention of Na^+ ion decreases with increase in the ionic

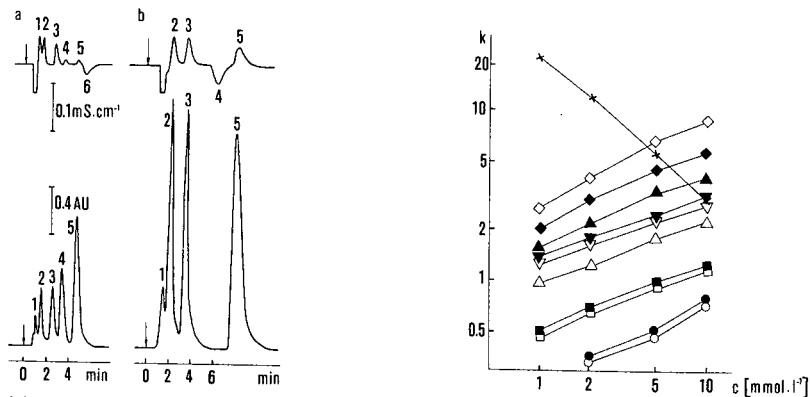


Fig. 1. Chromatograms of organic anions separated by isocratic ion-exclusion chromatography. Microcolumn: CGC (150 \times 1 mm I.D.), packed with Separon SGX C_{18} (5 μm), dynamically modified with SDS. Mobile phase: 5 mmol l^{-1} ammonium sulphate in deionized water (pH 7); flow-rate, (a) 2 and (b) 1.3 $\mu\text{l s}^{-1}$. Detection: upper trace, conductivity; lower trace, UV at 260 nm. Peaks: (a) 1 = benzenesulphonate, 2 = toluenesulphonate, 3 = 3,4-dimethylbenzenesulphonate, 4 = 1-naphthalenesulphonate, 5 = 2-naphthalenesulphonate, 6 = sodium ion; (b) 1 = benzoate, 2 = 4-methylbenzoate, 3 = 3,4-dimethylbenzoate, 4 = sodium ion, 5 = 1-naphthylacetate.

Fig. 2. Dependence of the capacity ratio (k) of organic anions on the molarity of ammonium sulphate in the mobile phase (c) at pH 7. Solutes: \bullet , benzenesulphonate; \blacksquare , toluenesulphonate; \blacktriangledown , 3,4-dimethylbenzenesulphonate; \blacktriangle , 1-naphthalenesulphonate; \blacklozenge , 2-naphthalenesulphonate; \circ , benzoate; \square , 4-methylbenzoate; ∇ , 3,4-dimethylbenzoate; \triangle , 1 naphthoate; \diamond , 1-naphthylacetate; \times , sodium ion. Other conditions as in Fig. 1.

strength of the mobile phase. The negative tangent of this dependence in log-log coordinates is close to unity, which indicates a common ion-exchange mechanism for Na^+ retention. In the system used, the retention of Li^+ ion was found to be identical with that of Na^+ ion, whereas the retention of Cs^+ ion was about 1.3 times that of Na^+ ion. Such a low selectivity for alkali metal ions was also observed earlier for C_{18} silica-based sorbents dynamically modified with alkyl sulphonates¹¹. Assuming the selectivity coefficient for $\text{Na}^+ - \text{NH}_4^+$ ion exchange to be close to unity, the exchange capacity can be calculated as the product of the column dead volume, the concentration of ammonium ions in the mobile phase and the capacity ratio of the Na^+ ion. This gives a value of about $5 \mu\text{equiv.}$ for the microcolumn used.

The retentions of aromatic anions increase with increase in the salt concentration from 1 to 10 mmol l^{-1} (Fig. 2). Similar dependences were found in an earlier study¹⁰ for the same or similar solutes, with the concentration of sodium sulphate varying from 20 to 400 mmol l^{-1} . In the latter instance, the anionic groups of the sorbent originated solely from dissociation of residual silanol groups. Calculations based on previous measurements¹² led to about $0.5 \mu\text{equiv.}$ of dissociated silanols in the volume of C_{18} silica reversed phase, which is equivalent to the volume of the microcolumn packing used in this study.

The isocratic elution of aromatic sulphonic acids also demonstrates the need for solving the "general solution problem". For example for a concentration of ammonium sulphate in the mobile phase of 1 mmol l^{-1} , the capacity ratio (k) for benzenesulphonate is near to zero and k for anthraquinone-2-sulphonate is 40.

Previous paragraphs lead to the following conclusions essential for the study of the gradient elution of organic anions: (1) dynamic modification of the C_{18} silica support with dodecylsulphate increases substantially the number of fixed anionic groups on the stationary phase surface; and (2) the retentions of organic anions on the sorbent used increase with increase in the salt concentration at both low and high ionic strengths.

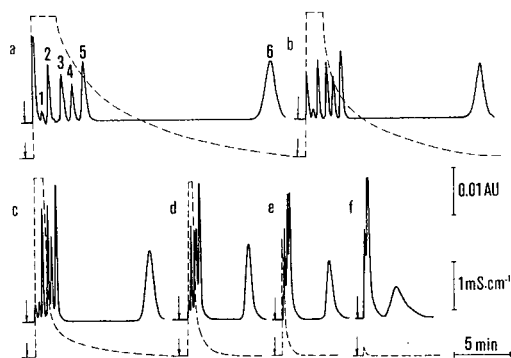


Fig. 3. Dependence of internal gradient profile on the concentration of ammonium sulphate in the injected solution. Mobile phase delivered by pump: deionized water adjusted to pH 7 with ammonia solution, conductivity $12 \mu\text{S cm}^{-1}$. Full-line peaks and concentrations in the injected solution (mmol l^{-1}): 1 = benzenesulphonate (1); 2 = 4-methylbenzenesulphonate (1); 3 = 3,4-dimethylbenzenesulphonate (1); 4 = 1-naphthalenesulphonate (0.2); 5 = 2-naphthalenesulphonate (0.2); 6 = 2-anthraquinonesulphonate (0.02). Broken line: conductivity of the column effluent. Concentration of ammonium sulphate in the injected solution: (a) 3; (b) 1; (c) 0.3; (d) 0.1; (e) 0.03; (f) 0 mol l^{-1} . Other conditions as in Fig. 1a.

Internal gradient

An internal gradient of decreasing ionic strength was obtained by injection of ammonium sulphate solution (pH 7) on to the microcolumn. The mobile phase delivered by the pump was deionized water adjusted to pH 7 with ammonia solution. The conductivity of this mobile phase was $12 \mu\text{S cm}^{-1}$. Keeping the volume injected at $3 \mu\text{l}$, the variation of the salt concentration in the solution introduced influences the profile of internal gradients of decreasing ionic strength obtained (Fig. 3). Here, the gradient profile was monitored with the conductivity detector (broken line). The solution conductivity can be converted into an approximate salt concentration if the conductivity of a 1 mmol l^{-1} solution of ammonium sulphate is considered to be $234 \mu\text{S cm}^{-1}$.

The observed variability of the salt elution profile with salt concentration in the solution injected cannot be explained only by overloading of column ion-exchange capacity (*e.g.*, ref. 13). In the present instance, the column behaves as a mixer in which washing out of salt corresponds to slower kinetics than that of solute equilibration between the mobile and stationary phases. The influence of precolumn volumes can be eliminated as the microcolumn is fitted directly to the sampling valve (see Experimental). Further, if a microcolumn of the same dimensions packed with non-porous glass beads $6 \mu\text{m}$ in diameter was fitted instead of the separation microcolumn, the salt concentration dropped to the steady-state level within about one dead volume even when the highest concentrations were injected. A rigorous explanation of the observed salt elution profile would require further investigations beyond the scope of this work.

Nevertheless, the variable internal gradient of decreasing ionic strength obtained has a practical value. The injected solution contained also aromatic sulphonates detectable by the UV detector (Fig. 3, full line). An increase in the salt concentration in the sample solution leads to an increase in gradient time and, consequently, to increased retention times of solutes. Simultaneously, the average steepness of the gradient decreases with increasing salt concentration. In agreement with the theory of gradient elution¹, a lower steepness is reflected by an increase in the peak widths.

The gradient profiles in Fig. 3 indicate that for all the concentrations of the salt in the sample, the lowest elution strength occurs at the very beginning of the chromatogram. In other words, the solute is most strongly retained at the moment of injection at the top of the column. These conditions are favourable for on-column solute preconcentration. Fig. 4 shows examples of chromatograms obtained with a sample volume of $60 \mu\text{l}$ (*i.e.*, two thirds of the microcolumn void volume). Fig. 4a represents the chromatogram of aromatic sulphonates under conditions similar to those for Fig. 3a. It shows good solute focusing even for the first eluted compounds. The solutes are eluted in the peaks which have volumes less than that of the sample. Hence the conditions are advantageous for trace analysis. Chromatograms similar to Fig. 4a were also obtained when aromatic sulphonates were injected in concentrated solutions of NaCl, KCl, NH_4Cl , KNO_3 , NaNO_3 , Na_2SO_4 , NaClO_4 and CH_3COONa .

UV-absorbing organic anions comprise a number of analytically important groups of compounds, *e.g.*, sulphonated dyes and their intermediates, nucleotides and pesticides. Fig. 4b shows the on-column focusing and gradient elution of a model mixture of some plant growth regulators (derivatives of acetic acid). Under the condi-

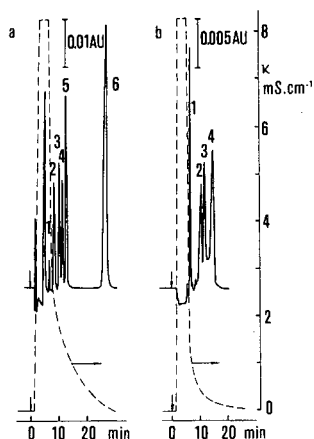


Fig. 4. On-column preconcentration and gradient elution of organic anions. Sample volume, $60\mu\text{l}$. (a) Ammonium sulphate concentration in the injected solution, 3 mol l^{-1} . Peaks and concentrations in the injected solution ($\mu\text{mol l}^{-1}$): 1 = benzenesulphonate (100), 2 = 4-methylbenzenesulphonate (100), 3 = 3,4-dimethylbenzenesulphonate (100), 4 = 1-naphthalenesulphonate (20), 5 = 2-naphthalenesulphonate (20), 6 = 2-anthraquinonesulphonate (2). (b) Ammonium sulphate concentration in the injected solution, 0.1 mol l^{-1} . Detector wavelength, 280 nm . Peaks and concentrations in the injected solution (mg l^{-1}): 1 = indole-3-acetate (0.5), 2 = 2,4-dichlorophenoxyacetate (1), 3 = 1-naphthoxyacetate (2), 4 = 2-(2,4-dichlorophenoxy)propionate (2). Other conditions as in Fig. 3.

tions used, the 3-indolylbutyrate is coeluted with 2,4-dichlorophenoxyacetate. All the compounds shown were injected at concentrations of about 1 mg l^{-1} . The chromatogram shows that the detection limit is by about 1–2 orders of magnitude lower than the concentrations injected. Dilution of the sample solution by adding salt solution is not significant as it represents as little as *ca.* 3% of the sample volume if saturated salt solution is used.

CONCLUSIONS

The experiments described provide evidence that a variable internal gradient of decreasing mobile phase ionic strength can be generated by injecting concentrated salt solution on to a column packed with a suitably modified sorbent provided that the isocratic pump delivers dilute salt solution. In agreement with the isocratic measurements, such a gradient leads to a continuous decrease in the retention of organic ions on a sorbent having both hydrophobic sites and ionic groups of charge sign similar to that of the solute.

The principle was verified with a number of anionic solutes employing several salts in the injected sample solution. According to the theory developed for isocratic conditions⁹, it should also be applicable to cationic solutes provided that the sorbent in the column contains positively charged groups.

This new form of internal gradient offers great flexibility of the control of gradient time and steepness by the adjustment of the salt concentration in the injected sample solution. The widest applicability of the method can be seen in the gradient separation and trace analysis of organic ions by microcolumn LC.

REFERENCES

- 1 P. Jandera and J. Churáček, *Gradient Elution in Column Liquid Chromatography*, Elsevier, Amsterdam, 1985.
- 2 K. Šlais and V. Preussler, *J. High Resolut. Chromatogr. Chromatogr. Commun.*, 10 (1987) 82.
- 3 K. Šlais and R. W. Frei, *Anal. Chem.*, 59 (1987) 376.
- 4 A. Hirose and D. Ishii, *J. Chromatogr.*, 387 (1987) 416.
- 5 K. Šlais, M. Krejčí and D. Kouřilová, *J. Chromatogr.*, 352 (1986) 179.
- 6 K. Šlais, M. Krejčí, J. Chmelíková and D. Kouřilová, *J. Chromatogr.*, 388 (1987) 179.
- 7 P. Jandera and J. Churáček, *Gradient Elution in Column Liquid Chromatography*, Elsevier, Amsterdam, 1985, pp 21 and 157.
- 8 C. A. Pohl and E. L. Johnson, *J. Chromatogr. Sci.*, 18 (1980) 442.
- 9 S. Afrashtehfar and F. Cantwell, *Anal. Chem.*, 54 (1982) 2422.
- 10 P. Jandera, J. Churáček and J. Bartošová, *Chromatographia*, 13 (1980) 485.
- 11 R. L. Smith, Z. Iskandarani and D. J. Pietrzyk, *J. Liq. Chromatogr.*, 7 (1984) 1935.
- 12 E. M. Thurman, *J. Chromatogr.*, 185 (1979) 625.
- 13 P. Gareil, L. Personnaz, J. P. Feraud and M. Caude, *J. Chromatogr.*, 192 (1980) 53.

CHROM. 21 328

FORMIC ACID AS A MILDER ALTERNATIVE TO TRIFLUOROACETIC ACID AND PHOSPHORIC ACID IN TWO-DIMENSIONAL PEPTIDE MAPPING

D. J. POLL* and D. R. K. HARDING

Separation Science Unit, Department of Chemistry and Biochemistry, Massey University, Palmerston North (New Zealand)

(First received October 17th, 1988; revised manuscript received January 18th, 1989)

SUMMARY

In reversed-phase chromatography of peptides, formic acid has been shown to successfully replace the stronger traditional trifluoroacetic and phosphoric acids. Detection of non-aromatic peptide at lower wavelength is not impaired and being volatile the acid is easily removed, enabling further studies of the peptides. Also in ion-exchange chromatography (the first step of a two-dimensional approach) formic acid works well with a sulphonic acid ion-exchange resin.

INTRODUCTION

Trifluoroacetic acid (TFA) is widely used in modern chromatography, particularly in the reversed-phase high-performance liquid chromatography (RP-HPLC) of peptides and proteins¹. Nevertheless this acidic material ($pK_a = 0.6$) is not used without concern. A recent study² has shown that 0.1% TFA in water at pH 2 in the presence of methanol or acetonitrile can result in loss of up to 50% of the initial reversed-phase loading on the stationary phase. In addition, the complete removal of trifluoroacetate from potentially useful therapeutic peptides is not readily achieved by techniques such as gel filtration³. Thus, despite its extensive analytical use, TFA may not prove to be the mobile phase modifier of choice for preparative chromatography of peptides and proteins destined for pharmaceutical use.

Phosphoric acid either alone⁴ or titrated with hydroxide⁵ or amines like triethylamine⁶ to a pH in the range 2–4 is another popular mobile phase ion pair reagent. However the usefulness of sodium, potassium or ammonium phosphate is limited by their solubility in reversed-phase buffers containing an organic solvent. For example, these salts begin to precipitate at approximately 40% acetonitrile. Triethylammonium or triethanolammonium phosphate is preferred in this respect. However these salts are not volatile and their use therefore often requires a further processing step.

A special place among the buffer components is held by ammonium bicarbonate⁷. It has been employed for (semi)preparative work because it can be removed by

freeze drying. This buffer however loses carbon dioxide to the atmosphere and consequently the pH rises easily to values over 9. Buffers at this pH are detrimental to expensive silica-based HPLC columns even with the use of precolumns.

Formic acid ($pK_a = 3.75$) also has been employed in the liquid chromatography of peptides and proteins¹. While it does not appear to enjoy the popularity of trifluoroacetic acid or phosphate it has nevertheless been used in the RP-HPLC of peptides and proteins in a parallel fashion, *i.e.*, alone⁸ or with counter ions such as ammonium⁸, triethylammonium⁹ or pyridinium¹⁰. Used alone formic acid should prove to be a useful buffer component because of its volatility and decreased acidity. Criticisms that are levelled at formic acid systems relative to TFA or phosphate systems include lower degrees of resolution¹¹ and recovery¹² plus inapplicability of UV detection at 220 nm¹⁰. This paper presents results from peptide mapping and two-dimensional chromatographic experiments that illustrate the usefulness of formic acid in these areas of HPLC.

EXPERIMENTAL

Apparatus

Three sets of apparatus were used in this study. A Pharmacia fast protein liquid chromatography (FPLC) system was used for HR 5/5 Mono Q, Mono S and PepRPC columns (50 × 5 mm I.D.). Detection at 280 nm was carried out with a single-path UV-1 monitor.

A Waters Assoc. HPLC system was used with a Vydac Protein C₄ column (250 × 4.6 mm I.D.). This system consisted of two M6000A solvent delivery units, an M680 controller and a U6K universal liquid chromatographic injector, coupled to an M450 variable-wavelength UV spectrophotometer (Waters Assoc.) and an Omniscribe two-channel chart recorder (Houston Instruments, Austin, TX, U.S.A.).

An LKB system using LKB 2150 pumps, an LKB 2152 LC controller and an LKB 2157 autosampler were also used. An LKB 2151 variable-wavelength detection monitor was used with the LKB 2134-216 Ultropac column (250 × 4.6 mm I.D., TSK ODS-120, T5 μm).

Reagents

The following reagents were used: Milli Q water, acetonitrile (BDH HiPerSolv., Prod.No. 15252); formic acid [May & Baker, Pronalys AR (98–100%)]; ammonium hydroxide (J. T. Baker, Analysed Reagent); sodium hydroxide (May & Baker, Volucon); hydrochloric acid (BDH, Convol); ammonium chloride was produced *in situ*.

All buffers were filtered and degassed through 0.45-μm filters (Millipore) for HPLC, while the buffers for FPLC were filtered using 0.2-μm filters. Samples were filtered through Gelman ACRO™ TC 13 filters (0.2 μm). Reversed-phase buffers were prepared in the usual way. For the Mono S and Mono Q experiments, buffer A was prepared as described in Figs. 8 and 9. The resultant apparent pH readings were as follows: Mono Q, buffer A, pH 10.72; Mono S, buffer A, pH 3.04. Buffer B was prepared by titrating the appropriate component to neutrality. The designated amount of acetonitrile was added. No adjustment was made for apparent pH shift. A few ml of water was added to achieve the final desired volume. The resultant apparent pH readings were as follows: Mono Q, buffer B, pH 6.95; Mono S, buffer B, pH 8.50.

Note that 30% acetonitrile with 1 M sodium chloride is close to the limit of this one phase system. Currently we use 20% acetonitrile without any problems.

HSA was normal serum albumin (human) U.S.P. Albutein® 25% from Alpha Therapeutic Co.; lysozyme (egg white) was obtained from Sigma (Prod. No. 6876); bovine serum albumin (BSA) was also obtained from Sigma (Prod. No. A7638); methionine human growth hormone (Met-hGH) was obtained from Genentech; sheep liver phosphofructokinase (PFK) was obtained from Mrs. K. J. Rutherford (Massey University) and trypsin was obtained from Sigma (Prod. No. T8003).

Methods

The tryptic digestions were performed as follows: trypsin was added (1 mg trypsin/100 mg protein) to the protein dissolved in 1% ammonium bicarbonate solution. The digest was then left for 4 h at 37°C, after which it was treated again with another dose of trypsin and left for 16 h at 37°C. The chromatographic conditions are reported in the figure legends.

RESULTS AND DISCUSSION

Glajch *et al.*² have recently presented more evidence as to the detrimental effect of TFA on reversed-phase columns and the subsequent effects it can have on protein separations. Nevertheless, TFA and phosphoric acid are widely used. In the area of thin-layer chromatography, it is customary to check purity by running more than one eluent system. Obviously this concept carries over to HPLC. The results discussed below go some way to furthering this concept with respect to formic acid as a viable

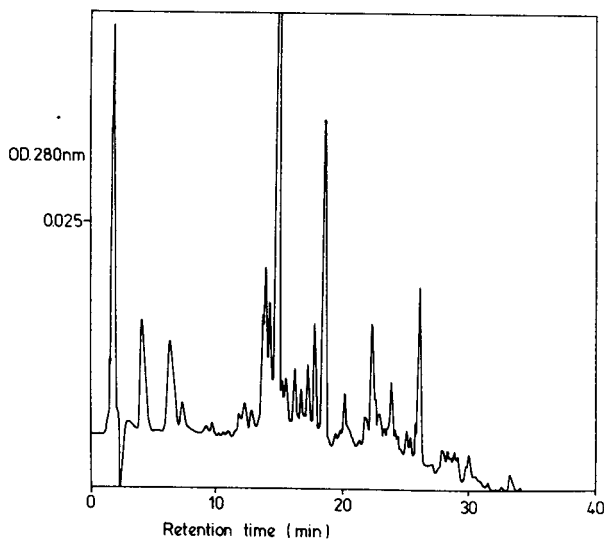


Fig. 1. HSA digest on a PepRPC HR 5/5 column. Conditions: buffer A, 0.1% formic acid-acetonitrile (19:1) and buffer B, 0.1% formic acid-acetonitrile (1:4); gradient, 0-100% B in 60 min at 0.5 ml/min; chart, 0.5 cm/min.

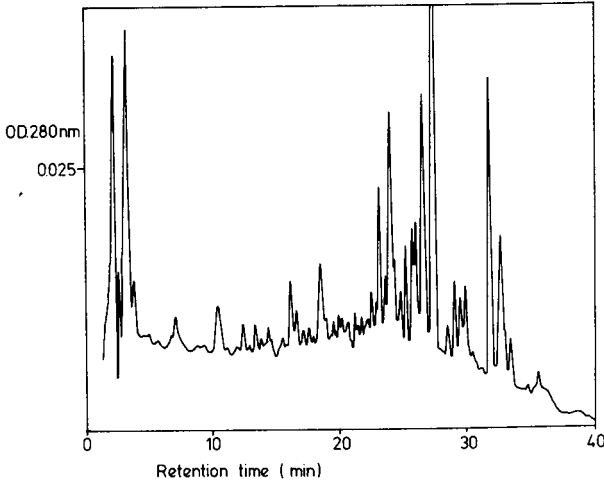


Fig. 2. Sheep liver PFK digest on PepRPC HR 5/5 column. Conditions as in Fig. 1.

alternative to other acids. Its applicability to the two-dimensional mapping of protein hydrolysates is also presented.

Figs. 1 and 2 illustrate the use of formic acid with trypsin hydrolysates of a commercial blood product and a sheep liver enzyme at 280 nm with a PepRPC column. Similarly the mapping of a recombinant protein in Fig. 3 illustrates good resolution on a Vydac C_4 column at the same wavelength. Figs. 4–6 show that signif-

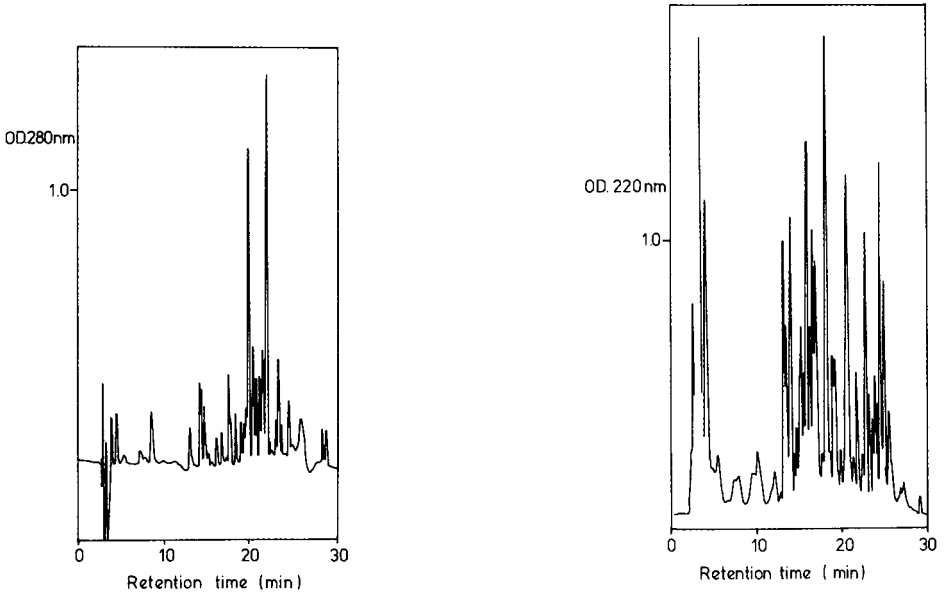


Fig. 3. Met-hGH digest on a Vydac Protein C_4 column (250×4.6 mm I.D.). Conditions: buffers and chart as for Fig. 1. Gradient: 0–100% B in 45 min at 1 ml/min.

Fig. 4. BSA digest on a Vydac Protein C_4 column (250×4.6 mm I.D.). Conditions as in Fig. 3.

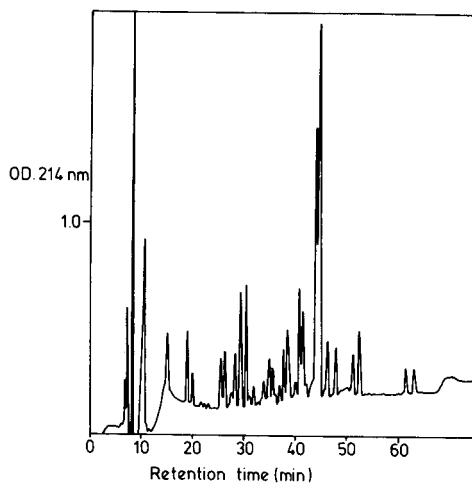
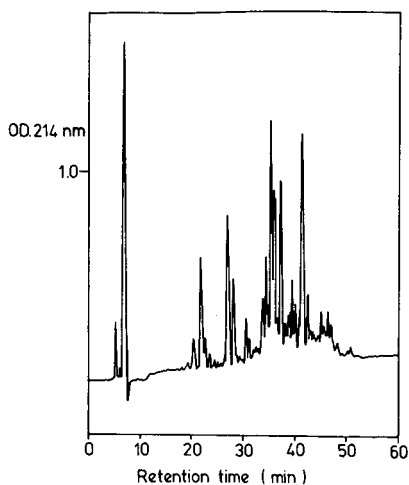


Fig. 5. Lysozyme digest on an Ultropac column (250×4.6 mm I.D.). Conditions: buffers as in Fig. 1; gradient 0–60% B in 60 min; chart, 2 mm/min.

Fig. 6. Met-hGH digest on an Ultropac column (250×4.6 mm I.D.). Conditions as in Fig. 5 except gradient, 0–60% B for 60 min then 60–100% B for 15 min.

icant resolution is maintained at lower wavelengths with a variety of hydrolysates on either a C_4 or a C_{18} column. Fig. 7 compares the performance of formic acid and phosphoric acid in a system that has all other components identical. The similarities are apparent and thus in this case illustrate the comparability of the two acids with the exception of volatility in favour of formic acid.

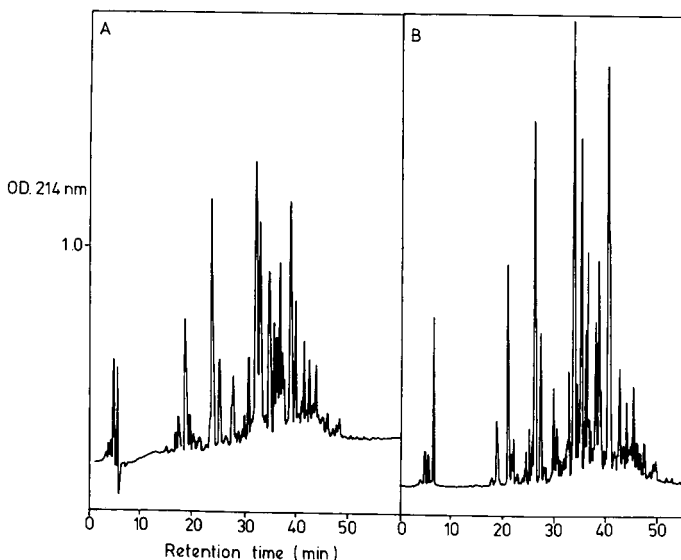


Fig. 7. HSA digest on an Ultropac column (250×4.6 mm I.D.). Conditions: (A) as in Fig. 6; (B) identical except for buffer A, 0.1% H_3PO_4 in water–acetonitrile (19:1) and buffer B 0.1% H_3PO_4 in water–acetonitrile (1:4).

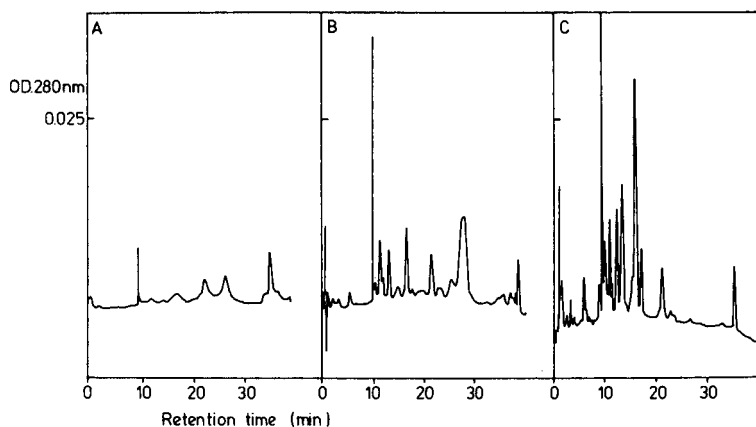


Fig. 8. HSA digest on a Mono S HR 5/5 column. Conditions: (A) as in (C) without acetonitrile; (B) as in (C) but 15% acetonitrile; (C) buffer A, 0.05 *M* formic acid in water-acetonitrile (7:3) and buffer B, 0.05 *M* sodium formate + 1 *M* sodium chloride in water-acetonitrile (7:3); gradient, 0–100% B in 30 min at 1 ml/min; chart, 2 mm/min.

Fig. 8 outlines the beneficial effect of using a formic acid system in conjunction with acetonitrile on a Mono S cation-exchange column. With the limitation noted above as to the concentration limit of the acetonitrile, the effect of organic modifier in this case is obvious. This effect has been noted in other systems employing ion exchange media for peptide separations^{13,14}. Similarly a Mono Q anion-exchange column (Fig. 9) can be used for mapping experiments of lysozyme and HSA. Fig. 10

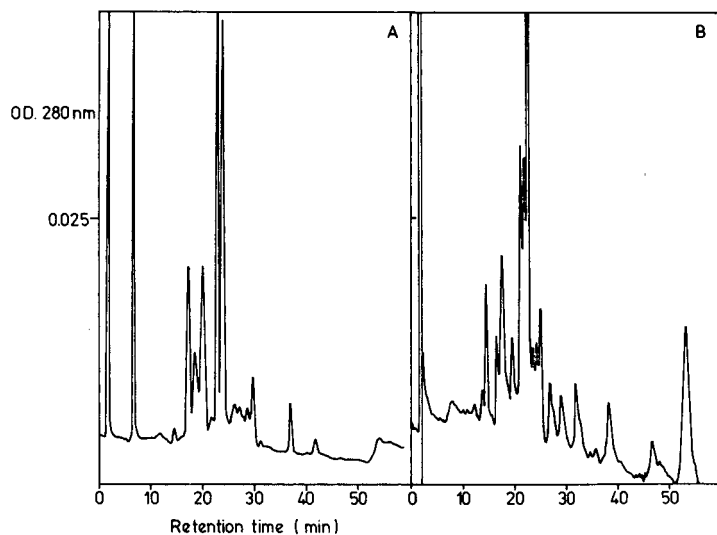


Fig. 9. Lysozyme (A) and HSA (B) digests on a Mono Q HR 5/5 column. Conditions: buffer A, 0.05 *M* ammonium hydroxide-acetonitrile (7:3) and buffer B, 0.05 *M* ammonium chloride + 1 *M* sodium chloride-acetonitrile (7:3); gradient, 0–25% B in 60 min then to 100% B in 10 min at 1 ml/min; chart, 2 mm/min.

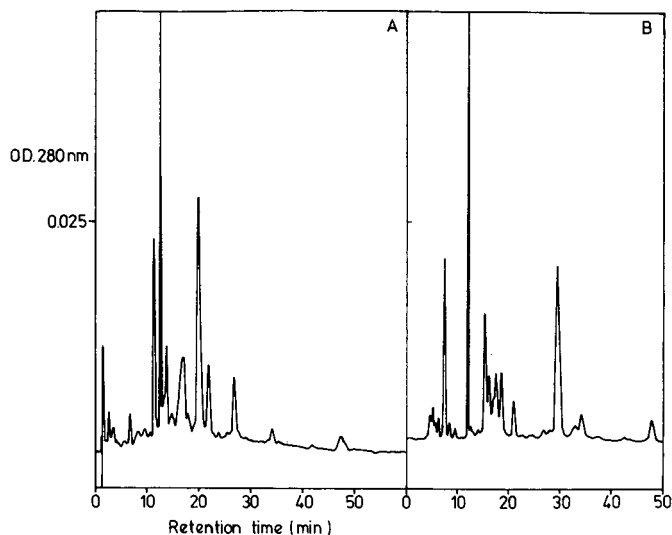


Fig. 10. HSA (A) and lysozyme (B) digests on a Mono S HR 5/5 column. Conditions: buffer A, 0.05 *M* formic acid–acetonitrile (7:3) and buffer B, 0.05 *M* sodium formate + 1 *M* sodium chloride–acetonitrile (7:3) gradient and chart as in Fig. 9.

illustrates the separation of the same materials on a Mono S column. With the idea of combining two-dimensional chromatography with peptide mapping, a digest of BSA was run on the Mono S column (Fig. 11A) using the formic acid–acetonitrile system. The success of this analytical run led to scaling-up and trapping of six peaks (Fig. 11B). These peaks were then analysed under reversed-phase conditions (Fig. 12).

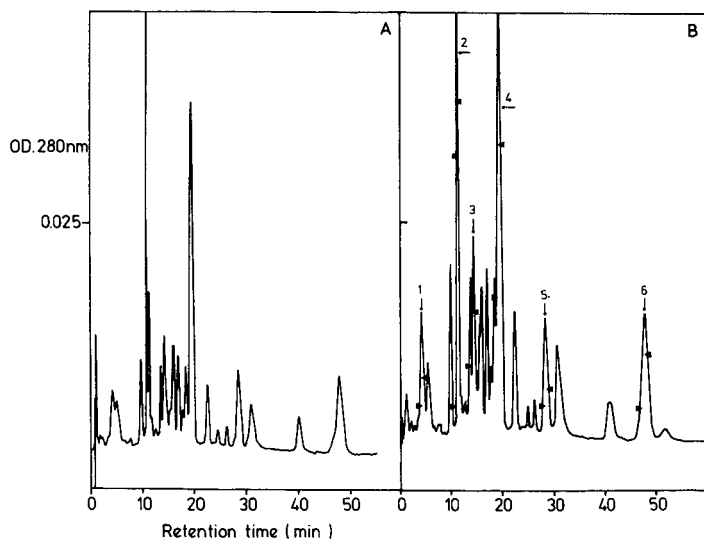


Fig. 11. BSA digest on a Mono S HR 5/5 column. Conditions: as in Fig. 10. (A) 300 μ g BSA digest; (B) 2 mg BSA digest with peaks trapped as indicated.

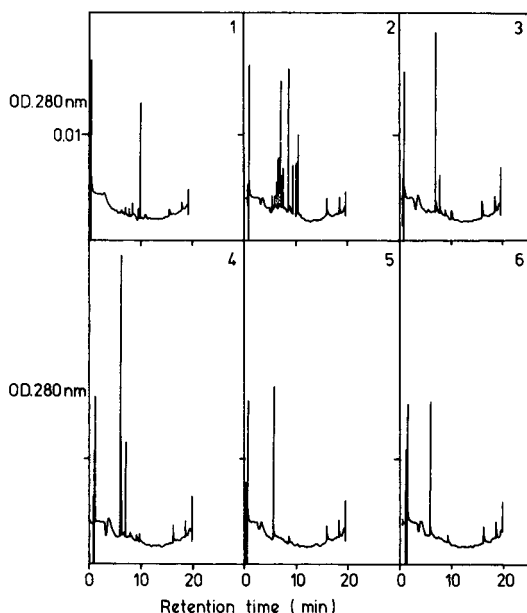


Fig. 12. Peaks 1-6 from Fig. 11B BSA digest run on a PepRPC HR 5/5 column. Conditions: buffers and chart as in Fig. 1; gradient, 0-100% B in 20 min at 1 ml/min.

With the exception of peak 2 all peaks were relatively clean and could be used for other analytical techniques such as amino acid analysis, sequencing or electrophoretic gels. The similarity of the retention times in Fig. 12 compared to the distinctly different retention times of Fig. 11B points out the obvious advantages of the two-dimensional approach.

In summary, this paper goes some way toward addressing the criticisms against the use of formic acid in high-performance chromatography. The figures above illustrate that formic acid can be used at low wavelengths with good resolution. With the exception of the MonoQ experiment, in all of the above experiments formic acid was used. Of particular importance with respect to Fig. 12 is the fact that even if formic acid had not been used in the ion-exchange step of the two-dimensional mapping, its use for the reversed-phase step constitutes a desalting method with a volatile buffer.

ACKNOWLEDGEMENTS

The authors gratefully acknowledge the support of the Medical Research Council of New Zealand. Fruitful discussions with Dr. W. S. Hancock, Genentech, Inc. are also acknowledged. Mrs. K. Rutherford (Massey University) was kind enough to supply a sample of sheep liver PFK for this study. The authors thank Genentech, Inc. for the sample of Met-hGH. The loan of the LKB equipment and the Ultropac column from Pharmacia (Australia) through Mr. R. Devine (New Zealand office) is also acknowledged.

REFERENCES

- 1 W. S. Hancock (Editor), *Handbook of HPLC for the Separation of Amino Acids, Peptides, and Proteins*, Vols. I and II, CRC Press, Boca Raton, FL, 1984.
- 2 J. L. Glajch, J. J. Kirkland and J. Köhler, *J. Chromatogr.*, 384 (1987) 81.
- 3 W. S. Hancock, Genentech, South San Francisco, CA, personal communication.
- 4 W. S. Hancock, C. A. Bishop, R. L. Prestidge, D. R. K. Harding and M. T. W. Hearn, *J. Chromatogr.*, 153 (1978) 391.
- 5 A. J. Banes and G. W. Link, *J. Chromatogr.*, 326 (1985) 419.
- 6 W. S. Hancock and J. T. Sparrow, *J. Chromatogr.* 206 (1981) 71.
- 7 D. R. Knighton, D. R. K. Harding, J. R. Napier and W. S. Hancock, *J. Chromatogr.*, 249 (1982) 193.
- 8 A. N. Staratt and M. G. Stevens, in W. S. Hancock (Editor), *Handbook of HPLC for the Separation of Amino Acids, Peptides, and Proteins*, Vol. II, CRC Press, Boca Raton, FL, 1984, p. 255.
- 9 A. Guyon-Gruaz, D. Raulais and P. Rivaille, in W. S. Hancock (Editor), *Handbook of HPLC for the Separation of Amino Acids, Peptides, and Proteins*, Vol. II, CRC Press, Boca Raton, FL, 1984, p. 213.
- 10 J. W. van Nispen and P. S. L. Janssen, in W. S. Hancock (Editor), *Handbook of HPLC for the Separation of Amino Acids, Peptides, and Proteins*, Vol. II, CRC Press, Boca Raton, FL, 1984, p. 229.
- 11 D. H. Coy, in W. S. Hancock (Editor), *Handbook of HPLC for the Separation of Amino Acids, Peptides, and Proteins*, Vol. II, CRC Press, Boca Raton, FL, 1984, p. 197.
- 12 D. D. Blevins, M. F. Burke and V. J. Hruby, in W. S. Hancock (Editor), *Handbook of HPLC for the Separation of Amino Acids, Peptides, and Proteins*, Vol. II, CRC Press, Boca Raton, FL, 1984, p. 137.
- 13 M. Dizdaroglu and M. G. Simic, *J. Chromatogr.*, 195 (1980) 119.
- 14 M. Dizdaroglu, *J. Chromatogr.*, 334 (1985) 49.

CHROM. 21 340

DETERMINATION OF POLYCYCLIC AROMATIC HYDROCARBONS IN LUBRICATING OIL BASE STOCKS USING HIGH-PERFORMANCE LIQUID CHROMATOGRAPHY AND GAS CHROMATOGRAPHY–MASS SPECTROMETRY

J.-P. F. PALMENTIER^a, A. J. BRITTEN, G. M. CHARBONNEAU and F. W. KARASEK

Chemistry Department, University of Waterloo, Waterloo, Ontario N2L 3G1 (Canada)

(First received September 28th, 1988; revised manuscript received January 23rd, 1989)

SUMMARY

A high-performance liquid chromatography (HPLC) method has been developed for the separation of aromatic compounds from the saturated hydrocarbons in lubricating oil base stocks and the further separation of polycyclic aromatic hydrocarbons (PAHs) into fractions based on the number of fused rings. Aromatic compounds were separated from the saturated hydrocarbons by HPLC using a silica column. The aromatic compounds were then backflushed onto an amine derivatized silica column using a six-port two-position switching valve. The PAHs were separated according to the differing number of fused rings. Further analysis by high-resolution gas chromatography–low-resolution mass spectrometry with a fused-silica DB-5 capillary column showed the presence of various parent and alkylated PAHs in the lubricating oil base stocks and 10W30 oil at the part per billion (10^9) level.

INTRODUCTION

Polycyclic aromatic hydrocarbons (PAHs) are a group of compounds with structures based on fused benzene rings. PAHs differ in the number and position of the fused rings and may contain heteroatoms such as oxygen, nitrogen and sulfur¹. There has been an increased interest in the identification and quantitation of PAHs in the environment and fossil fuels because of their carcinogenic properties². PAHs are present in lubricating oils in the part per billion to part per trillion concentration range with the alkylated PAHs present in greater abundance than their unalkylated parent PAHs^{3,4}.

Lubricating oils are composed of normal paraffin hydrocarbons, isoparaffins, naphthenes, aromatics, and some oxygen and sulfur compounds. They are divided into two base stock types, one naphthenic (aromatic), the other paraffinic (aromatic with a large number of alkyl side groups). The composition of a base stock depends

^a Present address: Ontario, Ministry of the Environment, Laboratory Services Branch, Drinking Water Organics–Mass Spectrometry Unit, P.O. Box 213, Rexdale, Ontario M9W 5L1, Canada.

on its origin and the extent of refinement. Base oil stocks are blended together to form specific lubricating oils prior to incorporation of additives. Lubricating oils are treated to remove PAHs because they form sludges and acids in car engines⁵.

The analysis of fossil fuels for PAHs is difficult because they are composed of mostly hydrocarbons which interfere with the analysis of the PAHs. Many techniques have been developed to solve this problem. An open column technique was used for the separation of aliphatic and aromatic compounds in diesel fuel⁶. Aliphatic hydrocarbons were eluted from a silica gel column using pentane. The aromatic compounds were eluted using benzene and the effluent was concentrated before analysis by gas chromatography (GC) using an ion trap detector. A number of PAHs in the sample were identified but were not separated into fractions based on the number of fused rings.

HPLC has also been used for the separation of PAHs. Wise *et al.*⁴ have studied normal-phase and reversed-phase high-performance liquid chromatography (HPLC) columns for the separation of PAHs. They compared the retention characteristics of the μ Bondapak NH₂ and μ Bondapak C₁₈ columns against literature values for silica and alumina columns for the separation of PAHs. The μ Bondapak NH₂ column separated PAHs into compound classes according to the increasing number of fused rings. All PAHs with three fused rings including alkyl substituted derivatives have similar retention on this column, unlike silica columns where addition of alkyl side groups causes them to elute later than their unalkylated parent-PAHs. The μ Bondapak C₁₈ column separated PAHs in a manner similar to silica and alumina columns, but alkyl-substituted PAHs also have increased retention.

Many HPLC techniques have been developed to separate PAHs from the bulk of the aliphatic hydrocarbons. A 4-port 2-position switching valve was used in a study on the separation of components of various petroleum products⁷. Saturated compounds and olefins eluted together from the column, then the flow was reversed (backflush) to elute the aromatic compounds from the column. This resulted in a fast analysis with a sharper peak for the aromatic compounds which without backflush would have eluted as a broad tailing peak. Polar compounds did not elute from the column.

Dark⁸ used an NH₂-derivatized silica column with backflush for the separation and quantitation of crude oil. The NH₂ column gave a better separation of the aromatics than the silica column. The backflush was performed after the aromatic compounds were eluted from the column (rather than after elution of the saturated compounds). This gave a good separation of aromatic from polar compounds, but a poor separation of saturated from aromatic compounds.

Davies *et al.*⁹ used an automated on-line HPLC-GC technique for the analysis of PAHs in diesel exhaust particulates. An HPLC system was used to separate the aromatic compounds from the alkanes on a silica column. Then, a 10-port valve interface was used to backflush the aromatic compounds onto a GC column through a retention gap after the alkanes had left the system. The aromatics were transferred to the GC column as a single peak and analyzed by GC using flame ionization detection. PAHs were identified in the aromatic fraction but were not resolved according to the number of fused rings.

An on-line HPLC column-switching technique was used for the separation and quantitation of paraffins, olefins, naphthenes and aromatics (PONA) in gasoline and

kerosene products¹⁰. Two switching valves and five columns were used to isolate the olefins and aromatics from the saturated compounds. Aromatic compounds and olefins were later eluted separately using the switching valves. Separation and identification of the aromatic compounds was not achieved.

Analysis of commercial lubricating oils for PAHs is very difficult. This paper demonstrates the separation of PAHs from the bulk of the aliphatic compounds using a single injection HPLC technique and the identification of PAHs by using GC-mass spectrometry (MS) and retention indices.

EXPERIMENTAL

Glassware, sample and standard preparation

All glassware was washed with detergent using ultrasonic agitation (30 min) and rinsed three times with tap water, twice with distilled water, and dried overnight at 230°C. Glassware was pre-rinsed with organic solvents. All solvents were distilled in glass, UV-grade from Caledon Labs. (Georgetown, Canada). PAH standards were purchased from Aldrich (Montreal, Canada) or Chem Service (West Chester, PA, U.S.A.) and had a minimum purity of 97%. A PAH standard solution was prepared by weighing 20 mg of each of ten PAHs into a 100-ml volumetric flask. The solution was made to volume with hexane and 2–5 ml of dichloromethane. The spiked oil sample was prepared by weighing 1 mg of each of four PAH standards: naphthalene, phenanthrene, chrysene, and picene into a volumetric flask and the flask made to volume with diluted base oil C4. The solution was sonicated (30 min) and then filtered using a disposable filter disk (Zetapor 25 mm, 0.45 μm porosity, Supelco, Bellefonte, PA, U.S.A.). The base oil samples A1, A2, C3, C4 (Imperial Oil) and 10W30 oil (Canadian Tire, API SFC-CC 28-8213-2) were prepared by weighing 50 mg of the oil into a 100-ml volumetric flask, and making to volume with hexane.

Semi-preparative HPLC

HPLC solvents were filtered and degassed using an aspirator vacuum filtering flask. Hexane was dried with molecular sieves (8–12 mesh, activated type 4A, J. T. Baker) for 24 h prior to filtration.

The instrument used in the HPLC fractionation was a Varian 5000 HPLC system with Vista CDS 402 integrator for recording and manipulating data on floppy disk. Samples were injected using an automated Rheodyne injector with a 100- μl injection loop. A six-port two-position switching valve was used for flow reversal. Semi-preparative $\mu\text{Porasil}$ silica (250 mm \times 7.8 mm I.D., 10 μm particle size, Waters Assoc., Milford, MA, U.S.A.) and $\mu\text{Bondapak}$ amine (250 mm \times 7.8 mm I.D., 10 μm particle size, Waters Assoc.) columns were used. A Hewlett-Packard 1037A refractive index (RI) detector was positioned between an ultra-violet (UV) detector and the waste collection valve (Fig. 1). Solvent gradient and flow-rate changes were used as shown in Table I.

Fractions collected from the HPLC were concentrated by rotary evaporation under reduced pressure to near dryness. The contents were transferred to calibrated "Reacti-vials" (Pierce). Flasks were rinsed three times with benzene and their contents transferred to the vials. Samples were reduced in volume to 10 μl using a gentle stream of high-purity nitrogen gas.

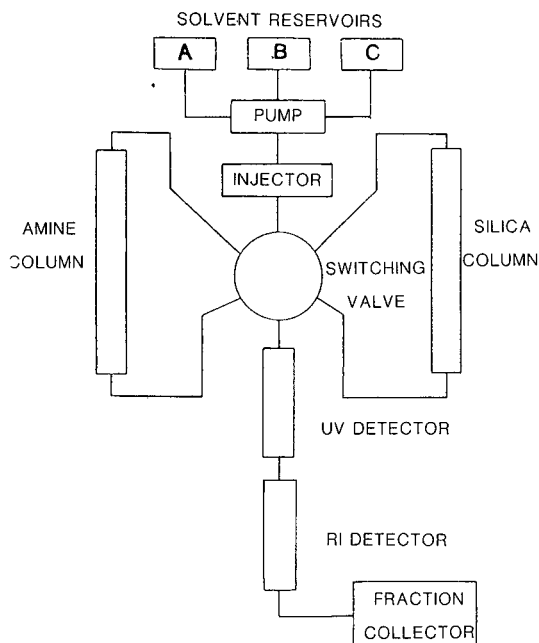


Fig. 1. HPLC block diagram.

TABLE I

SOLVENT GRADIENT AND FLOW-RATES USED IN HPLC FRACTIONATION OF THE OILS

HEX = hexane, DCM = dichloromethane, ACN = acetonitrile.

<i>Time (min)</i>	<i>Solvent</i>	<i>Flow-rate (ml/min)</i>
0	100% HEX	1
13.5	100% HEX	1
14.0	100% HEX	2.5
35.0	100% HEX	2.5
40.0	50% HEX 50% DCM	2.5
45.0	100% DCM	2.5
45.5	95% DCM 5% ACN	2.5
46.0	90% DCM 10% ACN	2.5
51.0	90% DCM 10% ACN	2.5
51.5	95% DCM 5% ACN	2.5
52.0	100% DCM	2.5
55.0	50% DCM 50% HEX	2.5
58.0	100% HEX	2.5
64.5	100% HEX	2.5
65.0	100% HEX	1.0

GC analysis

Initial fraction analysis was performed on a Hewlett-Packard 5880A GC system using cool on-column injector, flame ionization detector and DB-5 fused-silica capillary column (30 m \times 0.32 mm I.D., J&W Scientific, Rancho Cordova, CA, U.S.A.).

GC-MS analysis

A Hewlett-Packard 5987A GC-MS system in the positive ion, electron impact (EI) ionization and linear scanning (50–500 a.m.u.) modes was used for analysis of the HPLC fractions. The system consisted of a 5880A gas chromatograph, 5987A mass spectrometer, HP 1000 data system, cool on-column injector and a DB-5 fused-silica capillary column (30 m \times 0.32 mm I.D.). Temperature programming for GC and GC-MS consisted of an initial temperature of 80°C held for 1 min and ramped up at 3.5°C/min to 300°C and held for 10 min. The GC-MS computer system contained a mass spectral library searching system based on Probability Based Matching (PBM) and a reference file of 70 000 EI spectra for the identification of unknowns.

Compound identification was performed by using the PBM search system on the EI mass spectrum and the PAHs retention index system developed by Lee and Vassilaros¹¹ and Vassilaros *et al.*¹². A retention window of ± 0.2 retention index units was used for provisional identification of PAHs. Positive isomer identification could not be done without standards. Where more than one isomer could be the correct compound, all were listed in the table.

RESULTS AND DISCUSSION

Determination of backflush time

Aromatic compounds were separated from the saturated hydrocarbons in base oil C4 by HPLC using a μ Porasil silica column and hexane. The flow-rate was varied until baseline separation of saturated and aromatic compounds was achieved. The optimum flow-rate was found to be 1 ml/min, and the separation was monitored on UV and RI detectors as shown in Fig. 2. An RI detector was used to monitor the separation of aromatic from saturated compounds because both show a response on the RI detector. Only the aromatic compounds show a response on the UV detector.

A silica column was used to separate the aromatic from the saturated compounds, but further resolution of the aromatics from each other using this column was poor. After the aromatics were separated from the saturated hydrocarbons, they were backflushed as a narrow plug onto the μ Bondapak amine column (using a six-port two-position switching valve) where they were separated according to the differing number of fused rings. The optimum backflush time was found to be 13.3 min. Once the backflush time was determined, the RI detector was removed from the HPLC set-up.

Optimization of HPLC separation of PAHs

Solvent gradient and flow-rate changes were used to further improve and speed up the separation of the PAHs. The components of the PAH standard solution were separated on the HPLC system using the solvent gradient and fractions were collected according to the UV detector signal in Fig. 3. The valleys in the HPLC-UV chromatogram were used as rough fraction cut points.

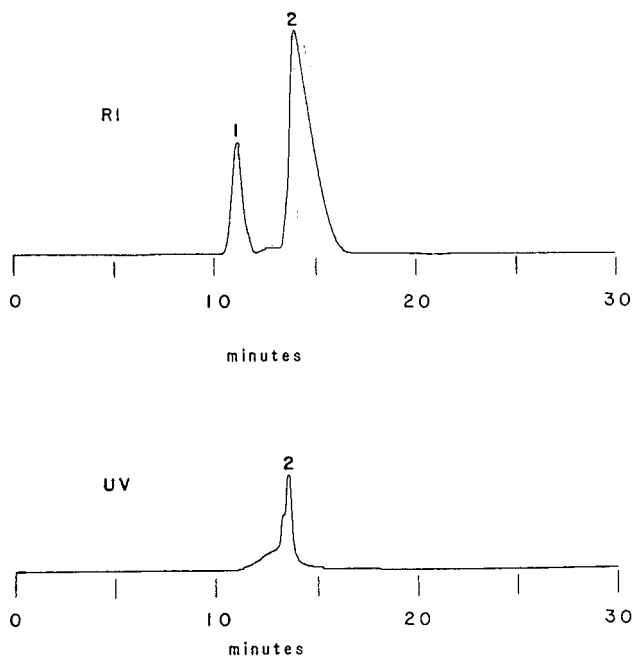


Fig. 2. HPLC separation of aromatic compounds (2) from saturated hydrocarbons (1) using a μ Porasil silica column (250 mm \times 7.8 mm I.D.) with hexane at 1 ml/min. Separation was monitored on RI and UV (254 nm) detectors.

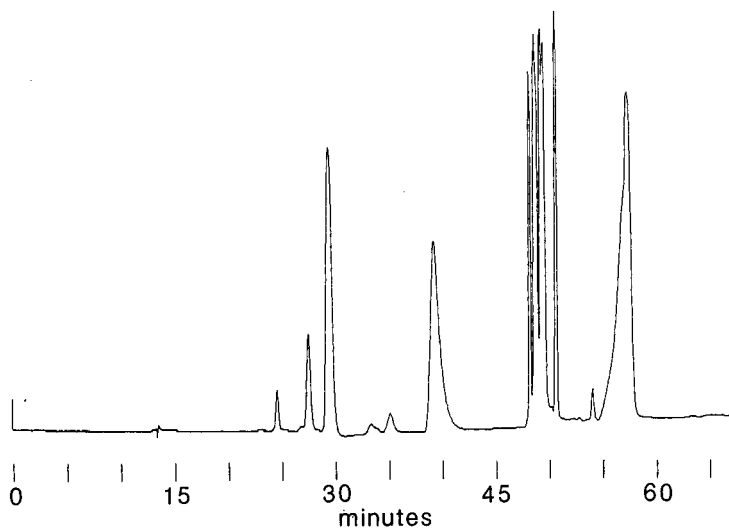


Fig. 3. HPLC-UV chromatogram. Separation of components of the PAH standard solution using the μ Porasil silica column (250 mm \times 7.8 mm I.D.), backflush, μ Bondapak amine column (250 mm \times 7.8 mm I.D.) and solvent gradient.

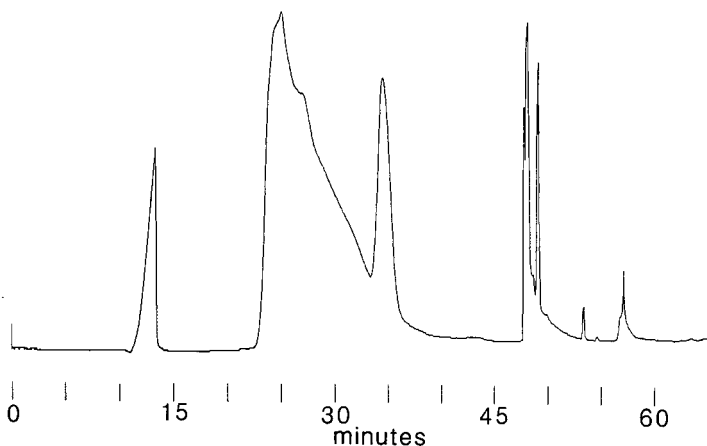


Fig. 4. HPLC-UV chromatogram. Separation of spiked base oil sample using the μ Porasil silica column (250 mm \times 7.8 I.D.), backflush, μ Bondapak amine column (250 mm \times 7.8 mm I.D.) and solvent gradient.

TABLE II

PROVISIONALLY IDENTIFIED COMPOUNDS FOUND IN FRACTION TWO OF BASE OIL A1 BY USING GC-MS AND RETENTION INDICES

See Fig. 5.

Peak No.	Compound ^a	Retention index	MW
1	Dibenzothiophene	295.4	184
2	Phenanthrene	300.0	178
3	C2-Fluorene	308.3	194
4a	Methyldibenzothiophene/methylnaphthothiophene	312.2	198
4b	8-Methylnaphtho[1,2- <i>b</i>]thiophene	315.8	198
4c	1-Methyldibenzothiophene/ 6-methylnaphtho[1,2- <i>b</i>]thiophene	319.6	198
5	4-Methylphenanthrene/1-methylantracene	323.3	192
6a	4,6-Dimethyldibenzothiophene	329.2	212
6b	C2-Dibenzothiophene/naphthothiophene	332.2	212
6c	2,8-Dimethyldibenzothiophene/ 3,7-dimethyldibenzothiophene	335.8	212
6d	C2-Dibenzothiophene/naphthothiophene	338.4	212
7a	C2-Phenanthrene/anthracene	341.5	206
7b	C2-Phenanthrene/anthracene	342.6	206
7c	C2-Phenanthrene/anthracene	344.6	206
8a	C3-Dibenzothiophene/naphthothiophene	346.5	226
8b	C3-Dibenzothiophene/naphthothiophene	348.9	226
8c	C3-Dibenzothiophene/naphthothiophene	350.2	226
8d	C3-Dibenzothiophene/naphthothiophene	351.4	226
8e	C3-Dibenzothiophene/naphthothiophene	354.6	226
8f	C3-Dibenzothiophene/naphthothiophene	356.7	226
9	C3-Phenanthrene/anthracene	359.5	220
10a	C4-Dibenzothiophene/naphthothiophene	361.9	240
10b	C4-Dibenzothiophene/naphthothiophene	366.6	240
10c	C4-Dibenzothiophene/naphthothiophene	368.6	240
10d	C4-Dibenzothiophene/naphthothiophene	370.5	240
10e	C4-Dibenzothiophene/naphthothiophene	374.9	240
10f	C4-Dibenzothiophene/naphthothiophene	377.1	240

^a - / represents possible isomers.

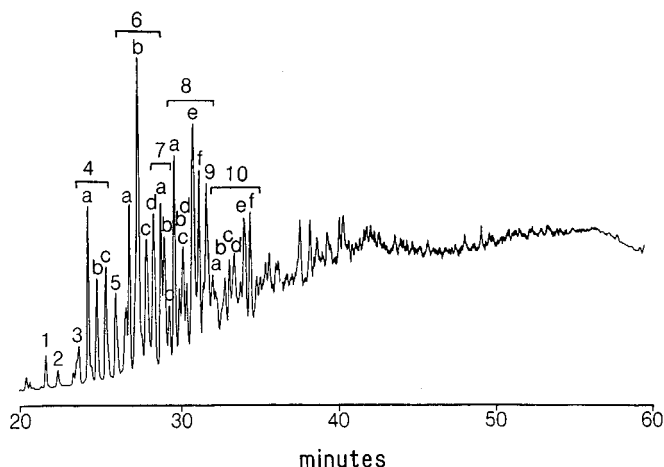


Fig. 5. GC-FID chromatogram. Separation of fraction 2 of base oil A1 on a DB-5 (30 m \times 0.32 mm I.D.) column using the temperature programme from 80°C hold 1 min to 300°C at 3.5°C/min hold 10 min.

Base oil C4 was spiked with four PAHs: naphthalene, phenanthrene, chrysene, and picene, representing 2 to 5 fused ring PAHs, respectively. The sample fractions were collected according to the UV trace (Fig. 4) and the rough fraction cut times determined using the PAH standard. The final fraction cut times obtained were 20–30.5, 40, 50, and 65 min.

Analysis of the base oils

A series of four base oils samples (A1, A2, C3 and C4) were separated on the HPLC system and fractions were collected using the optimized HPLC parameters. The aromatic composition of the four base oils was seen to be different according to

TABLE III

PROVISIONALLY IDENTIFIED COMPOUNDS FOUND IN FRACTION 3 OF BASE OILS A1, A2 AND 10W30 OIL USING GC-MS AND RETENTION INDICES

Compound ^a	Retention index			
	A1	A2	10W30	MW
2-/3-/8-Methylbenzo[<i>b</i>]naphtho[2,1- <i>d</i>]thiophene			407.6	248
2-/3-/8-/9-Methylbenzo[<i>b</i>]naphtho[2,1- <i>d</i>]thiophene	407.7			248
C2-Benzonaphthothiophene			424.9	262
C2-Benzonaphthothiophene	427.0			262
C3-Benzonaphthothiophene			441.2	276
C3-Benzonaphthothiophene		442.1		276
C3-Benzonaphthothiophene	443.2			276
C3-Benzonaphthothiophene	446.3			276
C3-Benzonaphthothiophene		451.3		276
C4-Benzonaphthothiophene	456.4			290
C4-Benzonaphthothiophene	464.5			290

^a - / represents possible isomers.

their UV traces. Base oils A1 and A2 appeared to have greater proportion of PAHs than C3 and C4, assuming similar UV response.

Base oil A1 was separated by HPLC and the fractions were collected. GC-MS analysis of fractions 1 and 4 of base oil stock A1 showed an absence of PAHs. Fraction 2 of base oil A1 contained 27 PAHs having three fused rings including a C2-fluorene, dibenzothiophene, alkylated dibenzothiophenes/naphthothiophenes, phenanthrene and alkylated phenanthrenes/anthracenes (Table II, Fig. 5). Six alkylated benzonaphthothiophenes (four fused rings) were found in fraction 3 (Table III). Eleven PAHs having three fused rings were found in fraction 2 of base oil A2, similar to those in fraction 2 of base oil A1 (Table IV). Two alkylated dibenzonaphtho-

TABLE IV

PROVISIONALLY IDENTIFIED COMPOUNDS FOUND IN FRACTION 2 BASE OIL A2 AND 10W30 OIL USING GC-MS AND RETENTION INDICES

Compound ^a	Retention index		
	A2	10W30	MW
1-Methylfluorene		288.8	180
4-Methyldibenzothiophene	312.7	312.6	198
2-Methyldibenzothiophene/3-methyldibenzothiophene	316.2		198
3-Methylphenanthrene	319.6		192
2-Methylphenanthrene		320.1	192
1-Methylphenanthrene		324.0	192
3-Ethyldibenzothiophene	328.5		212
C2-Dibenzothiophene/naphthothiophene		329.4	212
3,6-Dimethyldibenzothiophene/2-ethyldibenzothiophene	332.8		212
Methoxyanthracene		334.5	208
3,8-Dimethyldibenzothiophene	336.1		212
C2-Dibenzothiophene/naphthothiophene	338.4		212
C2-Phenanthrene/anthracene		339.5	206
C2-Phenanthrene/anthracene	342.0		206
C2-Phenanthrene/anthracene		342.5	206
C2-Phenanthrene/anthracene		343.0	206
C2-Phenanthrene/anthracene		343.8	206
C2-Phenanthrene/anthracene		345.0	206
C3-Dibenzothiophene/naphthothiophene	346.9	347.0	226
C3-Dibenzothiophene/naphthothiophene	349.7		226
C3-Dibenzothiophene/naphthothiophene		350.0	226
C3-Dibenzothiophene/naphthothiophene	354.3		226
C3-Phenanthrene/anthracene		359.0	220
C3-Phenanthrene/anthracene		361.9	220
C4-Phenanthrene/anthracene		377.1	234
C4-Phenanthrene/anthracene		380.5	234
9,10-Dimethyl-3-ethylphenanthrene		381.7	234
Unidentified		465.2	231
Unidentified		474.3	231
Unidentified		481.6	231
Unidentified		485.4	231
Unidentified		494.4	231

^a - / represents possible isomers.

phenes (four fused rings) were found in fraction 3 (Table III). Again, no PAHs were found in fraction 1 or 4 and no PAHs were found in either base oil C1 or C4.

Analysis of 10W30 oil

A commercial 10W30 oil was analyzed in the same manner as the lubricating oil base stocks. No PAHs were found in fractions 1 and 4 of the sample. Fraction 2 contained 18 PAHs including methylfluorene, alkylated dibenzothiophenes/naphthothiophenes, alkylated phenanthrenes/anthracenes, a methoxyanthracene, and five unidentified compounds with molecular weight 231 (Table IV). Three alkylated benzophenothiophenes were found in fraction 3 (Table III).

CONCLUSION

Baseline separation of saturated and aromatic compounds in the lubricating oil base stocks was achieved by using an HPLC system equipped with a silica column. PAHs in the aromatic fraction were subsequently separated into fractions based on the increasing number of fused rings using an amine derivatized silica column. To perform both separations, an HPLC method was developed using a single injection analysis, two semi-preparative HPLC columns, a six-port two-position switching valve and a solvent gradient. The separation can be completed in 65 min. This HPLC system can also be automated for the rapid and routine analysis of oils.

The separation of PAHs into compound class fractions according to the increasing number of fused rings was demonstrated using the spiked base oil sample. Base oil analyses demonstrated the effectiveness of the method since fraction 2 of the oils A1, A2 and 10W30 contained only PAHs having three fused rings, while fraction 3 of these oils contained PAHs having four fused rings. In total, 67 PAHs were provisionally identified at low-ppb concentrations in the oil samples A1, A2 and 10W30 by using GC-MS analysis with PBM library search and the use of retention indices. No PAHs were found in base oils C3 and C4. This result correlates with the low signal strength observed in their UV traces when compared with base oils A1 and A2.

ACKNOWLEDGEMENTS

This work was supported by Imperial Oil Ltd. Research, a division of Esso Petroleum Canada.

REFERENCES

- 1 F. W. Karasek and F. I. Onuska, *Open Tubular Column Gas Chromatography in Environmental Sciences*, Plenum Press, New York, 1984, pp. 196-216.
- 2 F. W. Karasek and J. A. Sweetman, in F. W. Karasek, S. Safe and O. Hutzinger (Editors), in *Mass Spectrometry in Environmental Sciences*, Plenum Press, New York, 1985, pp. 195-207.
- 3 R. A. Brown and T. D. Searl, K. H. Altgelt and T. H. Gouw (Editors), in *Chromatography of Petroleum Analysis*, New York, 1979, p. 390.
- 4 S. A. Wise, S. N. Chester, H. S. Hertz, L. R. Hilpert and W. E. May, *Anal. Chem.*, 49 (1977) 2306.
- 5 G. A. Purdy, *Petroleum: Prehistoric to Petrochemicals*, Copp's Clark Pub., Toronto, 1957, pp. 62, 66, 228, 252, 372.
- 6 P. T. Williams, G. E. Andrews, K. D. Bartle, P. Bishop and P. Watkins, *Biomed. Environ. Mass Spectrom.*, 15 (1988) 517.

- 7 J. C. Suatoni and R. E. Swab, *J. Chromatogr. Sci.*, 13 (1975) 361.
- 8 W. A. Dark, *J. Liq. Chromatogr.*, 5 (1982) 1645.
- 9 I. L. Davies, M. W. Raynor, P. T. Williams, G. E. Andrews and K. B. Bartle, *Anal. Chem.*, 59 (1987) 2579.
- 10 P. C. Hayes Jr. and S. D. Anderson, *J. Chromatogr.*, 437 (1988) 365.
- 11 M. L. Lee and D. L. Vassilaros, *Anal. Chem.*, 51 (1979) 768.
- 12 D. L. Vassilaros, R. C. Kong, D. W. Later and M. L. Lee, *J. Chromatogr.*, 252 (1982) 1.

CHROM. 21 364

ADSORPTION CHROMATOGRAPHY ON CELLULOSE

IV. SEPARATION OF D- AND L-TRYPTOPHAN AND D- AND L-METHYL-TRYPTOPHAN ON CELLULOSE WITH AQUEOUS SOLVENTS^a

A. O. KUHN and M. LEDERER*

Institut de Chimie Minérale et Analytique, Université de Lausanne, Lausanne (Switzerland)
and

M. SINIBALDI

Istituto di Cromatografia del CNR, Casella Postale 10, 00016 Monterotondo Scalo (Rome) (Italy)

(Received November 15th, 1988)

SUMMARY

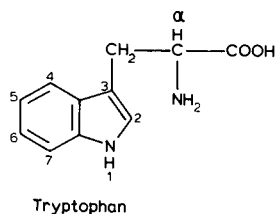
Differences in R_F values between D- and L-tryptophan on cellulose paper, developed with water, were observed already in 1954 and now several variables of this separation, such as modifications to the tryptophan molecule, the temperature and salting-out have been examined. Differences were found in the mechanism of the process compared with the systems described by Yuasa *et al.* [*Chromatographia*, 21 (1986) 79], who separated amino acid enantiomers on cellulose with pyridine–ethanol–water mixtures.

INTRODUCTION

The chiral properties of cellulose were first described in 1952 by Dalglish¹, who obtained separations of the D- and L-forms of kynurenine, hydroxykynurenines and hydroxyphenylalanines with a “partition” solvent, namely butanol–acetic acid–water. Soon afterwards Weichert² showed that D- and L-tryptophans had different R_F values when developed on cellulose paper with water (L-form, $R_F = 0.53$; D-form, $R_F = 0.55$). This was also reported by Yuasa *et al.*³. Later, cellulose derivatives were preferred for chiral resolutions, especially cellulose triacetate and cellulose tribenzoate (for a review, see ref. 4). Relatively few workers, *e.g.*, Yuasa and co-workers^{3,5}, used underivatized cellulose as a chiral stationary phase with partition solvents. They also pointed out that “native” cellulose had advantages for the preparative separation of amino acid pairs.

In a survey of the adsorptive properties of cellulose from aqueous solutions^{6,7}, we obtained “baseline” separations with substituted tryptophans on cellulose thin-layers which would be impossible on cellulose paper, as shown by Weichert², and we report our findings here.

^a Presented at the *International Symposium on Chromatography, Rehovot, November 14–17, 1988.*



Salting-out with ammonium sulphate in the eluent

When water is used as the eluent, the difference in R_F values in thin-layer chromatography (TLC) between the D- and L-forms is between 0.06 and 0.08. These values have at best a precision of ± 0.01 , but usually 0.02. Hence exact measurements would be illusory. However, it is evident from Table I that the separation decreases with increasing ammonium sulphate concentration. The general decrease in R_F values is probably due to two effects: the higher polarity of the eluent and the dehydration of the cellulose, owing to the presence of ammonium sulphate. We suggest that dehydration affects the lower chiral discrimination.

When lithium chloride solutions are used as eluents, we observe the same tendency with increasing concentration, but the effect is less than with ammonium

TABLE I

R_F VALUES OF OPTICALLY ACTIVE TRYPTOPHANS AT ROOM TEMPERATURE WITH DIFFERENT ELUENTS

Compound	Eluent						
	Water	Acetic acetic (2%)	Ammonium sulphate solution				
			0.66 M	1.0 M	2.0 M	2.65 M	4.0 M
DL-Tryptophan:							
D-Isomer	58	—	57	52	47	35	
L-Isomer	52(s) ^a	—	52(s)	45(s)	42(s)	31(s)	25
DL-1-Methyltryptophan:							
Spot 1	58		55	50 ^b	37 ^b		
Spot 2	52	57	50	46 ^b	34 ^b	28	13
DL-5-Methyltryptophan:							
Spot 1	50	46	42	39	29	26	
Spot 2	42(s)	40(s)	34	32(s)	24(s)	21(s)	10
DL-6-Methyltryptophan:							
Spot 1	47	42	43	38	27	22	
Spot 2	39(s)	38(s)	35(s)	32(s)	23(s)	19(s)	08
DL-7-Methyltryptophan:							
Spot 1	52		45	41 ^b	30 ^b	26 ^b	
Spot 2	46(s)	46	39(s)	37 ^b (s)	26 ^b (s)	21 ^b (s)	10
DL- α -Methyltryptophan	72	67	67	64	55	51	—

^a s = Slight streaking.

^b Critical separations.

TABLE II

COMPARISON OF LITHIUM CHLORIDE AND AMMONIUM SULPHATE SOLUTIONS AS ELUENTS FOR D- AND L-TRYPTOPHAN AT ROOM TEMPERATURE

Eluent	Concentration (M)	hR_F	
		D-Tryptophan	L-Tryptophan
Lithium chloride	0.5	55	48
	2.4	48	41
	4.7	37	33
Ammonium sulphate	0.66	57	52
	2.0	47	42
	4.0	25	25

sulphate. To illustrate this, the two salts are compared in Table II.

Phosphate buffers of pH 8.8 and 3.0 were also examined. Table III shows that the separations are very similar to those obtained in ammonium sulphate or in lithium chloride. A good separation is shown in Fig. 1.

EXPERIMENTAL

Cellulose thin layers (Merck Cellulose, Art. No. 5577) were developed by the ascending technique in small jars. The development took 10–30 min, depending on the salt concentration in the eluent. Development took place either at room temperature or in thermostatically controlled ovens or cooling cabinets.

The spots were revealed either with iodine vapour or by dipping into an acetone solution of ninhydrin, with subsequent heating with a hair dryer to full colour formation.

TABLE III

 R_F VALUES OF SUBSTITUTED TRYPTOPHANS IN PHOSPHATE BUFFERS

Buffers: 0.7 M orthophosphoric acid in 100 ml of water adjusted with potassium hydroxide to pH 8.8 or 3.0. Temperature, 40°C.

Compound	pH 8.8		pH 3.0	
	D-form	L-form	D-form	L-form
D-Tryptophan	0.66		0.66	
DL-Tryptophan	0.66	0.60	0.65	0.59
DL-1-Methyltryptophan	0.66	0.59	0.65	0.59
DL-5-Methyltryptophan	0.54	0.47	0.54	0.47
DL-6-Methyltryptophan	0.53	0.47	0.54	0.47
DL- α -Methyltryptophan		0.75		0.75



Fig. 1. Chromatogram on a Merck cellulose thin layer developed at room temperature with 0.5 *M* lithium chloride solution. The spots were revealed with iodine vapour. D = D-tryptophan; DL = DL-tryptophan; 1 = DL-1-methyltryptophan; 5 = DL-5-methyltryptophan; 6 = DL-6-methyltryptophan; 7 = DL-7-methyltryptophan; α = DL- α -methyltryptophan.

RESULTS AND DISCUSSION

Development with pure water

The R_F values of tryptophan and some substituted tryptophans are given in Table I. The difference between the D- and L-forms of tryptophan is greater than that reported by Weichert² on cellulose, as thin layers offer both a larger surface area owing to the smaller particle size and a more favourable sorbent to solvent ratio. Thus we obtained two distinct spots on the thin layer, whereas this does not occur on the usual filter-papers, such as Whatman No. 1 and 3MM.

Compounds with a methyl group on the benzene ring, *i.e.*, 5-, 6- and 7-methyltryptophan, are all more strongly adsorbed than the parent compound, but the differences in R_F values between the D- and L-forms are of the same order as for tryptophan.

A methyl group on the nitrogen atom of the indole ring does not lower the R_F

TABLE IV

EFFECT OF TEMPERATURE ON THE hR_F VALUES OF OPTICALLY ACTIVE TRYPTOPHANS WITH WATER AS ELUENT

Compound	hR_F			
	1°C	7°C	40°C	63°C
D-Tryptophan	46	49	62	75
L-Tryptophan	40(ss)	43(ss)	57	71
D-1-Methyltryptophan	46	49	64	76
L-1-Methyltryptophan	41(ss)	43(ss)	60	71
D-5-Methyltryptophan	35	39	54	63
L-5-Methyltryptophan	28(ss)	32(ss)	46	55
D-6-Methyltryptophan	31	37	52	63
L-6-Methyltryptophan	23	29(s)	44	56
D-7-Methyltryptophan	—	—	56	66
L-7-Methyltryptophan	—	69	49	61
α -Methyltryptophan	62		76	82

^a s = Streaking; ss = strong streaking.

values of the two optical isomers, but a methyl group in the α -position decreases the adsorption and seems to hinder the separation of the two isomers.

Development with acetic acid

At a lower pH with 2% acetic acid, most separations are either reduced or do not occur (Table I).

Effect of temperature

Tables IV–VIII show the R_F values obtained at different temperatures, between the lowest possible (between 0 and -10°C , depending on the salt and its concentra-

TABLE V

EFFECT OF TEMPERATURE ON THE hR_F VALUES OF OPTICALLY ACTIVE TRYPTOPHANS IN 0.5 M LITHIUM CHLORIDE AS ELUENT

Compound	hR_F			
	-5°C	22°C	40°C	63°C
D-Tryptophan	46	55	66	71
L-Tryptophan	37(s)	48(s)	60(s)	67
D-1-Methyltryptophan	49	55	67	71
L-1-Methyltryptophan	40(s)	48(s)	61(s)	67
D-5-Methyltryptophan	32	41	54	61
L-5-Methyltryptophan	21	31	44	53
D-6-Methyltryptophan	32	41	53	61
L-6-Methyltryptophan	21	32	44	54
D-7-Methyltryptophan	33	44	57	65
L-7-Methyltryptophan	25	37	49	60
α -Methyltryptophan	68	69	77	81

^a s = Streaking.

TABLE VI

EFFECT OF TEMPERATURE ON THE hR_F VALUES OF OPTICALLY ACTIVE TRYPTOPHANS IN 2.4 M LITHIUM CHLORIDE AS ELUENT

Compound	hR_F^a						
	$-10^\circ C$	$-5^\circ C$	$1^\circ C$	$7^\circ C$	$22^\circ C$	$40^\circ C$	$63^\circ C$
D-Tryptophan	32	32	35	36	48	58	67
L-Tryptophan	25(s)	24(s)	29(s)	31(s)	41(s)	51	61
D-1-Methyltryptophan	33	33	34	35	48	57	65
L-1-Methyltryptophan	25	26	29	29	41	51	60
D-5-Methyltryptophan	21	22	23	25	36	45	53
L-5-Methyltryptophan	13(s)	15(s)	16(s)	18(s)	28(s)	36(s)	45
D-6-Methyltryptophan	20	21	21	23	33	43	55
L-6-Methyltryptophan	13(s)	15(s)	15	16	25	35	48
D-7-Methyltryptophan	21	22	—	—	38	46	58
L-7-Methyltryptophan	15	17	—	—	31	39	52
α -Methyltryptophan	50	53	53	56	64	70	78

^a s = Streaking.

tion) and $63^\circ C$. There is little difference in the separation of the optical isomers at low and higher temperatures up to $40^\circ C$. At $63^\circ C$ some chromatograms show a decrease in the separation of the enantiomers, and this is most pronounced at high lithium chloride concentrations.

However, the separations are essentially the same over a wide temperature range. There is certainly no sign of inverted sequences, as observed in many other systems. From the point of view of obtaining good separations, there is an improvement in the compactness of the spots at $40^\circ C$. We suggest that this is due to a faster establishment of equilibrium during development.

TABLE VII

EFFECT OF TEMPERATURE ON THE hR_F VALUES OF OPTICALLY ACTIVE TRYPTOPHANS IN 4.7 M LITHIUM CHLORIDE AS ELUENT

Compound	hR_F		
	$22^\circ C$	$40^\circ C$	$61^\circ C$
D-Tryptophan	37	50	59
L-Tryptophan	33	45	59
D-1-Methyltryptophan	35	47	57
L-1-Methyltryptophan	31	44	57
D-5-Methyltryptophan	22	32	42
L-5-Methyltryptophan	17	28	38
D-6-Methyltryptophan	24	33	46
L-6-Methyltryptophan	20	29	46
D-7-Methyltryptophan	26	37	50
L-7-Methyltryptophan	22	34	50
α -Methyltryptophan	51	63	72

TABLE VIII

EFFECT OF TEMPERATURE ON hR_F VALUES OF OPTICALLY ACTIVE TRYPTOPHANS IN 0.76 *M* AMMONIUM SULPHATE AS ELUENT

Compound	hR_F				
	$-5^\circ C$	$1^\circ C$	$22^\circ C$	$40^\circ C$	$63^\circ C$
D-Tryptophan	39	40	50	63	75
L-Tryptophan	33(s)	35(s)	44(s)	57	71
D-1-Methyltryptophan	37	40	50	59	69
L-1-Methyltryptophan	33(s)	35	44	54	66
D-5-Methyltryptophan	27	28	38	49	61
L-5-Methyltryptophan	20(s)	21(s)	31(s)	42	54
D-6-Methyltryptophan	23	25	39	46	62
L-6-Methyltryptophan	17	19	32	39	56
D-7-Methyltryptophan	25	—	—	49	—
L-7-Methyltryptophan	21	—	—	44	—
α -Methyltryptophan	59	57	65	70	83

^a s = Striking.

DISCUSSION

Separations of the enantiomeric tryptophans can be achieved on cellulose with an R_F difference of about 0.06, over a wide range of salt concentrations and temperatures. Substitution of methyl groups on the benzene ring (positions 5, 6 and 7) or on the indole ring (position 1) does not alter this separation appreciably. There is no separation when the α -carbon is substituted with a methyl group. We therefore have a very simple and cheap chromatographic system, which produces "baseline" separations over a wide range of conditions.

It is interesting to compare these separations with some similar ones reported recently. Yuasa and co-workers^{3,5} used cellulose as a chiral support with a "partition solvent" consisting of pyridine-ethanol-water, both in columns and on thin layers. The R_F differences on thin-layer plates were 0.05 for several pairs of aromatic amino acids, *i.e.*, of the same order as we observed with aqueous solvents. However, they found that separation is possible only in a relatively narrow range of solvent mixtures, where the ratios of pyridine + water to water were 3-4. They also found that the separation "was clearly enhanced with a decrease in the temperature and with an increase in the hydrophobicity". Hence their system had very different parameters to ours.

Another interesting comparison can be made with the results of Büyüktimkin and Buschauer⁸, who separated by TLC the enantiomers of amino acids as their (*S*)-(+)-naproxen derivatives on silica gel plates (non-chiral). They obtained well separated spots with ten different pairs of amino acid enantiomers. The R_F differences were in the range 0.03-0.10, most being between 0.05 and 0.07. Further, Günther⁹ has reported numerous chiral separations on Chiralplates (Macherey, Nagel & Co., Düren, F.R.G.). Most separations showed differences in R_F values of 0.09-0.11. Hence the separations that we obtained seem comparable to those with other systems as far as separation ability is concerned, but offer the advantages of simplicity and robustness.

REFERENCES

- 1 C. E. Dalgleish, *J. Chem. Soc.* (1952) 3940.
- 2 R. Weichert, *Acta Chem. Scand.*, 8 (1954) 1542.
- 3 S. Yuasa, A. Shimada, M. Isoyama, T. Fukuhara and M. Itoh, *Chromatographia*, 21 (1986) 79.
- 4 A. Ichida and T. Shibata, in M. Zief and L. J. Crane (Editors), *Chromatographic Chiral Separations*, Marcel Dekker, New York, 1988, pp. 219–243.
- 5 T. Fukuhara, M. Isoyama, A. Shimada, M. Itoh and S. Yuasa, *J. Chromatogr.*, 387 (1987) 562.
- 6 A. O. Kuhn and M. Lederer, *J. Chromatogr.*, 406 (1987) 389.
- 7 A. O. Kuhn and M. Lederer, *J. Chromatogr.*, 440 (1988) 165.
- 8 N. Büyüktimkin and A. Buschauer, *J. Chromatogr.*, 450 (1988) 281.
- 9 K. Günther, *J. Chromatogr.*, 448 (1988) 11.

CHROM. 21 353

SEPARATION OF *cis* AND *trans* ISOMERS OF UNSATURATED FATTY ACIDS BY HIGH-PERFORMANCE LIQUID CHROMATOGRAPHY IN THE SILVER ION MODE

WILLIAM W. CHRISTIE* and GRACE H. McG. BRECKENRIDGE

Hannah Research Institute, University of Glasgow, Ayr KA6 5HL (U.K.)

(Received November 10th, 1988)

SUMMARY

High-performance liquid chromatography in the silver ion mode has been adapted for the analysis of positional and geometrical isomers of fatty acids, and especially for the determination of *trans* unsaturation in fats and oils. The stationary phase consisted of an ion-exchange medium, which was a silica gel matrix with bonded sulphonic acid moieties, loaded with silver ions. Fatty acids were converted into phenacyl esters so that UV detection at 242 nm could be used. The mobile phase for the separation of *trans*- and *cis*-monoenoic isomers was 1,2-dichloroethane-dichloromethane (1:1, v/v), and 0.5% of acetonitrile was added in order to elute geometrical isomers of linoleic and linolenic acids. Gradient elution was employed for mixtures containing a full range of components. Provided that the column temperature was kept constant, the retention times were reproducible over long periods of time, and the response of the detector was related in a rectilinear manner to the molar proportion of each fatty acid, irrespective of the structure. Monoenoic isomers from commercially hydrogenated soybean oil were identified by gas chromatography-mass spectrometry of picolinyl ester derivatives. The method was applied to natural fats containing *trans* double bonds, *i.e.*, sheep adipose tissues from three sites, to commercial margarines and cooking fats, and to soybean oil, rapeseed oil and a fish oil at various times during hydrogenation.

INTRODUCTION

A number of methods have been devised for the separation and/or determination of *cis* and *trans* isomers of unsaturated fatty acids (reviewed elsewhere¹), but none of these is entirely satisfactory. Infrared spectrometry has been much used for this purpose², but gas chromatography (GC) on long packed columns or capillary columns of fused silica with highly polar liquid stationary phases now appears to be generally preferred. The effectiveness of the latter procedure has been widely debated³⁻¹⁹, however, as it is not always easy to distinguish between peaks representing *cis*- and *trans*-monoenes.

Silver ion chromatography is also a useful technique for separating geometrical

isomers of fatty acids (as the methyl ester derivatives) for subsequent analysis by GC, but the thin-layer chromatographic (TLC) procedures used hitherto have limited resolution, and are costly and messy²⁰. On the other hand, a stable ion-exchange column loaded with silver ions has been developed for high-performance liquid chromatography (HPLC)²¹ that has proved of value in the simplification of complex mixtures of fatty acids of natural origin for subsequent identification by GC-mass spectrometry (MS)²²⁻²⁴ and for separating molecular species of triacylglycerols²⁵. The procedures are rapid, reproducible and give clean fractions, uncontaminated by silver ions. Applications of this column to the isolation and determination of fatty acids containing *trans* double bonds in samples of natural and industrial origin are described in this paper.

EXPERIMENTAL

Materials and reagents

Lipid standards and reagents were supplied by Sigma (Poole, U.K.). All solvents were of AnalaR or HPLC grade and were supplied by FSA Scientific Apparatus (Loughborough, U.K.). Margarines and cooking fats were commercial brands and were purchased in a local supermarket. Adipose tissue samples were obtained from a freshly killed sheep of the Institute flock. Partially hydrogenated oils were donated by Dr. G. Thaxton of Van den Berghs & Jurgens (Purfleet, U.K.). Mixtures of the geometrical isomers of linoleic and linolenic acids were prepared from the parent compounds by nitric oxide-catalysed isomerization²⁶. The reaction time was varied by trial and error to optimize the yield of products.

High-performance liquid chromatography

The HPLC equipment and the silver ion column were as described previously²². In brief, a Spectra-Physics (St. Albans, U.K.) Model 8700 solvent-delivery system was used, together with a Pye Unicam (Cambridge, U.K.) PU 4025 UV detector operated at 242 nm. A column (250 × 4.6 mm I.D.) of Nucleosil 5SA (kindly donated by Applied Chromatography Systems, Macclesfield, U.K.) was flushed with 1% ammonium nitrate solution at a flow-rate of 0.5 ml/min for 1 h, then with distilled water at 1 ml/min for 1 h. Silver nitrate (0.2 g) in water (1 ml) was injected on to the column via the Rheodyne valve in 50- μ l aliquots at 1-min intervals; silver began to elute from the column after about 10 min, and 20 min after the last injection the column was washed with methanol for 1 h, then with 1,2-dichloroethane-dichloromethane (1:1, v/v) for 1 h.

For most of the analytical work, the column temperature was maintained at 38°C in a thermostated oven. 1,2-Dichloroethane-dichloromethane (1:1, v/v) (mixture A) at a flow-rate of 1.5 ml/min was the mobile phase for the separation of isomeric monoenes, and the same solvent with the addition of 0.5% acetonitrile (mixture B) at a flow-rate of 0.75 ml/min was employed for isomeric dienes and trienes. With samples containing a wide range of components, such as hydrogenated fats, the column was eluted with solvent A for 13 min, then changed in one step to A-B (75:25) with a gradient to 100% B over 20 min.

Derivatization

Lipids were hydrolysed with 1 M potassium hydroxide in 90% ethanol at room temperature overnight. After acidification and extraction, the free fatty acids were converted into the phenacyl derivatives as described by Wood and Lee²⁷. Prior to HPLC analysis, phenacyl esters were purified by elution from a Bond Elut NH₂ column with hexane-diethyl ether (9:1, v/v). The methyl ester derivatives of the fatty acids were prepared from lipid samples by sodium methoxide-catalysed transesterification²⁸. Picolinyl ester derivatives were prepared as described elsewhere²⁹; in brief, the mixed anhydride of each fatty acid with trifluoroacetic acid was reacted with 3-(hydroxymethyl)pyridine (10-fold molar excess) in the presence of 4-dimethylaminopyridine (1.2 molar proportion) as catalyst.

Gas chromatography and gas chromatography-mass spectrometry

For analytical purposes, a Carlo Erba (Crawley, U.K.) Model 4130 capillary gas chromatograph, fitted with split/splitless injection, was equipped with a capillary column 25 m × 0.22 mm I.D.) of fused silica coated with Carbowax 20M (Chrompak, London, U.K.). The temperature was programmed from 165°C (held for 3 min) at 4°C/min to 195°C (held for 20 min). Hydrogen was the carrier gas. Components were quantified by electronic integration. The derivatives were submitted to GC-MS as described elsewhere³⁰ (except that the upper temperature of the column was 10°C lower), *i.e.*, a fused-silica capillary column (25 m × 0.2 mm I.D.), coated with a cross-linked (5% phenylmethyl) silicone (Hewlett-Packard, Wokingham, U.K.), with helium as carrier gas, was programmed from 60 to 220°C at 50°C/min then to 250°C at 1°C/min. The column outlet was connected directly to the ion source of a Hewlett-Packard 5970 mass-selective detector, operated at an ionization energy of 70 eV.

RESULTS AND DISCUSSION

Many different derivatives of fatty acids have been employed for the separation of fatty acids by HPLC³¹, and strongly UV-absorbing esters such as the phenacyl derivatives have the advantage that they can be detected with some sensitivity by their absorbance at 242 nm. In addition, the detector response is to the molar proportion rather than the weight proportion of the compound. Phenacyl derivatives were therefore used here.

Preliminary experience with the silver ion column indicated that excellent results were obtainable with chlorinated solvents as the mobile phase^{21,25}. Dichloromethane gave the best results but was too volatile alone, so 1,2-dichloroethane-dichloromethane (1:1, v/v) was employed initially. This gave baseline separations of the phenacyl derivatives of 9-*trans*-, 11-*trans*-, 9-*cis*- and 11-*cis*-octadecenoic acids. Standard mixtures containing these components were used to check the linearity of the detector response. Initially, this was found to be variable, as were the elution times of the compounds. As the strength of complex formation between the silver ions and double bonds is known to be affected appreciably by temperature³², the column was placed in a thermostated oven. It seems probable that better results would be obtained if this were maintained at a sub-ambient temperature, but 38°C was the lowest stable temperature possible with the equipment available. When the column temperature was

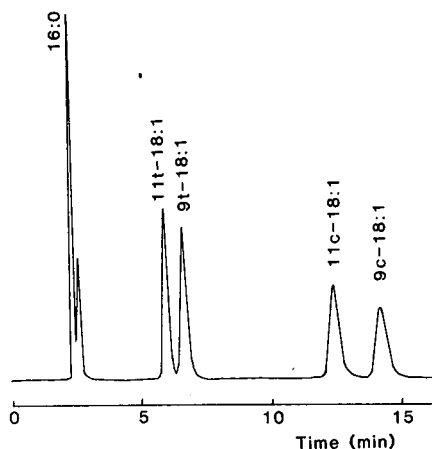


Fig. 1. Separation of the phenacyl derivatives of 16:0, 11*t*-18:1, 9*t*-18:1, 11*c*-18:1 and 9*c*-18:1 by HPLC in the silver ion mode. The column temperature was 38°C and the mobile phase was 1,2-dichloroethane-dichloromethane (1:1, v/v) at a flow-rate of 1.5 ml/min with detection at 242 nm.

kept constant in this way, the response of the detector to all fatty acid derivatives was found to be the same and constant, and relative to mass was rectilinear and passed through the origin (0–200 µg), while the elution times were constant over long periods of use of the column. The nature of the separation obtained with the standard mixture is illustrated in Fig. 1. Excellent resolution is achieved and the peak shapes are close to symmetrical. The results of a comparison of the composition of this standard mixture with that determined by the HPLC procedure (isocratic elution) are listed in Table I. It can be seen that the agreement is indeed excellent and that the standard deviations are small.

Large numbers of positional and geometrical isomers of monoenoic fatty acids are produced during the hydrogenation of vegetable oils and an application of the separation procedure to partially hydrogenated soybean oil is illustrated in Fig. 2.

TABLE I

COMPARISON BETWEEN THE ACTUAL COMPOSITIONS (%) OF STANDARD MIXTURES (DETERMINED GRAVIMETRICALLY) AND THOSE DETERMINED BY ISOCRATIC AND GRADIENT HPLC PROCEDURES (MEAN ± STANDARD ERROR OF FOUR DETERMINATIONS)

c = cis; *t* = trans.

Isocratic elution scheme			Gradient elution scheme		
Fatty acid	Actual	Found	Fatty acid	Actual	Found
16:0	35.13	34.79 ± 0.16	16:0	7.26	6.97 ± 0.04
11 <i>t</i> -18:1	9.91	9.71 ± 0.12	<i>trans</i> -Monoenes	13.04	12.91 ± 0.03
9 <i>t</i> -18:1	22.52	22.18 ± 0.32	<i>cis</i> -Monoenes	13.04	12.21 ± 0.03
11 <i>c</i> -18:1	9.91	10.04 ± 0.50	Dienes	33.15	35.16 ± 0.15
9 <i>c</i> -18:1	22.52	23.29 ± 0.25	Trienes	33.52	32.74 ± 0.15

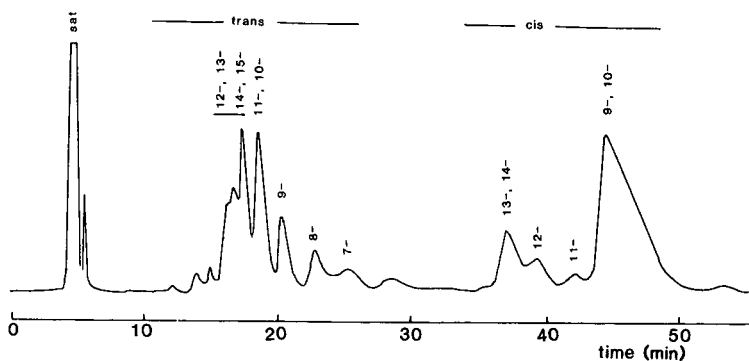


Fig. 2. Separation of the phenacyl derivatives of the saturated and monoenoic fatty acids from hydrogenated soybean oil by HPLC in the silver ion mode. Experimental condition as in the legend to Fig. 1. Abbreviation: sat = saturated fatty acids.

Relatively few standards are available for identification purposes, so peaks were collected as they eluted and were converted into the picolinyl ester derivatives for examination by GC-MS^{30,33}. With such a complex mixture, some overlap is inevitable, but most of the main products were identified and are labelled in Fig. 2. A systematic study of the migration of isomeric octadecenoates on thin layers of silicagel impregnated with silver nitrate indicated a sinusoidal relationship between double bond position and complex formation with the silver ions, with double bonds in positions 5–7 being retained most strongly and those in positions 11–13 being affected less strongly than adjacent isomers³⁴. A broadly similar phenomenon appears to be seen with the silver ion HPLC column in this work. Whereas a superficially similar chromatographic trace was obtained with an HPLC column containing silica gel impregnated with silver nitrate in work reported from another laboratory, the order of elution of the individual components was reportedly different (isomers were not identified by unequivocal means, however)³⁵.

In some samples, fatty acids with a conjugated diene system (predominantly the 9-*cis*,11-*trans* isomer) tended to co-elute with the last of the *trans*-monoenes. A similar phenomenon has been noted with some silver ion TLC systems³⁶.

Similarly, geometrical isomers of linoleic and linolenic acids, the most abundant polyenoic fatty acids in seed oils, are not available commercially, but mixtures can be prepared from the parent compounds by nitric oxide-catalysed isomerization. After conversion to the phenacyl derivatives, the various components eluted slowly with chlorinated solvent alone as the mobile phase, but addition of only 0.5% of acetonitrile speeded up the separation appreciably. The separation achieved with the isomeric dienes derived from linoleic acid is shown in Fig. 3A. Three peaks are apparent, the last of which is the natural 9-*cis*,12-*cis* isomer; the first must be 9-*trans*,12-*trans*-octadecadienoate, and the second peak is presumably a mixture of the 9-*cis*,12-*trans* and 9-*trans*,12-*cis* compounds. The separations are better than those reported from HPLC in the reversed-phase mode²⁷. With the geometrical isomers of linolenic acid and the same isocratic HPLC system, six peaks emerge, the first of which is presumably the all-*trans* isomer and the last the all-*cis* isomer (Fig. 3B). Eight isomers should be formed in the reaction. A substantial amount of chemical degradative work would be

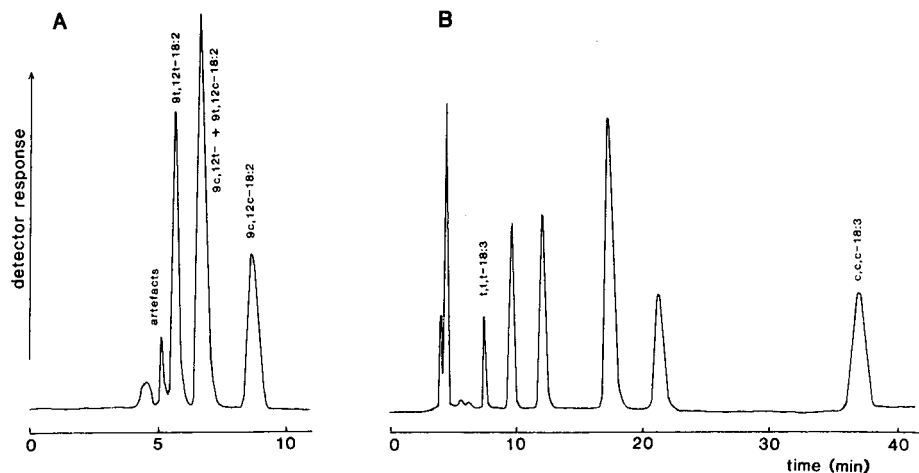


Fig. 3. Separation of the phenacyl derivatives of the geometrical isomers of (A) linoleic and (B) linolenic acids by HPLC in the silver ion mode. The column temperature was 38°C and the mobile phase was 1,2-dichloroethane–dichloromethane–acetonitrile (49.75:49.75:0.5, v/v/v) at a flow-rate of 0.75 ml/min with detection at 242 nm. Note the change of scale on the time axis.

necessary to identify the remaining isomers. In this instance, the resolution was better than that attained by capillary GC³⁷. The potential of the system for the isolation of related isomers, from insect pheromones for example, is obvious.

Although all-*trans*-octadecatrienoate tended to elute with the *cis*-dienes, this was not a problem in practice with samples of hydrogenated fats containing dienoic and trienoic fatty acids. A gradient elution scheme was adapted from the isocratic mobile phases used for monoenes and polyenes for the separation of such mixtures. As discussed above, the response of the detector to different fatty acids is constant, as only the phenacyl group affects this. Provided that the temperature of the column was kept constant, the elution times were reliable. The accuracy and reproducibility were determined by analysing a standard mixture of palmitic, oleic, linoleic and linolenic acids that had been isomerized with nitric oxide as the catalyst. The results (listed in Table I) show excellent agreement between the theoretical and actual value with small standard errors. When the system was applied to real samples, a spurious but constant peak was obtained in blank runs and tended to coincide with the main diene peak. This was eliminated mathematically in calculating the results.

The system can be used to determine the relative proportions of different geometrical isomers in oils and fats of natural or commercial origin. Some examples are listed in Table II. The adipose tissue from ruminant animals contains fatty acids with *trans* double bonds that are formed during biohydrogenation in the rumen. The data obtained here are higher than the mean values recorded elsewhere³⁸, but results from individual sheep can vary appreciably. As a check, samples were also analysed by capillary GC on a column that did not differentiate between geometrical isomers, and the results were mutually consistent.

Several commercial margarines and cooking fats that were examined using the procedure were found to contain between 4.5 and 20.6% of *trans*-monoenes. In these

TABLE II
FATTY ACID COMPOSITIONS (MOL%) OF SOME OILS AND FATS CONTAINING *trans*-UNSATURATION

Source	Fatty acids				
	Saturated	<i>trans</i> -Monoenes	<i>cis</i> -Monoenes	Dienes	Trienes
Sheep adipose tissues:					
Intestinal	60.2	8.2	27.4	3.4	0.8
Subcutaneous	52.5	7.3	36.1	4.1	
Perirenal	61.1	7.2	24.9	6.8	
Margarines:					
A	43.6	17.2	22.8	13.4	3.0
B	45.8	20.6	17.5	12.7	3.4
C	44.8	6.2	39.5	8.3	1.3
D	43.5	4.5	41.9	8.6	1.5
Cooking fats:					
E	42.4	18.8	17.8	20.2	0.7
F	21.3	11.1	44.9	16.2	6.5
Hydrogenated soybean oil:					
Start	13.3	2.0	23.7	53.1	7.8
Mid-point	16.7	25.9	38.1	17.4	1.9
End	28.9	51.0	17.5	2.6	
Hydrogenated rapeseed oil:					
Start	10.0	1.5	54.1	26.2	8.3
Mid-point	9.5	4.9	51.5	23.4	10.7
End	13.8	12.8	56.5	12.7	4.2
Hydrogenated fish oil:					
Start	44.5	4.0	38.6	12.9	
Mid-point	44.3	10.0	32.2	14.6	
End	39.5	16.3	18.6	25.6	

samples, the *trans*-monoenes are formed as by-products of the catalytic hydrogenation process used to alter the physical properties of native vegetable or fish oils. To demonstrate the efficacy of the HPLC methodology, it was applied to some oils taken at various stages of a commercial hydrogenation process. In each instance, the content of *trans*-monoenoic fatty acids is low just after the start of hydrogenation and rises rapidly as the reaction progresses, although the absolute degree of hydrogenation varied among the samples. The soybean oil received much more processing than did the rapeseed oil, which has already a high content of monoenoic fatty acids. The proportion of *trans* fatty acids in the former rises quickly until it is half of the total, while the content of di- and trienoic acids in the soybean oils decreases at the same rate over the period, as expected. With the hydrogenated fish oil, the analytical results indicate only part of the process as the tetra- to hexaenoic components are not eluted by the HPLC system used here. However, there is a rise in the content of *trans*-monoenes as the reaction progresses together with increases in the proportion of dienoic components presumably, formed by partial hydrogenation of the polyunsaturated fatty acids. Hydrogenated fish oils are notoriously difficult to analyse

because of the wide range of chain lengths and positional isomers in the fatty acid constituents. It should be possible to extend the gradient elution system to obtain a more comprehensive analysis with such samples. Again, a broad check on the data by GC gave consistent results.

In continued use over 18 months, the column lost some of its resolving power. This could be restored in part by washing the column with polar solvents such as methanol-acetonitrile mixtures and by injecting fresh silver nitrate on to the column at 1-2 monthly intervals. It was eventually necessary to replace the column.

HPLC in the silver ion mode, with a column of the type described here, therefore has the capacity to provide an alternative means to those in use elsewhere for the separation and analysis of fatty acids with *trans* unsaturation in fats and oils. It may also be of value for the isolation of positional and geometrical isomers for structural or other studies.

ACKNOWLEDGEMENTS

This work was supported in part by a Ministry of Agriculture, Fisheries and Food Grant No. N272. Dr. R. Burt of the Ministry proffered useful advice and encouragement.

REFERENCES

- 1 H. B. S. Conacher, *J. Chromatogr. Sci.*, 14 (1976) 405.
- 2 S. P. Kochhar and J. B. Rossell, *Int. Analyst*, No. 5 (1987) 23.
- 3 C. R. Scholfield, in E. A. Emken and H. J. Dutton (Editors), *Geometrical and Positional Fatty Acid Isomers*, American Oil Chemists' Society, Champaign, IL, 1978, p. 95.
- 4 A. Strocchi, *Riv. Ital. Sostanze Grasse*, 63 (1986) 99.
- 5 A. Strocchi, C. Mariani, F. Camurati, E. Fedeli, S. Baragli, P. Gamba, L. Giro and L. Motta, *Riv. Ital. Sostanze Grasse*, 61 (1984) 499.
- 6 E. G. Perkins, T. P. McCarthy, M. A. O'Brien and F. A. Kummerow, *J. Am. Oil Chem. Soc.*, 54 (1977) 279.
- 7 E. S. van Vleet and J. G. Quinn, *J. Chromatogr.*, 151 (1978) 396.
- 8 J. Sampugna, L. A. Pallansch, M. G. Enig and M. Keeney, *J. Chromatogr.*, 249 (1982) 245.
- 9 H. T. Slover and E. Lanza, *J. Am. Oil Chem. Soc.*, 56 (1979) 933.
- 10 E. Lanza and H. T. Slover, *Lipids*, 16 (1981) 260.
- 11 L. Svensson, L. Sisfontes, G. Nyborg and R. Blomstrand, *Lipids*, 17 (1982) 50.
- 12 J-L. Sebedio and R. G. Ackman, *J. Am. Oil Chem. Soc.*, 60 (1983) 1986.
- 13 A. A. Spark and M. Ziervogel, *J. High Resolut. Chromatogr. Chromatogr. Commun.*, 5 (1982) 206.
- 14 H. B. S. Conacher, J. R. Iyengar and J. L. Beare-Rogers, *J. Assoc. Off. Anal. Chem.*, 60 (1977) 899.
- 15 K. E. J. Dittmar, H. Heckers and F. W. Melcher, *Fette-Seifen-Anstrichm.*, 80 (1978) 297.
- 16 L. Gildenberg and D. Firestone, *J. Assoc. Off. Anal. Chem.*, 68 (1985) 46.
- 17 K. C. Lin, M. J. Marchello and A. G. Fischer, *J. Food Sci.*, 49 (1984) 1521.
- 18 D. M. Ottenstein, D. A. Bartley and W. R. Supina, *J. Chromatogr.*, 119 (1976) 401.
- 19 D. M. Ottenstein, L. A. Witting, P. H. Silvis, D. J. Hometchko and N. Pelick, *J. Am. Oil Chem. Soc.*, 61 (1981) 390.
- 20 W. W. Christie, *Lipid Analysis*, Pergamon, Oxford, 2nd ed., 1982.
- 21 W. W. Christie, *J. High Resolut. Chromatogr. Chromatogr. Commun.*, 10 (1987) 148.
- 22 W. W. Christie, E. Y. Brechany and K. Stefanov., *Chem. Phys. Lipids*, 46 (1988) 127.
- 23 K. Stefanov, K., M. Konaklieva, E. Y. Brechany and W. W. Christie, *Phytochemistry*, 27 (1988) 3495.
- 24 W. W. Christie, E. Y. Brechany and V. K. S. Shukla, *Lipids*, in press.
- 25 W. W. Christie, *J. Chromatogr.*, 454 (1988) 273.
- 26 W. W. Christie, *J. Labelled Compd. Radiopharm.*, 16 (1979) 263.
- 27 R. Wood and T. Lee, *J. Chromatogr.*, 254 (1983) 237.

- 28 W. W. Christie, *J. Lipid Res.*, 23 (1982) 1072.
- 29 W. W. Christie and K. Stefanov, *J. Chromatogr.*, 392 (1987) 259.
- 30 W. W. Christie, E. Y. Brechany, S. B. Johnson and R. T. Holman, *Lipids*, 21 (1986) 657.
- 31 W. W. Christie, *High-Performance Liquid Chromatography and Lipids*, Pergamon, Oxford, 1987.
- 32 L. J. Morris, *J. Lipid Res.*, 7 (1966) 717.
- 33 W. W. Christie, E. Y. Brechany and R. T. Holman, *Lipids*, 22 (1987) 224.
- 34 F. D. Gunstone, I. A. Ismail and M. Lie Ken Jie, *Chem. Phys. Lipids*, 1 (1967) 376.
- 35 R. Battaglia and D. Frohlich, *Chromatographia*, 13 (1980) 428.
- 36 W. W. Christie, *Biochim. Biophys. Acta*, 316 (1973) 204.
- 37 H. Rakoff and E. A. Emken, *Chem. Phys. Lipids*, 31 (1982) 215.
- 38 W. W. Christie, *Prog. Lipid Res.*, 17 (1978) 111.

CHROM. 21 253

SEPARATION OF MAJOR PHOSPHOLIPID CLASSES BY HIGH-PERFORMANCE LIQUID CHROMATOGRAPHY AND SUBSEQUENT ANALYSIS OF PHOSPHOLIPID-BOUND FATTY ACIDS USING GAS CHROMATOGRAPHY

MARKUS SEEWALD* and HANS M. EICHINGER

Versuchsstation Thalhhausen, Lehrstuhl für Tierzucht der Technischen Universität München, D-8051 Kranzberg (F.R.G.)

(Received June 1st, 1988; revised manuscript received January 2nd, 1989)

SUMMARY

A sensitive high-performance liquid chromatographic method for the separation of major phospholipid (PL) classes in biological materials is described. Using this method it was easy to separate P-cholin, P-ethanolamine, P-serine, P-inositol, cardiolipin, sphingomyelin, lyso-P-choline and lyso-P-ethanolamine from skeletal and cardiac muscle samples. The method is based on the simultaneous use of a pH gradient and a polarity gradient. This procedure can easily be modified to optimize the separation of PLs from very different tissues. Subsequent analysis of the PL-bound fatty acids (FAs) by gas chromatography resulted in a well separated FA pattern. Following this FA separation it was possible to recalculate the specific PL content in the original sample.

INTRODUCTION

Phospholipids (PLs) are components of biological membranes with various compositions of the polar head groups and the ester-linked fatty acids (FAs). The physiological properties of membranes, such as consistency, thickness, fluidity and associated functions, are influenced by these structural differences¹. For example, in a normal mammalian muscle cell the following major PL classes are present in various amounts²: P-choline (PC), P-ethanolamine (PE), P-serine (PS), P-inositol (PI), cardiolipin (C), plasmalogen PC and plasmalogen PE. However, the isolation and quantitation of the PL content in complex samples such as muscle is difficult, especially since the PL exist in very small amounts.

Several methods for the separation of PL from a variety of tissues have been reported. Most procedures employ thin-layer chromatography (TLC)³. A common stationary phase for TLC separation is silica gel or alumina⁴. However, modified materials such as diethylaminoethylsilica gel have also been used successfully⁵. Most TLC methods employing mobile phases with mixtures of chloroform–methanol–water are often modified with small amounts of acetic acid, ammonia solution and other

solvents⁶. Detection of PL spots involves oxidation with sulphuric acid or staining with reagents such as molybdenum blue for choline-containing PL⁶. Subsequent determination of the PL content requires methods such as densitometry⁴ or colorimetric measurement of PL phosphorus⁷. Qualitative analysis of TLC procedures in PL studies is simple, cheap and gives good results, but detailed quantification is extremely time consuming and requires extensive technical equipment.

To a more limited extent, column chromatographic⁸ and in recent years high-performance liquid chromatographic (HPLC) techniques have also been applied to the separation of PLs⁹. The methods range from the analysis of PL molecular species with reversed-phase columns^{10,11} to investigations that deal with the analysis of major PL classes using either gradient^{12,13} or isocratic elution systems^{14,15}.

For example, Nissen and Kreysel¹⁶ used a silica gel column and a polarity gradient consisting of acetonitrile and water and were able to separate C, PI, PS, PE, PC and sphingomyelin (S); however, baseline separation was not easily or reliably established. Therefore, with their method efficient collection of the PL fractions was not possible. In contrast, Hurst and Martin¹⁷ investigated an isocratic mobile phase with acetonitrile and methanol containing 1% phosphoric acid on a silica column. This method was developed to separate PL from soya extracts where cardiolipin was not to be isolated. Using this method, cardiolipin is eluted with the solvent front. In general, the high proportion of phosphoric acid in the mobile phase causes technical problems with valve systems. Hence, the methods described to date are inappropriate for the one-step separation of PLs in complex tissues such as muscle.

In this paper we describe an HPLC method for the separation of all major PL classes from biological material and the subsequent accurate gas chromatographic (GC) determination of individual PL-bound fatty acids.

EXPERIMENTAL

Reagents, standards and apparatus

All chemicals were purchased from Merck (Darmstadt, F.R.G.) and PL standards and fatty acid methyl ester (FAME) standards from Sigma (Taufkirchen, F.R.G.). HPLC analysis of PLs was performed on a Merck-Hitachi HPLC system (655A liquid chromatograph, 655A variable-wavelength UV monitor and 655A processor), coupled with a 25 cm × 0.4 cm I.D. Si 60 (5 µm) cartridge (LiChrocard, Merck) and a fraction collector (Model 201, Gilson, Villiers-le-Bel, France). GC analysis of FAMES was achieved using a Hewlett-Packard (Waldbronn, F.R.G.) system (5890 gas chromatograph, split injection, flame ionization detector, 7673 A autosampler, 3393A integrator), equipped with a capillary column (Durabond-Wax, 0.15 µm, 30 m × 0.25 mm I.D.; ICT, Frankfurt, F.R.G.). TLC was performed with Merck pre-coated silica gel 60 F₂₅₄ plates (20 cm × 20 cm; 0.25 mm layer).

Tissue samples and extraction of total lipids

Total lipids were extracted from musculus longissimus dorsi (m.l.d.) near the thirteenth rib, from musculus semimembranosus (m.s.) and from the left heart ventricle (h.v.) of eighteen pigs (average mass 40 kg) using the procedures described by Folch *et al.*¹⁸ and Hallermayer¹⁹. Immediately after slaughtering, samples were weighed (approximately 5 g) in a 100-ml centrifuge tube and quickly homogenized

with 35 ml of chloroform–methanol (1:1, v/v). Following centrifugation for 5 min at 4000 g, the supernatant was collected in a graded extraction burette. This procedure was repeated twice. To the combined supernatants 25 ml of 0.58% sodium chloride solution were added and mixed by inversion. This resulted in a clear two-phase separation with the lower chloroform phase containing the total lipids. An aliquot of the solution containing the lipids was evaporated under nitrogen at 35°C. The resulting total lipid extract was then ready for further analysis.

HPLC analysis

Total lipid extracts were diluted in chloroform–methanol (2:1, v/v) and 20 μ l containing 2 mg of each sample were injected directly into the HPLC unit. Peaks were identified by comparison with the retention times of standard PLs and verification was accomplished by co-injection with standards. A solvent system was established that was based on the simultaneous use of a pH gradient and a polarity gradient. This system consisted of several steps: (1) elution with acetonitrile for 5 min; (2) elution with acetonitrile containing 0.2% phosphoric acid for 10 min; and (3) between the 15th and 25th min elution with acetonitrile containing 0.2% phosphoric acid changing continuously to methanol containing 0.2% phosphoric acid. These changes to the mobile phase were made without interruption of the flow. The flow-rate was constant at 1 ml/min. The eluted lipids were detected at 205 nm at room temperature. The PL fractions were collected automatically (electronic peak detection) and then prepared for further analysis. Elution times varied only within 3%. Complete equilibration of the system was achieved within 30 min. The purity of the individual PL fractions was checked by TLC on silica gel plates using chloroform–methanol–water (75:22:3, v/v/v) as the solvent.

Transesterification

The PL-bound FAs were converted into FAMES according to the procedure of Shehata *et al.*²⁰. The single PL fractions were evaporated from the mobile phase and 0.5 ml of a solution of 0.5 M methanolic sodium methylate, light petroleum and diethyl ether (1.5:6:2.5, v/v/v) was added. The solution was gently mixed and left at room temperature for 3 min. Using this procedure, transesterification of the fatty acids was determined by TLC to be nearly 100%. With S, complete esterification can only be performed by the boron trifluoride method or appropriate acidic methanolysis²¹.

Gas chromatography

A 2- μ l sample of each PL fraction was automatically injected into the gas chromatograph with a splitting ratio of 1:50. The temperature program used started at 100°C, was increased at 10°C/min to 240°C, and then held for 3 min at 240°C. The injection port temperature was 240°C and the detector temperature 250°C. The hydrogen flow-rate in the column was 1.8 ml/min. Peaks were identified by comparison with standards and by a common spiking procedure²². The amount of each fatty acid was calculated using an internal standard method; C₁₇ was selected as the internal standard because in several test runs, of all PLs from the meat samples none of this fatty acid could be detected.

$$\frac{n \cdot \Phi MW_{FA} \cdot 100}{MW_{PL}} = \% FA_{PL}$$

(6) Determination of the absolute amount of PL:

$$\frac{\mu g_{\Sigma FA}}{\% FA_{PL}} \cdot 100 = \text{absolute amount of PL in } \mu g/\text{mg total extract}$$

RESULTS

A baseline separation of C, PI, PS, PE, PC, S, lyso-P-ethanolamine (LPE) and lyso-P-choline (LPC) was achieved in less than 50 min. Figs. 1 and 2 show the clear separation of these PLs. Hence, automatic fraction collection was possible, which allowed further analysis of the individual PLs by GC. Triglycerides and other non-polar lipids eluted with the solvent front and did not disturb the PL separation. The retention times of the individual PLs were highly reproducible [coefficient of variation (C.V.) < 1%], and C.V.s of the peak areas in the linear range were between 0.8% (PC) and 3.8% (S).

The resolution of this method makes the quantitative comparison of individual PL contents possible. For example the PL composition of total lipid extracts of different tissues of pigs were found to be significantly different (Table I). PC and PE were the predominant fractions. The LPC and LPE fractions represented the plasmalogen content of the respective PIs. The lysis was assumed to be partly an effect of the low pH of the mobile phase.

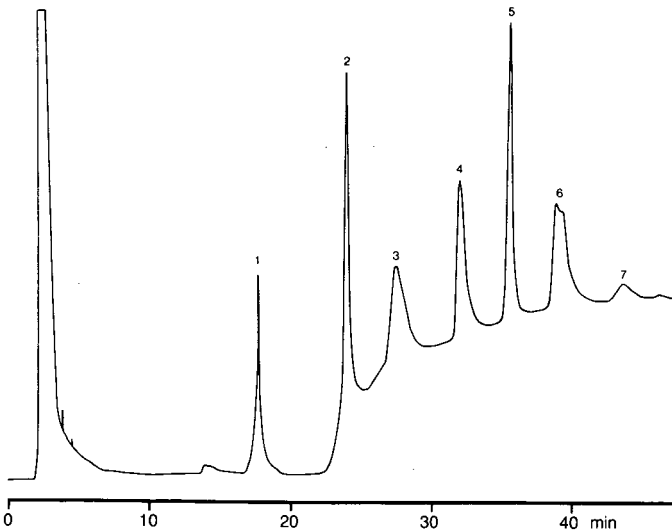


Fig. 1. HPLC of phospholipid standards: 1 = 4 μ g cardiolipin; 2 = 5 μ g P-inositol; 3 = 5 μ g P-serine; 4 = 4 μ g P-ethanolamine; 5 = 6 μ g lyso-P-ethanolamine; 6 = 5 μ g P-choline; 7 = 3 μ g sphingomyelin.

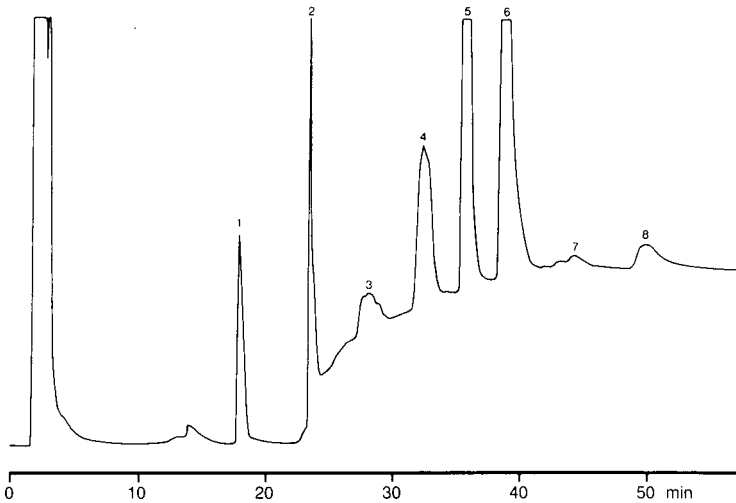


Fig. 2. HPLC of a phospholipid separation from pig muscle extract (m.l.d.); 1 = cardiolipin; 2 = P-inositol; 3 = P-serine; 4 = P-ethanolamine; 5 = lyso-P-ethanolamine; 6 = P-choline; 7 = sphingomyelin; 8 = lyso-P-choline.

The GC analysis of FAMES was completed in 15 min. The elution of the FAMES corresponded to their chain length and the number of double bonds within each molecule (Figs. 3 and 4). The retention times and the evaluation of the quantitative internal standard method were highly reproducible: the C.V.s of peak amounts were

TABLE I

PHOSPHOLIPID COMPOSITION (%) OF THE TOTAL LIPID EXTRACTS OF DIFFERENT TISSUES OF PIGS ($n = 18$)

Phospholipid	Parameter ^a	m.l.d. (a)	m.s. (b)	h.v. (c)	a:b ^b	a:c ^b	b:c ^b
Cardiolipin	LSM	16.20	12.40	13.80			
	SE	1.80	1.84	1.78			
P-Inositol	LSM	10.10	8.20	7.20	*	*	
	SE	0.60	0.60	0.58			
P-Serine	LSM	8.40	7.30	5.70		*	
	SE	0.65	0.65	0.63			
P-Ethanolamine	LSM	11.30	12.60	17.50		**	*
	SE	1.13	1.13	1.10			
Lyso-P-ethanolamine	LSM	11.00	11.10	14.70		**	**
	SE	0.90	0.90	0.90			
P-Choline	LSM	27.30	30.60	19.20		*	**
	SE	2.21	2.21	2.14			
Sphingomyelin	LSM	6.70	7.90	6.30			
	SE	0.96	0.96	0.93			
Lyso-P-choline	LSM	9.00	9.90	15.60		*	*
	SE	1.20	1.20	1.16			

^a LSM = least-square mean; SE = standard error.

^b * $P < 0.05$; ** $P < 0.01$.

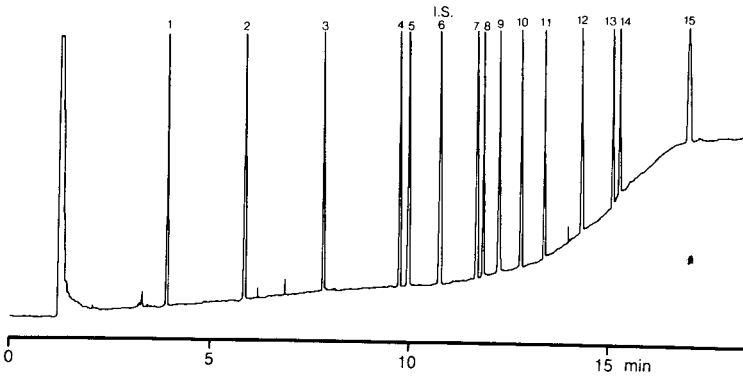


Fig. 3. Separation of FAME standards by GC: 1 = $C_{10:0}$; 2 = $C_{12:0}$; 3 = $C_{14:0}$; 4 = $C_{16:0}$; 5 = $C_{16:1}$; 6 = $C_{17:0}$ [internal standard (I.S.)]; 7 = $C_{18:0}$; 8 = $C_{18:1}$; 9 = $C_{18:2}$; 10 = $C_{18:3}$; 11 = $C_{20:0}$; 12 = $C_{20:4}$; 13 = $C_{22:0}$; 14 = $C_{22:1}$; 15 = $C_{24:0}$. Each peak represents 30 ng of substance.

between 0.2% ($C_{18:0}$) and 1.1% ($C_{14:0}$). Quantitation of the FA composition of different PLs was therefore possible. For example, the FA compositions of the same PL isolated from different tissues were significantly different (Table II). The predominant FAs of PLs isolated from the musculus longissimus dorsi and the cardiac muscle were $C_{16:0}$, $C_{18:0}$, $C_{18:1}$, $C_{18:2}$ and $C_{20:4}$.

Phosphorimetry showed a PL content in the total lipid extract of 41.4% for the musculus longissimus dorsi, 39.8% for the musculus semimembranosus and 66.7% for the cardiac muscle. In comparison, the PL contents in the total lipid extracts calculated via FAs were 36.8% for the musculus longissimus dorsi, 38.7% for the musculus semimembranosus and 71.2% for the cardiac muscle.

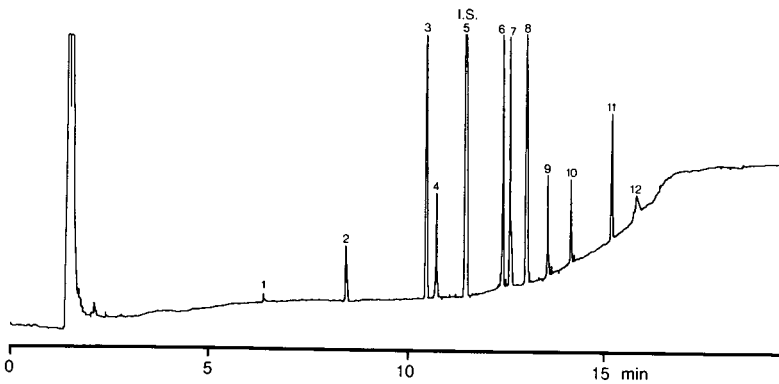


Fig. 4. GC separation of FAMES from the P-choline fraction of pig muscle (m.l.d.) after transesterification: 1 = $C_{12:0}$; 2 = $C_{14:0}$; 3 = $C_{16:0}$; 4 = $C_{16:1}$; 5 = $C_{17:0}$ (I.S.); 6 = $C_{18:0}$; 7 = $C_{18:1}$; 8 = $C_{18:2}$; 9 = $C_{18:3}$; 10 = $C_{20:0}$; 11 = $C_{20:4}$; 12 = $C_{22:0}$.

TABLE II

FATTY ACID COMPOSITION (%) OF CARDIOLIPIN AND P-ETHANOLAMINE ISOLATED FROM MUSCULUS LONGISSIMUS DORSI (m.l.d.) AND LEFT HEART VENTRICE (h.v.) OF THE PIG

Fatty acid	Cardiolipin			P-Ethanolamine		
	m.l.d.	h.v.	Diff. ^a	m.l.d.	h.v.	Diff. ^a
10:0	0.2	0.5		0.1	1.0	
12:0	0.2	0.0		0.2	0.2	
14:0	2.5	2.1		1.2	0.6	
16:0	20.3	7.8	**	8.3	7.5	
16:1	3.5	4.8		1.1	0.8	
18:0	10.0	6.6		33.7	33.6	
18:1	24.4	11.5	**	14.7	7.8	**
18:2	32.3	61.1	**	20.8	15.2	**
18:3	0.9	1.7		1.0	1.1	
20:0	2.1	0.6	*	0.7	0.4	
20:4	3.2	2.6		16.6	30.7	**
22:0	0.3	0.2		0.5	0.5	
22:1	0.0	0.3		1.0	0.5	
24:0	0.0	0.1		0.1	0.2	

^a * $P < 0.05$; ** $P < 0.01$.

DISCUSSION

The method described here for the isolation of PLs and the subsequent determination of FA contents has several major advantages. It allows one to work in a preparative manner and to collect all peaks with the necessary high purity for further quantitative analysis. The very easy preparation of the samples eliminates time-consuming pre-cleaning or pre-separation steps with the total lipid extracts. There is also no need for any derivatization procedures for increased detector sensitivity. The total PL separation can be carried out in a closed system with only one column and without further technical effort. Plasmalogen derivatives of choline and ethanolamine can be determined automatically because the corresponding lyso products are produced at low pH of the mobile phase, as proposed by Kawasaki *et al.*²⁵. Therefore, no subsequent hydrolysis with concentrated hydrochloric acid²⁶ is necessary. In order to detect naturally occurring lyso products we used first a gradient system at pH 6.8, where only after treatment with concentrated HCl fumes were lyso products detected (Fig. 5).

The coupled analysis of PL-bound FA using GC not only provides information about the average FA pattern of the individual PLs, but also allows a precise determination of the original amount of PLs. UV sensitivity also depends on the number of double bonds in the PL-bound FA molecules, hence the calibration of the HPLC-UV detection signal is only valuable in the rare case of a uniform FA pattern. Different FA patterns of PL standards and samples certainly influence the quantitative results. Other available techniques such as micro phosphorimetric methods are very time consuming, not easy to handle and show much larger variations. However, we

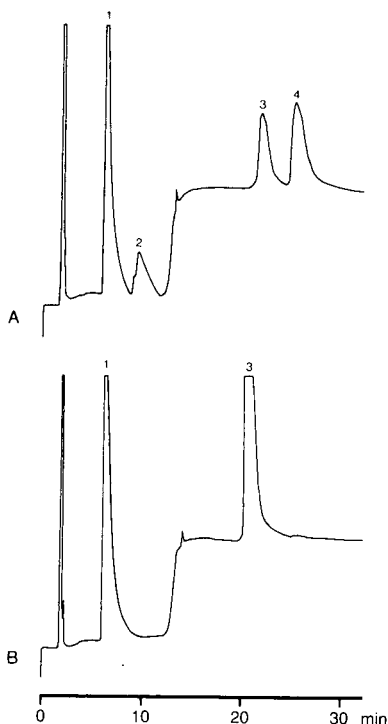


Fig. 5. HPLC of P-choline (1) and P-ethanolamine (3) and the appropriate plasmalogens lyso-P-choline (2) and lyso-P-ethanolamine (4) after treatment (A) with and (B) without concentrated HCl fumes. Mobile phase, initially 100% acetonitrile, changing between the 8th and 11th min to methanol-water (9:1). Flow-rate, constant at 1 ml/min. Lipids were detected at 205 nm at room temperature after separation on a 12.5 cm \times 0.4 cm I.D. (5 μ m) NH_2 -cartridge (LiChrocard).

found a good correlation ($r = 0.85$) between the calculated amounts of PLs from HPLC-GC and those obtained by phosphorimetry. Nevertheless, the recalculation of the PL content from the FA pattern appears to be more precise and useful in many instances.

It was possible to work in a preparative manner and to use large amounts of samples without technical problems. The very small amount of phosphoric acid in the mobile phase did not cause valve sticking or sealing problems and in general the overall column stability was high.

A further advantage of the method described here is the possibility to easily modify the method for specific needs. For example, if the user is more interested in the PLs which elute late, such as PC and PE, there is the possibility of creating a gradient with an earlier polarity shift and/or a lower pH. If there is more interest in PLs which elute early, such as C and PI, the gradient can simply be shortened in the second half in order to save time.

Finally, the amounts and patterns of PLs and FAs from different tissues of pigs obtained by our method were comparable to the results obtained by other workers using different methods²⁷.

In conclusion, the procedure described is a sensitive, rapid and flexible method for the determination of PLs and FAs in mammalian muscle and can easily be adapted to other biological materials.

ACKNOWLEDGEMENTS

We thank Petra Sölch for excellent technical assistance, Heimo Scherz and Franz Heinzl for expert analytical help and Karin Markert for typing the manuscript. This work was supported by the Hanns-Seidel-Stiftung and the Deutsche Forschungsgemeinschaft.

REFERENCES

- 1 L. A. Morson and M. T. Clandinin, *Nutr. Res.*, 5 (1985) 1113.
- 2 H. M. Eichinger, M. Seewald and P. A. Iaizzo, in J. F. Quirke and H. Schmid (Editors), *Control and Regulation of Animal Growth*, PUDOC, Wageningen, 1988, pp. 191–200.
- 3 W. W. Christie, *Z. Lebensm.-Unters.-Forsch.*, 181 (1985) 171.
- 4 F. M. Helmy and M. H. Hack, *J. Chromatogr.*, 374 (1986) 61.
- 5 U. H. Do and S.-L. Lo, *J. Chromatogr.*, 381 (1986) 233.
- 6 E. Stahl, *Dünnschicht-Chromatographie*, Springer, Berlin, Göttingen, Heidelberg, 1962.
- 7 P. R. Gentner and A. Haasemann, *Fette-Seifen-Anstrichm.*, 9 (1979) 357.
- 8 N. Zöllner, *Untersuchung und Bestimmung der Lipoide im Blut*, Springer, Berlin, Heidelberg, New York, 1965.
- 9 K. Aitzetmüller, *Fette-Seifen-Anstrichm.*, 8 (1984) 318.
- 10 M. Kito, H. Takamura, H. Narita and R. Urade, *J. Biochem.*, 98 (1985) 327.
- 11 A. D. Postle, *J. Chromatogr.*, 415 (1987) 241.
- 12 L. A. Dethloff, L. B. Gilmore and G. E. R. Hook, *J. Chromatogr.*, 382 (1986) 79.
- 13 P. Juaneda and G. Rocquelin, *Lipids*, 21 (1986) 239.
- 14 A. G. Andrews, *J. Chromatogr.*, 336 (1984) 139.
- 15 G. M. Patton, J. M. Fasulo and S. J. Robins, *J. Lipid Res.*, 23 (1982) 190.
- 16 H. P. Nissen and H. W. Kreysel, *J. Chromatogr.*, 276 (1983) 29.
- 17 W. J. Hurst and R. A. Martin, *J. Am. Oil Chem. Soc.*, 61 (1984) 1462.
- 18 J. M. Folch, G. H. Less and S. Sloane, *J. Biol. Chem.*, 226 (1957) 497.
- 19 R. Hallermayer, *Dtsch. Lebensm.-Rundsch.*, 10 (1976) 356.
- 20 A. Y. Shehata, J. deMan and J. C. Alexander, *Can. Inst. Food Technol. J.*, 3(3) (1970) 85.
- 21 R. C. Gaver and C. C. Sweeley, *J. Am. Oil Chem. Soc.*, 42 (1965) 294.
- 22 M. Seewald, H. M. Eichinger and H. Scherz, *Meat Sci.*, 19 (1987) 101.
- 23 P. R. Gentner, I. Dieterich and M. Bauer, *Fette-Seifen-Anstrichm.*, 1 (1982) 15.
- 24 C. H. Fiske and Y. Subbarow, *J. Biol. Chem.*, 66 (1925) 375.
- 25 T. Kawasaki, J. Kambayashi, M. Sakon, T. Ohshiro and T. Mori, *Thromb. Res.*, 42 (1986) 461.
- 26 S. S. Chen and A. J. Kou, *J. Chromatogr.*, 232 (1982) 237.
- 27 H. J. Oslage, U. Petersen and A. Seher, *Fette-Seifen-Anstrichm.*, 85 (1983) 177, 215, 295.

CHROM. 21 313

ANALYSIS OF WARFARIN AND ITS METABOLITES BY REVERSED-PHASE ION-PAIR LIQUID CHROMATOGRAPHY WITH FLUORESCENCE DETECTION

Y. W. J. WONG^a and P. J. DAVIS*

Division of Medicinal Chemistry, College of Pharmacy, University of Texas at Austin, Austin, TX 78712 (U.S.A.)

(Received January 11th, 1989)

SUMMARY

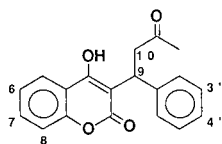
A high-performance liquid chromatographic method was developed for the determination of warfarin and its metabolites (diastereomeric warfarin alcohols and 6-, 7-, 8-, 4'- and 3'-hydroxywarfarin) in microbial cultures. Ion-pair chromatography with tetrabutylammonium ion as the counter ion allowed for the complete resolution of all compounds at pH 7.5 on a reversed-phase (C₁₈) column, thus permitting direct fluorescence detection without the use of post-column pH switching techniques. Analysis of cell suspension cultures of the fungus *Cunninghamella elegans* (ATCC 36112) indicated that this organism metabolizes warfarin to all known mammalian metabolites, plus the previously unreported 3'-hydroxywarfarin. Detection limits for all compounds were in the low nanogram range.

INTRODUCTION

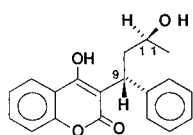
Warfarin [3-(α -acetylbenzyl)-4-hydroxycoumarin, **1**; Fig. 1] has been used extensively both as a rodenticide¹ and as a clinically effective oral anticoagulant². More recently, this compound has been exploited as a probe to study the multiplicity of cytochrome P-450 isozymes from a variety of mammalian sources³⁻⁶. Because of its clinical, pharmacological and biochemical importance, a number of sophisticated chromatographic methods have been developed to quantitate warfarin (**1**) and its metabolites (**2-11**) in various biological matrices⁷⁻¹¹.

Most notable of these analytical methods are the high-performance liquid chromatographic (HPLC) assay of Fasco and co-workers^{7,8} and the gas chromatographic-mass spectrometric (GC-MS) assay of Bush *et al.*¹¹. The HPLC method of Fasco utilizes either an isocratic⁷ or gradient⁸ elution technique with UV absorption detection at 313 nm. While offering high selectivity and complete resolution of all metabolites, this assay suffers from the inherent sensitivity limitation of UV photometric

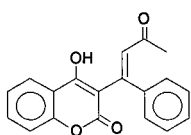
^a Present address: Department of Pharmacology, Division of Clinical Pharmacology, University of Texas Health Science Center at San Antonio, San Antonio, TX 78284, U.S.A.



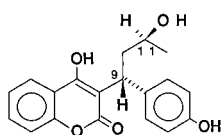
1. Warfarin
2. 6-Hydroxywarfarin
3. 7-Hydroxywarfarin
4. 8-Hydroxywarfarin
5. 4'-Hydroxywarfarin
6. 3'-Hydroxywarfarin
7. 9-Hydroxywarfarin
8. 10-Hydroxywarfarin



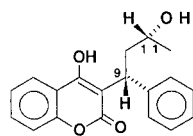
9. RS/SR-Alcohol
(9R,11S- Shown)



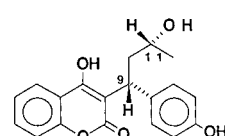
11. Dehydrowarfarin



12. RS/SR-Int. Std. A
(9R,11S- Shown)



10. RR/SS-Alcohol
(9R,11R- Shown)



13. RR/SS-Int. Std. B
(9R,11R- Shown)

Fig. 1. Structures of warfarin (1), warfarin metabolites (2–11) and internal standards (12, 13).

detection. The GC–MS assay of Bush *et al.*¹¹ employs a high-resolution capillary column to achieve separation of all compounds. Although excellent sensitivity is afforded by MS selected ion detection, specialized instrumentation and deuterated internal standards are required for warfarin and each metabolite.

Warfarin exhibits a strong native fluorescence¹²; thus, HPLC separation with fluorescence detection should make possible the sensitive analysis of warfarin and its metabolites. In most reports, however, full exploitation of warfarin's fluorescence has been precluded by the use of acidic mobile phases which quench the fluorescence⁹. This problem can be resolved by using post-column pH-switching techniques which alter the pH of the mobile phase with post-column reagents as it enters the detector, and has been described for the normal-phase HPLC determination of warfarin and its metabolites^{9,10}. However, such methods are not suitable for the analysis of microbial cultures with high concentrations of residual warfarin in comparison to levels of warfarin metabolites. Since warfarin elutes before its metabolites in normal-phase chromatography, the large amount of warfarin introduced would overload the HPLC column and interfere with the quantitation of the metabolites.

Ion-suppression techniques with acidic mobile phases have been used for reversed-phase HPLC of warfarin and its analogues which are 4-enols and thus act as

weak acids. At neutral pH these compounds are totally ionized and do not chromatograph efficiently on reversed-phase columns. Ion-pair chromatography with a cationic counter ion and a mobile phase buffered at pH 7.5 to afford complete ionization of all analytes offers an alternative approach for the chromatography of these compounds. The use of mobile phases at a pH above 6.5 also permits direct fluorescence detection without the experimental complexity of post-column pH-switching techniques. This method has been described previously for the analysis of coumarin rodenticide residues in animal tissue¹³ and rodenticide concentrates¹⁴. The present report describes the development of a highly sensitive reversed-phase ion-pair HPLC method with direct fluorescence detection for the analysis of warfarin (**1**) and its major metabolites (**2-6**, **9**, **10**) in microbial culture.

EXPERIMENTAL

Chemicals and reagents

All reagents are analytical reagent grade or higher in quality. Solvents for HPLC were HPLC grade (OmniSolv, MCB Manufacturing Chemists, Cincinnati, OH, U.S.A.). Racemic warfarin was obtained from Sigma (St. Louis, MO, U.S.A.). Tetrabutylammonium phosphate (1.0 M solution) was purchased from Aldrich (Milwaukee, WI, U.S.A.). Phenolic warfarin metabolites [6-, 7-, 8-, 4'- and 3'-hydroxywarfarin (**2-6**)] were synthesized by the methods of Hermodson *et al.*¹⁵ or Bush and Trager¹⁶. Dehydrowarfarin (**11**) was prepared by cuprous chloride oxidation of warfarin⁸. Warfarin alcohols (**9**, **10**) and the internal standard 4'-hydroxywarfarin alcohols (**12**, **13**) were synthesized by sodium borohydride reduction of warfarin (**1**) and 4'-hydroxywarfarin (**5**) respectively in water¹⁷. It should be noted that warfarin is racemic, based upon the presence of a chiral center at C-9; thus, reduction at C-11 (with the generation of a second chiral center) yields two chromatographically resolvable diastereomeric sets of enantiomers. Consequently, compounds **9** and **12** (Fig. 1) depict their respective 9*R*,11*S*/9*S*,11*R*-racemates (only one enantiomer is shown for convenience), while compounds **10** and **13** depict their respective 9*R*,11*R*/9*S*,11*S*-racemates (again, only one enantiomer is shown in each case for convenience). The mass spectrum of the synthetic 4'-hydroxywarfarin alcohol (**12/13**) was consistent with that expected for this compound¹⁸, and was used as the internal standard without further purification.

*Preparation of cell suspensions of *Cunninghamella elegans* (ATCC 36112)*

The fungus *Cunninghamella elegans* (ATCC 36112) was maintained on refrigerated (4°C) slants of Sabouraud-maltose agar (Difco, Detroit, MI, U.S.A.) and transferred to fresh slants every six months to maintain viability. This fungus was grown according to a two-stage fermentation procedure. The surface growth of a slant was used to inoculate one Stage-1 Bellco-Delong flask (1 l) containing 200 ml of growth medium. The medium used in these experiments consisted of the following: dextrose, 20 g; soybean meal (20 mesh; Capitol Feeds, Austin, TX, U.S.A.), 5 g; sodium chloride, 5 g; potassium phosphate (dibasic), 5 g; yeast extract (Difco), 5 g; distilled water, 1000 ml; pH adjusted to 7.0 with 6 M hydrochloric acid. The medium was sterilized in individual flasks at 121°C for 15 min. After inoculation, the Stage-1 flask was incubated for 72 h at 27°C and 250 rpm in a G-25 Environmental Shaker (New Bruns-

wick Scientific Co., Edison, NJ, U.S.A.) at which time 10 ml of growth was used to inoculate each Stage-2 flask (1 l) containing 200 ml of fresh medium. After incubation for 24–48 h, the fungal cells were harvested by filtration, rinsed by resuspension in distilled water followed by filtration. This process was repeated three times. Each cell suspension culture was prepared by suspending 4 g of cell pellets in 20 ml of pH 6.7 phosphate buffer (0.5 M) in a 125-ml Bellco-Delong flask. After pre-incubation for 1 h under the conditions specified above, 6 mg of warfarin as the potassium salt in 200 μ l sterile water was added to each flask to give a final substrate concentration of 0.3 mg/ml of buffer, and the incubation was resumed. One whole flask of cell suspension was harvested at 2, 6, 12, 24 and 48 h after substrate addition. Samples were filtered to remove fungal cells, and filtrates were stored at -20°C until analysis.

Instrumentation and HPLC conditions

HPLC was conducted using a Beckman Model 110A pump with a Schoeffel Model FS 970 fluorometric detector. The excitation wavelength was 290 nm and emission was measured in the presence of an emission filter (No. 389). A Hitachi model 100-10 variable-wavelength UV detector was also used for certain experiments, as specified (wavelength 310 nm). Chromatograms were recorded with a Hewlett-Packard Model 3390A reporting integrator. The mobile phase consisted of methanol–tetrahydrofuran–1.0 M aqueous TBA⁺–5 mM aqueous ammonium phosphate (pH 7.5) (30:7:1:62) and was prepared by filtering individual components through glass filter pads, GF/F grade (Whatman, Clifton, NJ, U.S.A.), mixing and degassing ultrasonically before use. The 5 mM ammonium phosphate buffer was prepared by adjusting the pH of a 5 mM potassium phosphate solution to pH 7.5 with ammonium hydroxide. The column was a Beckman ODS 5- μ m (C₁₈), 250 \times 4.5 mm I.D., eluted at a solvent flow-rate of 1.0 ml/min.

Excitation and emission spectra of warfarin were generated on an Aminco-Bowman spectrophotofluorimeter (American Instrument Co., Silver City, MD, U.S.A.).

Extraction of warfarin and metabolites

The extraction method was designed for pH 6.7 microbial cell suspensions. The sample filtrate (4 ml), distilled water (200 μ l), and the internal standard (4'-hydroxy-warfarin alcohols, 400 ng as the potassium salt in 100 μ l of water) were added to an extraction tube (125 \times 16 mm). The solution was extracted with 10% dichloromethane in cyclohexane (2 \times 4 ml). The organic layer was removed by an aspirator and discarded. The residual aqueous phase was then extracted with ethyl acetate (5 ml). The organic layer was then back extracted with 0.1 M potassium hydroxide (2 ml), and the organic layer discarded. The aqueous phase was acidified with 5 M hydrochloric acid (1 ml) and extracted with diethyl ether (5 ml). The ethereal layer was taken to dryness under nitrogen, and reconstituted with 250 μ l of mobile phase. A total of 50–200 μ l of this solution was injected into the chromatograph.

Preparation of standard curves

A standard solution containing all alcohol and phenolic warfarin metabolites (2–6, 9, 10) was prepared by dissolving 5 mg of each metabolite in 1000 ml of water with the aid of a minimum amount of 0.1 M potassium hydroxide. This solution

(1000 ng/200 μ l) was further diluted to give four additional solutions containing 400, 200, 80 and 40 ng of each metabolite in 200 μ l. Standard curves were constructed using five blank cell suspension filtrate samples of 4.0 ml each spiked with 200 μ l of one of the five standard solutions. These samples were subjected to the extraction and HPLC analysis described above. The resultant peak area ratios (metabolite/internal standard) were plotted *versus* metabolite concentration in ng/ml (Fig. 3).

Selection of excitation wavelength

A solution of warfarin, its phenolic metabolites and warfarin alcohols at a concentration of 100 ng/ml in mobile phase was prepared. A total of 250 μ l of this solution was injected into the HPLC system. The peak area as recorded on the integrator was taken as the detector response for each compound at a specific excitation wavelength. The excitation wavelengths investigated ranged from 280 to 325 nm. The detector response for each compound then was normalized to the optimal excitation wavelength at 290 nm (Table I).

TABLE I

RELATIVE FLUORESCENCE INTENSITY OF WARFARIN AND METABOLITES AS A FUNCTION OF EXCITATION WAVELENGTHS

Compound	Normalized fluorescence intensity ^a							
	Excitation wavelength (nm)							
	280	285	290	295	300	310	320	325
Warfarin (1)	64	93	100	91	78	47	21	16
6-Hydroxywarfarin (2)	61	92	100	94	83	49	25	20
7-Hydroxywarfarin (3)	78	104	100	88	82	63	33	25
8-Hydroxywarfarin (4)	61	92	100	93	81	42	17	11
4'-Hydroxywarfarin (5)	73	111	100	91	76	48	22	17
3'-Hydroxywarfarin (6)	78	103	100	88	74	45	22	15
RS/SR-Warfarin alcohol (9)	67	97	100	95	80	49	23	17
RR/SS-Warfarin alcohol (10)	54	80	100	79	68	44	19	15

^a Each value was normalized for the fluorescence response at the excitation and emission wavelength of 290 and >389 nm, respectively.

RESULTS AND DISCUSSION

Ion-pair chromatography

Preliminary experiments using methanol, pH 7.5 phosphate buffer, and a reversed-phase C₁₈ column showed that tetrabutylammonium ion (TBA⁺) could be used as a counter ion for the ion-pair chromatography of warfarin and its metabolites. With the exception of 6- and 7-hydroxywarfarin which co-eluted, baseline resolution of all compounds was achieved with excellent peak shape. The selectivity of an ion-pair chromatographic system is controlled by the stationary phase, the pH of the mobile phase, the organic modifiers, and the nature of the counter ion. In an attempt to resolve the 6- and 7-hydroxywarfarin, these parameters were systematically al-

tered while monitoring the selectivity of the chromatographic system. No selectivity effect was observed as the concentration of the TBA^+ was increased, but the capacity factor of all compounds increased accordingly. In addition, very little improvement was obtained with either a C_8 column as the stationary phase, or with tetramethylammonium ion (TMA^+) as the counter ion. Increasing the pH beyond 8.0 yielded a gradual improvement in resolution; at pH 10, an almost baseline resolution of 6- and 7-hydroxywarfarin was achieved. The use of a pH above 7.5 is, however, not feasible because of silica dissolution and column deterioration.

Variation in the organic modifiers yielded the desired resolution. Among the organic modifiers investigated, tetrahydrofuran provided unusual selectivity, and a mixture of methanol and tetrahydrofuran ultimately afforded complete resolution of all analytes. The final chromatographic system chosen consists of a $5\text{-}\mu\text{m}$ C_{18} stationary phase, with a mobile phase consisting of methanol-tetrahydrofuran- 1.0 M tetrabutylammonium phosphate- 5 mM ammonium phosphate (pH 7.5) (30:7:1:62) (Fig. 2). The aliphatic hydroxywarfarin metabolites (7 and/or 8) were not included because analytical standards were not available. Dehydrowarfarin (11) was also not included in the final assay because this metabolite does not exhibit fluorescence in the mobile phase.

An anticipated difficulty encountered with this chromatographic system was the gradual deterioration of column performance over a two-week period. As described by Gloor and Johnson¹⁹, a mobile phase pH of 7.5 (representing the pH limit of column stability) in combination with TBA^+ as the counter ion (although at a concentration much higher than that used in the current study) accelerate column degeneration. The problem was overcome by using a guard column ($75 \times 4.5\text{ mm}$ I.D.) packed with silica ($40\text{ }\mu\text{m}$), installed between the HPLC pump and injector to presaturate the mobile phase with silica.

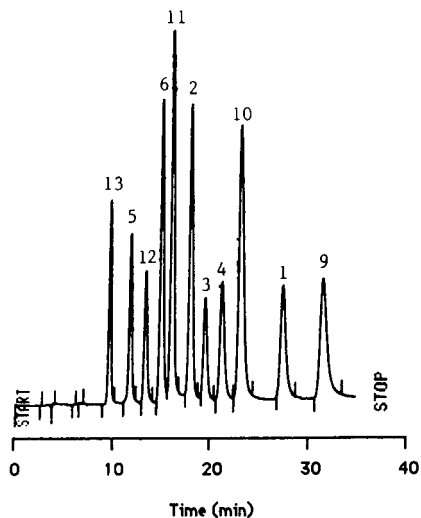


Fig. 2. Reversed-phase ion-pair HPLC separation of warfarin (1), metabolite standards (2-6, 9, 10), and internal standard (11, 12). See text for chromatographic conditions. Structure numbers are as specified in Fig. 1.

Selection of excitation wavelength

In order to exploit the sensitivity of fluorimetric detection, careful determination of the optimum excitation and emission wavelengths was undertaken. Analysis of the excitation/emission spectrum of warfarin generated with the Aminco-Bowman spectrofluorimeter indicated maximum emission at 395 nm when excited at 325 nm in the mobile phase, in close agreement with the wavelengths selected by Hunter²⁰ for the fluorescent detection of warfarin. However, preliminary HPLC investigations with these excitation and emission wavelengths showed that fluorimetric detection did not produce superior sensitivity over UV photometric detection, probably because the fluorimetric detector and spectrofluorimeter employed different lamp sources to provide energy of excitation. While the spectrofluorimeter was equipped with an xenon arc lamp, the HPLC fluorimetric detector relied on a deuterium lamp which provided very little excitation energy beyond 300 nm. The optimal wavelength of excitation for the HPLC fluorescence detector in use was subsequently determined experimentally. This was carried out by monitoring the fluorescence response of the detector for each compound at different excitation wavelengths between 280 and 325 nm. The results shown in Table I indicate that the best overall sensitivity was obtained with excitation at 290 nm. An even greater sensitivity would be obtainable on a detector equipped with a different lamp source because the emission spectrum of warfarin generated with the spectrofluorimeter indicates that the quantum yield can be doubled by excitation at 325 nm.

Extraction procedures

While offering excellent resolution of all compounds, this HPLC method did not allow for the quantitation of *RS/SR*-warfarin alcohol (9) in some microbial cultures with concentrations of residual warfarin substantially higher than those of its metabolites. This is because warfarin eluted just prior to this metabolite and the two chromatographic peaks tended to overlap at high warfarin concentration. Consequently, an extraction scheme was developed which preferentially removed warfarin from the microbial cultures, but allowed the metabolites to be recovered during a subsequent extraction step.

The use of cyclohexane to selectively extract warfarin from microsomal mixtures at pH 5.8 was reported by Bush *et al.*¹¹. Preliminary investigations showed that at pH 6.7 (the pH at which microbial metabolic studies were conducted), warfarin could be selectively extracted using cyclohexane containing a small amount of methylene chloride, and several experiments were carried out to optimize this extraction. Table II lists the protocols examined for extracting buffer solutions spiked with warfarin and metabolites (which would mimic the microbial cell suspension milieu). The results shown in Table II indicate that the most successful treatment developed for the removal of the majority of residual warfarin is to initially extract samples with 10% methylene chloride in cyclohexane. The metabolites could then be recovered quantitatively from the aqueous phase by a single extraction with ethyl acetate. Since over 80% of warfarin is removed before final analysis by HPLC, *SR/RS*-warfarin alcohol could then be accurately quantitated.

Calibration, accuracy and precision

Calibration plots of individual metabolites were constructed by the method of

TABLE II

EFFICIENCY OF WARFARIN REMOVAL AND METABOLITE EXTRACTION *VERSUS* EXTRACTION PROTOCOL

Extraction conditions ^a	Percentage of theoretical remaining in aqueous phase						
	Warfarin (1)	6-Hydroxy-warfarin (2)	7-Hydroxy-warfarin (3)	8-Hydroxy-warfarin (4)	4'-Hydroxy-warfarin (5)	3'-Hydroxy-warfarin (6)	SS/RR-Warfarin alcohol (10)
1	72	99	99	100	98	102	100
2	46	99	98	97	106	101	98
3	15	101	104	98	105	102	104
4	1	0	0	0	0	0	0

^a Extraction conditions: (1) 1 × 4 ml 5% dichloromethane in cyclohexane; (2) 2 × 4 ml 5% dichloromethane in cyclohexane; (3) 2 × 4 ml 10% dichloromethane in cyclohexane; (4) 1 × 4 ml ethyl acetate.

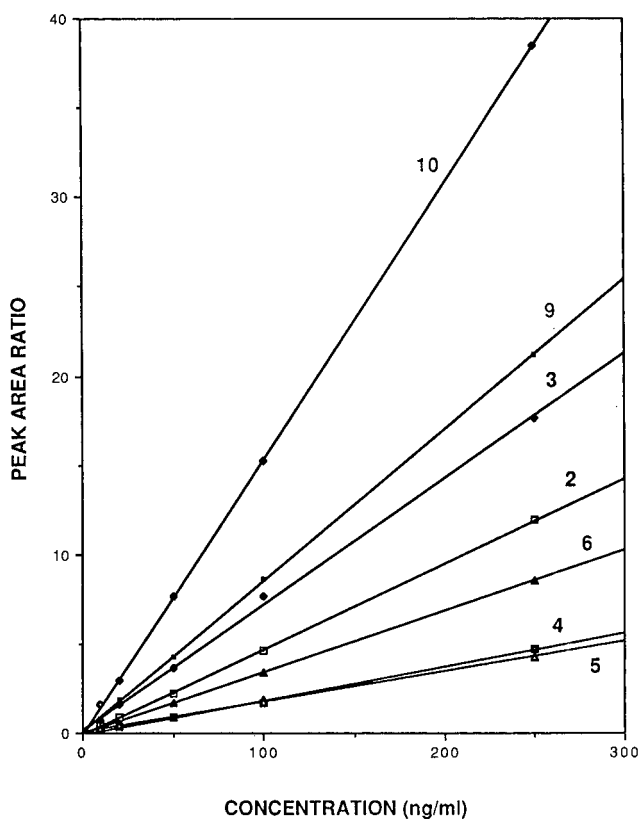


Fig. 3. Calibration plots for warfarin metabolites over the concentration range of 10–250 ng/ml. Numbering as in Fig. 1.

TABLE III

STATISTICAL ANALYSIS OF STANDARD CURVES GENERATED FOR WARFARIN METABOLITES ($n = 5$)

Compound	r^2	Slope \pm S.D.	Intercept \pm S.D.
6-Hydroxywarfarin (2)	0.9971	0.0506 \pm 0.0026	-0.2358 \pm 0.0949
7-Hydroxywarfarin (3)	0.9958	0.0778 \pm 0.0046	-0.0110 \pm 0.1945
8-Hydroxywarfarin (4)	0.9976	0.0195 \pm 0.0015	-0.0331 \pm 0.0625
4'-Hydroxywarfarin (5)	0.9941	0.0177 \pm 0.0009	0.0673 \pm 0.0865
3'-Hydroxywarfarin (6)	0.9987	0.0365 \pm 0.0024	-0.0465 \pm 0.0641
RS/SR-Warfarin alcohol (9)	0.9974	0.0911 \pm 0.0051	-0.0937 \pm 0.1828
RR/SS-Warfarin alcohol (10)	0.9986	0.1628 \pm 0.0076	-0.3891 \pm 0.2269

internal standardization with 4'-hydroxywarfarin alcohol as the internal standard (tentatively assigned as the RS/SR-4'-hydroxywarfarin alcohol (12) by reference to the elution order of SS/RR- and SR/RS-warfarin alcohols). Linear calibration plots were obtained for all metabolites (Fig. 3), and the calculated linear regression parameters for each metabolite are shown in Table III. The regression coefficients (r^2) for all compounds were better than 0.99 indicating good linearity. The coefficient of variation (C.V.) ($n = 5$) of the peak area ratio at each calibration point was less than 10% for all compounds indicating good precision. The accuracy of the assay was determined by duplicate analyses of samples containing standard amounts of metabolites. Deviation from the true value at all concentration levels was less than 10% for each metabolite (Table IV). Although the lowest calibration point of this assay was 10 ng/ml for all metabolites, levels as low as 1 ng/ml were detectable.

Analysis of microbial cell suspension of *Cunninghamella elegans* (ATCC 36112)

Fig. 4 shows typical chromatograms obtained from the analysis of cell suspension cultures of the fungus *Cunninghamella elegans* (ATCC 36112) (72 h incubation, sample and blank). It is evident that this organism metabolized warfarin to all known mammalian metabolites of this agent plus the previously unreported 3'-hydroxywar-

TABLE IV

RECOVERY OF WARFARIN METABOLITES FROM CELL SUSPENSION CULTURES OF *CUNNINGHAMELLA ELEGANS*

Concentration (ng/ml)	Metabolite recovered (theoretical percentage)						
	6-Hydroxywarfarin (2)	7-Hydroxywarfarin (3)	8-Hydroxywarfarin (4)	4'-Hydroxywarfarin (5)	3'-Hydroxywarfarin (6)	RR/SS-Warfarin alcohol (10)	RS/SR-Warfarin alcohol (9)
250	102, 103	98, 103	102, 98	100, 99	99, 100	97, 101	102, 97
150	108, 94	104, 94	106, 94	106, 97	107, 95	106, 101	100, 100
100	97, 106	97, 106	99, 98	95, 101	98, 99	101, 103	100, 101
50	103, 106	96, 106	99, 101	99, 101	101, 100	101, 95	100, 105
25	93, 104	90, 96	104, 97	102, 101	101, 112	92, 90	92, 94
12.5	93, 104	90, 96	99, 104	109, 104	101, 112	90, 96	90, 104

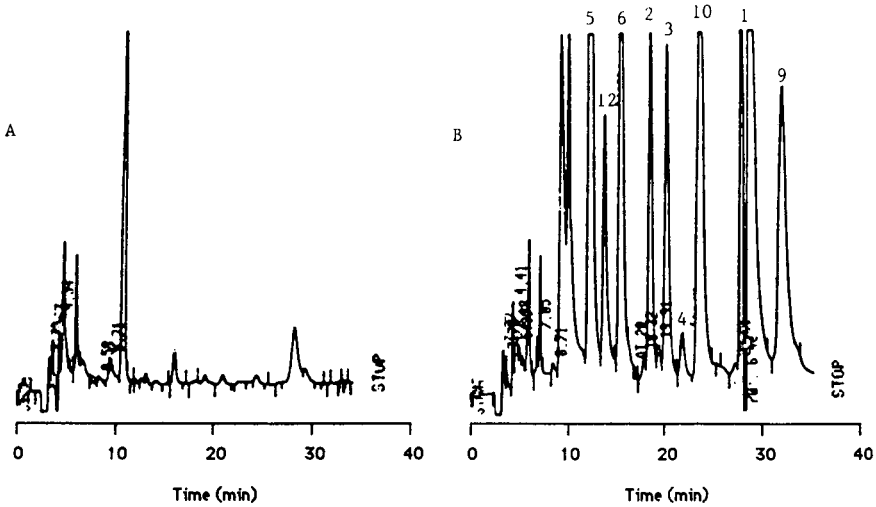


Fig. 4. HPLC analysis of warfarin metabolism by cell suspension cultures of *Cunninghamella elegans* (ATCC 36112). (A) Culture blank; (B) culture extract after 72 h incubation. Numbering as in Fig. 1.

farin. This suggests that this particular fungus possesses a drug metabolizing system quite similar to that found in mammalian species in terms of the metabolism of this important therapeutic agent and metabolic probe. The time course for the production of warfarin metabolites by *Cunninghamella elegans* (ATCC 36112) as monitored by this assay is shown in Fig. 5. The isolation and full structural characterization of each metabolite present will be the subject of a separate publication.

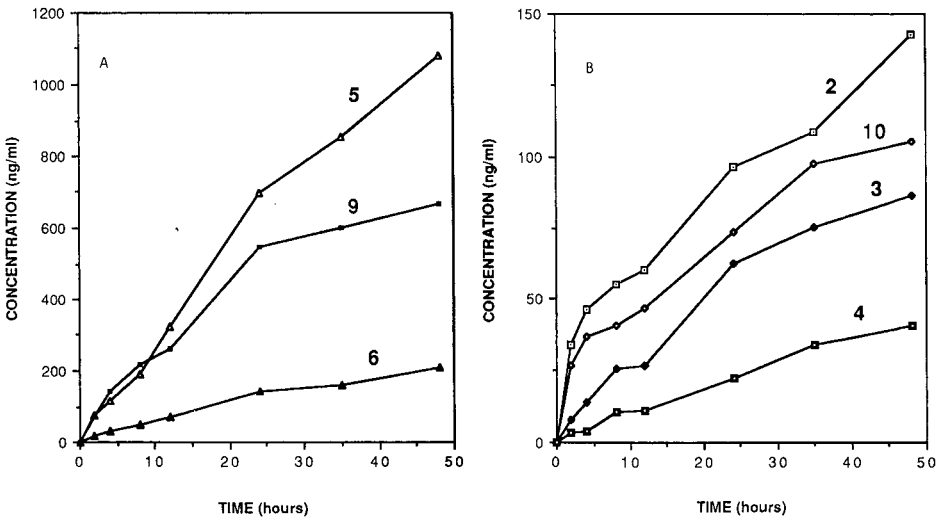


Fig. 5. Time-course profiles for the generation of warfarin metabolites using cell suspension cultures of *Cunninghamella elegans*. (A) Major metabolites (200–1000 ng/ml); (B) minor metabolites (25–150 ng/ml). Numbering as in Fig. 1.

ACKNOWLEDGEMENTS

The research was executed by James Wong in partial fulfillment of the requirements for the Ph.D. degree, and was supported in part by PHS/NIH Grant R01-ES04200.

REFERENCES

- 1 W. B. Jackson, P. J. Spear and C. G. Wright, *Pest Control*, 39 (1971) 13.
- 2 R. A. O'Reilly and P. M. Aggeler, *Pharmacol. Rev.*, 22 (1970) 36.
- 3 W. R. Porter, C. Wheeler and W. F. Trager, *Biochem. Pharmacol.*, 30 (1981) 3099.
- 4 L. S. Kaminsky, M. J. Fasco and F. P. Guengerich, *Methods Enzymol.*, 74 (1981) 262.
- 5 L. S. Kaminsky, F. P. Guengerich, G. A. Dannan and S. D. Aust, *Arch. Biochem. Biophys.*, 25 (1983) 398.
- 6 A. E. Rettie, L. Heimark, R. T. Mayer, M. D. Burke, W. F. Trager and M. R. Juchau, *Biochem. Biophys. Res. Commun.*, 126 (1985) 1013.
- 7 M. J. Fasco, L. J. Piper and L. S. Kaminsky, *J. Chromatogr.*, 131 (1977) 365.
- 8 M. J. Fasco, M. J. Cashin and L. S. Kaminsky, *J. Liq. Chromatogr.*, 2 (1979) 565.
- 9 S. H. Lee, L. R. Field, W. N. Howald and W. F. Trager, *Anal. Chem.*, 53 (1981) 467.
- 10 C. Banfield and M. Rowland, *J. Pharm. Sci.*, 73 (1984) 1392.
- 11 E. D. Bush, L. K. Low and W. F. Trager, *Biomed. Mass Spectrom.*, 10 (1983) 395.
- 12 M. Corn and R. Berberich, *Clin. Chem.*, 13 (1967) 126.
- 13 K. Hunter, *J. Chromatogr.*, 270 (1983) 277.
- 14 W. A. Trujillo, *J. Liq. Chromatogr.*, 3 (1980) 1219.
- 15 M. A. Hermondson, W. M. Barker and K. P. Link, *J. Med. Chem.*, 14 (1971) 167.
- 16 E. Bush and W. F. Trager, *J. Pharm. Sci.*, 72 (1983) 830.
- 17 K. K. Chan, R. J. Lewis and W. S. Trager, *J. Med. Chem.*, 15 (1972) 1265.
- 18 W. F. Trager, R. J. Lewis and W. A. Garland, *J. Med. Chem.*, 13 (1970) 1196.
- 19 R. Gloor and E. L. Johnson, *J. Chromatogr. Sci.*, 15 (1977) 413.
- 20 K. Hunter, *J. Chromatogr.*, 270 (1983) 267.

CHROM. 21 341

SEPARATION OF FUNGAL STEROLS BY NORMAL-PHASE HIGH-PERFORMANCE LIQUID CHROMATOGRAPHY

APPLICATION TO THE EVALUATION OF ERGOSTEROL BIOSYNTHESIS INHIBITORS

GARY A. PEACOCK* and MICHAEL W. GOOSEY^a

Dow Chemical Co. Ltd., Biochemistry Department, Letcombe Laboratory, Letcombe Regis, Wantage, Oxfordshire (U.K.)

(First received September 9th, 1988; revised manuscript received January 24th, 1989)

SUMMARY

An isocratic normal-phase high-performance liquid chromatographic method is reported which can separate radio-labelled sterols produced *in vitro* by cell-free extracts of the phytopathogenic fungus, *Ustilago maydis*. The method is rapid with typical analysis times of 15–20 min. It allows a reproducible separation of at least 7 radio-labelled sterols which have been identified by gas chromatography–mass spectrometry and enzyme inhibitor studies. This method can be used to obtain quantitative data on the inhibitory action of potential fungicides that disrupt ergosterol synthesis, and in favourable cases, the precise enzyme involved.

INTRODUCTION

Sterols are an important constituent in fungal cell membranes. Ergosterol is the predominant fungal sterol, even though it is not synthesised by some fungi such as the *Pythiaceae* family¹. This is in contrast to plant and mammalian membranes in which C-24 alkylated sterols and cholesterol are the predominant sterols respectively².

Ergosterol is present in the phospholipid bilayer of the fungal membrane. Because of its structure and amphiphilic nature, ergosterol is thought to increase the membrane microviscosity; *cf.* cholesterol in mammalian systems³. This property alters the fluidity and molecular motion of other lipids⁴, which may in turn modulate the activity of membrane-bound enzymes such as chitin synthetase and ATPase's⁵. Thus, ergosterol biosynthesis is essential for maintenance of normal growth and physiological status of the fungal cell.

An important and growing class of fungicides owe their fungitoxicity to the inhibition of ergosterol biosynthesis. Examples of such compounds include the triazoles⁶, pyrimidines⁷ and phenylpropylamines⁸.

* Present address: Shell Research Ltd., Sittingbourne Research Centre, Sittingbourne, Kent, U.K.

Researchers are increasingly interested in the qualitative and quantitative aspects of enzyme inhibition by antifungal compounds. This has led to the development of chromatographic methods capable of separating sterol intermediates and ergosterol.

Early methods used conventional silicic acid column chromatography⁹, but only partial resolution of some sterol intermediates was achieved with retention times of 2–3 days. Thin-layer chromatography (TLC) has also been extensively employed¹⁰, although it suffers from certain disadvantages such as low loading capacities, relatively low resolution, and difficulty in the recovery of the purified compounds.

Gas-liquid chromatography (GLC) has been widely used over the last two decades in the analysis of free sterols and their derivatized esters¹¹. Patterson¹², investigated structure–retention relationships of sterols in GLC. The great advantage of GLC over other chromatographic techniques is that it is ideal for interfacing with mass spectrometry (MS)¹³, giving highly specific and sensitive detection coupled with structural information.

However, there are disadvantages of GLC such as: many sterols are thermally unstable, sample recovery is difficult or impossible, where sample recovery is possible the low column loading prohibits preparative separations, and detection of radiolabelled sterols is difficult to achieve.

High-performance liquid chromatography (HPLC) has inherent advantages over TLC and GLC; chromatographic separation times are usually measured in minutes, HPLC is a non-destructive technique allowing easy collection of separated analytes, and it has greater potential for accomplishing difficult separations because it can utilize a larger range of separation mechanisms, *viz.* absorption, partition, reversed-phase partition, chemisorption, gel permeation, ion exchange and ion-pair formation. The application of HPLC to the analysis of sterols has increased over the last ten years, with most workers employing reversed-phase systems (*e.g.* ref. 14). Where radiolabelled sterols have been separated, the radioactivity was determined by eluent fraction collection and subsequent liquid scintillation counting.

Hansbury and Scallen¹⁵ reported a three step procedure for separating complex mixtures of sterol intermediates in cholesterol biosynthesis in which both reversed-phase HPLC and normal-phase HPLC were utilised. Evershed *et al.*¹⁶ commented that the problem with HPLC was the lack of resolution of different steryl esters, making it difficult to assign unambiguous identifications of components in complex mixtures; the lack of a strong chromophore meant that the UV detection of steryl esters have relatively poor detection limits, requiring 10–50 mg of each component for analysis. The majority of sterol separations by HPLC have been applied to sterols occurring in mammalian systems, *e.g.* cholesterol and its precursors. An HPLC method describing the separation and detection of squalene, 2,3-epoxysqualene, lanosterol and other sterols in the ergosterol biosynthesis pathway has not been reported.

In this study we report an isocratic normal-phase HPLC system using an on-line radiochemical HPLC detector. It is a rapid, sensitive method capable of separating and quantifying radioactive non-saponifiable lipids formed from cell-free extracts of the phytopathogenic fungus *Ustilago maydis*. This technique was used to determine the activity of commercial ergosterol biosynthesis inhibitors.

EXPERIMENTAL

Apparatus

High-performance liquid chromatography. The chromatography was performed with an HPLC system consisting of two high-pressure pumps (Models 510 and 600A; Waters Assoc., Milford, MA, U.S.A.), an automatic sample injector (WISP; Waters Assoc.) and a radioactivity HPLC monitor (Model LB 506C; Berthold U.K., Leeds, U.K.). For spectrophotometric detection a variable-wavelength UV detector (Model LC55, Perkin-Elmer, Beaconsfield, U.K.) was used. The HPLC column was stainless steel (250 × 4.6 mm) packed with Hypersil 3 μm silica (Hichrom, Reading, U.K.) and heated to 35°C for all analyses. A stainless-steel guard column (10 × 4.6 mm) packed with Hypersil 5 μm silica was used as an on-line filter.

Radioactivity detector. A Berthold LB506C radioactivity chromatography system was used to measure the radiolabelled sterols separated by HPLC. The high-energy window channel was employed to measure carbon-14 with a liquid flow-through cell (0.5 ml) used throughout. The counting efficiency was typically 40-50%, as determined by liquid scintillation counting in a Beckman (Fullerton, CA, U.S.A.) LS1800 counter, and the cpm were converted into dpm using the following formulae: $\text{dpm} = \text{counts} \times \text{total flow-rate through the cell (ml/min)}/\text{counting efficiency} \times \text{active cell volume (ml)}$.

Gas chromatography-mass spectrometry. Samples for mass analysis were produced by parallel enzyme assays using DL-mevalonic acid in one assay, and DL-[2-¹⁴C]-mevalonic acid in the other. The radiochromatogram of the ¹⁴C-labelled sterols was used to determine the areas of peak collection for the unlabelled eluent. Each sample was evaporated to dryness under nitrogen before conversion to the trimethylsilyl (TMS) derivatives prior to mass analysis. The TMS derivatives were formed by adding pyridine (50-μl) and bis(trimethylsilyl)trifluoroacetamide (BSTFA) (199 μl) before heating the sealed tube for 30 min at 60°C.

The derivatized samples were separated and analysed in a Finnigan 1020 automated GC-MS system (incorporating a Data General Nova 3 computer); the GC system was fitted with a 30 m × 0.32 mm I.D. J & W Scientific silica column coated with 0.25-μm DB-1, and a splitless injector with a flush 30 s after sample injection to remove residual gases. The end of the column was introduced directly into the mass spectrometer analyser chamber. The system was operated under the following conditions: helium pressure 11 lbs./in.²; injector temperature 300°C; GC temperature 75-300°C at 3°C/min. The mass spectrometer was set to scan 40-650 a.m.u. per nominal second with an ionizing voltage of 70 eV. The filament was switched on 250 s after injection of the sample into the gas chromatograph.

Chemicals and reagents

Dichloromethane, *n*-hexane and methanol were of HPLC grade (Romil Chemicals, Loughborough, U.K.), magnesium chloride (MgCl₂), manganese chloride (MnCl₂), potassium hydroxide (KOH), and pyridine were analytical grade. The following chemicals, co-factors, buffers and HPLC standards were all obtained from Sigma, Poole, U.K., BSTFA + 1% trimethylchlorosilane (TMCS), flavin adenine dinucleotide (FAD), reduced nicotinamide adenine dinucleotide phosphate (NADPH), S-adenosyl methionine *p*-toluenesulphonate (SAM), adenosine triphos-

phate (ATP), ethylenediaminetetraacetic acid (EDTA), N-2-hydroxyethylpiperazine-N-2-ethanesulphonic acid (HEPES), phenylmethyl sulphonyl fluoride (PMSF), dithiothreitol (DTT), squalene, lanosterol and ergosterol. DL-[2-¹⁴C]mevalonic acid DBED (N,N-dibenzylethylenediamine salt) (48.6 mCi/mmol) was obtained from Dupont (U.K.), New Research Products, Stevenage, U.K.

Tolnaftate, prochloraz and fenpropimorph were obtained from Sandoz, Vienna, Austria, Schering Agrochemicals, Saffron Walden, U.K. and Dr. Maag, 8157 Dielsdorf, Switzerland, respectively.

All aqueous solutions of co-factors and reagents were prepared in double-distilled water. The scintillation fluid used was Beckman ReadySafe liquid scintillation cocktail.

Biosynthesis and extraction of radiolabelled compounds

Fungal cultures. Sporidia of *Ustilago maydis* (103760:CMI, 1963) were maintained on potato dextrose agar (Oxoid, CM139) slopes. Liquid cultures (1 l) of *U. maydis* in 2.8-l Erlenmeyer flasks were grown in YED media (1.5% D-glucose, 0.3% yeast extract) and shaken in a rotary incubator at 120 rev./min at 25°C for 15–18 h. The cells (sporidia) were harvested by centrifugation at 1390 g for 20 min and washed three times with equal volumes of homogenisation media at 4°C.

Preparation of the cell-free enzyme system. The washed cells were suspended in 25 ml of homogenisation media (50 mM HEPES pH 7.4, 1 mM EDTA, 5 mM DTT and 10 mg/100 ml each of soybean trypsin inhibitor and PMSF), and an equal volume of glass beads, 0.2 mm diameter. The cells were then disrupted by two 45-s periods of homogenisation at 4°C in a bead beater (Biospec Products). The resultant homogenate was centrifuged at 10 000 g for 15 min and the supernatant (S₁₀) used for enzyme assays.

Enzymic assay. The standard reaction mixture for measuring incorporation of DL-[2-¹⁴C]mevalonic acid into non-saponifiable lipids was: 0.5 ml tissue (S₁₀) (8–12 mg protein/ml), 3 mM DL-[2-¹⁴C]mevalonic acid (0.2 μCi/assay), 1.7 mM NAD, 3.5 mM ATP, 1.7 mM NADPH, 1.7 mM S-adenosyl-L-methionine, 0.17 mM FAD, 3.5 mM MgCl₂ and 3.5 mM MnCl₂ in a total volume of 0.575 ml. The assay vials were incubated with shaking at 30°C for 3 h. The reaction was terminated by the addition of 15% KOH in ethanol (0.5 ml). The mixture was heated at 70°C for 30 min and then extracted with two 1-ml aliquots of *n*-hexane to remove the non-saponifiable lipids. The combined hexane extracts were then evaporated to dryness under nitrogen. The extracted lipids were re-dissolved in 200 μl of *n*-hexane prior to HPLC analysis.

Chromatographic procedure

Standard solutions of squalene, lanosterol and ergosterol in dichloromethane were found to give an acceptable UV absorption at 245 nm. In an effort to minimise extra-column band broadening effects the guard column was directly coupled to the head of the analytical column, and the connective stainless-steel tubing (1.5 mm × 0.13 mm I.D.) was kept as short as possible. Various mobile phases were tested and 0.025% methanol in dichloromethane was found to give the best separation in a reasonable time (15–20 min) for routine sample analysis. The samples in *n*-hexane (200 μl) were transferred to sealed autosampler vials fitted with limited volume inserts and screw tops with PTFE septa. A volume of 190 μl was taken by the auto sampler and injected onto the HPLC column.

When monitoring radiolabelled samples the on-line radioactivity detector was connected in place of the variable wavelength UV detector, via a mixing "T" block, into which the liquid scintillation cocktail was pumped at a rate of 3.5 ml/min. The stainless-steel connective tubing leading to the radioactivity detector was crimped every 6 mm to ensure complete mixing of the scintillant with the column eluent before entering the 0.5 ml flow-through cell.

All mobile phase combinations were mixed, passed through a 0.2- μ m membrane filter (Anachem, Luton, U.K.) under vacuum and used immediately at a flow-rate of 1.0 ml/min. Chromatographic retention data were expressed as capacity ratios: $k' = (t_R - t_0)/t_0$, where t_R and t_0 are the retention times of the analyte and a non-retained compound respectively. The shape of each peak was assessed by measuring the peak asymmetry factor (AF). This was calculated by dropping a perpendicular from the peak maximum and measuring the distance from this line to the leading edge (a) and the trailing edge (b) at the 10% peak-height level ($AF = b/a$).

Statistical treatment of results

Results are expressed as mean \pm S.E.M. with the number of replicate experiments given in parentheses. Radiochromatograms are from a typical experiment performed in duplicate.

RESULTS AND DISCUSSION

Although a high proportion of the literature methods employ reversed-phase systems, the lipophilicity of the sterols under investigation suggested that a normal-

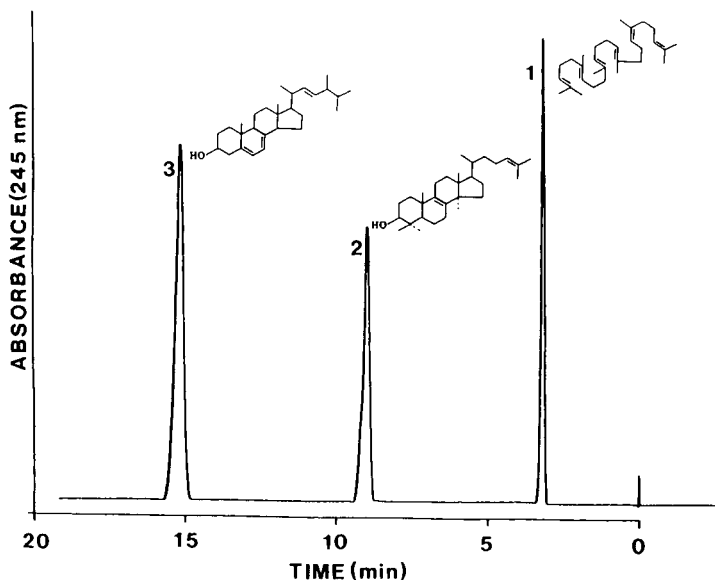


Fig. 1. HPLC separation of a mixture of (1) squalene (2 g), (2) lanosterol (0.8 g) and (3) ergosterol (0.8 g). The column (25 cm \times 4.6 mm I.D.) contained 3 μ m Hypersil silica and the mobile phase was 0.025% methanol in dichloromethane at 1 ml/min. Detection was by UV using a Perkin-Elmer LC55 detector at 245 nm.

phase system might be more efficient. Method development was carried out using standard solutions of squalene, lanosterol and ergosterol, with UV detection at a compromise wavelength of 245 nm. Note that squalene is virtually unretained under the conditions used to obtain the chromatogram shown in Fig. 1. Although this could be thought to be undesirable (as all retained solutes would elute at this point in the chromatogram), this does not cause any problems in practice: MS showed that the 0–4 min portion of the eluent collected after injection of authentic samples contained mobile phase and squalene only. Good separation of squalene, lanosterol and ergosterol (see Fig. 1) was achieved using a mobile phase of dichloromethane with 0.025% methanol and was therefore used throughout this study. The ergosterol peak symmetry shown in Fig. 1 demonstrates reasonable column performance for the longest retained peaks under the chromatographic conditions chosen.

A cell-free extract of *U. maydis* converted DL-[2- 14 C]mevalonic acid into non-saponifiable lipids as previously reported for *Saccharomyces cerevisiae*^{17,18}. However, previous studies with cell-free biosynthetic systems have separated and identified few sterols. The methods used have been either GLC¹⁷ or TLC¹⁸. In the former study¹⁷ only two peaks were identified by radio-GC whilst five radioactive peaks were found using silicic acid column chromatography. The latter study of Gadher *et al.*¹⁸ was able to show the TLC separation of squalene, 2,3-epoxysqualene and three classes of sterols; 4,4-dimethylsterols, 4 α -methylsterols and 4-desmethylsterols. The normal-phase HPLC method reported herein can resolve squalene, 2,3-epoxysqualene and at least 9 radio-labelled peaks, of which 7 have been identified as sterols (see Fig. 2). The peak identities in Table II were assigned in the following way; peaks 1, 2, 4, 5, 7 and 8 gave mass spectra that are identical to reference spectra from authentic samples. Peaks 3 and 6 were identified by mass fragmentation analysis and will be reported elsewhere.

Interestingly, this method has resulted in the identification of a relatively pure peak of radio-labelled ergosterol; co-crystallization of this peak ($t_R = 15$ min 18 s)

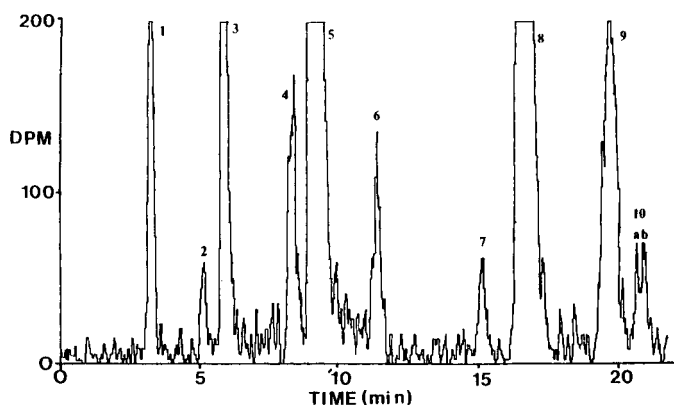


Fig. 2. A typical radiochromatogram of the 14 C-labelled non-saponified lipids formed from incubating [14 C]mevalonic acid with cell-free extracts of *U. maydis*. The peak identities are given in Table II. Chromatographic conditions were as in Fig. 1, except for the substitution of a Berthold LB 506C HPLC radio-monitor as the detector.

TABLE I

CHROMATOGRAPHIC DATA FOR A 3- μ m HYPERSIL COLUMN WHEN USED WITH SQUALENE, LANOSTEROL AND ERGOSTEROL

Chromatographic conditions: a stainless-steel column (25 cm \times 4.6 mm I.D. packed with 3- μ m Hypersil silica) was used with a mobile phase of 0.025% methanol in dichloromethane at a flow-rate of 1 ml/min. A Perkin-Elmer LC55 UV detector was used at 245 nm. t_R = retention time, k' = capacity factor, N = number of theoretical plates, AF = asymmetry factor and R_s = resolution. t_0 = 2.7 min.

Solute	Parameter				
	t_R	k'	N	AF	R_s
Squalene	3.1	0.15	41	1.2	19.7
Lanosterol	9.0	2.33	5208	1.5	13.8
Ergosterol	15.2	4.6	8264	2.0	

with authentic ergosterol gave a constant specific activity at approximately 75% of the initial radioactivity (Table III). The implications of the complete conversion of [14 C]mevalonate to [14 C]ergosterol with regard to the preferred sterol biosynthetic pathway in *U. maydis* will be discussed in a further report. The proposed biochemical pathway from squalene to ergosterol in fungi has been recently reviewed by Mercer¹⁹.

Of the total radioactivity added as [14 C]mevalonic acid, $33 \pm 4\%$ ($n=6$) was recovered in the non-saponifiable extract, indicating good conversion of radiolabel into sterols. Indeed this figure is an underestimate of the true conversion of radiolabel into sterol because only the L-isomer and not the D-isomer of mevalonic acid is the natural precursor for sterol synthesis. Thus since the racemate DL-[2- 14 C]mevalonic

TABLE II

MS ANALYSIS OF THE HPLC RADIO-LABELLED PEAKS IN FIG. 3

Radio-labelled peak	Compounds identified	t_R (HPLC) (min)	m/e
1	Squalene	3.60	410
2	2,3-epoxysqualene	5.13	426
3	4,4-dimethylergosta-8-ene-3 β -ol	6.3	428
4	24-methylene-24,25 dihydrolanosterol	8.5	440
5	lanosterol	9.5	426
6	4-methylergosta-8,24(28)-diene	11.3	412
7	Ergosterol	15.3	396
8	Fecosterol	16.6	398
	Episterol	16.6	398
9	ND ^a	20.3	-
10a	ND	21.1	-
10b	ND	21.3	-

^a ND = not determined.

TABLE III

IDENTIFICATION OF RADIOLABELLED ERGOSTEROL IN THE HPLC PEAK AT t_R 15 min 18 s, BY INVERSE ISOTOPE DILUTION

50 mg of authentic ergosterol was added to a sample of peak t_R 15 min 18 s, dissolved in acetone and crystallised from acetone/water.

Number of crystallisations with authentic ergosterol	Specific activity (dpm/mg)
0	3096
1	2633
2	2345
3	2332

acid was used in this study a radiolabelled conversion of 66% has probably been achieved. The rate of synthesis of ergosterol from [^{14}C]mevalonic acid *in vitro* is 0.020 ± 0.014 ($n=5$) nmol/mg protein/h (assuming 5 moles of ^{14}C are incorporated into 1 mole of ergosterol with the loss of one ^{14}C as $^{14}\text{CO}_2$ in a C-4 demethylation step and 75% of the "ergosterol" peak $t_R = 15$ min 18 s, is authentic ergosterol). The specific rate of ergosterol synthesis, reported in this study, is similar to that of sterol synthesis found in mammalian systems, e.g. cholesterol synthesis in rat liver peroxisomes and microsomes is 0.087 and 0.135 nmol/mg protein/h respectively²⁰.

It should be noted however, that sporidial cultures of *U. maydis* greater than 24 h rapidly lose the ability to synthesise ergosterol and even episterol and other C-4 demethyl sterols. For example, a 10 000 g supernatant fraction from a ten day old culture of *U. maydis* gave 90% of non-saponifiable fraction as squalene with the remaining 10% being lanosterol²¹. No other radiolabelled sterols were detected. The ability to synthesise ergosterol appears to be synchronized with the metabolically active growing phase of the fungi.

The results of the inhibitor studies support the proposed identity of the radiolabelled sterols. Thus, tolnaftate, which inhibits the enzyme squalene monooxygenase²² abolished most of the sterols at a concentration of 50 μM (Fig. 3a). The squalene peak is increased from 2% of the non-saponified lipids to 89.5% (Table IV) and the lanosterol peak is reduced from 58.5% to 8.3%. The peak at $t_R = 16.4$ min represents less than 2% of the radioactivity in the non-saponified extract and was not further characterized. The percentage radioactivity recovered in the non-saponified extract is decreased from 33 to 21.2%. This decrease, in the presence of tolnaftate, has been noted several times and may suggest that a regulatory feedback mechanism may exist when squalene concentrations are increased to a particular level or alternatively tolnaftate, at 50 μM , partially inhibits an earlier step in squalene synthesis. Further experiments are needed to support the above suggestions. However, this result shows that tolnaftate can inhibit squalene monooxygenase from a phytopathogenic fungus, albeit at a higher concentration compared to the inhibition of squalene monooxygenase in a mycopathogenic fungus such as *Candida albicans*²².

The fungicide prochloraz, which is a C-14 demethylase inhibitor, completely abolished the ergosterol and fecosterol/episterol peaks at a concentration of 10 μM (Fig. 3b). A large increase in squalene and a relatively small increase in lanosterol is

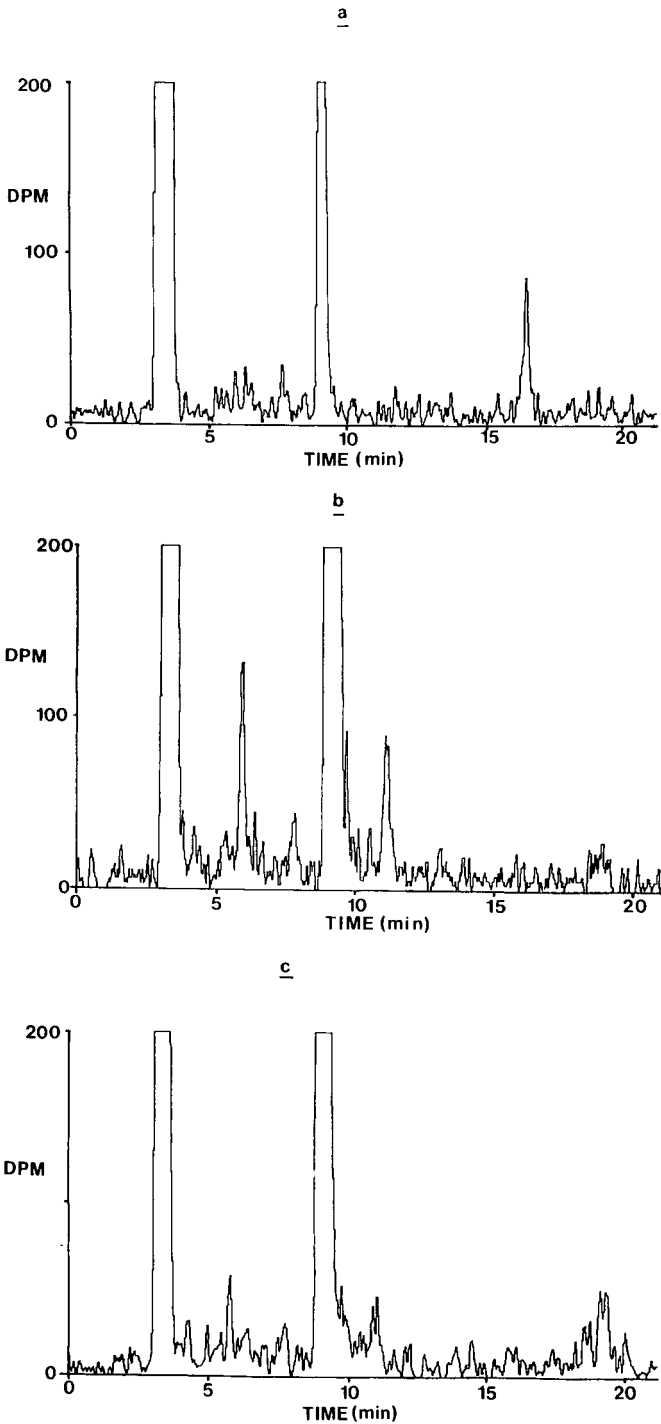


Fig. 3. Radiochromatograms of ^{14}C -labelled non-saponified lipids formed from incubating $[^{14}\text{C}]$ mevalonic acid with cell-free extracts of *U. maydis* in the presence of (a) $50\ \mu\text{M}$ tolnaftate, (b) $10\ \mu\text{M}$ prochloraz and (c) $10\ \mu\text{M}$ fenpropimorph.

TABLE IV

EFFECT OF 3 ANTIFUNGAL COMPOUNDS ON THE CONVERSION OF DL-[2-¹⁴C]MEVALONIC ACID TO NON-SAPONIFIED LIPIDS

The *in vitro* enzymic assay was as described in the experimental section but included 5 μ l of the test compound in acetone. Acetone (5 μ l) alone, had no effect on the incorporation of radioactivity into the non-saponified lipids.

Treatment	% Radioactivity recovered in non-saponified extract ^a	Distribution of radioactivity in the non-saponified extract ^b (%)		
		Squalene	Lanosterol	Episterol/ fecosterol
Control	33.0	2.0	58.5	25.3
Tolnaftate (50 μ M)	21.2	89.5	8.3	0
Prochloraz (10 μ M)	32.6	32.0	65.2	0
Fenpropimorph (10 μ M)	28.3	25.1	73.2	0

^a The figures represent the % radioactivity recovered in the non-saponified extract compared to the total radioactivity added as DL-[2-¹⁴C]mevalonic acid.

^b The figures are of % radioactivity in the respective sterol fractions compared to the total radioactivity recovered in the non-saponified extract.

observed (See Table IV). The 4,4-dimethyl-5 α -ergosta-8-ene-3- β -ol and 24-methylene-24,25-dihydrolanosterol peaks were reduced by 45 and 37% respectively. Although this altered profile supports the view that the primary mode of action of prochloraz is inhibition of the C-14 demethylation of 24-methylene-24,25-dihydrolanosterol (or lanosterol in yeast) at the concentration used in this study (10 μ M), partial inhibition of the C-24 methylation of lanosterol may occur.

Fenpropimorph gave similar results (see Fig. 3c). The ergosterol and fecosterol/episterol peaks were completely abolished. The squalene and lanosterol peaks are similarly increased as seen with prochloraz (Table IV). The 4,4-dimethyl-5 α -ergosta-8-ene-3- β -ol and 24-methylene-24,25-dihydrolanosterol peaks decreased by 80% and 50% respectively.

The interpretation of this altered profile is not straightforward; at a concentration of 10 μ M fenpropimorph may have inhibited the Δ^{14} -reductase step, which appears to reduce 4,4-dimethyl-5 α -ergosta-8,14-diene-3 β -ol to 4,4-dimethyl-5 α -ergosta-8-ene-3 β -ol in our system, since the latter sterol was almost abolished. This would be in agreement with the work of Baloch and Mercer²³ who showed that in *Saccharomyces cerevisiae*, fenpropimorph inhibited the Δ^{14} -reductase step at high concentrations (IC₅₀ = 2.3 μ M) whereas at lower concentrations (IC₅₀ = 13 nM) was preferentially inhibited. However this interpretation of the altered sterol profile should be cautioned since there was no evidence for the accumulation of $\Delta^{8,14}$ - or Δ^8 -sterols, which does occur in fungal cellular liquid cultures when treated with fenpropimorph²⁴. In the cell-free system in this study, the accumulation of a $\Delta^{8,14}$ -sterol may have occurred but was not resolved or detected under the experimental conditions used.

Thus although the altered sterol profiles support the proposed modes of action

of the three fungicides tested at a single dose in this study, more informative data can be achieved by testing compounds in a dose-response manner. Consequently the enzyme that is exquisitely sensitive to inhibition may be identified by the sequential return of sterol peak(s) to control levels. This enables IC_{50} values (the concentration at which a known sterol peak is reduced by 50%) to be calculated for a given compound *e.g.* tolinaftate has an $IC_{50} = 4 \mu M$ for inhibition of lanosterol synthesis and fenpropimorph and $IC_{50} = 220 nM$ for inhibition of episterol synthesis in *U. maydis*²¹. Although these values cannot be regarded as "absolute" IC_{50} values for the enzymes responsible for synthesizing lanosterol and episterol, they can be used to determine relative potencies for a series of structurally-related compounds. The precise enzyme inhibited, however, can only be definitively proven by single enzyme studies, yielding "accurate" K_i inhibition constants and the type of inhibition involved.

CONCLUSION

In conclusion, the isocratic normal-phase HPLC method reported here can separate radio-labelled sterols produced in cell-free extracts of *U. maydis* in a rapid and reproducible manner. This method can be used to obtain quantitative data on the inhibitory action of potential fungicides that disrupt ergosterol biosynthesis. The enzyme(s) involved in the inhibition may also be identified by observing the altered sterol profiles, although it is accepted that single enzyme studies are required to ultimately prove specific enzyme inhibition. This HPLC system is currently being used to clarify and provide further experimental evidence for the proposed sterol biosynthetic pathway in phytopathogenic fungi.

ACKNOWLEDGEMENTS

The authors would like to thank Dr. W. Greenaway, Department of Plant Sciences, University of Oxford, for providing GC-MS analysis and Drs. M. Jung, P. F. S. Street and R. Baloch (Dow Chemical Co. Ltd., Letcombe Laboratories) for helpful discussions at various times throughout this study.

REFERENCES

- 1 S. G. Wood and D. Gottlieb, *Biochem. J.*, 170 (1978) 335.
- 2 P. Benveniste, *Ann. Rev. Plant Physiol.*, 37 (1986) 275.
- 3 C. Tanford, *Biochem. Soc. Trans.*, 15 (1987) 15.
- 4 G. Deinum, H.V. Langen, G.V. Ginkel and Y.K. Levine, *Biochemistry*, 27 (1988) 852.
- 5 A. Duran and E. Cabib, *J. Biol. Chem.*, 253 (1978) 4419.
- 6 J. A. Quinn, T. T. Fujimoto, A. R. Egan and S. H. Shaber, *Pestic. Sci.*, 17 (1986) 357.
- 7 H. D. Sisler, N. N. Ragsdale and W. F. Waterfield, *Pestic. Sci.*, 15 (1984) 167.
- 8 A. Kerkenaar, J. M. Van Rossum, G. G. Versluis and J. W. Marsman, *Pestic. Sci.*, 15 (1984) 177.
- 9 I. D. Frantz, *J. Lipid Res.*, 4 (1963) 176.
- 10 T. J. Scallen, M. V. Srikantaiah, H. B. Shridlant and E. Hansbury, *FEBS Lett.*, 15 (1972) 227.
- 11 R. P. Evershed, N. Spooner, M. C. Prescott and L. J. Goad, *J. Chromatogr.*, 440 (1988) 23.
- 12 G. W. Patterson, *Anal. Chem.*, 43 (1971) 1165.
- 13 R. P. Evershed and L. J. Goad, *Biochem. Environ. Mass Spectrom.*, 14 (1987) 131.
- 14 J.-P. Bianchini, E. M. Gaydou, J.-C. Sigoillot and G. Terrom, *J. Chromatogr.*, 329 (1985) 231.
- 15 E. Hansbury and T. J. Scallen, *J. Lipid Res.*, 21 (1980) 921.

- 16 R. P. Evershed, V. L. Male and L. J. Goad, *J. Chromatogr.*, 400 (1987) 187.
- 17 T. Kato and Y. Kawase, *Agric. Biol. Chem.*, 40 (12), (1976) 2379.
- 18 P. Gadher, E. I. Mercer, B. C. Baldwin and T. E. Wiggins, *Pestic. Biochem. Physiol.*, 19 (1983) 1.
- 19 E. I. Mercer, *Pestic. Sci.*, 15 (1984) 133.
- 20 S. L. Thompson, R. Burrows, R. J. Laub and S. K. Krisans, *J. Biol. Chem.*, 262 (1987) 17420.
- 21 M. W. Goosey and G. A. Peacock, unpublished data.
- 22 N. S. Ryder and M. C. Dupont, *Biochem. J.*, 230 (1985) 765.
- 23 R. I. Baloch and E. I. Mercer, *Phytochem.*, 26 (1987) 663.
- 24 R. Baloch, personal communication.

CHROM. 21 386

USE OF LIQUID CHROMATOGRAPHY IN THE SYNTHESIS OF ISOLUMINOL-LABELLED MEDROXYPROGESTERONE ACETATE AND ZERANOL

H. KOEHLER, L. LAROCQUE and S. SVED*

Bureau of Drug Research, Health Protection Branch, Health and Welfare Canada, Ottawa, Ontario K1A 0L2 (Canada)

(First received November 11th, 1988; revised manuscript received February 3rd, 1989)

SUMMARY

A high-performance liquid chromatographic (HPLC) method for monitoring the syntheses of two isoluminol-labelled drugs, medroxyprogesterone acetate (MPA) and zeranol, has been developed. MPA and the ketone derivative of zeranol, zearalanone, were conjugated to N-(4-aminobutyl)-N-ethylisoluminol through the carboxymethyl oxime derivative of the drug by using the N-succinimide ester as an intermediary. Reaction mixtures were sampled periodically and chromatographed directly by HPLC on a silica gel column, by using isocratic elution with mixtures of hexane-ethanol-acetic acid in several different proportions. The degree of reaction completion was determined by comparison of the peak area of the initial reactant to that present at sampling time. MPA oxime production was found to be complete after 15 min; 97.0% of the oxime was converted to succinimide ester in 24 h; 99.0% of the available ester reacted within 2.5 h to form the final labelled product. Zearalanone oxime production was found to be complete after 2 h; 93.3% of the oxime was converted to the activated ester within 24 h; 89.6% of available ester had reacted in 30 min to form the final labelled product. The chromatography can be performed in real time, permitting modification in the conditions of the reaction while in progress.

INTRODUCTION

Luminescence immunoassay (LIA), a novel technique in which the labelled ligand bears a chemiluminescent group, is gaining popularity. One of the reasons for its increasing popularity is that, although the labelled ligand, and sometimes even the labelling reagent, are often unavailable commercially, they can be synthesized with relative ease in an average chemical laboratory.

Quantitation and identification of synthesized products have commonly been achieved with purification by recrystallization and weighing, followed by mass spectrometry (MS) or nuclear magnetic resonance (NMR)¹⁻³. The required purification procedures, although well established, are often lengthy and difficult to perform. Such a method is therefore not suitable for following the reaction progress.

Traditionally, thin-layer chromatography has been used to monitor reactions⁴ with acceptable results. However, this procedure suffers from several disadvantages:

(1) the results are only qualitative; (2) partially reacted material may be driven to completion during spotting of the plates⁵, thus giving false impressions of the reaction kinetics; (3) plates contaminated by normal laboratory atmosphere may obscure the results⁶.

High-performance liquid chromatography (HPLC) has been effectively utilized in the quality control and purification of luminogenic labels^{7,8}. This prompted us to examine HPLC for monitoring the progress of reactions involved in the synthesis of chemiluminescent labels. Immediate information on purity, yield, and identification of sample components is obtained through analysis of the crude reaction mixture at the start and finish of each intermediate step. In this way, the necessity for tedious purification procedures can be eliminated.

In this paper, the HPLC technique developed for monitoring the isoluminol derivatization of two drugs, zeranol (Ralgro) and medroxyprogesterone acetate (MPA) (Provera), is presented (Fig. 1).

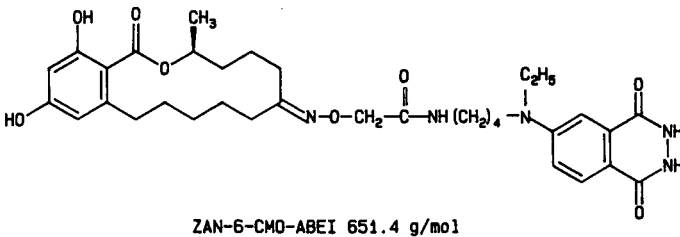
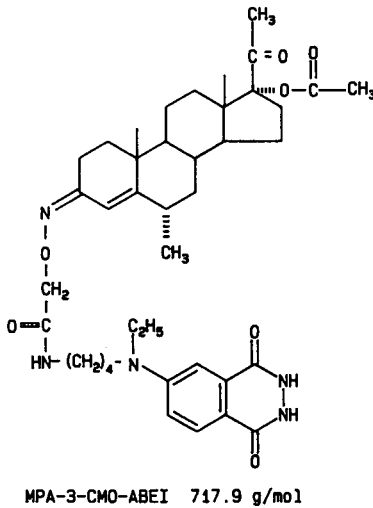


Fig. 1. Structural formulae of isoluminol-labelled medroxyprogesterone acetate (MPA-3-CMO-ABEI) and zeranol (ZAN-6-CMO-ABEI). Zearalanone (the ketone form of zeranol) was used to form the carboxymethyl oxime derivative.

EXPERIMENTAL

Chemicals

Zeranol and zearalanone (ZAN) were kindly provided by the International Minerals and Chemical Corporation (Terre Haute, IN, U.S.A.), and MPA by Upjon (Kalamazoo, MI, U.S.A.). Carboxymethoxylamine hemihydrochloride, N-hydroxysuccinimide and 1,3-dicyclohexylcarbodiimide were purchased from Aldrich (Milwaukee, WI, U.S.A.), and N-(4-aminobutyl)-N-ethylisoluminol (ABEI) from Sigma (St. Louis, MO, U.S.A.). Other reagents of analytical grade were obtained from various commercial sources.

Apparatus

The following apparatus were used: HPLC, a Waters Assoc. liquid chromatography system consisting of a Model 6000A solvent delivery system, Model U6K injector, and Model 440 ultraviolet detector; NMR, Bruker AM-400, measuring protons at 400.13 MHz; MS, Finnigan MAT, Model 4610, used in the chemical ionization (CI) mode, with solid probe at 260°C.

Preparation of MPA-3-carboxymethyloxime-ABEI

The procedure used was a modification of the ones described by Jansen *et al.*^{8,9} and Cornette *et al.*¹⁰. A solution of MPA (0.5 mmol) in pyridine (15.0 ml) was reacted with carboxymethoxylamine (CMO) hemihydrochloride (450 mg, equivalent to 4 mmol CMO), with stirring for 15 min at room temperature. The pyridine was removed in a rotary evaporator under reduced pressure. The residue was taken up in cold 0.1 M HCl (30 ml), and the acidified oxime was extracted in ethyl acetate (3 × 40 ml). The combined extracts were washed with water (3 × 15 ml), and dried with anhydrous sodium sulphate. The solvent was evaporated as above, leaving MPA-3-CMO as a white foam (250 mg yield).

MPA-3-CMO (68.9 mg, 0.15 mmol) was dissolved in anhydrous dimethylformamide (1.5 ml). Anhydrous N-hydroxysuccinimide (17.3 mg, 0.15 mmol) was added and stirred to dissolve. The solution was cooled to 0°C and 1,3-dicyclohexylcarbodiimide (30.95 mg) was added. After 24 h at room temperature, the activated ester supernatant was syphoned off with a Pasteur pipette from the crystalline dicyclohexylurea by-product.

To the activated ester solution was added dropwise 1 equivalent of ABEI dissolved in 0.2 M sodium dihydrogenphosphate (3.0 ml, final pH 7.5). Ethyl acetate (6.0 ml) was added and the resulting clear two-phase reaction mixture was stirred for 2.5 h. The organic layer was collected, and the aqueous phase was washed with ethyl acetate (2 × 3.0 ml). The organic extracts were combined, dried by adding anhydrous sodium sulphate, filtered and evaporated leaving MPA-CMO-ABEI (81 mg) as a yellow syrup.

Preparation of ZAN-6-CMO-ABEI

The isoluminol-labelled zeranol was prepared by the method of Jansen *et al.*⁹ using ZAN as starting material and four-fold excess equivalents of CMO hemihydrochloride. The final product was extracted in ethyl acetate (1.0 ml), dehydrated by mixing with sodium sulphate, filtered and evaporated to *ca.* 0.2 ml, yielding fine pale yellow crystals at 4°C.

Chromatographic procedure

Normal-phase HPLC was performed with a column (15 cm × 4.6 mm I.D.) of silica gel, particle size 5 μm (S5W, Chromatography Sciences, Montreal, Canada). Four different combinations of hexane-ethanol-acetic acid were used under the following conditions: 92:8:0.5 (v/v/v) at 2.0 ml/min for monitoring the reaction kinetics of MPA, MPA-3-CMO, and MPA-3-CMO-activated ester; 75:25:0.5 (v/v/v) at 2.0 ml/min for MPA-3-CMO-ABEI; 95:5:0.5 (v/v/v) at 2.0 ml/min for ZAN and ZAN-6-CMO; and 80:20:0.5 (v/v/v) at 3.0 ml/min for ZAN-6-CMO-activated ester and ZAN-6-CMO-ABEI. Column eluent was monitored at 254 nm for MPA and its derivatives, and at 313 nm for ZAN and its derivatives.

At each stage of preparation, samples (1 μl) of the reaction mixture were removed for HPLC analysis starting at time 0 h and continuing periodically until the reaction reached a steady state. The percent completion of each reaction was estimated from the peak area ratios of the starting material at the beginning and the end of the reaction. Overall yields were calculated by using the expected and actual weights of the finished products.

For both drugs the starting material, the oxime and the finished product were identified by MS and NMR. The identity of the activated ester peak on HPLC was assumed from its rate of formation, with the simultaneous disappearance of the starting materials.

RESULTS

Reaction progress was monitored by HPLC as described in the Experimental section. For each drug, at least two mobile phases were required for adequate separation of all derivatives (Table I). The oxime of both drugs, and the ester of MPA, were found to elute as double peaks representing *syn*- and *anti*-isomers at the oxime nitrogen. The presence of the two isomers was confirmed by NMR. Two peaks close together, near 4.5 ppm, were present at a ratio of approximately 2:1 in both

TABLE I

CAPACITY FACTORS (k') OF MEDROXYPROGESTERONE ACETATE, ZEARALANONE AND THEIR DERIVATIVES

Column: silica gel, 5 μm, 150 × 4.6 mm I.D. Mobile phase A: hexane-ethanol-acetic acid (92:8:0.5, v/v/v), 2.0 ml/min; mobile phase B: hexane-ethanol-acetic acid (75:25:0.5, v/v/v), 2.0 ml/min; mobile phase C: hexane-ethanol-acetic acid (95:5:0.5, v/v/v), 2.0 ml/min; mobile phase D: hexane-ethanol-acetic acid (80:20:0.5, v/v/v), 3.0 ml/min.

Derivative	MPA		ZAN	
	A	B	C	D
Drug	3.0	—	1.8	—
Oxime	2.1, 2.6 ^a	1.0	2.4, 2.9 ^a	1.3
Succinimide ester	6.3, 7.6 ^a	1.4	12.0	1.8
Final product				
Drug-CMO-ABEI	—	2.7	—	4.3

^a Two isomers (*syn* and *anti*).

MPA-3-CMO-ABEI and ZAN-6-CMO-ABEI, representing the methylene protons of the CMO residue.

Oxime formation

The oximes of MPA and ZAN were prepared by reacting each drug with a 4–8 fold excess carboxymethoxylamine in pyridine at room temperature. Excess pyridine had a tendency to interfere with chromatography, but this could be controlled by diluting the reaction mixture 1:400 in hexane and injecting 20 μ l. Based on comparison of initial reactant to residual amounts, MPA-3-CMO production was found to be complete within 15 min in presence of 4 mmol CMO (Fig. 2A and B). MPA was well separated from MPA-3-CMO, forming a shoulder on the descending side of the oxime doublet (Fig. 2C). The limit of detection of residual MPA from amongst the oxime trailing peak was estimated to be approximately 5% of the total oximes.

The formation of ZAN-6-CMO was also rapid at a CMO:ZAN ratio of 4 (Fig. 3). Over 70% of ZAN had reacted in 15 min, and the reaction was essentially 100% complete after 2 h at room temperature.

The oxime was purified by evaporating the reaction mixture, partitioning the residue between ethyl acetate and an excess of cold 0.1 M HCl and evaporating the extract. In these conditions, no hydrolysis of the oxime was observed as seen by the

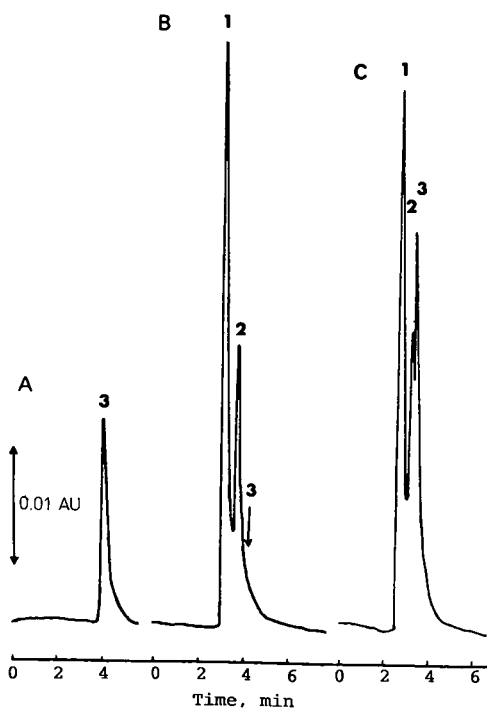


Fig. 2. Reaction of MPA with carboxymethoxylamine. Reaction times: (A) 0 h; (B) 0.25 h; (C) MPA and MPA-3-CMO. Peaks: (1) and (2), MPA-3-CMO (*syn* and *anti* isomers), (3) MPA. Chromatographic conditions: column, silica gel (5 μ m particles, 150 \times 4.6 mm I.D.). Mobile phase, hexane-ethanol-acetic acid (92:8:0.5, v/v/v), at 2.0 ml/min. Detection at 254 nm.

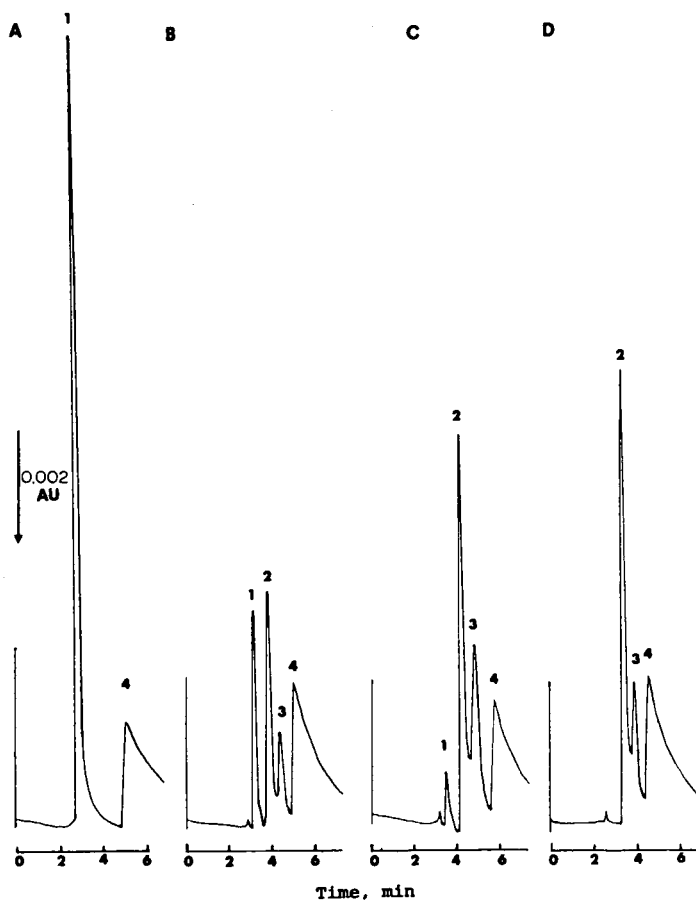


Fig. 3. Reaction of zearalanone with carboxymethoxylamine. Reaction times: (A) 0 h; (B) 0.25 h; (C) 1 h; (D) 2 h. Peaks: (1) ZAN; (2) and (3) ZAN-6-CMO (*syn* and *anti* isomers); (4) pyridine. Mobile phase, hexane-ethanol-acetic acid (95:5:0.5, v/v/v). Detection at 313 nm. Other conditions as in Fig. 2.

absence of either zeranone or ZAN on chromatographing the extract. Based on final weights, recovery of oxime product was 100% for MPA-3-CMO, and 87.1% for ZAN-6-CMO (Table II).

Formation of the succinimide ester

This reaction was accomplished using N-hydroxysuccinimide in the presence of dicyclohexylcarbodiimide. Upon reaction, both oxime peaks disappeared and were replaced by the succinimide ester peaks as illustrated in Fig. 4 for MPA. For both drugs, a steady state was reached within 24 h. In this time period, based on peak areas, 97.0% of the MPA-3-CMO and 93.3% of ZAN-6-CMO had reacted.

Formation of the labelled product

The succinimide ester derivative of each drug was reacted with a slight excess of ABEI in a two-phase system consisting of dibasic phosphate and ethyl acetate. Both

TABLE II
RECOVERY OF MPA AND ZERANOL DERIVATIVES

Compound	MW	Weight (mg)	mmol	% yield
Zearalanone	320.4	160.1 ^a	0.4997	—
ZAN-6-CMO	393.6	171.2 ^b	0.4350	87.1
ZAN-6-CMO	393.6	50.0 ^a	0.1270	—
ZAN-6-CMO-ABEI	651.9	50.4 ^b	0.0773	60.9
MPA	386.5	192.7 ^a	0.4986	—
MPA-3-CMO	459.7	246.0 ^b	0.5351	107.3
MPA-3-CMO	459.7	72.0 ^a	0.1566	—
MPA-3-CMO-ABEI	718.0	81.0 ^c	0.1128	72.0

^a Starting material.

^b By extraction and recrystallization.

^c By preparative HPLC and evaporation.

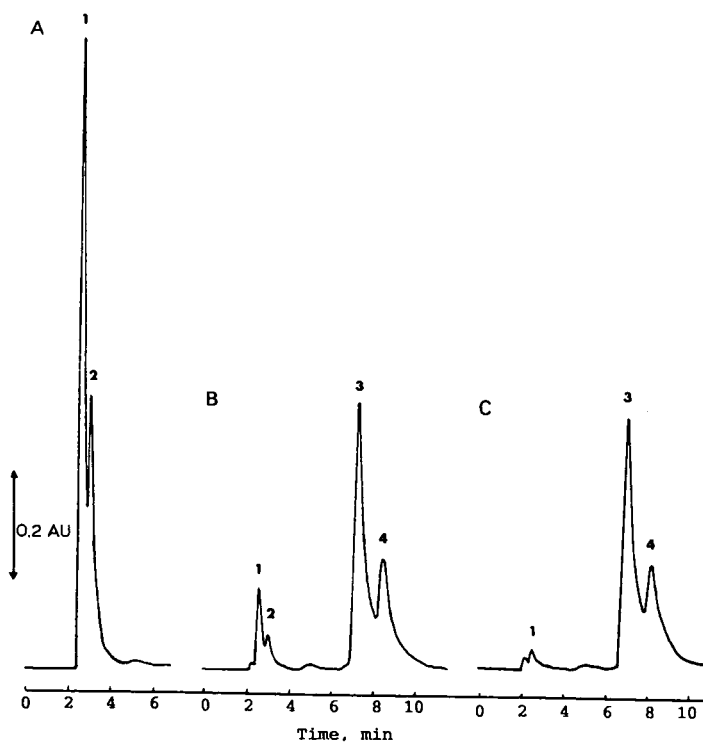


Fig. 4. Reaction of MPA-3-CMO with N-hydroxysuccinimide. Reaction times: (A) 0 h; (B) 6 h; (C) 23 h. Peaks: (1) and (2) MPA-3-CMO (*syn* and *anti* isomers); (3) and (4) MPA-3-CMO-N-succinimide ester (*syn* and *anti* isomers). Chromatographic conditions as in Fig. 2.

succinimide ester peaks reacted to form a single peak of labelled drug as shown in Fig. 5 for MPA. No attempts were made to separate the two isomers. Labelling of MPA was found to reach steady state within 2.5 h with 99.0% of available MPA-3-CMO-N-succinimide ester reacted. Extraction with ethyl acetate afforded 78.4% recovery of the total labelled MPA present in the reaction mixture, as monitored by HPLC. The identity of the product was confirmed by MS in the chemical ionization (CI) mode, showing the $[M + 1]$ peak at m/z 718.8, and by NMR, showing the aromatic protons of isoluminol (two doublets at 7 and 8 ppm and a singlet at 7.2 ppm), the CMO methylene protons at 4.5 ppm (*syn* and *anti*, see above) and the aliphatic and steroid protons between 0 and 2.2 ppm.

ZAN-6-CMO-succinimide ester was reacted with ABEI for only 30 min. HPLC analysis of the reaction mixture at this time revealed 89.6% reaction of the available ZAN ester. The efficiency of the extraction of the total labelled ZAN was 72.8%, similar to that of MPA. The final labelled product was fairly pure, with only two small contaminating peaks observable by HPLC analysis.

Fig. 6 illustrates the rates of formation of MPA-3-CMO, MPA-3-CMO-N-succinimide ester and MPA-3-CMO-ABEI from their respective precursors, based on HPLC measurement of the starting material (drug, oxime or activated ester) remaining at different sampling times. The oxime production (top curve) was rapid; steady state was achieved within the shortest sampling period. Production of esterified oxime (bottom curve) was much more gradual taking 23 h for the complete reaction.

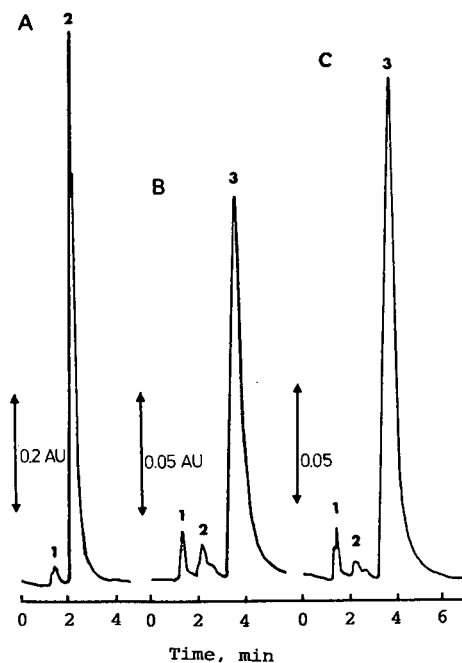


Fig. 5. Reaction of MPA-3-CMO-N-succinimide with ABEI. Reaction times: (A) 0 h; (B) 1.5 h; (C) 2.5 h. Peaks: (1) MPA-3-CMO; (2) MPA-3-CMO-N-succinimide ester (*syn* and *anti* isomers); (3) MPA-3-CMO-ABEI. Mobile phase, hexane-ethanol-acetic acid (75:25:0.5, v/v/v). Other conditions as in Fig. 2.

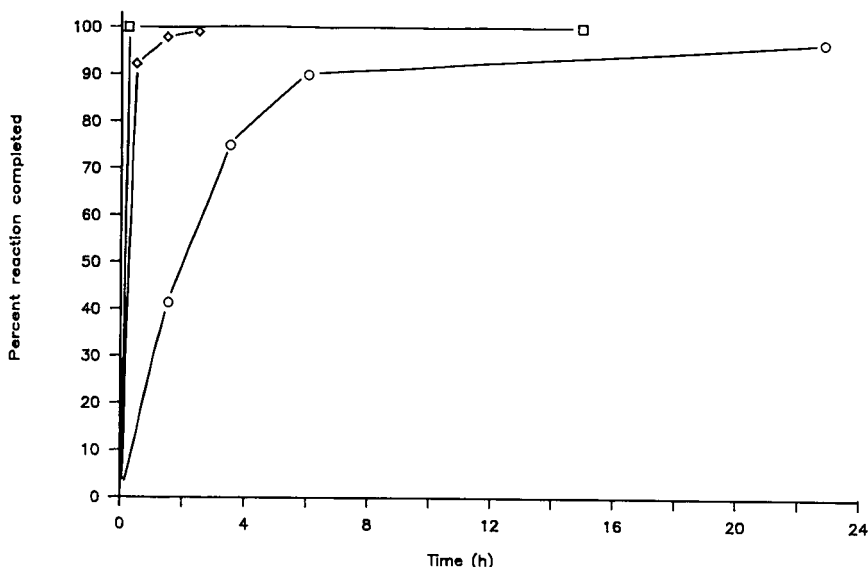


Fig. 6. Reaction profile of the formation of medroxyprogesterone acetate derivatives, estimated from the disappearance of the starting material. (□) MPA-3-CMO; (◇) MPA-3-CMO-ABEI; (○) MPA-3-CMO-N-succinimide ester.

Conjugation to ABEI (middle curve) was intermediate taking 2.5 h for completion. Eventually, each reaction achieved close to 100% yield.

Based on final weights of the products, the yields of both labelled drugs from the oxime were acceptably high: 72.0% for MPA and 60.9% for ZAN (Table II).

DISCUSSION

Monitoring reaction progress by HPLC is a novel technique. HPLC has traditionally proved useful in the isolation, quantitation, and identification of compounds. Here, it was shown to be a viable alternative to conventional monitoring procedures such as thin-layer chromatography. With real-time monitoring by HPLC, quantitative information on product quality and yield is obtained more rapidly, optimum time required for each reaction may be established and low yield can immediately be traced to its source. Thus, the procedure may be quickly modified and improved.

Normal phase chromatography was preferred in most of this work, as this gave good separations, and required only a small number of different mobile phases for all the reactants and products involved. Additionally, the organic mobile phase was compatible with the reaction and extraction (mostly ethyl acetate) for direct injection of the aliquots. Nevertheless, for the final purification of the labelled drug before LIA, a reversed-phase system was found preferable.

The isocratic HPLC system utilized here, although simple, was effective in resolving each of the compounds synthesized. Two mobile phases were, however, required for each drug. Improved monitoring might be achieved with gradient-elution HPLC such that all derivatives of a drug would be analyzed in a single system.

HPLC was effective in monitoring the oxime production of both drugs. The two isomers, *syn* and *anti*, were well separated. Thus, preparative HPLC could be used for separating them, should this be necessary. Separation between the MPA and its oximes was not baseline but still adequate to detect approximately 5% residual drug. With this technique it was found that the time needed for complete synthesis was only 15 min for MPA-3-CMO, and 2 h for ZAN-6-CMO. Others have found that progesterones and ZAN required much longer incubation times, ranging between 16 and 48 h⁸⁻¹⁰.

Recovery of MPA-3-CMO was slightly better than that of ZAN-6-CMO. This may have been due to the use of ethyl acetate for extracting the former as opposed to chloroform used for the latter oxime. Both oximes were found to be more soluble in ethyl acetate than in either chloroform or ether, solvents recommended by other authors^{6,7}.

The conjugation of the activated MPA to ABEI required 2.5 h for completion, although at 30 min it was over 90% complete. The analogous reaction with ZAN, terminated at 30 min, twice the length of time suggested by Jansen *et al.*⁹, was also close to 90% complete. Final yield for both drugs based on weights, was slightly lower than expected from chromatography results, due mainly to losses during extraction.

Final labelled products were found to be reasonably pure. Major impurities such as residual reactants were probably minimized since reactions were monitored and allowed to proceed to completion. Nevertheless, prior to use in an immunoassay the labelled drug must be further purified, otherwise, traces of unconjugated drug or luminescent material could cause interference⁸.

Some limitations have been observed with HPLC. It cannot be used for absolute quantitation of the reaction products unless standards are available to establish retention time and detector response. Preliminary synthesis followed by crystallization, is, therefore, still necessary to provide acceptably pure standards. Nevertheless, the speed and amount of information obtained by HPLC, with or without pure standards, exceed most other available systems.

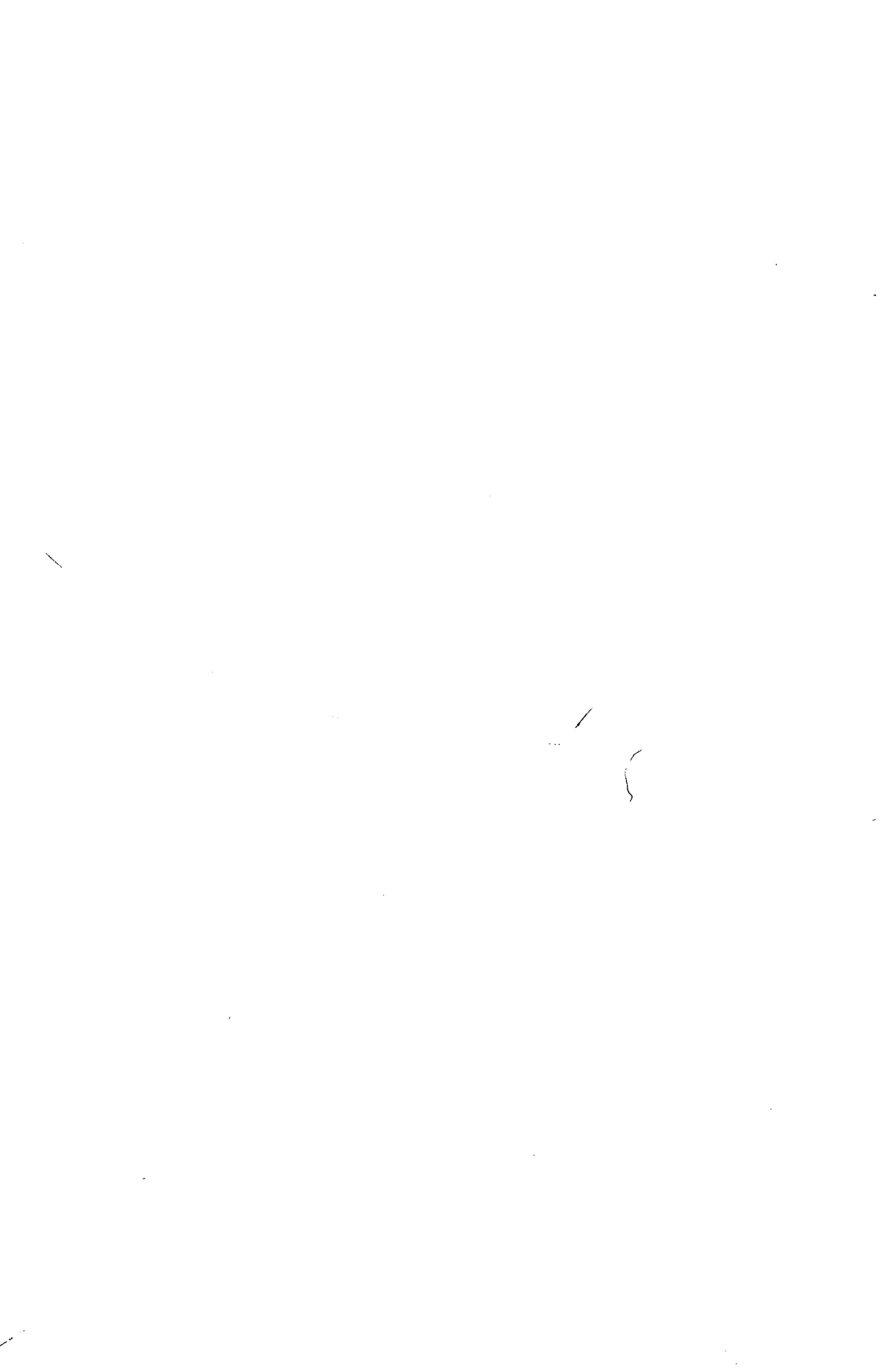
ACKNOWLEDGEMENTS

The authors thank the following people from the Bureau of Drug Research, Health and Welfare Canada: Dr. B. Dawson for providing the NMR spectra, Dr. J. Zamecnik and Mr. J. C. Ethier for the MS identifications, and Dr. J. C. K. Loo for his technical advice. We also thank Upjohn Co., Kalamazoo, MI, U.S.A. for the gift of MPA, and International Minerals and Chemical Co., Terre Haute, In, U.S.A. for their gift of zeranol and ZAN.

REFERENCES

- 1 A. Belanger, P. Brassard, S. Laquerre and Y. Merand, *Can. J. Chem.*, 65 (1987) 1392.
- 2 M. Pazzagli, J. B. Kim, G. Messeri, G. Martinazzo, F. Kohen, F. Franceschetti, G. Moneti, R. Salerno, A. Tommasi and M. Serio, *Clin. Chim. Acta*, 115 (1981) 277.
- 3 H. R. Schroeder, R. C. Bogulaski, R. J. Carrico and R. T. Buckler, *Methods Enzymol.*, 57 (1978) 424.
- 4 G. G. S. Dutton, K. B. Gibney, P. E. Reid and K. N. Slessor, *J. Chromatogr.*, 20 (1965) 163.
- 5 M. S. J. Dallas, *J. Chromatogr.*, 48 (1970) 193.
- 6 R. F. McGregor and M. Khan, *Clin. Chim. Acta*, 14 (1966) 844.
- 7 E. H. J. M. Jansen, R. H. van den Berg, R. Both-Miedema, C. Enkelaar-Willemsen and G. Zomer, *Anal. Chim. Acta*, 205 (1988) 175.

- 8 E. H. J. M. Jansen, R. H. van den Berg, C. Enkelaar-Willemsen and G. Zomer, *J. Chromatogr.*, 437 (1988) 268.
- 9 E. H. J. M. Jansen, R. H. van den Berg, G. Zomer, C. Enkelaar-Willemsen and R. W. Stephany, *J. Vet. Pharmacol. Therap.*, 9 (1986) 101.
- 10 J. C. Cornette, K. Kirton and G. W. Duncan, *Clin. Endocrinol. Metab.*, 33 (1971) 459.



CHROM. 21 337

DETERMINATION OF PRESERVATIVES IN COSMETIC PRODUCTS

II. HIGH-PERFORMANCE LIQUID CHROMATOGRAPHIC IDENTIFICATION

N. DE KRUIJF*, A. SCHOUTEN, M. A. H. RIJK and L. A. PRANOTO-SOETARDHI

TNO-CIVO Food Analysis Institute, Department of Toxicological Analysis, P.O. Box 360, 3700 AJ Zeist (The Netherlands)

(First received December 6th, 1988; revised manuscript received January 18th, 1989)

SUMMARY

A high-performance liquid chromatographic (HPLC) procedure is presented for the separation and identification of preservatives that are listed in the current EEC Council Directive on cosmetic products or have been permitted in the past. The method consists of an extraction of acidified cosmetics with methanol, and separation of the extracts by HPLC. Using two isocratic and two gradient reversed-phase HPLC systems, 47 preservatives were characterized by their retention times. The preservatives in three commercial cosmetic products were tentatively identified by the procedure described. The HPLC procedure is suitable for confirmation of the presence of preservatives in cosmetic products as indicated by a previously reported thin-layer chromatographic procedure. In general this method will permit the routine detection of preservatives in cosmetics in an approximate concentration of 0.01% (w/w).

INTRODUCTION

Preservatives are antimicrobial agents that are widely used in cosmetics to protect the health of the consumer, as well as to maintain the potency and stability of the product formulations. Combinations of two or more preservatives are often used to increase the ability of the system to withstand microbial contamination and to widen the range of microorganisms against which the cosmetic is protected¹⁻⁴.

The European Economic Community (EEC) Council Directive on cosmetics includes a positive list of preservatives for cosmetics. At present some 60 preservatives or groups of related preservatives are either definitively or provisionally permitted in cosmetics at specified maximum concentrations. Methods for the identification and quantification of these preservatives in cosmetic products are necessary for checking compliance with the EEC Directive.

A screening procedure based on a combination of thin-layer chromatography (TLC) and high-performance liquid chromatography (HPLC) was developed to identify the preservatives listed. In a previous paper a TLC procedure was presented that

enables the preliminary identification of many of the preservatives mentioned in the current EEC Council Directive on cosmetic products or which have been permitted in the past⁵. This paper describes a HPLC procedure that is suitable for confirmation of the presence of preservatives in cosmetic samples as indicated by the TLC procedure.

The use of HPLC for the analysis of preservatives permitted by the EEC Council Directive on cosmetic products has been previously described⁶⁻¹⁴. Most of this literature is concerned with a narrow range of related preservatives, and none of these methods enables the simultaneous determination of a wide range of unrelated preservatives in cosmetics. The HPLC procedure presented here is suitable for the separation and identification of many of the preservatives currently permitted by the EEC Council Directive on cosmetic products. The method consists of a simple sample preparation procedure and the separation of the preservatives using two isocratic and two gradient reversed-phase HPLC systems.

EXPERIMENTAL

Apparatus

The HPLC system used was a SP 8100 ternary liquid chromatograph (Spectra-Physics, San Jose, CA, U.S.A.), equipped with an SP 8110 autosampler, an SP 8440 variable-wavelength UV detector and an SP 4100 computing integrator.

Reagents and materials

Methanol, acetonitrile, tetrahydrofuran (unstabilized) and water used for the HPLC mobile phases were HPLC grade.

All preservatives were commercial grade. In a previous publication⁵ EEC names and synonyms for these preservatives were tabulated along with the maximum authorized concentrations as specified in the EEC Council Directive on cosmetic products.

All other chemicals and solvents employed were of reagent-grade quality and were used without further purification.

The cosmetic samples, a hand cream, a face powder and a night cream, were obtained from local outlets.

Preparation of samples and standards

A test portion of *ca.* 1 g of sample was weighed into a 50-ml glass tube fitted with a screw cap. After addition of 0.5 ml of 4 M formic acid and 9.5 ml of methanol, the tube was closed and vigorously shaken for 1 min. If required, the mixture was gently heated in a water-bath maintained at 60°C, to melt any lipid phase and to facilitate the extraction of preservatives into the methanol phase. The extract was stored overnight. If necessary the mixture was filtered using a disposable filter holder. A 2-ml aliquot of the clear sample solution was pipetted into a 5-ml sample vial.

Reference solutions, each containing 0.1 mg/ml of a mixture of methanol and 4 M formic acid (19:1), were prepared for all preservatives.

Chromatographic system 1

A 125 mm × 4.6 mm I.D. stainless-steel column slurry-packed with 5- μ m Zorbax C₈ (DuPont, Wilmington, DE, U.S.A.) was used under ambient conditions.

Mobile phase A was prepared as follows: 1.13 g of disodium hydrogen phosphate dihydrate and 2.88 g of 85% orthophosphoric acid were mixed with 1 l water. Mobile phase B was acetonitrile. The gradient profile was as follows:

Initial	80% A	20% B
Linear, 15 min to	70% A	30% B
Linear, 10 min to	40% A	60% B
Isocratic, 10 min at	40% A	60% B
Return, 2 min to	80% A	20% B
Reequilibrate, 5 min at	80% A	20% B

The flow-rate was 2.0 ml/min. The UV detector was set at 280 nm with 0.04 a.u.f.s. The injection volume was 10 μ l.

Chromatographic system 2

A 125 mm \times 4.6 mm I.D. stainless-steel column slurry-packed with 5- μ m Nucleosil 5 C₁₈ (Macherey-Nagel, Düren, F.R.G.) was used under ambient conditions. The mobile phase was acetonitrile-methanol-tetrahydrofuran-water (5:2:1:12). The flow-rate was 1.5 ml/min. The UV detector was operated at 280 nm with 0.16 a.u.f.s. The injection volume was 10 μ l.

Chromatographic system 3

A 125 mm \times 4.6 mm I.D. stainless-steel column slurry-packed with 5- μ m ODS Hypersil (Shandon Southern, Runcorn, U.K.) was used under ambient conditions. The mobile phase was acetate buffer-acetonitrile (9:1). The acetate buffer contained 6.35 g sodium acetate trihydrate and 20 ml 96% acetic acid per litre water. The flow-rate was 2.0 ml/min. The UV detector was set at 240 nm with 0.08 a.u.f.s. The injection volume was 10 μ l.

Chromatographic system 4

A 125 mm \times 4.6 mm I.D. stainless-steel column slurry-packed with 10- μ m μ Bondapak C₁₈ (Waters Assoc., Milford, MA, U.S.A.) was used under ambient conditions. Mobile phase A was prepared by dissolving 5.84 g sodium chloride and 1.01 g sodium heptanesulphonate in 1 l water. To this solution 10 ml of 96% acetic acid were added. Mobile phase B was prepared as follows: 5.84 g sodium chloride and 1.01 g sodium heptanesulphonate were dissolved in 100 ml water. To this solution 900 ml of methanol and 10 ml of 96% acetic acid were added. The gradient profile was as follows:

Initial	70% A	30% B
Isocratic, 4 min at	70% A	30% B
Linear, 8 min to	35% A	65% B
Isocratic, 6 min at	35% A	65% B
Linear, 4 min to	0% A	100% B
Isocratic, 3 min at	0% A	100% B
Return, 3 min to	70% A	30% B
Reequilibrate, 5 min at	70% A	30% B

The flow-rate was 2.5 ml/min. The UV detector was set at 264 nm with 0.16 a.u.f.s. The injection volume was 10 μ l.

RESULTS AND DISCUSSION

All preservatives mentioned in the current EEC Council Directive on cosmetic products, except thiomersal, phenylmercury and germall II, for which no reference material was available, were examined by the procedure described. In addition, a number of preservatives permitted previously but now deleted from the Directive were included in the investigation⁵.

Of the preservatives investigated, L-usnic acid, D-usnic acid, zinc pyrithione, germall 115, potassium metabisulphite and sodium iodate were found to be insoluble in methanol-4 M formic acid (19:1), while others were not determined properly by means of the HPLC methods. These preservatives were either eluted too early or too late from the chromatographic columns, or were not detectable by UV detection at the wavelengths applied. The HPLC procedure consisting of the four chromatographic systems described above permitted the characterization of 47 preservatives. The chromatographic behaviour of these preservatives is summarized in Table I. Some preservatives give a large major peak as well as one or more minor peaks, indicating that impurities were present in some of the preservative reference materials. In these cases only the major peak is listed in Table I. Kathon CG, however,

TABLE I
RETENTION TIMES FOR PRESERVATIVES CHROMATOGRAPHED ON FOUR HPLC SYSTEMS

System 1: column, Zorbax C₈ (5 μ m), 125 mm \times 4.6 mm I.D.; mobile phase, phosphate buffer-acetonitrile gradient; flow-rate, 2.0 ml/min; detection, UV at 280 nm. System 2: column, Nucleosil 5 C₁₈ (5 μ m), 125 mm \times 4.6 mm I.D.; mobile phase, acetonitrile-methanol-tetrahydrofuran-water (5:2:1:12); flow-rate, 1.5 ml/min; detection, UV at 280 nm. System 3: column, ODS Hypersil (5 μ m), 125 mm \times 4.6 mm I.D.; mobile phase, acetate buffer-acetonitrile (9:1); flow-rate, 2.0 ml/min; detection, UV at 240 nm. System 4: column, μ Bondapak C₁₈ (10 μ m), 125 mm \times 4.6 mm I.D.; mobile phase, methanol-water containing sodium heptanesulphonate, sodium chloride and acetic acid ion-pair gradient; flow-rate, 2.5 ml/min; detection, UV at 264 nm.

EEC No. ^a		Preservative	Retention times (min)			
I	II		System 1	System 2	System 3	System 4
2.13	2.41	Pyrrithione disulphide	1.3	1.3	1.5	1.7
-	2.34	8-Hydroxyquinoline	1.5	1.4	-	2.1
1.12	1.12	<i>p</i> -Hydroxybenzoic acid	2.1	1.6	1.9	1.8
1.39	2.45	Kathon CG ^b	2.4/2.1	1.6	2.5/1.5	2.0/0.9
1.34	2.51	Benzyl alcohol	3.5	3.4	4.1	2.3
1.29	2.43	Phenoxyethanol	5.4	2.4	7.4	3.2
-	2.40	Sodium pyrithione	5.5	1.8	-	1.8
1.4	1.4	Sorbic acid	5.9	2.6	7.8	4.6
1.1	1.1	Benzoic acid	6.3	2.6	6.6	4.5
1.12	1.12	Methylparaben	7.3	2.9	10.0	5.3
1.3	1.3	Salicylic acid	7.9	1.4	2.6	4.3
1.13	2.4	Dehydroacetic acid	8.1	3.0	9.6	4.8
2.2	2.3	Chlorphenesin	8.2	3.0	21.0	7.1
1.20/2.7	2.18	Bronidox	8.9	3.6	7.4	2.8

TABLE I (continued)

EEC No. ^a		Preservative	Retention times (min)			
I	II		System 1	System 2	System 3	System 4
2.14	2.56	Phenoxypropanol	9.1	3.4	18.2	6.3
1.12	1.12	Ethylparaben	12.2	4.5	29.3	9.7
1.1	1.1	Methyl benzoate	16.5	6.2	—	10.2
1.22	2.24	2,4-Dichlorobenzyl alcohol	17.4	8.0	—	12.0
1.24	2.26	<i>p</i> -Chloro- <i>m</i> -cresol	19.0	8.6	—	11.5
1.12	1.12	Propylparaben	19.1	7.8	—	12.5
1.26	2.32	<i>p</i> -Chloro- <i>m</i> -xyleneol	22.5	13.6	—	13.8
1.1	1.1	Ethyl benzoate	22.6	11.0	—	12.6
1.38	2.37	4-Isopropyl-3-methylphenol	23.1	13.8	—	13.6
1.12	1.12	Butylparaben	23.2	14.5	—	14.7
1.7	1.7	<i>o</i> -Phenylphenol	23.5	15.0	—	13.3
2.19	2.6	Benzylparaben	23.7	16.4	—	14.7
1.32	2.49	Climbazol	25.4	—	—	14.2
—	2.12	Sorbic acid, isopropyl ester	25.4	18.0	—	15.4
—	2.33	Dichloro- <i>m</i> -xyleneol	25.5	29.9	—	16.1
1.1	1.1	Propyl benzoate	25.8	20.8	—	15.2
—	2.29	Dichlorophene	26.2	50.4	—	17.1
2.9	2.17	Chlorophene	27.3	54.7	—	17.5
1.1	1.1	Benzyl benzoate	28.0	42.9	—	17.8
1.1	1.1	Butyl benzoate	28.2	40.5	—	18.0
1.23	2.25	Triclocarban	29.6	—	—	22.4
1.25	2.28	Triclosan	29.8	—	—	22.0
—	2.21	Tetrabromo- <i>o</i> -cresol	30.0	—	—	22.9
—	2.27	Halocarban	30.6	—	—	22.8
1.37	2.20	Bromophen	31.4	—	—	23.5
1.6	1.6	Hexachlorophene	33.3	—	—	24.4
1.21	2.19	Bronopol	—	—	1.38	—
2.3	2.9	Dibromopropamide, diisethionate	—	—	—	12.8
2.20	2.7	Hexamidine, diisethionate	—	—	—	13.3
1.15	2.8	Dibromohexamidine, diisethionate	—	—	—	15.3
2.24	2.31	Chlorhexidine, digluconate	—	—	—	16.4
2.24	2.31	Chlorhexidine · 2HCl	—	—	—	16.6
2.15	2.53	Benzethonium chloride	—	—	—	23.5

^a According to EEC Commission Directive 86/199/EEC of March 26th, 1986 (I); according to EEC Council Directive 82/368/EEC of May 17th, 1982 and EEC Commission Directive 83/496/EEC of September 22nd, 1983 (II).

^b Kathon CG contains two active ingredients, and therefore two major peaks are obtained using systems 1, 3 and 4; the retention times of these peaks are presented in order of decreasing peak heights.

consists of 1.15% 5-chloro-2-methyl-4-isothiazolin-3-one, 0.35% 2-methyl-4-isothiazolin-3-one, 25% magnesium nitrate and 73.5% water¹⁵. As this preservative system contains two active ingredients, two major peaks were obtained, using systems 1, 3 and 4, both of which are listed in Table I in order of descending peak height.

Chromatographic system 1 is considered to be the basic screening method. Therefore, the results in Table I are given in order of ascending retention time as obtained with this system. Using this gradient procedure, many preservatives of widely different polarities are eluted. In addition, other cosmetic constituents that might interfere in the determination of the preservatives investigated are also eluted using

chromatographic system 1. Final conclusions concerning the presence of preservatives in cosmetic products can therefore be drawn only after comparison of the results from this HPLC method with the results from both the other HPLC methods and the previously reported TLC procedure⁵. The method is based on a previously described isocratic HPLC method for the determination of hexachlorophene and related bactericides in deodorant preparations¹⁶. The basic screening procedure is particularly useful for the simultaneous determination of *o*-phenylphenol, 2,4-dichlorobenzyl alcohol, triclocarban, *p*-chloro-*m*-cresol, triclosan, *p*-chloro-*m*-xylenol, bromophen, 4-isopropyl-3-methylphenol and hexachlorophene.

By means of chromatographic system 2 a better resolution for the neutral preservatives of medium polarity is achieved. The method is suitable for the simultaneous determination of phenoxyethanol, phenoxypropanol, methylparaben, ethylparaben, propylparaben, butylparaben and benzylparaben. Combinations of these preservatives are often used in cosmetics¹⁷.

A number of polar preservatives that are eluted rather early when the basic screening method (system 1) is used can be resolved by means of chromatographic system 3. This method is particularly suitable for the simultaneous determination of the acid preservatives 4-hydroxybenzoic acid, salicylic acid, benzoic acid and sorbic acid.

Chromatographic system 4 has been included in the screening procedure because it enables the determination of the cationic preservatives dibromopropamide, hexamidine, dibromohexamidine and chlorhexidine, as well as of the quaternary ammonium compound benzethonium chloride. Many preservatives of greatly varying polarities are eluted using this ion-pair gradient system, and therefore the results obtained are also very useful to corroborate the initial identifications made on the basis of retention times obtained with the other chromatographic systems. The method is derived from a previously described method for the determination of basic preservatives in cosmetics⁹. At first the suitability of this previously reported method for the determination of hexamidine, dibromohexamidine, dibromopropamide and chlorhexidine was investigated. These initial experiments showed, however, that these preservatives gave poorly reproducible peak shapes. Sometimes fronting peak shapes were obtained, indicating an instability of the HPLC separation system. Therefore some modifications were introduced. It was found that more reproducible results and symmetrical peaks were obtained when sodium ions were added to the mobile phase constituents, and also a well defined quantity of acetic acid (1%) instead of adjusting the pH of the aqueous part and the apparent pH of the organic part of the mobile phase to 3.5. The addition of an excess of sodium ions to the mobile phase also has a stabilizing effect on the ion-pair HPLC separation system. A comprehensive study on the effect of the counter-ion concentration in the mobile phase on both pairing ion adsorption and solute retention in reversed-phase ion-pair chromatography has been reported by Bartha *et al.*¹⁸. In addition, the gradient profile was adjusted to enable an optimum separation of all determinable preservatives.

The column used for the determination of the cationic preservatives was μ Bondapak C₁₈. Several other reversed-phase materials, *viz.*, ODS Hypersil, RSIL C₁₈ LL, Zorbax C₈ and Nucleosil 5 C₁₈, were also evaluated. It appeared that satisfactory results were obtained only with a μ Bondapak C₁₈ column. A similar result was obtained by Gaffney *et al.*¹⁹, who investigated the determination of chlorhexidine in urine,

For the identification of preservatives in unknown cosmetic formulations the following procedure proved to be most effective. The sample solutions were subjected to the complete HPLC screening procedure. The retention times of the major peaks in the chromatograms obtained were measured. Unknown preservatives were then tentatively identified by comparing these retention times with those obtained for reference substances under similar conditions (Table I). As the retention behaviour of solutes in HPLC determinations is strongly dependent on the type, the brand and the history of the stationary phase applied, and in addition rather sensitive to slight changes in several specified conditions, the retention times presented in Table I have to be regarded as indicative of the relative retention behaviour and the order of elution of the preservatives investigated using the four HPLC separation systems. Therefore, the sample solutions were subsequently analysed again by means of the appropriate chromatographic systems, together with standards of the preservatives tentatively identified in these samples. The retention times thus obtained were used to corroborate the initial identifications. The preliminary conclusions based on these results were used to confirm the presence of preservatives in the cosmetic samples as indicated by a previously reported TLC procedure⁵.

The HPLC methods described have potential application not only in the identification but also in the quantification of preservatives. Although no attempt has been made in this study to optimize the sample preparation procedure, initial experiments indicated a satisfactory recovery of most investigated preservatives from cosmetics. The HPLC methods, as described, can therefore also be used to estimate the amount of a preservative that is possibly identified in a cosmetic product.

The HPLC procedure was applied to three cosmetic products previously investigated by means of the above-mentioned TLC procedure. To illustrate the practical operation of the HPLC screening procedure a detailed description of the identification of the preservatives in a commercial hand cream is given below.

The hand cream sample was subjected to the complete HPLC procedure. The chromatograms obtained using the four HPLC systems are shown in Figs. 1–4. The HPLC analyses of the cosmetic products were performed immediately after the analysis of the preservative reference materials. In this manner the retention times for standards and samples were obtained under practically identical conditions and initial identifications can be made on the basis of retention times.

As is seen in Fig. 1, using HPLC system 1 three major peaks are obtained for the hand cream sample. By comparing the retention times with those of standards (Table I), tentative peak identifications were made (Table II). Also in the chromatogram obtained by means of HPLC system 2 (Fig. 2) three major peaks are observed. The first peak (retention time 0.9 min) was found to result from an unknown compound. The retention time of this early-eluting peak does not correspond to that of any of the preservatives investigated. On the basis of the retention time (4.6 min) the second peak was tentatively identified as ethylparaben. By comparison of the sample peak height with that of the ethylparaben reference solution, the injected amount of ethylparaben represented by the peak was found to be about 1.1 μg , which corresponds to an ethylparaben level in the hand cream of *ca.* 0.11% (w/w). The third peak (retention time 8.0 min) may originate from either propylparaben or 2,4-dichlorobenzyl alcohol. The presence of 2,4-dichlorobenzyl alcohol in the hand cream can be excluded on the basis of the results obtained using HPLC system 1. In the chroma-

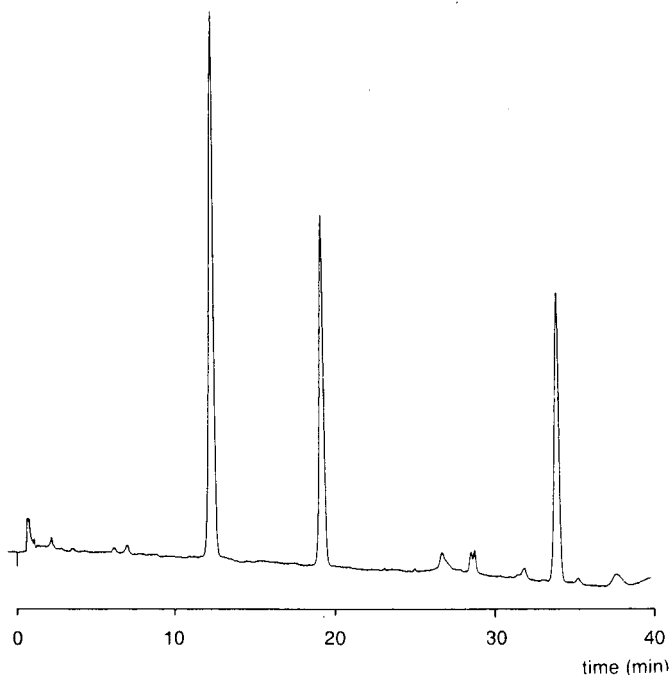


Fig. 1. Chromatogram of a hand cream extract obtained with system 1. Column: Zorbax C_8 ($5\ \mu\text{m}$), $125\ \text{mm} \times 4.6\ \text{mm}$ I.D. Mobile phase: phosphate buffer-acetonitrile gradient; flow-rate, $2.0\ \text{ml/min}$. Injection volume: $10\ \mu\text{l}$. Detection: UV at $280\ \text{nm}$; sensitivity, $0.04\ \text{a.u.f.s.}$

ogram obtained with this HPLC method (Fig. 1) no peak appears to be present having the approximate retention time of 2,4-dichlorobenzyl alcohol. In this manner the third peak in the chromatogram obtained by means of HPLC system 2 was tentatively identified as propylparaben. The propylparaben content of the hand cream represented by the peak was found to be about 0.07% (w/w). The possible presence of *p*-chloro-*m*-cresol as indicated by HPLC system 1 (Table II) is not confirmed by the results obtained by means of HPLC system 2.

Using HPLC system 3 only one large peak was obtained, with a retention time corresponding to that of ethylparaben (Fig. 3). The chromatogram obtained confirms that the hand cream investigated did not contain significant amounts of polar preser-

TABLE II

INITIAL IDENTIFICATION OF CHROMATOGRAPHIC PEAKS OBTAINED FOR A HAND CREAM USING SYSTEM 1

Peak No.	Retention time (min)	Possible identity
1	12.2	Ethylparaben
2	19.0	<i>p</i> -Chloro- <i>m</i> -cresol, propylparaben
3	33.8	Hexachlorophene

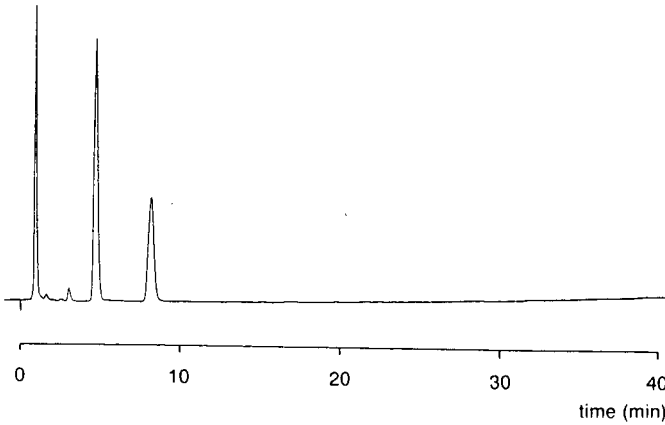


Fig. 2. Chromatogram of a hand cream extract obtained with system 2. Column: Nucleosil 5 C₁₈ (5 μ m), 125 mm \times 4.6 mm I.D. Mobile phase: acetonitrile-methanol-tetrahydrofuran-water (5:2:1:12); flow-rate, 1.5 ml/min. Injection volume: 10 μ l. Detection: UV at 280 nm; sensitivity, 0.16 a.u.f.s.

vatives, such as acid preservatives, that elute rather early when using the basic screening method (system 1), and that cannot be distinguished on the basis of the retention times obtained with HPLC system 1. The presence of ethylparaben and propylparaben in the hand cream is confirmed again by means of HPLC system 4. In the chro-

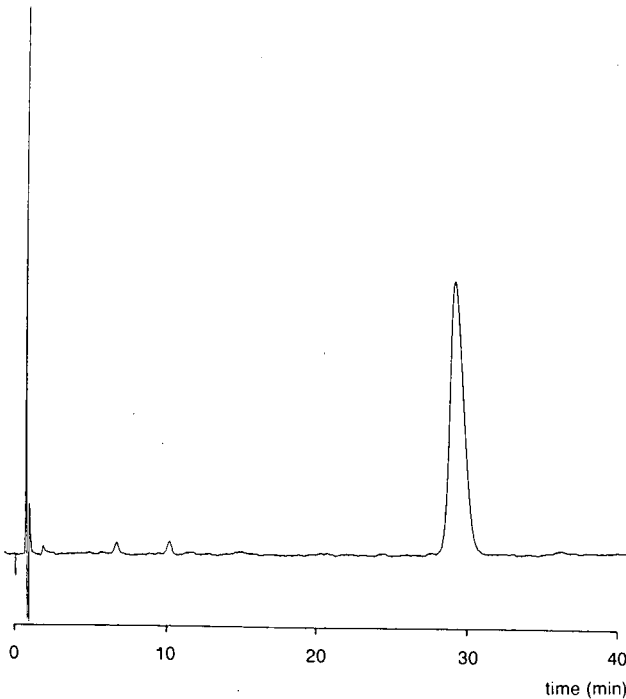


Fig. 3. Chromatogram of a hand cream extract obtained with system 3. Column: ODS Hypersil (5 μ m), 125 mm \times 4.6 mm I.D. Mobile phase: acetate buffer-acetonitrile (9:1); flow-rate, 2.0 ml/min. Injection volume: 10 μ l. Detection: UV at 240 nm; sensitivity, 0.08 a.u.f.s.

matogram obtained with this ion-pair gradient system (Fig. 4) two major peaks are observed with retention times corresponding to those of ethylparaben and propylparaben. As no peak was found to be present in this chromatogram having the approximate retention time of hexachlorophene, the possible presence of this preservative as indicated by HPLC system 1 was not confirmed.

In summary, the results obtained by means of the complete HPLC procedure indicate the presence of ethylparaben (*ca.* 0.11%) and propylparaben (*ca.* 0.07%) in the hand cream sample. These findings confirm the results of a previously reported TLC procedure⁵. Using this TLC procedure, parabens were tentatively identified in the hand cream. Ethylparaben and propylparaben are not separated using the TLC procedure. In addition, the reaction of these related preservatives to the detection reagents applied and their behaviour under UV radiation were found to be very similar. Therefore, ethylparaben and propylparaben cannot be distinguished by means of the TLC procedure. The HPLC procedure, however, permits the identification of the individual parabens. This detailed description of the identification of preservatives in a commercial hand cream demonstrates that the initial identifications made on the basis of the TLC procedure are confirmed and supplemented by the results of the HPLC procedure, and that a final identification of the preservatives present in a cosmetic sample is achieved by an independent comparison of the results obtained for a cosmetic product by means of the TLC procedure and the HPLC procedure with results obtained for reference substances.

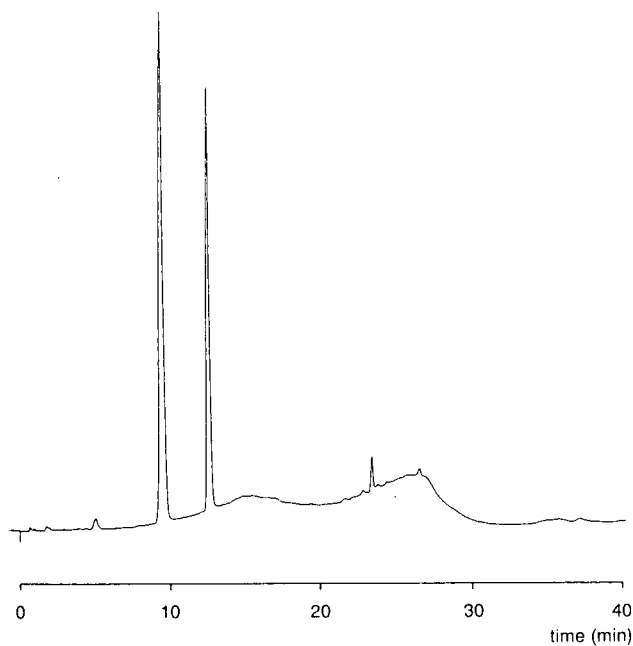


Fig. 4. Chromatogram of a hand cream extract obtained with system 4. Column: μ Bondapak C_{18} (10 μ m), 125 mm \times 4.6 mm I.D. Mobile phase: methanol-water containing sodium heptanesulphonate, sodium chloride and acetic acid ion-pair gradient; flow-rate, 2.5 ml/min. Injection volume: 10 μ l. Detection: UV at 264 nm; sensitivity, 0.16 a.u.f.s.

TABLE III

QUALITATIVE DETERMINATION OF PRESERVATIVES IN COMMERCIAL COSMETIC PRODUCTS

Cosmetic product	Preliminary identifications		Final identifications
	TLC procedure ⁵	HPLC procedure	
Hand cream	Parabens	Ethylparaben Propylparaben	Ethylparaben Propylparaben
Night cream	<i>p</i> -Hydroxybenzoic acid ^a Cationic compound ^a Parabens	<i>p</i> -Hydroxybenzoic acid Hexamidine Methylparaben	<i>p</i> -Hydroxybenzoic acid Hexamidine Methylparaben
Face powder	Parabens Benzoic acid ^a Benzyl benzoate ^a	Methylparaben Propylparaben	Methylparaben Propylparaben

^a Conclusion not clear, but the presence of this compound cannot be excluded.

In a similar manner the preservatives present in a night cream and a face powder sample were identified. The results obtained are summarized in Table III.

In conclusion, the present study has shown that the HPLC screening procedure described that consists of four separation systems, enables the characterization of 47 preservatives by their retention times. It is suitable for confirmation of the presence of preservatives in cosmetic products as indicated by a previously reported TLC procedure. In principle, the HPLC methods described can also be used for the quantitation of preservatives in cosmetics.

In general this HPLC procedure will permit the routine detection of preservatives in cosmetics in an approximate concentration of 0.01% (w/w).

ACKNOWLEDGEMENTS

Thanks are due to the Commission of the European Communities (Directorate General for the Environment, Consumer Protection and Nuclear Safety) for permission to publish this work, and to Mr. J. L. Collin and Mr. G. Gontier for continued interest and support.

REFERENCES

- 1 M. S. Parker, in J. J. Kabara (Editor), *Cosmetic and Drug Preservation*, Marcel Dekker, New York, 1984, p. 389.
- 2 R. A. Cowen and B. Steiger, *Cosmet. Toiletries*, 92 (1977) 15.
- 3 W. E. Rosen and P. A. Berke, *J. Soc. Cosmet. Chem.*, 24 (1973) 663.
- 4 B. Croshaw, *J. Soc. Cosmet. Chem.*, 28 (1977) 3.
- 5 N. de Kruijf, M. A. H. Rijk, L. A. Pranoto-Soetardhi and A. Schouten, *J. Chromatogr.*, 410 (1987) 395.
- 6 H.-J. Schmahl and R. Matissek, *Fresenius' Z. Anal. Chem.*, 307 (1981) 392.

- 7 R. Matissek, *Z. Lebensm.-Unters.-Forsch.*, 176 (1983) 95.
- 8 L. Gagliardi, A. Amato, G. Cavazzuti, V. Zagarese, E. Gattavecchia and D. Tonelli, *J. Chromatogr.*, 294 (1984) 442.
- 9 B. Wyhowski de Bukanski and M. O. Masse, *Int. J. Cosmet. Sci.*, 6 (1984) 283.
- 10 L. Gagliardi, A. Amato, A. Basili, G. Cavazzutti, E. Gattavecchia and D. Tonelli, *J. Chromatogr.*, 315 (1984) 465.
- 11 L. Gagliardi, A. Amato, A. Basili, G. Cavazzutti, E. Gattavecchia and D. Tonelli, *J. Chromatogr.*, 325 (1985) 353.
- 12 L. Gagliardi, A. Amato, A. Basili, G. Cavazzutti, E. Federici, F. Chimenti, M. G. Casanova, E. Gattavecchia and D. Tonelli, *J. Chromatogr.*, 348 (1985) 321.
- 13 R. Matissek, *Z. Lebensm.-Unters.-Forsch.*, 183 (1986) 273.
- 14 R. Matissek, R. Nagorka and M. Daase, *Lebensmittelchem. Gerichtl. Chem.*, 42 (1988) 111.
- 15 C. Wright, E. Gingold, S. Venitt and C. Crofton-Sleigh, *Mutat. Res.*, 119 (1983) 35.
- 16 J. Rooselaar and D. H. Liem, *De Ware(n)-Chemicus*, 10 (1980) 144.
- 17 T. E. Haag and D. F. Loncrini, in J. J. Kabara (Editor), *Cosmetic and Drug Preservation*, Marcel Dekker, New York, 1984, p. 63.
- 18 A. Bartha, H. A. H. Billiet, L. de Galan and G. Vigh, *J. Chromatogr.*, 291 (1984) 91.
- 19 M. H. Gaffney, M. Cooke and R. Simpson, *J. Chromatogr.*, 306 (1984) 303.

CHROM. 21 334

CHARACTERIZATION OF INDIRECT PHOTOMETRY FOR THE DETERMINATION OF INORGANIC ANIONS IN NATURAL WATER BY ION CHROMATOGRAPHY

N. CHAURET and J. HUBERT*

Chemistry Department, Université de Montréal, P.O. Box 6128, Station A, Montreal, Quebec, H3C 3J7 (Canada)

(Received January 11th, 1989)

SUMMARY

A high-performance liquid chromatographic method based on indirect photometric detection is described for the analysis of inorganic anions in natural waters. Up to ten anions can be analyzed simultaneously with detection limits at the nanogram level. The working range covers three decades in concentration and the short term stability is around 1% for most anions. The validity of the method is proven by an inter-laboratory study and by the analysis of certified samples. The main advantages of this method over ion chromatography with suppressed conductivity detection are its simple response standardization and its simplicity as it involves conventional high-performance liquid chromatography equipment.

INTRODUCTION

The determination of inorganic anions in natural water is becoming increasingly important as it allows a better understanding of environmental pollution. The standard methods used are usually based on a specific reaction for each species (*e.g.*, colorimetric or electrochemical reactions¹). When a large number of determinations are required, the application of specific reactions for anions becomes time consuming and the possibility of the simultaneous separation, identification and quantification of several anions is then of interest. Ion chromatography with suppressed conductivity detection is one of the most popular methods that satisfy these objectives². However, the technique involves chromatographic equipment that is very specific to the determination of ionic species, such as a suppression column, an ionic separation column and a conductivity detector. Also, as conductivity is sensitive to temperature, a temperature controller is often needed. Recently, efforts have been made to avoid the use of a suppression column, as it introduces an additional dead volume and needs special care such as periodic regeneration. The use of a low-conductivity eluent was found to allow omission of the suppression column^{3,4}, but it still requires the use of a specific detector.

In this paper, an indirect photometric chromatographic method with an ultra-

violet detector is described for the determination of inorganic anions. Although the theoretical aspects of the technique are now well known⁵, its application to the analysis of real samples has not been widely reported. The purpose of this work was to characterize the method in terms of sensitivity, detection limits, working range and stability in order to define its possibilities and limitations for the determination of several important inorganic anions. The analysis of natural waters was also investigated and the validity of the method was established by inter-laboratory studies and by comparison with quality control samples.

EXPERIMENTAL

Instrumentation

The liquid chromatograph used consisted of a Waters Assoc. (Bedford, MA, U.S.A.) Model 510 pump and a Model 481 variable-wavelength UV detector. A Model 7125 six-port high-pressure switching injection valve (Rheodyne, Cotati, CA, U.S.A.) was used with a 500- μ l injection loop. A Waters IC Pak (25 μ m) guard column (0.5 cm \times 0.6 cm I.D.) was inserted before the separation column (15 cm \times 0.4 cm I.D.) which was packed with PRPX-100 polystyrene-divinylbenzene anion exchanger (10 μ m, 200 μ equiv./g) (Hamilton, Reno, NV, U.S.A.).

Data acquisition was performed with an integrator (Shimadzu, Kyoto, Japan) or via a digital voltmeter connected with an IEEE-488 card (Capital Equipment, Burlington, NY, U.S.A.) to a IBM-XT microcomputer. In this instance Nelson Analytical (Cupertino, CA, U.S.A.) (3000 series chromatographic data system) was used for peak processing.

Reagents and procedures

The water used for the preparation of the various solutions was distilled and passed through a Millipore (Bedford, MA, U.S.A.) Milli-Q purification system. Standard solutions (1000 mg/l) of fluoride, nitrite, chloride, nitrate, bromide, phosphate, sulfate, iodide, propionate, acetate, formate and carbonate were prepared by dissolving appropriate amounts of analytical-reagent grade sodium or potassium salts in pure water. These solutions were kept in polypropylene bottles and were diluted daily to give the multi-anion solutions required. Prior to the analysis, the solutions were filtered through a 0.45- μ m filter (25-mm HAWP or HVLP filter; Millipore).

The eluents were prepared daily from 0.1 *M* potassium hydrogenphthalate solution prepared from the analytical-reagent grade salt. The pH of the mobile phase was adjusted with 0.1 *M* sodium hydroxide solution. The mobile phases were filtered through a 0.45- μ m filter (47-mm HAWP or HVLP) and degassed in a ultrasonic bath before use.

Samples

Samples of natural water (river or lake) were kept at 4°C in polypropylene bottles before and after analysis.

RESULTS AND DISCUSSION

Practical considerations

Selectivity. Various analytical methods have been used to determine the most important inorganic anions in natural water, *viz.*, fluoride, chloride, nitrite, nitrate, phosphate, sulphate and iodide¹. However, in contrast to these methods, chromatography is not based on a specific reaction for each analyte but on separation. It is therefore important during the method development to consider all species likely to be present. Among the various anions, carbonate is an important anion to take into account and, based on water analyses reported by Jones and Tarter⁶, bromide could also be a potential interferent. Low-molecular-weight organic acids that could elute in a relatively short time and interfere in inorganic determinations also need to be considered. Brocco and Tappa⁷ found traces of acetic, formic and propionic acids in rain water.

All these species were taken into consideration when optimizing the chromatographic separation.

Sensitivity. In indirect photometry, the signal S produced by the UV detector when an analyte anion A^- elutes in an eluent containing E^- species is given by

$$S = l(\epsilon_{E^-} C_{E^-} - \epsilon_{A^-} C_{A^-})$$

where l = optical path length, ϵ = molar absorptivity and C = concentration. For maximum sensitivity, ϵ_{A^-} should be zero. Most inorganic anions are transparent above 220 nm and a higher detection wavelength should therefore be chosen.

Another important point in indirect photometry is to obtain a "background" absorbance between 0.2 and 0.8 for the eluent species at the detection wavelength in order to minimize the spectrophotometric error. An absorbance range that is steady near the detection wavelength is also needed in order to minimize the imprecision of the wavelength.

pH of the eluent. Two types of interferences are often observed in the determination of inorganic anions by indirect photometric chromatography. The first arises from carbonate, which may be present in large amounts in natural waters. The simplest way to eliminate carbonate is to use an eluent at $\text{pH} < 6$ so that the anion will be fully protonated.

The second type of interference is that resulting from the system peak, the presence of which seems to be due to the elution of neutral molecules of the eluent on injection of a water sample⁸. These molecules are believed to be retained on the chromatographic column by a reversed-phase mechanism, as about 85% of a low-capacity ion-exchange column is unfunctionalized (*i.e.*, does not have any ionized group)⁹. The retention time of this peak depends on a large number of parameters (nature and concentration of the eluent, pH of the mobile phase, presence of a modifier in the eluent, etc.). Its existence can be a real problem if it overlaps with an analyte peak or if it appears late in the chromatogram and increases the time of analysis. To avoid this peak, the eluent must be completely ionized at the pH chosen.

Optimization of the chromatographic system

Keeping all the above practical considerations in mind, the chromatographic

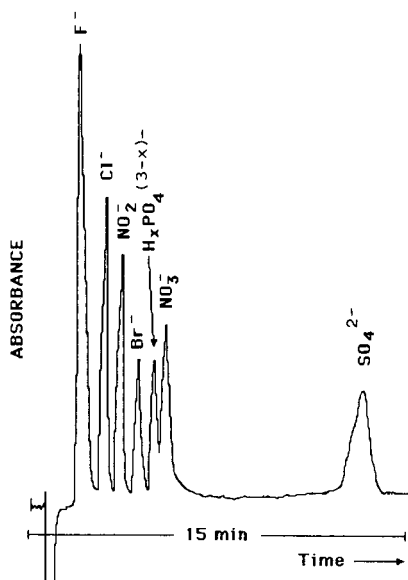


Fig. 1. Typical separation of inorganic anions by indirect photometry chromatography. For experimental conditions, see Table I.

system was optimized in terms of separation and detection. Three commonly used organic anions were considered as UV-active eluent species: *p*-hydroxybenzoate, *p*-toluenesulfonate and phthalate. The best separation conditions were found with phthalate at a concentration of 0.8 mM at pH 6.8. The detection wavelength was set at 265 nm. A typical separation obtained under these conditions is shown in Fig. 1. The separation with *p*-toluenesulfonate could not be easily optimized and good detection with *p*-hydroxybenzoate in the eluent could not be obtained.

The only anion of interest that could not be determined using these conditions was iodide, as its elution time was too long. It was observed that carbonate, formate and acetate, if present at low concentrations, would not interfere with any determination as they elute between fluoride and chloride (Fig. 2). Propionate was found to co-elute with bromide but probability of finding both species in natural water is low. If a peak appears at the elution time of bromide or propionate, it would always be possible to modify the pH of the mobile phase slightly so that the degree of ionization of the propionic acid would change and the propionate would elute at a different time. Interference from the system peak was avoided because at this pH, phthalate is fully ionized. The optimum conditions are reported in Table I.

Analytical performances

Sensitivity. An interesting point in indirect photometry is the standardization of a UV-transparent solute response. In fact, if we consider the elution of an analyte, this species will displace an equivalent concentration of a UV-active eluent species as required by electroneutrality. The sensitivity, in terms of peak area per unit concentration expressed in normality, is then independent of the nature of the analyte. This behavior was studied and the results obtained were 730, 700, 750 and 750 mV s/mN

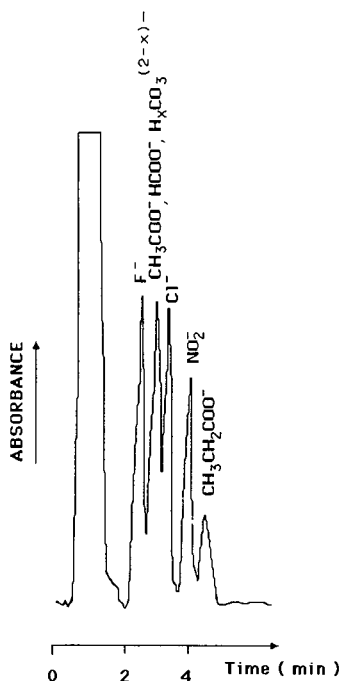


Fig. 2. Retention of organic anions potentially present in natural waters. For experimental conditions, see Table I.

for Cl^- , NO_2^- , Br^- and NO_3^- , respectively. From these results, it was clear that the response of a known solute could be used to evaluate the concentration of other unknown analytes with an accuracy of $\pm 10\%$ without the need to calibrate for each species.

Detection limits. The detection limits, DL , were evaluated according to Foley and Dorsey¹⁰, i.e., $DL = 3\sigma_b/4$, where σ_b is the noise-to-signal ratio. The results obtained are given in Table II and are compared with those reported by the U.S. Environmental Protection Agency (EPA) in their test method using ion chromatography with suppressed conductivity detection².

The results indicate that indirect photometry is comparable to ion suppressed conductivity as far as the detection limits are concerned.

TABLE I

OPTIMUM CONDITIONS FOR THE SEPARATION OF INORGANIC ANIONS

Operation	Parameter	Value
Separation	Phthalate concentration (mM)	0.8
	pH	6.8
	Flow-rate (ml/min)	1.2
	Injection volume (μl)	500
Detection	Wavelength (nm)	265
	Response time (s)	1

TABLE II
DETECTION LIMITS FOR INORGANIC ANIONS

Anion	Detection limit (ng)	
	Indirect photometry ^a	Conductivity with suppression ^b
F ⁻	1	1
Cl ⁻	1	1
NO ₂ ⁻	3	1
NO ₃ ⁻	4	6
H _x PO ₄ ^{(3-x)-}	21	18
SO ₄ ²⁻	4	20

^a The volume injected was 500 μ l.

^b The volume injected was 100 μ l. The experimental conditions were as described in the test method approved by the EPA for the determination of inorganic anions in water by ion chromatography: chromatographic system, Dionex; eluent, 0.003 M NaHCO₃-0.0024 M Na₂CO₃; regeneration solution, 0.0125 M H₂SO₄.

Short-term stability. The short-time stability was evaluated from the results obtained with five injections of a multi-anion solution at ca. 2 mg/l of each species. Table III gives the results obtained at a 95% confidence level.

The short-time stability was acceptable for most anions. The poorest results were obtained for nitrate and phosphate, and can be explained by the small difference between their elution times. As the separation was optimized assuming bromide could be present, the composition of the mobile phase was chosen so that phosphate would elute between nitrate and bromide. As bromide is uncommon in natural waters, once its absence has been confirmed it is possible to modify the composition of the mobile phase slightly to improve the separation of phosphate and nitrate, and this would result in better quantification.

Working range. For the analysis of a multi-anion solution, it was found that the maximum concentration or amount that could be injected was limited by saturation of the capacity of the column, resulting in poor peak shapes. The term "working range" is then more appropriate than "linear range".

TABLE III
SHORT-TERM STABILITY AND WORKING RANGE

Anion	Short-term stability (%) ^a	Upper limit (μ g)
F ⁻	1.0	2
Cl ⁻	2.8	2
NO ₂ ⁻	0.5	2
NO ₃ ⁻	3.5	2.5
H _x PO ₄ ^{(3-x)-}	5.0	4
SO ₄ ²⁻	2.7	1.5

^a The results are reported at a 95% confidence level and were evaluated with five measurements.

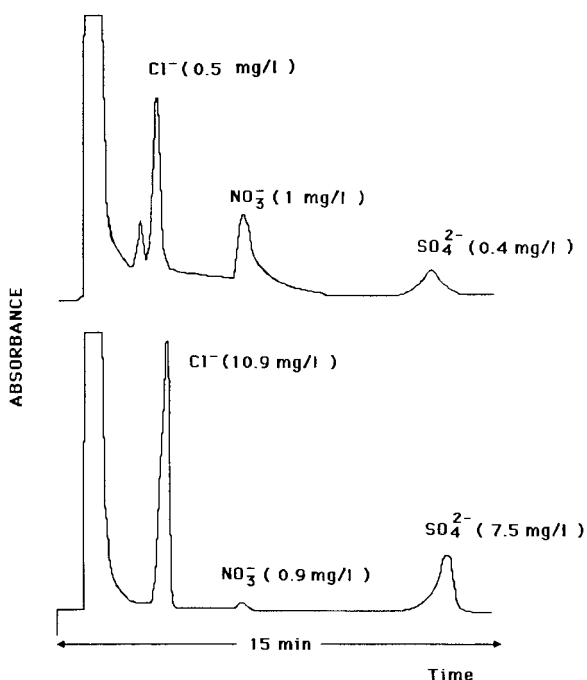


Fig. 3. Analysis of lake water by indirect photometry chromatography. For experimental conditions, see Table I.

In Table III the maximum amounts of a multi-anion solution that could be injected on to the chromatographic column are reported. It is important to note that if resolution is not affected by the peak shape, higher concentrations could be injected as the relationship between peak area and concentration is linear over these limits.

Analysis of natural water

In order to examine the suitability of the method for the determination of inorganic anions, several types of natural water were analysed, an inter-laboratory study was conducted and certified samples were analysed.

Examples of chromatograms obtained for lake and river water samples are illustrated in Fig. 3. As expected, when a large amount of hydrogencarbonate was present in the sample, it interfered with the chloride determination (Fig. 4). Decreasing the pH of the mobile phase could prevent the ionization of the hydrogencarbonate. In these particular instances, the analysis needs to be repeated. First an analysis was made using the optimum conditions for separation and then a second separation at lower pH was performed to eliminate the carbonate interference. The interference from hydrogencarbonate is a disadvantage in our method and in the EPA method by ion chromatography with suppressed conductivity detection.

In order to evaluate the accuracy of the method, an inter-laboratory study was undertaken. Nine lake water samples were analysed by 46 laboratories (university, industrial, government and private laboratories) and the results were compared. In most instances the determinations were done by ion chromatography with suppressed

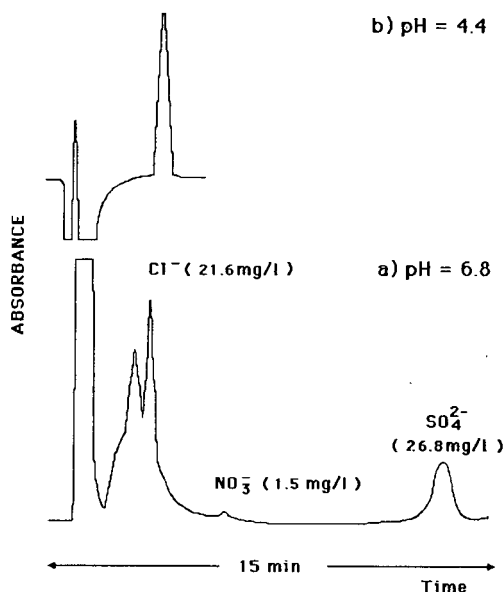


Fig. 4. Analysis of river water by indirect photometry chromatography. (a) For experimental conditions, see Table I. (b) The carbonate interference was removed by decreasing the pH of the mobile phase from 6.8 to 4.4.

TABLE IV

INTER-LABORATORY RESULTS

Sample No.	Anion ^a	Concentration (mg/l)		Standard deviation (mg/l) ^b	Confidence interval (95%) (mg/l)
		Median	Obtained		
1	Cl ⁻	0.495	0.5040	0.0006	0.501–0.506
	NO ₂ ⁻ /NO ₃ ⁻ /N	0.210	0.217	0.007	0.19–0.25
	SO ₄ ²⁻	0.360	0.37	0.01	0.33–0.41
2	Cl ⁻	0.765	0.432	0.003	0.42–0.44
	NO ₂ ⁻ /NO ₃ ⁻ /N	0.067	0.058	0.002	0.049–0.067
	SO ₄ ²⁻	1.01	0.61	0.01	0.57–0.65
3	Cl ⁻	0.865	0.45	0.03	0.3–0.6
	NO ₂ ⁻ /NO ₃ ⁻ /N	0.106	0.096	0.002	0.087–0.105
	SO ₄ ²⁻	3.10	2.95	0.07	2.6–3.2
4	Cl ⁻	10.9	10.6	0.2	9.7–11.5
	NO ₂ ⁻ /NO ₃ ⁻ /N	0.223	0.164	0.006	0.14–0.19
	SO ₄ ²⁻	7.49	7.7	0.1	7.3–8.1
5	Cl ⁻	0.543	0.553	0.009	0.51–0.59
	NO ₂ ⁻ /NO ₃ ⁻ /N	0.17	0.14	0.01	0.10–0.18
	SO ₄ ²⁻	4.87	4.70	0.07	4.4–5.0
7	Cl ⁻	4.66	4.135	0.004	4.12–4.15
	NO ₂ ⁻ /NO ₃ ⁻ /N	0.066	0.072	0.003	0.06–0.08
	SO ₄ ²⁻	5.95	6.0	0.1	5.6–6.4
9	Cl ⁻	11.6	11.3	0.1	10.9–11.7
	NO ₂ ⁻ /NO ₃ ⁻ /N	0.164	0.14	0.01	0.10–0.18
	SO ₄ ²⁻	15	14.4	0.2	13.5–15.3

^a NO₂⁻/NO₃⁻/N: the concentrations of nitrite and nitrate are expressed as nitrogen.

^b The standard deviation was obtained for three measurements.

conductivity detection using the experimental procedures recommended by the EPA. Nitrite and nitrate were often determined by other standard techniques (spectrophotometry, Technicon AutoAnalyzer, liquid chromatography). In Table IV the results of the inter-laboratory study are given and are compared with the values obtained by indirect photometric chromatography. Two major differences were observed. In general, the agreement between our results and the median is good except for chloride and sulphate in sample 2 and chloride in sample 3. These discrepancies could not be explained by contamination or by co-elution of two analytes, as the values obtained were lower than expected. It also could not be attributed to a loss of sample (leak in the injector), as all anions in the same sample did not show lower concentrations. In our laboratory, the concentrations found by external calibration were corroborated by standard additions. The discrepancies obtained could not be explained. Fortunately, all other samples analysed were found to have concentrations in the expected range.

The validity of the method was also established by the analysis of EPA certified samples. As reported in Table V, in all instances the concentrations obtained by our method were in the range of the confidence intervals given by the EPA. Only fluoride, chloride, nitrate and sulphate were detected in the natural water analysed and it was confirmed by this study of certified samples that as far as these anions are concerned good accuracy could be obtained.

CONCLUSION

The results clearly indicate that indirect photometry is comparable to ion chromatography with suppressed conductivity for the determination of inorganic anions, but has the advantages of being simpler and more versatile. The method was successfully used for the analysis of natural waters.

TABLE V
ANALYSIS OF EPA CERTIFIED SAMPLES

<i>Anion^a</i>	<i>Value^b</i>	<i>True value (mg/l)</i>	<i>Mean recovery (mg/l)</i>	<i>Confidence interval (95%) (mg/l)</i>
N-NO ₃ ⁻	C	0.14	0.14	0.11-0.17
	O		0.139	
P-PO ₄ ³⁻	C	0.35	0.35	0.33-0.37
	O		0.325	
F ⁻	C	2.75	2.7	2.5-3.0
	O		2.69	
N-NO ₃ ⁻	C	10.30	10.2	9.5-11.0
	O		10.1	
Cl ⁻	C	17.8	18.0	16.1-19.9
	O		18.0	
SO ₄ ²⁻	C	7.2	7.0	5-9
	O		7.3	

^a N-NO₃⁻: The concentration of nitrate is expressed as nitrogen. P-PO₄³⁻: The concentration of phosphate is expressed as phosphorus.

^b C = certified; O = obtained.

ACKNOWLEDGEMENTS

The authors thank the National Science and Engineering Council of Canada (NSERC) and the Fonds pour la Formation des Chercheurs et d'Aide à la Recherche du Québec for financial support. One of us (N.C.) thanks NSERC for a scholarship.

REFERENCES

- 1 Environnement du Canada, *Manuel des Méthodes Analytiques*, Direction de la Qualité de l'Eau, Ottawa, 1987.
- 2 *Annual Book of ASTM Standards, Part 31, Water*, ASTM, Philadelphia, PA, 1984, Method 300, pp. 300.0.1–300.0.5.
- 3 G. Schmuckler, *J. Chromatogr.*, 313 (1984) 47.
- 4 D.T. Gjerde, J.S. Fritz and G. Schmuckler, *J. Chromatogr.*, 186 (1979) 509.
- 5 H. Small and T.E. Miller, *Anal. Chem.*, 54 (1982) 462.
- 6 V.K. Jones and J.G. Tarter, *Am. Lab. (Fairfield, Conn.)*, 50 (1985) 418.
- 7 D. Brocco and R. Tappa, *J. Chromatogr.*, 367 (1986) 240.
- 8 P.E. Jackson and P.R. Haddad, *J. Chromatogr.*, 346 (1985) 125.
- 9 D.P. Lee, *J. Chromatogr. Sci.*, 22 (1984) 327.
- 10 J. P. Foley and J. G. Dorsey, *Chromatographia*, 18 (1984) 503.

CHROM. 21 351

ISOCRATIC ELUTION OF SODIUM, AMMONIUM, POTASSIUM, MAGNESIUM AND CALCIUM IONS BY ION-EXCHANGE CHROMATOGRAPHY

HISAKUNI SATO

Laboratory of Analytical Chemistry, Faculty of Engineering, Yokohama National University, Tokiwadai 156, Hodogaya-ku, Yokohama-shi, 240 (Japan)

(Received January 16th, 1989)

SUMMARY

Isocratic elution conditions for five cationic species were investigated using conductivity and UV absorption detectors. Using several kinds of eluents and silica and styrene-divinylbenzene separating columns, the detection sensitivity, separation efficiency, separation time, system peak interference, etc., were examined. As a result, two types of eluents were concluded to be useful: a solution of benzylamine, citric acid and N-hydroxyethylenediamine-N,N',N'-triacetic acid (EDTA · OH) and a solution of 1,1'-di-*n*-heptyl-4,5'-bipyridinium (DHBP) ion and citric acid. When the former eluent is used, monovalent cations are separated clearly and divalent cations can be eluted without being captured in the column. With a slightly lower precision, divalent cations at the parts per million level can also be determined. The latter eluent is suitable mainly for determining Mg^{2+} and Ca^{2+} ions with no interference from heavy metal ions. The separation of monovalent ions was poor with a commercially available separation column, but the detection sensitivity with a UV absorption detector was higher than that with the benzylamine eluent. Several examples of application are shown.

INTRODUCTION

Monovalent sodium, ammonium and potassium ions and divalent magnesium and calcium ions are found together in various aqueous samples such as environmental waters and biological fluids, and often all these species need to be determined. Although ion-exchange chromatography is usually suitable for multi-component analysis, the simultaneous determination of these monovalent and divalent cations by isocratic elution is not easy because of their very different properties. Therefore, since the development of ion chromatography¹ many studies^{2–6} have concerned monovalent and divalent species under separate elution conditions. However, when monovalent cations are eluted with dilute nitric acid or hydrochloric acid, any divalent cations, when present, are captured in the column and as a result the effective ion-exchange capacity of the column is reduced. To eliminate this drawback, it is necessary to use a precolumn to prevent divalent sample cations from entering to the separation column or to clean up the column frequently. Even when only monovalent

cations are to be determined, elution conditions that prevent divalent cations from being in the column are desirable. Small and Miller³ proposed a column switching method by using two separating columns and switching them to change the flow path during the elution. However, this method is generally not easy to use. If a gradient elution method is used, it will be easy to elute monovalent and divalent species successively. However, suitable detection methods are difficult to establish.

A few methods have been reported for handling monovalent and divalent species simultaneously by isocratic elution with the use of a universal UV spectrophotometric (hereinafter referred to as a UV) detector. Miyazaki *et al.*⁷ reported a simultaneous determination method for alkali metal, ammonium, magnesium and calcium ions by combining a silica gel-based cation-exchange column with a copper sulphate eluent. In this method, however, a column having a high theoretical plate number (more than about 5000) is needed to separate monovalent cations if calcium ions are to be eluted within a reasonable time (*e.g.*, 20 min). Sherman and Danielson⁸ reported that the simultaneous determination of monovalent and divalent species could be effected by using a styrene-divinylbenzene (St-DVB)-based cation exchanger (500 $\mu\text{equiv./g}$, 5 μm), a cerium(III) eluent and indirect absorption detection. In our experiments with this method with a column packed with an ordinary sulphonated St-DVB resin, it was found to be effective for separating Na^+ , K^+ , Mg^{2+} , and Ca^{2+} , but NH_4^+ and K^+ overlapped and could not be separated, and a system peak appeared between the peaks of Mg^{2+} and Ca^{2+} at some sample pH values and interfered with their determination. Further, in the method using these metal ion solutions as eluent, various divalent metal ions appear in the vicinity of the peak of Mg^{2+} , and no effective method for masking them could be found.

In order to find novel approaches that permit the isocratic elution of sample species from Na^+ to Ca^{2+} and their determination with a conductivity or UV absorption detector, we have studied extensively various eluents and combinations of separation columns. As the elution system for eluting monovalent and divalent cations isocratically, combinations of a monovalent ion and a strong complex-forming agent, or of a divalent cation and a comparatively weak complex-forming agent, were chosen. Complex-forming agents are necessary for accelerating the elution of the divalent cations.

Eluting ions are required to effect good separations and to have a low equivalent conductivity or large UV absorption. In addition, the exchange capacity and the base material of the ion exchanger are important factors. From such viewpoints, a Li^+ , tetrabutylammonium, anilinium, benzylammonium and trimethylbenzylammonium ions were selected as the monovalent eluting ions and EDTA or analogous compounds were used as the complex-forming agents. Hexamethylenediammonium, cyclohexanediammonium, hexamethonium, *m*-phenylenediammonium and diheptylbipyridinium ions were used as divalent eluting ions combined with citric acid.

Using these diverse eluents and silica and St-DVB separating columns, we examined the detection sensitivity, separation efficiency, separation time, system peak interference, etc. As a result, two elution types have been concluded to be useful: a combination of benzylamine with citric acid and N-hydroxyethylenediamine-N,N'-triacetic acid ($\text{EDTA} \cdot \text{OH}$), and a combination of 1,1'-di-*n*-heptyl-4,5'-bipyridinium (DHBP) ion and citric acid. This paper describes these methods and gives examples of applications to some common samples.

EXPERIMENTAL

Equipment

The liquid chromatograph consisted of a pump system (Tosoh, CCPM, metal-free model), a conductivity detector (Tosoh, CM-8000) and a UV-visible detector (Tosoh, UV-8000). To inject the sample, a Rheodyne loop injector (100- μ l loop) was used. The separation columns were a Tosoh IC cation (St-DVB, low exchange capacity, 50 \times 4.6 mm I.D.), a Tosoh IC cation SW (silica gel, medium exchange capacity, 50 \times 4.6 mm I.D.), a Tosoh SCX (St-DVB, ordinary exchange capacity, 50 \times 4.6 mm I.D.) and stainless-steel columns packed with cation exchangers manufactured by Tosoh (sulphonated St-DVB, 4% DVB, average diameter 11 μ m, exchange capacity 24, 50 and 85 μ equiv./ml).

Reagents

Various amines, DHP bromide and EDTA \cdot OH were obtained from Tokyo Kasei Kogyo. All other reagents were of guaranteed grade and used without further processing. Distilled, deionized water was used. Benzylamine-type eluents were prepared from solutions 100 mM of benzylamine, EDTA \cdot OH and citric acid by mixing them in various proportions by volume. To prepare DHPB-type eluents, 2.572 g ($5 \cdot 10^{-4}$ mol) of DHPB-bromide were dissolved in 80 ml of water, the solution was allowed to flow through an anion-exchange column (20 \times 100 mm bed) which had been converted to the citrate ion form by running 200 ml of 1 M sodium citrate solution beforehand, and the column was eluted with water to give 500 ml of solution (DHPB 10 mM, pH 8.0). To use this solution as an eluent, it was diluted with an appropriate amount of citric acid.

The sample ion solutions used were aqueous solutions of NaCl, KCl and NH_4Cl and dilute HCl solutions of MgO and CaCO_3 .

Chromatographic operation

The eluent flow-rate was 1.0 ml/min. Elution was performed mostly at room temperature (15–25°C). The cell of the conductivity detector was maintained at 35°C.

RESULTS AND DISCUSSION

Benzylamine-EDTA \cdot OH-citric acid type eluents

Benzylammonium ion allows monovalent cations to be separated at weakly acidic or neutral pH⁹. If this species is combined with EDTA and used with a sulphonated St-DVB column for separation, Ca^{2+} ions are eluted first, followed by monovalent cations and then Mg^{2+} ions. In this instance, even if the benzylamine to EDTA ratio, pH, etc., are varied, the peak of Ca^{2+} appears too fast, and is deformed by the overlapping system peak, so the determination of Ca^{2+} is difficult because the complex formation constant of EDTA with Ca^{2+} ions¹⁰ is too large. If the determination of Ca^{2+} is not necessary, this method may be useful for the determination of monovalent cations and Mg^{2+} ion.

EDTA \cdot OH¹⁰ was selected as a complex-forming agent as it does not have such a large difference as EDTA in the complex formation constants between Ca^{2+} and Mg^{2+} ions. It was found that Ca^{2+} ions are eluted early and overlap with K^+ with the

use of a combination of benzylamine and EDTA · OH alone when the pH is adjusted to nearly 6.5 so as to allow Mg^{2+} ions to be eluted within a moderate time. On the other hand, with a combination of benzylamine and citric acid alone, Ca^{2+} ions are eluted following Mg^{2+} at pH 6–7, so the overall elution time becomes long. Ca^{2+} can be eluted rapidly by using a relatively concentrated eluent, but the separations of monovalent ions are unsatisfactory. Hence, a long time is required between the elution of the monovalent group and the divalent group. Addition of EDTA · OH makes it possible for Ca^{2+} to be eluted before Mg^{2+} . Based on this finding, the eluent system benzylamine–EDTA · OH–citric acid was examined. Separations of Na^+ , NH_4^+ , K^+ , Ca^{2+} and Mg^{2+} are good, and high sensitive detection by either UV absorption or conductivity is possible.

Ion retention time vs. eluent composition. When a 15-cm separation column packed with 50 μ equiv./ml of sulphonated St–DVB is used, monovalent cations can be separated with a 5 mM or lower concentration of benzylammonium ions. The elution time for each ion depends on the ratios of the three components, benzylamine, EDTA · OH and citric acid, the total concentration and the ion-exchange capacity of the column. Further, with UV detection, it is not preferable to raise the benzylamine concentration too high so as not to reduce the detection sensitivity. The background absorbance of 5 mM benzylammonium is about 1.2 at the peak wavelength in the vicinity of 257 nm, just falling within the limits of the linear response of the detector used. Fig. 1 shows the retention time of each ion when the ratio of EDTA · OH to citric acid is varied with the benzylammonium ion concentration fixed at 5 mM.

The retention times of the monovalent ion vary very little. When the total concentration of citric acid and EDTA · OH is fixed at 2 mM and their ratio is varied from 2:0 to 1:1, the eluent pH varies from 6.12 to 7.32. In this instance, the retention time of Mg^{2+} ions varies slightly. When the citric acid to EDTA · OH ratio is fixed at

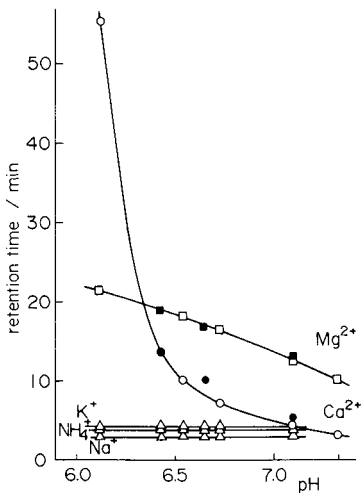


Fig. 1. Relationship between the retention time of cations and the pH of the benzylamine–EDTA · OH–citric acid eluent. Δ , monovalent cations; \square , \blacksquare , Mg^{2+} ; \circ , \bullet , Ca^{2+} ; concentration of benzylamine, 5.0 mM (constant). \square , \circ , Total concentration of EDTA · OH and citric acid 2.0 mM; \blacksquare , \bullet , citric acid to EDTA · OH ratio = 3:1.

3:1 and the total concentration is changed, the retention behaviour of Mg^{2+} is similar, and so can be regarded as almost determined by the pH. On the other hand, the retention time of Ca^{2+} varies significantly with increasing pH. When the citric acid to $\text{EDTA} \cdot \text{OH}$ ratio is 3:1–2.5:1 and the pH is 6.5–6.7, five ion species are separated and eluted within 20 min. Fig. 2 shows a typical chromatogram for alkali metal ions, including Rb^+ and Cs^+ ions, Ca^{2+} and Mg^{2+} ions. As Rb^+ and Cs^+ are not present in ordinary samples, they can be utilized as internal standards. Ca^{2+} is eluted earlier than Mg^{2+} owing to the complex-forming effect of $\text{EDTA} \cdot \text{OH}$. In spite of the later elution of Mg^{2+} than Ca^{2+} , the peak of Mg^{2+} is sharper than that of Ca^{2+} , reflecting a smaller interaction between Mg^{2+} and $\text{EDTA} \cdot \text{OH}$.

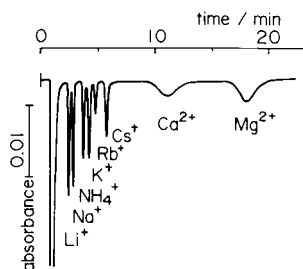


Fig. 2. Typical chromatogram of alkali metal, ammonium, magnesium and calcium ions using benzylamine– $\text{EDTA} \cdot \text{OH}$ –citric acid eluent and UV detection. Eluent, benzylamine (5.0 mM)– $\text{EDTA} \cdot \text{OH}$ (0.475 mM)–citric acid (1.425 mM) (pH 6.6); flow-rate, 1.0 ml/min. Column, 150 \times 4.6 mm I.D., sulphonated St–DVB, 50 $\mu\text{equiv./ml}$. Sample, each ion $1 \cdot 10^{-4}$ M except for Rb^+ ($5 \cdot 10^{-5}$ M); 100 μl . Detection: UV absorption at 257 nm.

Conductivity detection and UV detection. The equivalent conductivity of benzylammonium ions (ca. 30 $\mu\text{S/cm}$) is lower than that of Li^+ and peaks of Na^+ , NH_4^+ and K^+ appear in the direction of increasing conductivity. With equal molar concentrations, the peak height of Na^+ is as small as about half of that of NH_4^+ . Mg^{2+} and Ca^{2+} partially form complexes and their apparent equivalent conductivities are very small, so their peaks appear in the direction of decreasing conductivity. Fig. 3 shows an example of such behaviour. Benzylammonium ion has a local absorption maximum in the vicinity of 257 nm. At a concentration of 5 mM, the background absorption at this wavelength falls within the limit of the linear response of detectors in common use. The larger the molar absorption coefficient, the greater is the detection sensitivity of the detector. However, with too large a background absorption, the apparent sensitivity may become low¹¹. Moreover, at shorter wavelengths, citric acid and $\text{EDTA} \cdot \text{OH}$ show large absorption. Therefore, it was concluded that the local maximum in the vicinity of 257 nm was a suitable detection wavelength. In this instance, absorption detection and conductivity detection methods show approximately similar sensitivity responses when recorded at the same attenuation of the integrator. With respect to the relatively large peak intensity of divalent species, conductivity detection is superior to indirect UV detection. However, the indirect UV method has the advantage that all peaks appear in one direction and the tailing of the first dip peak originated by the sample injection is smaller than that with conductivity detection.

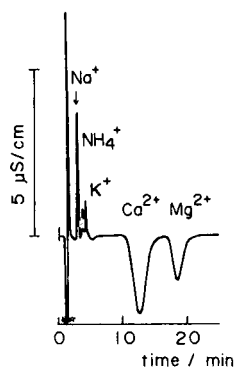


Fig. 3. Chromatogram of a river water sample. Eluent as in Fig. 2. Sample, Tama river water, 100 μ l. Result: Na^+ 20.3, NH_4^+ 2.1, K^+ 5.9, Ca^{2+} 19.2 and Mg^{2+} 4.6 mg/l.

Influence of temperature, hydrogen ion concentration, heavy metal ions, etc. As can be seen from Figs. 2 and 3, the peaks of divalent ions are wider than those of monovalent ions. This seems to show an influence of complex formation reactions which are fairly slow. The column temperature was changed from room temperature (20°C) to 40°C; the peak widths of Ca^{2+} and Mg^{2+} were unchanged, but elution of Mg^{2+} was slightly faster. In addition, the peaks of NH_4^+ and K^+ began to approach each other at *ca.* 35°C and the detection sensitivity for NH_4^+ became low. Hence a temperature of 20–30°C is the most suitable for both separation and detection. With increase in temperature, the NH_4^+ detection sensitivity is reduced probably because the dissociation constant of NH_4^+ increases with increasing temperature. However, this assumption is uncertain as the retention time does not change with temperature. The presence of hydrogen ions in the sample has no effect when the pH is above 2. Heavy metal ions (Ni, Co, Zn, Cd, Pb, etc.) are eluted faster than the Na^+ ion, and have no influence except at very high concentrations. The presence of EDTA below 10^{-3} M does not affect the elution of Mg^{2+} and Ca^{2+} .

A problem is that once the eluent has stopped flowing and is then switched on after a lapse of time, it takes a long time for the baseline to stabilize. If a solution of double the concentration is allowed to flow for a short period, the baseline stabilization is faster.

Quantification. Table I summarizes the results for four repetitive analyses of a 100- μ l sample solution containing $2 \cdot 10^{-4}$ M Na^+ , K^+ , Ca^{2+} and Mg^{2+} using UV detection. The reproducibility of the peak heights is fairly good for each ion.

The peak area is good for Na^+ and K^+ but poor for Ca^{2+} and Mg^{2+} , possibly owing to the larger peak widths. In the range $0\text{--}2 \cdot 10^{-4}$ M concentration of each ion, the peak areas show good linearity. The peak height of Na^+ is not proportional to the concentration at concentrations above $1 \cdot 10^{-4}$ M.

Applications. Fig. 3 shows a chromatogram for a river water sample obtained with conductivity detection. All ions from Na^+ to Mg^{2+} are present at a level suitable for the present method. The sample water was only filtered with a 0.1- μ m membrane filter and then injected. In this example, the content of NH_4^+ is high. Fig. 4 shows a chromatogram of milk obtained with indirect UV detection. The sample was first

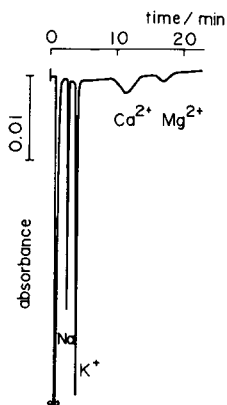


Fig. 4. Chromatogram of milk. Eluent as in Fig. 2. Sample, cow milk filtered with an ultrafiltration membrane, diluted 100-fold with water, 100 μ l. Result: Na^+ 0.43, K^+ 1.57, Ca^{2+} 0.34 and Mg^{2+} 0.057 g/l.

filtered through an ultrafiltration membrane (Tosoh, UNISEP) and diluted 100-fold with water. "Non-bound" calcium and magnesium were separated.

Diheptylbipyridinium-citric acid type eluents

To determine divalent cations by ion-exchange chromatography, the conductivity detection method using the ethylenediammonium ion as eluent is well known. If ions from Na^+ to Ca^{2+} are to be handled simultaneously, ethylenediammonium, hexamethylenediammonium, etc., cannot be used because a system peak appears in the vicinity of the peaks of monovalent sample ions.

As a divalent eluting ion showing UV absorption, *m*-phenylenediamine has been used, but because it is easily oxidized and unstable in air, its application is difficult. For this reason, we searched extensively for stable divalent ions other than metal ions, and found that the DHBP ion is effective when a silica-based separation column is used. This eluting ion cannot be used with St-DVB-based cation exchangers because of the strong absorption behaviour.

DHBP is a quaternary ammonium ion, available commercially as the bromide, and is in the form of a divalent ion over a wide pH range. In this work, to separate Ca^{2+} and Mg^{2+} ions from other divalent metal ions, it was converted to the citrate, to which a further excess of citric acid was added to give an eluent of suitable pH. With water alone as the solvent, the separations of Na^+ and K^+ were poorer. When 10% (v/v) of acetonitrile was added, clear separations were obtained. The addition of acetonitrile hardly affected the separation of divalent ions.

Ion retention time vs. eluent composition. The characteristics of DHBP-citric acid eluents vary with the concentration of DHBP, the total concentration of citric acid and the pH. If no electrolyte is added other than DHBP and citric acid, the pH is determined approximately by the mixing ratio of DHBP and citric acid. Fig. 5 shows the retention time of monovalent and divalent cations *versus* the pH of the DHBP-citric acid eluent prepared by varying the citric acid concentration with a constant DHBP concentration of 1 mM. A pH of 5.6 was obtained with an aqueous solution of DHBP bromide containing no citric acid. It is considered that the acidic pH

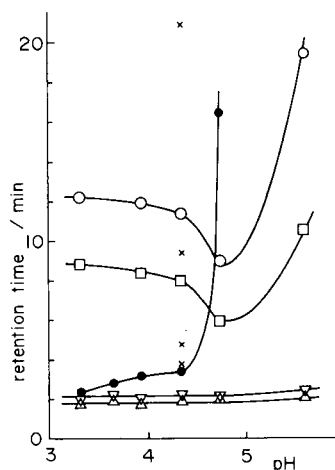


Fig. 5. Relationship between the retention time of cations and the pH of the DHBP-citric acid eluent. Eluent, DHBP (1.0 mM)-citric acid (variable) + 10% (v/v) acetonitrile. Δ , Na^+ ; ∇ , K^+ ; \square , Mg^{2+} ; \circ , Ca^{2+} ; \bullet , ghost peak; \times , Zn^{2+} , Ni^{2+} , Co^{2+} , Mn^{2+} (from bottom to top).

is due to dissolved carbon dioxide. In this experiment, all eluents contained 10% (v/v) of acetonitrile. For reference, the retention times of some divalent heavy metal ions are also shown in Fig. 5.

Fig. 5 shows that the retention time of monovalent ions hardly depends on pH, indicating that the complex formation with citrate ions can be ignored. NH_4^+ has been omitted from Fig. 5 because of its significant overlap with Na^+ . The slope of the $\log k'$ vs. $\log C$ plots for Na^+ and K^+ at pH 4.6 is about -0.53 , indicating that ion exchange of monovalent ions with divalent ions has occurred.

As the pH decreases, Mg^{2+} and Ca^{2+} first elute faster, but then more slowly again. The probable reason is that the accelerating effect of the complex formation with increasing citrate ion concentration and the retarding effect of the complex dissociation with decreasing pH are in competition.

With the aqueous DHBP bromide solution, the elution of Ca^{2+} is slow and hardly practical. On addition of citric acid to reduce the pH from 5 to 3, elution of Ca^{2+} becomes faster and more practically useful. However, this addition of citric acid causes a system peak to appear and its retention time decreases with decreasing pH. The slope of the $\log k'$ vs. $\log C$ plots is -0.82 , corresponding to the dissociation state of citrate ions between monovalent and divalent species. At pH 4–4.5, the system peak appears between K^+ and Mg^{2+} and does not affect their determination. The reason for the appearance of the system peak will be described elsewhere. An eluent pH of 4–4.5 (1 mM DHBP citrate + 1 mM citric acid) is suitable. The lower the DHBP concentration, the smaller the background absorption becomes, and hence higher sensitivities can be achieved by changing the detection wavelength toward higher absorption. However, with 0.5 mM DHBP, it takes about 23 min for Ca^{2+} to elute, and in this respect it can be concluded that a DHBP concentration of about 1 mM is suitable for the faster elution of Ca^{2+} .

Fig. 6 shows a typical chromatogram for Na^+ , K^+ , Mg^{2+} and Ca^{2+} obtained

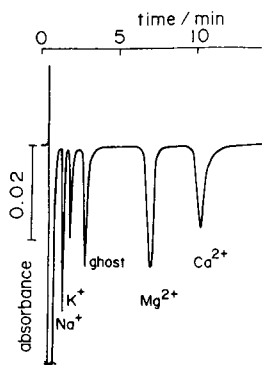


Fig. 6. Typical chromatogram of sodium, potassium, magnesium and calcium ions using DHBP–citric acid eluent and UV detection. Eluent, DHBP citrate (1.0 mM)–citric acid (1.0 mM) (pH 4.3); flow-rate, 1.0 ml/min. Column, IC cation SW. Sample, each ion $0.8 \cdot 10^{-4} M$, 100 μ l. Detection, UV absorption at 300 nm.

with the elution conditions determined as described above. The presence of NH_4^+ ion can be ascertained as the peaks of Na^+ and NH_4^+ are separated from each other by using two SW columns in series. If it becomes possible to use a column with a higher theoretical plate number, it will be possible to separate Na^+ , NH_4^+ and K^+ .

UV detection and conductivity detection. The solution of DHBP shows a UV absorption peak in the vicinity of 262 nm and the molar absorption coefficient is about $2.4 \cdot 10^4$. When a 1 mM solution of DHBP is used as the eluent, it is necessary to hold the background absorption at the detection wavelength below about 1, and therefore, a wavelength of about 300 nm is appropriate. If the linear response region of the detector can be widened, it will be possible to achieve higher detection sensitivities at a wavelength below 300 nm. A conductivity detector also can be used. With 1 mM DHBP citrate + 1 mM citric acid, the background conductivity is as low as 137 $\mu\text{S}/\text{cm}$, so that the equivalent conductivity of DHBP^{2+} ions is very small. For this reason, the detection sensitivity for monovalent ions is high. With divalent ions, peaks appear in the direction toward decreasing conductivity. This effect is the same as with the benzylamine-type eluents mentioned above and the appearance of both positive and negative peaks is inconvenient. Moreover, the detection sensitivity for divalent ions is slightly lower than that with UV detection and therefore, in general, the UV detection method is more advantageous.

Influence of temperature and heavy metal ions. With increasing temperature, separations of monovalent ions become poor, as with benzylamine-type eluents. At 27°C, Na^+ and K^+ are separated from each other, but at 45°C they overlap. A suitable temperature is 20–30°C. The peaks of Mg^{2+} and Ca^{2+} are sufficiently sharp at room temperature. Heavy metal ions elute at positions that vary with the pH of the eluent. In most instances, specific heavy metal ions can be eluted so that they do not overlap with the peaks of Mg^{2+} and Ca^{2+} . If they coexist in large amounts, EDTA may be added so that they can be eluted faster. With tap water samples, a peak which seems to be Fe^{2+} appears in the vicinity of the peak of Mg^{2+} . If EDTA (acid form) is added to the sample water in a small amount as a solid, and the solution is mixed well, filtered and then injected, the interfering peak disappears.

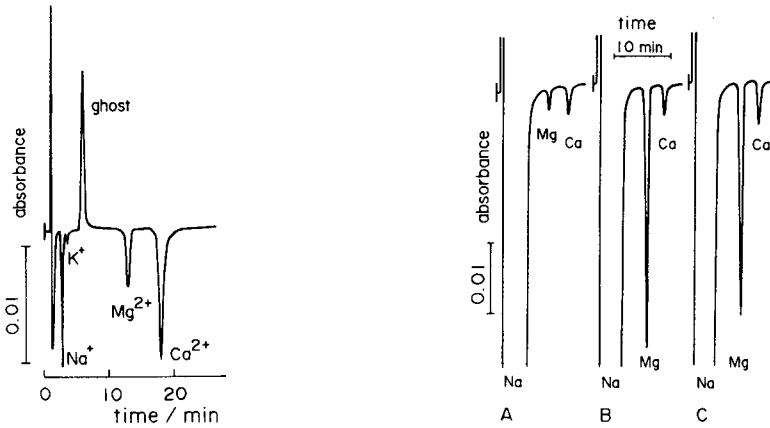


Fig. 7. Chromatogram of a mineral water. Elution conditions as in Fig. 6. Sample, commercial mineral water, 100 μ l. Result: Na^+ 12.7, K^+ 2.4, Mg^{2+} 6.8 and Ca^{2+} 39.1 mg/l.

Fig. 8. Chromatograms of raw salt samples. Elution conditions as in Fig. 6. Samples, raw salt for industrial use from Mexico, Australia and China, aqueous solutions filtered with a 0.1- μ m membrane filter, 100 μ l. Results: (A) Mexico, Mg^{2+} 0.146, Ca^{2+} 0.397 ppt; (B) Australia, Mg^{2+} 2.05, Ca^{2+} 0.470 ppt; and (C) China, Mg^{2+} 2.69, Ca^{2+} 1.008 ppt.

Quantification. Calibration graphs were obtained by using 1 mM DHBP citrate + 1 mM citric acid-type eluent within the range $0\text{--}2 \cdot 10^{-4}$ M Na^+ , K^+ , Mg^{2+} and Ca^{2+} . The peak area for each ion showed good linearity. At concentrations above $1 \cdot 10^{-4}$ M, the peak heights of Na^+ and K^+ deviated from a linear relation with concentration.

Applications. Fig. 7 shows a chromatogram of a commercial mineral water, which was injected without any treatment. Fig. 8 shows chromatograms obtained by applying the present method to the determination of Mg^{2+} and Ca^{2+} in raw salt samples, although it is not an example with conditions allowing the determination of both monovalent and divalent species. Suitable amounts of solid samples were dissolved in water and filtered with a 0.1- μ m membrane filter. This example makes use of the advantage of indirect UV detection in that the tailing of a large peak due to Na^+

TABLE I

REPRODUCIBILITY OF PEAK HEIGHT AND PEAK AREA WITH BENZYLAMINE ELUENT
Four replicate analyses with $2 \cdot 10^{-4}$ M samples and UV detection; all values relative.

Parameter	Na^+	K^+	Ca^{2+}	Mg^{2+}
Peak height				
Average	1.1855	0.9108	0.2105	0.2590
Standard deviation	0.0030	0.0016	0.0024	0.0028
Peak area				
Average	0.2003	0.1919	0.3954	0.4016
Standard deviation	0.0010	0.0017	0.0101	0.0076

is less than that with conductivity detection. This indicates the possibility that Ca^{2+} and Mg^{2+} in raw salts for industrial use can be determined simply and with good precision.

CONCLUSION

It was difficult to find elution conditions that allow Na^+ , K^+ , NH_4^+ , Mg^{2+} and Ca^{2+} to be determined with equal precision. The methods with monovalent eluting ions are mainly suitable for the determination of monovalent sample ions, and the methods with divalent eluting ions are suitable mainly for the determination of divalent sample ions. However, if benzylamine-EDTA · OH-citric acid eluent is used, divalent sample ions can be eluted without being retained in the column. With a slightly lower precision, their determination is also possible.

DHBP-citric acid eluents are disadvantageous in that the separation of monovalent ions is poor and NH_4^+ can hardly be identified. Moreover, polymer-type packing agents cannot be used in the column. These eluents are suitable mainly for determining divalent Mg^{2+} and Ca^{2+} ions while circumventing the interference of heavy metal ions. However, the detection sensitivity is higher than with benzylamine or many other amines.

REFERENCES

- 1 H. Small, T. S. Stevens and W. C. Bauman, *Anal. Chem.*, 47 (1975) 1801.
- 2 J. S. Fritz, D. T. Gjerde and R. M. Becker, *Anal. Chem.*, 52 (1980) 1519.
- 3 H. Small and T. E. Miller, Jr., *Anal. Chem.*, 54 (1982) 462.
- 4 H. Shintani, *J. Chromatogr.*, 341 (1985) 53.
- 5 M. Ishikawa, M. Yamamoto, Y. Masui, K. Hayakawa, M. Miyazaki, H. Nakazawa and M. Fujita, *Bunseki Kagaku*, 35 (1986) 309.
- 6 N. T. Basta and M. A. Tabatabai, *J. Environ. Qual.*, 14 (1985) 450.
- 7 M. Miyazaki, K. Hayakawa and S.-G. Choi, *J. Chromatogr.*, 323 (1985) 443.
- 8 J. H. Sherman and N. D. Danielson, *Anal. Chem.*, 59 (1987) 490.
- 9 R. C. L. Foley and P. R. Haddad, *J. Chromatogr.*, 366 (1986) 13.
- 10 L. G. Sillén and A. E. Martell, *Stability Constants of Metal-Ion Complexes*, Chemical Society, London, 1964.
- 11 Y. Yokoyama and H. Sato, *J. Chromatogr. Sci.*, 26 (1988) 11.

CHROM. 21 323

CAPILLARY GAS CHROMATOGRAPHIC-MASS SPECTROMETRIC DETERMINATION OF ACID HERBICIDES IN SOILS AND SEDIMENTS

TADASHI TSUKIOKA*

Nagano Research Institute for Health and Pollution, 1978, Komemura, Amori, Nagano-shi, Nagano (Japan)
and

TETSURO MURAKAMI

Department of Chemical Engineering, Kogakuin University, 1-24-2, Nishishinjuku, Shinjuku-ku, Tokyo (Japan)

(First received January 11th, 1988; revised manuscript received January 11th, 1989)

SUMMARY

A capillary gas chromatographic method with selected-ion monitoring (GC-SIM) was applied to eight common herbicides: 2-(4-chloro-*o*-tolyl-oxy)propionic acid, 3,6-dichloro-2-methoxybenzoic acid, 2-methyl-4-chlorophenoxyacetic acid, 2,3,6-trichlorobenzoic acid, 2,4-dichlorophenoxyacetic acid, 3,5,6-trichloro-2-pyridyloxyacetic acid, 2,4,5-trichlorophenoxyacetic acid and α -(2-methyl-4-chlorophenoxy)butyric acid. The method involves extraction with saturated calcium hydroxide solution, esterification with pentafluorobenzyl bromide, clean-up with a silica gel column and determination by capillary GC-SIM. Recoveries from soil and sediment are over 89% (with the exception of 77% for TBA) with coefficients of variation below 5% ($n = 7$). The method is suitable for the simultaneous determination of the eight herbicides in environmental samples with high sensitivity and accuracy.

INTRODUCTION

Phenoxyalkanoic, benzoic acid-derived and pyridyloxy herbicides have a selective killing effect on broadleaf weeds and are therefore widely used in agriculture and forestry. These herbicides are marketed in the form of esters, salts or acids. After application, they can enter water flow systems, with the possibility of environmental pollution. Hence it is desirable to have a method for the simultaneous determination of multiple components in environmental samples. The purpose of this work was to develop such a method applicable to herbicides in samples at concentrations of the order of micrograms per kilogram.

Many methods¹⁻¹⁵ of analysis have been reported for phenoxyalkanoic and benzoic acid-derived herbicides in soils and sediments. For pyridyloxy herbicides, only one method¹⁶ has been presented for environmental water and none for soil or sediment.

Several methods of extracting herbicides from soils or sediments have been

proposed. Khan¹ used a mixture of acidified acetone and *n*-hexane, Abbott *et al.*² one of dilute sulphuric acid and diethyl ether and Cotterill³ saturated calcium hydroxide solution.

Herbicides extracted from environmental samples, except esters, are insufficiently volatile or too highly polar for gas chromatographic (GC) analysis. It is therefore necessary to decrease their polarity and to make them more volatile by methylation using diazomethane^{1,4,5} boron trichloride-methanol⁶, or iodomethane^{3,7} Chau and Terry⁸ adopted derivatization to halogenated alkyl esters and halogenated aromatic esters such as the pentafluorobenzyl ester to increase the sensitivity of sample herbicides towards electron-capture detection (ECD) in GC. Bertrand *et al.*¹⁵ adopted (cyanoethyl)dimethylsilylation.

In most determinations of extracted herbicides the samples were cleaned up by liquid-liquid partition or column chromatography before being subjected to GC-ECD. Capillary GC-ECD¹⁴ and capillary GC-mass spectrometry (GC-MS) have recently come into use.

This investigation was undertaken in order to establish a suitable method for the simultaneous determination of these compounds in soils and sediments. The examination was focused on the applicability of pentafluorobenzylation as a method for the pre-treatment of environmental samples and the application of high-selectivity GC-selected-ion monitoring (SIM) to the determination of acid herbicides. The method proposed here has proved to have adequate sensitivity, accuracy and selectivity.

EXPERIMENTAL

Reagents

3,5,6-Trichloro-2-pyridyloxyacetic acid (triclopyr), triethylammonium 3,5,6-trichloro-2-pyridyloxyacetate (triclopyr-TEA) and butoxyethyl 3,5,6-trichloro-2-pyridyloxyacetate (triclopyr-BE) were obtained from Dow Chemical Japan, 2,4-dichlorophenoxyacetic acid (2,4-D), 2,4,5-trichlorophenoxyacetic acid (2,4,5-T) and 2-methyl-4-chlorophenoxyacetic acid (MCP) from Wako, 2,3,6-trichlorobenzoic acid (TBA) from Takeda Chemical, 3,6-dichloro-2-methoxybenzoic acid (dicamba) from King Chemical, α -(2-methyl-4-chlorophenoxy)butyric acid (MCPB) and 2-(4-chloro-*o*-tolylxy)propionic acid (MCPB) from Yashima Chemical, 2,3,4,5,6-pentafluorobenzyl bromide (PFB) from Tokyo Kasei and *p*-terphenyl-*d*₁₄ from MSD Isotopes, Canada.

Silica gel (Wako Gel S-1) was activated by heating at 130°C for 12 h before use. Ultrabond 20M, a polyethylene glycol GC packing, was obtained from Ultra Scientific. OV-1 (methylsilicone) and OV-17 (mixed methyl- and phenylsilicone) were obtained in the form of wide-bore capillary columns (15 m × 0.53 mm I.D.), with the silicones chemically bonded, from Gasukuro Kogyo.

n-Hexane, benzene, dichloromethane and acetone were of the grade suitable for the detection of pesticide residues. All the other reagents were of guaranteed grade.

Apparatus

The GC-MS instrument used was a Model JMS-D300 from Japan Electron Optics Laboratory and the ultrasonic cleaner was a Model UT-20 (26 kHz, 300 W) from Kokusai Denki.

Measurement conditions

The conditions for GC were as follows: column temperature, 230°C; injection port temperature, 250°C; and carrier gas (helium) flow-rate, 15 ml/min. Three columns were tested for applicability as described later.

The conditions for SIM-MS were as follows: ion multiplier voltage, 1.8 kV; and ion source and enricher temperature, 250°C. Experiments to select suitable monitor ions and ionization voltages were conducted as described later.

Experiments performed to develop the standard procedure

Extraction conditions were determined as follows: to 20 g of soil sample 5 µg of each acid herbicide were added and after 1 h, 2 g of calcium hydroxide and 100 ml of distilled water were added. The mixture was extracted several times by sonication for various times in the range 10–60 min and the recovery for each herbicide was determined.

To select a suitable esterifying agent, the following three experiments were conducted using 10 µg of each acid herbicide: (1) methylation was conducted using 2 ml of a diethyl ether solution of diazomethane; (2) esterification with trifluoroethanol (TFE) was conducted at 80°C for 1 h using 0.25 ml of boron trifluoride (BF₃)–TFE; (3) esterification with PFB was conducted at 60°C for 3 h and at 25°C for 1–24 h.

To select clean-up conditions, 10 µg of the PFB esterification product of each herbicide was loaded on to a 10 mm I.D. column containing silica gel and eluted with 100 ml of benzene–*n*-hexane (10:90); no ester species were found in the eluate. The esters were completely eluted with 100 ml of benzene–*n*-hexane (55:45).

Interferences from similar substances which might be extracted from the initial soil sample by dichloromethane were examined for the following substances: 2,4-dichlorophenol, 2,4,5-trichlorophenol, pentachlorophenol, salicylic acid, benzoic acid, 2,4-dichlorophenyl 3-methoxy-4-nitrophenyl ether, *p*-nitrophenyl 2,4,6-trichlorophenyl ether and 2,4-dichlorophenyl *p*-nitrophenyl ether. For this examination 100 µg of each substance were added to 100 ml of distilled water prior to extraction with dichloromethane and esterification.

To select the MS conditions, PFB esterification products were prepared, as follows, according to Lee and Chau's method¹³ (different from the standard procedure because a larger amount of herbicide was to be handled for preparation purposes). Amounts of 1 mg each of MCP, dicamba, MCP, TBA, 2,4-D, triclopyr, 2,4,5-T and MCPB were placed in a 5-ml vial, 3 ml of acetone were added and then 30 µl of 30% (w/v) potassium carbonate solution and 200 µl of 5% (v/v) PFB solution in acetone were added. The mixture was allowed to react at 60°C for 3 h and the reaction products were extracted with 20 ml of *n*-hexane. The products were identified by electron impact (EI) MS measurements using the usual technique adopted for the selection of MS conditions.

For GC using the conditions given above, a column packed with Ultrabond 20M and wide-bore columns with chemically bonded OV-1 or OV-17 were examined. For MS using the predetermined conditions given above, monitor ions and ionization voltages (15–30 and 70 eV) were sought that would be susceptible to as little interference and capable of providing as high sensitivity as possible.

Standard procedure

The standard procedure consists of four steps: extraction, esterification, clean-up and determination.

Extraction. About 20 g of sample are weighed into a 300-ml centrifuge tube and 2 g of calcium hydroxide and 100 ml of distilled water are added. The mixture is stirred with a glass rod and extracted by sonication for 30 min. The sample is centrifuged at 2000 g for 10 min and the extract is filtered under suction through a glass-fibre filter paper into a beaker. Extraction is repeated once in the same way with 100 ml of distilled water. The combined extracts are transferred into a separating funnel, acidified to a pH below 1 with 9 M sulphuric acid and extracted twice for 3 min with 50 ml of dichloromethane. The dichloromethane extract solution is washed with 50 ml of 5% (w/v) sodium chloride solution, dehydrated with anhydrous sodium sulphate, transferred into a 200-ml oval flask and evaporated to dryness on a rotary evaporator.

Esterification. The residue is dissolved in 4 ml of acetone in the flask, 30 μ l of 30% (w/v) potassium carbonate solution and 200 μ l of 5% (v/v) PFB solution in acetone are added and the solution is allowed to stand for 5 h at room temperature for esterification to proceed. The solution is evaporated to dryness on a rotary evaporator and the residue is dissolved in about 20 ml of *n*-hexane in a 50-ml separating funnel. The solution is washed twice with 10 ml of 5% (w/v) sodium chloride solution, dehydrated with anhydrous sodium sulphate and concentrated to less than 5 ml in a Kuderna–Danish concentrator.

Clean-up. A silica gel column is prepared by packing a 10 mm I.D. column with a slurry of 3 g of silica gel in *n*-hexane. The concentrate is transferred on to this column, washed with 100 ml of benzene–*n*-hexane (10:90) and eluted with 100 ml of benzene–*n*-hexane (55:45).

Determination. The eluate is concentrated to less than 5 ml in a Kuderna–Danish concentrator and, after adding 0.5 μ g of *p*-terphenyl-*d*₁₄ as an internal standard, further concentrated to 1 ml under a gentle stream of nitrogen. The sample is injected into the GC–SIM instrument for determination.

Blank tests are run using the same procedure.

RESULTS AND DISCUSSION

Investigation of extraction conditions for soil samples

The experimental investigation for establishing the extraction condition utilized Cotterill's method³, which extracts ester-type herbicides under a hydrolysis condition with alkali and may be regarded as efficient with respect to the number of operational steps.

The recovery obtained with extraction times of 30–60 min reached a constant value. One extraction run did not give a sufficient recovery but two successive runs were satisfactory. The extraction conditions adopted were 30-min sonication twice. It was noted that tricopyr-BE is hydrolyzed completely into triclopyr within 5 min.

Investigation of PFB esterification conditions

Diazomethane, which is unstable and explosive, could convert all eight acid herbicides into methyl esters. However, the methyl esters of MCP, TBA and MCP have such low boiling points that the efficiency of concentration is too low. BF₃–TFE

hardly reacts with MCPB, dicamba, MCP and TBA. PFB was found to effect smooth esterification with the formation of products with relatively high boiling points. It was therefore decided to adopt PFB as the esterifying agent.

Many methods have been reported for the esterification of acid herbicides with PFB. This investigation was conducted according to Lee and Chau's method¹³. However, at 60°C, the heating temperature employed for esterification in their method, additional peaks appeared in the blank chromatogram and the compounds responsible could not be removed from the blank sample by silica gel clean-up. We therefore lowered the heating temperature to 25°C. Heating durations of 4–16 h gave a constant formation ratio whereas heating for 16–24 h caused extraneous peaks at longer retention times. Hence, the optimum conditions were esterification with 5% (v/v) PFB solution in acetone at 25°C for 5 h.

Clean-up of PFB esterification products by silica gel column chromatography

A variety of substances in soils and sediments can be simultaneously extracted and esterified by PFB and cause interference in the determination of acid herbicides. Therefore, the esterification products were purified using a silica gel column. When eluted with 100 ml of benzene-*n*-hexane (10:90) no ester species were found in the eluate. However, the esters were completely eluted with 100 ml of benzene-*n*-hexane (55:45) (Fig. 1).

The clean-up procedure adopted was therefore as follows: the column was washed with 100 ml of benzene-*n*-hexane (10:90) to elute as many of the interfering compounds as possible and the esters were eluted with 100 ml of benzene-*n*-hexane (55:45).

All the phenols, acids and ethers tested with respect to interferences were completely removed by the silica gel clean-up or had sufficiently different GC retention times not to cause interference.

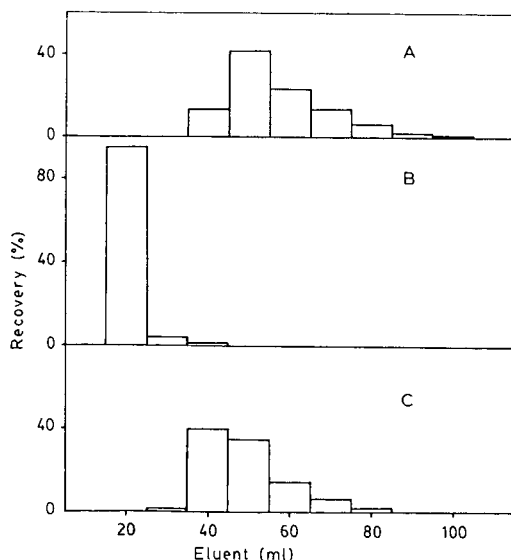


Fig. 1. Elution patterns of (A) MCPB-PFB, (B) TBA-PFB and (C) triclopyr-PFB.

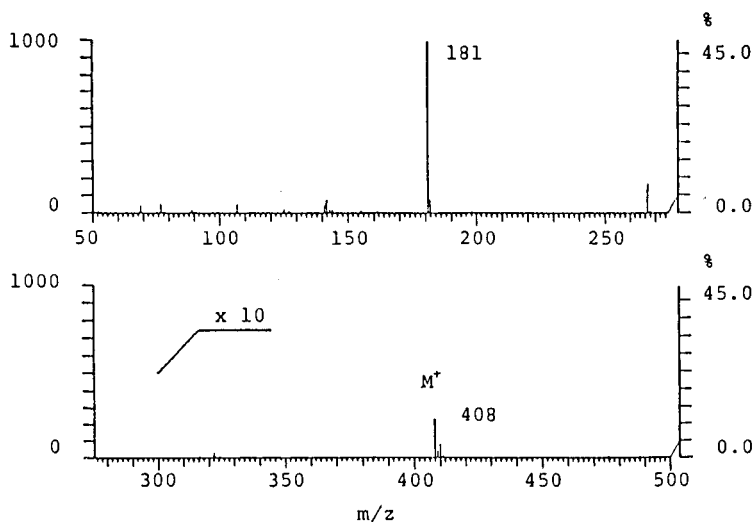


Fig. 2. EI mass spectrum of MCPB-PFB.

Formation and identification of products from reaction with PFB

Each compound was found to give its corresponding molecular ion as follows: m/z 394 (MCP), 400 (dicamba and 2,4-D), 380 (MCP), 404 (TBA), 406 (MCPB), 434 (2,4,5-T) and 435 (triclopyr). TBA and MCPB had a low tendency to form molecular ions, as shown in Figs. 2 and 3. For this reason ions other than molecular ions, *i.e.* at m/z 369 and 267, were adopted as monitoring ions for TBA and MCPB, respectively.

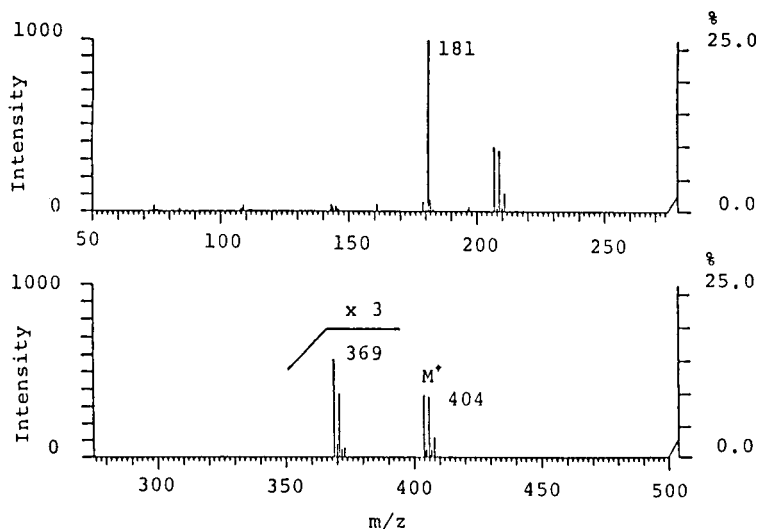


Fig. 3. EI mass spectrum of TBA-PFB.

Chromatography and detection

Lee and Chau¹³ used Ultrabond 20M as the GC column packing to separate ten PFB derivatives. We used the same packing for GC-SIM but found that it gave too high a background response to be applicable.

Next, we tried a wide-bore capillary column, which features a low background response, high-speed separation and almost the same sample injection volume as a packed column. A wide-bore column (15 m × 0.53 mm I.D.) chemically bonded with OV-17 was capable of almost completely separating all eight acid herbicides in 6 min.

The monitoring ions for determination were selected by measuring the EI mass spectra of each PFB ester and taking into account the fragment intensity and selectivity. The following monitoring ions were selected: m/z 267 (MCPB), 369 (TBA), 380 (MCP), 394 (MCP), 400 (2,4-D and dicamba), 434 (2,4,5-T) and 435 (triclopyr).

The ionization voltage that allows the monitoring ion to give the highest sensitivity was examined in the range 15–30 and 70 eV; 27.5 eV was found to give the highest sensitivity.

Calibration and recovery

The calibration graphs, obtained for 0.05, 0.10, 0.25, 0.50 and 1.0 µg of each acid herbicide, were linear over the concentration range examined. The detection limits were 0.5 µg/kg for MCP, MCPB and TBA, 1.0 µg/kg for 2,4-D and triclopyr and 1.5 µg/kg for dicamba and 2,4,5-T.

Recovery experiments were carried out by adding 0.5 µg of each acid herbicide to 20 g of paddy field soil (ignition loss 18.4%) and applying the standard procedure to evaluate the recovery. The recoveries obtained were over 89%, except for TBA (77%), with coefficients of variation being less than 5%.

Table I summarizes the results obtained, indicating that the proposed method is satisfactory.

Application to actual samples

The proposed method was applied to soils and sediments ($n = 20$). Paddy field soils and sediments were found to contain MCP and 2,4-D at levels of 0.25–3.0 µg/kg,

TABLE I
RECOVERY OF ACID HERBICIDES FROM SOIL

Mean values ($n = 7$)

<i>Herbicide</i>	<i>Amount of sample (g)</i>	<i>Amount of herbicide added (µg)</i>	<i>Recovery (%)</i>	<i>Coefficient of variation (%)</i>	<i>Detection limit (µg/kg)</i>
MCP	20.0	0.5	92.5	3.4	0.5
Dicamba	20.0	0.5	92.7	4.3	1.5
MCPB	20.0	0.5	94.3	3.5	0.5
TBA	20.0	0.5	77.5	3.2	0.5
2,4-D	20.0	0.5	90.1	4.1	1.0
Triclopyr	20.0	0.5	89.0	3.7	1.0
Triclopyr-TEA	20.0	0.5	90.3	4.3	1.0
Triclopyr-BE	20.0	0.5	89.7	3.5	1.0
2,4,5-T	20.0	0.5	90.4	4.4	1.5
MCPB	20.0	0.5	89.2	4.5	0.5

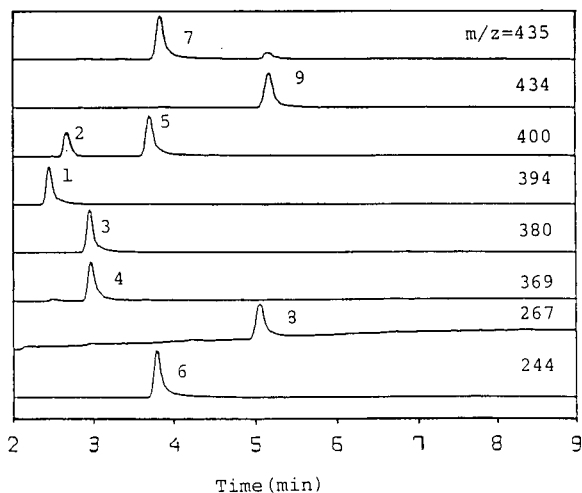


Fig. 4. SIM chromatogram of a standard mixture of acid herbicides. Peaks: (1) MCP; (2) dicamba; (3) MCP; (4) TBA; (5) 2,4-D; (6) *p*-terphenyl; (7) triclopyr; (8) MCPB; (9) 2,4,5-T.

and turf soils taken from around the laboratory were found to contain TBA, triclopyr, MCP and dicamba at levels of 9–100 $\mu\text{g}/\text{kg}$. Figs. 4 and 5 show examples of SIM chromatograms for acid herbicides and for soil taken from around the laboratory, respectively.

Similar determinations were made using GC-ECD, but the appearance of a large number of interfering peaks required an analysis time for one sample of more than 1 h, with analytical values higher than those given by the proposed method.

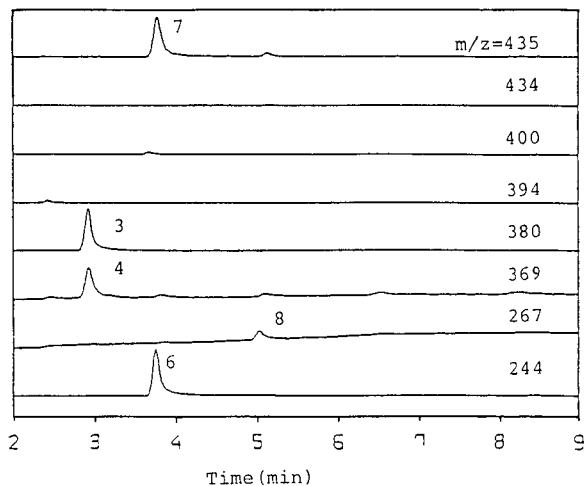


Fig. 5. SIM chromatogram of turf soil from near the laboratory. Peaks as in Fig. 4.

ACKNOWLEDGEMENTS

The authors thank Miss Maria Miyajima and Professor Isao Matuzaki for helpful suggestions.

REFERENCES

- 1 S. U. Khan, *J. Assoc. Off. Anal. Chem.*, 58 (1975) 1027.
- 2 D. C. Abbott, H. Egan, E. W. Hammond and J. Thomson, *Analyst (London)*, 89 (1964) 480.
- 3 E. G. Cotterill, *Analyst (London)*, 107 (1982) 76.
- 4 S. F. Howard and G. Yip, *J. Assoc. Off. Anal. Chem.*, 54 (1971) 970.
- 5 L. E. St. John, Jr. and D. J. Lisk, *J. Dairy Sci.*, 50 (1967) 582.
- 6 W. H. Gutermann and D. J. Lisk, *J. Agric. Food Chem.*, 11 (1963) 301.
- 7 A. P. Thio, M. J. Kornet, H. S. I. Tan and D. H. Tompkins, *Anal. Lett.*, 12 (1979) 1009.
- 8 A. S. Y. Chau and K. Terry, *J. Assoc. Off. Anal. Chem.*, 59 (1976) 633.
- 9 H. Agemian and A. S. Y. Chau, *Analyst (London)*, 101 (1976) 732.
- 10 J. D. Gaynor and D. C. Mactavish, *Analyst (London)*, 107 (1982) 700.
- 11 E. G. Cotterill, *J. Chromatogr.*, 171 (1979) 478.
- 12 M. A. Sattar and J. Paasirvirta, *Anal. Chem.*, 51 (1979) 598.
- 13 H. B. Lee and A. S. Y. Chau, *J. Assoc. Off. Anal. Chem.*, 66 (1983) 1023.
- 14 H. B. Lee, Y. Stokker and A. S. Y. Chau, *J. Assoc. Off. Anal. Chem.*, 69 (1986) 557.
- 15 M. J. Bertrand, A. W. Ahmed, B. Sarrasin and V. N. Mallet, *Anal. Chem.*, 59 (1987) 1302.
- 16 T. Tsukioka, R. Takeshita and T. Murakami, *Analyst (London)*, 111 (1986) 145.

CHROM. 21 345

RAPID HIGH-PERFORMANCE LIQUID CHROMATOGRAPHIC SEPARATION OF BARLEY MALT α -AMYLASE ON CYCLOBOND COLUMNS

CYNTHIA A. HENSON*

U.S.D.A. Agricultural Research Service, Cereal Crops Research Unit, Department of Agronomy, University of Wisconsin, 1575 Linden Dr., Madison, WI 53706 (U.S.A.)

and

JULIE M. STONE

Department of Agronomy, University of Wisconsin, 1575 Linden Dr., Madison, WI 53706 (U.S.A.)

(First received November 15th, 1988; revised manuscript received January 24th, 1989)

SUMMARY

A procedure for separation of α - and β -amylases was developed which results in their complete resolution in less than 20 min. A cyclodextrin stationary phase column was equilibrated in 10 mM phosphoric acid at pH 7.0. Purified barley malt α - or β -amylases, mixtures of both, or crude malt extracts were injected. β -Amylase did not bind to the column and was rapidly eluted with water or buffer. α -Amylases specifically bind to the immobilized dextrin. Optimal elution of α -amylase was achieved with a 10-ml gradient from 0 mg/ml β -cyclodextrin (cycloheptaamylose) in buffer to 12 mg/ml β -cyclodextrin in 15% aqueous methanol, followed by flushing with 20 ml of 12 mg/ml β -cyclodextrin in 15% aqueous methanol. Elution buffer containing β -cyclodextrin at pH values from 6.0 to 7.0 was not as effective in eluting α -amylase as was cyclodextrin in aqueous methanol. Inclusion of methanol in the gradient resulted in enhanced recoveries of α -amylase. α -Amylase did not bind to the column at pH values higher than 7.0. This procedure should be useful for rapid separation of plant α - and β -amylases, separation of pullulanases or debranching enzymes from other carbohydrases, and purification of α -amylases.

INTRODUCTION^a

The use of high-performance liquid chromatography (HPLC) has, within the last decade, become commonplace in protein chemistry. The rapid separations achievable with HPLC combined with the power of affinity chromatography can result in separation and purification of proteins in a few days.

Affinity chromatography of plant amylases was accomplished in 1933 using

^a Mention of a proprietary product does not constitute a guarantee or warranty of the product by the U.S. Department of Agriculture and does not imply its approval to the exclusion of other suitable products.

starch as the enzyme-specific ligand¹. Cyclohexaamylose-bonded Sepharose, to which sweet potato β -amylase specifically adsorbs², as well as cycloheptaamylose³ and glycogen⁴ bound to Sepharose have been used successfully for purification of cereal amylases. Although these resins provide a very powerful tool in protein purification, the bonded ligand responsible for the biospecificity bleeds off the column with repeated use.

Commercially available cyclodextrin-bonded silica HPLC resins which are stable in both aqueous and organic mobile phases have been recently developed for use in separation of optical isomers [*e.g.*, D,L-amino acids; (\pm)-barbital derivatives] and structural isomers (*e.g.*, α - and β -naphthoflavones; *o*, *m*, *p*-xylenes)^{5,6}. These columns are available with cyclohexaamylose, cycloheptaamylose or cyclooctaamylose chemically bonded to a spherical silica gel support through a non-nitrogenous (*i.e.* amines or amides) spacer arm.

We report here the use of a commercially available affinity column (Cyclobond I) for the separation and purification of carbohydrases commonly found in plant tissues—including α -amylase, β -amylase, and pullulanase (debranching enzyme). The main advantages of using HPLC over conventional open column chromatography are that separations of various carbohydrases can be achieved in 20 min rather than 6–8 h and that very stable bonded phases for separation are available.

EXPERIMENTAL

Enzyme sources

Preparation of purified α -amylases. Barley (*Hordeum vulgare* cv. Morex) malt was ground with a VirTis homogenizer in extraction buffer (40 mM Tris, pH 8.0, containing 1 mM CaCl₂) with a ratio of 5 ml buffer/1 g malt. The extract was centrifuged at 6000 *g* for 40 min (4°C). Supernatants were heated at 70°C for 15 min to inactivate β -amylase. After clarification by centrifugation at 15 000 *g* for 15 min, heated supernatants were chromatofocused on a Polybuffer exchanger 94 column (71 × 1.5 cm) equilibrated with 25 mM imidazole, pH 7.4. Elution was with a 1:10 dilution of Polybuffer 74, pH 4.0. α -Amylase activities were detected as described before⁷. The fractions containing high *pI* α -amylase activities were pooled, dialyzed against 40 mM Tris, pH 8.0 containing 1 mM CaCl₂, and then concentrated with an Amicon YM-10 membrane.

Preparation of crude malt extract. Morex malt was ground in extraction buffer. Grinding ratios of 5:1 were used when extracting pullulanase and 10:1 when extracting other carbohydrases. The homogenates were centrifuged at 12 000 *g* for 15 min (4°C), and then dialyzed against extraction buffer.

Purified barley malt β -amylase (No. 13440) was purchased from Serva (Westbury, NY, U.S.A.) and solubilized in extraction buffer (0.5 mg β -amylase/ml). Pullulanase (P-2138) and bovine serum albumin (BSA) (A-7906) were purchased from Sigma (St. Louis, MO, U.S.A.).

Enzyme assays

Total amylolytic activities were assayed with soluble starch as the substrate. Reducing sugars were detected with 3,5-dinitrosalicylic acid⁷. Assays using soluble starch as the substrate detect α -amylase, β -amylase, and debranching or pullulanase

type enzymes. Starch azure assays, which are specific for α -amylase in the presence of β -amylase, were conducted as described in Henson and Stone⁸. Pullulanase was assayed with 2% pullulan as the substrate. Detection was with the dinitrosalicylic acid technique used for total amylolytic assays.

Chromatography

HPLC-grade phosphoric acid, 85%, was purchased from Fisher Scientific (Fair Lawn, NJ, U.S.A.). Phosphoric acid was passed through a C₈ column (Aquapore Octyl RP-300) to remove impurities prior to use as a mobile-phase component. HPLC-grade methanol, ChromAR, was purchased from Mallinckrodt (Paris, KY, U.S.A.). β -Cyclodextrin (C-4767) was purchased from Sigma.

All separations were done at 25°C (FIATron TC-50 temperature controller) using a Shimadzu LC-6A liquid chromatograph. The separation column, Cyclobond I (10 × 0.46 cm), was obtained from Advanced Separation Technologies, Whippany, NJ, U.S.A. An OH-100 Aquapore guard column (Brownlee Labs., Santa Clara, CA, U.S.A.) was used. The flow-rate was 2 ml/min. The gradient was composed of 0–100% B in 5 min followed by 13 min of 100% B. The composition of solvents A and B varied as described in the figure legends. All solvents and protein solutions were filtered through a 0.45- μ m membrane prior to chromatography. The column was cleaned between injections with 100% methanol.

RESULTS AND DISCUSSION

The effects of mobile phase composition on binding and elution of amylases were investigated (Fig. 1). Effects of pH on column selectivity were determined from pH 6.0 to 8.0 in 10 mM phosphate buffer. Data in Fig. 1a–c were obtained using the same pH buffer for both equilibration and elution. A gradient of 0–12 mg β -cyclodextrin/ml equilibration buffer was used for elution (see figure legends). At low pH (6.0 and 6.5), both α - and β -amylase were tightly bound to the column (Fig. 1a and b). At high pH (7.5 and 8.0), both amylases eluted in the void volume (Fig. 1a and b). Fig. 1c shows chromatography under what was determined to be the optimal conditions for separation of α - and β -amylase. These conditions were column equilibration at pH 7.0 and elution with a gradient of β -cyclodextrin in pH 8.0 phosphate buffer. Even though this was optimal, repeated use of elution gradients at pH 8.0 was considered unsuitable because of the instability of the silica resin.

Aqueous–organic mobile phases are commonly used with cyclodextrin stationary phases and frequently result in altered selectivities or retention times. Effects of methanol addition to the β -cyclodextrin gradient, made in unbuffered water, are shown in Fig. 1d. While the retention of either α - or β -amylase was not greatly altered, the addition of an organic modifier resulted in better peak resolution (Fig. 1d) and a 28% greater recovery of the amylolytic activity. Optimal conditions for separation of α - and β -amylase were determined to be on a column equilibrated with 10 mM phosphoric acid at pH 7.0, followed by elution with a gradient of 0–100% solvent B (12 mg β -cyclodextrin/ml of 15% methanol in water) and a 13-min flush with 100% B. Under these conditions approximately 75% of the α -amylase activity applied to the column was recovered in fractions 19–22.

Separation on Cyclobond columns is the result of formation of inclusion

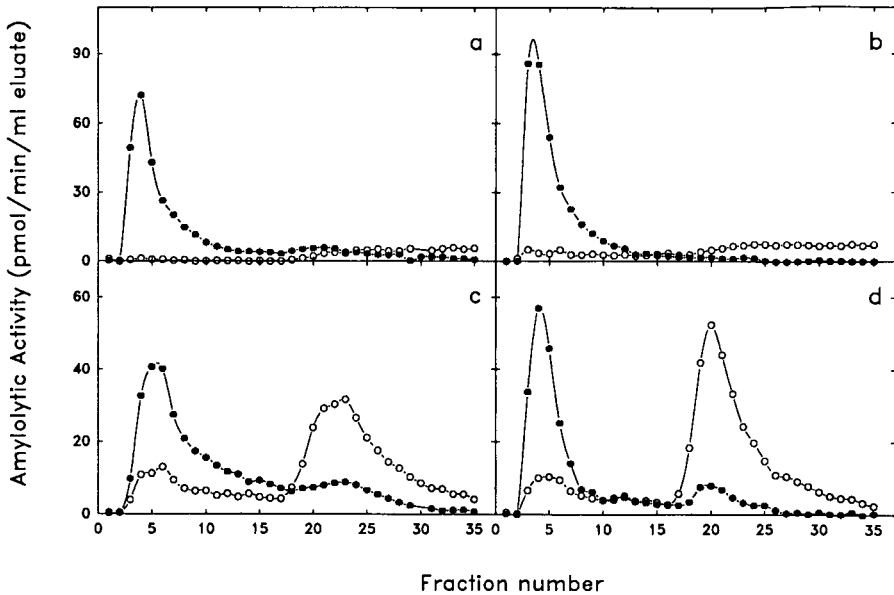


Fig. 1. Chromatography of purified barley malt α - and β -amylases on a cyclodextrin-bonded HPLC column. Solvent A was 10 mM phosphoric acid at varying pH values. Solvent B was 12 mg β -cyclodextrin per ml solvent A or aqueous methanol. The gradient was 0–100% B in 5 min and was followed by 13 min flush with 100% B. (a) Purified α -amylase, solvent A was pH 6.5 (○) or 7.5 (●), solvent B was solvent A containing cyclodextrin; (b) purified β -amylase, solvent A was pH 6.5 (○) or 7.5 (●), solvent B was solvent A containing cyclodextrin; (c) purified α -amylase (○) and β -amylase (●) solvent A was pH 7.0 and solvent B was 12 mg β -cyclodextrin/ml pH 8.0 phosphate buffer; (d) same as (c) except solvent B was β -cyclodextrin made in 15% aqueous methanol rather than in solvent A.

complexes between the adsorbed compound and the hydrophobic cavity of the cyclodextrin⁹. Typical compounds which can form inclusion complexes with the hydrophobic cavity of the cyclodextrin ring range from small inorganic ions to aromatic compounds such as substituted benzene isomers and enantiomeric organometallic compounds. The decreased retention of a solute in the presence of an organic modifier is due to competition for the hydrophobic cavity of the cyclodextrin⁹. As the concentration of organic modifier increases, a solute's interaction with the cyclodextrin is decreased until it is eventually no longer retained. It is likely that the binding of at least some of the α -amylase is due to an exposed aromatic amino acid forming an inclusion complex with the cyclodextrin cavity. Indeed, it has been demonstrated that at least one non-catalytically essential tryptophanyl residue is involved in the binding of β -cyclodextrin to α -amylase¹⁰.

As previous data were obtained with partially purified high *pI* α -amylases and highly purified β -amylases, we next tested the separation of carbohydrases from crude barley malt. Using the previously defined optimal conditions, all of the malt α -amylases, both high and low *pI* isozymes, were bound to the column (Fig. 2a; open circles). The first peak of amylolytic activity detected is β -amylase free of contaminating α -amylase. This peak of activity corresponds well with the β -amylase "standard" shown in Fig. 1d. The second peak of activity detected with dinitrosalicylic

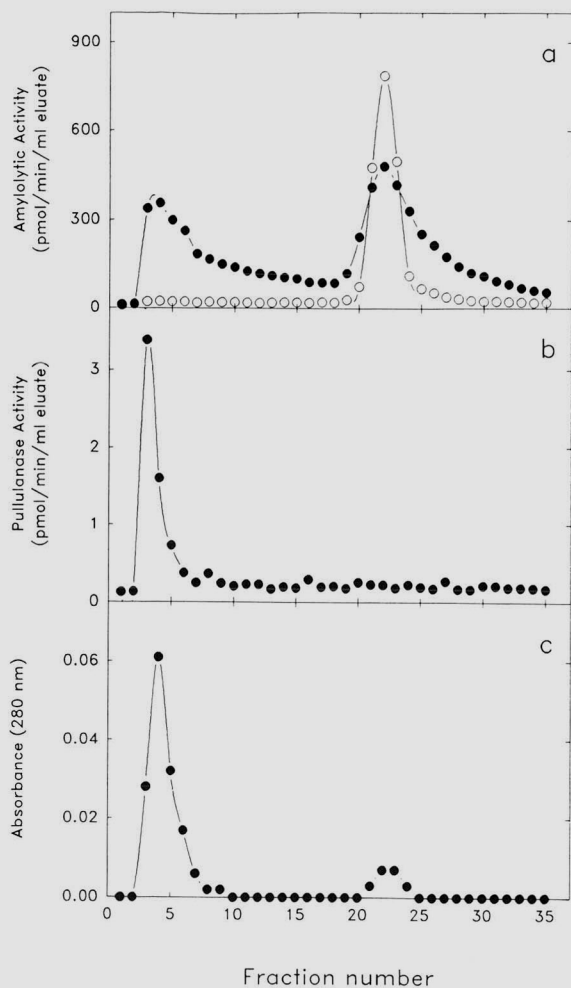


Fig. 2. Chromatography of crude barley malt extract on a cyclodextrin-bonded HPLC column. Solvent A was 10 mM phosphoric acid at pH 7.0. Solvent B was 12 mg β -cyclodextrin/ml 15% aqueous methanol. The gradient was from 0–100% B in 5 min and was followed by 13 min flush with 100% B. (a) α -Amylase activity measured with the starch azure assay (\circ), total amylolytic activity measured as reducing sugar production from soluble starch (\bullet); (b) pullulanase or debranching enzyme activity; (c) elution profile of malt proteins.

acid coelutes with the α -amylase “standard” (Fig. 1d), and with the single peak of endolytic amylase activity detected by the starch azure assay. Hence, the second peak in Fig. 2a is α -amylase. The α -amylase recovered in the second peak migrated as a single band on a sodium dodecyl sulfate polyacrylamide gel (SDS-PAGE) (Fig. 3) and thus was purified to homogeneity by chromatography of crude malt extracts on the cyclobond column.

Pullulanase, or debranching enzyme, is present in crude malt extracts in low levels although much greater activities are found in unkilned malt and in tissues of other plants. Malt pullulanase does not bind to the β -cyclodextrin ring of the

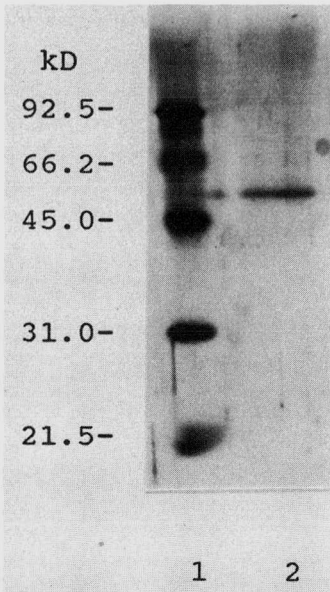


Fig. 3. SDS-PAGE¹⁴ of crude barley malt extract proteins eluted in fractions 19–22. Lane 1 contains molecular weight standards (in order of decreasing molecular weight: phosphorylase B, BSA, ovalbumin, carbonic anhydrase, soybean trypsin inhibitor). Lane 2 contains the α -amylase that was eluted in fractions 19–22 when a crude malt extract was injected.

Cyclobond column and is eluted in the void volume as is β -amylase (Fig. 2b). In contrast, *Enterobacter aerogenes* pullulanases eluted as three distinct peaks with k' values of 1, 2.33, and 5.33 (data not shown). The barley malt and bacterial pullulanases we have chromatographed elute prior to and separate from the α -amylases.

A protein elution profile ($A_{280\text{nm}}$) from a crude malt injection is shown in Fig. 2c. The majority of the protein eluted near the void volume, as did β -amylase. The actual void volume, calculated from the elution of bovine serum albumin (Fig. 4), was 3.0 ml.

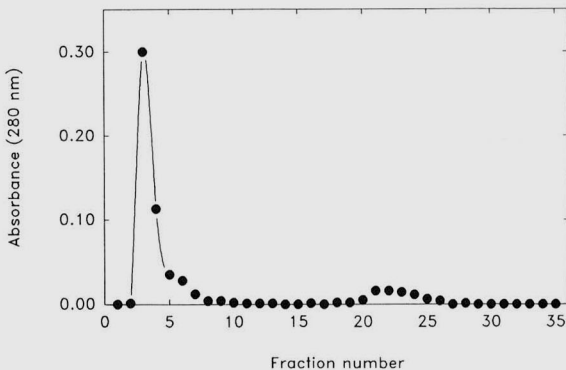


Fig. 4. Chromatography of BSA on cyclodextrin-bonded HPLC column. Elution conditions were the same as in Fig. 2.

BSA was selected as a void volume marker as it is similar in molecular weight (66 000) to both malt α - and β -amylase (45 000 and 65 000 daltons, respectively)^{11,12}. Additionally, BSA was not expected to bind to the carbohydrate ligand. Over 98% of the protein absorbing at 280 nm eluted in the first six fractions. A slight increase in absorbance was also detected in fractions 21–24. Apparently, this preparation of BSA contains some protein which, based on its ability to specifically bind β -cyclodextrin, either contains a carbohydrate binding site or has exposed aromatic amino acid residues capable of binding the Cyclobond resin. The void volume value is in excellent agreement with the value (2.95 ml) determined by injecting water while pumping a mixed mobile phase and detecting the peak via a change in refractive index¹³. Setting $V_0 = 3.0$, then $k' = 1.33$ for purified β -amylase (Fig. 1d) and 1.67 when separated from a crude malt mixture (Fig. 2a). Similarly, $k' = 6.67$ for partially purified α -amylase (Fig. 1d) and 7.33 in a crude malt extract (Fig. 2a).

In conclusion, the use of cycloheptaamylose-bonded HPLC columns results in complete separation of malt α -amylases from β -amylases and pullulanase or debranching enzyme in less than 20 min. The stability of this affinity resin is a significant advantage over the amine-coupled resins commonly used in open column chromatography. We have injected over 300 crude plant samples onto this column with no detectable loss of selectivity or binding capacity. The application of cyclodextrin-bonded phases for separation of other carbohydrate binding proteins or other proteins with exposed aromatic amino acid residues remains to be exploited.

ACKNOWLEDGMENTS

This research was supported by the U.S.D.A. Agricultural Research Service and the University of Wisconsin, Madison, WI, U.S.A.

REFERENCES

- 1 O. Holmbergh, *Biochem. Z.*, 258 (1933) 134–140.
- 2 P. Vretblad, *FEBS Lett.*, 47 (1974) 86–89.
- 3 M. P. Silvanovich and R. D. Hill, *Anal. Biochem.*, 73 (1976) 430–433.
- 4 R. Tkachuk, *FEBS Lett.*, 52 (1975) 66–68.
- 5 D. W. Armstrong, W. DeMond, A. Alal, W. L. Hinze, T. E. Riehl and K. H. Bui, *Anal. Chem.*, 57 (1985) 234–237.
- 6 D. W. Armstrong, *J. Liq. Chromatogr.*, 7 (1984) 353–376.
- 7 C. A. Henson, S. H. Duke and W. L. Koukkari, *Plant Cell Physiol.*, 27 (1986) 233–242.
- 8 C. A. Henson and J. M. Stone, *J. Cereal Sci.*, 8 (1988) 39–46.
- 9 D. W. Armstrong and W. DeMond, *J. Chromatogr. Sci.*, 22 (1984) 411–415.
- 10 R. M. Gibson and B. Svensson, *Carlsberg Res. Commun.*, 51 (1986) 295–308.
- 11 F. Kerhardy, I. Hara-Nishimura, M. Nishimura and J. Daussant, *Electrophoresis*, 8 (1987) 144–148.
- 12 C. Lauriere, M. Lauriere and J. Daussant, *Physiol. Plant.*, 67 (1986) 481–483.
- 13 D. W. Armstrong, W. DeMond and B. P. Czech, *Anal. Chem.*, 57 (1985) 481–484.
- 14 U. K. Laemmli, *Nature (London)*, 227 (1970) 680–685.

CHROM. 21 348

QUANTITATIVE ANALYSIS OF THORIUM IN PLUTONIUM USING REVERSED-PHASE LIQUID CHROMATOGRAPHY AND SPECTROPHOTOMETRIC DETECTION

VIRGINIA T. HAMILTON*, W. DALE SPALL, BARBARA F. SMITH and EUGENE J. PETERSON
Chemical and Laser Sciences Division, CLS-1, MS G740, Los Alamos National Laboratory, Los Alamos, NM 87545 (U.S.A.)

(First received September 5th, 1988; revised manuscript received January 12th, 1989)

SUMMARY

We have developed a method for separating and quantitating trace amounts of thorium in plutonium using a C_{18} reversed-phase column, an eluent containing 2-hydroxyisobutyric acid as a complexant followed by post-column reaction with Arsenazo III, and an absorbance measurement at 656 nm. The method is linear over the range 1–50 $\mu\text{g/ml}$ thorium and can detect thorium as low as 0.2 $\mu\text{g/ml}$. Precision is 3% relative standard deviation at the 4 $\mu\text{g/ml}$ level. The method is simple, rapid, and precise and does not involve preliminary extraction or precipitation of thorium from plutonium or other potential contaminants.

INTRODUCTION

The separation of neutral metal chelates and organometallics by high-performance liquid chromatography (HPLC) is well documented^{1–4}, but the methodology has not been applied to the separation of actinides except in a few cases^{5–9}. We have developed a reversed-phase liquid chromatographic analytical method for separating and quantitating thorium in plutonium to replace a precipitation method currently in use in our laboratory¹⁰ as well as to continue our studies of actinide separations. Barkley *et al.*⁵ reported that Th^{4+} and U^{6+} were selectively absorbed by reversed phases in the presence of 2-hydroxyisobutyric acid and, depending on the conditions of the mobile phase, could be well resolved from the rare earths and many transition metals. We studied the effect of modifying the mobile phase to optimize the resolution of thorium (4+) from plutonium (3+, 4+) to quantitate directly trace amounts of Th^{4+} in strong acid dissolutions of plutonium oxide and plutonium metal.

The chromatograph used for this work was configured so that the system components making contact with radioactive solutions, *i.e.* injection port, injection valve, separatory column, membrane reactor (Dionex, Sunnyvale, CA, U.S.A.), and photometer, were confined to an open-front radiation containment box. The eluent was pumped isocratically. Although gradient elution may provide better resolution of analytes, it was not studied as part of this work because the resolution obtained from isocratic elution was satisfactory and because this method was developed for

automated, routine analyses of many samples for which gradient equilibration periods are not desirable.

EXPERIMENTAL

Instrumentation

The chromatograph was a modified Dionex 4000 system consisting of various modules. The Dionex 4000 p.s.i. pump was operated isocratically at a flow-rate of 1.5 ml/min (1400–1600 p.s.i.). The sample was introduced by a Dionex 4000 p.s.i. injection valve plumbed for 50 μ l sample uptake. The column was a μ Bondapak C₁₈ reversed-phase column (300 \times 3.9 mm I.D., Waters Assoc., Milford, MA, U.S.A.) used at room temperature. A Dionex reagent delivery module and a membrane reactor were used for delivery and post-column mixing of the color reagent, Arsenazo III, with the eluent stream. The flow-rate of the Arsenazo solution into the membrane reactor was 0.6 ml/min. The detector was a Dionex UV-VIS fixed-wavelength photometer monitoring at 656 nm with an Ealing 12.7-mm diameter, 11.5-nm band pass filter used in place of one of the standard photometer filters. Usual photometer attenuation was 0.2 a.u.f.s. A Spectra Physics 4270 integrator, operating with appropriate settings, was used to determine peak areas and retention times.

Reagents

The mobile phase was a 0.3 M solution of 96% 2-hydroxyisobutyric acid (HIBA, Aldrich, Milwaukee, WI, U.S.A.) in 0.2 M reagent-grade NH₄Cl, adjusted to pH 4.0 with reagent-grade NH₄OH. The concentration of Arsenazo III [2,2'-(1,8-dihydroxy-3,6-disulfonaphthylene-2,7-bisazo)bisbenzenearsonic acid, Aldrich], was $1.5 \cdot 10^{-4}$ M. Stock and working solutions were made by dissolving these reagents as received in 18 M Ω -cm deionized water. Before use, the working eluent was filtered first through a 0.45- μ m pore cellulose acetate filter (Millipore, Bedford, MA, U.S.A.) then through a 0.2- μ m polycarbonate filter (Biorad Labs., Richmond, CA, U.S.A.). The Arsenazo III solution was not filtered. The eluent reservoir was kept under nitrogen pressure of 3 p.s.i. to prevent the formation of bubbles in the pump and column. The Dionex reagent delivery module was pressurized with nitrogen at 40 p.s.i. to send the Arsenazo III to the membrane reactor for mixing with the column effluent stream.

Analyte solutions

Thorium standard solutions were made from a 1000 μ g/ml stock in 10% HNO₃ (Spex Industries, Edison, NJ, U.S.A.). Plutonium solutions were made from a dissolution of plutonium metal diluted to a concentration of 1017 μ g/ml in 1% HNO₃. Americium (3+) and neptunyl (NpO₂⁺) stock solutions were made from acidic dissolutions of the metal oxides. Uranyl (UO₂²⁺) solutions were made from 1000 μ g/ml uranium in 10% HNO₃ (Spex). All other metal solutions were prepared from commercially available acidic, aqueous standards by dilution in filtered eluent. A pH range of 3.0–3.5 was noted for the analyte solutions.

RESULTS AND DISCUSSION

The use of post-column derivatization and detection of Arsenazo III metal

complexes has several advantages over direct detection techniques. The color reagent provides favorable selectivity for detection because of its reactivity with the metals of interest at pH 4 and its lack of reactivity with many other metals. The high extinction coefficients of Arsenazo III complexes of thorium and plutonium give more than sufficient sensitivity at low concentrations of these analytes. Such high sensitivity is desirable so that the amounts of radioactive materials required for analysis can be kept to a minimum.

Initial absorbance measurements made with a diode array spectrophotometer showed an absorbance increase in the wavelength region 600–700 nm when a solution of thorium in Arsenazo III was measured against a solution of Arsenazo III. We used 656 nm as the detection wavelength because it is midway in this broad absorbance range. The Ealing 12.7-mm diameter, 656-nm interference filter was chosen for its small size as well as its 11.5-nm band pass, a feature we considered advantageous as it provides more signal than does a narrower band pass.

Selection of the mobile phase complexant, HIBA, was based on the work of Barkley *et al.*⁵ They found that the selective adsorption of thorium (4+) and uranium (6+) in the presence of only HIBA obviated the inclusion of an organic modifier in the eluent. We held the concentration of the complexant at levels which would insure that the thorium complex contained four ligands and would be a neutral species¹¹. Addition of organic solvents such as acetonitrile or methanol decreased the retention times of both the thorium and plutonium peaks, as found by Barkley *et al.* Ammonium chloride was added to the eluent to increase mobile phase polarity and to reduce the tailing of the peaks, thereby increasing the resolution of thorium from plutonium. We altered the pH, the HIBA concentration, and the salt concentration in the mobile phase to optimize the resolution of thorium from plutonium. The conditions yielding the best resolution values were used for investigations of linearity, reproducibility, and interferences of the method.

Because the maximum buffer capacity of HIBA is at pH 4.04 (Beilstein Index, 3313), we began our evaluation at that pH. Results of eluent pH adjustments to pH 4.0 made with either NaOH or NH₄OH were compared using resolution values (Table Ia). The *R* value of 1.29 from the NH₄OH adjusted eluent was somewhat better than the *R* value of 1.08 from the NaOH adjusted eluent. This difference in *R* value may result from the effects of different ionic strengths.

The effect of varying eluent pH from 3.0 to 5.0 was determined by resolution value. Eluent at pH 4.0 yielded an *R* value of 1.39, whereas eluents at the other pH levels yielded *R* values from 0.76 to 1.12 (Table Ib). Thorium and plutonium peaks were not resolved at all when the eluent was at pH 5.0.

To determine which concentration of HIBA yielded the best resolution, we compared five HIBA complexant concentrations ranging from 0.15 *M* to 0.425 *M*. Resolution values ranged from 1.22 to 1.53 for HIBA concentrations of 0.2 *M* through 0.425 *M* (Table Ic). Although any HIBA concentration in this range can adequately resolve the thorium from the plutonium, the 0.3 *M* concentration was selected as the analytical concentration because it kept the system pressure below 1500 p.s.i. while providing reasonable retention times and peak shapes of the analytes (Fig. 1).

We thought that making the eluent more polar might improve the resolution of thorium from plutonium. Comparisons were made of the *R* values calculated from 0.2 *M* concentrations of NaCl and NH₄Cl in the eluent. Because 0.2 *M* NH₄Cl yielded the

TABLE I
RESOLUTION VALUES OF Th⁴⁺ FROM Pu⁴⁺ FOR VARIOUS CONDITIONS OF THE ELUENT

<i>Parameter</i>	<i>R Value</i>
(a) pH Adjuster	
NH ₄ OH	1.29
NaOH	1.08
(b) Eluent pH	
3.0	0.76
3.5	1.12
4.0	1.39
4.5	0.93
(c) HIBA concentration	
0.15 <i>M</i>	1.22
0.2 <i>M</i>	1.49
0.3 <i>M</i>	1.39
0.375 <i>M</i>	1.40
0.425 <i>M</i>	1.53
(d) Eluent salt	
NH ₄ Cl (0.2 <i>M</i>)	1.39
NaCl (0.2 <i>M</i>)	1.29

higher *R* value of 1.39, it was used as the eluent for the linearity, sensitivity and precision studies (Table Id).

Increasing the temperature in the separation column from room temperature to 40°C had no effect on the resolution of Th⁴⁺ from Pu⁴⁺. Because no changes were seen, further temperature studies were not pursued. Also, no improvement in sensitivity was noted when the concentration of Arsenazo III was doubled from 1.5 · 10⁻⁴ *M* to 3.0 · 10⁻⁴ *M*.

Once optimum mobile phase conditions were determined, linearity studies of Th⁴⁺ concentration *versus* integrated peak areas were done at three photometer sensitivity settings. A minimum of five concentrations of thorium was used to calculate the correlation coefficients at each sensitivity setting. In all cases, the correlation coefficients were greater than 0.99 for thorium concentrations between 1.0 and 50.0 µg/ml (Table II).

The lowest detectable concentration of thorium was determined by analyzing Th⁴⁺ solutions to the level at which Th⁴⁺ could no longer be discerned from the baseline. The lowest concentration detectable was 0.2 µg/ml at the 0.1 a.u.f.s. photometer setting.

Reproducibility of thorium quantitation was established by analyzing a 4.0 µg/ml Th⁴⁺ control solution for 12 days over a period of 3 weeks. Variables in the system during the time these data were collected included a column replacement and three eluent batch changes. For the twelve determinations, an average concentration of 4.06 mg/ml with an S.D. of 0.12 µg/ml and a relative standard deviation (R.S.D.) of 2.96% were calculated.

Analyses of 5 µg/ml solutions of thorium in increasing amounts of plutonium showed that interference of thorium quantitation by plutonium begins when the

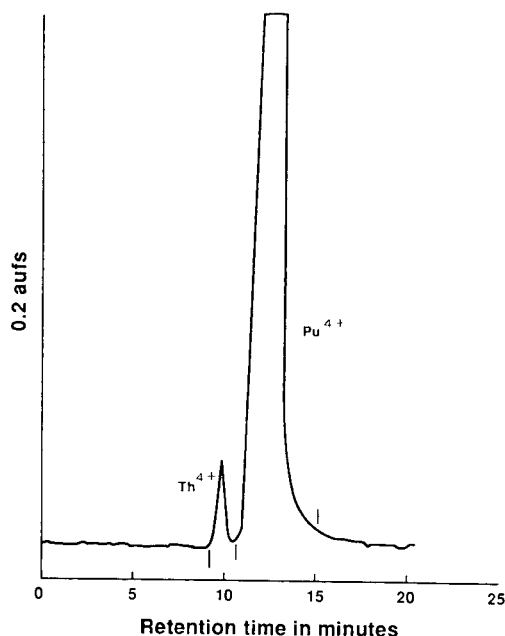


Fig. 1. Chromatogram of 5 $\mu\text{g/ml}$ Th^{4+} and 470 $\mu\text{g/ml}$ Pu^{4+} in 0.3 M HIBA in 0.2 M NH_4Cl , pH 4 with NH_4OH . Post-column reaction with $1.5 \cdot 10^{-4}$ M Arsenazo III; detection at 656 nm, 0.2 a.u.f.s.

plutonium concentration exceeds 500 $\mu\text{g/ml}$. At this point, the increasing base width of the plutonium peak begins to affect the base of the thorium peak (Fig. 1). Although appropriate integrator settings can correct this problem, analyses for thorium in greater than 500 $\mu\text{g/ml}$ plutonium should be done by using standards containing matching amounts of plutonium or by standard additions of thorium.

The efficiency of the column as measured by the height equivalent to a theoretical plate (HETP) of the thorium peak is not as high a might be expected, with values *ca.* 0.2 mm being the average HETP seen with the analytical conditions. We believe the reason for the relatively low efficiencies lies in several factors, which include the mass transfer rate of the complex onto the column, the labile nature of the adsorbed thorium complex arising from the dynamic equilibrium between the adsorbed species and the ligand in the mobile phase, and peak broadening arising from the apparatus necessary for post column derivatization. In spite of the relatively low column efficiency, the degree of resolution between thorium and plutonium is sufficient for high precision analysis.

An equilibration period of up to 2 days was needed for some concentrated solutions of plutonium which contained both Pu^{3+} and Pu^{4+} to allow time for oxidation from Pu^{3+} to Pu^{4+} . Chromatograms of fresh plutonium solutions made from a stock solution in 1% HNO_3 showed two peaks: a small, early peak eluting between 2 and 3 min and a much larger peak eluting after thorium. When the same solution was analyzed the next day, the early Pu^{3+} peak was diminished, whereas the later Pu^{4+} peak had increased proportionately (Fig. 2). Because the dilutions were made in the pH 4 eluent, it appears that it took some time for any Pu^{3+} to oxidize to

TABLE II
LINEARITY RESULTS

	0.1 a.u.f.s.	0.2 a.u.f.s.	0.5 a.u.f.s.
Range ($\mu\text{g/ml}$)	10–10.0	1.0–20.0	2.0–50.0
Correlation coefficient	0.9939	0.9988	0.9995

Pu^{4+} . In the presence of HIBA at pH 4, evidence of plutonium polymerization was not seen.

Studies of interferences by other metals were done using most of the Group IIIB–Group IVA metals at concentrations of $10 \mu\text{g/ml}$, and fourteen lanthanide metals at concentrations ranging from 2 to $50 \mu\text{g/ml}$. Interferences by the actinides, UO_2^{2+} , NpO_2^+ , Pu^{3+} , Pu^{4+} , and Am^{3+} were also studied (Fig. 3). Arsenazo III complexes were observed with Y^{3+} , Fe^{3+} , Pb^{2+} , the actinides and the lanthanides (Table III), though the detection sensitivity of lanthanides decreased with increasing atomic number (Fig. 4). All metals reacting with Arsenazo III eluted well before the Th^{4+} peak except Pu^{4+} and UO_2^{2+} , which eluted later.

The possibility of thorium hydrolysis and polymer formation was considered. The method for preparing the solutions for analysis was intended totally to preclude the formation of polymeric species. The solutions were prepared by acid dissolution of the metals, where the acid concentrations were at least 10%. An aliquot of this solution was added to the eluent solution, which contained 0.3 M HIBA. The formation

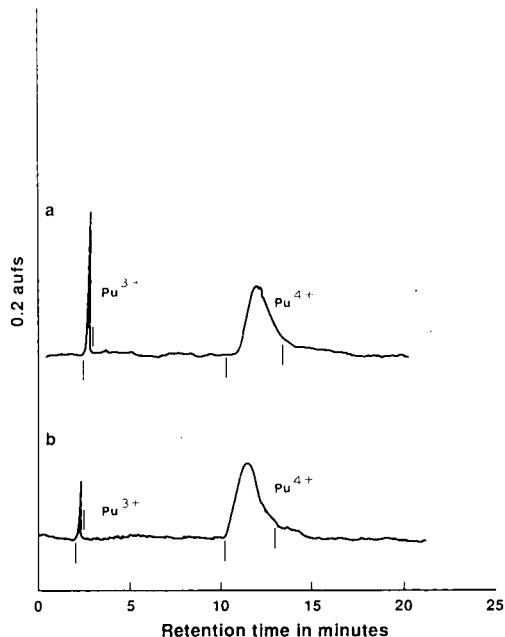


Fig. 2. (a) Chromatogram of $10 \mu\text{g/ml}$ plutonium in eluent; (b) chromatogram of same dilution analyzed the next day. Conditions as in Fig. 1.

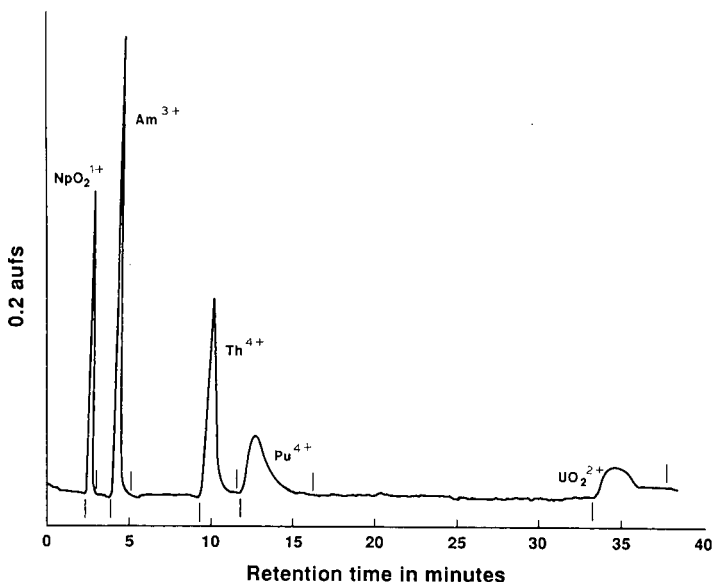


Fig. 3. Chromatogram of 6 $\mu\text{g/ml}$ NpO_2^+ , 5 $\mu\text{g/ml}$ Am^{3+} , 10 $\mu\text{g/ml}$ Th^{4+} , Pu^{4+} , and UO_2^{2+} in eluent. Conditions as in Fig. 1.

constants for the complexation reaction dominate the chemistry of the solution and completely block polymerization reactions of the thorium¹¹. It has been reported that in the pH range used for analysis, the formation of $\text{Th}(\text{OH})^{3+}$ ($\beta_1 = 2.98$) occurs slowly and that polymeric species are minor constituents¹². In the presence of HIBA ligand, which has a higher formation constant than hydroxide with Th^{4+} , ($\beta_1 =$

TABLE III
REACTIONS OF METALS ANALYZED IN REVERSED-PHASE SYSTEM

Rx: (-), no complex forming reaction with Arsenazo III; (+) complex forming reaction with Arsenazo III.

Metal	Rx	Metal	Rx	Metal	Rx
Sc^{3+}	-	In^{3+}	-	Nd^{3+}	+
Ti^{4+}	-	Sn^{4+}	-	Sm^{3+}	+
V^{5+}	-	Sb^{3+}	-	Eu^{3+}	+
Cr^{6+}	-	Hf^{4+}	-	Gd^{3+}	+
Mn^{2+}	-	Ta^{5+}	-	Tb^{3+}	+
Fe^{3+}	+	W^{6+}	-	Dy^{3+}	+
Zn^{2+}	-	Re^{7+}	-	Ho^{3+}	+
Ga^{3+}	-	Pt^{4+}	-	Er^{3+}	+
Ge^{4+}	-	Tl^{1+}	-	Tm^{3+}	+
Y^{3+}	+	Pb^{2+}	+	Yb^{3+}	+
Zr^{4+}	-	Bi^{3+}	-	Lu^{3+}	+
Nb^{5+}	-	Al^{3+}	-	Np^{5+}	+
Mo^{6+}	-	La^{3+}	+	Am^{3+}	+
Rh^{3+}	-	Ce^{3+}	+	U^{6+}	+
Pd^{2+}	-	Pr^{3+}	+	$\text{Pu}^{3+,4+}$	+
Ag^+	-				

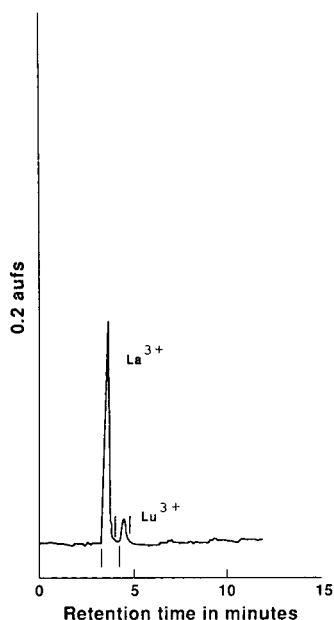


Fig. 4. Chromatogram of 2 $\mu\text{g/ml}$ La^{3+} and 50 $\mu\text{g/ml}$ Lu^{3+} in eluent. Conditions as Fig. 1.

4.43)¹¹, no polymerization occurs. Integrated areas from peaks from our reproducibility study remained constant over a 3-week period, which when considered with the pH of the stock solution and the probable thorium species present, precludes any significant loss of the thorium due to polymerization.

CONCLUSION

The data obtained from this HIBA reversed-phase separation system indicate that it is very useful for detecting thorium in plutonium because of its simplicity, sensitivity, and precision. Continued work may provide better understanding of the complexations and column interaction which occur, and may lead to improved routine separations of the actinides and lanthanides.

ACKNOWLEDGEMENTS

We thank Gordon Jarvinen for helpful discussions about HIBA metal complexes, and Nathana Haines for editing this manuscript.

REFERENCES

- 1 J. W. O'Laughlin, *J. Liq. Chromatogr.*, 7 (1984) 127–204.
- 2 B. R. Willeford and H. Veening, *J. Chromatogr.*, 251 (1982) 61–88.
- 3 G. Schwedt, *Chromatographia*, 12 (1979) 613–619.
- 4 C. A. Tollinche and T. H. Risby, *J. Chromatogr. Sci.*, 16 (1978) 448–454.
- 5 D. J. Barkley, M. Blanchette, R. M. Cassidy and S. Elchuk, *Anal. Chem.*, 58 (1986) 2222–2226.

- 6 R. Morales, C. S. Bartholdi and P. T. Cunningham, *Talanta*, 35 (1988) 461–464.
- 7 E. P. Horwitz, W. H. Delphin, C. A. A. Bloomquist and G. F. Vandegrift, *J. Chromatogr.*, 125 (1976) 203–218.
- 8 E. P. Horwitz and C. A. A. Bloomquist, *J. Inorg. Nucl. Chem.*, 35 (1973) 271–284.
- 9 C. H. Knight, R. M. Cassidy, B. M. Recoskie and L. W. Green, *Anal. Chem.*, 56 (1984) 474–478.
- 10 K. S. Bergstresser and M. E. Smith, *LA-1839*, Los Alamos Scientific Laboratory, Sept. 1954.
- 11 L. Magon, A. Bismondo, L. Maresca, G. Tomat and R. Portanova, *J. Inorg. Nucl. Chem.*, 35 (1973) 4237–4243.
- 12 P. L. Brown, J. Ellis and R. N. Sylva, *J. Chem. Soc., Dalton Trans.*, (1983) 31–34.

Note

Influence of the cellulose content of cellulose gels on the electrophoretic mobility

MIECZYSLAW WRÓŃSKI

Department of Chemical Technology and Environmental Protection, University of Łódź, Nowotki 18, Łódź (Poland)

(First received November 22nd, 1988; revised manuscript received January 24th, 1989)

It is generally accepted that the relationship between electrophoretic mobility, u , apparent charge, z , and molecular mass, M , may be represented by

$$u = azM^{-b} \quad (1)$$

where a and b are constants. Hais¹ found $b = 1$ for derivatives of hydroxycoumarin. From the mobilities of metal complexes and aromatic acids, Jokl² derived the equation

$$u = 14.7zM^{-\frac{1}{2}} - 0.29 \quad (2)$$

Offord³, on the basis of an extensive study of peptides, found $b = 2/3$. An investigation of electrophoretic mobilities on cellulose gel strips⁴ resulted in $b = 1/2$ for mercapto acids and 0.85 for trithiocarbonates. The experiments were always carried out in the presence of a standard, because only corrected or relative values of mobility can be introduced into the equation. On the other hand, the interaction between the support media and migrating substances was not taken into account.

In order to explain the contribution of the sieving effect and adsorption on cellulose gel, it is necessary to determine the electrophoretic mobility at different cellulose concentrations. The mobility in polyacrylamide gel is given by the well known Ferguson equation⁵:

$$\log u = \log u_0 - kc \quad (3)$$

where u_0 is the electrophoretic mobility at zero concentration, k the retardation coefficient and c the gel concentration. It has been found, however, that in cellulose gel the results better fit the equation

$$u = u_0/(1 + kr) \quad (4)$$

where r is the ratio of cellulose to water content and k is a constant that may be called the apparent partition coefficient.

EXPERIMENTAL

The preparation of cellulose gel strips was carried out as described previously⁶ using viscose at different dilutions. Samples of 100 g of viscose (11.6% cellulose content) were diluted one after the other with 5, 20, 50, 90, 150 and 200 ml of water containing 2, 4, 6, 8, 10 and 12 g of ethylenediamine, respectively. Sheets of glass-fibre paper were immersed in the viscose solution, pressed between two glass plates and set aside for 1 day. The strips thus obtained were washed with water, 3% (w/w) hydrochloric acid, 10% (w/w) sodium sulphite and 0.001 *M* Na₂EDTA and stored in 50% (v/v) ethylene glycol. Part of each viscose solution was placed in a test-tube and, after solidification, washed with water. The cellulose content was then determined by drying to constant weight at 105°C. The ratios of cellulose to water content (*r*) in the prepared strips were 0.175, 0.159, 0.135, 0.124, 0.105 and 0.080, respectively.

Buffer of pH 6.7 consisted of triethanolamine (20 g/l)–boric acid (40 g/l)–Na₂EDTA (2 g/l)–H₂EDTA (0.5 g/l)–ethylene glycol (50 ml/l). Buffer of pH 11.6 was prepared by equilibrating 200 ml of octane and 15 ml of triethylamine with 800 ml of 5% (v/v) ethylene glycol. Aqueous phase was used as a buffer and the organic phase as a cooling bath.

The electrophoresis was performed as described previously⁶ on vertical strips at 18°C and a voltage gradient of 40 V/cm. The electroosmotic flow was determined by means of ethylenethiourea, visualized with mercurated fluorescein⁴.

RESULTS AND DISCUSSION

According to eqn. 4 the reciprocal of mobility should bear a straight-line relationship to the ratio *r*:

$$\frac{1}{u} = \frac{1}{u_0} + \frac{kr}{u_0} \quad (5)$$

By plotting $1/u$ versus *r* it is possible to determine graphically, as demonstrated in Fig. 1, both u_0 and *k*. The values determined are summarized in Table I. The relationship between $\log(u_0/z)$ and $\log M$ is shown in Fig. 2.

The results indicate that the carboxylic acids (1–11, Table I) have reduced mobility compared with sulphonic acids (12–26). Comparison of the mobilities of 3-mercaptopropionic acid and 2-mercaptoethanosulphonic acid, methyl red and methyl orange and phenol red and phenolphthalein leads to the conclusion that the real charge of a sulphonic group must be higher than that of a carboxylic group in spite of their equal formal charges.

The best approximation relating the molecular mass to the mobility at zero cellulose concentration can be expressed for carboxylic acids by

$$u_0 = (330 \pm 10)zM^{-\frac{2}{3}} \quad (6)$$

and for sulphonic acids by

$$u_0 = (463 \pm 29)zM^{-\frac{2}{3}} \quad (7)$$

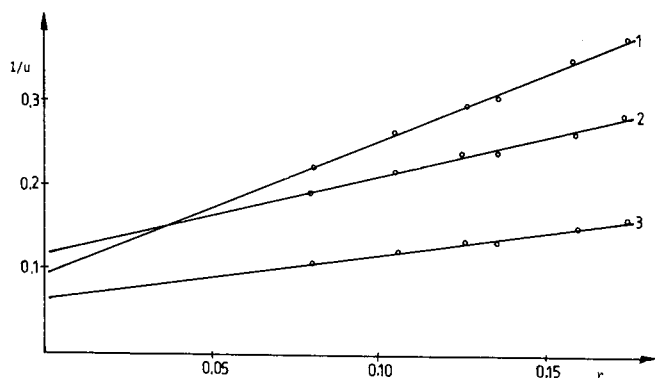


Fig. 1. Relationship between reciprocal values of electrophoretic mobility, kV min cm^{-2} , and the ratio r of cellulose to water content in cellulose gel. 1 = Methyl orange (pH 6.7); 2 = phenol red (pH 6.7); 3 = phenol red (pH 11.6).

TABLE I

ELECTROPHORETIC MOBILITY, u_0 ($\text{cm}^2 \text{min}^{-1} \text{kV}^{-1}$), AT ZERO GEL CONCENTRATION, APPARENT CHARGE, z , AND APPARENT PARTITION COEFFICIENT, k

No.	Ionic species	pH	z	u_0	k
1	3-Mercaptopropionic acid	6.7	1	16.0	4.3
2	Thiobenzoic acid	6.7	1	12.4	4.9
3	Thiomalic acid	6.7	2	20.8	5.5
4	Mercaptionicotinic acid	6.7	1	11.0	4.7
5	Thiosalicylic acid	6.7	1	11.8	5.0
6	Acetylcysteine	6.7	1	10.8	4.9
7	Captopril	6.7	1	9.8	6.5
8	Methyl red	11.6	1	7.1	7.9
9	Glutathione	6.7	1	7.5	6.2
10	Fluorescein	6.7	2	13.4	13.2
11	Phenolphthalein	11.6	2	12.5	6.0
12	2-Mercaptoethanesulphonic acid	6.7	1	18.0	6.3
13	Naphthionic acid	6.7	1	11.8	9.3
14	2-Hydroxynaphthionic acid	6.7	1	11.1	9.2
15	Methyl orange	11.6	1	11.2	19
16	Methyl orange	6.7	1	10.6	17
17	Alizarin red	6.7	2	20.0	16
18	7-Iodo-8-hydroxyquinoline-5-sulphonic acid	11.6	2	17.2	9.6
19	Phenol red	6.7	1	8.3	7.6
20	Phenol red	11.6	2	15.9	8.8
21	Chlorophenol red	11.6	2	15.4	11.0
22	Thymol blue	6.7	1	7.5	9.3
23	Thymol blue	11.6	2	13.2	10.0
24	Thorin	11.6	3	21.3	9.7
25	Bromothymol blue	11.6	2	15.4	12.3
26	Bromophenol blue	6.7	2	14.3	12.9

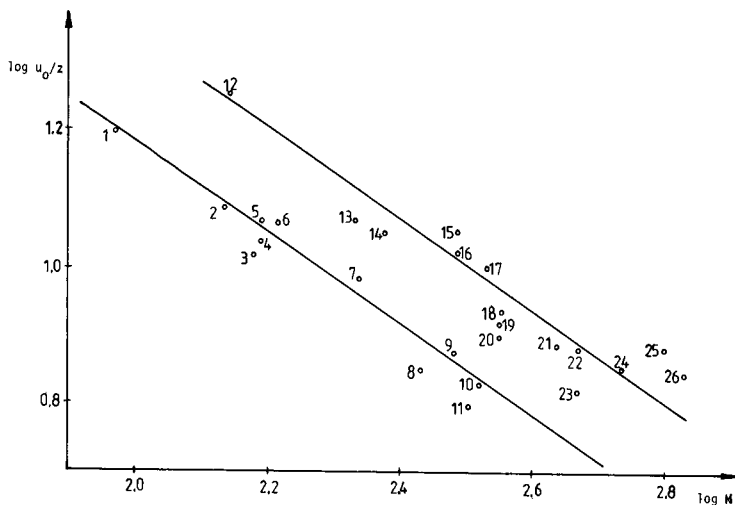


Fig. 2. Relationship between the logarithm of electrophoretic mobility, u_0 , at zero gel concentration divided by the apparent charge, z , and the logarithm of molecular weight, M . The numbers correspond to those in Table I.

The results are in general agreement with those presented by Offord³, who also found that the sulphonic group in cysteic acid enhances the mobility more than a carboxylic one.

The constant k in eqn. 4 represents the resistance resulting from interaction between the cellulose chains and a moving substance. It follows from Table I that the k values for sulphonic acids are higher than those for carboxylic acids.

Apart from a few compounds, such as fluorescein, methyl orange and methyl red, there is a distinct increase in k values with increasing molecular mass, indicating a sieving effect. For a reliable determination of molecular weight on basis of k values, it is obviously necessary to differentiate between a sieving effect and adsorption. An approach involving comparison of k and R_F values (Whatman 2 paper) was not satisfactory, with the exception of methyl orange, the high k value of which is in accordance with a low R_F value of 0.30. The other substances listed in Table I have R_F values between 0.6 and 0.98 but do not show any clear relationship with k values.

Let us now consider the influence of cellulose content on electrophoretic resolution expressed by difference in mobilities:

$$u_2 - u_1 = \frac{u_{02}}{1 + k_2 r} - \frac{u_{01}}{1 + k_1 r} \quad (8)$$

The resolution is equal to zero when $u_2 = u_1$, and then $r = r_0$:

$$r_0 = \frac{u_{02} - u_{01}}{k_2 u_{01} - k_1 u_{02}} \quad (9)$$

For example, the point of intersection of the mobilities of methyl orange and phenol red at pH 6.7 is 0.038.

The function $u_2 - u_1 = f(r)$ passes the maximum at $r = r_{\max}$:

$$r_{\max} = \frac{(k_2 u_{02})^{0.5} - (k_1 u_{01})^{0.5}}{k_2 (k_1 u_{01})^{0.5} - k_1 (k_2 u_{02})^{0.5}} \quad (10)$$

For example, for methyl orange and phenol red $r_{\max} = 0.17$ and for captopril and acetylcysteine $r_{\max} = 0.087$.

REFERENCES

- 1 I. M. Hais, *Chem. Listy*, 49 (1955) 709.
- 2 V. Jokl, *J. Chromatogr.*, 13 (1964) 451.
- 3 R. E. Offord, *Nature (London)*, 211 (1966) 591.
- 4 M. Wroński, *J. Chromatogr.*, 288 (1984) 206.
- 5 K. A. Ferguson, *Metabolism*, 13 (1964) 985.
- 6 M. Wroński, *J. Chromatogr.*, 261 (1983) 127.

Note

Chromatographic studies of metal complexes

V. Thin-layer chromatography of some octahedral cobalt(III) and nickel(II) complexes

R. K. RAY*

Department of Chemistry, Rama Krishna Mission Vivekananda Centenary College, Rahara-743186,
24-Parganas (North), West Bengal (India)

MADHAB K. BANDYOPADHYAY

Department of Physics, Rama Krishna Mission Vivekananda Centenary College, Rahara-743186,
24-Parganas (North), West Bengal (India)

and

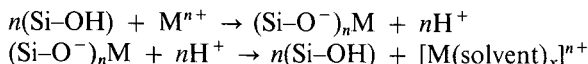
GEORGE B. KAUFFMAN

Department of Chemistry, California State University, Fresno, CA 93740 (U.S.A.)

(First received March 14th, 1988; revised manuscript received January 21st, 1989)

A number of studies have been made of the adsorption of complex cations on silica gel¹, and considerable evidence has accumulated that silica gel behaves as a weak cation-exchange resin². The surface of silica gel consists of silanol (Si-OH) sites on which hydrogen atoms may be exchanged for cations in a reasonably predictable manner³. Dugger *et al.*⁴ have tabulated entropy, enthalpy and free-energy change values for the exchange reaction between the metal ions and the hydrogen atoms of the silanol group of the silica gel. The mechanism of the separation of different metal cations on silica gel may therefore be considered to occur according to the following steps:

- (1) adsorption of metal cations on Si-OH groups;
- (2) desorption of metal cations by acids or by salts⁵⁻⁸;
- (3) migration of metal cations due to solvation⁹:



Strong binding is thus observed between the metal cation (M^{n+}) and the silanol anion (Si-O^-) of the silica gel, which resists the movement of the metal cation through the silica gel. Therefore, any explanation for the movement of a given cation should be sought in the electrical and other properties (*e.g.*, surface tension¹⁰, viscosity¹⁰, and dielectric constant¹⁰⁻¹²) of the solvent used to cause the cationic species to migrate through the anionic silica gel. Other workers¹⁰⁻¹² have attempted to correlate the movement of cationic complexes in terms of R_F values with surface tension, viscosity

or dielectric constant considered individually. Interestingly, a linear relationship exists between the R_F values of cations and the dielectric constant/viscosity ratio for organic solvents.

In this paper we show that the movement of complex cations is dependent on the joint effect of the surface tension of the developer and the anionic conductance of the electrolytes present in different developers.

EXPERIMENTAL

Materials

The complex compounds were prepared according to published procedures¹³⁻¹⁶. Their purity was established by conventional chemical analysis and spectral measurements.

Procedures

Merck silica gel G was slurred with distilled water (2 parts of water to 1 part of adsorbent) and spread on 0.25-mm thick glass thin-layer chromatographic (TLC) plates. The plates were dried in air, heated at 105–110°C for 1 h and stored in a desiccator as recommended by Stahl¹⁷. As R_F values depend on the thickness of the adsorbent, we tried to maintain a thickness of 0.25 mm for the silica gel throughout this investigation. Chromatographic chambers were saturated with developer solvents for 2 days. Each complex was dissolved in water and the solution was spotted at a starting point 5 cm above the lower edge of the plate. The developer was allowed to travel 13–14 cm from the point of application. R_F values were reproducible to within ± 0.02 unit.

Aqueous solutions of NaCl, NaBr, NaI, NaNO₂, NaNO₃, Na₂SO₄ and Na₂S₂O₃ were used as developer solvents. Developer concentrations of 0.2 and 0.1 M were used for the separation of cobalt(III) and nickel(II) complexes, respectively. Sodium sulphide solution was used as a spray reagent to detect the cobalt(III) complexes (the spots turned black) and an ethanolic solution of dithiooxamide (rubeanic acid) for the nickel(II) complexes (the spots turned blue).

RESULTS AND DISCUSSION

On the basis of electrophoresis, Mazzei and Lederer¹⁸ measured the mobilities of [Co(NH₃)₆]³⁺, [Co(en)₃]³⁺, [Co(dip)₃]³⁺ and [Co(*o*-phen)₃]³⁺ ions (en = ethylenediamine; dip = dipyriddy; *o*-phen = *o*-phenanthroline) in several types of salt solutions and found a marked effect of ion association on the mobility of the complexes. They did not give a detailed discussion of the mechanism of association. In TLC studies, however, Lederer and Battilotti¹⁹ employed the same cobalt(III) complexes used in the electrophoresis studies but different stationary phases (alumina, silica gel and cellulose-sulphonate) and various concentrations of electrolyte developers. They concluded that not only do the eluent anions form ion pairs with cobalt(III) complexes, but also ion-pair formation occurs between the stationary phase material (silica gel) and the developer electrolyte. Further, Lederer and Polcaro²⁰ studied the behaviour of inorganic anions on alumina and demonstrated that strong adsorption is due not to an ion-exchange process but to ion-pair formation, which favours the separation.

TLC and filter-paper chromatography have also shown that as the concentra-

TABLE I

VALUES OF ANIONIC CONDUCTANCE AND SURFACE TENSION FOR SODIUM SALT SOLUTIONS AT 25°C AND R_F VALUES AT 25°C FOR $[\text{Ni}(\text{en})_3]^{2+}$, $[\text{Co}(\text{NH}_3)_6]^{3+}$, $[\text{Co}(\text{bigH})_3]^{3+}$ AND $[\text{Co}(\text{en})_3]^{3+}$

Values of anionic conductance were calculated by subtracting the ionic conductance of Na^+ from the equivalent conductance of the corresponding sodium salts.

Developer ^a	A_i	$S - S_w^b$	$\frac{S - S_w}{A_i}$	R_F			
				$[\text{Ni}(\text{en})_3]^{2+}$	$[\text{Co}(\text{NH}_3)_6]^{3+}$	$[\text{Co}(\text{bigH})_3]^{3+}$	$[\text{Co}(\text{en})_3]^{3+}$
I^-	67.9	0.1	0.0015	0.21			
Br^-	68.0	0.14	0.0020	0.23			
Cl^-	65.6	0.17	0.0025	0.30			
NO_3^-	57.0	0.12	0.0021	0.24			
NO_2^-	54.0	0.112	0.0021	0.24			
$\text{S}_2\text{O}_3^{2-}$	121.0	0.40	0.0033	0.41			
SO_4^{2-}	49.0	0.27	0.0055	0.62			
I^-	66.45	0.20	0.0030		0.30	0.30	0.26
Br^-	65.55	0.26	0.0039		0.38	0.33	0.31
Cl^-	63.05	0.34	0.0054		0.46	0.42	0.39
NO_3^-	53.55	0.24	0.0045		0.40	0.38	0.34
NO_2^-	56.55	0.20	0.0035		0.34	0.32	0.29
$\text{S}_2\text{O}_3^{2-}$	110	0.70	0.0064		0.53	0.50	0.57
SO_4^{2-}	43.05	0.54	0.0125		0.85	0.80	0.78

^a Developer concentrations were 0.1 and 0.2 M for $[\text{Ni}(\text{en})_3]^{2+}$ and cobalt(III) complexes, respectively.

^b S = Surface tension of the electrolyte solution; S_w = surface tension of pure water. Values were obtained from International Critical Tables²⁸.

tion of the electrolyte in a given developer increases, the R_F value of a particular complex cation also increases^{21,22}. With an increase in concentration of a given developer electrolyte, the anionic conductance of the developer solution decreases. As TLC involves electrostatic processes, some relationship between the anionic conductance of electrolyte developers and the mobility of a given complex cation may exist^a. In TLC and paper chromatography, the mobility of the complexes is shown by their R_F values. In fact, a direct connection between R_F values of the complex cation and the joint effect of the anionic conductance of the electrolyte and the surface tension of the developer solvent is observed (see Table I).

In order to minimize any further chemical reaction that might occur between the complex cation and the developer electrolyte^{22,23} or between the complex cation and the stationary phase^{3,5,23,24}, we used only octahedral complexes. Any change in R_F values may then be attributed to the differences in the equivalent conductance of the developer solution. However, the change in R_F values in different electrolyte developers of the same concentration does not seem to bear any simple relationship to the anionic conductance. However, in most instances, the R_F values decrease with an increase in conductance (see Table I).

The most striking exception is with $\text{Na}_2\text{S}_2\text{O}_3$ as developer. The equivalent

^a Some workers prefer the direct use of salt activity as a measure of the interaction of the anions present in the developer solvent with the cations adsorbed on the chromatographic support. However, anionic conductance may be used at least as an indirect measure of such an interaction.

conductance of 0.1 M $\text{Na}_2\text{S}_2\text{O}_3$ is almost double that of 0.1 M NaI , so the R_F value of a given complex should have been much less in the former developer. However, the experimental results reveal the reverse order. It may be pointed out that the surface tension of $\text{Na}_2\text{S}_2\text{O}_3$ solutions (expressed as the excess over the surface tension of pure water) is much greater than that of NaI solutions at the same concentrations.

Surface tension facilitates the migration of the complex cation. Hence the greater the surface tension of the developer, the higher will be the R_F value. However, once again, no simple relationship exists between R_F values and surface tension.

Although an increase in the surface tension of the developer solvent generally causes an increase in R_F values, this is not strictly followed, as revealed by considering the R_F values of a given complex in the Na_2SO_3 and $\text{Na}_2\text{S}_2\text{O}_3$ systems. The surface tension (expressed as the excess over that of pure water) of $\text{Na}_2\text{S}_2\text{O}_3$ solution is much higher than that of Na_2SO_4 solution of the same concentration, but every complex exhibited lower R_F values in $\text{Na}_2\text{S}_2\text{O}_3$ than in Na_2SO_4 developer.

Therefore, the different R_F values of a given complex cation in different electrolytes should be attributed to the joint effect of the surface tension ($S - S_w$, where S is the surface tension of the electrolyte solution and S_w is that of pure water) and the anionic conductance (A_i) of the developer ion. This hypothesis is supported by the fact that the $[\text{Ni}(\text{en})_3]^{2+}$ ion shows the same R_F value in NaNO_2 and NaNO_3 developers, which, incidentally, also have the same $(S - S_w)/A_i$ values as well. Therefore, the variation in R_F values with $(S - S_w)/A_i$ is linear, at least for the $[\text{Co}(\text{en})_3]^{3+}$, $[\text{Co}(\text{NH}_3)_6]^{3+}$, $[\text{Co}(\text{bigH})_3]^{3+}$ and $[\text{Ni}(\text{en})_3]^{2+}$ systems (bigH = biguanide) (see Figs. 1-4).

R_F values of the same octahedral complexes were also measured with several potassium salts (KCl , KBr , KI , KNO_3 , KNO_2 , and K_2SO_4) as eluents in order to observe whether changing the cation of the developer electrolyte affects this linear relationship. We found that the R_F values change only slightly (Table II) from the values obtained with the corresponding sodium salts as eluents (Table I). At any rate,

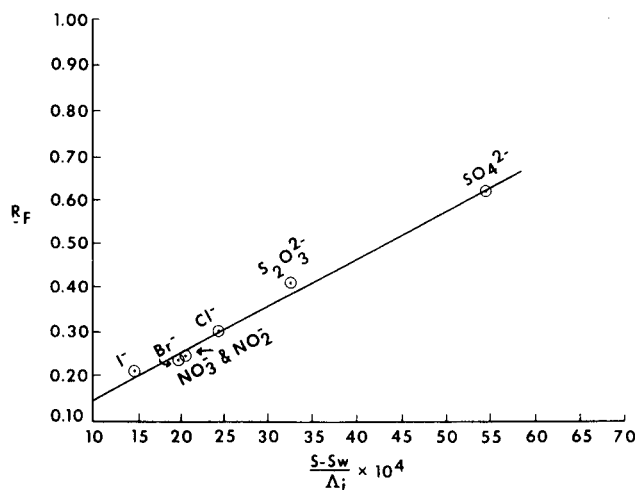


Fig. 1. Variation of R_F for $[\text{Ni}(\text{en})_3]^{2+}$ with $(S - S_w)/A_i$ values for different electrolyte solutions.

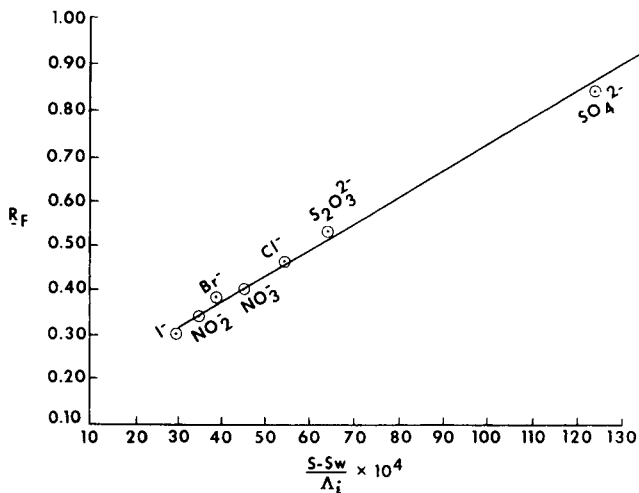


Fig. 2. Variation of R_F for $[Co(NH_3)_6]^{3+}$ with $(S-S_w)/A_i$ values for different electrolyte solutions.

the linear relationship between R_F and $(S-S_w)/A_i$ was also found with potassium salts as eluents.

Jenkins and Monk²⁵ and later De and Dutta²⁶ reported that the ion-associated constants of some cationic cobalt(III) complexes with halides and sulphate ions decrease with increase in the equivalent conductance of the complex salts. They also evaluated the ion-association constants of $[Co(en)_3]^{3+}$ and $[Co(bigH)_3]^{3+}$ with halides and sulphate ions and observed the order²⁵⁻²⁷ $I^- < Br^- < Cl^- < SO_4^{2-}$. The movement of a cationic complex on a silica gel bed may be attributed to ion-pair formation between the complex cation and the anion of the electrolyte present in the developer, so that the overall effective charge of the complex cation is considerably reduced^{19,21,24}.

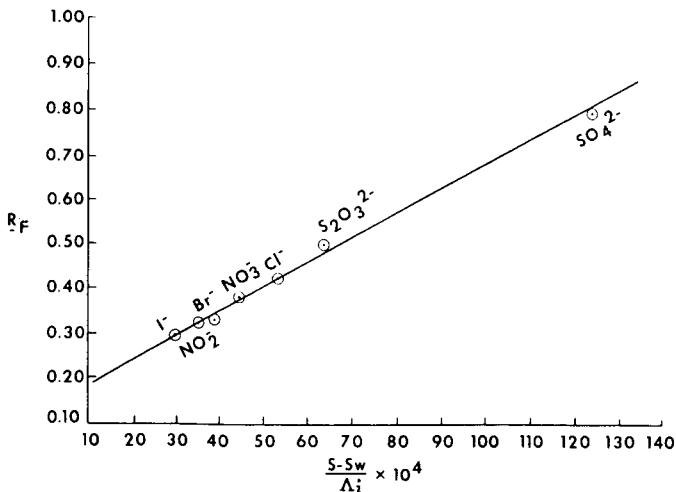


Fig. 3. Variation of R_F for $[Co(bigH)_3]^{3+}$ with $(S-S_w)/A_i$ values for different electrolyte solutions.

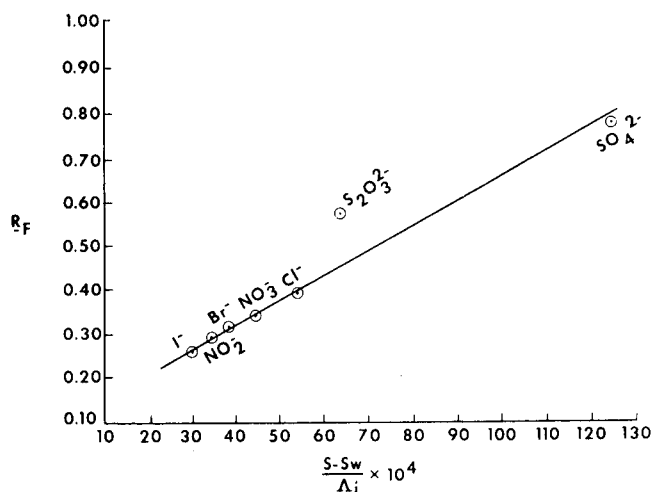
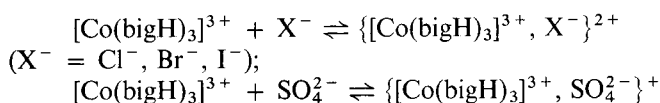


Fig. 4. Variation of R_F for $[\text{Co}(\text{en})_3]^{3+}$ with $(S - S_w)/A_i$ values for different electrolyte solutions.



As the increase in equivalent conductance of the developer solution reduces the ion-pair formation between the complex cation and the anion²⁵⁻²⁷, R_F values should decrease with increase in equivalent conductance. This investigation supports this view if proper account is taken of the effect of surface tension.

TABLE II

VALUES OF ANIONIC CONDUCTANCE AND SURFACE TENSION FOR POTASSIUM SALT SOLUTIONS AT 25°C AND R_F VALUES AT 25°C FOR $[\text{Ni}(\text{en})_3]^{2+}$, $[\text{Co}(\text{NH}_3)_6]^{3+}$, $[\text{Co}(\text{bigH})_3]^{3+}$ AND $[\text{Co}(\text{en})_3]^{3+}$

Values of anionic conductance calculated by subtracting the ionic conductance of K^+ from the equivalent conductance of the corresponding potassium salts.

Developer ^a	A_i	$S - S_w^b$	$\frac{S - S_w}{A_i}$	R_F			
				$[\text{Ni}(\text{en})_3]^{2+}$	$[\text{Co}(\text{NH}_3)_6]^{3+}$	$[\text{Co}(\text{bigH})_3]^{3+}$	$[\text{Co}(\text{en})_3]^{3+}$
I^-	63.3	0.168	0.0026	0.26	0.34	0.33	0.31
Br^-	64	0.270	0.0042	0.30	0.42	0.39	0.36
Cl^-	60.9	0.301	0.0049	0.36	0.47	0.44	0.43
NO_2^-	50.2	0.22	0.0044	0.34	0.44	0.41	0.38
NO_3^-	53.0	0.21	0.0040	0.31	0.40	0.39	0.37
SO_4^{2-}	48.2	0.51	0.0106	0.67	0.81	0.79	0.80

^a Developer concentrations were 0.2 M for all complexes.

^b S = Surface tension of the electrolyte solution; S_w = surface tension of pure water. Values were obtained from International Critical Tables²⁸.

ACKNOWLEDGEMENTS

We are indebted to Dr. Dwijesh Majumdar, Department of Physics, Rama Krishna Mission Vivekananda Centenary College, Rahara, for his keen interest in this work. We are also indebted to the referee for valuable suggestions for the improvement of this paper.

REFERENCES

- 1 L. H. Reyerson and R. E. Clark, *J. Phys. Chem.*, 40 (1936) 1055.
- 2 F. Helfferich, *Ion Exchange*, McGraw-Hill, New York, 1962.
- 3 R. L. Burwell, Jr., R. G. Pearson, G. L. Haller, P. B. Tjok and S. P. Chock, *Inorg. Chem.*, 4 (1965) 1123.
- 4 D. L. Dugger, J. H. Stanton, B. N. Irby, B. L. McConnell, W. W. Cummings and P. W. Maatman, *J. Phys. Chem.*, 68 (1964) 757.
- 5 R. L. Dutta, R. K. Ray and G. B. Kauffman, *Coord. Chem. Rev.*, 28 (1979) 23.
- 6 M. Lederer, *J. Chromatogr.*, 6 (1961) 437, 518.
- 7 L. Ossicini and M. Lederer, *J. Chromatogr.*, 17 (1965) 387.
- 8 H. M. Irving, *Q. Rev. Chem. Soc.*, 5 (1951) 200.
- 9 W. C. Brown, *Nature (London)*, 143 (1939) 377.
- 10 A. Paul and P. B. Janardhan, *Bull. Chem. Soc. Jpn.*, 40 (1967) 1131.
- 11 A. M. Ghe and A. Placucci, *Ann. Chim. (Rome)*, 49 (1959) 1769.
- 12 M. Qureshi and M. A. Khan, *Talanta*, 13 (1966) 117.
- 13 P. Rây, *Chem. Rev.*, 61 (1961) 313.
- 14 W. G. Palmer, *Experimental Inorganic Chemistry*, Cambridge University Press, Cambridge, 1959, p. 530.
- 15 J. B. Work, *Inorg. Synth.*, 2 (1946) 221.
- 16 H. M. State, *Inorg. Synth.*, 6 (1960) 200.
- 17 E. Stahl, *Thin Layer Chromatography: A Laboratory Handbook*, George Allen and Unwin, London, 2nd ed., 1969.
- 18 M. Mazzei and M. Lederer, *J. Chromatogr.*, 31 (1967) 196.
- 19 M. Lederer and M. Battilotti, *J. Chromatogr.*, 89 (1974) 380.
- 20 M. Lederer and C. Polcaro, *J. Chromatogr.*, 84 (1973) 379.
- 21 R. K. Ray and G. B. Kauffman, *J. Chromatogr.*, 442 (1988) 381.
- 22 R. L. Dutta and R. K. Ray, *J. Indian Chem. Soc.*, 51 (1974) 187.
- 23 R. K. Ray, *Analyst (London)*, submitted for publication.
- 24 T. Baba and H. Yoneda, *Bull. Chem. Soc. Jpn.*, 43 (1970) 2478.
- 25 I. L. Jenkins and C. B. Monk, *J. Chem. Soc.*, (1951) 68.
- 26 M. K. De and R. L. Dutta, *J. Indian Chem. Soc.*, 52 (1975) 67.
- 27 F. Basolo and R. G. Pearson, *Mechanisms of Inorganic Reactions*, Wiley, New York, 2nd ed., 1967, p. 37.
- 28 E. W. Washburn (Editor), *International Critical Tables of Numerical Data: Physics, Chemistry and Technology*, Vols. III-VII, McGraw-Hill, New York, London, 1928, 1929, 1930.

Note

Use of absorbance ratios in densitometric measurements for the characterization and identification of natural products of pharmacological interest

M. I. WALASH^a and O. M. SALAMA^{*b}

Faculty of Pharmacy, Mansoura University, Mansoura (Egypt)

and

M. M. BISHR

Islamic Centre for Medical Sciences, Ministry of Public Health, P.O. Box 5, Saffat 13001 (Kuwait)

(Received December 27th, 1988)

Developments in densitometric measurement techniques have greatly enhanced their value in the analysis of natural products such as alkaloids^{1,2}, coumarins^{3,4}, saponins⁵ and iridoids⁵. The improvements in detector systems (*e.g.*, multi-wavelength ultraviolet detectors) allow the unequivocal identification of various components.

This paper addresses the feasibility of the rapid and reliable identification of some common natural products by their characteristic R_F values, absorbance ratios and constants obtained by the use of a densitometer.

EXPERIMENTAL

Apparatus

A Shimadzu (Kyoto, Japan) CS-930 thin-layer chromatographic (TLC) scanning photodensitometer of high sensitivity and precision was used. Precoated silica gel G glass TLC plates were obtained from E. Merck (Darmstadt, F.R.G.).

Materials

Pharmaceutical-grade compounds (Table I) were checked according to different Pharmacopoeias^{5–10}. Solutions in methanol or chloroform (1 mg/ml) were prepared and were stable at 20°C for at least 2 months.

The following developing systems were used: ethyl acetate–methanol–water (100:13.5:10), toluene–ethyl acetate (93:7), chloroform–diethylamine (90:10), ethanol–acetic acid–water (60:30:10), methanol–ammonia solution (100:1.5), ethyl acetate–formic acid–acetic acid–water (100:11:11:27) and toluene–ethyl acetate–diethylamine (70:20:10).

^a Present address: Criminal Laboratory, Ministry of Interior, Kuwait, Kuwait.

^b Present address: Department of Phytochemistry, Islamic Centre for Medical Sciences, Ministry of Public Health, P.O. Box 5, Saffat 13001, Kuwait.

Procedure

Compounds representing different chemical classes were selected. Sample solutions contained 1 mg/ml of solute in methanol or chloroform. The sample size varied from 0.5 to 5 μ l, depending on the compound.

The sample solutions were spotted side-by-side on the origin. The plates were developed for a distance of 15 cm using the developing systems listed in Table III. The absorbances of all compounds were recorded at 220 and 254 nm and the absorbance ratios (K_1) were calculated. The compounds may be identified primarily by their K_1 values (Table I), then from measurements at the wavelength of maximum absorption for each compound the K_2 ratio were determined (Table II) to confirm the compound identities. Each compound was chromatographed as six separate spots on one plate in order to verify the reproducibility and precision.

RESULTS AND DISCUSSION

Traditionally, the identification and quantification of a solute separated by TLC and monitored with a UV detector at a single wavelength are based on the R_F values¹¹. However, if a solute is monitored at several wavelengths, the absorbances can be very different and reflect the UV-absorbing characteristics of the compound. Table III illustrates the results obtained by such a procedure after chromatographic development.

By selecting one of the wavelengths as a reference, absorbance ratios can be calculated. For colchicine, for instance 220 nm is selected as a reference wavelength. The calculated absorbance ratios will be the areas under the peaks at 254 and 220 nm (K_1) and 243 and 220 nm (K_2).

TABLE I

DATA OBTAINED BY CALCULATION FROM DENSITOMETRIC MEASUREMENT AND ARRANGED IN INCREASING ORDER OF (K_1) VALUES

K_1 = absorbance ratio, 254/220 nm (areas under the peaks).

Compound	K_1	Compound	K_1
Pilocarpine	0.028	Theobromine	1.32
Cinchonine	0.11	Theophylline	1.35
Cinchonidine	0.13	Harmaline	1.58
Yohimbine	0.30	Caffeic acid	1.60
Quinine	0.35	Quercetin	1.78
Eugenol	0.35	Berberine	1.81
Emetine	0.36	Psoralin	1.85
Codeine	0.37	Colchicine	1.95
Quinidine	0.38	Chlorogenic acid	1.95
Morphine	0.49	Anisaldehyde	2.41
Thymol	0.66	Papaverine	2.61
Heroin	0.71	Strychnine	2.93
Caffeine	0.99	Eserine	3.30
Methyl salicylate	0.99	Harmine	3.67
Brucine	1.01	α -Santonin	4.94
Vanillin	1.16		

TABLE II

DATA OBTAINED BY CALCULATION FROM DENSITOMETRIC MEASUREMENTS AND ARRANGED IN INCREASING ORDER OF K_2 VALUES

K_2 = absorbance ratio, $\lambda_{\max.}/220$ nm.

Compound	$\lambda_{\max.}$ ^a (nm)	K_2	Compound	$\lambda_{\max.}$ (nm)	K_2
Morphine	288	0.35	Colchicine	243	2.25
Cinchonine	303	0.41	Methyl salicylate	312	2.40
Codeine	290	0.41	Berberine	275	2.87
Cinchonidine	303	0.48	Caffeine	272	3.01
Heroin	282	0.85	Strychnine	262	3.04
Yohimbine	282	0.86	Quercetin	270	3.10
Thymol	278	1.08	Papaverine	247	3.50
Eugenol	283	1.08	Theophylline	273	3.76
Emetine	287	1.16	Theobromine	277	3.94
Quinine	238	1.17	Harmine	325	4.45
Psoralin	335	1.55	Caffeic acid	327	4.60
Quinidine	238	1.58	Anisaldehyde	297	5.50
Eserine	315	1.60	Chlorogenic acid	325	6.31
Harmaline	263	1.61	Pilocarpine ^b	—	—
Brucine	270	1.70	α -Santonin ^b	—	—
Vanillin	330	2.15			

^a $\lambda_{\max.}$ was measured directly *in situ* with the TLC scanner.

^b Compounds with no maxima other than 254 nm.

Under controlled conditions, the UV absorption spectrum is characteristic for a specific compound, and hence the absorbance ratios derived from it also characterize the compound. These absorbance ratios can be used in conjunction with R_F data to identify the compound (Table III).

It has also been found that the two absorbance ratios (*i.e.*, monitoring at three wavelengths) gave adequate information to discriminate and identify the compounds examined, even those displaying very similar absorbance profiles, *e.g.*, purine bases (caffeine, theophylline, theobromine), phenanthrene alkaloids (morphine, codeine) and quinoline alkaloids (quinine, quinidine, cinchonine, cinchonidine) (Tables 1–3).

For selective and final identification of a compound, a wavelength of maximum absorption should be used (Table II). Classification of the compounds tested into five groups according to the first absorbance ratio K_1 (254/220 nm) (Table I), *e.g.*, (A) 0–0.13, (B) 0.30–0.49, (C) 0.66–1.00, (D) 1.00–1.96 and (E) 2.00 and above, will give the primary identification of groups. The second measurement at $\lambda_{\max.}$ and calculation of the second ratio K_2 ($\lambda_{\max.}/220$ nm) (Table II) will give the complete identification of the compound tested.

Another classification of the compounds into groups can be done according to the K_2 values by arranging them in increasing order. However, we prefer to start with K_1 as it represents a general and primary measurement at two fixed wavelengths (220 and 254 nm) whereas K_2 involves different wavelengths according to the compound tested.

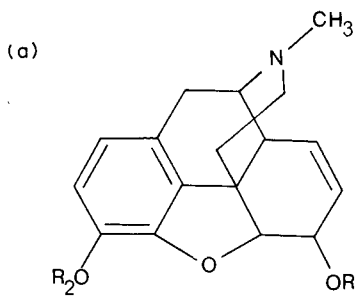
The composition of the solvent systems was varied to achieve optimum

TABLE III

DATA OBTAINED BY CALCULATION FROM DENSITOMETRIC MEASUREMENT AND CLASSIFIED ACCORDING TO DEVELOPING SOLVENT

Compound	K_1	K_2	A^a	R_F	B^b	M.W.	C^c
<i>Group I: developing solvent ethyl acetate-methanol-water (100:13.5:10)¹²</i>							
Caffeine	0.99	3.01	2.98	0.46	15.43	194	89.2
Theobromine	1.32	3.96	5.23	0.36	6.88	180	64.8
Theophylline	1.35	3.76	5.07	0.53	10.45	180	95.4
Colchicine	1.95	2.25	4.38	0.29	6.60	399	115.7
<i>Group II: developing solvent toluene-ethyl acetate (93:7)¹²</i>							
Eugenol	0.35	1.08	0.37	0.47	127	164	77.0
Thymol	0.66	1.08	0.71	0.52	73.2	150	78.0
Anisaldehyde	2.41	5.50	13.25	0.10	0.7	136	13.6
Methyl salicylate	0.99	2.40	2.37	0.82	34.6	152	124.6
Vanillin	1.16	2.15	2.49	0.25	10.0	152	38.0
Psoralen	1.85	1.55	2.86	0.30	10.5	186	55.8
α -Santonin	4.94	—	—	0.10	—	246	24.6
<i>Group III: developing solvent chloroform-diethylamine (90:10)¹²</i>							
Quinine	0.35	1.17	0.40	0.14	35.0	324	45.3
Quinidine	0.38	1.58	0.60	0.30	50.0	324	97.2
Cinchonine	0.11	0.41	0.04	0.38	950.0	294	111.7
Cinchonidine	0.13	0.48	0.06	0.24	400.0	294	70.5
<i>Group IV: developing solvent ethanol-acetic acid-water (60:30:10)¹³</i>							
Morphine ^d	0.49	0.35	0.17	0.27	158.8	303	81.81
Codeine ^d	0.37	0.41	0.15	0.40	266.6	317	126.80
Heroin ^e	0.71	0.85	0.60	0.35	58.3	423	253.80
<i>Group V: developing solvent methanol-ammonia solution (100:1.5)¹³</i>							
Harmaline	1.58	1.61	2.54	0.38	14.9	214	81.3
Harmine	3.67	4.45	16.33	0.68	4.2	212	144.1
<i>Group VI: developing solvent ethyl acetate-formic acid-acetic acid-water (100:11:11:27)¹²</i>							
3-hlorogenic acid	1.96	6.30	12.35	0.45	3.6	354	159.3
Caffeic acid	1.60	4.60	7.36	0.96	13.0	180	172.8
Quercetin	1.78	3.10	5.51	0.97	17.0	302	292.9
<i>Group VII: developing solvent toluene-ethyl acetate-diethylamine (70:20:10)¹²</i>							
Pilocarpine	0.028	—	—	0.10	—	208	20.8
Brucine ^e	1.01	1.70	1.71	0.23	13.5	466	107.1
Strychnine ^e	2.93	3.04	8.90	0.37	4.2	306	150.2
Yohimbine	0.30	0.86	0.26	0.49	188.5	354	92.0
Eserine	3.30	1.60	5.28	0.56	10.6	275	154.0
Emetine	0.36	1.16	0.41	0.56	136.5	480	268.8
Papaverine	2.61	3.50	9.13	0.62	6.8	339	210.1
Berberine	1.81	2.87	5.19	0.46	8.9	336	154.5

^a $A = K_1 K_2$.^b $B = hR_F/A$.^c $C = MW \times R_F$.^d Base monohydrate.^e Hydrochloride salt.

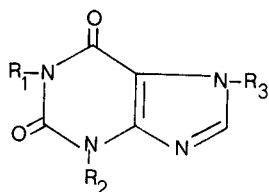


$R_1 = R_2 = H$ Morphine

$R_1 = H, R_2 = CH_3$ Codeine

$R_1 = R_2 = COCH_3$ Heroin

(b)

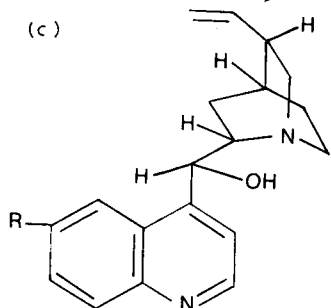


$R_1 = R_2 = R_3 = CH_3$ Caffeine

$R_1 = R_2 = CH_3, R_3 = H$ Theophylline

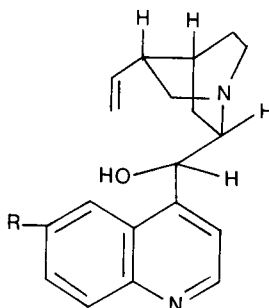
$R_1 = H, R_2 = R_3 = CH_3$ Theobromine

(c)



$R = OCH_3$ (-)-Quinine

$R = H$ (-)-Cinchonidine



$R = H$ (+)-Cinchonine

$R = OCH_3$ (+)-Quinidine

Fig. 1. Structures of compounds. (a) Phenanthrene alkaloids; (b) xanthine alkaloids; and (c) quinoline alkaloids.

chromatographic conditions. The compounds tested were detected and identified at a concentration of $0.5 \mu\text{g}/\mu\text{l}$ in methanol or chloroform solutions.

We tried to correlate the results obtained with the structures, and reached some interesting conclusions.

(a) Within the same group of structurally related compounds, *e.g.*, morphine, codeine and heroin^a (Fig. 1a), there is a difference in K_1 values. The presence of a methyl group in codeine reduces its K_1 value, whereas the diacetyl group in heroin increases its K_1 value. The K_2 and C values increase in the order given.

(b) For caffeine, theobromine and theophylline (Fig. 1b), there is an increase in K_1 (0.99, 1.32 and 1.35 respectively), even though theophylline and theobromine have the same molecular mass. The K_2 values increased in the order caffeine, theophylline and theobromine (3.01, 3.76 and 3.96, respectively). Also, the B values increased in the order theobromine, theophylline and caffeine (6.88, 10.45 and 15.43, respectively), and the C values in the order theobromine, caffeine and theophylline (64.8, 89.2 and 95.4, respectively) (Table III).

(c) Within the quinoline alkaloids, which include two pairs of isomers, *viz.*, (-)-quinine, (+)-quinidine and (-)-cinchonidine, (+)-cinchonine (Fig. 1c), the presence of the methoxy group in quinine and quinidine increases the K_1 and K_2 values. Whereas the K_1 and K_2 values give no sharp differentiation between the members of each pair, the B and C values (Table III) could be regarded as a guide for differentiating between the two pairs of isomers and also between the members of each pair with the same molecular mass.

To test the reliability of identification by this method, eight unknown samples were prepared by one of the investigators and analysed by another. The eight unknowns consisted of one compound from each of the seven classes (Table III) plus a compound that was not included in this study. An initial run for each compound placed them in a particular class. From the values of absorbance ratios (K_1), the primary identification was rapidly achieved. Then, confirmation by measurement at the maximum wavelength completed the identification.

REFERENCES

- 1 O. M. Salama and M. I. Walash, *Anal. Lett.*, 22 (1989), in press.
- 2 T. M. Sarg, M. M. El-Domiatiy, M. M. Bishr, O. M. Salama and A. R. El-Gindy, *Analyst (London)*, in press.
- 3 S. H. Hilal, A. S. Radwan, M. y. Haggag, F. R. Melek and O. D. El-Gindy, *Egypt. J. Pharm. Sci.*, 23 (1982) 203.
- 4 S. H. Hilal, A. S. Radwan and M. Y. Haggag, *Egypt. J. Pharm. Sci.*, 23 (1982) 365.
- 5 M. Vanhaelen and R. Vanhaelen-Fastré, *J. Chromatogr.*, 312 (1984) 497.
- 6 *British Pharmacopoeia 1988*, Her Majesty's Stationery Office, London, 1988.
- 7 *The Pharmacopoeia of the United States of America (USP XXI)*, U.S. Pharmacopoeial Convention, Rockville, MD, 1985.
- 8 *Pharmacopoeé Française*, Ordre National des Pharmaciens, Paris, 1974.
- 9 *Egyptian Pharmacopoeia*, Fouad I University Press, Cairo, 1953.
- 10 *European Pharmacopoeia*, Maisonneuve. Sainte-Ruffine, France 1985.
- 11 H. Wagner, S. Bladt and E. M. Zgainski, *Plant Drug Analysis, A Thin Layer Chromatography Atlas*, Springer, Berlin, Heidelberg, New York, Tokyo, 1984.
- 12 E. G. C. Clarke, *Isolation and Identification of Drugs*, Pharmaceutical Press, London, 1969.
- 13 E. Stahl, *Thin Layer Chromatography*, Springer, Berlin, Heidelberg, New York, 2nd ed., 1969.

^a Although heroin is not a natural compound, it is included because of its structural relationship to the phenanthrene alkaloids and its legal implications.

Note

Simple method for the preparation of spherical agarose and composite gel particles

ELENA PRESECAN

Institute of Hygiene and Public Health, R-3400 Cluj-Napoca (Romania)

HOREA PORUMB

Department of Biophysics, Medical and Pharmaceutical Institute, R-3400 Cluj-Napoca (Romania)

and

IOAN LASCU*

Department of Biochemistry, Medical and Pharmaceutical Institute, 6 Pasteur Street, R-3400 Cluj-Napoca (Romania)

(First received May 26th, 1988; revised manuscript received January 31st, 1989)

Agarose gel in spherical form is used extensively in chromatography and as a carrier for biocatalysts. The methods for obtaining agarose beads are based either on phase separation¹ or on gelation of an agarose solution after dispersion in an “oil” phase² or by spraying it in diethyl ether³. The last two methods are particularly attractive for the preparation of “tailor-made” agarose beads and composite beads on a laboratory scale, not only for determining the performance of new derivatives, but also for the preparation of moderate amounts (a few litres) of commercially available but expensive chromatographic materials. We describe here a modification of the latter technique; instead of applying pressure to force the agarose solution through a needle, we used an electrical paint blower for the generation of the agarose droplets.

EXPERIMENTAL

A 5% agarose solution was obtained by swelling the agarose overnight and then autoclaving it for 10 min at 120°C. This procedure is particularly useful for gel concentrations above 6%, when simple addition of agarose to boiling water does not suffice. For the preparation of composite gels, the hot agarose solution (200 ml) was mixed with either 30 g of wet hydroxyapatite (equivalent to about 10 g of dry material, prepared as described by Hirano *et al.*⁴), 15 g of activated carbon or 15 g of magnetite.

The set-up for producing the particles is shown in Fig. 1. The upper diethyl ether layer cools the agarose droplets before they reach and become accumulated into the aqueous layer at the bottom. To avoid gelation of the agarose solution in the blower, it was pre-heated by running hot distilled water through the blower before starting the experiment. The nozzle of the blower was fitted to the neck of the glass vessel by using a flexible rubber collar. During operation, the blower was contin-

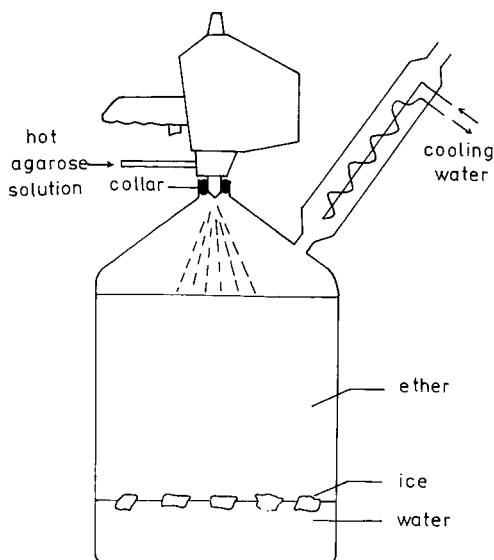


Fig. 1. Set-up for producing agarose beads using a paint blower.

uously moved from one side to another in order to avoid clumping of particles. In spite of this, the agarose beads tended to form a layer at the diethyl ether–water interface, which was dispersed by vigorously rotating the whole vessel after spraying about 50 ml of solution. Other mixing methods (magnetic stirring, bubbling of air) were found to be less efficient. The water phase was replaced after spraying about 300 ml of agarose solution. Finally, the beads were sorted according to size by passing them under a water jet through successive sieves of decreasing mesh size.

RESULTS AND DISCUSSION

With respect to the method described by Bengtsson and Philipson³ we made two improvements. The first was to use a closed container where the cooling with diethyl ether occurs. This ensures the safety of the procedure. Diethyl ether is highly flammable but it cannot be replaced with other organic solvent as it is convenient to have both a boiling point below or about the same as the gelation temperature of the agarose solution and a density lower than that of water. The second improvement was the use of a paint blower for generating the agarose droplets. The blower develops a considerable pressure, and therefore viscous solutions and thick suspensions can be conveniently handled. Professional paint blowers are inexpensive and offer the facility for varying the pressure, which makes it possible to obtain particles of predetermined size. In the experiments reported, the diameters of the particles obtained from a 5% agarose solution ranged between 50 and 400 μm . The addition of hydroxyapatite, activated carbon or magnetite did not have any significant effect on the size of the particles. The bead size distribution did not seem to be related to the agarose concentration or to be affected by the balancing of the blower, although a thorough investigation was not carried out. Beads cross-linked as described previous-

ly⁵ and liganded to Cibacron red 3B-P were successfully used in the purification of nucleoside diphosphate kinase from human erythrocytes (to be reported elsewhere).

The composite gels have not been tested yet. It is believed that the same set-up, with appropriate gelling solutions, could be useful for the preparation of spherical particles made of agarose-alginate, cellulose and other polymers, and of other composite gels.

REFERENCES

- 1 H. Pertoft and A. Hallén, *J. Chromatogr.*, 128 (1976) 125-131.
- 2 S. Hjertén, *Biochim. Biophys. Acta*, 79 (1964) 393-398.
- 3 S. Bengtsson and L. Philipson, *Biochim. Biophys. Acta*, 79 (1964) 399-404.
- 4 H. Hirano, T. Nishimura and T. Iwamura, *Anal. Biochem.*, 150 (1985) 228-232.
- 5 T. Porumb, H. Porumb, I. Lascu and I. Proinov, *J. Chromatogr.*, 319 (1985) 218-221.

Note

Improvement of a carbon–nitrogen elemental analyser for marine samples collected on glass-fibre filters

CHRISTIAN BECHEMIN^a, DANIEL DELMAS* and MARIE-JOSÉ GARET^b

CREMA L'Houmeau (CNRS/IFREMER), Case 5, 17137 Nieul-sur-Mer (France)

(First received October 31st, 1988; revised manuscript received January 30th, 1989)

In the marine environment, organic carbon and nitrogen are involved in biological, chemical and geochemical processes. The measurement of particulate organic carbon (POC) and nitrogen (PON) by high-temperature combustion, with subsequent separation and detection, is the most efficient and widely used method^{1–3}. In sea water, as particulate organic matter is very diluted (a few milligrams per litre), it is concentrated by filtration on pre-combusted glass-fibre filters. Thus, in contrast with the normal situation, our samples are a mixture of a small amount of organic matter with a large amount of glass-fibre, which melts during the high temperature combustion. Owing to this fact and depending on the equipment used, some specific analytical problems occur. However, the glass-fibre melting can be overcome by using lower temperatures, but erratic results are obtained^{4,5}. This depends on the nature of organic material and also on the combustion time, which is not generally adjustable for most elemental analysers. Therefore, we have tried to resolve the practical problem of high-temperature combustion in our apparatus.

EXPERIMENTAL

Several systems using the high-temperature oxidation process are available. In our laboratory we use a Carlo Erba Model 1500 elemental analyser.

Briefly, the sample, enclosed in a tin container, is introduced into the quartz oxidation column, which is maintained at 1020°C. The tin primes a “flash combustion” at about 1700°C; combustion products, carried by helium, pass through layers of catalysts. Then carbon dioxide and nitrogen are separated on a gas chromatographic column and detected by thermal conductivity. With our samples, the quartz oxidation reactor is damaged very rapidly and as a consequence the analysis costs are high.

Two facts can explain the damage to the quartz oxidation column: first, during the “flash combustion”, the temperature is increased in the combustion zone from 1020 to 1700°C (near the melting point of quartz), so the quartz tube is submitted to high thermal stress every 6 min. Second, ashes, tin oxides and mainly melting glass

^a Present address: LEC, Mus de Loup, 17390 La Tremblade, France.

^b Present address: ECOCEAN, 17000 La Rochelle Pallice, France.

filters (used to process our samples) mix with the top layer of catalyst. Therefore, when we remove the ash from the furnace after every 100 analyses, this residue has formed a very hard plug. The connection of this hard plug with the weakened zone of the quartz tube leads to breakage of the oxidation reactor after two or three cleanings.

Initially, Carlo Erba provided a nickel sheet to protect the quartz combustion tube against thermal stress, but unfortunately they no longer supply it, and anyway this nickel sheet does not prevent the plug formation in the top layer of catalyst.

In order to reduce this drawback, we have examined the use of a crucible in the oxidation reactor. The specific requirements were to protect the quartz column against thermal stress and to isolate the top layer of catalyst from ashes and melting products. However, such a modification to the system must not trap any carbon or nitrogen or hinder the flow of gases and carrier. This crucible also needs to be introduced and removed easily without any manipulation of the oxidation reactor.

Alundum is a refractory product made with 90% aluminium oxide (melting point 2015°C) Alundum crucibles are porous (5–20 μm) and show good chemical inertia. Moreover, pure aluminium oxide can be used as a catalyst instead of chromium oxide (Carlo Erba, technical information). We therefore tested this material in order to protect the oxidation reactor. The external diameter of the commercially available crucible is close to the internal diameter of the oxidation reactor, so it is necessary to file it in order to have 1 mm free space between the walls.

RESULTS

The use of alundum crucibles in the analysis of acetanilide standards had no effects on the carbon and nitrogen response factors or retention times (Table I).

As acetanilide is not representative of the more complex marine particulate organic matter, we tested the combustion efficiency of a large polymeric compound, chitin, a high-molecular-weight material widely distributed in marine samples. With the analytical conditions used here, with flash combustion and catalytic oxidation, the results showed that (i) the alundum crucibles and (ii) the melting glass filters do not

TABLE I

INFLUENCE OF ALUNDUM CRUCIBLE ON THE RESPONSE FACTORS (K , $\mu\text{g } \mu\text{V}^{-1} \text{s}^{-1}$) AND RETENTION TIMES ($t_{R,s}$) FOR ACETANILIDE STANDARDS

R.S.D. = relative standard deviation (%).

System	Parameter	Carbon		Nitrogen	
		K	t_R	K	t_R
No crucible	Mean ^a	$7.79 \cdot 10^{-4}$	179.0	$2.23 \cdot 10^{-3}$	105.2
	S.D.	$0.35 \cdot 10^{-4}$	1.8	$0.18 \cdot 10^{-3}$	0.4
	R.S.D. (%)	4.4	1.0	8.0	0.9
With crucible	Mean ^a	$7.76 \cdot 10^{-4}$	179.3	$2.33 \cdot 10^{-3}$	105.3
	S.D.	$0.25 \cdot 10^{-4}$	0.8	$0.12 \cdot 10^{-3}$	0.5
	R.S.D. (%)	3.3	0.4	5.1	0.5

^a $n = 6$.

TABLE II

CARBON AND NITROGEN CONTENTS (% w/w) AND CARBON/NITROGEN RATIO OF CHITIN (ASH = 5%) ANALYSED WITH AN ALUNDUM CRUCIBLE AND WITH OR WITHOUT A GLASS-FIBRE FILTER

System	Parameter	Carbon	Nitrogen	Carbon/nitrogen
	Theoretical value	44.92	6.54	6.86
Without glass-fibre	Mean ^a	44.26	6.50	6.83
	S.D.	0.40	0.31	0.28
	R.S.D. (%)	0.91	4.76	4.13
With glass-fibre ^b	Mean ^a	44.39	6.46	6.87
	S.D.	0.57	0.27	0.25
	R.S.D. (%)	1.29	4.14	3.62

^a $n = 10$.

^b The weight of glass-fibre represents at least ten times the mass of chitin analysed.

affect the combustion yield (Table II). Depending on the sample size, it is necessary to replace the crucible every 50–70 sample combustions. This is carried out in less than 1 min without any manipulation of the oxidation reactor. For samples free from glass-fibre filter (*e.g.*, sediments, organic standards) there is no problem in emptying the crucible and using it several times. With this slight modification we have performed 450 sample analyses during six working days without any significant change in the response factors (Table III). Now we currently analyse more than 1000 samples with the same quartz column and catalysts; as alundum crucibles are very inexpensive, the analysis costs are substantially decreased.

The use of an alundum crucible is not restricted to the Carlo Erba elemental analyser. If necessary, this crucible can be employed with other analysers and also with some mass spectrometers. Further, alundum refractory cement offers the possibility of making less expensive and more thermally resistant sample boats than the quartz type used with some elemental analysers such as the Perkin-Elmer models.

TABLE III

DAY-TO-DAY VALUES FOR CARBON (K_C , $10^{-4} \mu\text{g} \mu\text{V}^{-1} \text{s}^{-1}$) AND NITROGEN (K_N , $10^{-3} \mu\text{g} \mu\text{V}^{-1} \text{s}^{-1}$) RESPONSE FACTORS WITH ACETANILIDE STANDARD USING ALUNDUM CRUCIBLES AND THE SAME OXIDATION REACTOR

Response factor	Parameter	Days					
		17/3 ($n = 6$)	18/3 ($n = 8$)	22/3 ($n = 12$)	24/3 ($n = 3$)	28/3 ($n = 6$)	29/3 ($n = 6$)
K_C	Mean	6.95	6.75	6.88	6.89	6.94	6.60
	R.S.D. (%)	1.8	1.3	2.9	2.2	3.3	2.2
K_N	Mean	1.85	2.23	2.28	2.22	2.1	1.84
	R.S.D. (%)	5.5	6.4	7.6	7.0	2.9	6.2

ACKNOWLEDGEMENT

This work was partly funded by the PIREN.

REFERENCES

- 1 J. H. Sharp, *Mar. Chem.*, 1 (1973) 211.
- 2 M. D. MacKinnon, *Mar. Chem.*, 7 (1978) 17.
- 3 M. D. MacKinnon, in E. K. Duursma and R. Dawson (Editors), *Marine Organic Chemistry*, Elsevier, Amsterdam, 1981, pp. 415–443.
- 4 R. J. Gibbs, *J. Sediment Petrol.*, 47 (1977) 547.
- 5 M. J. Charles and M. S. Simmons, *Analyst (London)*, 111 (1986) 385.

Note

Large-volume spotting apparatus and its application to the semi-quantitative determination of organochlorine pesticides in tea

HAIBIN WAN

Tea Research Institute, Chinese Academy of Agricultural Sciences, Yunxi Road, Hangzhou (China)

(Received January 27th, 1989)

A simple and inexpensive field method for checking the level of organochlorine pesticide residues in tea is needed by tea-purchasing stations in China. Thin-layer chromatography (TLC) is suitable and different methods have been reported^{1,2}. However, the pesticides have to be extracted, and the extracts concentrated and purified prior to the TLC determination. The usual techniques cannot be applied by the workers in tea-purchasing stations, who have little experience in chemistry. To simplify the operation, a device that can apply a relatively large volume of sample to a TLC plate and can carry out clean-up and spotting in one step was developed.

EXPERIMENTAL

Apparatus

Figs. 1 and 2 show the apparatus, which consists of spotters made from medical syringes, hair dryers and a modified magnetic agitator. The tip of the spotter is made from a syringe needle by cutting off the long and thin part and filling the base part tightly with a bundle of cotton thread, and cotton. On spotting, the solution percolating through the tip is absorbed by the thin layer of a TLC plate. The flow of cool air from the hair dryer and the heat applied to the TLC plate by the magnetic agitator promote the evaporation of the solvents, and thus maintain the sample spot on the TLC plate at a certain size.

Procedure

Extraction and clean-up were based on the method described by Chen *et al.*³. The TLC determination was similar to that described by Laitem and Gaspar¹.

Ground tea (10 g) was soaked in 50 ml of hexane – acetone (9:1, v/v) and stirred for 30 min using the magnetic agitator. An aliquot of the extracts (5 ml) was washed with concentrated sulphuric acid (1 ml) in a stoppered test-tube. The upper phase was transferred to a spotter packed with alumina (2 cm³) and with the tip removed. After the liquid had been drawn off the adsorbent, the tip was added to the spotter, and the spotter was placed in the spotting apparatus with the tip right on the spotting position on the TLC plate. The heating unit of the magnetic agitator and the hair dryer were switched on. Hexane (4 ml) was added to the spotter. During spotting, the temperature of the TLC plate was maintained at *ca.* 60°C. When spotting was completed, a

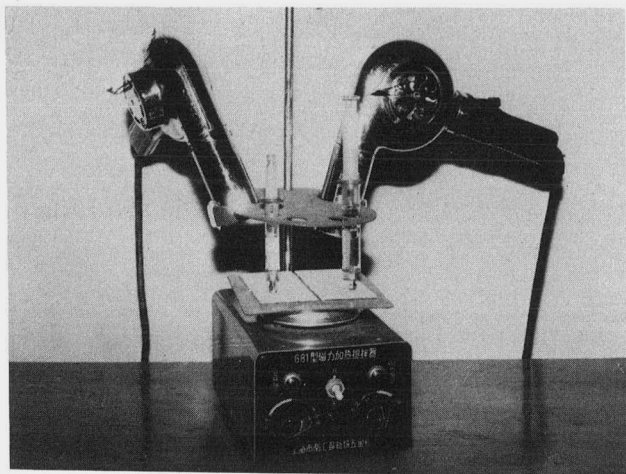


Fig. 1. Photograph of spotting apparatus.

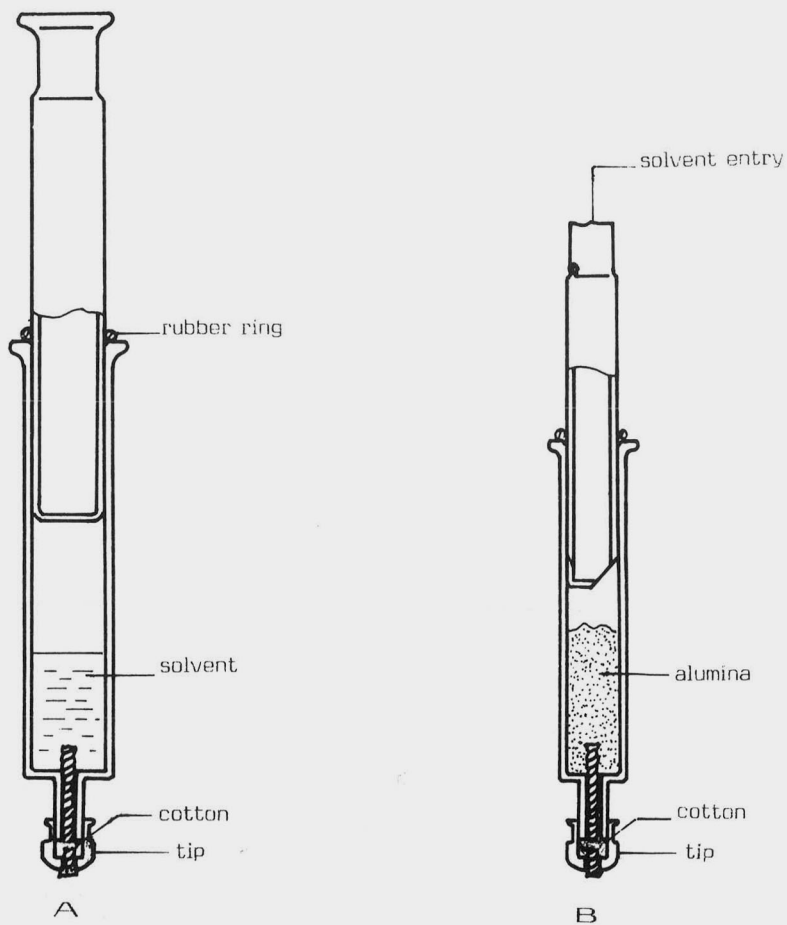


Fig. 2. Diagrams of spotters: (A) for liquid sample; (B) for clean-up.

standard solution (5 μ l) was spotted beside the sample spot on the TLC plate. The TLC plate was then developed. The residue level of the pesticide was estimated by comparing the spot size with that of the standard.

RESULTS AND DISCUSSION

The working principle of the device is similar to that described by Moosmann⁴, but the present device has little influence on the original spot size and the R_F value, and thus no extra modification of the TLC plates is needed. Also, the device can carry out column chromatography clean-up and spotting at the same time. Tea samples fortified with BHC (0.4 mg kg⁻¹) produced the same spot size as that of an equal amount of the standard. The time for analysing one sample is about 2 h.

To determine the influence of the relatively high temperature and prolonged flow of air on pesticides, several pesticides with different vapour pressures were spotted on a TLC plate using this device (0.4 μ g in 5 ml of acetone). The spots on the plate were scraped into a Pasteur pipette and the pesticides were eluted to a test-tube with acetone (5 ml). The recoveries were tested by gas-liquid chromatography. BHC, malathion, dimethoate and quinalphos all gave recoveries higher than 90%, whereas dichlorvos, which is very volatile, gave a recovery of less than 30%.

REFERENCES

- 1 L. Laitem and P. Gaspar, *Bull. Environ. Contam. Toxicol.*, 19 (1978) 264.
- 2 D. C. Abbot, J. O'G. Tatton and N. F. Wood, *J. Chromatogr.*, 42 (1969) 83.
- 3 Z.-M. Chen, H.-Q. Han, H.-B. Wan and R.-Z. Yeu, *Acta Sci. Circumst.*, 6 (1986) 278.
- 4 H. Moosmann, *J. Chromatogr.*, 209 (1981) 84.

Note

Traditional oriental medicines

I. Black Pearl: identification and chromatographic determination of some undeclared medicinal ingredients

A. BY, J. C. ETHIER, G. LAURIAULT, M. LeBELLE, B. A. LODGE*, C. SAVARD, W.-W. SY and W. L. WILSON

Drug Identification Division, Bureau of Drug Research, Health Protection Branch, Health and Welfare Canada, Tunney's Pasture, Ottawa, Ontario K1A 0L2 (Canada)

(First received July 15th, 1988; revised manuscript received February 9th, 1989)

Black Pearl is a round (10 mm diameter), black herbal pill that is labelled by the manufacturer on Grand Cayman Island as a herbal food supplement containing twenty-two herbs in a honey base. Its physical appearance as well as its smell and the list of ingredients on the label is very close to the traditional Chinese pill, Nan Lien Chui Fong Toukuwan¹. This study was initiated because, from past experience with Chui Fong², the presence of added prescription drugs was suspected. Primary regulatory concern with respect to a product of this nature can be satisfied by the demonstration of the presence of undeclared medicinal ingredients. However, the degree of regulatory response may require the evaluation of the health hazard associated with the product. Accordingly, estimates of the amounts of the medicinal ingredients and the average daily dosage associated with the use of the product may be required.

Although detailed and rigorous thin-layer chromatographic schemes and systems have been described^{3,4}, the use of the extraction method and thin-layer system used here is particularly applicable to ethnic medicines. From experience these products are formulated often to contain a steroidal anti-inflammatory, a diuretic and a sedative. The extraction method and thin-layer chromatographic system employed here has been found to be an efficient method for the identification of many of the substances found in ethnic medicines. In combination with direct probe mass spectrometry the identification of a wide variety of substances is facilitated.

The HPLC method was developed specifically for the determination of the added drugs found in Black Pearl pills. Sample preparation involved the crushing of the pill and extraction of the soluble material in solvent. The presence of other material did not interfere with the quantitation of the analyzed drugs by high-performance liquid chromatography (HPLC). The analysis revealed the presence of significant amounts of an anti-inflammatory (indomethacin), an analgesic (mefenamic acid), a tranquillizer (diazepam), and a diuretic (hydrochlorothiazide). Prolonged consumption of products such as Black Pearl containing undeclared amounts of prescription drugs may cause serious adverse health consequences².

EXPERIMENTAL

Drugs and chemicals

Ethyl acetate was distilled-in-glass grade (Caledon Labs., Georgetown, Canada). Methanol and acetonitrile were HPLC grade (J. T. Baker, Phillipsburg, NJ, U.S.A.). Monobasic potassium phosphate (J. T. Baker) and orthophosphoric acid (British Drug Houses, Toronto, Canada) were reagent grade. Water was obtained from a Nanopure II system (Barnstead, Boston, MA, U.S.A.). All drugs were obtained from the reference collection of the Health Protection Branch. The Black Pearl pills were obtained through investigative activities of the Health Protection Branch. The labels of all samples received carried no lot numbers but indicated the product originated in the British West Indies.

Thin-layer chromatography

Sample preparation. One pill was powdered and placed in a test tube to which was added about 2 ml of water and 2 ml of ethyl acetate. Dissolution was assisted by stirring with a glass rod. The mixture was centrifuged at approximately 400 g for 5 min using a bench-top centrifuge (Fisher Scientific, Ottawa, Canada) and approximately 0.5 ml of the ethyl acetate extract was applied manually to the plate with a disposable pipet.

Plates. Silica gel GHLF 0.25 mm plates (20 × 20 cm) were from Analtech, Newark, DE, U.S.A.

Solvents. System A was ethyl acetate, system B ethyl acetate-methanol (4:1, v/v).

Procedure. The plate was developed first in solvent system A. The bands were identified using short-wave UV light and the substances were extracted from the silica gel using ethyl acetate containing a small amount of methanol. The band corresponding in R_F to hydrochlorothiazide was extracted and the material obtained was redissolved in ethyl acetate and chromatographed using solvent system B.

Identification of substances

A 4610B quadrupole instrument (Finnigan MAT, San José, CA, U.S.A.) operating in electron impact mode was employed. Spectra were obtained by direct probe inlet of the residue obtained from the extraction of the thin-layer plate. Gas chromatographic introduction of the sample residues was precluded due to the wide range of volatility and polarity of the substances. Identification of the drug substances was made by comparison of the mass spectra obtained from the isolated materials with those obtained from authentic standards.

High-performance liquid chromatography

Instruments. The apparatus consisted of a Spectra-Physics (Santa Clara, CA, U.S.A.) SP8100 liquid chromatograph (with integral autosampler), a Spectra-Physics SP8440 UV-VIS detector (operated at 240 nm, because of the applicability of this wavelength to steroid detection) and a Spectra-Physics SP4200 computing integrator.

Conditions. The reversed-phase column which was operated at ambient temperature was an octyl coated silica of 10- μ m particle size, 250 × 4.6 mm, RP-8 Spheri-10 (Brownlee Labs, Santa Clara, CA, U.S.A.). The mobile phase was a two component system made from acetonitrile (A) and 0.05 M potassium dihydrogenphosphate pH

3.3 (B). The pH of the buffer was adjusted by the addition of concentrated phosphoric acid. The solvent gradient program was as follows, at a flow-rate of 1 ml/min:

<i>Time (min)</i>	<i>%A</i>	<i>%B</i>
0.00	15.0	85.0
10.00	15.0	85.0
12.00	50.0	50.0
40.00	50.0	50.0
50.00	70.0	30.0

Stock solutions. Stock solutions of indomethacin (1.33 mg/ml), mefenamic acid (1.63 mg/ml), diazepam (0.073 mg/ml) and hydrochlorothiazide (0.6 mg/ml) were prepared in methanol.

Standard solutions. Five solutions were prepared to contain the four drugs over the concentration ranges shown in Table I. The concentrations were based on preliminary chromatographic investigations.

Mixed standard. A mixed standard solution was prepared in methanol to contain each of the substances at one tenth of the concentration in the stock solution.

Sample preparation. Single pills were crushed in a pill crusher and transferred to a vial. Composite was weighed directly into the vial. The contents of the vial were then sequentially extracted using an ultrasonicator (10 min) with four 10-ml portions of methanol. The methanol extracts were combined in a 50-ml volumetric flask and the volume completed with methanol. About 2 ml of the solution was filtered through cotton and 10 μ l injected into the HPLC system using the autosampler.

RESULTS AND DISCUSSION

Initial chromatography of the tablet extracts in solvent system A indicated the presence of three bands corresponding in R_F to indomethacin, diazepam and hydrochlorothiazide. No other significant bands were detectable. As it was suspected that the band corresponding to the last substance was impure, the extracted material was re-chromatographed in solvent system B. Two distinct bands were then detected corresponding in R_F to hydrochlorothiazide and mefenamic acid. The R_F of the reference standard drugs on the two TLC systems are shown in Table I.

The retention times and relative responses of the same substances by HPLC are also shown in Table I. The linearity of the system was verified by injection of standard solutions. The detection of the four drugs was found to be linear over the required concentrations. A summary of the data and the minimum detectability of each drug is shown in Table I.

The extraction efficiency of the procedure was verified by analyzing the content of each of the drugs in unpooled sequential 10-ml methanol extracts. The results are shown in Table II. Greater than 95% of each of the drugs was extracted in the first and second extracts. The recovery of the method was determined by adding, to two weighed aliquots of a homogeneous composite, aliquots of a methanolic solution containing each of the four drugs. The amounts added corresponded to approximately 35 and 50% of the amount of each of the drugs originally found to be present.

TABLE I
TLC AND HPLC PROPERTIES OF REFERENCE SUBSTANCES

Drug	TLC		HPLC				
	R_F		t_R (min)	Relative response	Minimum detectability (mg/tablet)	Linearity	
	Solvent A	Solvent B				Concentration (mg/ml)	Correlation coefficient
Hydrochlorothiazide	0.42	0.64	7.76	0.09	0.5	0.0365–0.170	0.990
Diazepam	0.50	0.68	27.37	1.00	0.1	0.00515–0.0225	0.995
Indomethacin	0.14	0.21	29.55	0.6	0.2	0.085–0.360	0.999
Mefenamic acid	0.42	0.50	33.09	0.5	0.2	0.113–0.462	0.999

TABLE II
EXTRACTION EFFICIENCY

Drug	Recovery (% of total)			
	First extract	Second extract	Third extract	Fourth extract
Hydrochlorothiazide	72.9	23.2	3.9	0
Diazepam	65.0	30.0	4.5	0.6
Indomethacin	71.2	25.5	3.2	0.1
Mefenamic acid	66.8	29.6	3.2	0.4

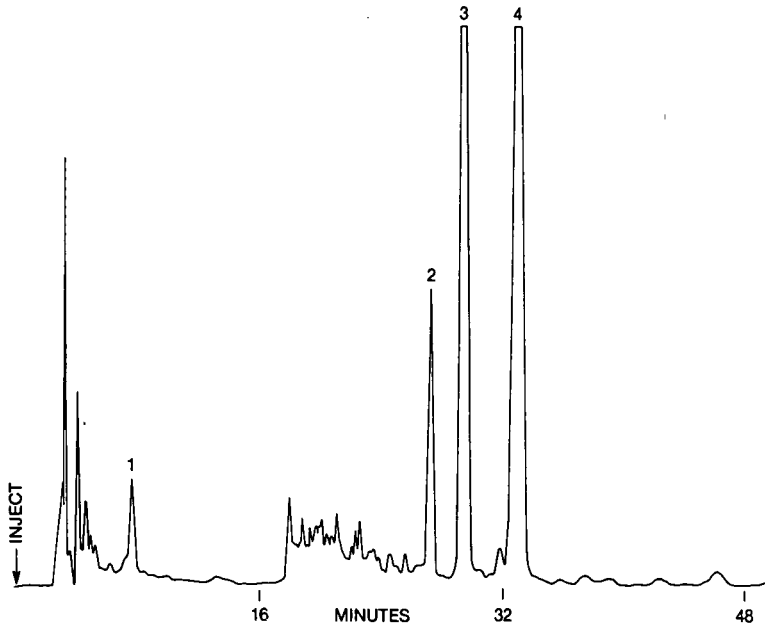


Fig. 1. HPLC profile of a Black Pearl pill containing hydrochlorothiazide (1), diazepam (2), indomethacin (3) and mefenamic acid (4).

Recovery of all four drugs was greater than 95%. The reproducibility of the analysis of tablet material was verified by determining the content of the four drugs in a finely ground homogeneous composite. The results (coefficients of variation) were 2, 6, 2 and 1% ($n = 6$) for hydrochlorothiazide, diazepam, indomethacin and mefenamic acid, respectively.

A chromatogram of the extract of a sample which contained the four added medicinal ingredients is shown in Fig. 1. A number of peaks due to unidentified substances will be noted. These may be other unidentified drugs or substances derived from the rather complex pill matrix.

One bottle containing twelve tablets was originally submitted for analysis. In all of the six tablets analyzed, the four drugs were found to be present. Fifty tablets taken from a different shipment were also submitted for analysis. From nine tablets analyzed, only two were found to contain the four drugs.

Subsequently, eight additional identical bottles of pills were received for analysis. One bottle contained 100 tablets and the remainder contained from 1 to 10 pills. From each bottle some pills (1 to 5) were analyzed quantitatively. The results of quantitative analysis of these eight batches of pills are shown in Table III, from which it can be clearly seen that there is a lack of homogeneity, suggesting a lack of quality

TABLE III
RESULTS OF ANALYSIS

Sample No.	Hydrochlorothiazide (mg/tablet)	Diazepam (mg/tablet)	Indomethacin (mg/tablet)	Mefenamic acid (mg/tablet)
1	2.50	0.47	5.88	7.79
	2.15	0.38	5.20	6.89
2	2.34	0.43	5.50	6.86
	2.15	0.36	5.39	7.21
3	1.94	0.41	5.41	7.14
	2.40	0.52	6.21	8.18
4	2.33	0.38	5.50	7.48
	2.26	0.42	5.75	7.91
5	2.05	0.44	5.85	7.56
	2.16	0.35	5.38	7.25
	1.82	0.40	5.28	6.98
6	2.00	0.47	6.18	8.21
7	— ^a	—	—	—
	—	—	—	—
	—	—	—	—
	—	—	—	—
8	1.64	0.35	4.09	5.19
	1.92	0.35	4.85	6.14
	1.36	0.30	3.69	4.54
	2.33	0.44	5.39	6.99
	2.34	0.35	4.74	5.88

^a Not detected.

control in the manufacturing process. Sample 7 is different from the others in that no detectable amounts of added drugs were found.

REFERENCES

- 1 S. Yuen and C. A. Lau-Cam, *J. Chromatogr.*, 329 (1985) 107.
- 2 C. A. Ries and M. A. Sahud, *J. Am. Med. Assoc.*, 231 (1975) 352.
- 3 A. C. Moffat (Editor), *Clarke's Isolation and Identification of Drugs*, The Pharmaceutical Press, London, 1986.
- 4 A. H. Stead, R. Gill, T. Wright, J. P. Gibbs and A. C. Moffat, *Analyst*, 107 (1982) 1106.

CHROM. 21 408

Note

Resolution of neuroactive non-protein amino acid enantiomers by high-performance liquid chromatography utilising pre-column derivatisation with *o*-phthaldialdehyde-chiral thiols

Application to 2-amino- ω -phosphonoalkanoic acid homologues and α -amino- β -N-methylaminopropanoic acid (β -methylaminoalanine)

MELVIN R. EUERBY* and LYNDA Z. PARTRIDGE

Department of Pharmaceutical Chemistry, School of Pharmacy, University of London, 29-39 Brunswick Square, London WC1N 1AX (U.K.)

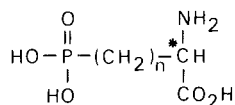
and

PETER B. NUNN

Department of Biochemistry, King's College London, Strand, London WC2R 2LS (U.K.)

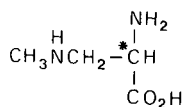
(First received November 28th, 1988; revised manuscript received February 14th, 1989)

Excitatory amino acid receptors have been classified into different subtypes^{1,2}. The N-methyl-D-aspartate (NMDA) receptors, which are activated by NMDA and blocked by 2-amino- ω -phosphonoalkanoic acids, are involved in synaptic excitation in the spinal cord and it has been proposed that they are activated physiologically by L-aspartate and/or L-glutamate². The use of the NMDA antagonists 2-amino- ω -phosphonoalkanoic acids [Fig. 1: 2-amino-4-phosphonobutanoic acid (2APB), **1a, b**; 2-amino-5-phosphonovaleric acid (2APV), **2a, b**; and 2-amino-7-phosphonoheptanoic acid (2APH), **3a, b**] are of considerable value in the investigation of amino



compound	n	optical configuration
1a	2	L-
1b	2	D-
2a	3	L-
2b	3	D-
3a	5	L-
3b	5	D-

Fig. 1. Structure of the 2-amino- ω -phosphonoalkanoic acids (asterisk denotes chiral centre).



compound	optical configuration
4a	L-
4b	D-

Fig. 2. Structure of MeDAP (asterisk denotes chiral centre).

acid-mediated synaptic excitation^{1,4}. The antagonist activity of these compounds resides with the D-enantiomers⁴, although previous biochemical studies employed racemic DL-mixtures^{1,4}. However, it is essential to establish the enantiomeric purity of these compounds. For example, although the D-(−)-enantiomer of 2APB acts as an antagonist at the NMDA receptor, its corresponding L-(+)-enantiomer is a potent synaptic depressant, possibly at another non-NMDA receptor site². The L-(+)-isomer of β-amino-β-methylaminopropanoic acid (MeDAP, Fig. 2) appears to act at the NMDA receptor and it became the focus of much interest in view of the high incidence of degenerative neural diseases on the Pacific island of Guam⁵. During World War II, the inhabitants were forced to consume large quantities of seeds from the false sago palm (*Cycas circinalis*), which is a natural source of MeDAP. Primates given repeated oral doses of MeDAP exhibited many signs characteristic of upper and lower motor systems disease together with associated neurodegenerative changes⁶. The neurotoxicity of MeDAP is associated with the L-(+)-enantiomer only^{7,8}.

It can be seen therefore that since both MeDAP and the 2-amino-ω-phosphonoalkanoic acid series are prepared synthetically^{4,9} as the racemate and then resolved, the enantiomeric purity of the resultant L- and D-enantiomers must be assessed prior to pharmacological or biochemical studies. To date, the optical purity of these compounds has been ensured by optical rotation measurements. However, this method is insensitive to contamination with small quantities of minor enantiomers arising from racemisation or incomplete resolution⁷.

Recently, we have described the use of an enantioselective high-performance liquid chromatographic (HPLC) determination of the non-NMDA agonists β-N-oxalyl-L-α,β-diaminopropanoic acid, γ-N-oxalyl-L-α,γ-diaminobutanoic acid and related compounds by a pre-column derivatisation technique, utilising *o*-phthalaldehyde (OPA) and chiral thiols to yield diastereoisomeric isoindole derivatives, which are separable by reversed-phase HPLC and detected using fluorimetry¹⁰. It was decided to extend this approach to the development of a new, enantioselective assay for the 2-amino-ω-phosphonoalkanoic acids and MeDAP.

EXPERIMENTAL

Reagents and chemicals

All chemicals and solvents were of analytical or HPLC grade. Ultra-pure water was obtained by means of a Milli-Q system (Millipore). OPA was purchased from

Sigma; N-acetyl-L-cysteine (NAC) and N-*tert.*-butyloxycarbonyl-S-benzyl-L-cysteine from Fluka. DL-, D- and L-2APB, 2APV, 2APH and L-MeDAP were obtained from Cambridge Biochemical Reserch. N-*tert.*-Butyloxycarbonyl-L-cysteine (BocC) was prepared as described by Buck and Krummen¹¹. Synthetic DL-, D- and L-MeDAP were prepared using an established method⁷.

Chromatographic systems

HPLC was performed using a Gilson gradient system (Anachem, Luton, U.K.) which consisted of two Model 301 single piston pumps (5-ml heads), a Rheodyne 7125 loop injector (20 μ l), a Model 801 pressure module and a Model 121 fluorescence detector fitted with OPA filters (excitation at 344 nm and emission at 443 nm). The gradient was controlled by an Apple IIe computer using Gilson gradient manager software.

Chromatograms were recorded on an LKB 2210 single channel recorder at a sensitivity of 10 mV, a chart speed of 5 mm/min and a fluorescence sensitivity of 0.2 and 0.5 range units for MeDAP and 2-amino- ω -phosphonoalkanoic acids respectively. A Spherisorb ODS II "EXCEL", 5 μ m (25 cm \times 4.6 mm I.D.) column was purchased from Hichrom (Reading, U.K.) and fitted with a guard column (5 cm \times 2 mm I.D.) packed with CO:PELL ODS sorbent (particle size 40 μ m; Hichrom).

Preparation of standard amino acids derivatives

Stock solutions of the individual enantiomers were prepared, freshly each day, in water at a concentration of 2.5–5.0 μ mol/ml. Standard mixtures were prepared by diluting the appropriate stock solutions with water to yield a final concentration of 60–250 nmol/ml and 150–450 nmol/ml for each individual enantiomer of the 2-amino- ω -phosphonoalkanoic acids and MeDAP respectively.

Mobile phases

Solvents A and B were prepared freshly every other day, filtered through a 0.22- μ m membrane filter and degassed by continuous purging with helium. Solvents A and B consisted of 50 mM sodium acetate (pH 7.1 and 6.8, adjusted with dilute acetic acid for the 2-amino- ω -phosphoalkanoic acids and MeDAP, respectively) and

TABLE I

CHROMATOGRAPHIC GRADIENT CONDITIONS FOR THE ANALYSIS OF 2-AMINO- ω -PHOSPHONOALKANOIC ACIDS AND MeDAP

Duration (min)	Solvent A:B	
	From	To
0–30	90:10	75:25
30–35	75:25	65:35
35–50	65:35	65:35
50–55	65:35	40:60
55–60	40:60	40:60
60–65	40:60	90:10
65–75	90:10	90:10

TABLE II
CHROMATOGRAPHIC GRADIENT CONDITIONS FOR THE ANALYSIS OF 2APB

Duration (min)	Solvent A:B	
	From	To
0-40	90:10	75:25
40-45	75:25	40:60
45-50	40:60	40:60
50-55	40:60	90:10
55-65	90:10	90:10

methanol, respectively. The flow-rate was 1 ml/min and the column pressure was approximately 1600 p.s.i. at the beginning of the gradient. The gradient elution programme employed for the separation of the enantiomers of 2APV, 2APH and MeDAP is shown in Table I and for 2APB in Table II.

Pre-column derivatisation procedure

The derivatisation reagents were freshly prepared every other day by dissolving 10 mg of OPA and 10 mg of the chiral thiol in 1 ml of HPLC-grade methanol (in order to preserve the optical purity of the chiral thiols, the alkaline borate buffer was added immediately prior to derivatisation). These reagents were stored at 4°C in the dark until use. The 2-amino- ω -phosphonoalkanoic acid and MeDAP solutions (20 μ l) were mixed with the derivatisation reagent (40 μ l) and borate buffer (60 μ l, pH 8.2, adjusted with 2 M sodium hydroxide), and incubated for 5 min at ambient temperature in the dark before immediate injection onto the column.

RESULTS AND DISCUSSION

The acidic 2-amino- ω -phosphonoalkanoic acids gave intensely fluorescent diastereoisomeric isoindole derivatives when reacted with OPA and the chiral thiol, BocC in alkaline conditions. At ambient temperature in the dark they reached their maximum fluorescence within 2-3 min and were stable for up to at least 10 min. The resultant diastereoisomeric isoindole derivatives were separable by reversed-phase HPLC using a 50 mM sodium acetate (pH 7.1)-methanol gradient (optimised for separation of acidic compounds) and a Spherisorb ODS II column as described previously for the ω -N-oxaly-diamino acid series¹⁰. It has previously been shown that this type of pre-column diastereoisomer formation induces no detectable degree of racemisation^{11,12}.

Using these conditions the commercially available racemic DL-2APV and DL-2APH (Table I) gave baseline separation for the D- and L-enantiomers, whereas those of the short chain homologue, 2APB, were not fully resolved (Tables I and III, and Fig. 3A). However, on employing a gradient with a lower rate of change of buffer-methanol, baseline separation was achieved (Tables II and III, and Fig. 3D). The reproducibility of the retention times and peak heights for the enantiomers of 2APB, 2APV and 2APH was better than 1% coefficient of variation (C.V.). The

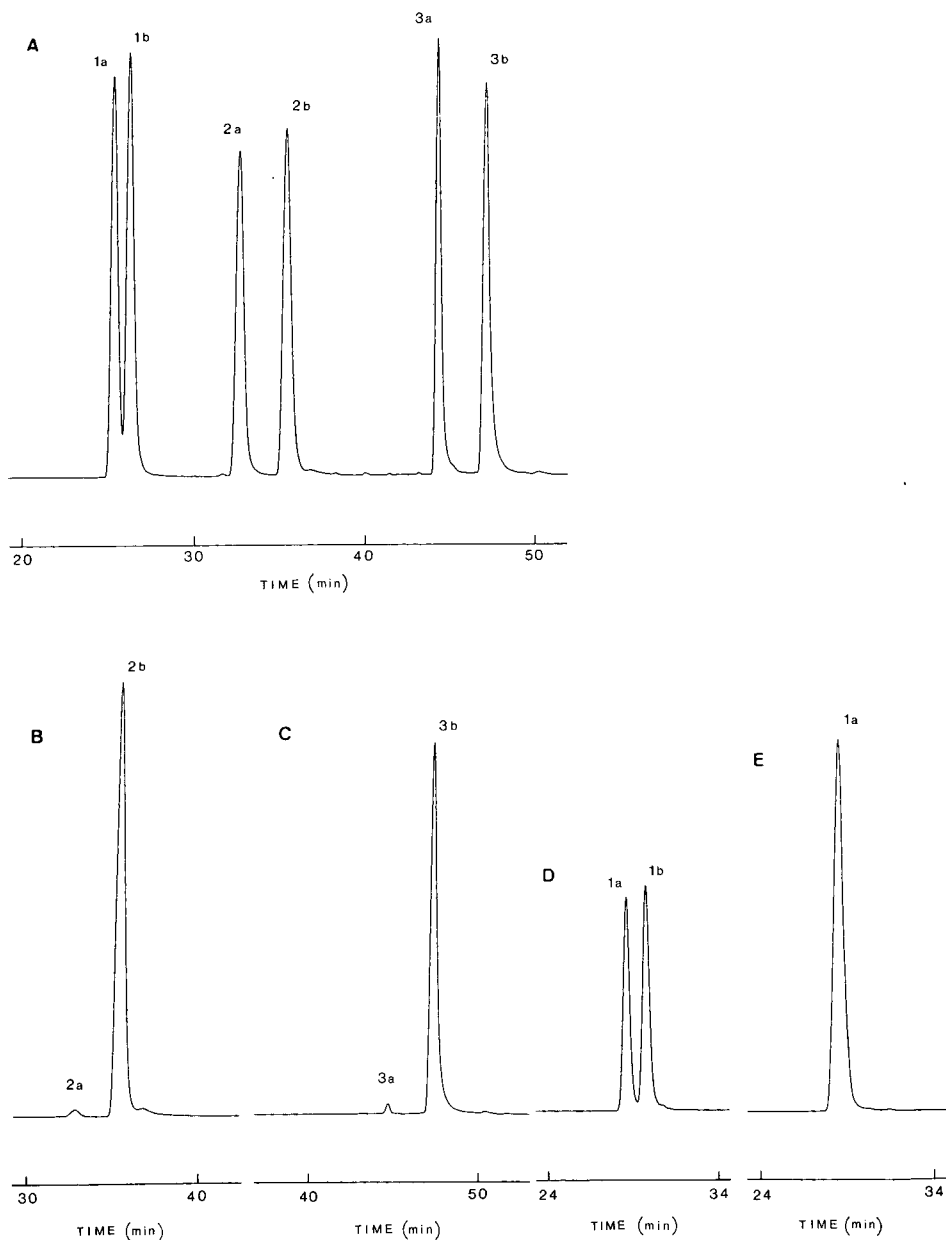


Fig. 3. HPLC of OPA-BocC derivatives of 2-amino- ω -phosphonoalkanoic acids on a Spherisorb ODS II "EXCEL" reversed-phase column. Chromatographic conditions as in the Experimental section. (A) Standard mixture of 2-amino- ω -phosphonoalkanoic acids using conditions as in Table I. Each peak corresponds to 500 pmol. (B and C) Commercial samples of D-2APV and D-2APH. (D) Standard mixture of DL-2APB using conditions as in Table II. Each peak corresponds to 300 pmol. (E) Commercial sample of L-2APB. Peaks: **1a, b** = L-, D-2APB; **2a, b** = L-, D-2APV; **3a, b** = L-, D-2APH.

TABLE III

SEPARATION OF DIASTEREOISOMERIC DERIVATIVES FORMED FROM 2-AMINO- ω -PHOSPHONOALKANOIC ACIDS–BocC AND MeDAP–NAC

$t_0 = 3.2$ min; k^* and R_s are the capacity and resolution factors, respectively, for a pair of enantiomers; chromatographic conditions are as in the Experimental section and Table I.

Compound	K_L^*	K_D^*	R_s
APB	6.97	7.28	1.04
APB ^a	7.88	8.13	1.64
APV	9.25	10.13	3.33
APH	12.94	13.88	3.77
MeDAP	10.25	9.48	4.33

^a Chromatographic conditions are as in the Experimental section and Table II.

calibration graph for the enantiomers of 2APB, 2APV and 2APH showed good linearity between peak height and concentration within the range of 0.2–1.1 nmol per injection ($r^2 > 0.997$). The limit of detection of the minor isomer was better than 0.1% and injection of a blank illustrated that there were no interfering peaks in the region of interest.

As observed with other OPA–BocC amino acids, the L-enantiomers eluted before their corresponding D-enantiomer^{10–12}. This result is probably due to the fact that the diastereoisomers from the D-enantiomers are capable of forming stronger intramolecular hydrogen bonds and therefore, being more lipophilic, are retained longer on the reversed-phase column than those formed from the L-enantiomers.

Commercial samples of the D- and L-enantiomers of 2APB, 2APV and 2APH were shown to be more than 98% optically pure and fell within the specification of the manufacturer (*i.e.*, see Fig. 3B, C and E). The use of this approach is ideally suited to the quality control assessment of the enantiomeric purity of these compounds as, in addition to the above results, we have shown that the pre-column derivatisation can be conveniently automated using a Gilson autosampler and injector (the BocC–OPA reagent is stable for at least 18 h at ambient temperature in amber vessels). The OPA–BocC reagent is added to the amino compound first, followed by the borate buffer just prior to derivatisation to avoid any possibility of racemisation of the chiral thiol.

In contrast to the acidic 2-amino- ω -phosphonoalkanoic acids and ω -N-oxalyl-diamino acids¹⁰, MeDAP is considerably more basic⁷. The use of the lipophilic chiral thiol BocC with synthetic DL–MeDAP resulted in separation of the diastereoisomers. However, compared to the 2-amino- ω -phosphonoalkanoic acid series, they eluted late in the chromatogram ($t_R = 60.00$ and 61.5 min for the L- and D-enantiomers, respectively) due to their increased lipophilic nature. In addition, on performing a blank, interfering peaks were shown to co-elute with the peaks of interest. On substituting the chiral thiol NAC for BocC, the diastereoisomers produced were less fluorescent and were eluted earlier than their corresponding BocC derivatives and free from interfering peaks. It was of interest to note that the NAC derivative of the D-enantiomer of MeDAP had a fluorescence intensity 1.50 times greater than the corresponding L-enantiomer for a racemic DL-mixture (optical rotation and circular dichroism measurements confirmed a 50:50 racemic mixture) whereas the UV

response (at 338 nm) to both derivatives was the same. In contrast, the BocC derivatives gave peaks of equal area for both enantiomers. This phenomenon of unequal fluorescence response was also observed by Buck and Krummen¹¹ for the amino compounds phenylalaninol and tryptophane but the difference in intensities was much lower than observed for the NAC derivatives of D- and L-MeDAP. The separation of the enantiomers achieved with the chiral thiol NAC was excellent (Table III and Fig. 4A) giving baseline separation and a limit of detection of the minor isomer of better than 0.1%. The elution order of the OPA-BocC derivatives of MeDAP was L- before the D-enantiomer whereas the order for the OPA-NAC derivatives was D- before the L-enantiomer. The order of elution with OPA-NAC derivatives has been previously related to the hydrophilicity of the amino acid. Hydrophilic amino acids result in the L-eluting before the D-enantiomer whereas the hydrophobic amino acids elute with the D- before the L-enantiomer¹¹.

The assay of MeDAP was highly pH dependent, using a mobile phase of pH values 6–7.1 a single peak was seen for each enantiomer. However, at pH values above

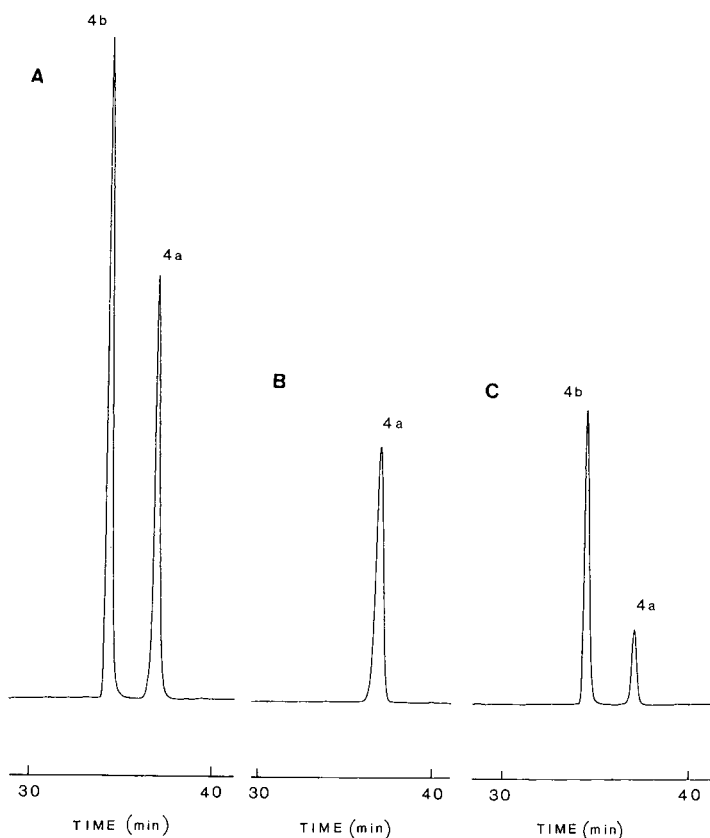


Fig. 4. HPLC of OPA-NAC derivatives of MeDAP (**4a**, **b**) on a Spherisorb ODS II "EXCEL" reversed-phase column. Chromatographic conditions as in Experimental section. (A) Standard mixture of DL-MeDAP (**4a** and **b**). Each peak corresponds to 1.5 nmol. (B) Commercially available L-MeDAP (**4a**). (C) Synthetically prepared D-MeDAP (**4b**).

7.1, two peaks are observed for each enantiomer, the second occurring very late in the "run" suggesting the additional production of a more lypophilic derivative (further investigations of these additional peaks are presently underway). Using a mobile phase of pH 6.8 the early-eluting peaks are reproducible (coefficients of variation of below 1% where obtained for the t_R and peak height) and the peak heights for each enantiomer responded linearly with concentration within the range 0.5–1.5 nmol (injected onto the column).

Synthetic and commercially available L-MeDAP contained no detectable levels of the D-enantiomer (Fig. 4B). However, the synthetic D-MeDAP produced by our laboratory contained 1.24% of the L-enantiomer. Whereas, D-MeDAP from another laboratory was shown to contain up to 20% of the L-enantiomer (Fig. 4C). During the synthesis, separation of the enantiomers from the racemic DL- α -N-acetyl-MeDAP is achieved by incubation with acylase-I which yields free L-MeDAP. This compound is separated from the impure α -N-acetyl-D-MeDAP by ion-exchange chromatography. The impure α -N-acetyl-D-MeDAP is resubjected to more acylase-I to remove further quantities of L-MeDAP⁷. The N-acetyl-D-MeDAP is then hydrolysed with acid to yield free D-MeDAP. The occurrence of considerable amounts of the L-enantiomer in the D-enantiomer suggests either racemisation in the hydrolysis stage or, more probably, an incomplete acylase-I reaction.

The HPLC assay described represents a specific and reproducible method ideally suited for quality control purposes for assessing the enantiomeric purity of the synthetically prepared NMDA agonist MeDAP, and antagonists, 2-amino- ω -phosphonoalkanoic acids.

ACKNOWLEDGEMENTS

We thank Professor W. A. Gibbons for support of this project and use of his laboratory facilities (M.R.E. and L.Z.P.), the C. W. Maplethorpe Trust for a research fellowship (to M.R.E.) and the Motor Neurone Disease Association for financial support (to P.B.N.).

REFERENCES

- 1 R. H. Evans, A. A. Francis, K. Hunt, D. J. Oakes and J. C. Watkins, *Br. J. Pharm.*, 67 (1979) 591.
- 2 C. W. Cotman and L. L. Iversen, *Trends Neurosci.*, 10 (1987) 263.
- 3 J. C. Watkins and H. J. Olverman, *Trends Neurosci.*, 10 (1987) 265.
- 4 J. Davies, A. A. Francis, A. W. Jones and J. C. Watkins, *Neurosci. Lett.*, 21 (1981) 77.
- 5 R. M. Garruto and Y. Yase, *Trends Neurosci.*, 9 (1986) 368.
- 6 P. S. Spencer, P. B. Nunn, A. Hugon, A. C. Ludolph, S. M. Ross, D. N. Roy and R. C. Robertson, *Science (Washington, D.C.)*, 237 (1987) 517.
- 7 A. Vega, E. A. Bell and P. B. Nunn, *Phytochemistry*, 7 (1968) 1885.
- 8 P. B. Nunn, M. Seelig, S. C. Zagorem and P. S. Spencer, *Brain Res.*, 410 (1987) 375.
- 9 J. R. Chamber and A. F. Isbell, *J. Org. Chem.*, 29 (1964) 832.
- 10 M. R. Euerby, P. B. Nunn and L. Z. Partridge, *J. Chromatogr.*, 466 (1989) 407.
- 11 R. H. Buck and K. Krummen, *J. Chromatogr.*, 387 (1987) 255.
- 12 M. R. Euerby, L. Z. Partridge and P. Rajani, *J. Chromatogr.*, 447 (1988) 392.

Note

Application of correlation chromatography to the investigation of biopolymers in wines

I. Sh. SHATIRISHVILI

Digomi Georgian Institute of Agriculture, Tbilisi (U.S.S.R.)

(First received October 3rd, 1988; revised manuscript received January 16th, 1989)

Correlation chromatography, a new variant of pyrolytic chromatography, was developed by Küllik *et al.* The method was found to be applicable, without any modifications, for the investigation of biopolymeric residues of wines. The solid residue was placed in a special instrument with temperature-programmed control (Institute of Chemistry, Estonian Academy of Sciences, Tallin, U.S.S.R.) and the temperature was raised stepwise in 10°C intervals. The resulting decomposition products were delivered at certain intervals (impulsively) by a special device designed to place the samples in a gas chromatograph equipped with an SE-30 capillary column. The detector recorded the composition of the decomposition products for about 1 min. The next impulsive delivery of the decomposition products obtained at a higher temperature was recorded in the form of a parallel chromatogram shifted with respect to the preceding one, etc. As a result, a two-dimensional chromatogram showing the changes with time in the composition of the tested sample decomposition products is obtained; this chromatogram can be recorded in direct and reverse order with respect to the time axis.

This method is useful for studying the residues of wines and wine raw materials from two points of view: first, to characterize the wines, and second, to obtain information about the biopolymers in wine. The residues of four kinds of Georgian wines, namely Kakhetinski (home-made), Kinzmarauli, Tibaani and Gurdjuani, were studied. A sample of the solid, dry residue from the wine, filtered through a membrane filter and consisting of biopolymers, was weighed (usually 2–4 mg) and placed on the boat of the receiver. Then the programming control was switched on and all the subsequent operations were performed automatically according to the given reference programme of the investigation. The reproducibility of the retention times was about 0.2 and of the peak heights about 1% according to the data of Küllik *et al.*¹. The chromatograms are normalized to 1 mg of residues to facilitate comparisons.

It is convenient to employ the following three modes to represent the results: isometric projection (direct and reverse), a set of one-dimensional cuts and a contour map.

The isometric projections are obtained by depicting all the chromatograms obtained in the process of the two-dimensional experiment (time, temperature) one over the other so that the second variable could increase (or decrease). A chroma-

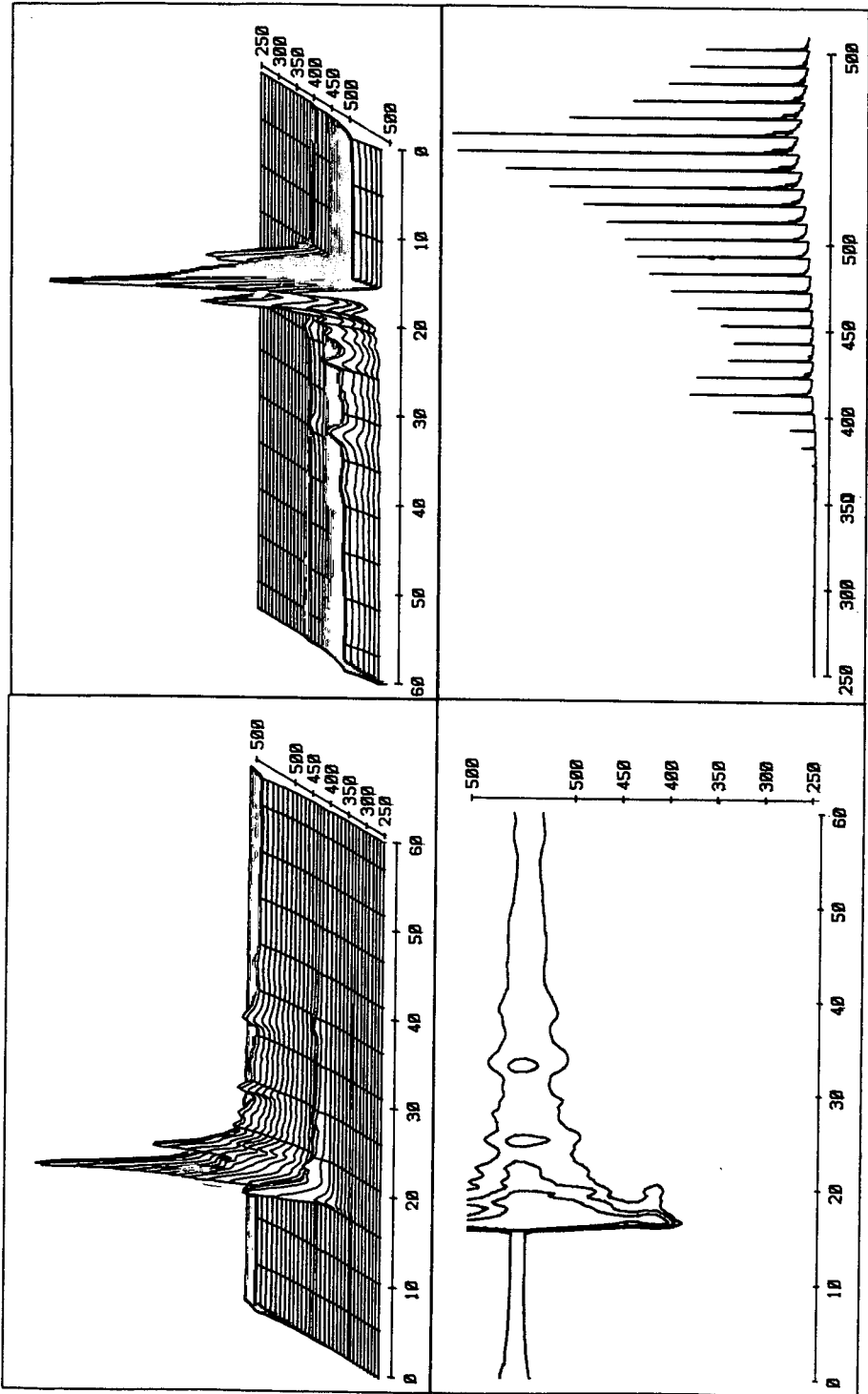


Fig. 1. Correlation chromatograms for Tibaani wine.

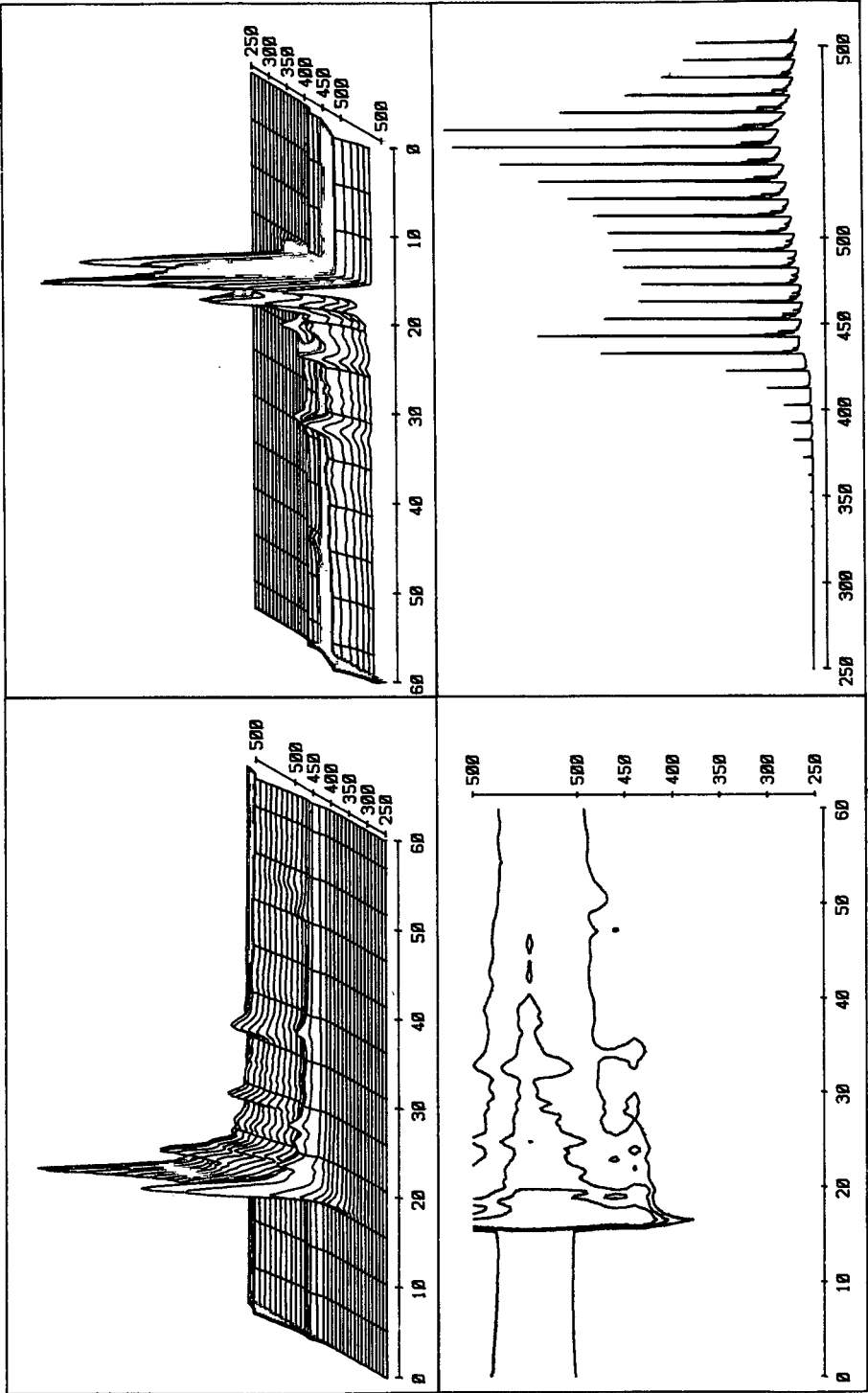


Fig. 2. Correlation chromatograms for Kinzmarituli wine.

togram situated above is shifted with respect to the one below it by a certain value determined mainly by convenience of representation. The isometric projections obtained through the above procedures are usually termed "three-dimensional", which is wrong as there are only two independent variables, time and temperature. The inverted isometric projection provides some additional information on peaks that are overlapped in the conventional representation of the data.

One-dimensional cuts can be obtained, for example, at heights of 0.1, 0.2, 0.3 or 0.5 relative to the maximum height using another useful technique. The temperature dependences of the formation of the separate components can be readily plotted with the use of one-dimensional cuts of the two-dimensional chromatograms.

If we determine the total area of all the peaks on the chromatograms, we obtain the total amount of all the gaseous products of pyrolysis, which contributes to the information acquired by thermogravimetry. For each particular peak data on the retention time and the corresponding peak heights for any of the points concerned are obtained. Using these data, one can calculate the areas of all the peaks and their proportions and obtain any individual chromatograms.

Finally, these experimental data can be used to obtain contour maps. If we cut the surface area of the two-dimensional chromatogram by the plane parallel to the x - y plane at a given height (0.1, 0.2, 0.5) and then project the plane of the cut line, we obtain a contour map. The resulting isolines exactly represent the positions of the peaks on the two-dimensional chromatogram.

Figs. 1 and 2 show the main types of correlation chromatograms for two kinds of wines, Tibaani and Kinzmariuli. A substantial difference in the general views of the chromatograms can be easily seen. Also, one can see the possibility for the temperature to be measured at the beginning of the decomposition of the biopolymer complexes of both kinds of wines. These temperatures differ substantially.

Correlation chromatograms of wine biopolymers could make it possible to identify the wines according to their grading features by using a "fingerprint" method. Also, it is possible to use factor analysis to describe the correlation chromatograms of wine.

Note

High-performance liquid chromatography of brassinosteroids in plants with derivatization using 9-phenanthreneboronic acid

KEIJI GAMOH*

Faculty of Education, Kochi University, 2-5-1 Akebono-cho, Kochi-shi 780 (Japan)
and

KUMIKO OMOTE, NAOKO OKAMOTO and SUGURU TAKATSUTO*

Department of Chemistry, Joetsu University of Education, Joetsu-shi, Niigata 943 (Japan)
(First received October 3rd, 1988; revised manuscript received January 24th, 1989)

Since the discovery of brassinolide (**1**) as a new plant growth hormonal steroid¹, a number of related steroids (general term brassinosteroids) have been found to occur in a wide variety of higher plants². The structures of some brassinosteroids are shown in Fig. 1. In a previous paper³, we described the microanalysis of brassinosteroids using a labelling technique with 1-naphthaleneboronic acid. Although the boronic acid was very useful as a labelling reagent for brassinosteroids that have two vicinal diol groups in both the A ring and the side-chain, the resulting naphthaleneboronates were detected with ultraviolet absorption at 280 nm. As a continuation of our research on microanalytical methods for brassinosteroids, we have screened a number of derivatizing reagents in the hope of developing a more sensitive and selective analytical method.

In this paper, we report the determination of brassinosteroids as bis-9-phenanthreneboronate derivatives by high-performance liquid chromatography (HPLC) with fluorimetric detection and its application to the identification of brassinosteroids in plant extracts.

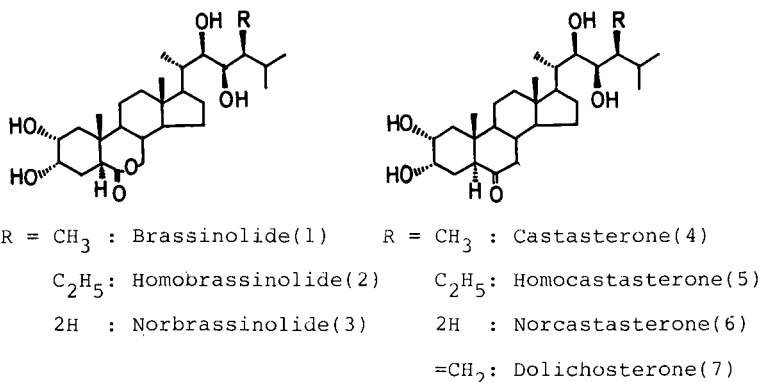


Fig. 1. Structure of brassinosteroids.

EXPERIMENTAL

Plant material

The bee-collected pollen of broad bean (*Vicia faba* L.) was obtained from China and was kindly supplied by Nippon Kayaku (Tokyo, Japan). Identification of the pollen was carried out by microscopic examination.

Rice-lamina inclination test

The procedure for the purification of brassinosteroids was based on the rice-lamina inclination test. The bioassay was carried out according to our previous method⁴ using etiolated seedlings of rice (*Oryza sativa* L. cv. Koshihikari).

Chemicals

Authentic brassinosteroids, brassinolide (**1**), 28-homobrassinolide (**2**), 28-norbrassinolide (**3**), castasterone (**4**), 28-homocastasterone (**5**), 28-norcastasterone (**6**) and dolichosterone (**7**) were synthesized in our laboratory⁵⁻⁷. 9-Phenanthreneboronic acid (PBA) was purchased from Kanto Chemical (Tokyo, Japan). All other reagents were of analytical-reagent grade.

Extraction of brassinosteroids

The broad bean pollen (25 g) was extracted with methanol (200 ml) for 1 week and then ethyl acetate-methanol (1:1, v/v) (200 ml) for 1 week. The combined extracts were concentrated below 30°C *in vacuo* and then partitioned between ethyl acetate (100 ml, twice) and water (100 ml). The organic layer was concentrated and further partitioned between *n*-hexane (100 ml) and methanol-water (9:1, v/v) (100 ml, twice). The aqueous methanol layer was concentrated and then partitioned between ethyl acetate (100 ml) and saturated sodium hydrogencarbonate solution (100 ml). The organic layer was dried over anhydrous magnesium sulphate, filtered and concentrated *in vacuo* to give a biologically active oil (240 mg).

Silica gel adsorption chromatography

The active oil (240 mg) was charged on to a column (200 mm × 10 mm I.D.) of silica gel (Merk Kieselgel 60, 70-230 mesh). Elution was carried out stepwise with chloroform (50 ml) and then chloroform-methanol (98:2, 50 ml; 95:5, 50 ml; 90:10, 50 ml; 85:15, 50 ml; 80:20, 50 ml). The eluates were collected in 25-ml fractions. One hundredth of each fraction was subjected to the bioassay. Biological activity appeared in the 5-10% methanol in chloroform eluates and these fractions were combined and concentrated *in vacuo* to give the active fraction (31.3 mg).

Preparative thin-layer chromatography

The active fraction (31.3 mg) was applied to a precoated silica gel plate (Merk Kieselgel 60 F₂₅₄ precoated plate, 20 × 20 cm², 0.25 mm film thickness). The plate was developed with chloroform-methanol (10:1). Silica gel was scraped off into ten bands and each was eluted with ethyl acetate. One hundredth of each fraction was subjected to the bioassay. The activity appeared in the region of $R_F = 0.2-0.4$ and these fractions were combined and concentrated *in vacuo* to give a partially purified fraction (2.8 mg). This active fraction was estimated to contain several micrograms of

brassinosteroids by the rice-lamina inclination test using brassinolide as a reference compound.

Derivatization

The standard mixture of the biologically active brassinosteroid fraction was dissolved in a small amount of acetonitrile (100 μ l). To the solution, 100 μ l of 9-phenanthreneboronic acid⁸ (1 mg/ml) in 1% (v/v) pyridine–acetonitrile was added. The mixture was heated at 70°C for 10 min. After cooling, several microlitres of the solution were injected directly into the analytical column (Fig. 2). The electron-impact (EI) mass spectrum of the bisphenanthreneboronate of brassinolide afforded a molecular ion at m/z 852 (Shimadzu GCMS-QP 1000A direct inlet system with EI ionization source; data not shown).

HPLC analysis

A Shimadzu Model LC-6A chromatograph equipped with a fluorimetric detector (Shimadzu Model RF-535) was employed (Excitation 305 nm, Emission 375 nm). A reversed-phase column of STR ODS-H (150 mm \times 4.0 mm I.D.) (Shimadzu Techno Research, Kyoto, Japan) was used at 45°C. Samples were injected into the column using a Rheodyne rotary valve 7125 syringe-loading injector. The optimum mobile phase for the separation of the brassinosteroid bisphenanthreneboronates was acetonitrile–water (90:10) at a flow-rate of 0.8 ml/min.

RESULTS AND DISCUSSION

HPLC analysis

For the separation of the brassinosteroid bisphenanthreneboronates, an STR ODS-H column was found to afford better resolution than several conventional ODS columns tested. We examined the detection limit of these brassinosteroid derivatives using the ODS column and acetonitrile–water as the mobile phase.

As shown in Fig. 3, the bisphenanthreneboronates of norbrassinolide (**3**), brassinolide (**1**), dolichosterone (**7**), norcastasterone (**6**), homobrassinolide (**2**), castasterone (**4**) and homocastasterone (**5**) afforded sharp peaks at 7.2, 8.6, 9.1, 10.0, 10.6, 12.1 and 15.1 min, respectively. The amounts of these brassinosteroids were 200 pg for **5**, 150 pg for **3**, **6** and **4**, 120 pg for **1** and **7** and 75 pg for **2**. The method presented using 9-phenanthreneboronic acid gave a detection limit for brassinolide 50 pg (*ca.* 500

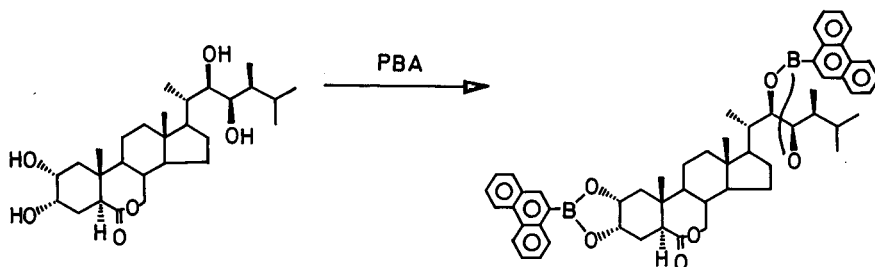


Fig. 2. Reaction of brassinolide with 9-phenanthreneboronic acid (PBA).

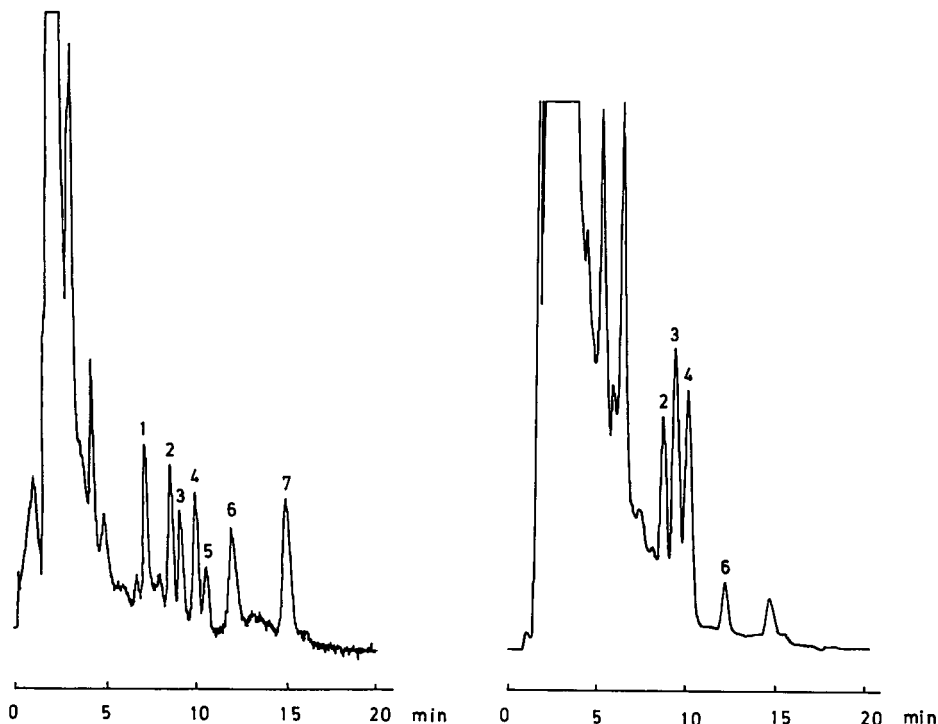


Fig. 3. Chromatogram of bisphenanthreneboronates of authentic brassinosteroids. Peaks: 1 = norbrassinolide (3); 2 = brassinolide (1); 3 = dolichosterone (7); 4 = norcastasterone (6); 5 = homobrassinolide (2); 6 = castasterone (4); 7 = homocastasterone (5). Conditions: STR ODS-H ($5\ \mu\text{m}$) column, $15\ \text{cm} \times 4.0\ \text{mm}$ I.D.; mobile phase, acetonitrile–water (9:1); flow-rate, $0.8\ \text{ml/min}$; temperature, 45°C .

Fig. 4. Chromatogram of bisphenanthreneboronates of natural brassinosteroids extracted from the pollen of broad bean. Peaks: 2 = brassinolide (1); 3 = dolichosterone (7); 4 = norcastasterone (6); 6 = castasterone (4). Conditions as in Fig. 3.

fmol) per injection with a signal-to-noise ratio of 3. A five-fold increase in detectability was observed when the fluorescence of the phenanthreneboronates was compared with UV absorption detection of the naphthaleneboronates.

Application

The method was applied to the identification and determination of brassinosteroids in the bee-collected pollen of the broad bean (*Vicia faba* L.). Although brassinosteroids have previously been reported in the pollen⁹, we examined independently the same pollen in this present study. The biologically active fraction ($280\ \mu\text{g}$) obtained from the pollen was derivatized with 9-phenanthreneboronic acid as described above and analysed by HPLC. As shown in Fig. 4, brassinolide (1), dolichosterone (7), norcastasterone (6) and castasterone (4) were determined. The amounts of these brassinosteroids were calculated by use of authentic samples for calibration and the results were summarized in Table I. The amount of brassinolide calculated was in good agreement with that reported using gas chromatography–mass spectrometry⁹.

TABLE I

AMOUNTS OF BRASSINOSTEROIDS IN THE POLLEN OF BROAD BEAN DETERMINED BY HPLC

<i>Brassinosteroid</i>	<i>Amount (ng/g)^a</i>
Brassinolide (1)	180.8 ± 3.1
Dolichosterone (7)	536.5 ± 4.5
Norcastasterone (6)	628.4 ± 3.6
Castasterone (4)	134.4 ± 2.2

^a Mean ± S.D. (n=4).

Hence it is possible to determine the other brassinosteroids in the pollen by the proposed HPLC method.

A recovery test was carried out by adding a mixture of 4 ng of brassinolide and 6 ng of castasterone to the divided extraction fraction. The samples were derivatized as described above and analysed by HPLC. The added compounds were recovered at a rate of more than 92% (n=4, coefficient of variation = 2.2%).

In conclusion, we have developed an HPLC method with fluorescence detection for the determination of brassinosteroids and demonstrated its usefulness in the identification of several brassinosteroids in broad bean pollen. As the bisphenanthreneboronate was found to be a sensitive and suitable derivative, simultaneous identification and determination of brassinosteroids in plant extracts could be performed by this HPLC method.

REFERENCES

- 1 M. D. Grove, G. F. Spencer, W. K. Rohwedder, N. B. Mandava, J. F. Worley, J. D. Warthen, Jr., G. L. Steffens, J. L. Flippen-Anderson and J. C. Cook, Jr., *Nature (London)*, 281 (1979) 216.
- 2 G. Adam and V. Marguardt, *Phytochemistry*, 25 (1986) 1787.
- 3 K. Gamoh, T. Kitsawa, S. Takatsuto, Y. Fujimoto and N. Ikekawa, *Anal. Sci.*, 4 (1988) 533.
- 4 S. Takatsuto, N. Yazawa, N. Ikekawa, T. Morishita and H. Abe, *Phytochemistry*, 22 (1983) 1393.
- 5 S. Takatsuto and N. Ikekawa, *J. Chem. Soc., Perkin Trans. 1*, (1983) 2133.
- 6 S. Takatsuto and N. Ikekawa, *Chem. Pharm. Bull.*, 30 (1982) 4181.
- 7 S. Takatsuto, N. Yazawa, M. Ishiguro, M. Morisaka and N. Ikekawa, *J. Chem. Soc., Perkin Trans. 1*, (1984) 139.
- 8 C. F. Poole, S. Singhawangcha, A. Zlatkis and E. D. Morgan, *J. High Resolut. Chromatogr. Chromatogr. Commun.*, 1 (1978) 96.
- 9 N. Ikekawa, F. Nishiyama and Y. Fujimoto, *Chem. Pharm. Bull.*, 36 (1988) 405.

CHROM. 21 415

Note

Liquid chromatographic separation of racemates on acetylated or carbamoylated β -cyclodextrin-bonded stationary phases

MINORU TANAKA* and TOSHIYUKI SHONO

Department of Applied Chemistry, Faculty of Engineering, Osaka University, Yamada-oka, Suita, Osaka 565 (Japan)

DAO-QIAN ZHU

Dalian Institute of Chemical Physics, Chinese Academy of Sciences, 129 Street, Dalian (China)
and

YOSHIHIRO KAWAGUCHI

NTT Opto-Electronics Laboratories, Morinosato, Wakamiya, Atsugi, Kanagawa 234-01 (Japan)

(First received January 17th, 1989; revised manuscript received February 15th, 1989)

Cyclodextrins (CDs) and their chemically modified derivatives have been the subject of numerous investigations and have been used for various purposes. It is well known that the chemical modification of CDs brings about changes in the depth of the CD cavity, in the hydrogen-bonding ability and in various other physical properties. In previous papers, we reported selectivity changes in solute retention after acetylation^{1–3} or carbamoylation⁴ of unmodified CD-bonded stationary phases in high-performance liquid chromatography (HPLC).

Recently, there has been considerable interest in separating racemates with CD-bonded stationary phases. The unmodified β -CD phases have been especially widely employed for this purpose^{5–12}. It is of great interest to investigate optical resolution with chemically modified CD stationary phases, because their selectivity change may be reflected in the separation of racemates. To our knowledge, only the separation of optical isomers of norgestrel on an acetylated β -CD stationary phase has been reported briefly⁶.

In this paper, we describe the preliminary HPLC separation of some racemates on acetylated or carbamoylated β -CD stationary phases.

EXPERIMENTAL

Preparation of β -CD stationary phases

Sodium salt of unmodified β -CD was coupled to 3-glycidoxypropyl silica (Gp-silica) in *N,N*-dimethylformamide at 130°C for 4 h¹³. The stationary phase thus obtained is denoted CD-Gp-silica after end-capping of the silanols with 1,1,1,3,3,3-hexamethyldisilazane in hexane. The amount of β -CD immobilized was evaluated to be 54.2 μ mol/g by elemental analysis.

CD-Gp-silica (2.0 g) was treated with acetic anhydride (8 ml) in dry pyridine (30

ml) at 45°C for 6 h. The acetylated stationary phase is denoted Ac-CD-Gp-silica.

CD-Gp-silica (2.5 g) was carbamoylated in pyridine (100 ml) at 30°C by adding methyl isocyanate (1 g) three times at intervals of 24 h. Similarly, CD-Gp-silica (2.5 g) was treated with phenyl isocyanate (2.4 g) in pyridine (80 ml) at 70°C for 10 h. The resulting methyl- or phenylcarbamoylated β -CD stationary phase is denoted Me-CD-Gp-silica or Ph-CD-Gp-silica, respectively.

Materials and chromatography

Silica gel (5 μ m) and β -CD were obtained from Wako (Osaka, Japan) and other chemicals of analytical-reagent grade from Wako, Tokyo Kasei (Tokyo, Japan) or Sigma (St. Louis, MO, U.S.A.).

The HPLC system used consisted of a Shimadzu (Kyoto, Japan) LC-6A pump and a Waters Assoc. (Milford, MA, U.S.A.) 440 UV detector operating at 254 nm. Each stationary phase was packed into a stainless-steel column (15 cm \times 4 mm I.D.) by the balanced-density slurry method. The flow-rate of the eluent [methanol-1% triethylammonium acetate (TEAA) mixtures] was 1.0 ml/min.

RESULTS AND DISCUSSION

In this study, the extent of separation between the two peaks of a racemate is represented by

$$R' = \frac{H - H'}{H} \cdot 100$$

where H and H' are the height of the first eluted peak and that of the valley between the two peaks, respectively, for a clear separation. In this definition, the greater the value of R' , the better is the resolution, and $R' = 100$ represents a complete separation of the two peaks.

Table I gives the R' values for eight pairs of dansylamino acid enantiomers together with their retention times (t_R) and separation factors (α) on both CD-Gp-silica and Ac-CD-Gp-silica in methanol-TEAA at pH 5.0. A decrease in retention was found for these solutes on CD-Gp-silica with increasing proportion of methanol in the eluent. A similar decrease in the retention also occurred as the pH of TEAA increased; the solute retention in methanol-TEAA (50:50) at pH 6.0 was about half with that at pH 5.0. Considering the separations of the enantiomers and the total analysis times, the optimum eluent was methanol-TEAA (50:50) at pH 5.0 for CD-Gp-silica, as indicated in Table I.

In chiral recognition and separation in chromatographic processes using unmodified CD, the interaction of the guest (solute) with the 2- or 3-hydroxy groups at the mouth of the CD cavity is considered to play an important role, in addition to a tight fit between the guest and the CD host¹⁰. Therefore, it is interesting to compare the separation before and after the chemical modification of these hydroxyl groups. In this work, acetylation and methyl- and phenylcarbamoylation were investigated, because each modified CD stationary phase could be obtained by treating the same unmodified phase and probably contained the same amount of CD. It is apparent from Table I that the acetylation of CD-Gp-silica considerably enhances the separation of

TABLE I

SEPARATION OF DANSYLAMINO ACID ENANTIOMERS ON β -CD STATIONARY PHASES BEFORE AND AFTER ACETYLATION IN METHANOL-TEAA (50:50) AT pH 5.0.

Dansylamino acid	Isomer	CD-Gp-silica			Ac-CD-Gp-silica			Ac-CD-Gp-silica ^a		
		t_R (min)	α	R'	t_R (min)	α	R'	t_R (min)	α	R'
α -Amino- <i>n</i> -butyric acid	L	8.70			17.25			9.36		
	D	9.30	1.08	22.4	19.92	1.15	94.4	10.71	1.17	98.7
Leucine	L	11.70			21.30			11.10		
	D	14.10	1.25	93.5	24.74	1.18	100	13.05	1.20	98.2
Methionine	L	9.75			17.85			10.50		
	D	10.56	1.09	49.7	19.75	1.12	80.2	11.70	1.15	88.3
Norvaline	L	9.06			16.20			9.24		
	D	9.69	1.09	28.1	18.15	1.13	90.0	10.44	1.15	94.8
Phenylalanine	L	16.95			31.95			15.00		
	D	18.96	1.14	72.9	36.90	1.14	91.7	17.01	1.15	95.6
Serine	L	7.95			14.40			10.23		
	D	8.49	1.09	34.7	16.50	1.17	94.8	11.91	1.19	100
Threonine	L	8.16			16.68			10.26		
	D	9.12	1.13	81.4	20.58	1.26	100	12.84	1.29	100
Valine	L	9.54			20.40			10.50		
	D	10.50	1.13	64.1	24.30	1.20	98.8	12.54	1.23	100

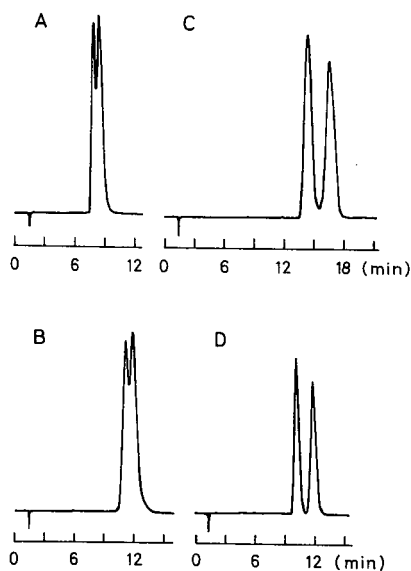
^a Eluted with methanol-TEAA (70:30) at pH 5.0.

Fig. 1. Enantiomeric separation of dansyl-D,L-serine on CD-Gp-silica in methanol-TEAA at pH 5.0, (A) (50:50) and (B) (40:60), and on Ac-CD-Gp-silica in methanol-TEAA at pH 5.0, (C) (50:50) and (D) (70:30).

TABLE II
SEPARATION OF ENANTIOMERS ON β -CD STATIONARY PHASES BEFORE AND AFTER CHEMICAL MODIFICATION
The methanol content and pH of TEAA in the eluent are given in parentheses.

Solute	CD-Gp-silica			Ac-CD-Gp-silica			Me-CD-Gp-silica			Ph-CD-Gp-silica		
	t_R (min)	α	R'	t_R (min)	α	R'	t_R (min)	α	R'	t_R (min)	α	R'
Alanine- β -naphthylamide		(30%, pH 5.1)		(10%, pH 4.5)			(20%, pH 4.95)			(30%, pH 5.1)		
	L	3.66	1.36	93.1	9.60	1.24	98.0	5.85	1.12	36.0	9.15	1.27
	D	4.41			11.55			6.45			11.34	50.5
α -Aminoethylbenzene				(0%, pH 5.1)			(0%, pH 4.95)					
	L			2.30	1.22	84.3	2.26					
	D			2.57			2.42					
α -Hydroxyethylferrocene		(30%, pH 5.1)		(30%, pH 5.0)								
		27.30 ^a	1.09	59.5	65.40 ^a	1.10	63.0					
		29.70			71.70							
Mandelic acid methyl ester				(0%, pH 5.0)								
	R			15.06	1.06	18.1						
	S			15.90								

^a Retention time of the first-eluted enantiomer.

the enantiomers for each dansylamino acid eluted with methanol-TEAA (50:50). Each solute, however, exhibited a relatively long retention time on Ac-CD-Gp-silica in this instance. Consequently, the methanol content in the eluent was changed from 50 to 70%, in order to reduce the retention [nearly comparable to that on CD-Gp-silica eluted with methanol-TEAA (50:50)]. This change resulted in a further improvement in separation, except for dansylleucine.

Fig. 1 shows typical liquid chromatograms for the separation of dansyl-D,L-serine. Fig. 1A and C represent the separation of the enantiomers on CD-Gp-silica and Ac-CD-Gp-silica, respectively, with methanol-TEAA (50:50) at pH 5.0. Apparently, the separation of the enantiomers is much better after the acetylation. The methanol concentration was adjusted to give the same retention time (*ca.* 12 min) for both CD stationary phases. As the result, the R' value decreased from 34.7 (Fig. 1A) to 25.9 (Fig. 1B) on CD-Gp-silica, whereas it increased from 94.8 (Fig. 1C) to 100 (Fig. 1D) on Ac-CD-Gp-silica. The enantiomers can be separated completely on the acetylated CD stationary phase with methanol-TEAA (70:30) at pH 5.0. Hence acetylation of CD-Gp-silica enhanced the chiral recognition for the dansylamino acid enantiomers, whereas both methyl- and phenylcarbamoylation removed it.

An attempt was also made to separate several other solutes, and some of the results are given in Table II. Although the eluent conditions were not identical, acetylation improved the enantiomeric separation for these solutes. In contrast, methyl- and phenylcarbamoylation resulted in a substantial decrease in the enantioselectivity of the modified CD stationary phases.

Unmodified CD-Gp-silica has many terminal hydroxyl groups produced by the deactivation of the unreacted 3-glycidoxypropyl groups with CD on Gp-silica (*ca.* 600 $\mu\text{mol/g}$). These hydroxyl groups are probably acetylated or carbamoylated in addition to those of the immobilized CD moiety. Moreover, the spacer arm linking CD to silica gel in CD-Gp-silica contains one hydroxyl group formed on coupling CD. It is also possible for this hydroxyl group to be acetylated or carbamoylated. In this context, it is reasonably accepted that the chemical modification of some and/or all of these hydroxyl groups affects the interaction between the solute and the stationary phase (the CD moiety and/or the non-CD-containing moiety) and that this brings about the considerable change in the enantioselectivity after the modification. Further work is needed for a more convincing explanation.

REFERENCES

- 1 Y. Kawaguchi, M. Tanaka, M. Nakae, K. Funazo and T. Shono, *Anal. Chem.*, 55 (1983) 1852.
- 2 M. Tanaka, Y. Kawaguchi and T. Shono, *J. Chromatogr.*, 267 (1983) 285.
- 3 M. Tanaka, Y. Kawaguchi, T. Shono, M. Uebori and Y. Kuge, *J. Chromatogr.*, 301 (1984) 345.
- 4 M. Tanaka, H. Ikeda and T. Shono, *J. Chromatogr.*, 398 (1987) 165.
- 5 W. L. Hinze, T. E. Riehl, D. W. Armstrong, W. DeMond, A. Alak and T. Ward, *Anal. Chem.*, 57 (1985) 237.
- 6 T. J. Ward and D. W. Armstrong, *J. Liq. Chromatogr.*, 9 (1986) 407.
- 7 K. G. Feitsma, B. F. H. Drenth and R. A. de Zeeuw, *J. Chromatogr.*, 387 (1987) 447.
- 8 J. H. Maguire, *J. Chromatogr.*, 387 (1987) 453.
- 9 P. Macaudiere, M. Caud, R. Rosset and A. Tambute, *J. Chromatogr.*, 405 (1987) 135.
- 10 S. M. Han, Y. I. Han and D. W. Armstrong, *J. Chromatogr.*, 441 (1988) 376, and references cited therein.
- 11 H. Y. Aboul-Enein, M. R. Islam and S. A. Bakr, *J. Liq. Chromatogr.*, 11 (1988) 1485.
- 12 J. I. Seeman, H. V. Secor, D. W. Armstrong, K. D. Timmons and T. J. Ward, *Anal. Chem.*, 60 (1988) 2120.
- 13 D. W. Armstrong, *U.S. Pat.*, 4 539 399, 1985.

Note

Milligram-scale separation of optical isomers of 2-pentafluoroethylalanine and 2-trifluoromethylalanine by medium-performance reversed-phase chromatography

JOHN W. KELLER* and KATSUHIRO NIWA^a

Department of Chemistry, University of Alaska Fairbanks, Fairbanks, AK 99775-0520 (U.S.A.)

(First received December 28th, 1988; revised manuscript received February 21st, 1989)

Reversed-phase separation of amino acid optical isomers using a copper(II)-amino acid mobile phase is now a standard analytical tool^{1,2}. We have previously used this method for analytical-scale optical resolutions of several polyfluoro 2,2-dialkylglycines using a copper(II)-L-phenylalanine mobile phase³. We report here a preparative version of this method in which a column packed with commercially available 40 μm reversed-phase silica was used to resolve milligram quantities of 2-pentafluoroethylalanine (PEA) and 2-trifluoromethylalanine (TMA).

PEA and TMA are analogues of isovaline and 2-methylalanine. The latter are major constituents of alamethicin-type cytotoxic polypeptides produced by soil fungi⁴ and are also substrates of the *Pseudomonas cepacia* 2,2-dialkylglycine decarboxylase⁵⁻⁷. The polyfluoro analogues, both racemic and optically active forms, are being investigated in our laboratory as potential inhibitors of the dialkylglycine decarboxylase or as components of synthetic peptides. The optical isomers of TMA have been prepared enzymatically in 98% enantiomeric excess by stereospecific hydrolysis of the N-trifluoroacetyl derivative by hog kidney aminoacylase^{3,8}. However, other polyfluoro dialkylglycines cannot be resolved this way. For example, the N-acyl derivatives of PEA and 2-trifluoromethyl-2-aminobutanoic acid³ are not hydrolyzed by hog kidney aminoacylase⁹. Thus we have developed a chromatographic method that resolves polyfluoro dialkylglycines on the preparative scale and requires only commonly available reagents and equipment.

MATERIALS AND METHODS

Racemic 2-pentafluoroethylalanine³ and 2-trifluoromethylalanine¹⁰ were prepared by literature methods.

Preparative chromatography was carried out with Baker octadecyl silica for flash chromatography (40- μm irregular particles). Bio-Rad Econocolumns (25 \times 1.5 cm or 7.3 \times 1.5 cm) equipped with a flow adaptor and a home-made constant-

^a Present address: Department of Industrial Chemistry, Faculty of Engineering, Gifu University, Gifu 501-11, Japan.

temperature jacket were slurry-packed (acetonitrile suspension, gravity flow), then equilibrated with mobile phase [2 mM L-phenylalanine, 1 mM copper(II) acetate, 3 mM potassium acetate adjusted to pH 4.4 with acetic acid, to which was added 2% (TMA) or 8% (PEA), v/v, acetonitrile]. Mobile phase was delivered with a Gilson Minipulse peristaltic pump through a Rheodyne Type 50 rotary injection valve. The eluate was monitored at 280 nm with a Gilson Holochrome detector.

During initial equilibration of the 7.3×1.5 cm column with mobile phase, phenylalanine concentrations in the eluate were determined spectrophotometrically after derivatization with *o*-phthaldialdehyde¹¹. Copper(II) concentrations in the eluate were determined by atomic absorption spectrometry¹².

Copper and phenylalanine were removed from collected fractions by passage through Dowex 50 (10×1 cm, H⁺), which does not bind the strongly acidic polyfluoro amino acids³. Eluate from the Dowex column containing the polyfluoro amino acid was dried *in vacuo* and the residue weighed.

Analytical high-performance liquid chromatography (HPLC) of fluoro amino acids was carried out at room temperature with a 250×4.6 mm C₁₈ silica column (Alltech/Applied Science 60130, 5 μ m) with eluate monitored as above. In some experiments the spectrophotometer output was digitized, stored, smoothed and plotted on an IBM-PC microcomputer equipped with a Data Translation DT-2805 A/D board and ASYST software.

RESULTS AND DISCUSSION

Reversed-phase columns must be loaded with copper by equilibration with the copper-amino acid mobile phase before they can be used for amino acid separation¹⁻³. Since the degree of copper loading on the column can affect retention and resolution¹, the equilibration process was studied first. The glass chromatography column facilitated observation of this process. It was observed that as copper(II)-L-phenylalanine mobile phase was pumped through the newly packed column, a dark blue zone appeared at the top of the column separated from the white lower portion by a narrow (3 mm) transition zone. As the equilibration progressed, the narrow transition zone moved downward until the column was completely blue.

Chemical analysis of the eluate during the equilibration process suggests that the blue zone of the column is the portion saturated with Cu(L-Phe)₂. During column equilibration the position of the transition zone and the concentrations of copper and phenylalanine in the eluate were measured periodically. The data from equilibration of a 7.3×1.5 cm packed bed of C₁₈ silica with copper(II)-L-phenylalanine mobile phase are shown in Fig. 1. These data indicate that, except for the first 100 ml, the eluate contained phenylalanine and copper in the nearly constant molar ratio of 2, suggesting that the major bound species is Cu(L-Phe)₂. The higher phenylalanine:copper ratio in the early part of the equilibration may have been caused by displacement of L-phenylalanine from Cu(L-Phe)₂ by higher-affinity silicate sites.

The equilibration data in Fig. 1 also allow the calculation of the ligand concentration on the copper-saturated column. Integration of the phenylalanine concentration curve in Fig. 1 reveals that a total of 1.1 mmol phenylalanine was bound during equilibration. Therefore, the ligand concentration in the packed column was 86 mM, which is significantly lower than that of amino acid ligands covalently linked to silica, which is typically 350-400 mM¹³.

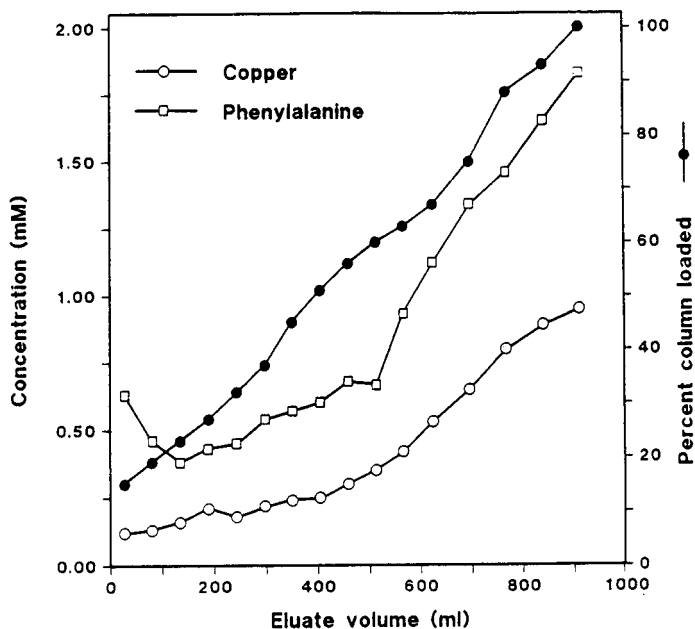


Fig. 1. Changes in eluate composition and column packing color during loading of a new 7.3×1.5 cm C_{18} column with copper(II)-L-phenylalanine mobile phase. Percent column loaded = $(L_b/L_t) \times 100$, where L_b = length of the blue portion and L_t = total length of the packed column.

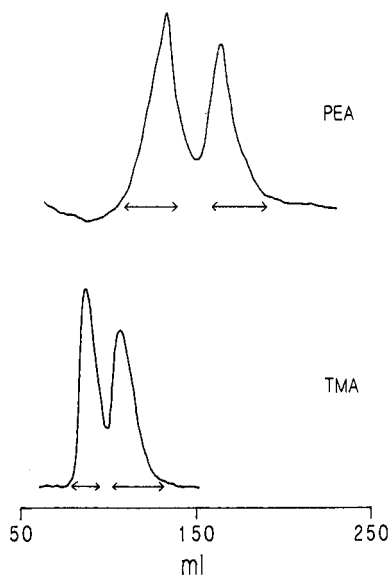


Fig. 2. Preparative chromatograms showing fractions combined for subsequent isolation. Samples: 4 mg of racemic PEA or TMA dissolved in 1 ml of mobile phase. Mobile phase: 2 mM L-phenylalanine, 1 mM copper(II) acetate, 3 mM potassium acetate to pH 4.4 with acetic acid containing 2% (TMA) or 8% (PEA) acetonitrile.

TABLE I

STRUCTURES, CAPACITY FACTORS (k'_1, k'_2) AND ENANTIOSELECTIVITIES ($\alpha = k/k'$) OF 2,2-DIALKYLGLYCINES ($R_1R_2CNH_2COOH$) IN COPPER(II)-L-PHENYLALANINE REVERSED-PHASE CHROMATOGRAPHY

Compound	R_1	R_2	Analytical			Preparative		
			k'_1, k'_2	α	Acetonitrile (%)	k'_p, k'_2	α	Acetonitrile (%)
2-Pentafluoroethylalanine (PEA)	CF_2CF_3	CH_3	5.0, 7.0	1.4	6	7.8, 9.7	1.2	2
2-Trifluoromethylalanine (TMA)	CF_3	CH_3	12.9, 16.0	1.2	12	12.3, 15.5	1.2	8

Temperature and sample size parameters were tested in preliminary experiments with a 7.3×1.5 cm column. It was found that the resolution increased as the operating temperature increased from 25 to 50°C; however, significant column degradation was observed at 50°C, thus an operating temperature of 40°C was chosen. Resolution was adequate at this temperature and the column was stable for weeks of daily operation. As expected, resolution decreased with increasing sample size; therefore the largest sample size consistent with a near-baseline resolution, 4 mg of racemic amino acid in 1 ml of solution, was chosen.

Typical chromatograms obtained when 4-mg samples of racemic PEA or TMA were applied to a copper-saturated 25×1.5 cm column are shown in Fig. 2 (see also Table I). As observed in HPLC separations, the PEA isomers were more strongly retained than the TMA isomers, probably because of the increased hydrophobicity of the pentafluoroethyl substituent³. By analogy to TMA, the early-eluting PEA isomer

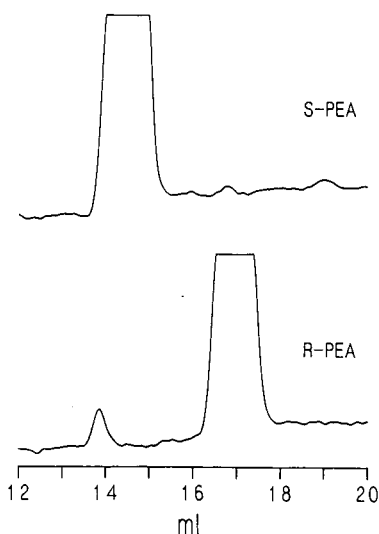


Fig. 3. Analytical HPLC of chromatographically resolved PEA isomers. Only the lowest 10% of the major peak is shown. Sample: 20 μ g; mobile phase as in Fig. 2 but with 12% acetonitrile.

is predicted to have the *S* configuration since this one has the smaller, less hydrophobic group in the pro-*S* position^{3,8,14}.

Nine PEA-samples (total 35 mg) were chromatographed; 17 and 14 mg respectively of the early- and late-eluting peaks were recovered from fractions combined as shown in Fig. 2. Optical-purity analysis of these samples by HPLC showed that the amino acid recovered from the early-eluting peak contained no measurable amounts of the late-eluting component; probably 0.1% of the minor isomer could have been observed above the baseline noise (Fig. 3). The late-eluting sample contained 5% of the early-eluting isomer.

Eight TMA samples (total 30 mg) were chromatographed, with 9 and 16 mg respectively recovered from the early (*S*) and late (*R*) eluting peaks (Fig. 2). HPLC analysis showed that the early (*S*) peak contained 0.5% of the *R* isomer and the late (*R*) peak contained 2.9% of the *S* isomer (Fig. 4).

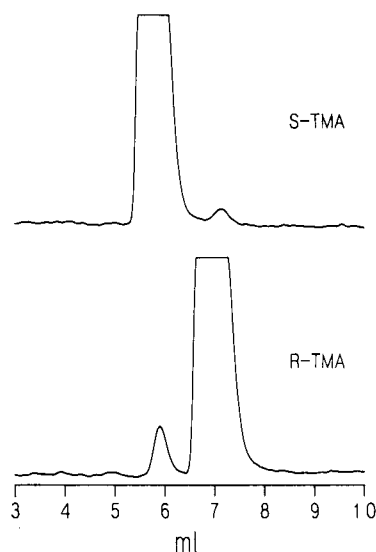


Fig. 4. Analytical HPLC of chromatographically resolved TMA isomers. Only the lowest 10% of the major peak is shown. Sample: 20 μ g; mobile phase as in Fig. 2 but with 6% acetonitrile.

This chromatographic method significantly improved the optical purity of the early-eluting (*S*) isomers of PEA and TMA compared to the *S*-TMA produced enzymatically, which contained 1% of the minor (*R*) isomer^{3,8}. However, the late-eluting (*R*) isomers of PEA and TMA both had lower optical purity (5.0% and 2.9% *S* isomer contamination, respectively) than the enzymatically produced *R*-TMA (1% *S*-TMA^{3,8}), although they were isolated from fractions taken from the apparent peak centers. This was probably caused by tailing of the early-eluting isomer. Therefore maximum optical purity of *R*-PEA or *R*-TMA could be obtained by collecting the early-eluting peak from chromatography of the racemic amino acid on a $\text{Cu}(\text{D-Phe})_2$ -loaded column.

Thus we have demonstrated the use of reversed-phase chromatography for preparation of milligram quantities of polyfluoro amino acids in high optical purity. This method should be useful for small-scale resolutions of some amino acids or for improving the optical purity of amino acids which have been partially resolved enzymatically. Successful application of the method requires subsequent separation of the resolved amino acid from phenylalanine.

REFERENCES

- 1 R. Wernicke, *J. Chromatogr. Sci.*, 23 (1985) 39.
- 2 S. Weinstein, *Angew. Chem., Int. Ed. Engl.*, 21 (1982) 218.
- 3 J. W. Keller and K. O. Dick, *J. Chromatogr.*, 367 (1986) 187.
- 4 H. Schmitt and G. Jung, *Justus Liebig's Ann. Chem.*, (1985) 321.
- 5 C. A. Lamartiniere, H. Itoh and W. B. Dempsey, *Biochemistry*, 10 (1971) 4783.
- 6 S. Sato, M. Honma and T. Shimomura, *Agric. Biol. Chem. (Tokyo)*, 42 (1976) 2341.
- 7 J. W. Keller and M. H. O'Leary, *Biochem. Biophys. Res. Commun.*, 90 (1979) 1104.
- 8 J. W. Keller and B. J. Hamilton, *Tetrahedron Lett.*, 27 (1986) 1249.
- 9 J. W. Keller and K. O. Dick, unpublished results.
- 10 H. N. Christensen and D. L. Oxender, *Biochim. Biophys. Acta.*, 74 (1963) 385.
- 11 V. K. Svedas, I. J. Galaev, I. L. Borisov and I. V. Berezin, *Anal. Biochem.*, 101 (1980) 188.
- 12 A. F. Greenberg, J. J. Connors and D. J. Jenkins (Editors), *Standard Methods for Examination of Water and Wastewater*, American Public Health Association, Washington, DC, 15th ed., 1981, p. 152.
- 13 P. Roumeliotis, K. K. Unger, A. A. Kurganov and V. A. Davankov, *J. Chromatogr.*, 255 (1983) 51.
- 14 J. W. Keller and C. S. Day, *Acta Crystallogr.*, 40C (1984) 1224.

Note

Isocratic reversed-phase high-performance liquid chromatographic assay for a cryptand-cryptate-free metal ion system

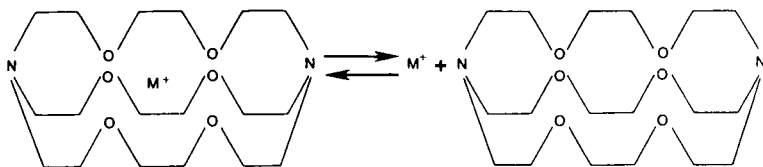
WILLIAM A. PETTIT*, BARBARA K. SWAILES and RICHARD E. PETERSON

Nuclear Medicine Service, Veterans Administration Medical Center and Department of Radiology, University of Iowa College of Medicine, Iowa City, IA 52246 (U.S.A.)

(First received December 6th, 1988; revised manuscript received February 27th, 1989)

Cryptands are metal ion complexing agents which consist of two bridgehead nitrogens connected by three ethoxy ether bridges. These compounds form inclusion complexes with a variety of metal ions¹. These complexes, known as cryptates, have varying stabilities dependent upon the relative sizes of the cryptand cavity and the metal ion, the type of solvating medium, and other factors²⁻⁴. Some potentially practical applications of cryptate complexes include removal of heavy metal ions from contaminated individuals⁵, and use as radionuclide carriers for blood flow measurements⁶ and in cancer therapy⁷.

Assay systems that have been used to determine the extent of cryptate formation from metal ions and cryptands are nuclear magnetic resonance^{8,9}, conductivity^{3,4,10}, and enthalpy and volume measurements^{10,11}. Recently developed chromatographic methods for assaying metal ion complexing molecules and their corresponding complexes were examined. A number of biogenic amines and some metal complexing species in this category have been separated by acidic solutions or buffers^{12,13}. These methods are not acceptable for our purposes since our principal objective was to evaluate the stability of cryptate complexes with a mobile phase which would not promote the equilibrium shown.



Cryptate complexes are known to decompose into the component species at acidic pH as a result of protonation of the bridgehead nitrogens⁸. The free electron pairs on the nitrogens are then unavailable for coordination with the encapsulated metal ion and the complex decomposes into cryptand and free metal ion. Alternatively, Bauer's method for the assay of acidic porphyrins using tetra-N-butylammonium hydroxide solution¹⁴ increased retention times of the components in our system significantly. Therefore, an organic mobile phase appeared most suitable for separation

of the organic components, *i.e.*, free cryptand and cryptate, followed by an aqueous phase of low pH to remove free metal ions¹⁵. In view of the potential utility of cryptands in clinical nuclear medicine, we report the development of a high-performance liquid chromatographic (HPLC) assay method for the individual components of a cryptand complexing system.

EXPERIMENTAL

The chromatographic system consisted of a Beckman Instruments (Fullerton, CA, U.S.A.) Model 116 pump, Model 166 UV detector, Model 170 radioisotope detector and Model 210A injector fitted with a 250- μ l loop. Detector outputs were monitored by a dual pen strip chart recorder. The column was a Hamilton (Las Vegas, NV, U.S.A.) PRP-1, 150 \times 4.1 mm I.D., of 5 μ m particle size. Barium chloride (¹³³Ba) was obtained from New England Nuclear (North Billerica, MA, U.S.A.). The cryptand, 4,7,13,16,21,24-hexaoxa-5,6-benzo-1,10-diazabicyclo[8.8.8]hexacosane (2B:2:2), was obtained from PCR (Gainesville, FL, U.S.A.) as a 50% toluene solution. Solvents used were HPLC-grade methanol and water that was purified by Milli-Q Plus system (Millipore, Bedford, MA, U.S.A.). The buffer used to elute free barium ions was prepared from reagent-grade chemicals and consisted of 14.1 mM citric acid, 5.88 mM sodium dihydrogen phosphate and 0.079 mM ethylenediamine tetraacetic acid (EDTA). The buffer was prepared at 10 fold concentration with 20% ethanol by volume. The buffer was diluted as needed and had a pH of 2.7. All solvents were filtered through a sintered glass filter prior to use. The column was protected by a PRP-1 pre-column. Standard methanol solutions were prepared for ultraviolet (UV) analysis from weighed samples of 2B:2:2 recovered from the toluene solution. Spectra were obtained on a Beckman DU-40 ultraviolet-visible spectrometer.

Complex formation

A weighed sample of 2B:2:2 was dissolved in 2 ml of HPLC-graded methanol. In a test tube 5–10 μ Ci ¹³³BA (20–40 μ l) was placed with a slight molar excess of cold BaCl₂ and evaporated to dryness. The methanol solution of 2B:2:2 was added to the BaCl₂ residue and the resulting mixture was mixed for 5 min. The solution was allowed to stand for 15 min. The methanol was then evaporated under a stream of nitrogen and the oily residue was extracted two times with 1 ml of methylene chloride. The extracts were dried over anhydrous sodium sulfate, decanted, and taken to dryness under a stream of nitrogen. The residue was dissolved in 2 ml of HPLC-grade methanol and filtered through a 0.45- μ m filter prior to analysis.

Method of chromatography

Methanol was used to elute 2B:2:2 and its corresponding complex with Ba²⁺. The column was then washed with the citrate-phosphate buffer to elute free barium ions. Sample size varied from 10–100 μ l. The flow-rate was 0.5 ml/min. The system was recycled between runs by washing the column with methanol-water (2:1).

HPLC column recoveries

Each component of the mixture in the complex equilibrium was subject to column recovery experiments using either the UV absorbance at 275 nm (2B:2:2) or

scintillation counting of radioactivity (complex and free Ba^{2+}). Counting standards and a standard curve generated from the UV absorbance of known concentrations of 2B:2:2 at 275 nm were used to determine percent recoveries of peaks eluted from the column. Scintillation counting of samples was performed on a Beckman gamma 4000.

RESULTS AND DISCUSSION

Both 2B:2:2 and the 2B:2:2 complex with barium ion were eluted from the column in methanol, with retention volumes of 5.5 ml and 1.5 ml respectively. The buffer (citric acid–dihydrogenphosphate–EDTA) quickly and efficiently removed barium ions, presumably as complexed salts. Barium was eluted with a retention volume of 7.0 ml once the solvent change was effected. Interestingly, free barium was not eluted from the column using methanol as a mobile phase. This result does not indicate any particular affinity for the stationary phase, but more likely reflects the reduced solubility of barium salts in methanol¹⁶. In addition, separation of the components of the equilibrium system using methanol, which is a weaker acid than water, indicates that the establishment of chemical equilibrium in methanol is slow, relative to the time required for the analysis. Cryptate complexes are known to be considerably more stable in methanol than in water¹. A typical elution pattern of a mixture containing all three components of the system under study is provided in Fig. 1. The results of the column recovery experiments are provided in Table I. Ultraviolet spectra of 2B:2:2 showed that absorbance at 275 nm was linear with concentration of 2B:2:2 over the range studied.

Our interest in the potential use of cryptate complexes of metal radionuclides for cancer therapy required the development of a convenient assay procedure for

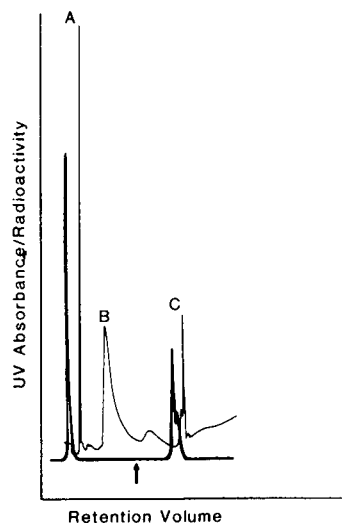


Fig. 1. Typical elution pattern of an equilibrium mixture of barium complex of 2B:2:2 (A), 2B:2:2 (B) and uncomplexed barium (c) represented by UV absorbance (—), and radioactivity (---). Arrow indicates point of mobile phase change.

TABLE I
HPLC COLUMN RECOVERIES (%)

Species	Trials	Recovery (%)
2B:2:2	6	87.5 ^a ± 1.53
Complex	8	101.8 ^{b,c} ± 1.91
Ba ²⁺	5	92.4 ^c ± 3.94

^a By UV absorbance at 275 nm.

^b Recovery consists of 74.9 ± 6.17% complex and 26.9 ± 5.67% excess free Ba²⁺.

^c By scintillation counting of ¹³³Ba.

determination of complex stabilities under various conditions. The method reported here is the first chromatographic assay developed for this system and is more convenient than the assay methods previously reported.

ACKNOWLEDGEMENTS

This work was supported by the Medical Research Service of the Veterans Administration and by a University of Iowa College of Medicine BSRG Grant.

REFERENCES

- 1 J. M. Lehn, *Struct. Bonding (Berlin)*, 16 (1973) 1.
- 2 R. T. Myers, *Inorg. Nucl. Chem. Lett.*, 16 (1980) 329.
- 3 J. M. Lehn and J. P. Sauvage, *J. Am. Chem. Soc.*, 97 (1975) 6700.
- 4 E. L. Yee, O. A. Gansow and M. J. Weaver, *J. Am. Chem. Soc.*, (1970) 2278.
- 5 W. H. Muller, W. A. Muller and U. Linznev, *Naturwissenschaften*, 64 (1977) 96.
- 6 K. A. Krohn, Y. Yano, T. F. Budinger and B. R. Moyer, *Radionuclide Generators: New Systems for Nuclear Medicine Applications*, Society of Nuclear Medicine, Washington, DC, 1984, pp. 199-213.
- 7 M. W. Brechbiel, O. A. Gansow, R. W. Atcher, J. Schlom, J. Esteban, D. Simpson and D. Colcher, *Inorg. Chem.*, 25 (1986) 2772.
- 8 A. Knochel, J. Oehler, G. Rudolf and V. Sinnwell, *Tetrahedron*, 33 (1977) 119.
- 9 E. Kauffmann, J. L. Dye, J. M. Lehn and A. I. Popov, *J. Am. Chem. Soc.*, 102 (1980) 2274.
- 10 N. Morel-Desrosiere and J. P. Morel, *Nouv. J. Chim.*, 8 (1984) 269.
- 11 M. H. Abraham, A. F. Danil de Namor and R. A. Schulz, *J. Chem. Soc. Faraday Trans. 1*, 76 (1980) 869.
- 12 P. Kontur, R. Dawson and A. Monjan, *J. Neurosci. Methods*, 11 (1984) 5.
- 13 L. W. O'Laughlin, *Anal. Chem.*, 54 (1982) 178.
- 14 J. Bauer, C. Linton and B. Norris, *J. Chromatogr.*, 445 (1988) 429.
- 15 B. D. Karcher and I. S. Krall, *J. Chromatogr. Sci.*, 25 (1987) 472.
- 16 A. M. Comey and D. A. Hahn, *Dictionary of Chemical Solubilities: Inorganic*, Macmillan, New York, 1921, pp. 81-88.

Note

Use of free-flow electrophoresis for the purification of components separated by ion-pair chromatography

R. KESSLER*, H. J. MANZ and G. SZÉKELY

Central Research, Ciba-Geigy Ltd., K-127.276, CH-4002 Basle (Switzerland)

(Received February 2nd, 1989)

After separation by ion-pair chromatography^{1–8}, isolated components still contain the ion-pair reagent (*e.g.*, tetrabutylammonium salts for anionic and heptanesulphonic acid for cationic substances), and if further characterization of a component by spectroscopic methods is necessary the ion-pair reagent has to be removed. If the substance is a large molecule there is no problem as a separation by dialysis, ultracentrifugation or gel chromatography is possible. However, if the substance is a small molecule, as with dyestuffs, the separation could be difficult. There is a need for a simple method that can quickly separate ion-pair reagents from small molecules. Here we describe a suitable purification method using free-flow electrophoresis^{9–17}.

PRINCIPLE

Flanked by the two electrolyte solutions with high ionic strength, the sample solution with low conductivity is admitted to the separation chamber (Fig. 1). Because of the stepwise field strength profile resulting from the different ionic strengths of the different solutions, sample ions migrate according to their charge at high speed to the boundaries formed by the sample solution and the electrolyte solutions. At these boundaries the sample ion will be slowed and thereby focused. With this simple separation principle, it is possible to separate anionic substances from cationic ion-pair reagents (*e.g.*, tetrabutylammonium) and cationic substances from anionic ion-pair reagents (*e.g.*, heptanesulphonic acid).

EXPERIMENTAL

All chemicals were purchased from Fluka (Buchs, Switzerland) and were of analytical-reagent grade. Free-flow electrophoresis was performed in an Elphor VaP 21 apparatus with a separation chamber of 100 × 250 × 0.8 mm (Bender and Hobein, Munich, F.R.G.). The separation method used was field-step electrophoresis^{14–17}. The conductivity of the anodic and cathodic electrolytes was 5 mS cm⁻¹, and that of the sample was 0.4 mS cm⁻¹. Experiments were performed in ammonium acetate buffer at pH 7.0 under 320 V and 100 mA. The flow of the buffer in the separation chamber was 8 ml per fraction per hour. As electrode buffer a solution of

0.04 *M* disodium hydrogenphosphate and 0.03 *M* potassium dihydrogenphosphate was pumped through both electrode compartments. The detection of the purified dyestuff was done with an adapted UV-scanner at 280 nm.

Thin-layer chromatography with silica gel 60 plates (Merck, Darmstadt, F.R.G.) was used to check the purity of the fractions from free-flow electrophoresis. The mobile phase was *n*-propanol–formic acid (8:2). The ion-pair reagent was detected with Cl_2/KI –starch¹⁸.

RESULTS

Free-flow electrophoresis is well suited to the preparative purification of components separated by ion-pair chromatography. Field-step electrophoresis allows a throughput of 50–100 mg h⁻¹. Even short residence times of about 60 s are sufficient to achieve complete separation of dyestuffs from the ion-pair reagent (Fig. 2). Afterwards the separation components still contain ammonium acetate buffer from the

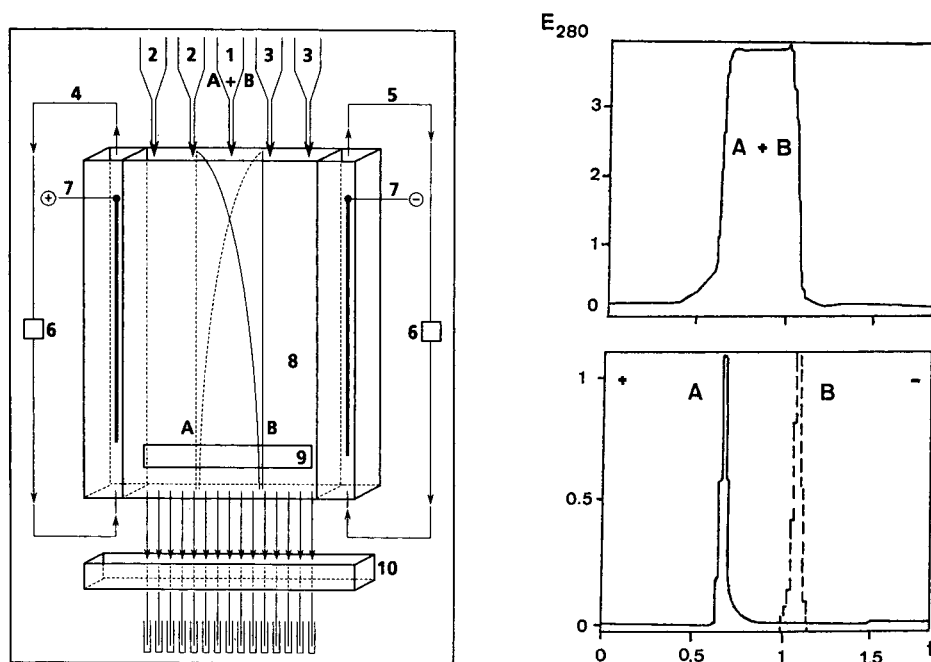


Fig. 1. Schematic diagram of the separation process. 1, Sample solution (mixture of dyestuff A with ion-pair reagent B); 2, anodic electrolyte; 3, cathodic electrolyte; 4, anodic electrode buffer; 5, cathodic electrode buffer; 6, electrode buffer pump; 7, electrodes (Pt); 8, separation chamber; 9, detection window; 10, fraction collector pump and fractions. Principle: the sample solution and the electrolytes are introduced at the top of the separation chamber consisting of two parallel plates. The electric field is applied perpendicular to the liquid flow. The charged molecules are deflected by the electrical field and are collected at the bottom through 90 outlet tubes.

Fig. 2. Separation of a dyestuff A⁻ (fluorescein) from the ion-pair reagent B⁺ (tetrabutylammonium). Above: the sample (mixture of 3 mg A and 30 mg B) is applied as a broad zone to the separation chamber. Below: separated zones A and B at the end of the separation chamber.

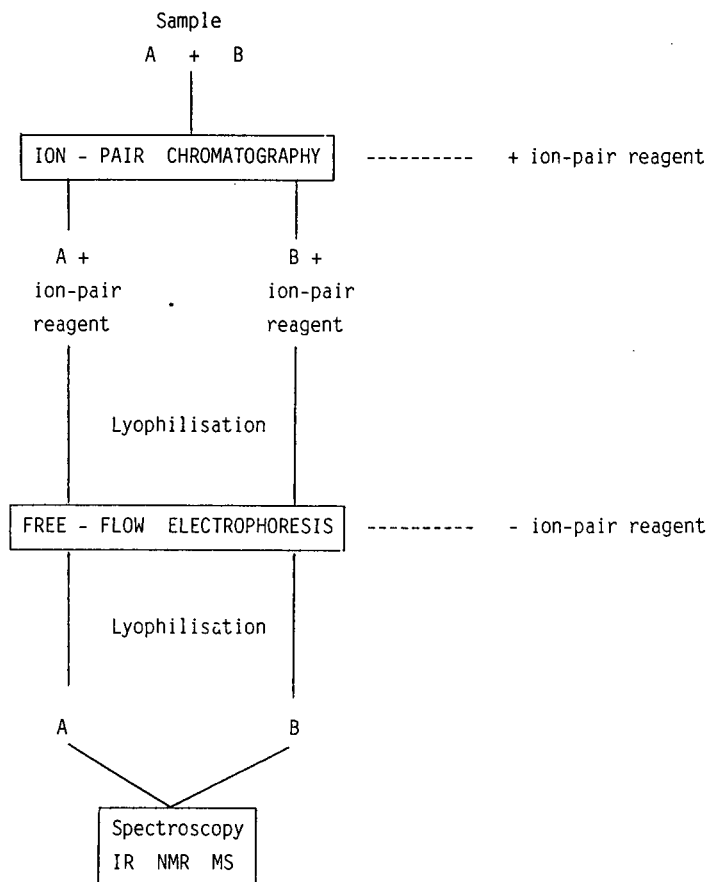


Fig. 3. Purification and isolation of dyestuffs by combination of ion-pair chromatography and free-flow electrophoresis.

electrophoresis, which can easily be removed by lyophilization. Substances purified in this way may be directly investigated using spectroscopic techniques (Fig. 3).

By means of free-flow electrophoresis, ion-pair chromatography can be used for the purification of components with similar molecular weight to the ion-pair reagent. This could be very helpful if the determination of the structures of dyestuffs and their impurities is necessary.

REFERENCES

- 1 S. Eksborg and G. Schill, *Anal. Chem.*, 45 (1973) 2092.
- 2 B. A. Persson, *Acta Pharm. Suec.*, 5 (1968) 343.
- 3 G. Schill, R. Modin and B. A. Persson, *Acta Pharm. Suec.*, 2 (1965) 119.
- 4 B. L. Karger, S. C. Su, S. Marchese and B. A. Persson, *J. Chromatogr. Sci.*, 12 (1974) 678.
- 5 B. A. Persson and B. L. Karger, *J. Chromatogr. Sci.*, 12 (1974) 521.
- 6 J. H. Knox and J. Jurand, *J. Chromatogr.*, 103 (1975) 311.
- 7 J. H. Knox and G. R. Laird, *J. Chromatogr.*, 122 (1976) 17.

- 8 J. C. Kraak and J. F. K. Huber, *J. Chromatogr.*, 102 (1974) 333.
- 9 W. Grassmann and K. Hannig, *Naturwissenschaften*, 37 (1950) 397.
- 10 K. Hannig, *Fresenius Z. Anal. Chem.*, 181 (1961) 244.
- 11 K. Wiek, *J. Chromatogr.*, 13 (1964) 111.
- 12 N. Seiler, J. Thobe and G. Werner, *Hoppe-Seyler's Z. Physiol. Chem.*, 351 (1970) 865.
- 13 E. Bidwell, G. W. R. Dike and K. W. E. Denson, *Br. J. Haematol.*, 12 (1966) 583.
- 14 H. Wagner and R. Kessler, *GIT Lab. Med.*, 7 (1984) 30.
- 15 S. A. Shukun, A. V. Gavryskin, V. N. Brezgunov and V. P. Zav'yalov, *Electrophoresis*, 6 (1985) 489.
- 16 R. Kuhn, H. Wagner, R. A. Mosher and W. Thormann, *Electrophoresis*, 8 (1987) 503.
- 17 A. Heydt, H. Wagner and H. L. Paul, *J. Virol. Methods*, 19 (1988) 13.
- 18 H. N. Rydon and P. W. G. Smith, *Nature (London)*, 169 (1952) 922.

Note

Purification of yeast killer toxin KT28 by receptor-mediated affinity chromatography

MANFRED SCHMITT and FERDINAND RADLER*

Institut für Mikrobiologie und Weinforschung, Johannes Gutenberg-Universität, Postfach 3980, D-6500 Mainz (F.R.G.)

(First received September 26th, 1988; revised manuscript received January 27th, 1989)

The ability of certain yeast strains of several genera to secrete protein or glycoprotein "killer toxins", lethal to other, sensitive yeast strains, is a well documented phenomenon¹. Most *Saccharomyces cerevisiae* killer strains belong to either the K₁, K₂ or K₃ class, in which the killer phenotype is dependent on the presence in the cell of two different double-stranded RNA species^{2,3}. Both of these RNA molecules are encapsulated by the same 88-kilodalton protein encoded by the larger L-A-dsRNA. The smaller M-dsRNA carries the information necessary for the production of killer toxin or its precursor protein⁴.

Although a considerable amount of information concerning the genetic basis of the killer phenomenon has been published⁴⁻⁷, comparatively little is known about the killer proteins and their mode of action. This lack of data is due, in part, to the instability of killer toxins (they are rapidly inactivated at pH values above pH 5 and temperatures above 30-35°C) and therefore few killer toxins have been successfully purified and characterized. The K₁-killer toxin of *S. cerevisiae* is a non-glycosylated 18-kilodalton α , β -heterodimer that, after initially binding to a linear β -1,6-D-glucan component of the cell wall, exerts its toxic effect via a specific, but as yet unknown, interaction with the cytoplasmic membrane of sensitive yeast cells^{8,9}. The killer toxin KT28 of *S. cerevisiae* differs from the killer groups K₁-K₃ in that it does not bind to glucans but to a 185-kilodalton mannoprotein constituent of yeast cell walls^{10,11}. It has already been shown that minor modifications to the structure of this mannoprotein prevent the binding of killer toxin KT28 to the cell walls of sensitive yeast strains and also that these modifications are sufficient to confer resistance to killer toxin KT28¹².

This paper describes how the specific binding of killer toxin KT28 to immobilized mannoprotein was utilized to develop a simple and effective method for the purification of this killer toxin, via a receptor-mediated affinity chromatographic technique.

EXPERIMENTAL

Microorganisms and culture media

For the production of killer toxin KT28, *Saccharomyces cerevisiae* strain 28 was cultivated in synthetic B-medium at pH 3.5¹⁰. Sensitive strains of *S. cerevisiae* (381 and X2180-1Aa, obtained from Dr. C. E. Ballou, Berkely, CA, U.S.A.) were grown in YEPD medium as described previously¹⁰. Methylene blue agar (2% glucose, 2% peptone, 1% yeast extract, 1.5% agar, 1.92% citric acid, 0.003% methylene blue, adjusted to pH 5.8 with K₂HPO₄) was used for the determination of killer toxin activity.

Production of killer toxin KT28 and measurement of killer toxin activity

S. cerevisiae strain 28 was grown in 20 l of B-medium (pH 3.5) for 72 h at 20°C. After centrifugation (5000 g, 30 min), the supernatant was concentrated by ultrafiltration (Sartorius type SM 12136, Amicon-PM10) to a volume of 20 ml and then dialysed against citrate-phosphate buffer (10 mM, pH 3.5) as described previously¹⁰. Killer toxin activity in this crude concentrate was assayed by the agar diffusion method¹³. After seeding the sensitive strain *S. cerevisiae* 381 (10⁵ cells) on to methylene blue agar plates, killer toxin KT28 (0.1 ml; crude concentrate) was pipetted into wells (10 mm diameter) cut into the agar and the plates were incubated for 72 h at 20°C. The presence of a growth-free zone around the wells is indicative of killer toxin activity. The activity of killer toxin KT28 is expressed in arbitrary units; one unit of KT28 activity corresponds to about 0.1 ng of purified protein¹¹.

Isolation and purification of the primary receptor for killer toxin KT28

The primary receptor for killer toxin KT28, a 185-kilodalton mannoprotein component of the yeast cell wall, was extracted from *S. cerevisiae* X2180-1Aa by first autoclaving (90 min, 121°C) the cells in citrate buffer (30 mM, pH 7.0) and then precipitating the mannan complex by addition of four volumes of ice-cold methanol¹¹. Following further fractionation of this extract with cetyltrimethylammonium bromide according to the method of Lloyd¹⁴, crude mannoprotein was purified by anion-exchange chromatography on Q-Sepharose followed by gel filtration on Superose 12 HR 10/30 as described previously¹¹.

Preparation of mannoprotein-CNBr-Sepharose and affinity chromatography of killer toxin KT28

CNBr-Sepharose 4B (1 g, Pharmacia) was soaked for 15 min in 50 ml HCl (1 mM), placed on a sintered-glass filter (Schott, size G 4, average pore size 10–16 µm) and rinsed successively with 200 ml of HCl (1 mM) and 5 ml of coupling solution (0.1 M NaHCO₃–0.5 M NaCl, pH 8.3). The gel was then mixed with 55 mg of purified mannoprotein (dissolved in 5 ml of coupling solution), gently shaken for 2 h at 20°C and washed with 15 ml of coupling solution on top of the sintered-glass filter. The carbohydrate content of the receptor bound to the gel matrix was determined indirectly by the phenol-sulphuric acid method as described previously¹¹. To inactivate remaining free binding sites on the CNBr-Sepharose, the gel was treated with ethanolamine (1 M, pH 8.0) for 2 h at 20°C and then washed three times with 15 ml of coupling solution and 15 ml of acetate buffer (0.1 M Na-acetate–0.5 M NaCl, pH

4.0). At a flow-rate of 1.0 ml min^{-1} , the mannoprotein–CNBr–Sephacryl gel was pumped into a glass column ($2.6 \times 1.6 \text{ cm I.D.}$) and equilibrated with ten column volumes of citrate–phosphate buffer (10 mM , $\text{pH } 3.5$). For affinity chromatography, 2 ml of crude, dialysed concentrate of killer toxin KT28 (specific activity $2.0 \cdot 10^4 \text{ U mg}^{-1} \text{ protein}$) was applied to the column and chromatographed with sodium citrate buffer (10 mM , $\text{pH } 3.5$, 4°C) at a flow-rate of 0.1 ml min^{-1} . Bound killer toxin was eluted by applying a linear gradient of $0\text{--}1 \text{ M NaCl}$ (40 ml) in sodium citrate buffer. Eluted fractions (1 ml) were collected and assayed for protein content and killer toxin activity. The protein content of the eluate was determined spectroscopically at a wavelength of 280 nm^{15} .

Sodium dodecyl sulphate-polyacrylamide gel electrophoresis (SDS-PAGE)

Following affinity chromatography, fractions that contained killer toxin KT28 were dialysed against sodium citrate buffer (10 mM , $\text{pH } 3.5$), lyophilized and then dissolved in sample buffer containing 2.5% (w/v) SDS and 5% (v/v) mercaptoethanol. The compositions of the sample and electrode buffer were as described previously¹⁰. Samples were then applied to an SDS gradient gel ($4\text{--}30\%$ acrylamide) and electrophoresed for 3.5 h at 150 V . After fixation in an aqueous solution of 25% (v/v) 2-propanol and 10% (v/v) acetic acid, the proteins were rendered visible by staining the gels with Coomassie Brilliant Blue [0.02% (w/v) in 7% (v/v) acetic acid].

RESULTS AND DISCUSSION

Mannoprotein is an important component of the yeast cell wall and constitutes the primary receptor for yeast killer toxin KT28¹¹. To enable the affinity chromatography of killer toxin to be performed, cell wall mannoprotein was purified and then covalently linked to CNBr-activated Sepharose 4B. Analysis of the carbohydrate content of the ligand, both before and after coupling mannoprotein to the gel matrix, revealed that about 20% of mannoprotein became covalently bound to the Sepharose gel.

Killer toxin KT28 bound specifically to the immobilized mannoprotein and could be eluted at a conductivity of approximately 7 mS in fractions 49–54 (Fig. 1). This affinity chromatographic procedure resulted in a 115-fold increase in killer toxin specific activity (from $2.0 \cdot 10^4$ to $2.3 \cdot 10^6 \text{ U mg}^{-1} \text{ protein}$).

The success of the technique described for purifying killer toxin KT28 was further demonstrated by SDS-PAGE (Fig. 2). In contrast to the crude preparation of killer toxin KT28, which contained several different protein components, purified killer toxin obtained by affinity chromatography was visible as a single band on SDS gels with an R_F value characteristic of the 16-kilodalton glycoprotein KT28.

Not only their instability to higher pH values, temperature and oxygen, but also their tendency to form aggregates causes problems and difficulties in the purification of yeast killer toxins^{16–18}. The affinity chromatographic technique described here, based on the biospecific interaction of killer toxin and its receptor, appears to be a simple and effective one-step method for the purification of yeast killer toxin. However, it is apparently insufficient to use preparations of immobilized yeast cell walls as the bound ligand, as only partial purification of killer toxin can then be achieved¹⁹. Obviously, for the successful purification of killer toxin, isolated and purified recep-

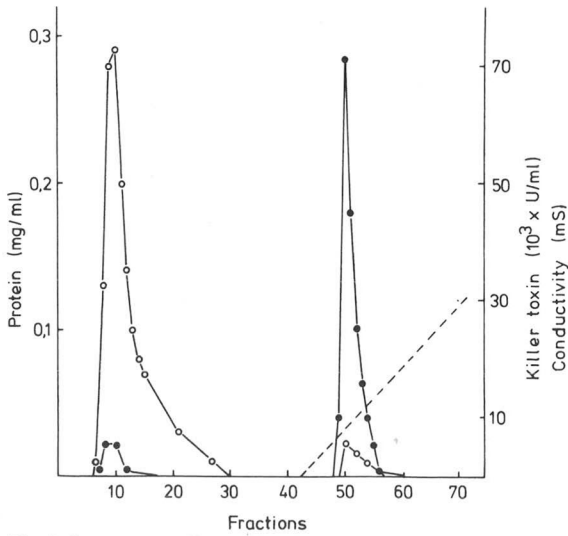


Fig. 1. Receptor-mediated affinity chromatography of killer toxin KT28 with a column of mannoprotein-CNBr-Sepharose 4B. ● = Killer toxin activity; ○ = protein concentration; broken line = conductivity.

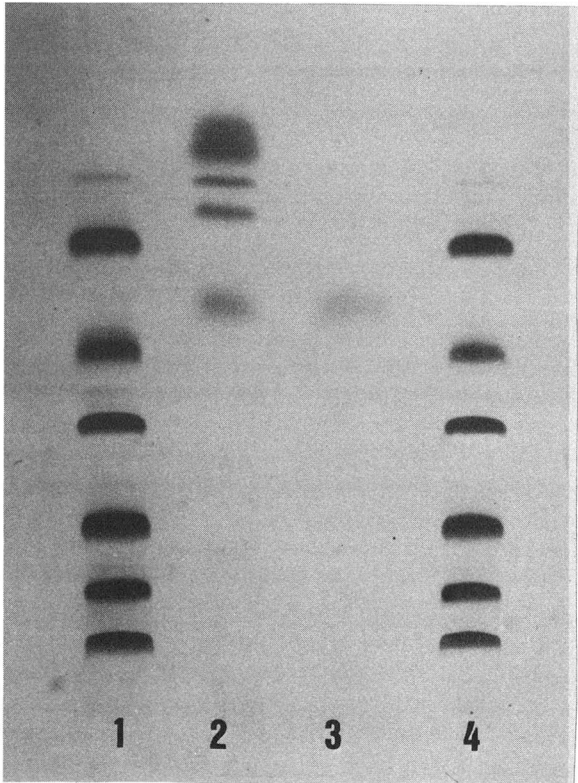


Fig. 2. SDS-PAGE of crude killer toxin KT28 before (lane 2) and after (lane 3) affinity chromatography with mannoprotein-CNBr-Sepharose 4B. Lanes 1 and 4, low-molecular-weight calibration proteins (from top to the bottom: α -lactalbumin, 14.2 kilodaltons; trypsin inhibitor, 20.1 kilodaltons; carbonic anhydrase, 29 kilodaltons; ovalbumin, 45 kilodaltons; albumin, 66 kilodaltons; phosphorylase B, 97.4 kilodaltons).

tors are required. Only the primary receptors for killer toxins K_1 ⁹ and KT28¹¹ have so far been identified, and it is not known whether other types of killer toxins are bound by these receptors¹². Hutchins and Bussey⁹ linked fungal pustulan to Sepharose and were able to purify the K_1 killer toxin of *S. cerevisiae* T158C by affinity chromatography, thereby demonstrating the affinity of K_1 to β -1,6-D-glucan, a component of the yeast cell wall. Similarly, we previously used mannoprotein linked to Sepharose to demonstrate the binding of killer toxin KT28 to cell wall mannoprotein¹¹. However, in these experiments, mannoprotein was linked to the Sepharose via the hydroxyl groups of the mannose side-chains essential for the binding activity of the KT28-receptor¹². Consequently, the affinity of the receptor for killer toxin KT28 was decreased and this made the purification of killer toxin on a preparative scale impossible.

In the experiments described here an affinity gel was used to which the purified receptors for KT28 had been linked covalently via their polypeptide chains, as the protein moiety of mannoprotein is known not to be involved in killer toxin binding¹¹. By introducing this modification, killer toxin KT28 could be purified 115-fold and separated from other extra-cellular proteins. The gel matrix of Sepharose itself does not bind the killer toxin; this was demonstrated with a CNBr-Sepharose in which all reactive groups had been blocked with ethanolamine.

Thus, it was shown that the presence of a specific receptor, cell wall mannoprotein, is essential for successful affinity chromatography of killer toxin KT28. We are optimistic that this procedure will provide an effective means for the selective purification of other yeast killer toxins and, possibly, other proteins with similar biological activities. One immediate candidate for purification by the affinity chromatography method is the killer toxin of *Debaryomyces hansenii*, which, like killer toxin KT28 of *S. cerevisiae*, is bound by the mannan fraction of the yeast cell wall²⁰.

REFERENCES

- 1 D. J. Tipper and K. A. Bostian, *Microbiol. Rev.*, 48 (1984) 125.
- 2 K. A. Bostian, J. A. Surgeon and D. J. Tipper, *J. Bacteriol.*, 143 (1980) 463.
- 3 R. B. Wickner, *Annu. Rev. Biochem.*, 55 (1986) 373.
- 4 T. W. Young, in A. H. Rose and J. S. Harrison (Editors), *The Yeasts*, Academic Press, New York, 2nd ed., 1987, p. 131.
- 5 R. Esteban and R. B. Wickner, *Genetics*, 117 (1987) 399.
- 5 M. El-Sherbeini and K. A. Bostain, *Proc. Natl. Acad. Sci. U.S.A.*, 84 (1987) 4293.
- 7 T. Fujimura and R. B. Wickner, *J. Biol. Chem.*, 263 (1988) 454.
- 8 K. A. Bostian, H. Bussey, Q. Elliot, V. Burn, A. Smith and D. J. Tipper, *Cell*, 36 (1984) 741.
- 9 K. Hutchins and H. Bussey, *J. Bacteriol.*, 154 (1983) 161.
- 10 P. Pfeiffer and F. Radler, *J. Gen. Microbiol.*, 128 (1982) 2699.
- 11 M. Schmitt and F. Radler, *J. Gen. Microbiol.*, 133 (1987) 3347.
- 12 M. Schmitt and F. Radler, *J. Bacteriol.*, 170 (1988) 2192.
- 13 J. M. Somers and E. A. Bevan, *Genet. Res.*, 13 (1969) 71.
- 14 K. O. Lloyd, *Biochemistry*, 9 (1970) 3446.
- 15 O. Warburg and W. Christian, *Biochem. Z.*, 310 (1941) 384.
- 16 D. R. Woods and E. A. Bevan, *J. Gen. Microbiol.*, 51 (1968) 115.
- 17 H. Bussey, *Nature New Biol.*, 235 (1972) 73.
- 18 G. E. Palfrey and H. Bussey, *Eur. J. Biochem.*, 93 (1979) 487.
- 19 V. Jirku, *Biotechnol. Lett.*, 8 (1986) 639.
- 20 S. Jenkner-Becherer, unpublished results.

Author Index

- Bandyopadhyay, M. K., see Ray, R. K. 383
- Barbaro, A. M., see Biagi, G. L. 121
- Barker, T.
— and Brown, S. D.
Resolution of a coeluting chromatographic pair using Kalman filtering 77
- Bechalany, A., see El Tayar, N. 91
- Bechemin, C.
—, Delmas, D. and Garet, M.-J.
Improvement of a carbon-nitrogen elemental analyser for marine samples collected on glass-fibre filters 399
- Beck, D. J., see Krishnamurthy, T. 209
- Belyakova, L. D., see Hradil, J. 143
- Bergren, M. S., see Foust, D. W. 161
- Berthod, A.
—, Chartier, F. and Rocca, J.-L.
Contribution of longitudinal diffusion to band broadening in liquid chromatography 53
- Biagi, G. L.
—, Pietrogrande, M. C., Barbaro, A. M., Guerra, M. C., Borea, P. A. and Cantelli Forti, G.
Study of the lipophilic character of a series of β -carbolines 121
- Bishr, M. M., see Walash, M. I. 390
- Blessington, B.
—, Crabb, N., Karkee, S. and Northage, A.
Chromatographic approaches to the quality control of chiral propionate anti-inflammatory drugs and herbicides 183
- Borea, P. A., see Biagi, G. L. 121
- Breckenridge, G. H. McG., see Christie, W. 261
- Britten, A. J., see Palmentier, J.-P. F. 241
- Brown, S. D., see Barker, T. 77
- Bushuk, W., see Sapirstein, H. D. 127
- By, A.
—, Ethier, J. C., Lauriault, G., LeBelle, M., Lodge, B. A., Savard, C., Sy, W.-W. and Wilson, W. L.
Traditional oriental medicines. I. Black Pearl: identification and chromatographic determination of some undeclared medicinal ingredients 406
- Callery, P. S., see Grubb, M. F. 191
- Cantelli Forti, G., see Biagi, G. L. 121
- Charbonneau, G. M., see Palmentier, J.-P. F. 241
- Chartier, F., see Berthod, A. 53
- Chauret, N.
— and Hubert, J.
Characterization of indirect photometry for the determination of inorganic anions in natural water by ion chromatography 329
- Christie, W. W.
— and Breckenridge, G. H. McG.
Separation of *cis* and *trans* isomers of unsaturated fatty acids by high-performance liquid chromatography in the silver ion mode 261
- Crabb, N., see Blessington, B. 183
- Däppen, R.
—, Karfunkel, H. R. and Leusen, F. J. J.
 π -Acceptor amide group for liquid chromatographic chiral separations with special emphasis on the 3,5-dinitrobenzoyl amide 101
- Davis, P. J., see Wong, Y. W. J. 281
- De Kruijf, N.
—, Schouten, A., Rijk, M. A. H. and Pranoto-Soetardhi, L. A.
Determination of preservatives in cosmetic products. II. High-performance liquid chromatographic identification 317
- Delmas, D., see Bechemin, C. 399
- Dziwiński, E., see Szymanowski, J. 197
- Eichinger, H. M., see Seewald, M. 271
- El Rassi, Z., see Melander, W. R. 3
- El Tayar, N.
—, Marston, A., Bechalany, A., Hostettmann, K. and Testa, B.
Use of centrifugal partition chromatography for assessing partition coefficients in various solvent systems 91
- Ethier, J. C., see By, A. 406
- Euerby, M. R.
—, Partridge, L. Z. and Nunn, P. B.
Resolution of neuroactive non-protein amino acid enantiomers by high-performance liquid chromatography utilising pre-column derivatisation with *o*-phthaldialdehyde-chiral thiols. Application to 2-amino- ω -phosphonoalkanoic acid homologues and α -amino- β -N-methylaminopropanoic acid (β -methylaminoalanine) 412
- Filfil, N. T., see Janini, G. M. 43
- Forti, G., Cantelli, see Biagi, G. L. 121
- Foust, D. W.
— and Bergren, M. S.
Analysis of solvent residues in pharmaceutical bulk drugs by wall-coated open tubular gas chromatography 161
- Fu, R., see Jin, Y. 153
- Gamoh, K.
—, Omote, K., Okamoto, N. and Takatsuto, S.
High-performance liquid chromatography of brassinosteroids in plants with derivatization using 9-phenanthreneboronic acid 424
- Garet, M.-J., see Bechemin, C. 399

- Gillespie, P. C., see Smith, M. A. 111
- Goosey, M. W., see Peacock, G. A. 293
- Grubb, M. F.
- and Callery, P. S.
Derivatization of N-methyl and cyclic amino acids with dimethylformamide dimethyl acetal 191
- Guerra, M. C., see Biagi, G. L. 121
- Hamilton, V. T.
- , Spall, W. D., Smith, B. F. and Peterson, E. J.
Quantitative analysis of thorium in plutonium using reversed-phase liquid chromatography and spectrophotometric detection 369
- Harding, D. R. K., see Poll, D. J. 231
- Henson, C. A.
- and Stone, J. M.
Rapid high-performance liquid chromatographic separation of barley malt α -amylase on cyclobond columns 361
- Horváth, Cs., see Melander, W. R. 3
- Hoshino, H., see Saitoh, T. 175
- Hostettmann, K., see El Tayar, N. 91
- Hradil, J.
- , Švec, F., Platonova, N. P., Belyakova, L. D. and Maroušek, V.
Gas chromatographic and sorption properties of macroporous methacrylate copolymers 143
- Huang, Z., see Jin, Y. 153
- Hubert, J., see Chauret, N. 329
- Huffer, M.
- and Schreier, P.
Analytical resolution of 4(5)-alkylated γ -(δ)-lactones by high-performance liquid chromatography on a silica-bonded chiral polyacrylamide sorbent. Chromatographic characterization of a stationary phase 137
- Isensee, R. K., see Krishnamurthy, T. 209
- Janini, G. M.
- and Filfil, N. T.
Optimization of the gas chromatographic separation of five-membered ring polyarenes with an admixed BPhBT liquid crystal-Dexsil 300 stationary phase 43
- Jarvis, B. B., see Krishnamurthy, T. 209
- Jin, Y.
- , Fu, R. and Huang, Z.
Use of crown ethers in gas chromatography 153
- Karasek, F. W., see Palmentier, J.-P. F. 241
- Karfunkel, H. R., see Däppen, R. 101
- Karkee, S., see Blessington, B. 183
- Kauffmann, G. B., see Ray, R. K. 383
- Kawaguchi, Y., see Tanaka, M. 429
- Keller, J. W.
- and Niwa, K.
Milligram-scale separation of optical isomers of 2-pentafluoroethylalanine and 2-trifluoromethylalanine by medium-performance reversed-phase chromatography 434
- Kessler, R.
- , Manz, H. J. and Székely, G.
Use of free-flow electrophoresis for the purification of components separated by ion-pair chromatography 444
- Kleinmann, I., see Plicka, J. 29
- Koehler, H.
- , Larocque, L. and Sved, S.
Use of liquid chromatography in the synthesis of isoluminol-labelled medroxyprogesterone acetate and zeranol 305
- Krishnamurthy, T.
- , Beck, D. J., Isensee, R. K. and Jarvis, B. B.
Mass spectral investigations on trichothecene mycotoxins. VII. Liquid chromatographic-thermospray mass spectrometric analysis of macrocyclic trichothecenes 209
- Kruijf, N. de, see De Kruijf, N. 317
- Kuhn, A. O.
- , Lederer, M. and Sinibaldi, M.
Adsorption chromatography on cellulose. IV. Separation of D- and L-tryptophan and D- and L-methyltryptophan on cellulose with aqueous solvents 253
- Kusz, P., see Szymanowski, J. 197
- Larocque, L., see Koehler, H. 305
- Lascu, I., see Presecan, E. 396
- Laurialt, G., see By, A. 406
- LeBelle, M., see By, A. 406
- Lederer, M., see Kuhn, A. O. 253
- Leusen, F. J. J., see Däppen, R. 101
- Lodge, B. A., see By, A. 406
- McCune, J. E., see Pirkle, W. H. 67
- Manz, H. J., see Kessler, R. 444
- Maroušek, V., see Hradil, J. 143
- Marston, A., see El Tayar, N. 91
- Melander, W. R.
- , El Rassi, Z. and Horváth, Cs.
Interplay of hydrophobic and electrostatic interactions in biopolymer chromatography. Effect of salts on the retention of proteins 3
- Murakami, T., see Tsukioka, T. 351
- Niwa, K., see Keller, J. W. 434
- Northage, A., see Blessington, B. 183
- Nunn, P. B., see Euerby, M. R. 412
- Okamoto, N., see Gamoh, K. 424
- Omote, K., see Gamoh, K. 424

- Palmentier, J.-P. F.
—, Britten, A. J., Charbonneau, G. M. and Karasek, F. W.
Determination of polycyclic aromatic hydrocarbons in lubricating oil base stocks using high-performance liquid chromatography and gas chromatography-mass spectrometry 241
- Partridge, L. Z., see Euerby, M. R. 412
- Peacock, G. A.
— and Goosey, M. W.
Separation of fungal sterols by normal-phase high-performance liquid chromatography. Application to the evaluation of ergosterol biosynthesis inhibitors 293
- Peterson, E. J., see Hamilton, V. T. 369
- Peterson, R. E., see Pettit, W. A. 440
- Pettit, W. A.
—, Swailes, B. K. and Peterson, R. E.
Isocratic reversed-phase high-performance liquid chromatographic assay for a cryptand-cryptate-free metal ion system 440
- Pietrogrande, M. C., see Biagi, G. L. 121
- Pirkle, W. H.
— and McCune, J. E.
Discussion of a controversial chiral recognition model 67
- Platonova, N. P., see Hradil, J. 143
- Plicka, J.
—, Svoboda, V., Kleinmann, I. and Uhlířvá, A.
Mathematical modelling of the peak in liquid chromatography 29
- Poll, D. J.
— and Harding, D. R. K.
Formic acid as a milder alternative to trifluoroacetic acid and phosphoric acid in two-dimensional peptide mapping 231
- Porumb, H., see Presecan, E. 396
- Pranoto-Soetardhi, L. A., see De Kruijf, N. 317
- Presecan, E.
—, Porumb, H. and Lascu, I.
Simple method for the preparation of spherical agarose and composite gel particles 396
- Pyżalski, K., see Szymanowski, J. 197
- Radler, F., see Schmitt, M. 448
- Rassi, Z. El, see Melander, W. R. 3
- Ray, R. K.
—, Bandyopadhyay, M. K. and Kauffman, G. B.
Chromatographic studies of metal complexes. V. Thin-layer chromatography of some octahedral cobalt(III) and nickel(II) complexes 383
- Rijk, M. A. H., see De Kruijf, N. 317
- Rocca, J.-L., see Berthod, A. 53
- Saitoh, T.
—, Hoshino, H. and Yotsuyanagi, T.
Separation of 4-(2-pyridylazo)resorcinolato metal chelates by micellar electrokinetic capillary chromatography 175
- Salama, O. M., see Walash, M. I. 390
- Sapirstein, H. D.
—, Scanlon, M. G. and Bushuk, W.
Normalisation of high-performance liquid chromatography peak retention times for computerised comparison of wheat prolamin chromatograms 127
- Sato, H.
Isocratic elution of sodium, ammonium, potassium, magnesium and calcium ions by ion-exchange chromatography 339
- Savard, C., see By, A. 406
- Scanlon, M. G., see Sapirstein, H. D. 127
- Schmitt, M.
— and Radler, F.
Purification of yeast killer toxin KT28 by receptor-mediated affinity chromatography 448
- Schouten, A., see De Kruijf, N. 317
- Schreier, P., see Huffer, M. 137
- Seewald, M.
— and Eichinger, H. M.
Separation of major phospholipid classes by high-performance liquid chromatography and subsequent analysis of phospholipid-bound fatty acids using gas chromatography 271
- Shatirishvili, I. Sh.
Application of correlation chromatography to the investigation of biopolymers in wines 420
- Shono, T., see Tanaka, M. 429
- Sinibaldi, M., see Kuhn, A. O. 253
- Šlais, K.
Sample-induced internal gradient of ionic strength in ion-exclusion microcolumn liquid chromatography 223
- Smith, B. F., see Hamilton, V. T. 369
- Smith, M. A.
— and Gillespie, P. C.
Ionization of DEAE-cellulose. Dependence of pK on ionic strength 111
- Spall, W. D., see Hamilton, V. T. 369
- Stone, J. M., see Henson, C. A. 361
- Švec, F., see Hradil, J. 143
- Sved, S., see Koehler, H. 305
- Svoboda, V., see Plicka, J. 29
- Swailes, B. K., see Pettit, W. A. 440
- Sy, W.-W., see By, A. 406
- Székely, G., see Kessler, R. 444
- Szewczyk, H., see Szymanowski, J. 197

- Szymanowski, J.
—, Kusz, P., Dziwiński, E., Szewczyk, H. and Pyżalski, K.
Degradation and analysis of polyoxyethylene monoalkyl ethers in the presence of acetyl chloride and ferric chloride 197
- Takatsuto, S., Gamoh, K. 424
- Tanaka, M.
—, Shono, T., Zhu, D.-Q. and Kawaguchi, Y.
Liquid chromatographic separation of racemates on acetylated or carbamoylated β -cyclodextrin-bonded stationary phases 429
- Tayar, N. El, see El Tayar, N. 91
- Testa, B., see El Tayar, N. 91
- Tsukioka, T.
— and Murakami, T.
Capillary gas chromatographic-mass spectrometric determination of acid herbicides in soils and sediments 351
- Uhlířová, A., see Plicka, J. 29
- Walash, M. I.
—, Salama, O. M. and Bishr, M. M.
Use of absorbance ratios in densitometric measurements for the characterization and identification of natural products of pharmacological interest 390
- Wan, H.
Large-volume spotting apparatus and its application to the semi-quantitative determination of organochlorine pesticides in tea 403
- Wilson, W. L., see By, A. 406
- Wong, Y. W. J.
— and Davis, P. J.
Analysis of warfarin and its metabolites by reversed-phase ion-pair liquid chromatography with fluorescence detection 281
- Wroński, M.
Influence of the cellulose content of cellulose gels on the electrophoretic mobility 378
- Yotsuyanagi, T., see Saitoh, T. 175
- Zhu, D.-Q., see Tanaka, M. 429

journal of
chromatography news section



**THE THIRTEENTH SYMPOSIUM ON
COLUMN LIQUID CHROMATOGRAPHY**

UNDER THE PATRONAGE OF
HER MAJESTY QUEEN SILVIA

STOCKHOLM, SWEDEN, JUNE 25-30, 1989

SCIENTIFIC PROGRAMME

Introductory Lecture

Prospects in Separation Science and Technology: The Future Role of Chromatography
Csaba Horváth

Review Lectures

Chromatography and Biotechnology
Fred Regnier

Novel Analytical and Preparative Chiral Separations
Wolfgang Lindner

The Role of Microcolumn Separation Methods in the Analysis
and Characterization of Femtomole Amounts of Biological
Macromolecules
Milos Novotny

Biomedical and Pharmaceutical Applications
Fritz Erni

Progress in Synthesis and Characterization of Stationary
Phases for Column Liquid Chromatography
Klaus Unger

Coupled Column Separations by LC-GC
Konrad Grob Jr

Keynote Lectures

Chemometrics and Chromatography
Optimization of Chromatographic Separations Using a
Combination of Optimization Software and Expert Systems
Peter Schoenmakers

Biomedical Applications
Approaches to Liquid-Chromatographic Separation in
Biomedical Analysis
Bengt-Arne Persson

Progress in Detection Techniques
Progress in Optical Detection Techniques
Edward Yeung

Field Flow Fractionation and Related Techniques
Advances in FFF
J. Calvin Giddings

Hydrodynamic Chromatography on Small Sized Non-Porous
Silica Gel Particles
Johan Kraak

Quantitative Structure Retention Relationships
Correlations between Chemical Structure of Noncongeneric
Solutes and Their Retention in Liquid Chromatography
Roman Kaliszán

Retention mechanisms

Utilization of Secondary Equilibria in LC
Hans Poppe

LC / MS — NMR — IR

On-Line MS in Chromatography and Electrophoresis
Jack Henion

Hyphenated Techniques in Micro-LC
Kiyokatsu Jinno

Chiral separations

Chiral Recognition in Hydrophobic Monolayer on Silica Gel in Reversed Phase LC
Shoji Hara

Interactions between Macromolecules and Small Molecules — Kinetic Aspects
Bengt Mannervik

Separations of Enantiomers Using Ion-Pair Chromatography
Curt Pettersson

Biopolymer separations

Structure-function Studies on Growth Factors: The Need for High Resolution Separations
E.C. Nice

Computers and Chromatography

Development and Optimisation of HPLC Methods by Computer-Assisted Mobile-Phase Mapping
Lloyd Snyder

Novel Approaches of Solid Phases

NMR-Imaging, a Tool for Optimization of Chromatographic Columns
Ernst Bayer

LC-Techniques in Neurochemistry

Microcolumn Separations in Neurochemistry
James W. Jorgenson

Preparative Chromatography

Theory of Non-Linear Chromatography
Georges Guiochon

Preparative Chromatography of Biopolymers
Csaba Horváth

Capillary Liquid Chromatography and Electrophoresis

High-Performance Electrophoresis in Adsorption- and Electroendosmosis-Free 0.025—0.05 μm Capillaries — A Versatile Analytical and Micropreparative Method with a Resolution Approaching the Theoretical Limit
Stellan Hjérten

Supercritical Fluid Chromatography

Possibilities and Limitations of SFC
Milton Lee

Novel Solid Phases

Polymer Coated Stationary Phases Based on Different Types of Inorganic Support Materials such as SiO_2 , Al_2O_3 , and ZrO_2 .
G. Schomburg

Coupled Column Separations

Improved Selectivity in Precolumn Sample Handling of Biological and Environmental Samples
Udo Brinkman

Closing Lecture

A Detailed Examination of the Kinetic Behavior of Protein Structural Changes in Chromatographic Systems
Barry L. Karger

The scientific programme comprises further about 60 lectures, over 400 posters, as well as discussion sessions.

Social programme

The symposium programme includes a welcome party, a reception in the form of a buffet dinner at the Stockholm City Hall, known all over the world as the setting for the annual Nobel Prize banquet. The symposium banquet will be held at a well-reputed restaurant, with a view of the old Royal Palace, in the city centre.

The traditional Wednesday excursions will, among other alternatives, be made to the old university city of Uppsala, with traditions from the Viking era, or by boat into the Stockholm archipelago, or to the Palace of Drottningholm, present residence of the Swedish Royal Family.

For accompanying persons, a full program will be arranged with visits to places of interest both within and outside Stockholm.

We can promise that it will be possible for you to discover the beauty of Stockholm and its surroundings and to feel the atmosphere of the Nordic light.

Attractive post-symposium tours will be arranged on request: for example to the glassblowers in Småland; to the midnight sun in Lapland; or even to Helsinki and Leningrad.

Invitation to "Last minute poster session".

You are invited to participate in the scientific programme by the registration of a last minute poster with deadline April 30. Please, require the Invitation Programme including abstract forms from the Conference secretariat.

For further information, please contact:

Conference secretariat

Stockholm Convention Bureau
CLC '89
Box 6911
S-102 39 Stockholm, Sweden
Tel. 46-8-23 09 90
Telex: S-11556
Telefax: 46-8-34 84 41

PUBLICATION SCHEDULE FOR 1989

Journal of Chromatography and Journal of Chromatography, Biomedical Applications

MONTH	J	F	M	A	M	J	J	A	S	O	N	D				
Journal of Chromatography	461 462 463/1	463/2 464/1	464/2 465/1 465/2	466 467/1 467/2	468 469 470/1 470/2	471 472/1 472/2 473/1	473/2 474/1 474/2 475	476 477/1 477/2	The publication schedule for further issues will be published later							
Bibliography Section		486/1		486/2		486/3		486/4								
Biomedical Applications	487/1	487/2	488/1 488/2	489/1 489/2	490/1 490/2	491/1	491/2	492/1 493/1					493/2			

INFORMATION FOR AUTHORS

(Detailed *Instructions to Authors* were published in Vol. 445, pp. 453–456. A free reprint can be obtained by application to the publisher, Elsevier Science Publishers B.V., P.O. Box 330, 1000 AH Amsterdam, The Netherlands.)

Types of Contributions. The following types of papers are published in the *Journal of Chromatography* and the section on *Biomedical Applications*: Regular research papers (Full-length papers), Notes, Review articles and Letters to the Editor. Notes are usually descriptions of short investigations and reflect the same quality of research as Full-length papers, but should preferably not exceed six printed pages. Letters to the Editor can comment on (parts of) previously published articles, or they can report minor technical improvements of previously published procedures; they should preferably not exceed two printed pages. For review articles, see inside front cover under Submission of Papers.

Submission. Every paper must be accompanied by a letter from the senior author, stating that he is submitting the paper for publication in the *Journal of Chromatography*. Please do not send a letter signed by the director of the institute or the professor unless he is one of the authors.

Manuscripts. Manuscripts should be typed in double spacing on consecutively numbered pages of uniform size. The manuscript should be preceded by a sheet of manuscript paper carrying the title of the paper and the name and full postal address of the person to whom the proofs are to be sent. Authors of papers in French or German are requested to supply an English translation of the title of the paper. As a rule, papers should be divided into sections, headed by a caption (e.g., Summary, Introduction, Experimental, Results, Discussion, etc.). All illustrations, photographs, tables, etc., should be on separate sheets.

Introduction. Every paper must have a concise introduction mentioning what has been done before on the topic described, and stating clearly what is new in the paper now submitted.

Summary. Full-length papers and Review articles should have a summary of 50–100 words which clearly and briefly indicates what is new, different and significant. In the case of French or German articles an additional summary in English, headed by an English translation of the title, should also be provided. (Notes and Letters to the Editor are published without a summary.)

Illustrations. The figures should be submitted in a form suitable for reproduction, drawn in Indian ink on drawing or tracing paper. Each illustration should have a legend, all the legends being typed (with double spacing) together on a *separate sheet*. If structures are given in the text, the original drawings should be supplied. Coloured illustrations are reproduced at the author's expense, the cost being determined by the number of pages and by the number of colours needed. The written permission of the author and publisher must be obtained for the use of any figure already published. Its source must be indicated in the legend.

References. References should be numbered in the order in which they are cited in the text, and listed in numerical sequence on a separate sheet at the end of the article. Please check a recent issue for the layout of the reference list. Abbreviations for the titles of journals should follow the system used by *Chemical Abstracts*. Articles not yet published should be given as "in press" (journal should be specified), "submitted for publication" (journal should be specified), "in preparation" or "personal communication".

Dispatch. Before sending the manuscript to the Editor please check that the envelope contains three copies of the paper complete with references, legends and figures. One of the sets of figures must be the originals suitable for direct reproduction. Please also ensure that permission to publish has been obtained from your institute.

Proofs. One set of proofs will be sent to the author to be carefully checked for printer's errors. Corrections must be restricted to instances in which the proof is at variance with the manuscript. "Extra corrections" will be inserted at the author's expense.

Reprints. Fifty reprints of Full-length papers, Notes and Letters to the Editor will be supplied free of charge. Additional reprints can be ordered by the authors. An order form containing price quotations will be sent to the authors together with the proofs of their article.

Advertisements. Advertisement rates are available from the publisher on request. The Editors of the journal accept no responsibility for the contents of the advertisements.

An authoritative review... highly recommended...

Optimization of Chromatographic Selectivity

A Guide to Method Development

by P. Schoenmakers, *Philips Research Laboratories, Eindhoven, The Netherlands*

(Journal of Chromatography Library, 35)

"The contents of this book have been put together with great expertise and care, and represent an authoritative review of this very timely topic... highly recommended to practising analytical chemists and to advanced students." (Jnl. of Chromatography)

"...an important contribution by a worker who has been in the field almost from its inception and who understands that field as well as anyone. If one is serious about method development, particularly for HPLC, this book will well reward a careful reading and will continue to be useful for reference purposes." (Mag. of Liquid & Gas Chromatography)

This is the first detailed description of method development in chromatography - the overall process of which may be summarized as: method selection, phase selection, selectivity optimization, and system optimization. All four aspects receive attention in this eminently readable book.

The first chapter describes chromatographic theory and nomenclature and outlines the method development process. Guidelines are then given for method selection and quantitative concepts for characterizing and classifying chromatographic phases. Selective separation methods (from both GC and LC) are

given - the main parameters of each method are identified and simple, quantitative relations are sought to describe their effects. Criteria by which to judge the quality of separation are discussed with clear recommendations for different situations. The specific problems involved in the optimization of chromatographic selectivity are explained. Optimization procedures, illustrated by examples, are described and compared on the basis of a number of criteria. Suggestions are made both for the application of different procedures and for further research. The optimization of programmed analysis receives special attention, and the last chapter summarizes the optimization of the chromatographic system, including the optimization of the efficiency, sensitivity and instrumentation.

Those developing chromatographic methods or wishing to improve existing methods will value the detailed, structured way in which the subject is presented. Because optimization procedures and criteria are described as elements of a complete optimization package, the book will help the reader to understand, evaluate and select current and future commercial systems.

Contents: 1. Introduction. 2. Selection of Methods. 3. Parameters Affecting Selectivity. 4. Optimization Criteria. 5. Optimization Procedures. 6. Programmed Analysis. 7. System Optimization. Indexes.

1986 1st repr. 1987 xvi + 346 pages
US\$ 110.50 / Dfl. 210.00
ISBN 0-444-42681-7



ELSEVIER SCIENCE PUBLISHERS

P.O. Box 211, 1000 AE Amsterdam, The Netherlands
P.O. Box 1663, Grand Central Station, New York, NY 10163, USA

scale 82